
IREX I

Performance of Iris Recognition Algorithms on Standard Images

Supplement to

NIST Interagency Report 7629

P. Grother, E. Tabassi, G. W. Quinn, W. Salamon

Information Access Division
National Institute of Standards and Technology



October 28, 2009

Release Notes

- ▷ The appendices in this document contain a complete set of results for each SDK tested in the IREX trial. This information is expected to be of most use to the IREX algorithm providers.
- ▷ Much of the tabulated content in this report was produced automatically. This involved the use of scripting tools to generate directly typesettable L^AT_EX content. This improves timeliness, flexibility and maintainability, and reduces transcription errors.
- ▷ Readers are asked to direct any correspondence to IREX AT NIST DOT GOV.

Disclaimer

Specific hardware and software products identified in this report were used in order to perform the evaluations described in this document. In no case does identification of any commercial product, trade name, or vendor, imply recommendation or endorsement by the National Institute of Standards and Technology, nor does it imply that the products and equipment identified are necessarily the best available for the purpose.

Errata

As of June 24, 2009 there are no errata.

Compiled Results for Implementation A1

On June 25, 2009, NIST invited the IREX participants to submit a description of the SDKs submitted for the IREX effort. The intent was to allow providers to describe and contrast the feature sets, optimization, operational suitability and availability of the primary and secondary SDKs. NIST indicated that any submitted text would appear verbatim (with typesetting) in draft and final versions of the IREX report and that it would be attributed to the organization. This was optional and NIST put no constraints on the content beyond a 600 word limit, and a statement that anything labelled as confidential or proprietary would be omitted.

The provider of SDK A1, Sagem, submitted the following to NIST - we are unable to validate this information.

The two SDKs provided by Sagem for IREX are experimental coding and matching methods and algorithms currently under development by Sagem R&D. They have been developed and tested on numerous databases obtained with almost all the iris acquisition devices currently available on various types of population and ethnicities.

After the localization of the iris area, the coding algorithm involves a set of Local Feature Jets (LFJ) which use various statistics and filters to describe the iris texture around points of interest. The LFJ are spread on the whole iris area with a fixed density, and their number can be influenced by the occlusions and pupil dilatation. A likely measure is proceeded in order to determine if each local descriptor is indeed located or on the iris. This step is accomplished by a statistical model and can correct errors made by the localization algorithm. An iris template then contains a variable number of vectors describing locally the texture.

The matching algorithm measures a distance between two sets of LFJ from two different irises. First, each LFJ from one set will be associated with its closest neighbor from the other set by a likelihood measure. A global measure of similarity can then be calculated between the two sets of LFJ. Additionally, the global geometric coherence of the LFJ associations is evaluated. A final distance is then calculated between the two sets of LFJ by combining the global similarity and the geometric score.

One important characteristic of this method is that since coding and matching scheme rely on local characteristics to associates points, it is less sensitive to iris segmentation and can cope with less accurate iris segmentation.

On August 17, 2009, NIST invited the IREX participants to submit a description their comments on an draft version of the IREX report. This was intended to allow participants to assist readers in the interpretation of a large and complicated testing effort. NIST indicated that any submitted text would appear verbatim (with typesetting) in the final version of the IREX report and that it would be attributed to the organization. Submission of content was optional and NIST put no constraints on the content beyond a word limit, and a statement that anything labelled as confidential or proprietary would be omitted.

The provider of SDK A1, Sagem, elected not to submit any information

A = SAGEM	B = COGENT	C = CROSSMATCH	D = CAMBRIDGE	E = L1	x1 = PRIMARY
F = RETICA	G = LG	H = HONEYWELL	I = IRITECH	J = NEUROTECHNOLOGY	x2 = SECONDARY
KIND 1 = RAW 640x480	KIND 3 = CROP	KIND 7 = CROP+MASK	KIND 16 = CONCENTRIC POLAR		

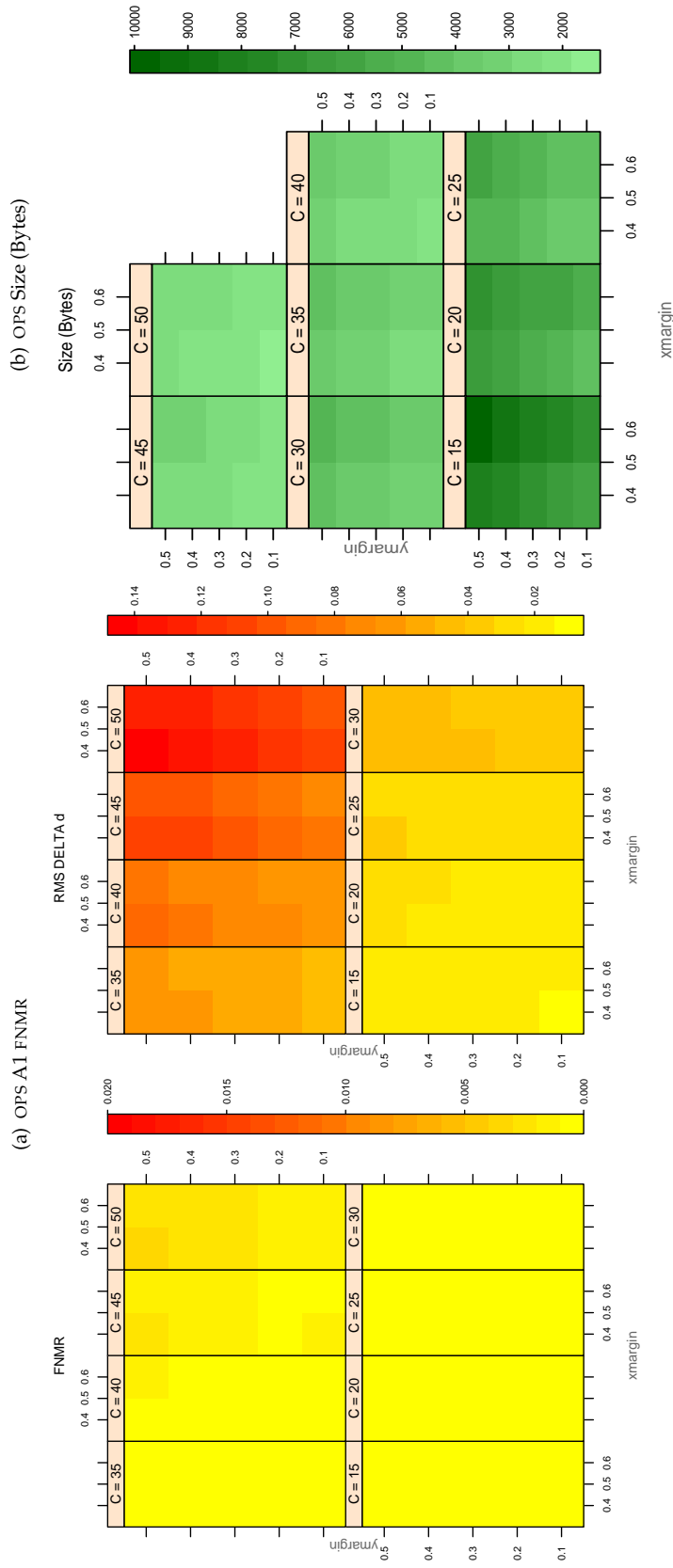


Table 1: For the IREX partition of the OPS database the plots at left show the dependence of cFNMR on the vertical and horizontal iris cropping margins for various compression ratios. This applies only for KIND 3 records. The margins are in units of iris radius. The use of conditional FNMR means that the plots exclude comparisons that were falsely rejected even before any compression was applied. On the **right side** is the rms difference between the crop+compress and the uncompressed comparison scores for each image pair. All computations are driven by the bounding box coordinates reported by the II SDK. The number of bits per pixel is $8/C$, where C is the compression ratio. The iris radius varies and because the cropping margins are fixed multiples of the radius the image size varies. The compressed size, in bytes, is the width times height divided by C . Values of cFNMR greater than 0.02 are shown as 0.02.

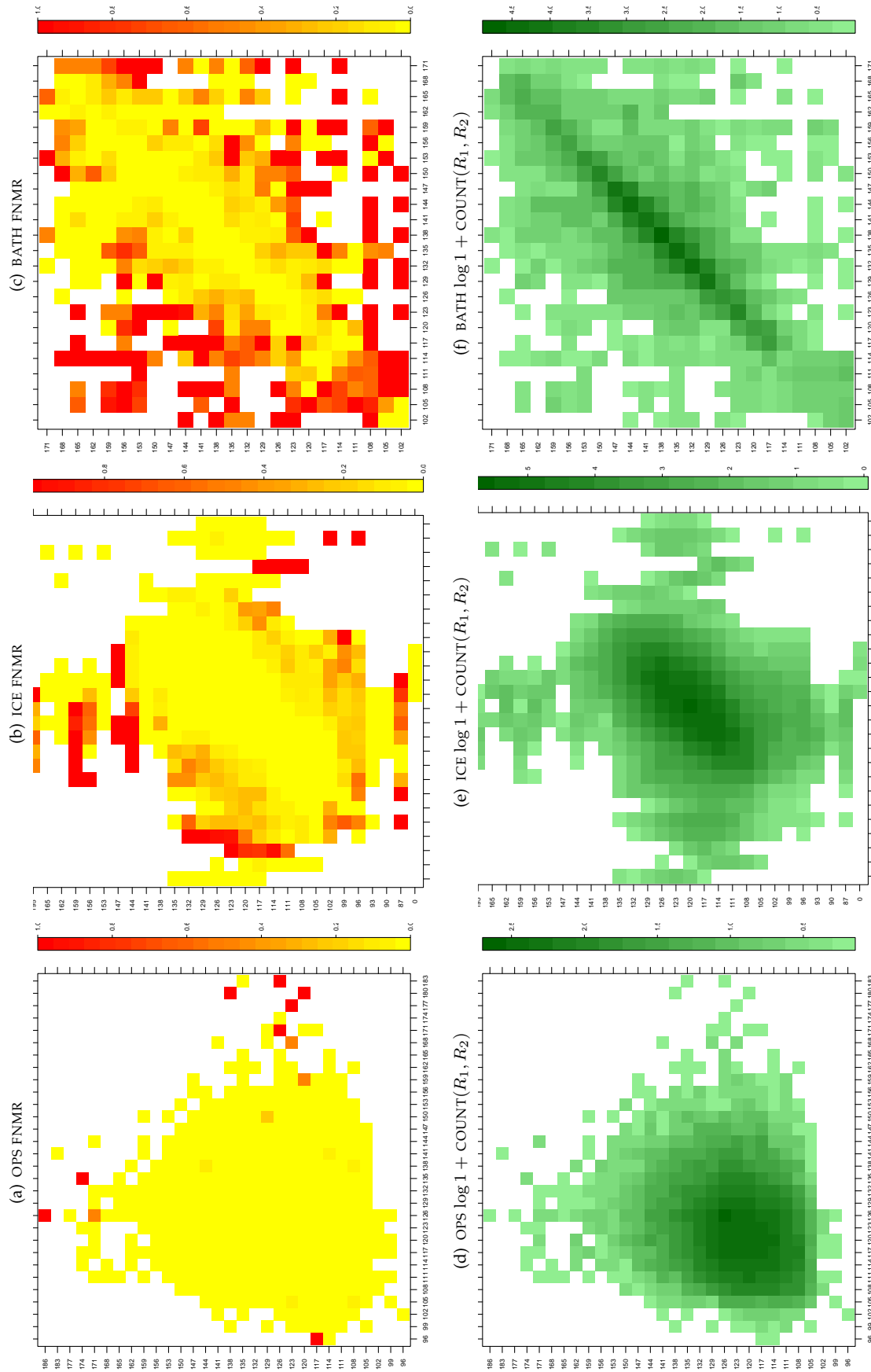


Table 2: For the three IREX databases: In the **top** row the color in each cell represents the occurrence of genuine comparisons with the given pair of radii. The *y*-axis represents enrollment samples with verification samples on the *x*-axis; In the **bottom** row the color scale plots $\log 1 + \text{COUNT}(R_1, R_2)$. The radii are quantized into three-pixel bins. The radii for DOD are on the range $96 \leq r \leq 186$ pixels. The radii for ICE are on the range $87 \leq r \leq 165$ pixels. The radii for BATH are on the range $100 \leq r \leq 170$ pixels.

A = SAGEM	B = COGENT	C = CROSSMATCH	D = CAMBRIDGE	E = L1	$x1$ = PRIMARY
F = RETICA	G = LG	H = HONEYWELL	I = IRITECH	J = NEUROTECHNOLOGY	$x2$ = SECONDARY
KIND 1 = RAW 640x480		KIND 3 = CROP		KIND 7 = CROP+MASK	KIND 16 = CONCENTRIC POLAR

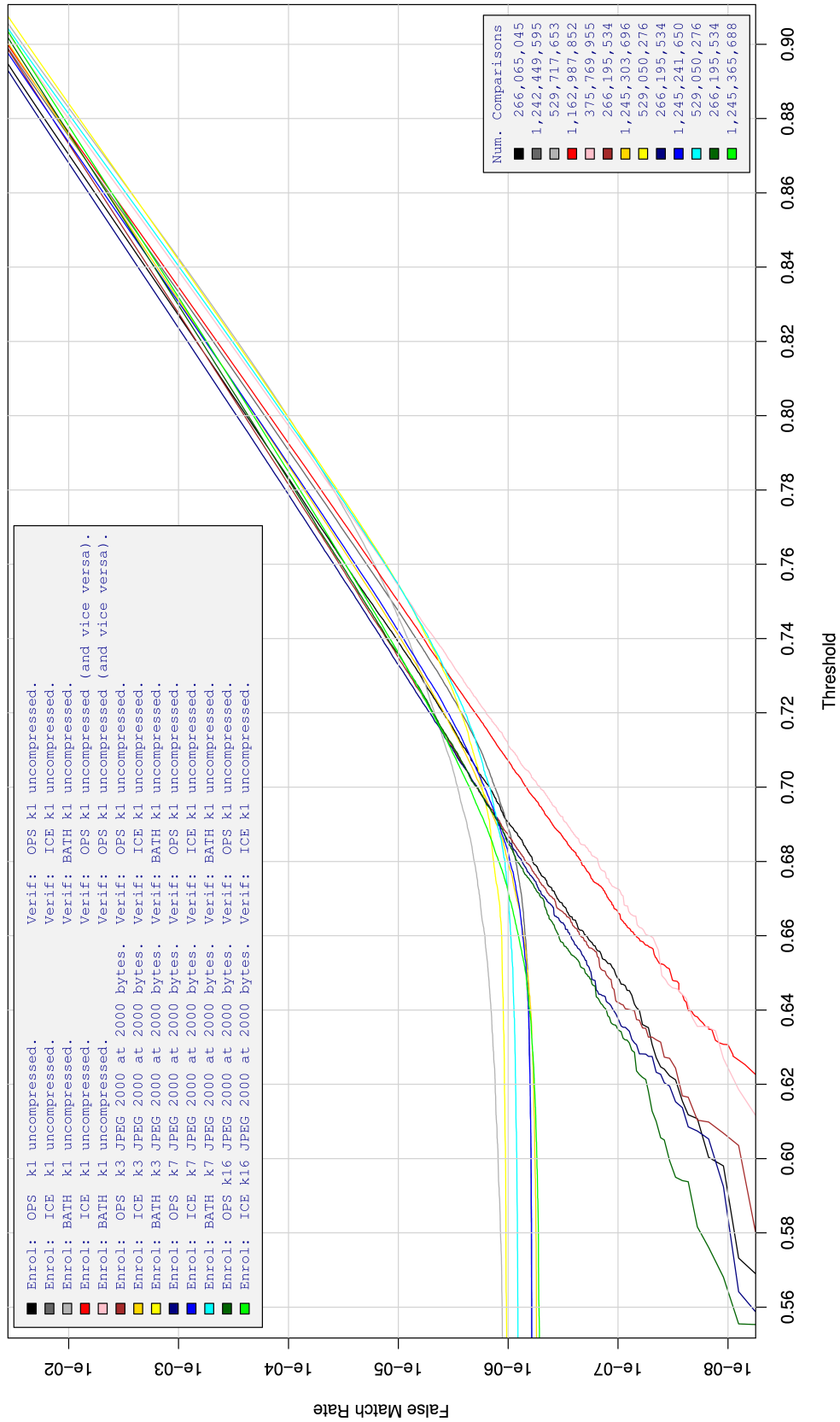


Table 3: For implementation A1, the dependency of FMR on threshold. for various combinations of enrollment and verification dataset, format, and compression.

A = SAGEM	B = COGENT	C = CROSSMATCH	D = CAMBRIDGE	E = L1	x1 = PRIMARY
F = RETICA	G = LG	H = HONEYWELL	I = IRITECH	J = NEUROTECHNOLOGY	x2 = SECONDARY
KIND 1 = RAW 640x480		KIND 3 = CROP		KIND 7 = CROP+MASK	
KIND 16 = CONCENTRIC POLAR					

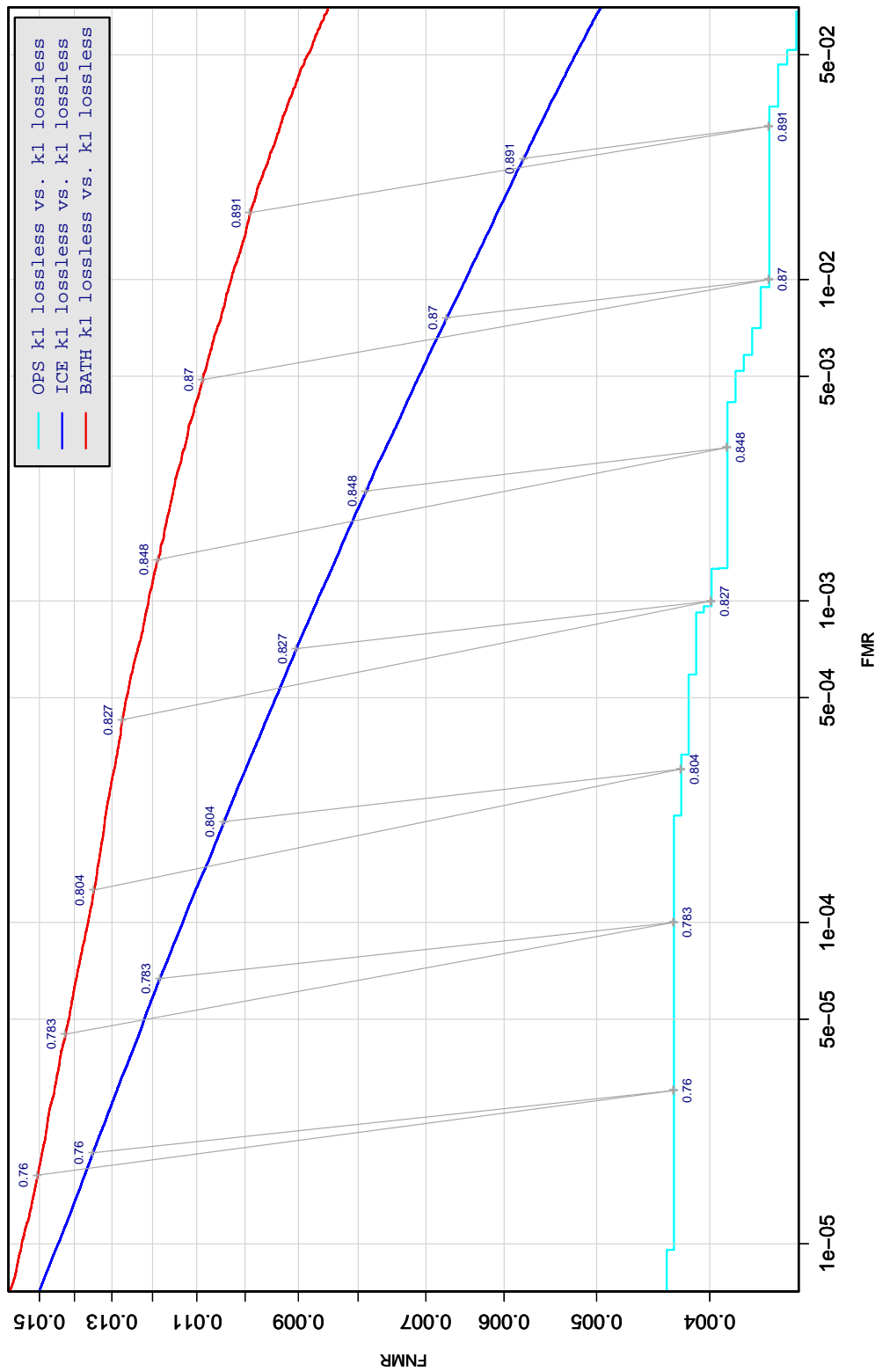


Table 4: DET curve for implementation A1 on three IREX databases. All comparisons are with uncompressed KIND 1 vs. KIND 1 images. The lines join points corresponding to the a fixed threshold. Non-vertical links indicate a change in FMR when the database changes. All results apply to native operation. Failures to produce a template i.e. FTE are ignored because the plots are intended to show *matching* effects, specifically to compare DET slopes and to show the effect of fixing a threshold.

A = SAGEM	B = COGENT	C = CROSSMATCH	D = CAMBRIDGE	E = L1	$x1$ = PRIMARY
F = RETICA	G = LG	H = HONEYWELL	I = IRITECH	J = NEUROTECHNOLOGY	$x2$ = SECONDARY
KIND 1 = RAW 640x480		KIND 3 = CROP	KIND 7 = CROP+MASK	KIND 16 = CONCENTRIC POLAR	

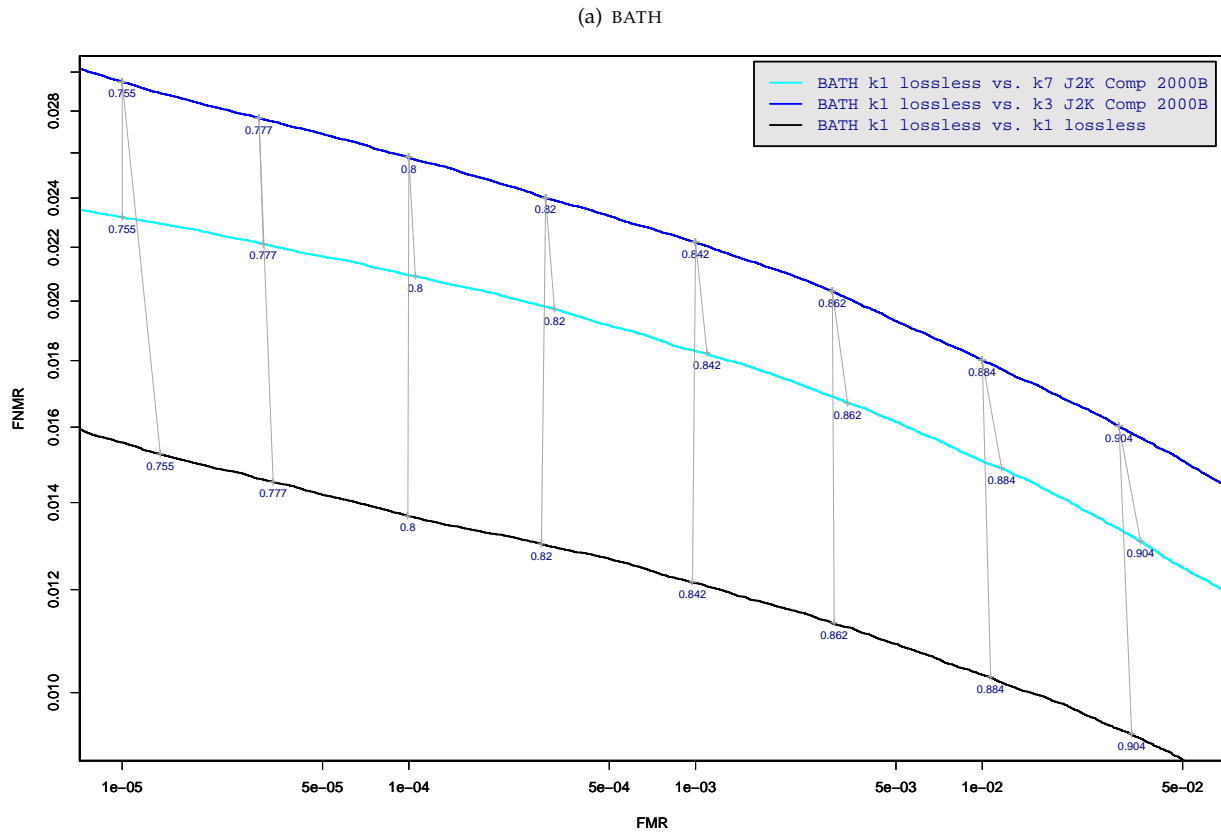


Table 5: DET curve for implementation A1 on the BATH database for the various supported KINDS . The DET characteristics are linked by lines joining points of equal threshold. Non-vertical links indicate a change in false acceptance when the data KIND changes. All results apply to native operation, and the effects of FTE are included.

A = SAGEM	B = COGENT	C = CROSSMATCH	D = CAMBRIDGE	E = L1	x1 = PRIMARY
F = RETICA	G = LG	H = HONEYWELL	I = IRITECH	J = NEUROTECHNOLOGY	x2 = SECONDARY
KIND 1 = RAW 640x480		KIND 3 = CROP		KIND 7 = CROP+MASK	
KIND 16 = CONCENTRIC POLAR					

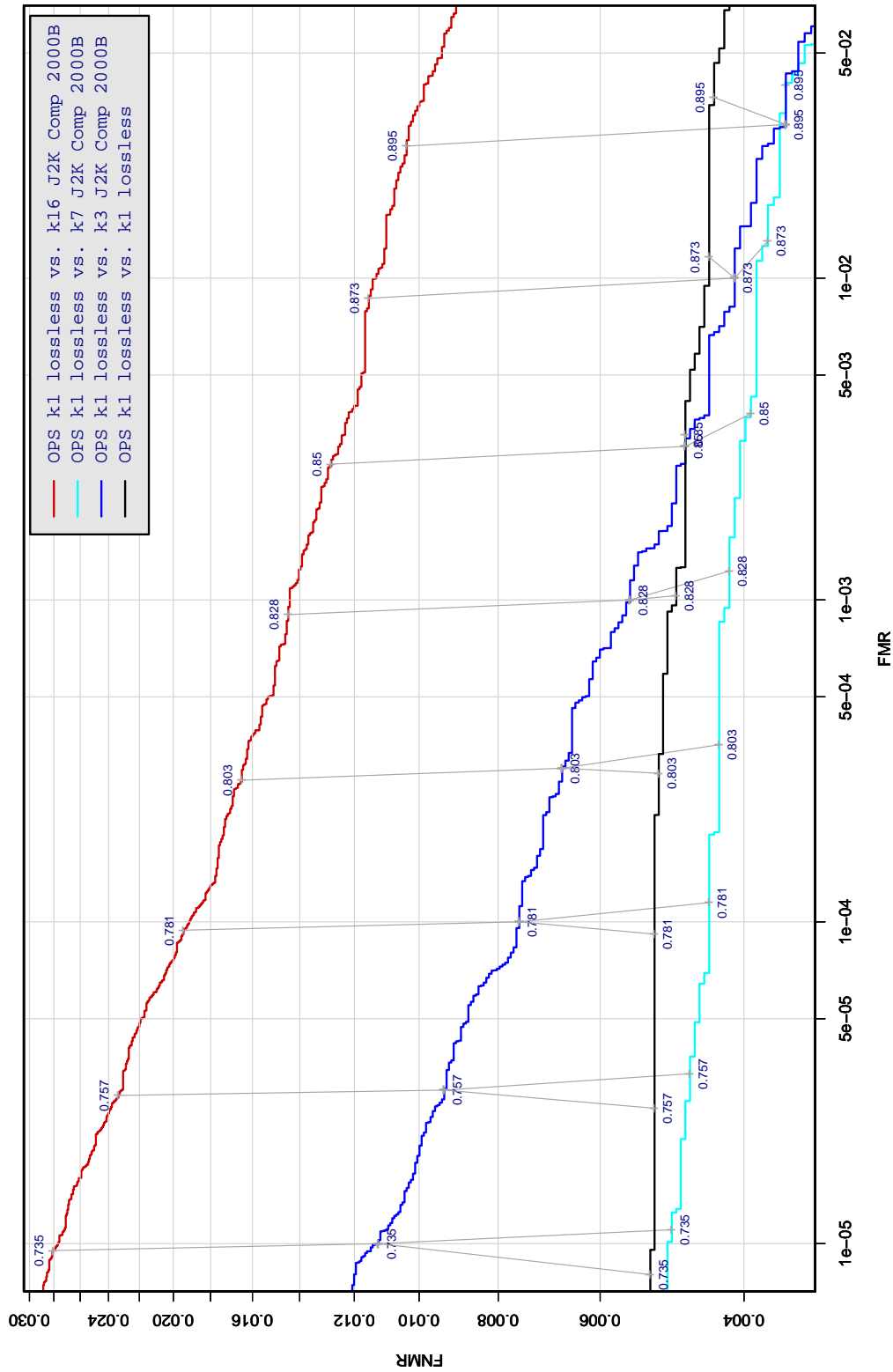


Table 6: DET curve for implementation A1 on the OPS database for the various supported KINDS . The DET characteristics are linked by lines joining points of equal threshold. Non-vertical links indicate a change in false acceptance when the data KIND changes. All results apply to native operation, and the effects of FTE are included.

A = SAGEM	B = COGENT	C = CROSSMATCH	D = CAMBRIDGE	E = L1	$x1$ = PRIMARY
F = RETICA	G = LG	H = HONEYWELL	I = IRITECH	J = NEUROTECHNOLOGY	$x2$ = SECONDARY
KIND 1 = RAW 640x480		KIND 3 = CROP	KIND 7 = CROP+MASK	KIND 16 = CONCENTRIC POLAR	

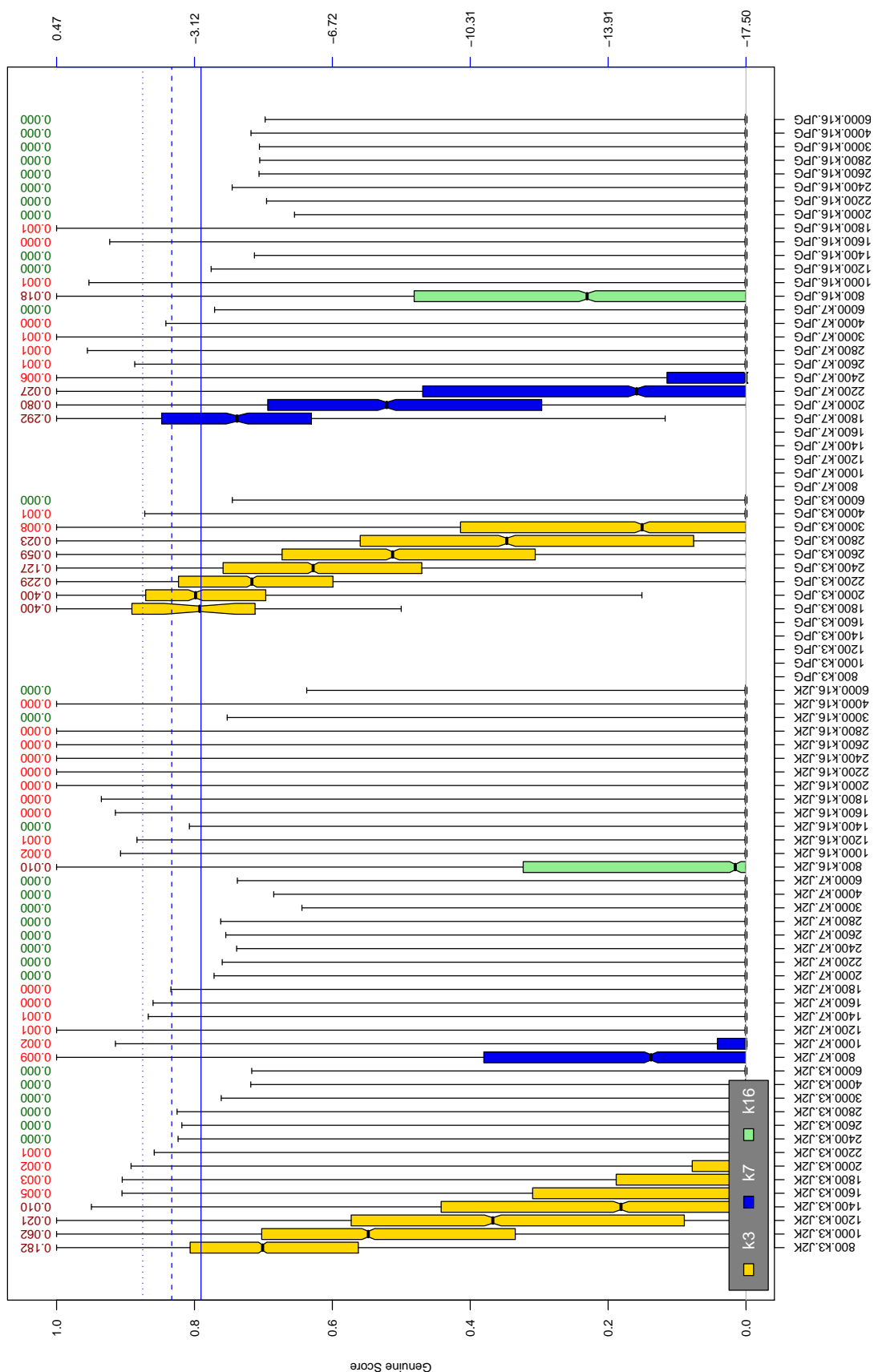
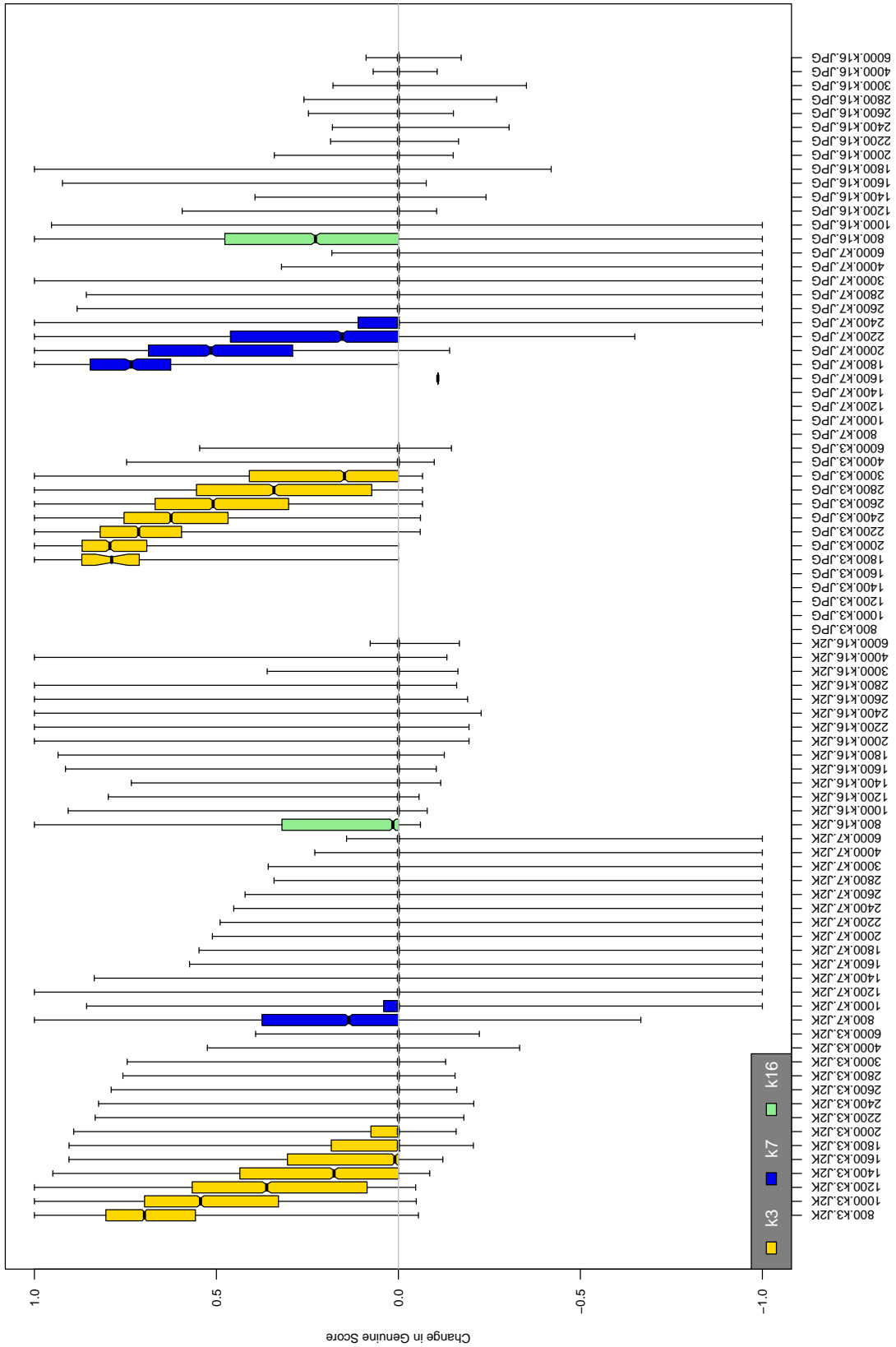


Table 7: The distribution of A1 native genuine comparison scores by size of the compressed image, KIND and the compression algorithm. The images are from the OPS dataset. The right axis scale gives the corresponding value for $d' = (s - \mu_I) / \sqrt{0.5(\sigma_I^2 + \sigma_C^2)}$ for genuine score s . The boxplots only include comparison scores if the uncompressed version of the same image was matched below the FMR = 0.001 threshold. Above the boxplots are FNMR values at FMR = 10^{-3} . The three blue lines correspond, from the top, to FMR of 10^{-2} , 10^{-3} , 10^{-4} . The lower grey line refers to the median score obtained from comparison of uncompressed KIND 3 images. Any comparison for which either template had not been generated is excluded. Note that the iris record size on the horizontal axis is not evenly spaced above 3000 bytes.

A = SAGEM	B = COGENT	C = CROSSMATCH	D = CAMBRIDGE	E = L1	$x1$ = PRIMARY
F = RETICA	G = LG	H = HONEYWELL	I = IRITECH	J = NEUROTECHNOLOGY	$x2$ = SECONDARY
KIND 1 = RAW 640x480		KIND 3 = CROP	KIND 7 = CROP+MASK	KIND 16 = CONCENTRIC POLAR	



A = SAGEM	B = COGENT	C = CROSSMATCH	D = CAMBRIDGE	E = L1	x1 = PRIMARY
F = RETICA	G = LG	H = HONEYWELL	I = IRITECH	J = NEUROTECHNOLOGY	x2 = SECONDARY
KIND 1 = RAW 640x480		KIND 3 = CROP	KIND 7 = CROP+MASK	KIND 16 = CONCENTRIC POLAR	

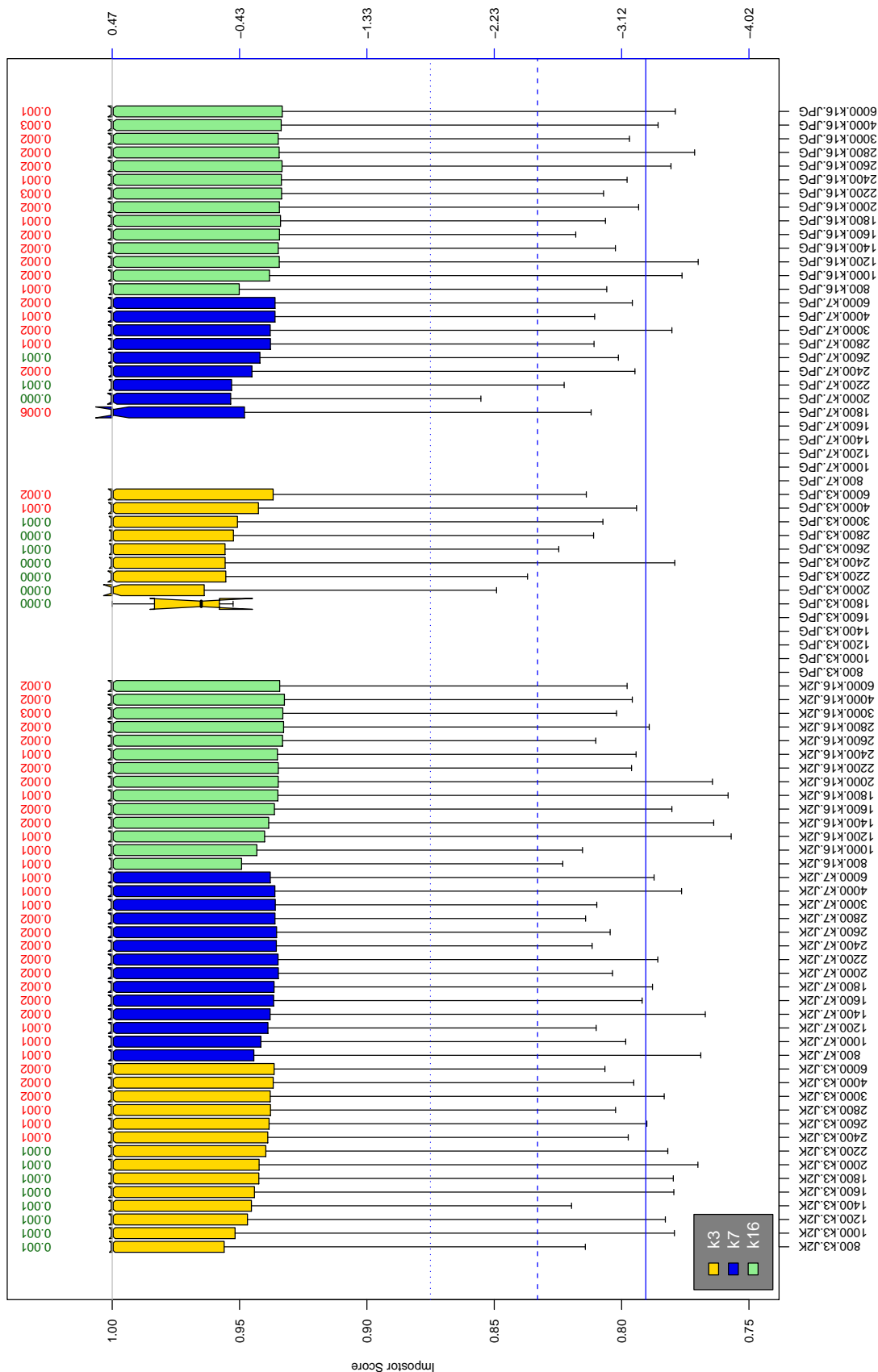


Table 8: The distribution of A1 native impostor comparison scores by size of the compressed image, KIND and the compression algorithm. The right axis scale gives the corresponding value for $d' = (s - \mu_1) / \sqrt{0.5(\sigma_1^2 + \sigma_2^2)}$ for impostor score s . The three blue lines correspond, from the top, to FMR of $10^{-2}, -3, -4$. The lower grey line refers to the median score obtained from comparison of uncompressed KIND 3 images. Any comparison involving a failed template is excluded. Above the boxplots are FMR values at the threshold that gives FMR = 10^{-3} on uncompressed images. These figures are computed from only 4000 comparisons so the FMR values and the tails of the impostor distribution are poorly characterized. Note that the iris record size on the horizontal axis is not evenly spaced above 3000 bytes.

A = SAGEM	B = COGENT	C = CROSSMATCH	D = CAMBRIDGE	E = L1	x_1 = PRIMARY
F = RETICA	G = LG	H = HONEYWELL	I = IRITECH	J = NEUROTECHNOLOGY	x_2 = SECONDARY
KIND 1 = RAW 640x480		KIND 3 = CROP	KIND 7 = CROP+MASK	KIND 16 = CONCENTRIC POLAR	

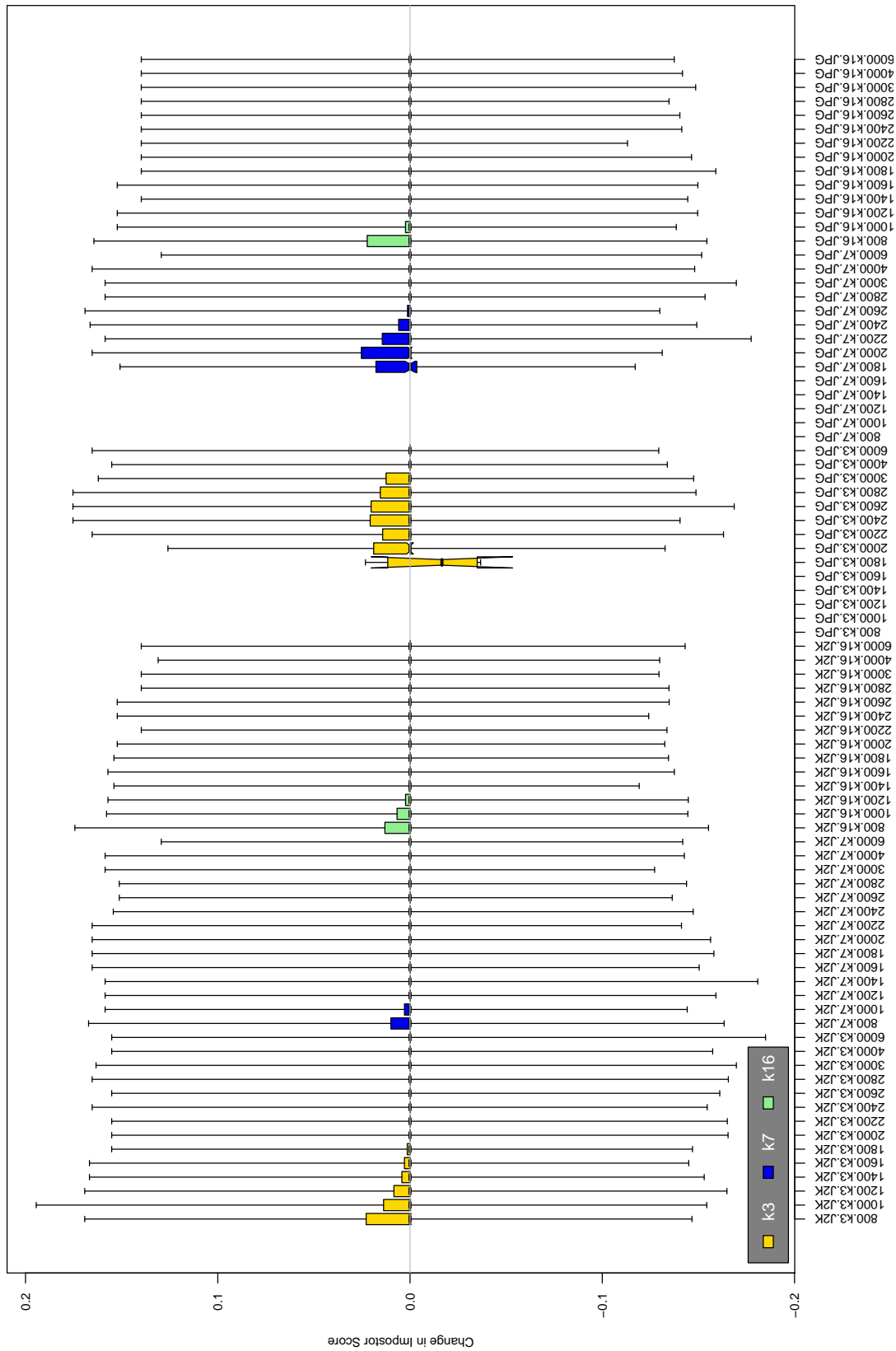


Table 9: The distribution of the increase in A1 native impostor comparison scores between the uncompressed “parent” and the compressed image, arranged by size, KIND and the compression algorithm. The images are from the OPS dataset. Any comparison involving a failed template is excluded. Note that the iris record size on the horizontal axis is not evenly spaced above 3000 bytes.

A = SAGEM	B = COGENT	C = CROSSMATCH	D = CAMBRIDGE	E = L1	x1 = PRIMARY
F = RETICA	G = LG	H = HONEYWELL	I = IRITECH	J = NEUROTECHNOLOGY	x2 = SECONDARY
KIND 1 = RAW 640x480		KIND 3 = CROP	KIND 7 = CROP+MASK	KIND 16 = CONCENTRIC POLAR	

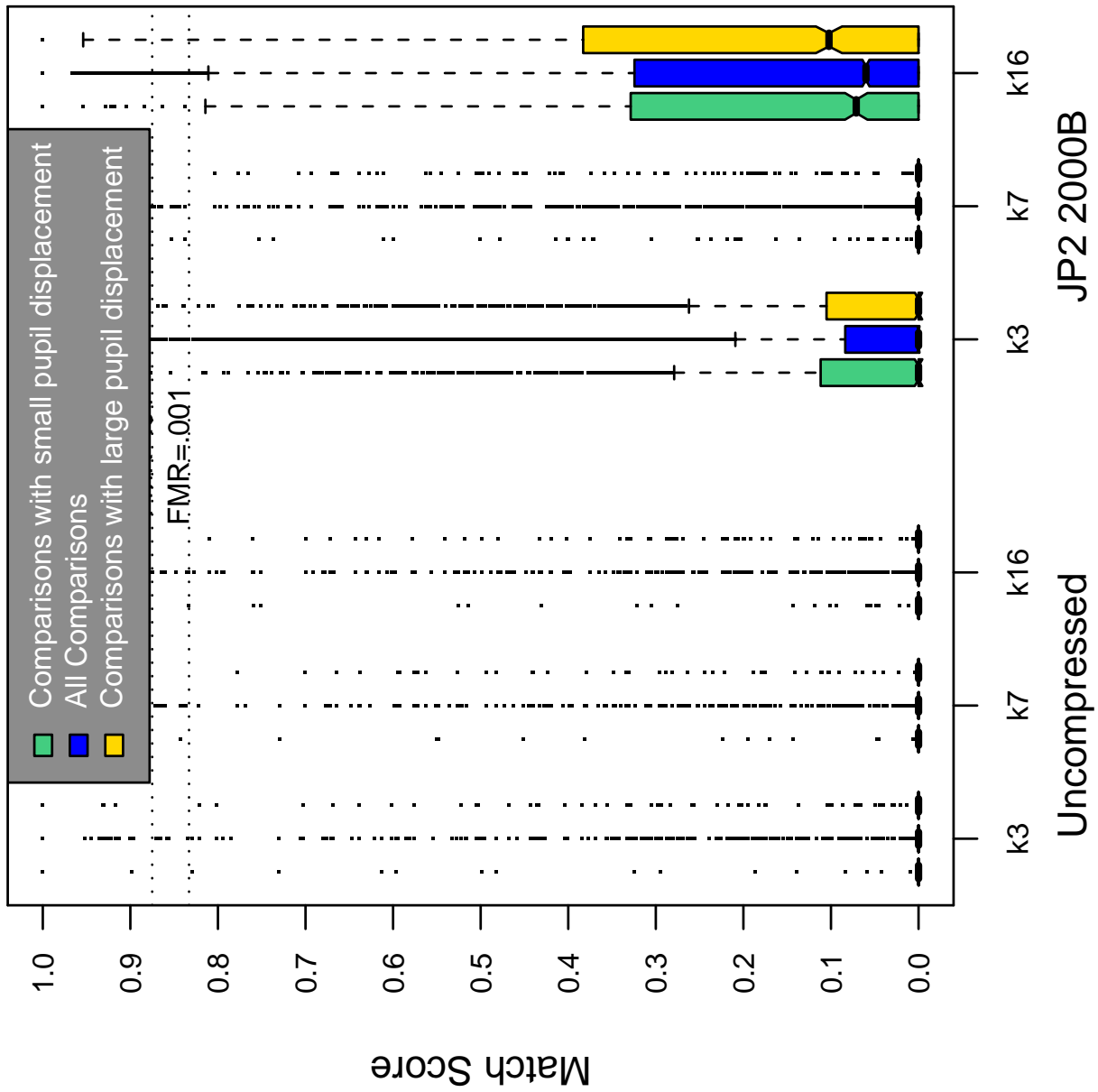


Table 10: Effect of pupil displacement on the genuine score distribution for A1

A = SAGEM	B = COGENT	C = CROSSMATCH	D = CAMBRIDGE	E = L1	x1 = PRIMARY
F = RETICA	G = LG	H = HONEYWELL	I = IRITECH	J = NEUROTECHNOLOGY	x2 = SECONDARY
KIND 1 = RAW 640x480		KIND 3 = CROP		KIND 7 = CROP+MASK	
				KIND 16 = CONCENTRIC POLAR	

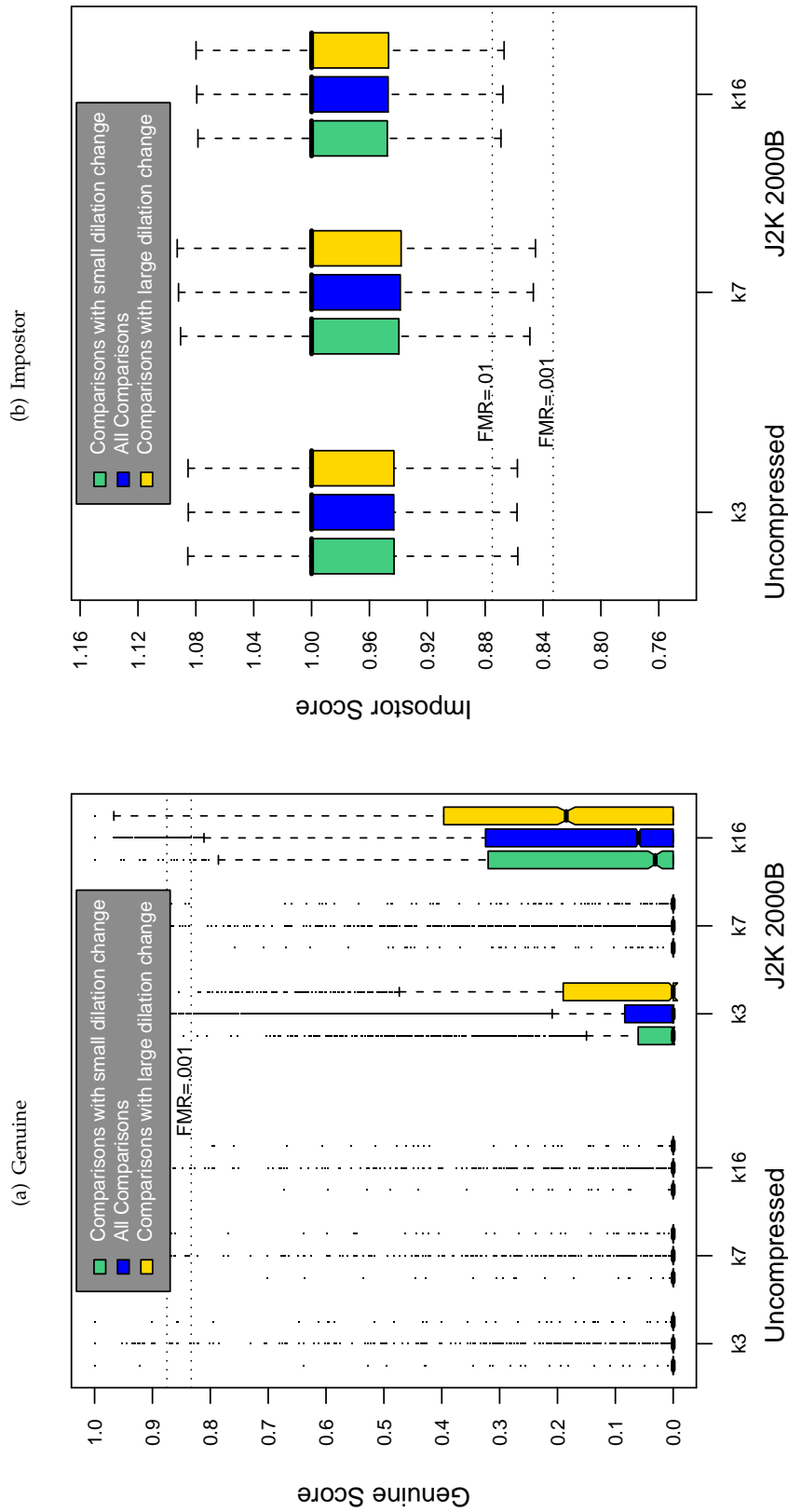


Table 11: The effect of dilation change on the two scores distributions for SDK A1.

A = SAGEM	B = COGENT	C = CROSSMATCH	D = CAMBRIDGE	E = L1	$x1$ = PRIMARY
F = RETICA	G = LG	H = HONEYWELL	I = IRITECH	J = NEUROTECHNOLOGY	$x2$ = SECONDARY
KIND 1 = RAW 640x480		KIND 3 = CROP	KIND 7 = CROP+MASK	KIND 16 = CONCENTRIC POLAR	

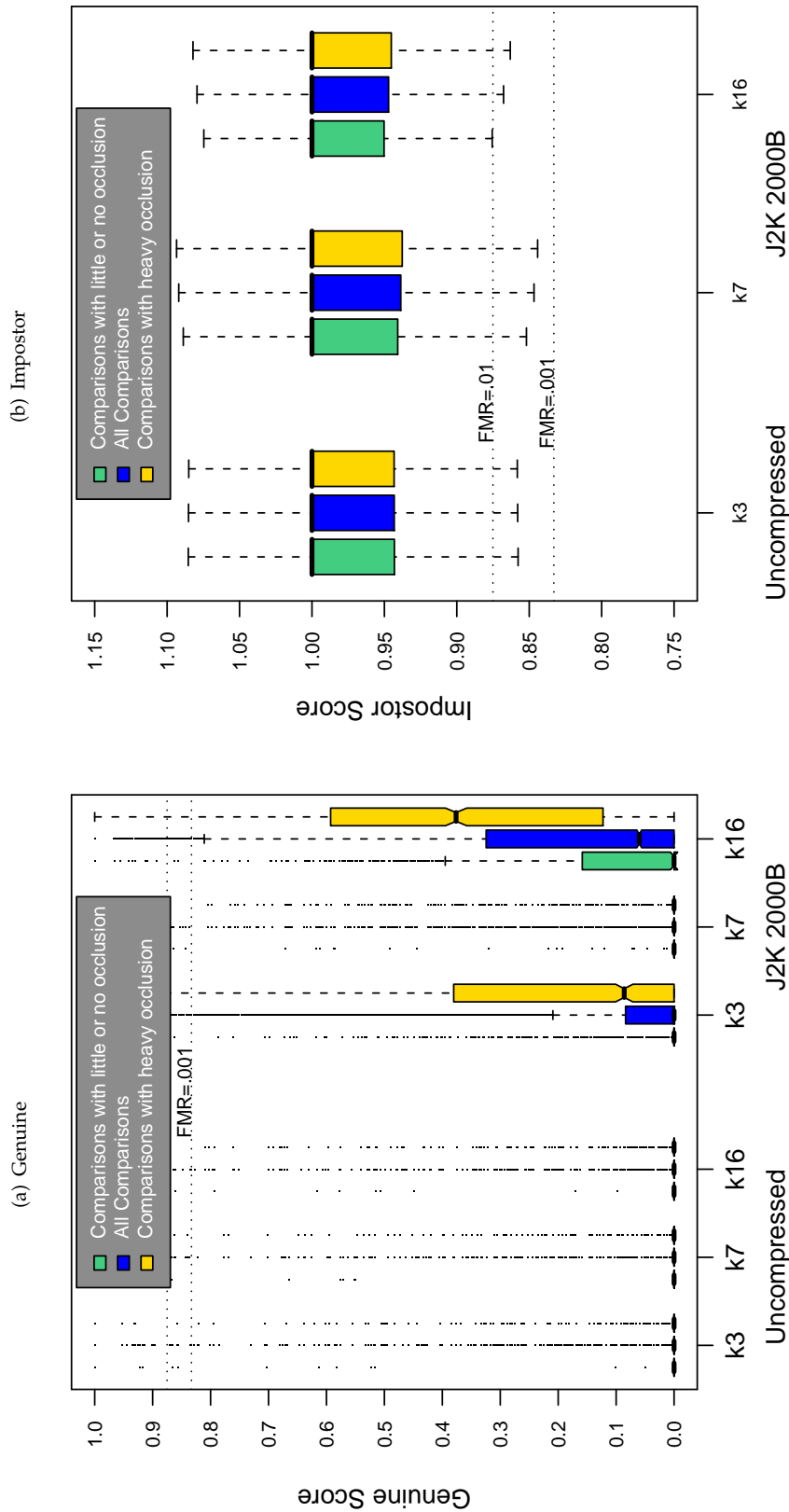
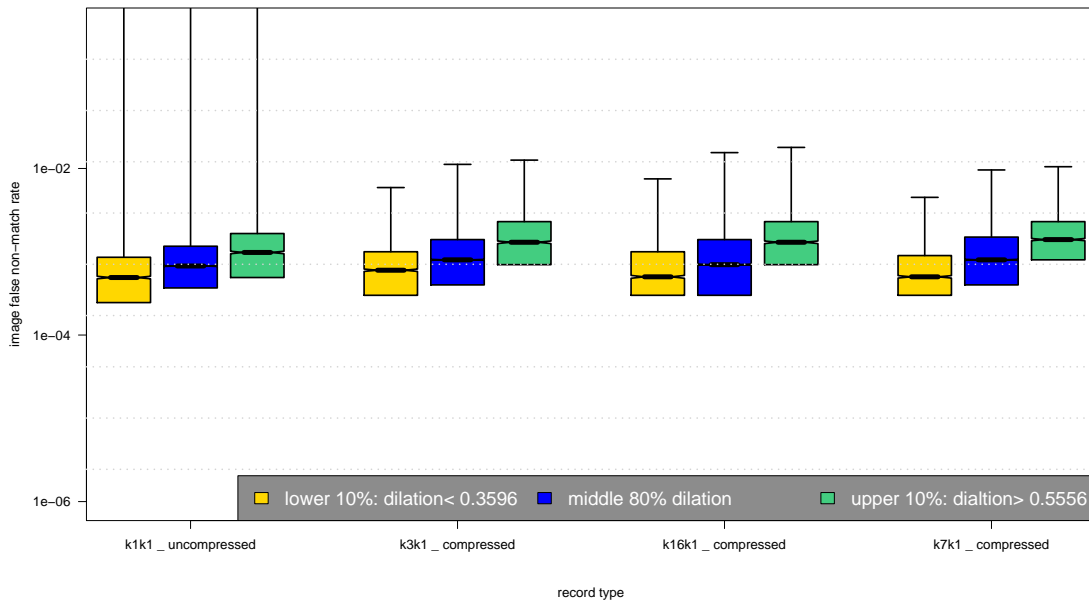
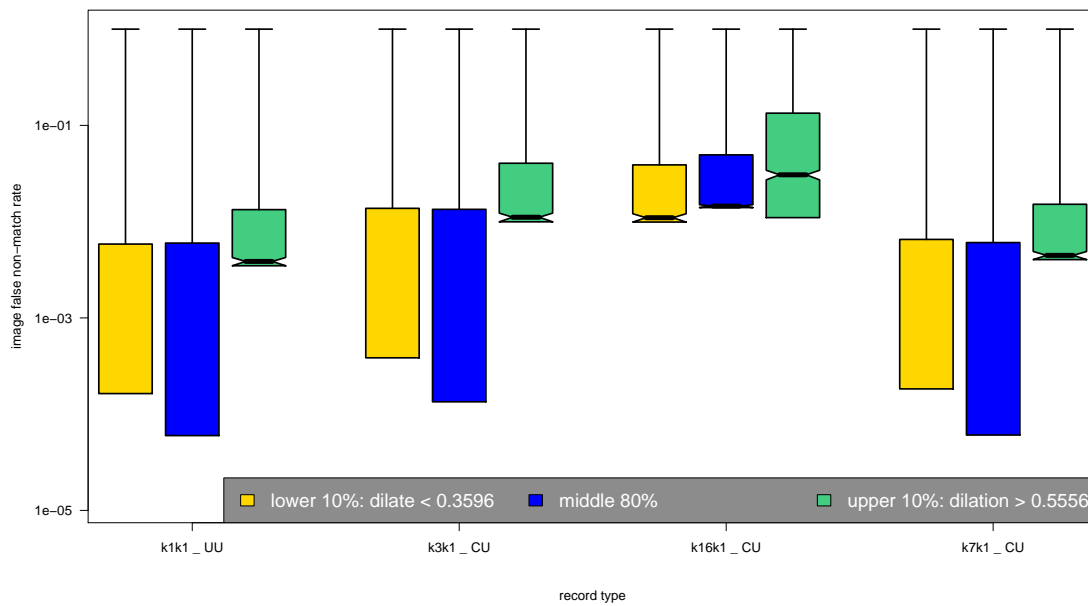


Table 12: The effect of eyelid occlusion on the two scores distributions for SDK A1.

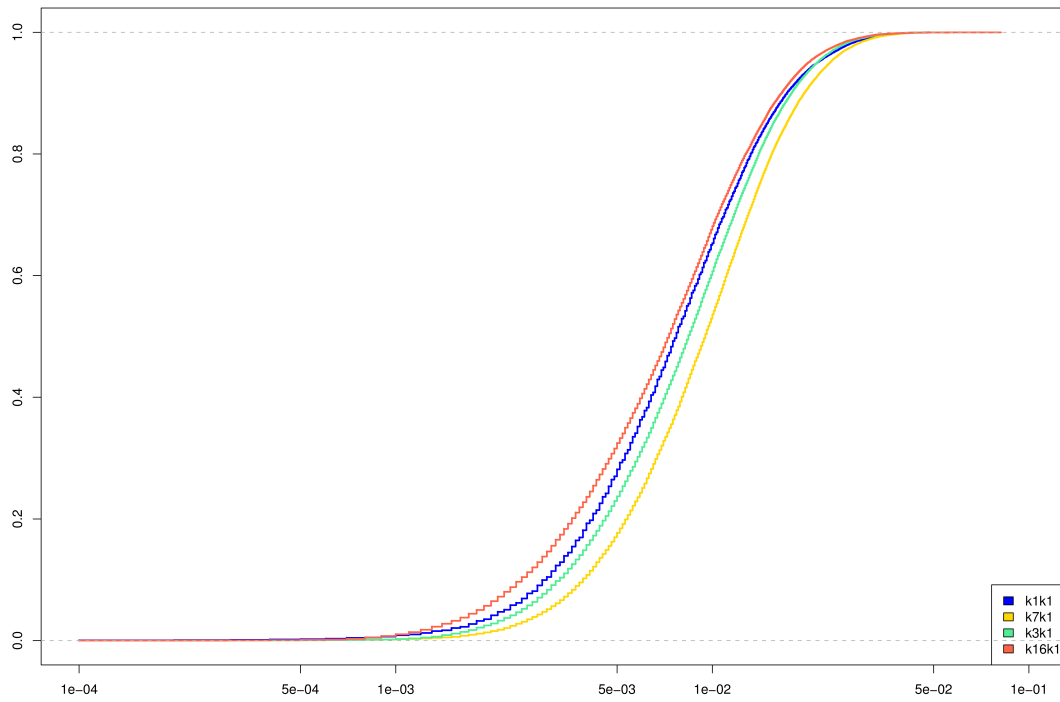
(a) iFMR using A1 dilation estimates



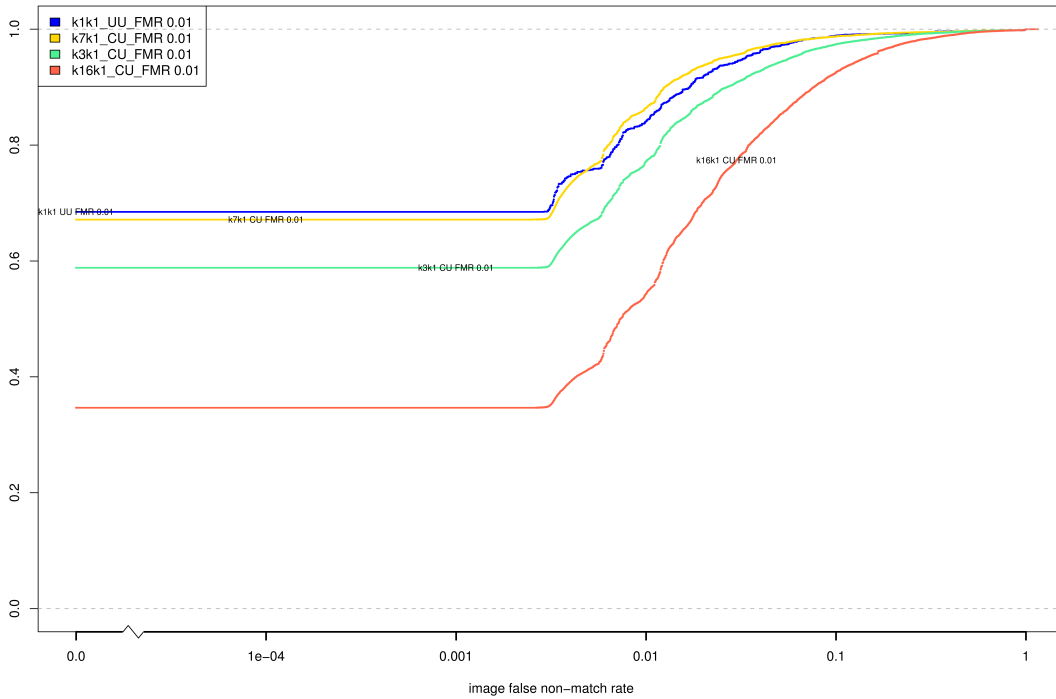
(b) iFNMR using A1 dilation estimates



(c) iFMR CDF



(d) iFNMR CDF



Compiled Results for Implementation A2

On June 25, 2009, NIST invited the IREX participants to submit a description of the SDKs submitted for the IREX effort. The intent was to allow providers to describe and contrast the feature sets, optimization, operational suitability and availability of the primary and secondary SDKs. NIST indicated that any submitted text would appear verbatim (with typesetting) in draft and final versions of the IREX report and that it would be attributed to the organization. This was optional and NIST put no constraints on the content beyond a 600 word limit, and a statement that anything labelled as confidential or proprietary would be omitted.

The provider of SDK A2, Sagem, submitted the following to NIST - we are unable to validate this information.

The two SDKs provided by Sagem for IREX are experimental coding and matching methods and algorithms currently under development by Sagem R&D. They have been developed and tested on numerous databases obtained with almost all the iris acquisition devices currently available on various types of population and ethnicities.

After the localization of the iris area, the coding algorithm involves a set of Local Feature Jets (LFJ) which use various statistics and filters to describe the iris texture around points of interest. The LFJ are spread on the whole iris area with a fixed density, and their number can be influenced by the occlusions and pupil dilatation. A likely measure is proceeded in order to determine if each local descriptor is indeed located or on the iris. This step is accomplished by a statistical model and can correct errors made by the localization algorithm. An iris template then contains a variable number of vectors describing locally the texture.

The matching algorithm measures a distance between two sets of LFJ from two different irises. First, each LFJ from one set will be associated with its closest neighbor from the other set by a likelihood measure. A global measure of similarity can then be calculated between the two sets of LFJ. Additionally, the global geometric coherence of the LFJ associations is evaluated. A final distance is then calculated between the two sets of LFJ by combining the global similarity and the geometric score.

One important characteristic of this method is that since coding and matching scheme rely on local characteristics to associates points, it is less sensitive to iris segmentation and can cope with less accurate iris segmentation.

On August 17, 2009, NIST invited the IREX participants to submit a description their comments on an draft version of the IREX report. This was intended to allow participants to assist readers in the interpretation of a large and complicated testing effort. NIST indicated that any submitted text would appear verbatim (with typesetting) in the final version of the IREX report and that it would be attributed to the organization. Submission of content was optional and NIST put no constraints on the content beyond a word limit, and a statement that anything labelled as confidential or proprietary would be omitted.

The provider of SDK A2, Sagem, elected not to submit any information

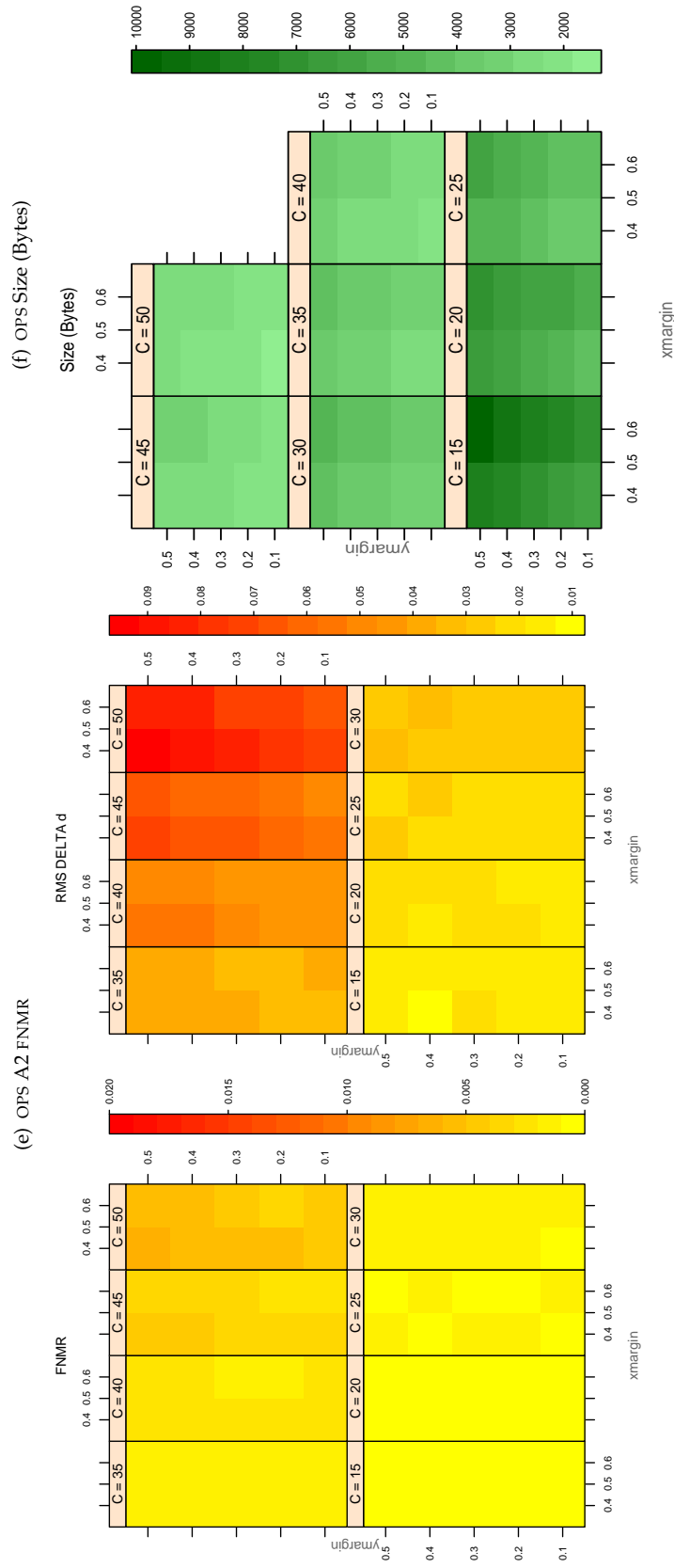


Table 13: For the IREX partition of the OPS database the plots at left show the dependence of cFNMNR on the vertical and horizontal iris cropping margins for various compression ratios. This applies only for KIND 3 records. The margins are in units of iris radius. The use of conditional FNMNR means that the plots exclude comparisons that were falsely rejected even before any compression was applied. On the **right side** is the rms difference between the crop+compress and the uncompressed comparison scores for each image pair. All computations are driven by the bounding box coordinates reported by the II SDK. The number of bits per pixel is $8/C$, where C is the compression ratio. The iris radius varies and because the cropping margins are fixed multiples of the radius the image size varies. The compressed size, in bytes, is the width times height divided by C . Values of cFNMNR greater than 0.02 are shown as 0.02.

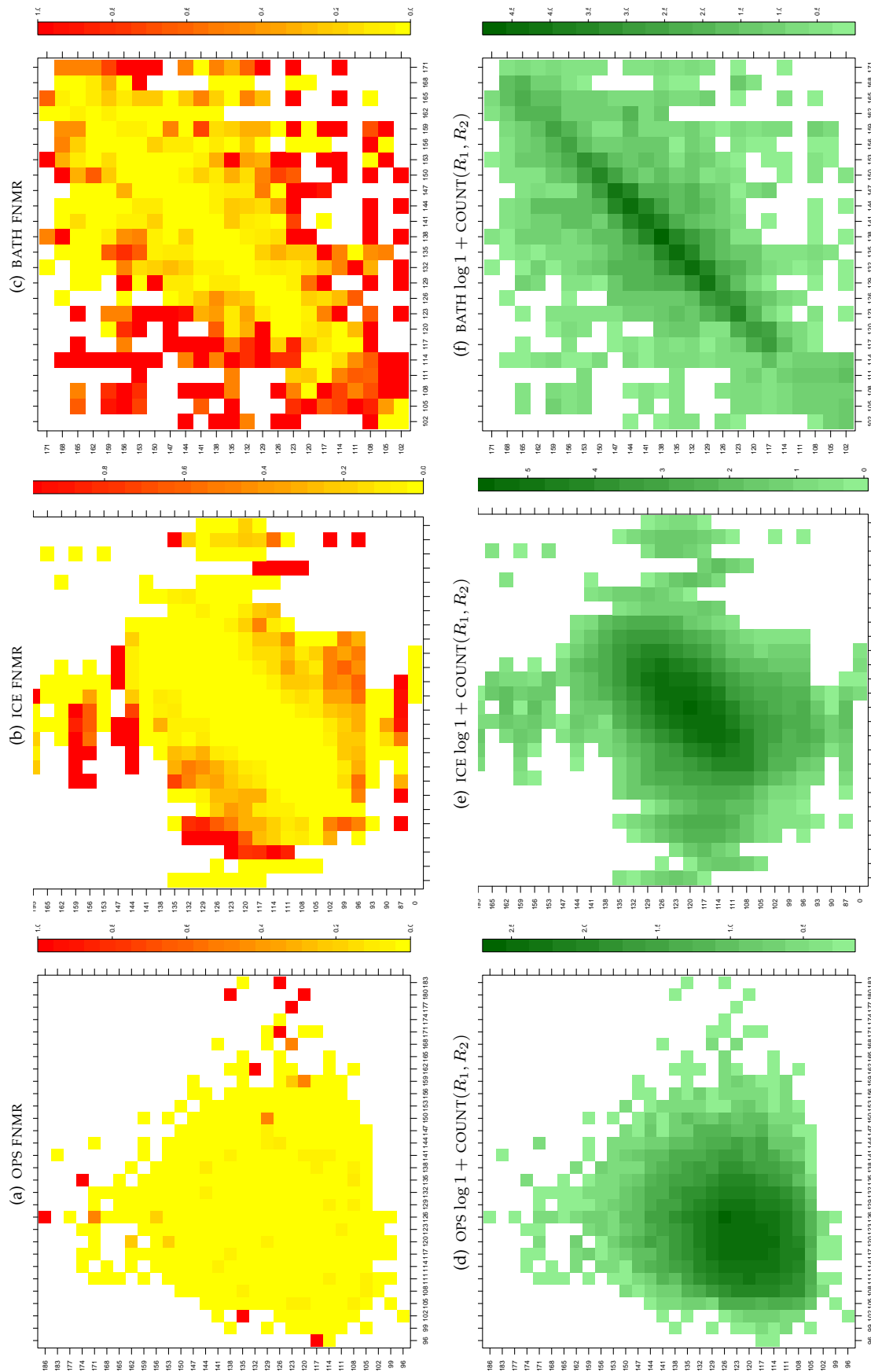


Table 14: For the three IREX databases: In the **top** row the color in each cell represents the occurrence of genuine comparisons with the given pair of radii. The *y*-axis represents enrollment samples with verification samples on the *x*-axis; In the **bottom** row the color scale plots $\log 1 + \text{COUNT}(R_1, R_2)$. The radii are quantized into three-pixel bins. The radii for DOD are on the range $96 \leq r \leq 186$ pixels. The radii for ICE are on the range $87 \leq r \leq 165$ pixels. The radii for BATH are on the range $100 \leq r \leq 170$ pixels.

A = SAGEM	B = COGENT	C = CROSSMATCH	D = CAMBRIDGE	E = L1	$x1$ = PRIMARY
F = RETICA	G = LG	H = HONEYWELL	I = IRITECH	J = NEUROTECHNOLOGY	$x2$ = SECONDARY
KIND 1 = RAW 640x480		KIND 3 = CROP	KIND 7 = CROP+MASK	KIND 16 = CONCENTRIC POLAR	

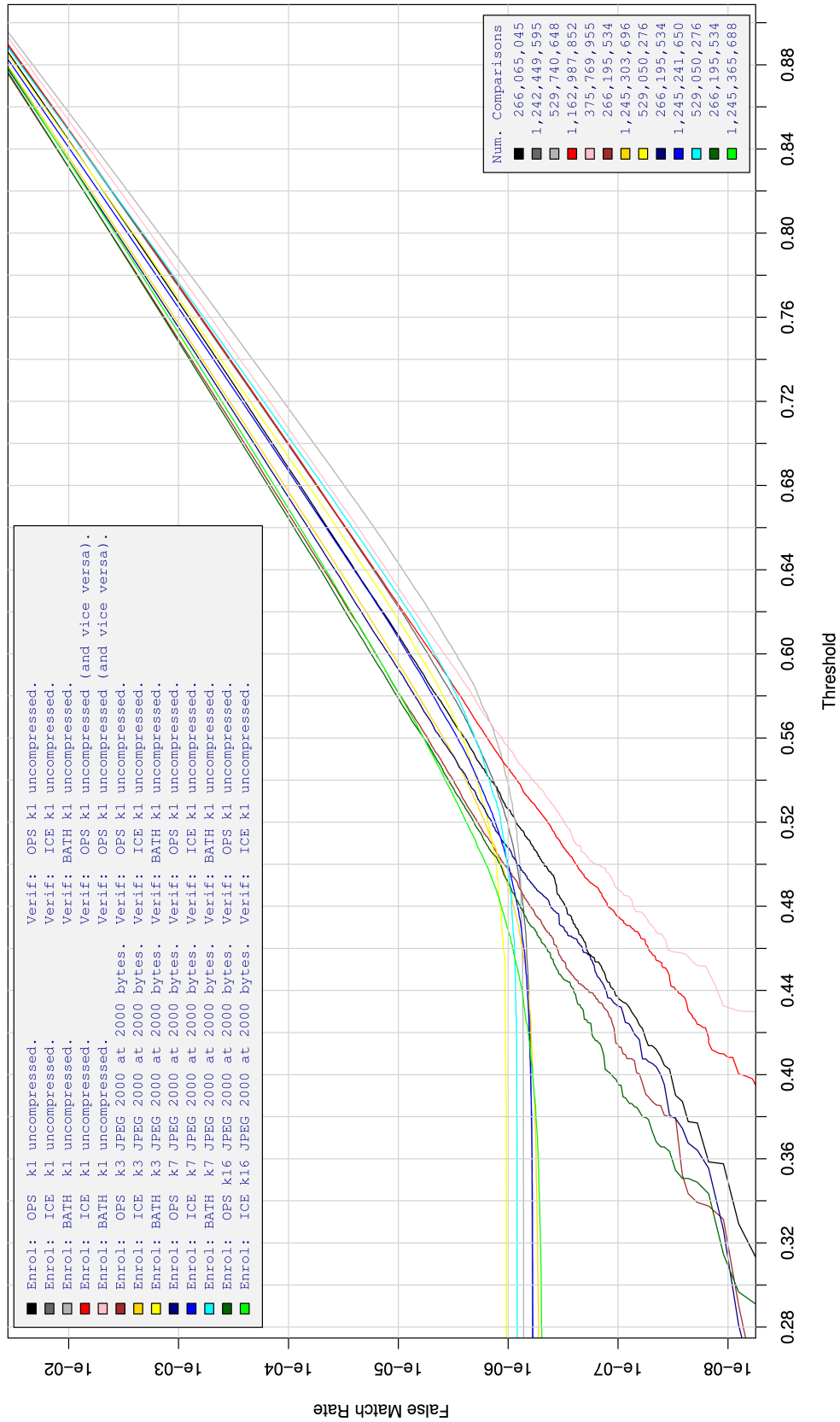


Table 15: For implementation A2, the dependency of FMR on threshold. for various combinations of enrollment and verification dataset, format, and compression.

A = SAGEM	B = COGENT	C = CROSSMATCH	D = CAMBRIDGE	E = L1	x1 = PRIMARY
F = RETICA	G = LG	H = HONEYWELL	I = IRITECH	J = NEUROTECHNOLOGY	x2 = SECONDARY
KIND 1 = RAW 640x480		KIND 3 = CROP		KIND 7 = CROP+MASK	
KIND 16 = CONCENTRIC POLAR					

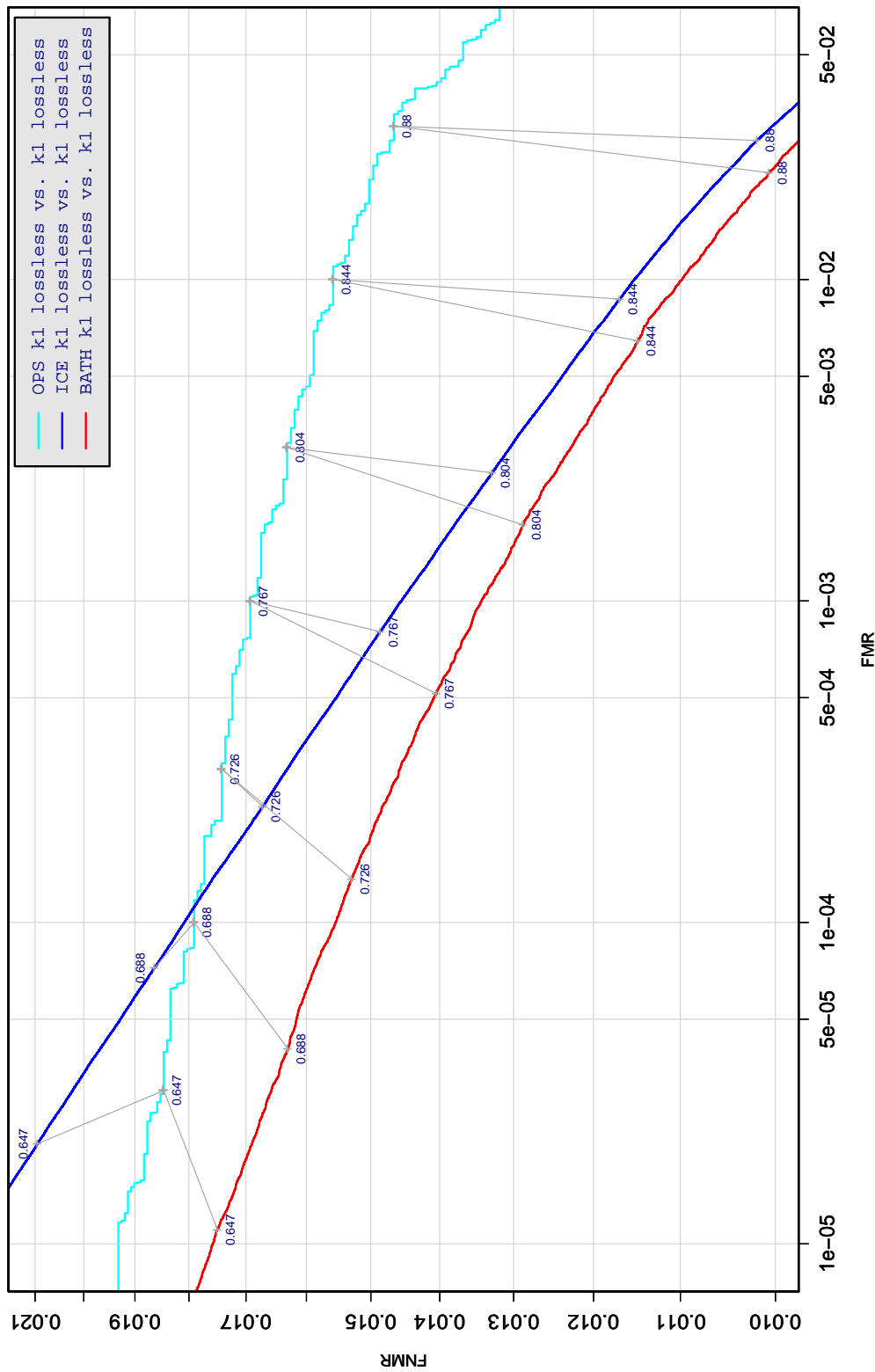


Table 16: DET curve for implementation A2 on three IREX databases. All comparisons are with uncompressed KIND 1 vs. KIND 1 images. The lines join points corresponding to the a fixed threshold. Non-vertical links indicate a change in FMR when the database changes. All results apply to native operation. Failures to produce a template i.e. FTE are ignored because the plots are intended to show *matching* effects, specifically to compare DET slopes and to show the effect of fixing a threshold.

A = SAGEM	B = COGENT	C = CROSSMATCH	D = CAMBRIDGE	E = L1	$x1$ = PRIMARY
F = RETICA	G = LG	H = HONEYWELL	I = IRITECH	J = NEUROTECHNOLOGY	$x2$ = SECONDARY
KIND 1 = RAW 640x480		KIND 3 = CROP	KIND 7 = CROP+MASK	KIND 16 = CONCENTRIC POLAR	

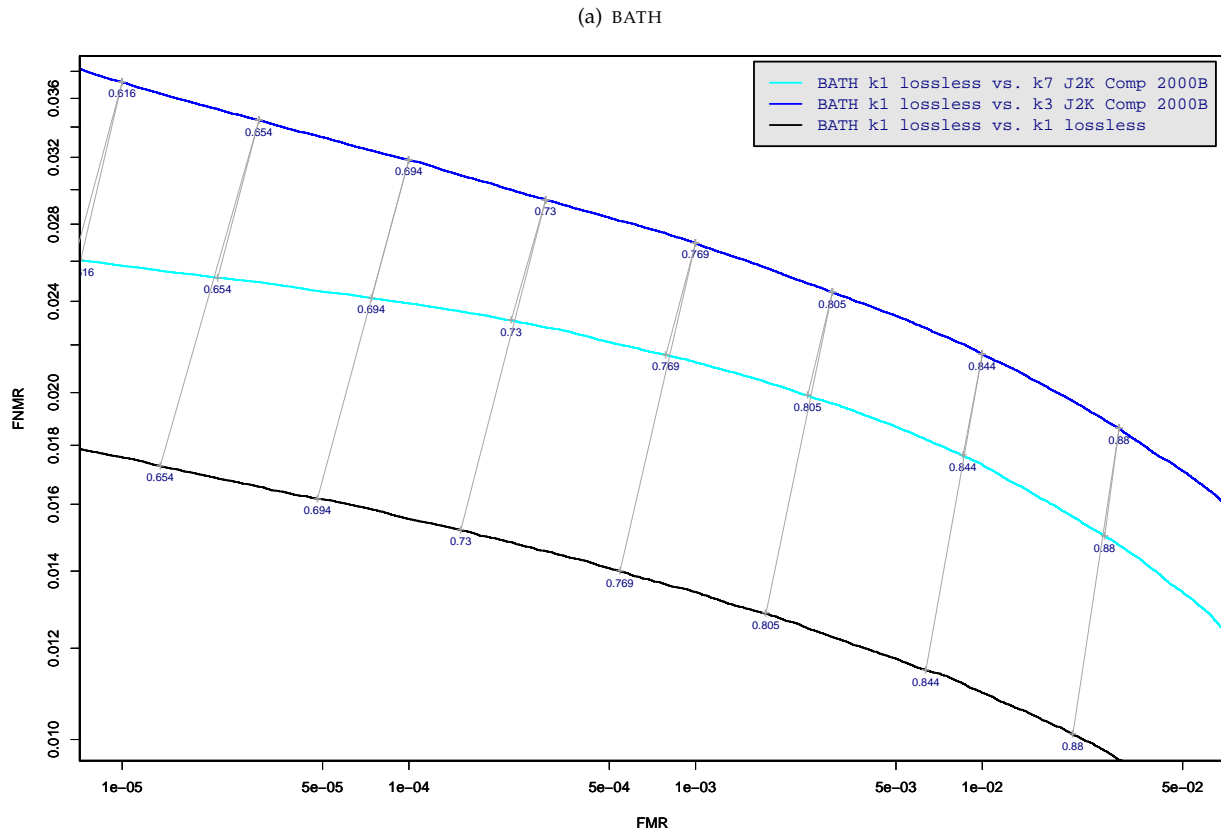


Table 17: DET curve for implementation A2 on the BATH database for the various supported KINDS . The DET characteristics are linked by lines joining points of equal threshold. Non-vertical links indicate a change in false acceptance when the data KIND changes. All results apply to native operation, and the effects of FTE are included.

A = SAGEM	B = COGENT	C = CROSSMATCH	D = CAMBRIDGE	E = L1	$x1$ = PRIMARY
F = RETICA	G = LG	H = HONEYWELL	I = IRITECH	J = NEUROTECHNOLOGY	$x2$ = SECONDARY
KIND 1 = RAW 640x480		KIND 3 = CROP		KIND 7 = CROP+MASK	KIND 16 = CONCENTRIC POLAR

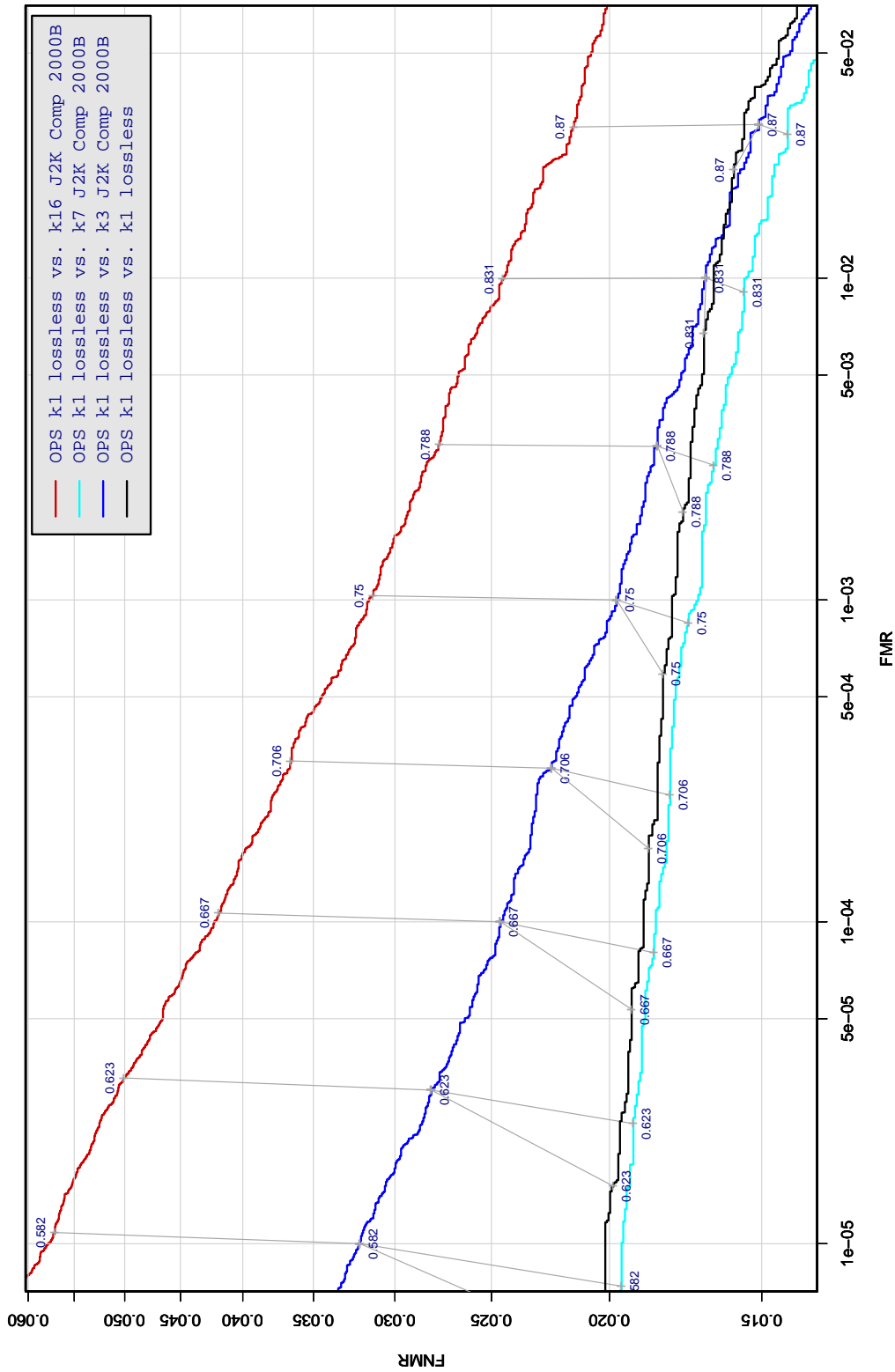


Table 18: DET curve for implementation A2 on the OPS database for the various supported KINDS . The DET characteristics are linked by lines joining points of equal threshold. Non-vertical links indicate a change in false acceptance when the data KIND changes. All results apply to native operation, and the effects of FTE are included.

A = SAGEM	B = COGENT	C = CROSSMATCH	D = CAMBRIDGE	E = L1	$x1$ = PRIMARY
F = RETICA	G = LG	H = HONEYWELL	I = IRITECH	J = NEUROTECHNOLOGY	$x2$ = SECONDARY
KIND 1 = RAW 640x480		KIND 3 = CROP	KIND 7 = CROP+MASK	KIND 16 = CONCENTRIC POLAR	

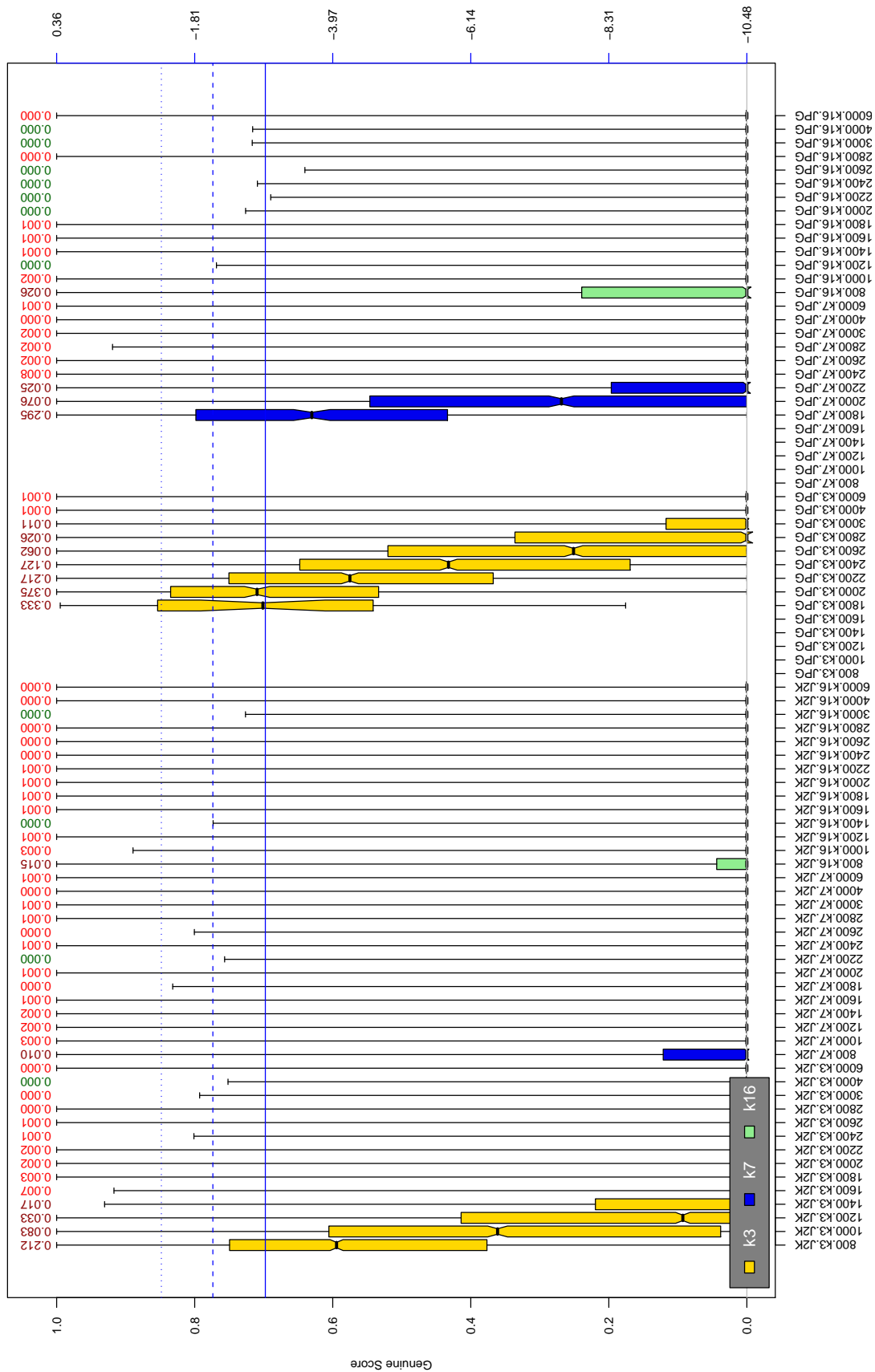


Table 19: The distribution of A2 native genuine comparison scores by size of the compressed image, KIND and the compression algorithm. The images are from the OPS dataset. The right axis scale gives the corresponding value for $d' = (s - \mu_I) / \sqrt{0.5(\sigma_I^2 + \sigma_G^2)}$ for genuine score s . The boxplots only include comparison scores if the uncompressed version of the same image was matched below the FMR = 0.001 threshold. Above the boxplots are FNMR values at FMR = 10^{-3} . The three blue lines correspond, from the top, to FMR of $10^{(-2, -3, -4)}$. The lower grey line refers to the median score obtained from comparison of uncompressed KIND 3 images. Any comparison for which either template had not been generated is excluded. Note that the iris record size on the horizontal axis is not evenly spaced above 3000 bytes.

A = SAGEM	B = COGENT	C = CROSSMATCH	D = CAMBRIDGE	E = L1	$x1$ = PRIMARY
F = RETICA	G = LG	H = HONEYWELL	I = IRITECH	J = NEUROTECHNOLOGY	$x2$ = SECONDARY
KIND 1 = RAW 640x480		KIND 3 = CROP	KIND 7 = CROP+MASK	KIND 16 = CONCENTRIC POLAR	

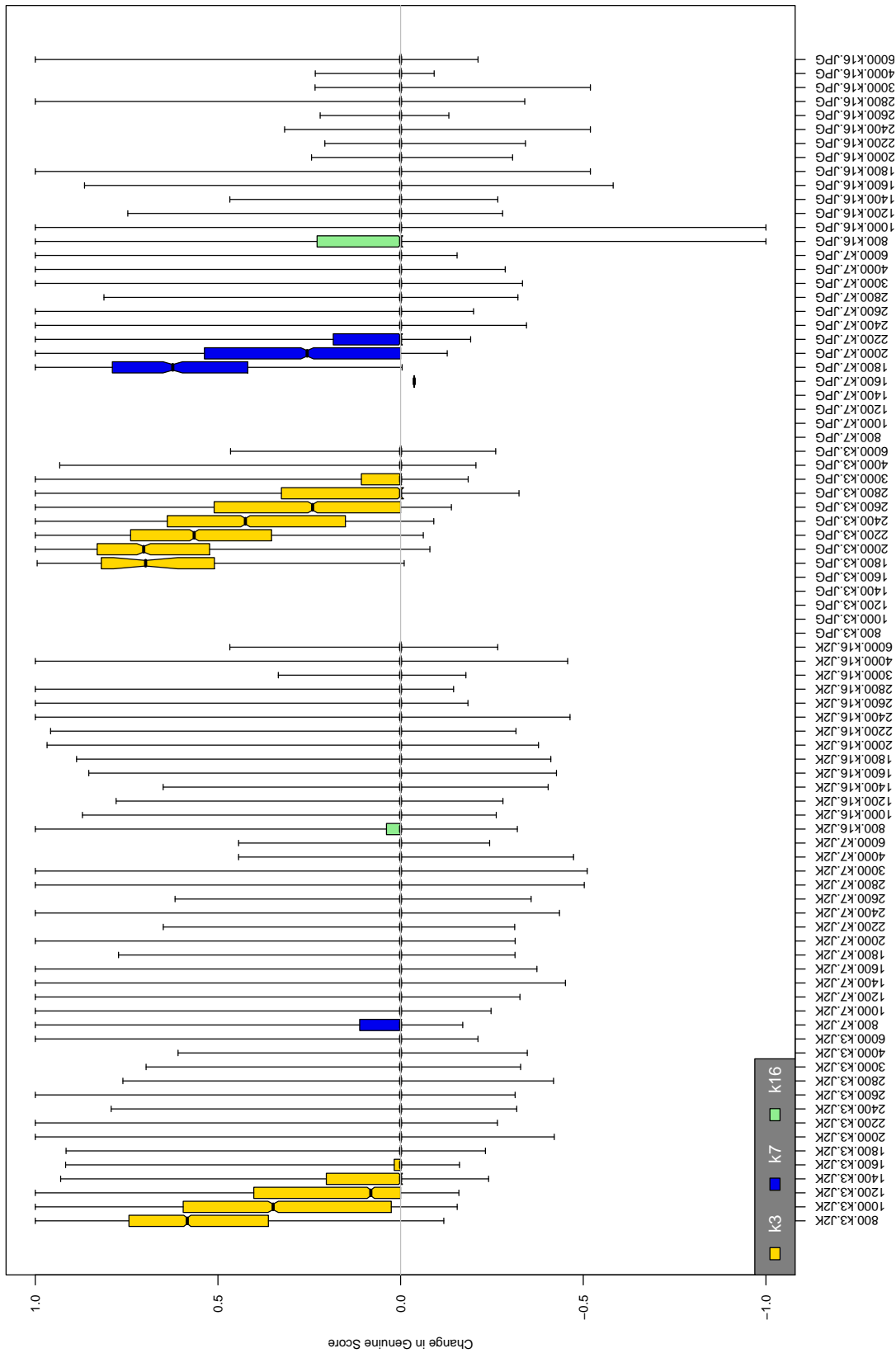


Table 20: The distribution of the *increase* in A2 native genuine comparison scores between the uncompressed “parent” and the compressed image, arranged by size, KIND and the compression algorithm. The images are from the OPS dataset. Any comparison involving a failed template is excluded. Note that the iris record size on the horizontal axis is not evenly spaced above 3000 bytes.

A = SAGEM	B = COGENT	C = CROSSMATCH	D = CAMBRIDGE	E = L1	x1 = PRIMARY
F = RETICA	G = LG	H = HONEYWELL	I = IRITECH	J = NEUROTECHNOLOGY	x2 = SECONDARY
KIND 1 = RAW 640x480		KIND 3 = CROP		KIND 7 = CROP+MASK	
KIND 16 = CONCENTRIC POLAR					

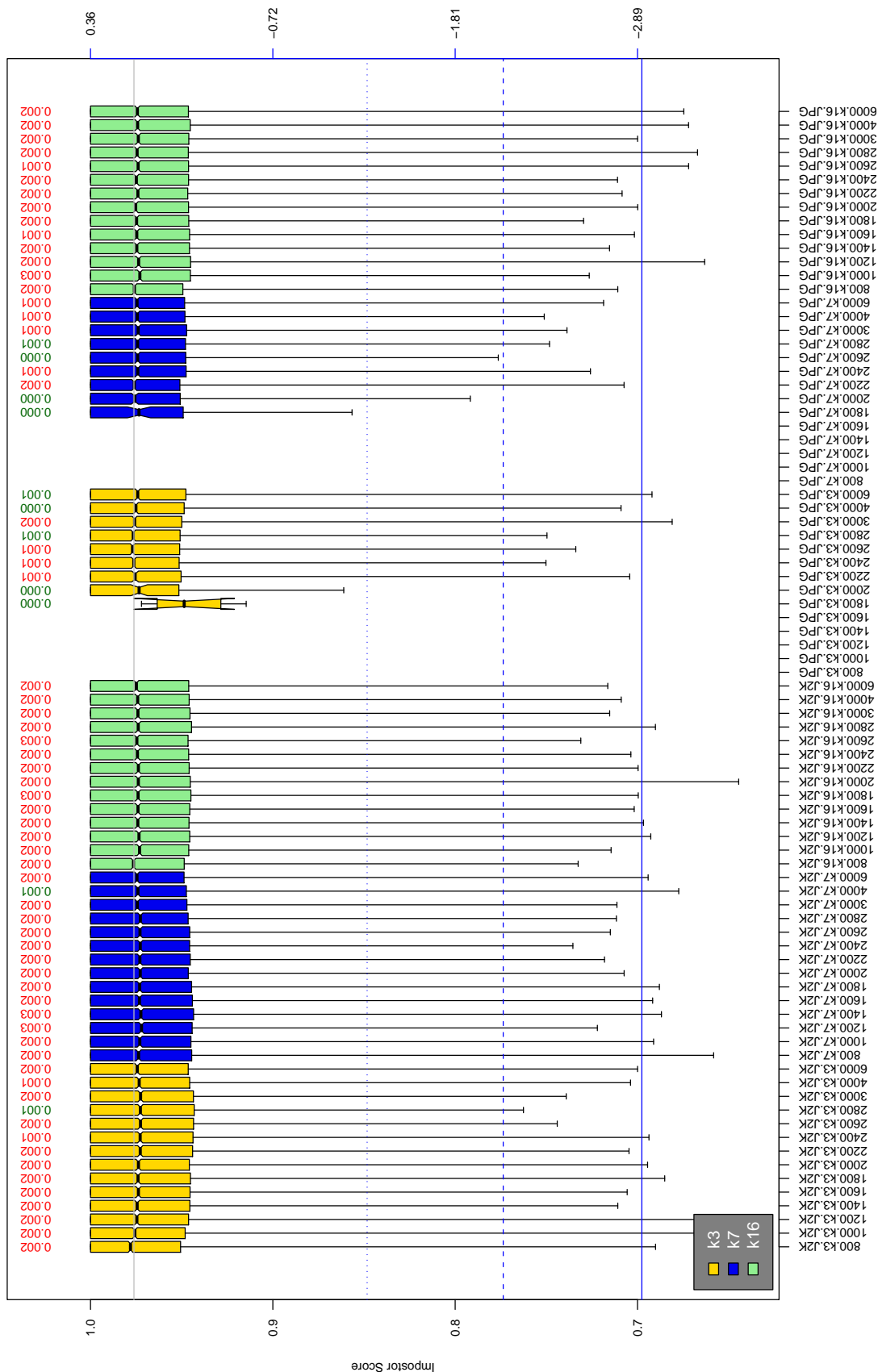


Table 21: The distribution of A2 native impostor comparison scores by size of the compressed image, KIND and the compression algorithm. The right axis scale gives the corresponding value for $d' = (s - \mu_1) / \sqrt{0.5(\sigma_1^2 + \sigma_2^2)}$ for impostor score s . The three blue lines correspond, from the top, to FMR of 10^{-2} , 10^{-3} , and 10^{-4} . The lower grey line refers to the median score obtained from comparison of uncompressed KIND 3 images. Any comparison involving a failed template is excluded. Above the boxplots are FMR values at the threshold that gives FMR = 10^{-3} on uncompressed images. These figures are computed from only 4000 comparisons so the FMR values and the tails of the impostor distribution are poorly characterized. Note that the iris record size on the horizontal axis is not evenly spaced above 3000 bytes.

A = SAGEM	B = COGENT	C = CROSSMATCH	D = CAMBRIDGE	E = L1	x_1 = PRIMARY
F = RETICA	G = LG	H = HONEYWELL	I = IRITECH	J = NEUROTECHNOLOGY	x_2 = SECONDARY
KIND 1 = RAW 640x480		KIND 3 = CROP	KIND 7 = CROP+MASK	KIND 16 = CONCENTRIC POLAR	

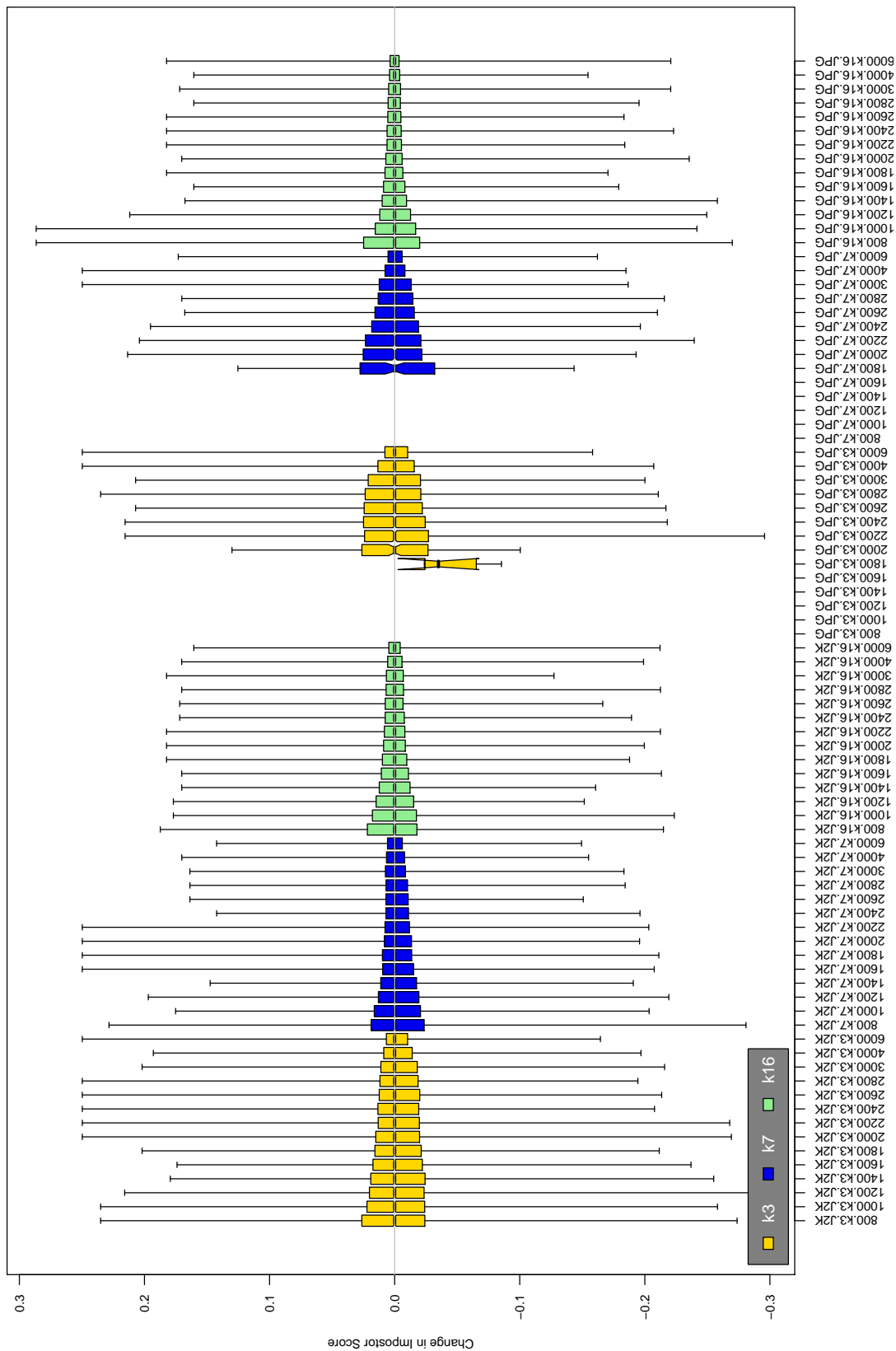


Table 22: The distribution of the increase in A2 native impostor comparison scores between the uncompressed “parent” and the compressed image, arranged by size, KIND and the compression algorithm. The images are from the OPS dataset. Any comparison involving a failed template is excluded. Note that the iris record size on the horizontal axis is not evenly spaced above 3000 bytes.

A = SAGEM	B = COGENT	C = CROSSMATCH	D = CAMBRIDGE	E = L1	x1 = PRIMARY
F = RETICA	G = LG	H = HONEYWELL	I = IRITECH	J = NEUROTECHNOLOGY	x2 = SECONDARY
KIND 1 = RAW 640x480		KIND 3 = CROP		KIND 7 = CROP+MASK	KIND 16 = CONCENTRIC POLAR

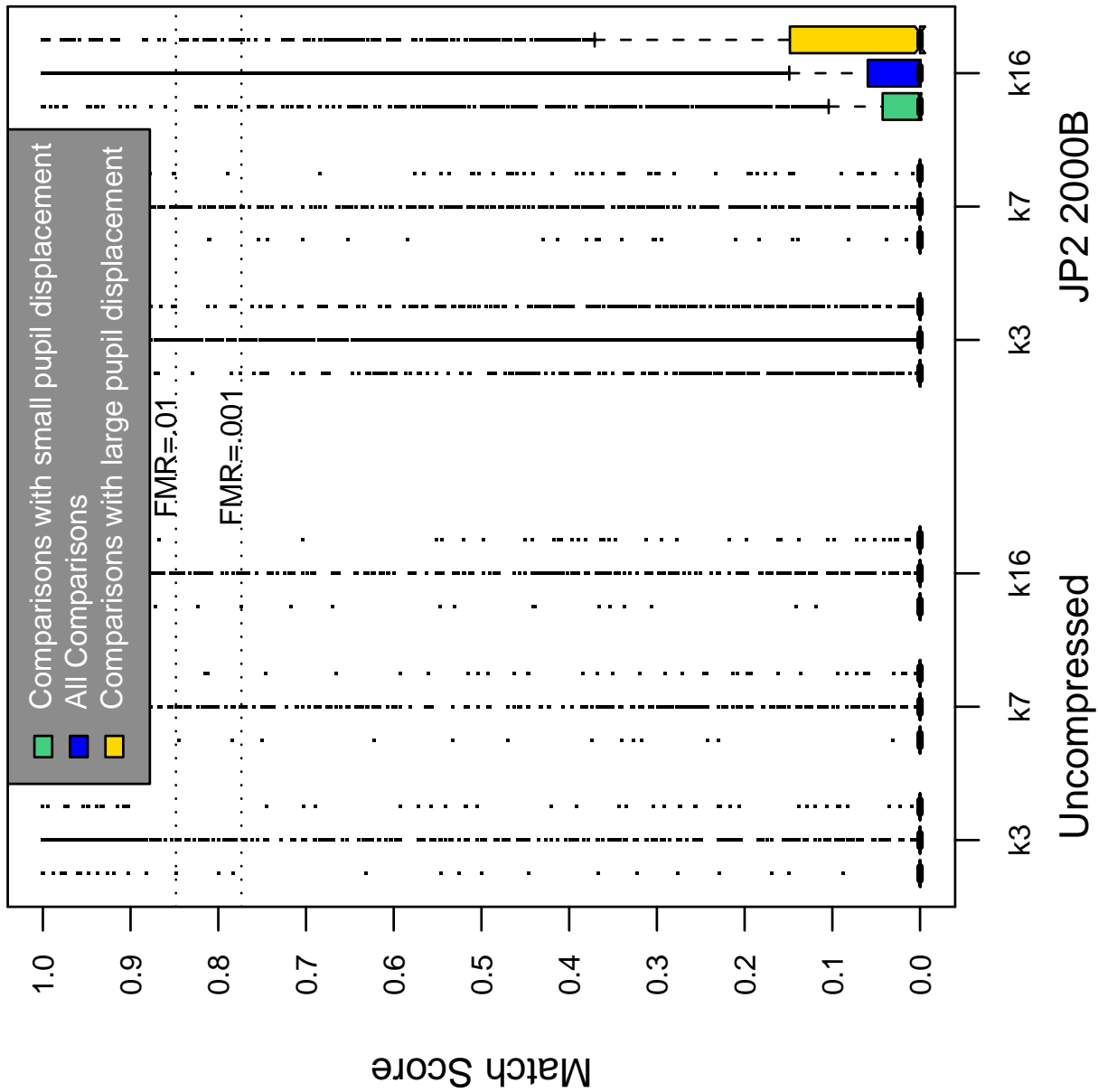


Table 23: Effect of pupil displacement on the genuine score distribution for A2

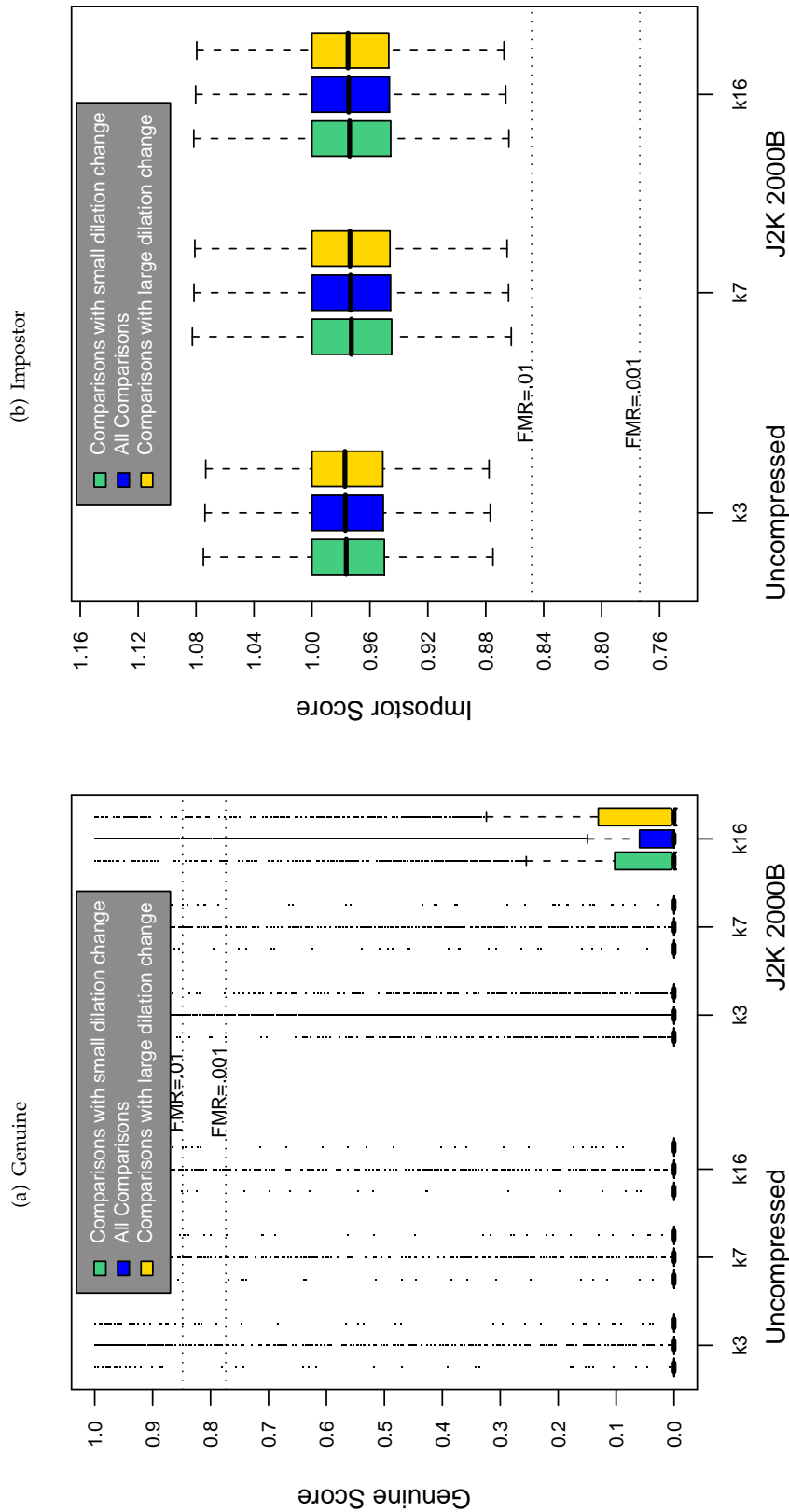


Table 24: The effect of dilation change on the two scores distributions for SDK A2.

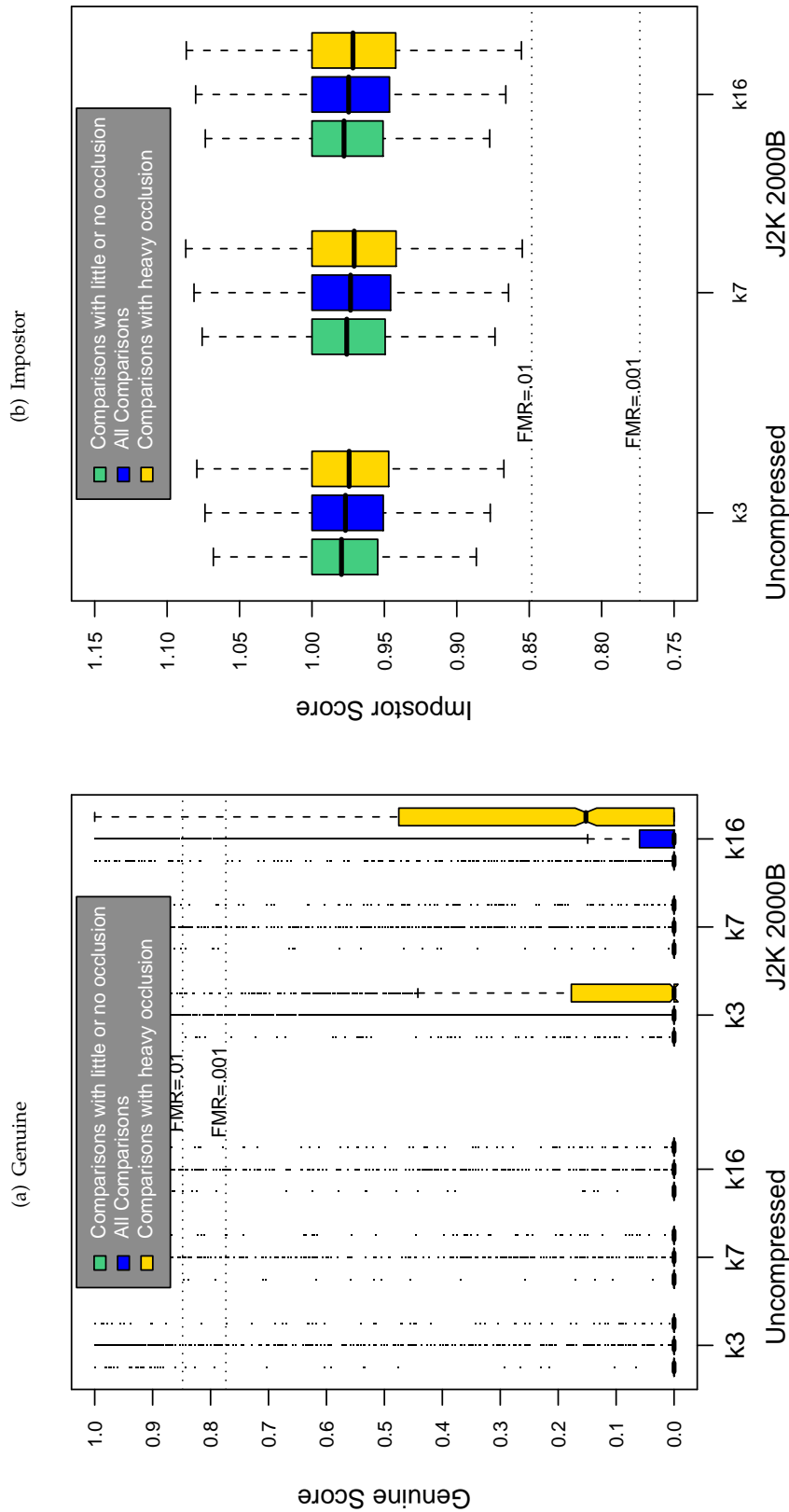
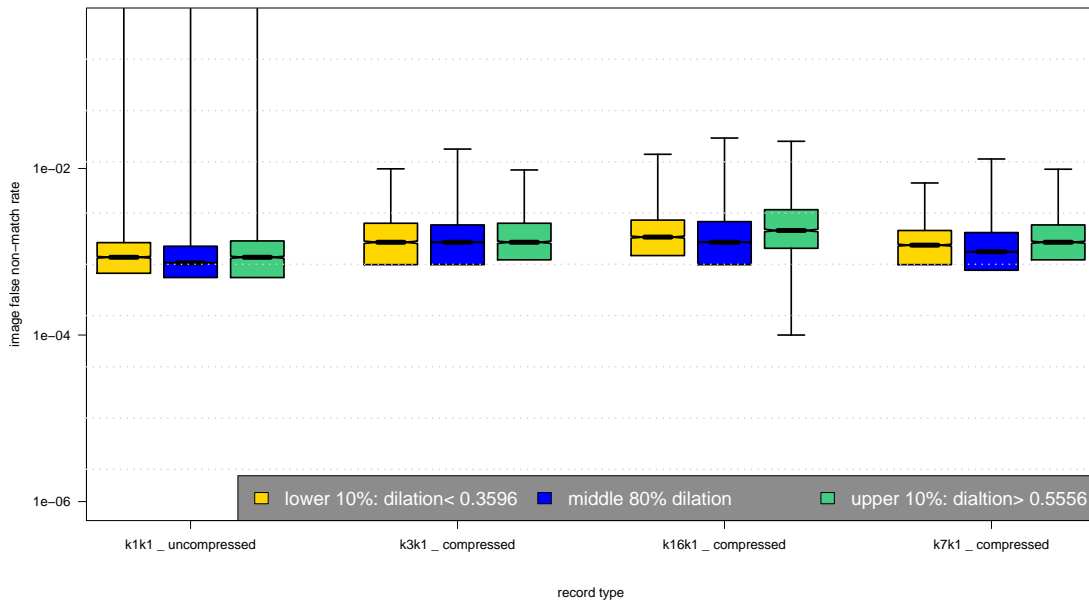
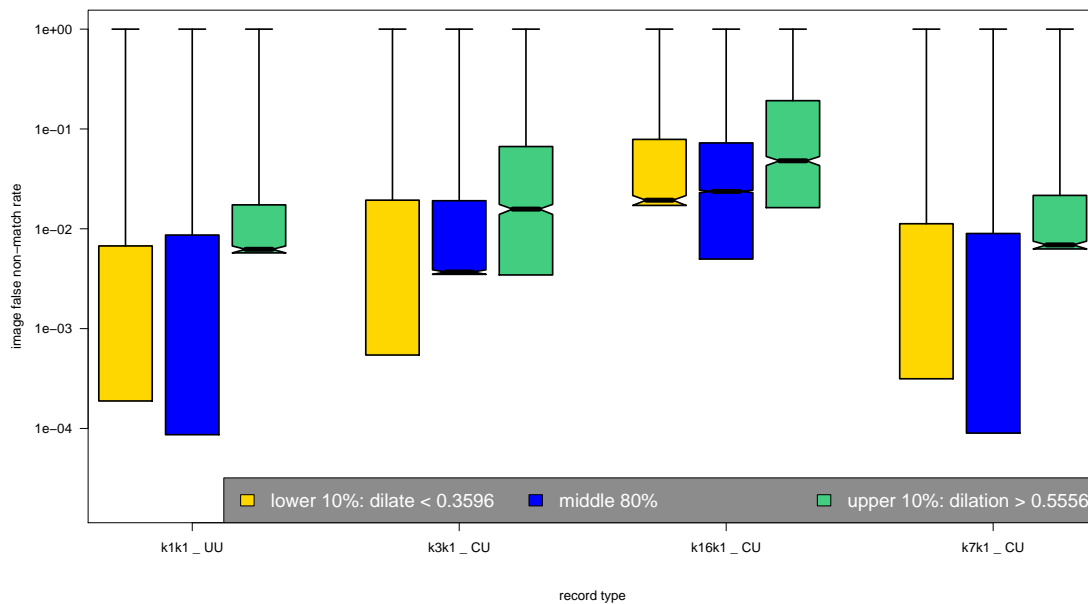


Table 25: The effect of eyelid occlusion on the two scores distributions for SDK A2.

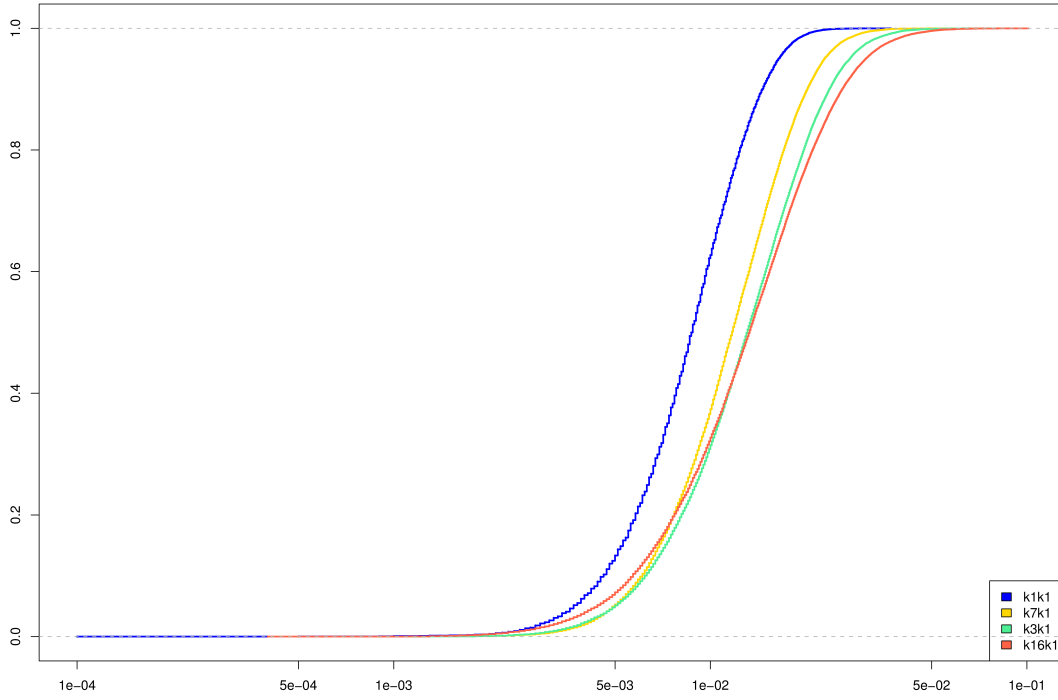
(a) iFMR using A1 dilation estimates



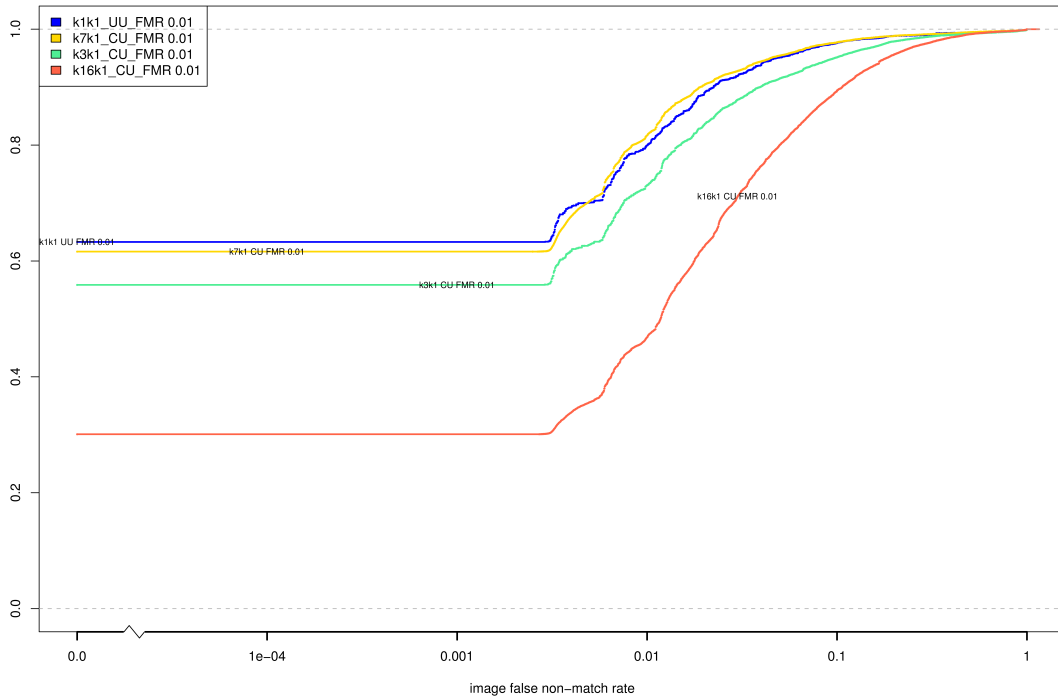
(b) iFNMR using A1 dilation estimates



(c) iFMR CDF



(d) iFNMR CDF



Compiled Results for Implementation B1

On June 25, 2009, NIST invited the IREX participants to submit a description of the SDKs submitted for the IREX effort. The intent was to allow providers to describe and contrast the feature sets, optimization, operational suitability and availability of the primary and secondary SDKs. NIST indicated that any submitted text would appear verbatim (with typesetting) in draft and final versions of the IREX report and that it would be attributed to the organization. This was optional and NIST put no constraints on the content beyond a 600 word limit, and a statement that anything labelled as confidential or proprietary would be omitted.

The provider of SDK B1, Cogent Systems, elected not to submit any information

On August 17, 2009, NIST invited the IREX participants to submit a description their comments on an draft version of the IREX report. This was intended to allow participants to assist readers in the interpretation of a large and complicated testing effort. NIST indicated that any submitted text would appear verbatim (with typesetting) in the final version of the IREX report and that it would be attributed to the organization. Submission of content was optional and NIST put no constraints on the content beyond a word limit, and a statement that anything labelled as confidential or proprietary would be omitted.

The provider of SDK B1, Cogent Systems, submitted the following to NIST - we make no comment on this information.

When kind 16 instances are involved, the matching performance of Cogent's IREX SDK is affected by a data decoding error. This is discussed in the following comments.

1. The error occurred during the process of decoding kind 48 format data. The decoding was not part of the feature extraction algorithms or matching algorithms.

During IREX testing, iris matching was performed on proprietary templates which were generated from iris data in different formats. In the case when iris data was provided in kind 16 format (unsegmented polar), the NIST test harness converted kind 16 data to kind 48 data (reconstructed rectilinear image). Cogent's template generator took the kind 48 data as input, decoded it get raw image, and performed feature extraction on raw image to produce the proprietary template that would be used for matching.

2. Matching accuracy was affected when one or both templates were generated from kind 16 / kind 48 data.

This includes the following:

- Results reported in Figure 26 (page 70)
 - Results listed under K16 in Table 9 (page 64)
 - Results listed under K16 in Table 10 (page 65)
 - Results listed under K16 in Table 11 (page 66)
 - Results listed under K16 in Table 14 (page 79)
3. Results on kind 1 (K1), kind 3 (K3), and kind 7 (K7) data were not affected.
 4. The kind 16 records generated by Cogent's SDK were not affected.

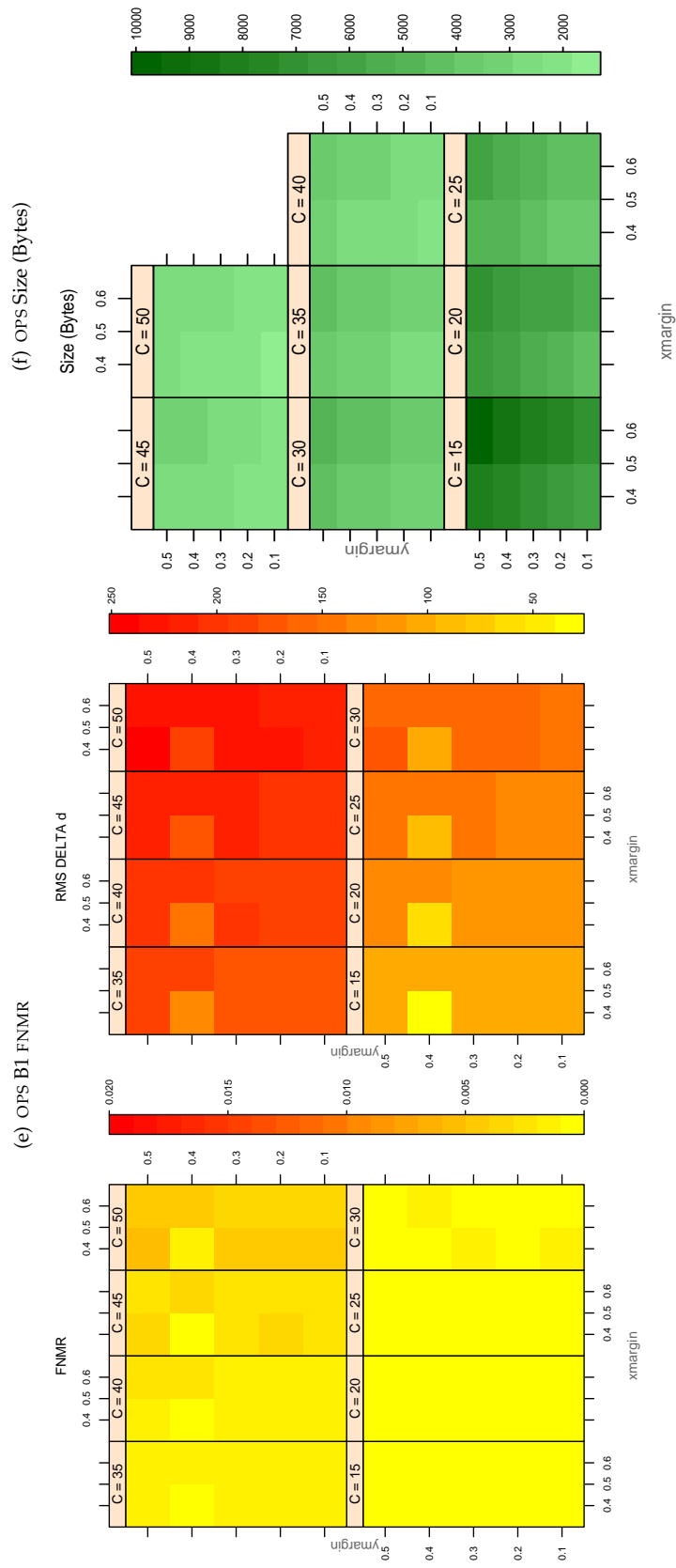


Table 26: For the IREX partition of the OPS database the plots at left show the dependence of cFNMR on the vertical and horizontal iris cropping margins for various compression ratios. This applies only for KIND 3 records. The margins are in units of iris radius. The use of conditional FNMR means that the plots exclude comparisons that were falsely rejected even before any compression was applied. On the **right side** is the rms difference between the crop+compress and the uncompressed comparison scores for each image pair. All computations are driven by the bounding box coordinates reported by the II SDK. The number of bits per pixel is $8/C$, where C is the compression ratio. The iris radius varies and because the cropping margins are fixed multiples of the radius the image size varies. The compressed size, in bytes, is the width times height divided by C . Values of cFNMR greater than 0.02 are shown as 0.02.

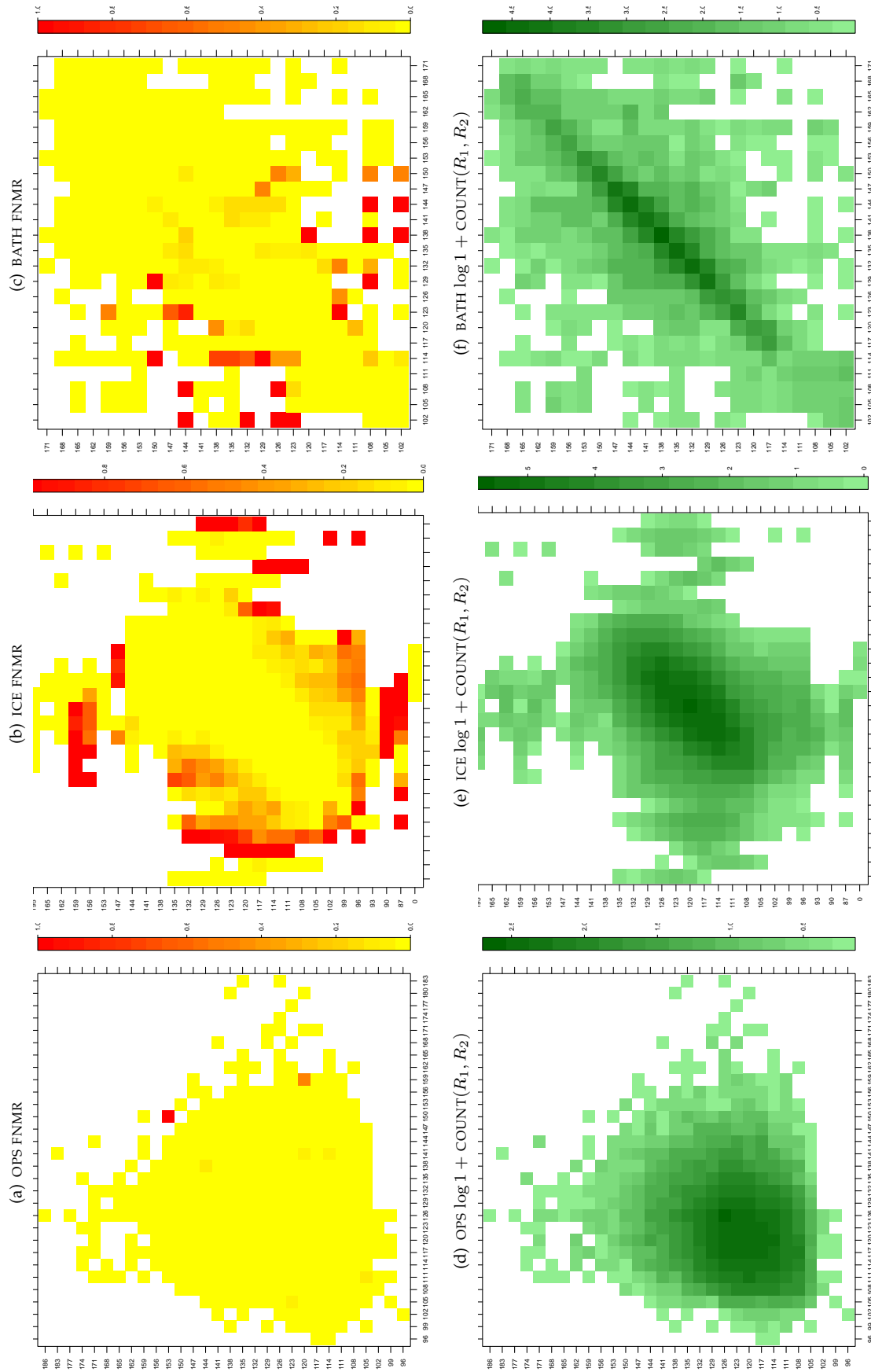


Table 27: For the three IREX databases: In the **top** row the color in each cell represents the occurrence of genuine comparisons with the given pair of radii. The *y*-axis represents enrollment samples with verification samples on the *x*-axis; In the **bottom** row the color scale plots $\log 1 + \text{COUNT}(R_1, R_2)$. The radii are quantized into three-pixel bins. The radii for DOD are on the range $96 \leq r \leq 186$ pixels. The radii for ICE are on the range $87 \leq r \leq 165$ pixels. The radii for BATH are on the range $100 \leq r \leq 170$ pixels.

A = SAGEM	B = COGENT	C = CROSSMATCH	D = CAMBRIDGE	E = L1	$x1$ = PRIMARY
F = RETICA	G = LG	H = HONEYWELL	I = IRITECH	J = NEUROTECHNOLOGY	$x2$ = SECONDARY
KIND 1 = RAW 640x480		KIND 3 = CROP	KIND 7 = CROP+MASK	KIND 16 = CONCENTRIC POLAR	

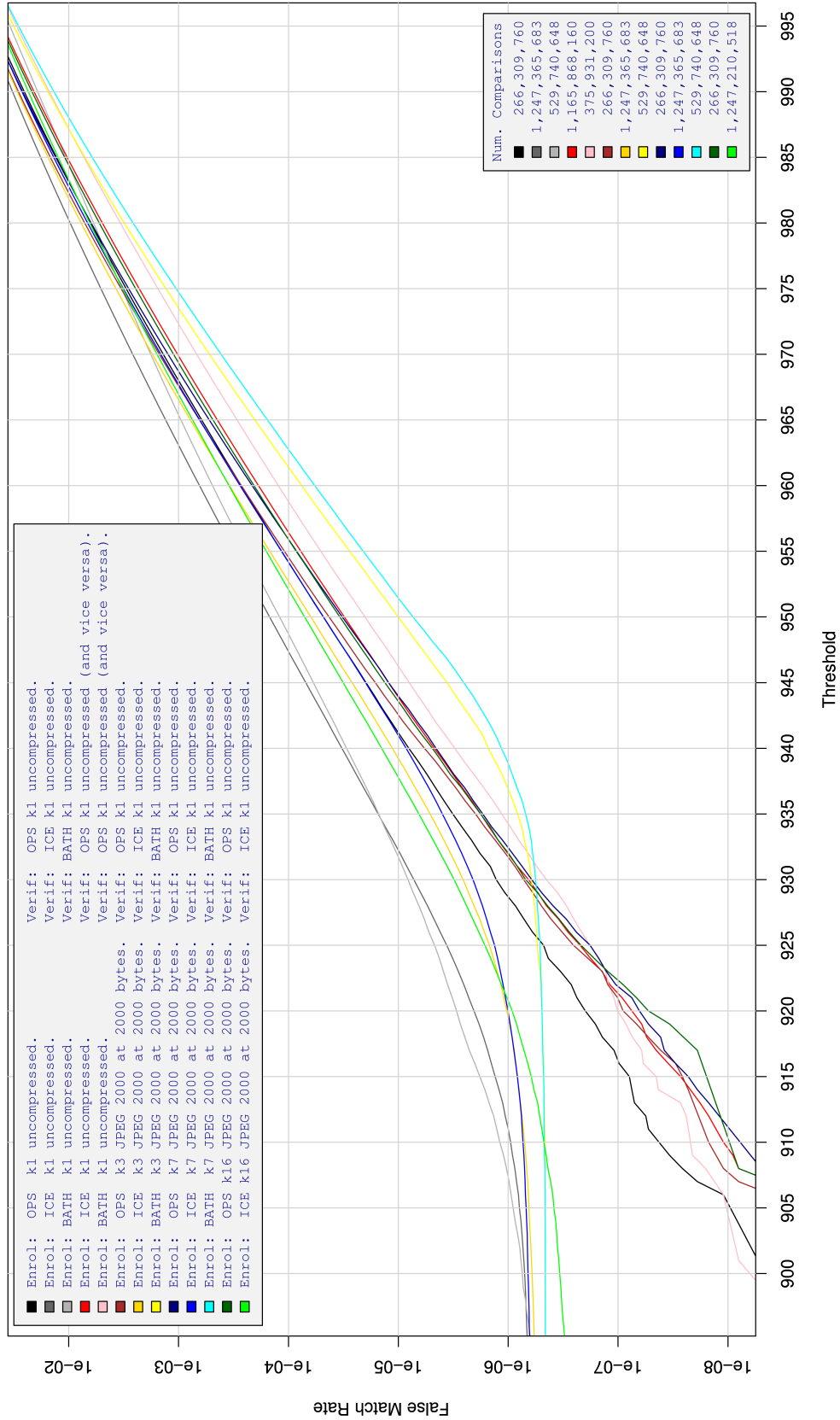


Table 28: For implementation B1, the dependency of FMR on threshold. for various combinations of enrollment and verification dataset, format, and compression.

A = SAGEM	B = COGENT	C = CROSSMATCH	D = CAMBRIDGE	E = L1	x1 = PRIMARY
F = RETICA	G = LG	H = HONEYWELL	I = IRITECH	J = NEUROTECHNOLOGY	x2 = SECONDARY
KIND 1 = RAW 640x480		KIND 3 = CROP		KIND 7 = CROP+MASK	
KIND 16 = CONCENTRIC POLAR					

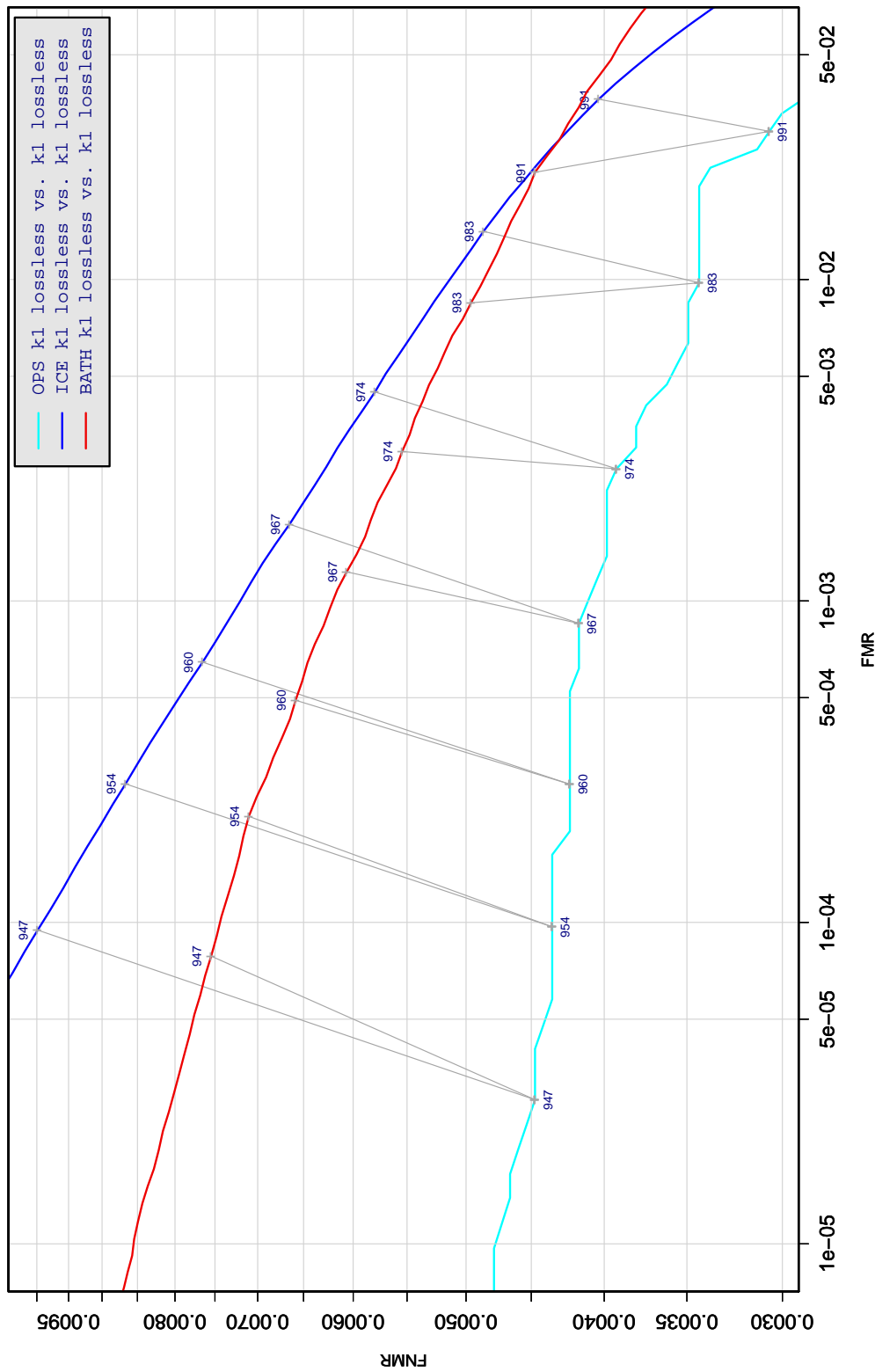


Table 29: DET curve for implementation B1 on three IREX databases. All comparisons are with uncompressed KIND 1 vs. KIND 1 images. The lines join points corresponding to the a fixed threshold. Non-vertical links indicate a change in FMR when the database changes. All results apply to native operation. Failures to produce a template i.e. FTE are ignored because the plots are intended to show *matching* effects, specifically to compare DET slopes and to show the effect of fixing a threshold.

A = SAGEM	B = COGENT	C = CROSSMATCH	D = CAMBRIDGE	E = L1	$x1$ = PRIMARY
F = RETICA	G = LG	H = HONEYWELL	I = IRITECH	J = NEUROTECHNOLOGY	$x2$ = SECONDARY
KIND 1 = RAW 640x480		KIND 3 = CROP	KIND 7 = CROP+MASK	KIND 16 = CONCENTRIC POLAR	

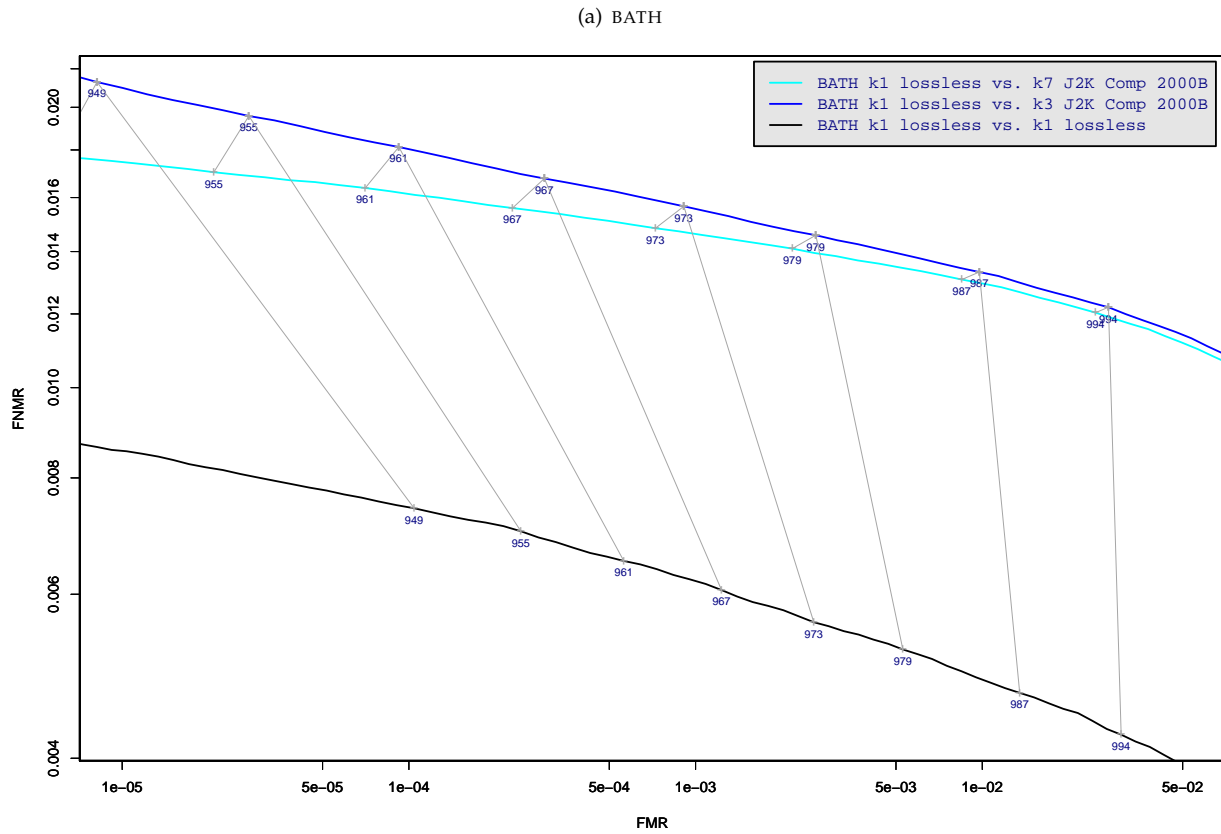


Table 30: DET curve for implementation B1 on the BATH database for the various supported KINDS . The DET characteristics are linked by lines joining points of equal threshold. Non-vertical links indicate a change in false acceptance when the data KIND changes. All results apply to native operation, and the effects of FTE are included.

A = SAGEM	B = COGENT	C = CROSSMATCH	D = CAMBRIDGE	E = L1	x1 = PRIMARY
F = RETICA	G = LG	H = HONEYWELL	I = IRITECH	J = NEUROTECHNOLOGY	x2 = SECONDARY
KIND 1 = RAW 640x480		KIND 3 = CROP	KIND 7 = CROP+MASK	KIND 16 = CONCENTRIC POLAR	

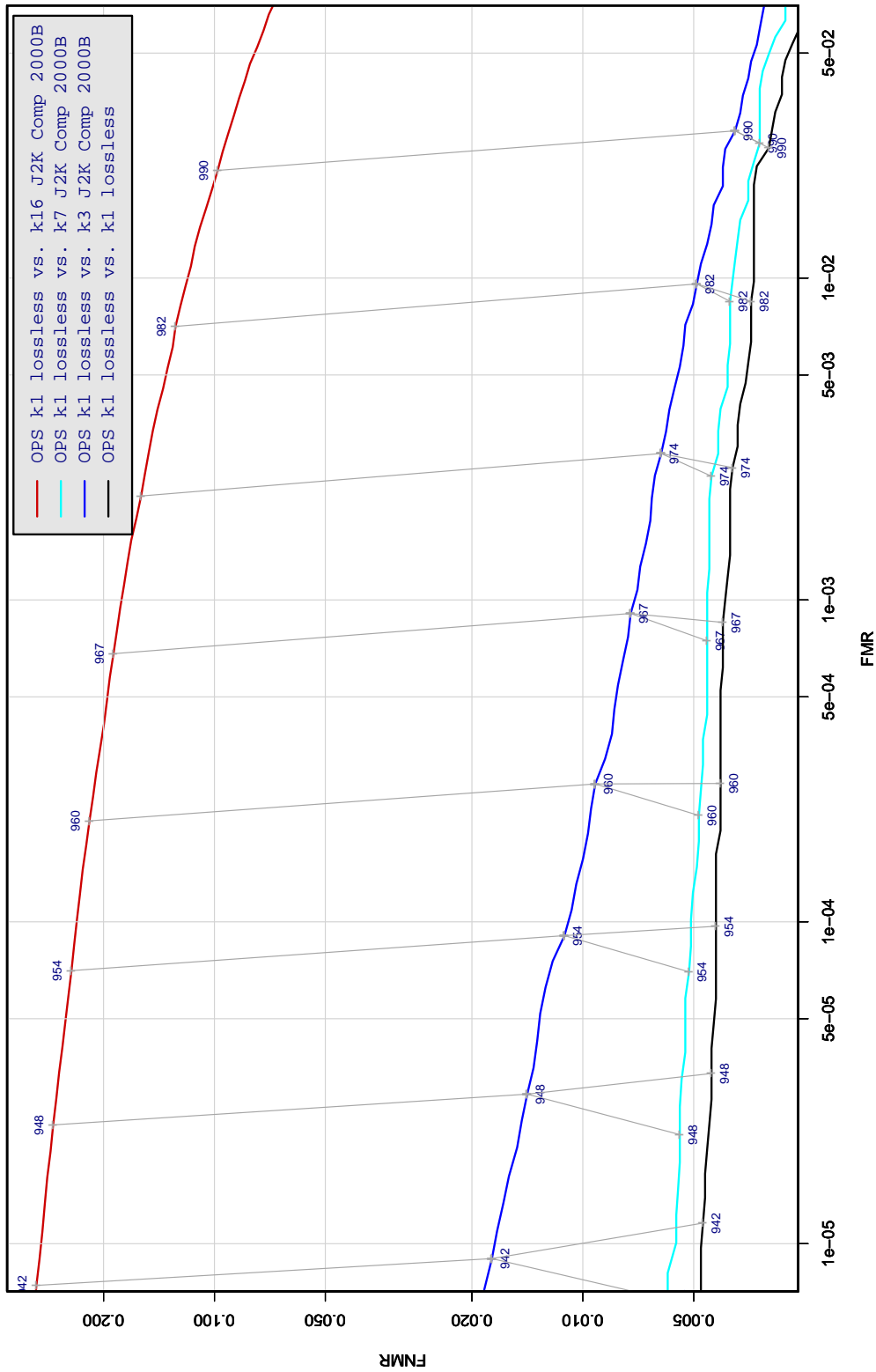


Table 31: DET curve for implementation B1 on the OPS database for the various supported KINDS . The DET characteristics are linked by lines joining points of equal threshold. Non-vertical links indicate a change in false acceptance when the data KIND changes. All results apply to native operation, and the effects of FTE are included.

A = SAGEM	B = COGENT	C = CROSSMATCH	D = CAMBRIDGE	E = L1	x1 = PRIMARY
F = RETICA	G = LG	H = HONEYWELL	I = IRITECH	J = NEUROTECHNOLOGY	x2 = SECONDARY
KIND 1 = RAW 640x480		KIND 3 = CROP	KIND 7 = CROP+MASK	KIND 16 = CONCENTRIC POLAR	

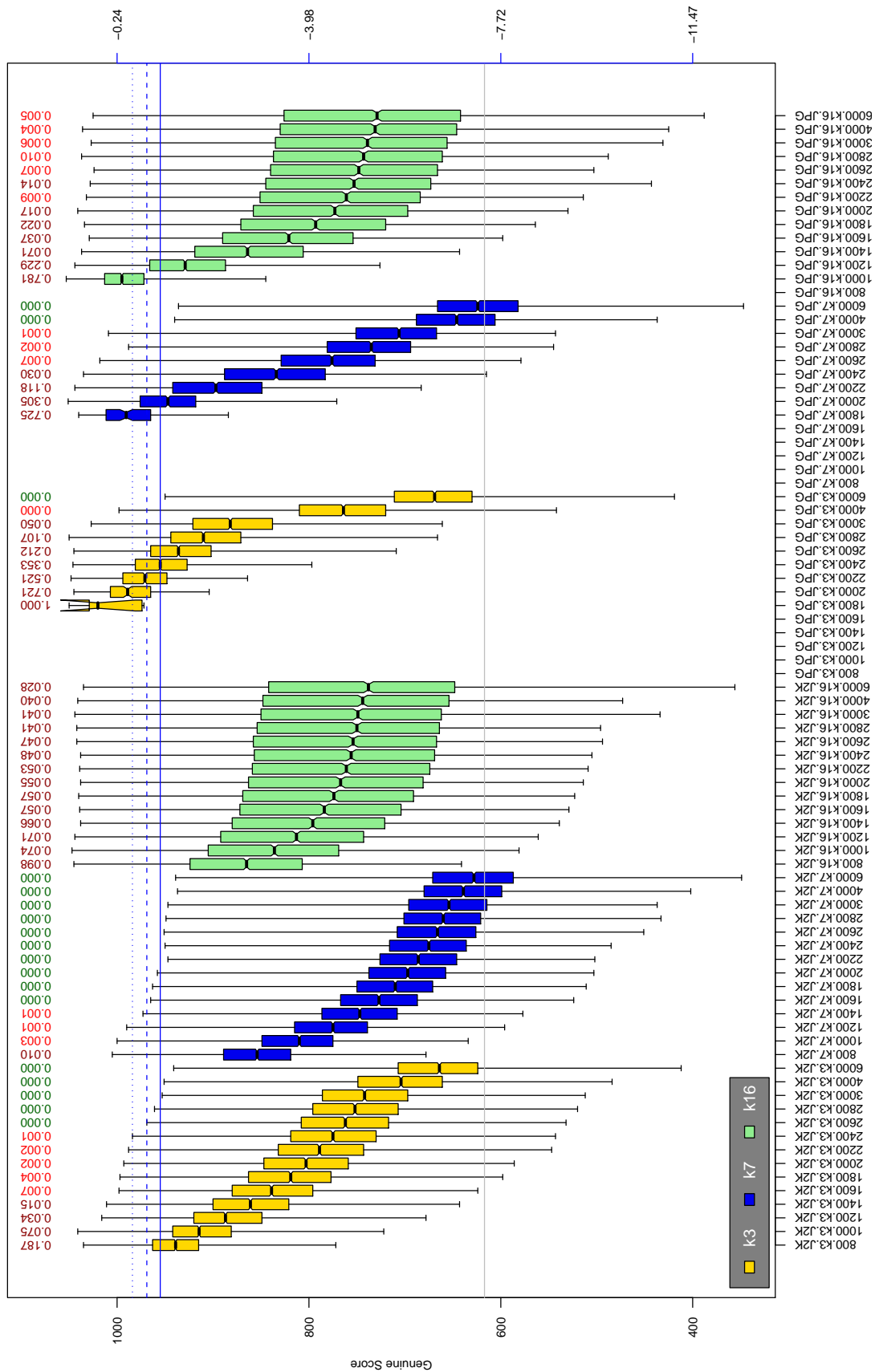


Table 32: The distribution of B1 native genuine comparison scores by size of the compressed image, KIND and the compression algorithm. The images are from the ops dataset. The right axis scale gives the corresponding value for $d' = (s - \mu_I) / \sqrt{0.5(\sigma_I^2 + \sigma_C^2)}$ for genuine score s . The boxplots only include comparison scores if the uncompressed version of the same image was matched below the FMR = 0.001 threshold. Above the boxplots are FNMR values at FMR = 10^{-3} . The three blue lines correspond, from the top, to FMR of $10^{-2}, -3, -4$. The lower grey line refers to the median score obtained from comparison of uncompressed KIND 3 images. Any comparison for which either template had not been generated is excluded. Note that the iris record size on the horizontal axis is not evenly spaced above 3000 bytes.

A = SAGEM	B = COGENT	C = CROSSMATCH	D = CAMBRIDGE	E = L1	$x1$ = PRIMARY
F = RETICA	G = LG	H = HONEYWELL	I = IRITECH	J = NEUROTECHNOLOGY	$x2$ = SECONDARY
KIND 1 = RAW 640x480		KIND 3 = CROP	KIND 7 = CROP+MASK	KIND 16 = CONCENTRIC POLAR	

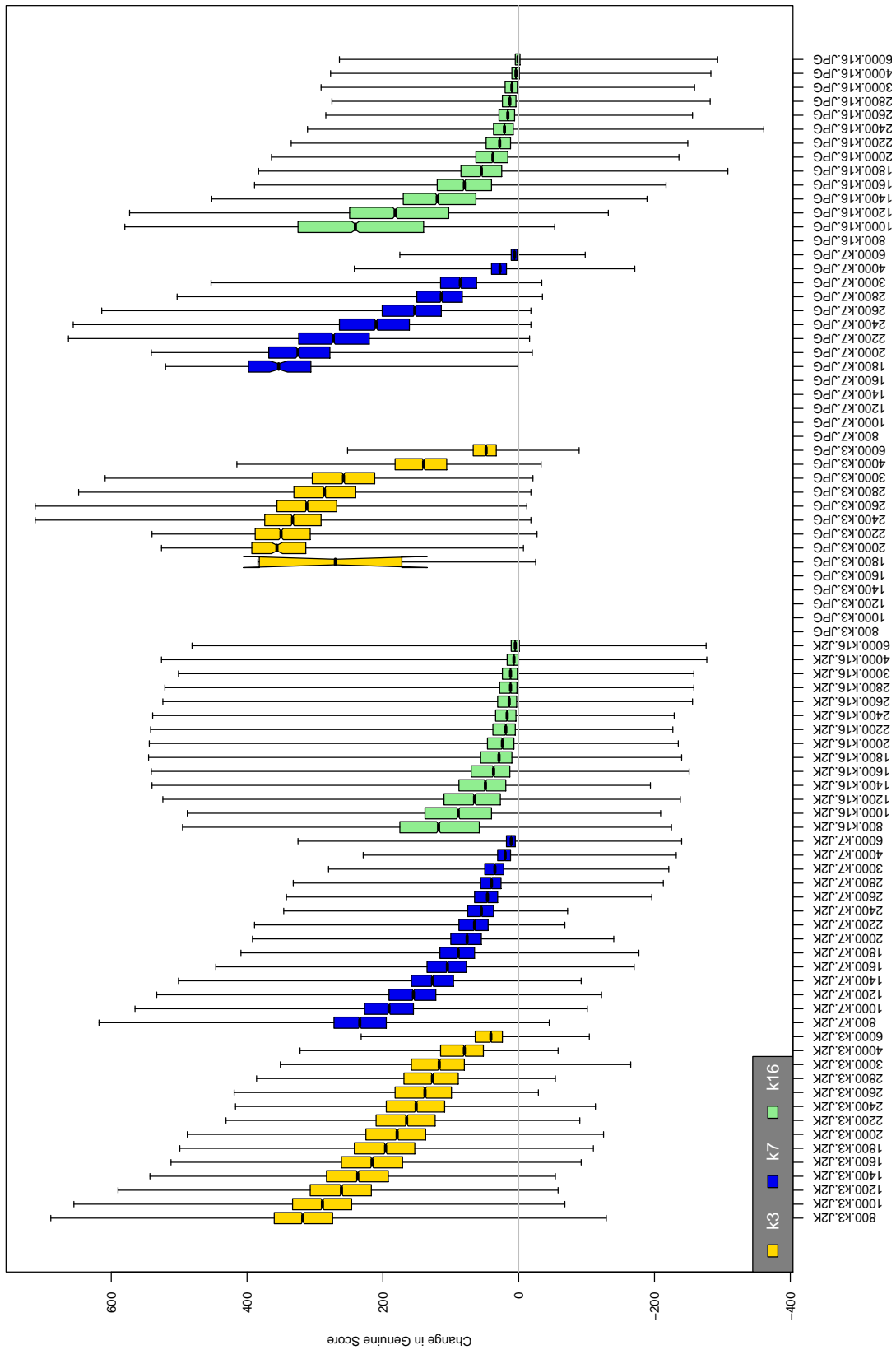


Table 33: The distribution of the *increase* in B1 native genuine comparison scores between the uncompressed “parent” and the compressed image, arranged by size, KIND and the compression algorithm. The images are from the OPS dataset. Any comparison involving a failed template is excluded. Note that the iris record size on the horizontal axis is not evenly spaced above 3000 bytes.

A = SAGEM	B = COGENT	C = CROSSMATCH	D = CAMBRIDGE	E = L1	x1 = PRIMARY
F = RETICA	G = LG	H = HONEYWELL	I = IRITECH	J = NEUROTECHNOLOGY	x2 = SECONDARY
KIND 1 = RAW 640x480		KIND 3 = CROP	KIND 7 = CROP+MASK	KIND 16 = CONCENTRIC POLAR	

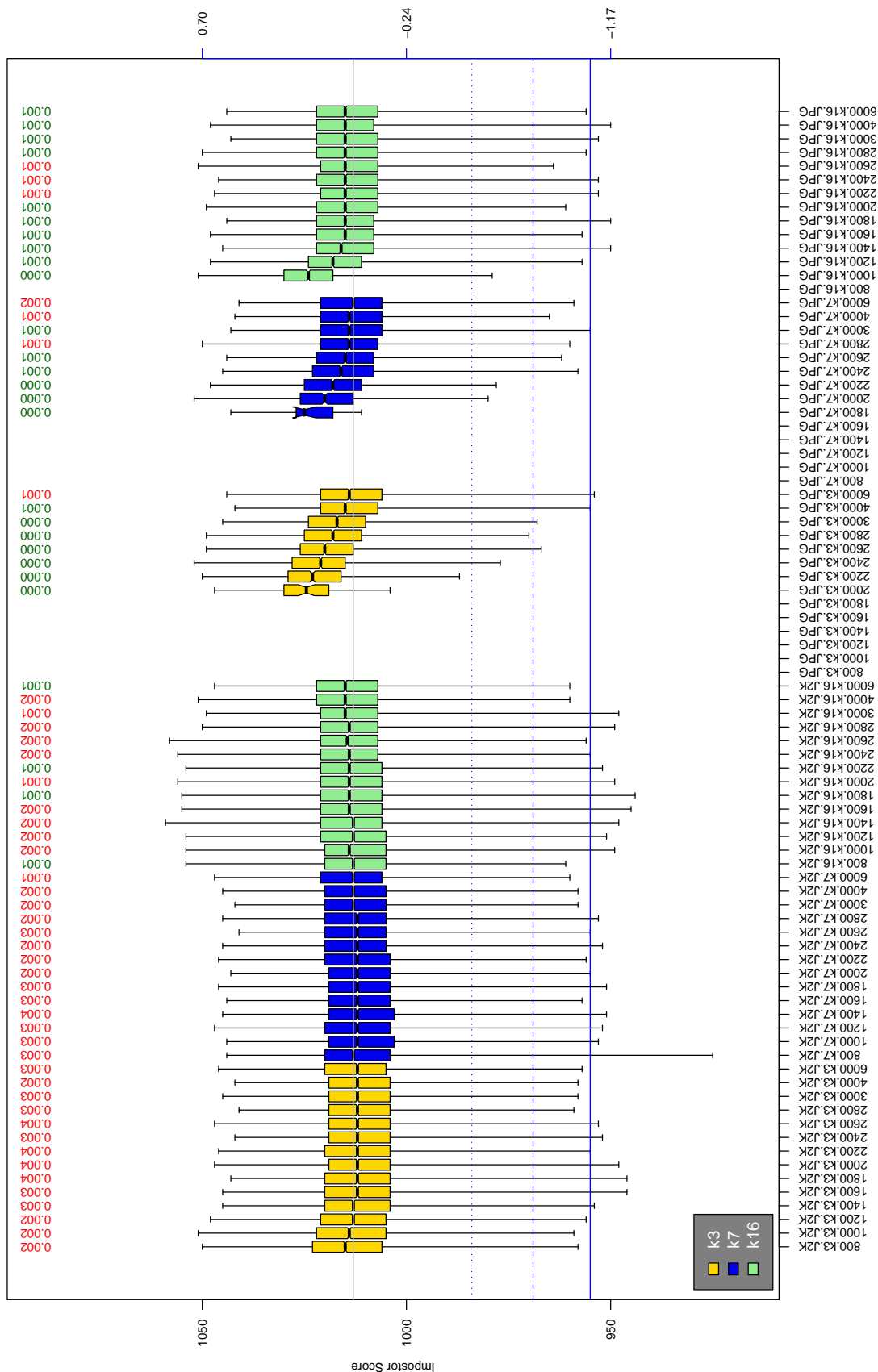


Table 34: The distribution of BI native impostor comparison scores by size of the compressed image, KIND and the compression algorithm. The right axis scale gives the corresponding value for $d' = (s - \mu_1) / \sqrt{0.5(\sigma_1^2 + \sigma_2^2)}$ for impostor score s . The three blue lines correspond, from the top, to FMR of 10^{-2} , -3 , -4 . The lower grey line refers to the median score obtained from comparison of uncompressed KIND 3 images. Any comparison involving a failed template is excluded. Above the boxplots are FMR values at the threshold that gives FMR = 10^{-3} on uncompressed images. These figures are computed from only 4000 comparisons so the FMR values and the tails of the impostor distribution are poorly characterized. Note that the iris record size on the horizontal axis is not evenly spaced above 3000 bytes.

A = SAGEM	B = COGENT	C = CROSSMATCH	D = CAMBRIDGE	E = L1	$x1$ = PRIMARY
F = RETICA	G = LG	H = HONEYWELL	I = IRITECH	J = NEUROTECHNOLOGY	$x2$ = SECONDARY
KIND 1 = RAW 640x480		KIND 3 = CROP		KIND 7 = CROP+MASK	KIND 16 = CONCENTRIC POLAR

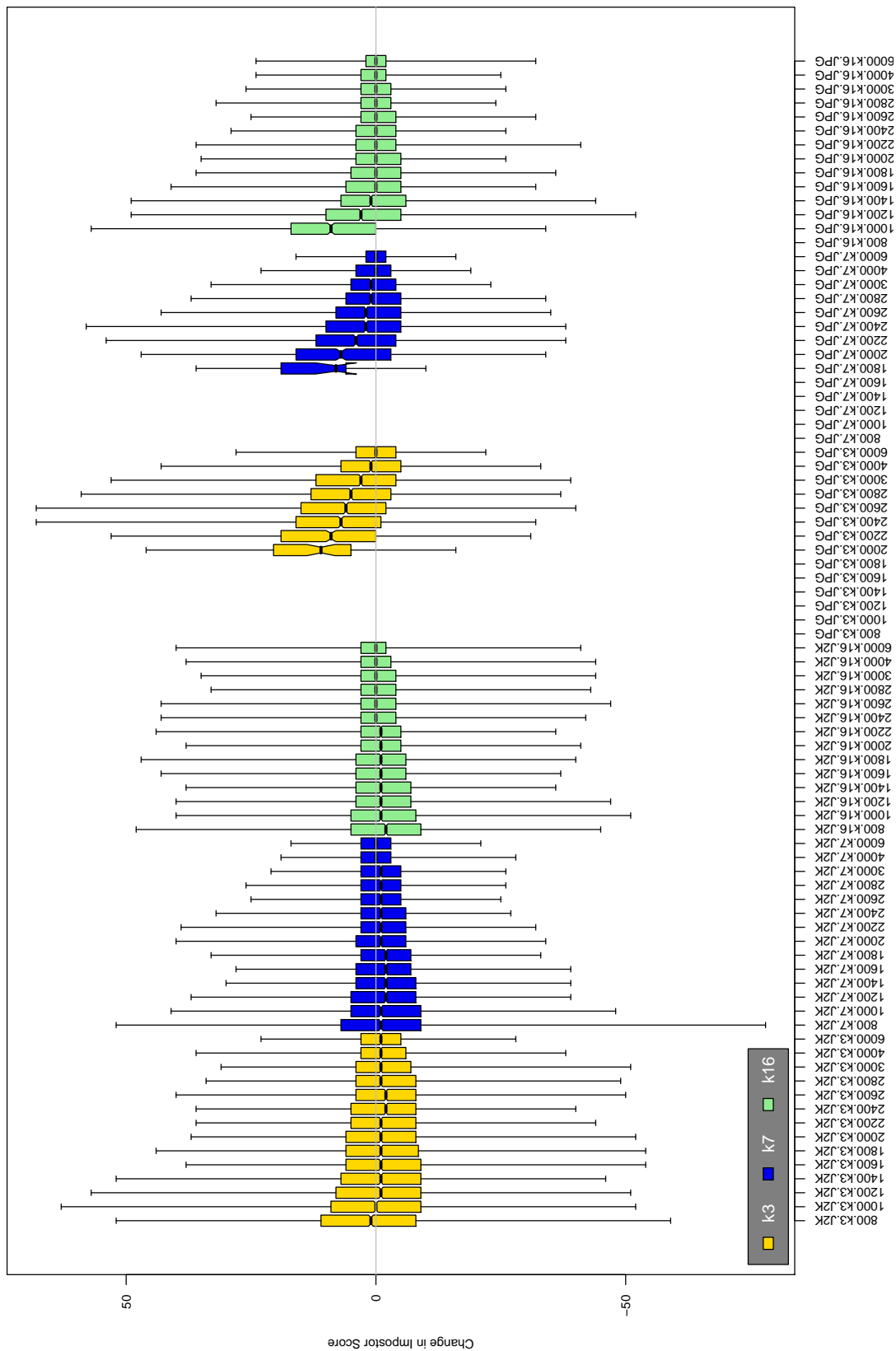


Table 35: The distribution of the increase in B1 native impostor comparison scores between the uncompressed “parent” and the compressed image, arranged by size, KIND and the compression algorithm. The images are from the OPS dataset. Any comparison involving a failed template is excluded. Note that the iris record size on the horizontal axis is not evenly spaced above 3000 bytes.

A = SAGEM	B = COGENT	C = CROSSMATCH	D = CAMBRIDGE	E = L1	x1 = PRIMARY
F = RETICA	G = LG	H = HONEYWELL	I = IRITECH	J = NEUROTECHNOLOGY	x2 = SECONDARY
KIND 1 = RAW 640x480		KIND 3 = CROP	KIND 7 = CROP+MASK	KIND 16 = CONCENTRIC POLAR	

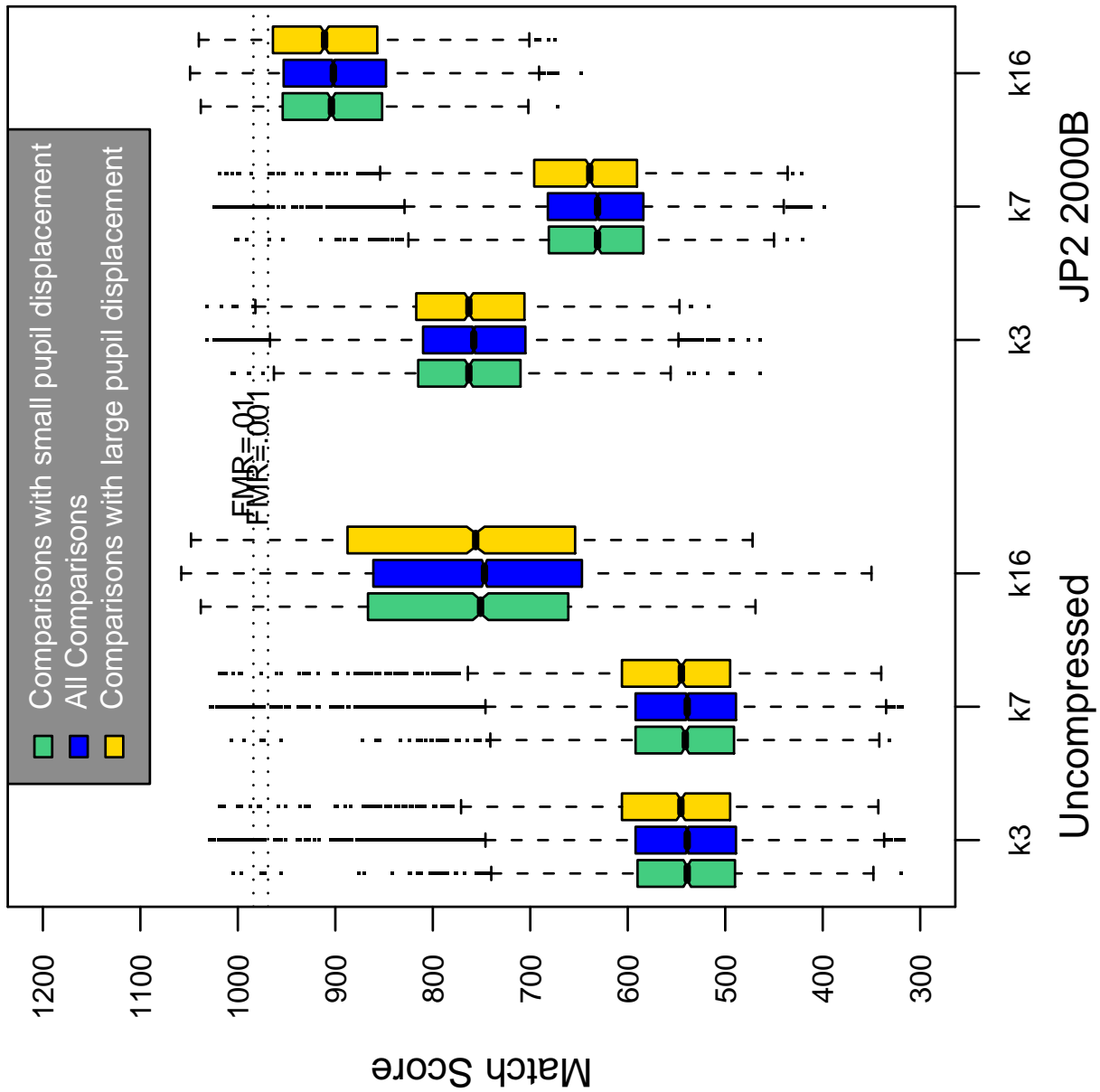


Table 36: Effect of pupil displacement on the genuine score distribution for B1

A = SAGEM	B = COGENT	C = CROSSMATCH	D = CAMBRIDGE	E = L1	x1 = PRIMARY
F = RETICA	G = LG	H = HONEYWELL	I = IRITECH	J = NEUROTECHNOLOGY	x2 = SECONDARY
KIND 1 = RAW 640x480		KIND 3 = CROP	KIND 7 = CROP+MASK	KIND 16 = CONCENTRIC POLAR	

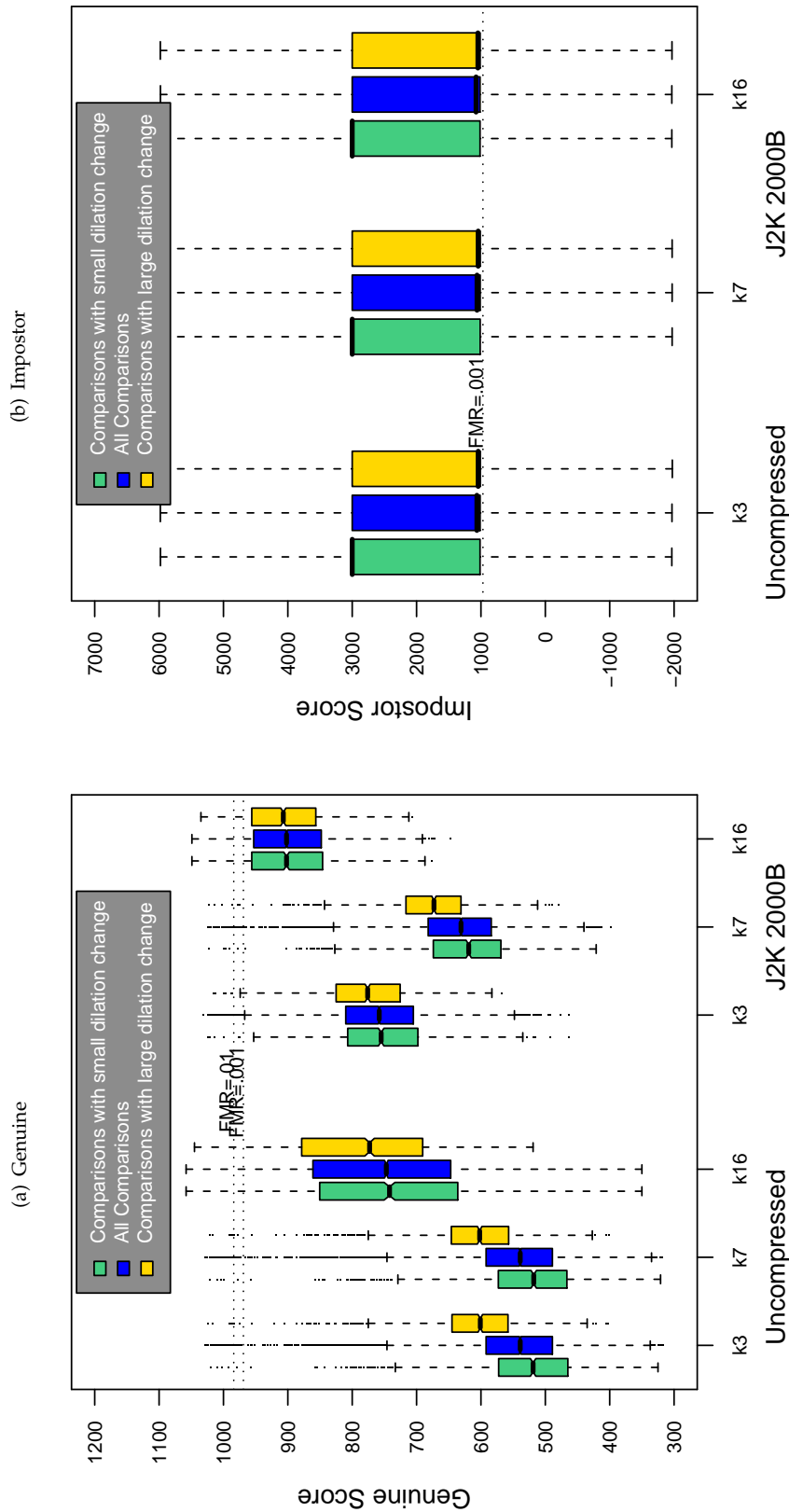


Table 37: The effect of dilation change on the two scores distributions for SDK B1.

A = SAGEM	B = COGENT	C = CROSSMATCH	D = CAMBRIDGE	E = L1	$x1$ = PRIMARY
F = RETICA	G = LG	H = HONEYWELL	I = IRITECH	J = NEUROTECHNOLOGY	$x2$ = SECONDARY
KIND 1 = RAW 640x480		KIND 3 = CROP	KIND 7 = CROP+MASK	KIND 16 = CONCENTRIC POLAR	

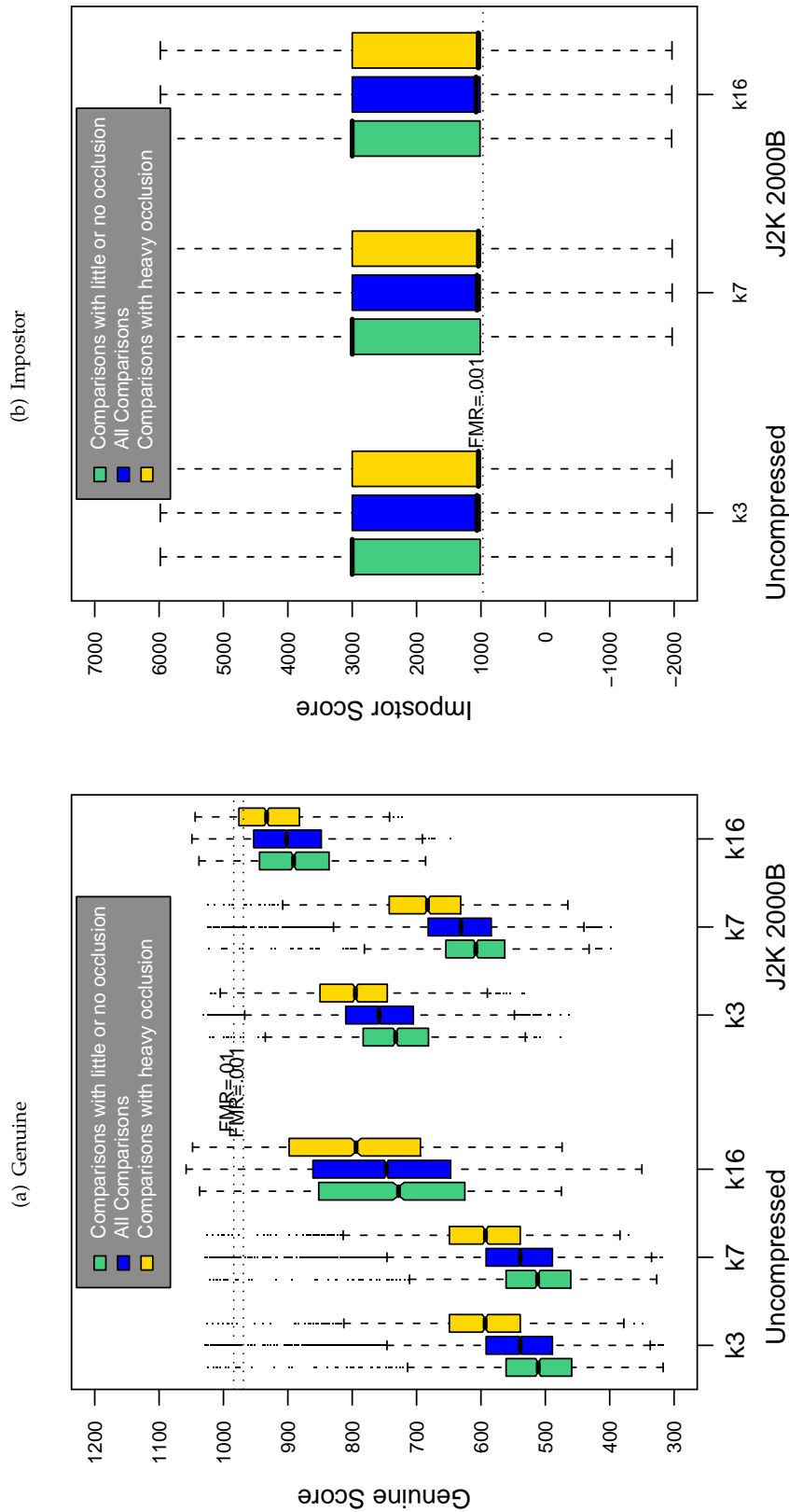
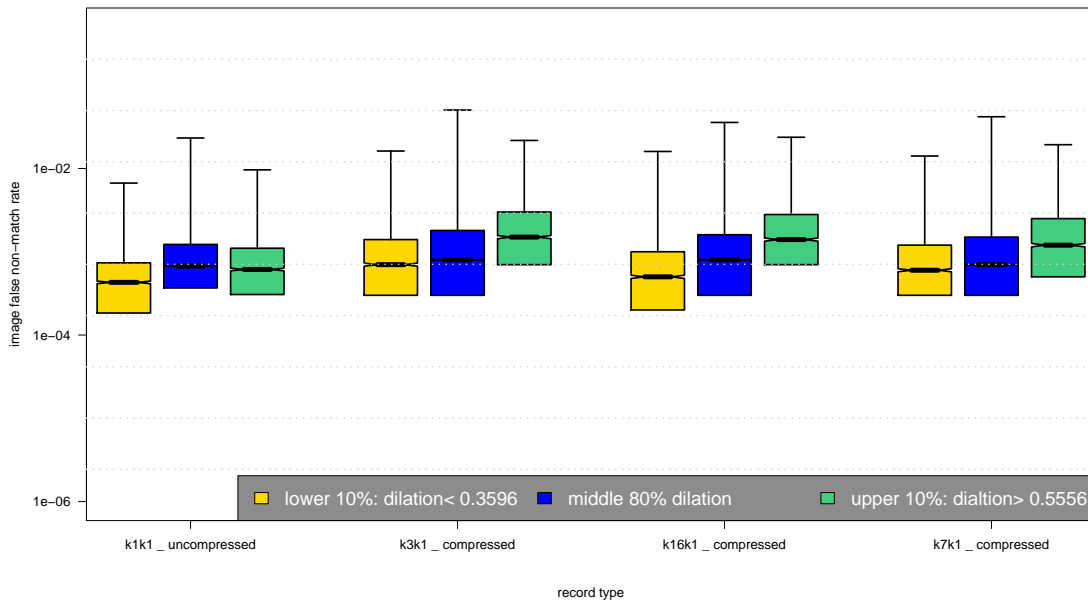


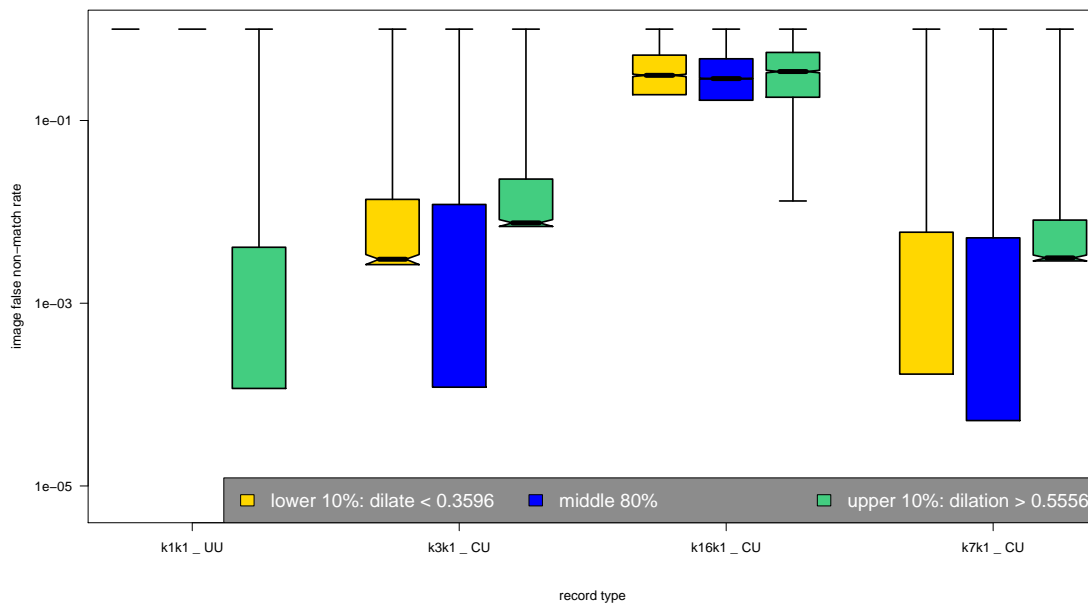
Table 38: The effect of eyelid occlusion on the two scores distributions for SDK B1.

A = SAGEM	B = COGENT	C = CROSSMATCH	D = CAMBRIDGE	E = L1	$x1$ = PRIMARY
F = RETICA	G = LG	H = HONEYWELL	I = IRITECH	J = NEUROTECHNOLOGY	$x2$ = SECONDARY
KIND 1 = RAW 640x480		KIND 3 = CROP	KIND 7 = CROP+MASK	KIND 16 = CONCENTRIC POLAR	

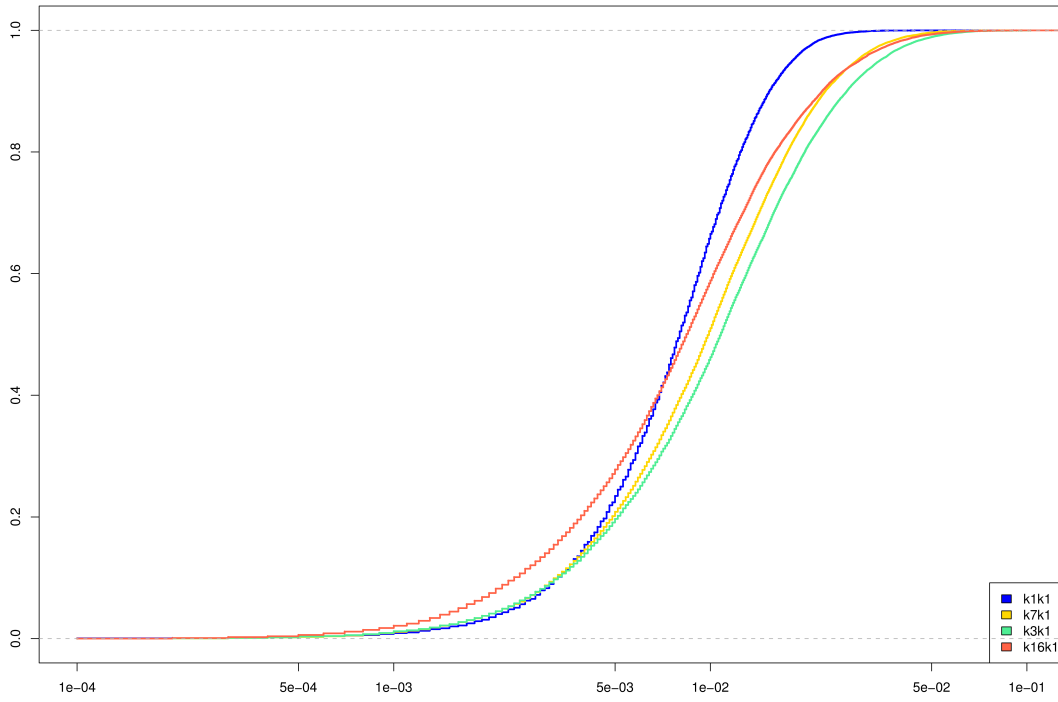
(a) iFMR using A1 dilation estimates



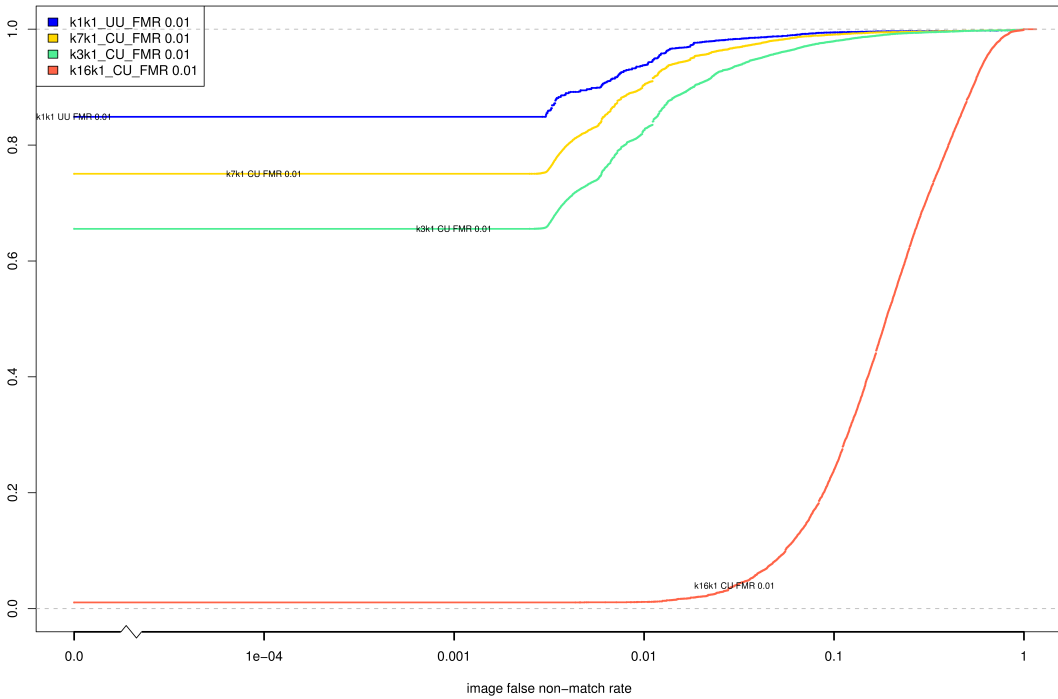
(b) iFNMR using A1 dilation estimates



(c) iFMR CDF



(d) iFNMR CDF



A = SAGEM	B = COGENT	C = CROSSMATCH	D = CAMBRIDGE	E = L1	x1 = PRIMARY
F = RETICA	G = LG	H = HONEYWELL	I = IRITECH	J = NEUROTECHNOLOGY	x2 = SECONDARY
KIND 1 = RAW 640x480		KIND 3 = CROP		KIND 7 = CROP+MASK	
				KIND 16 = CONCENTRIC POLAR	

Compiled Results for Implementation B2

On June 25, 2009, NIST invited the IREX participants to submit a description of the SDKs submitted for the IREX effort. The intent was to allow providers to describe and contrast the feature sets, optimization, operational suitability and availability of the primary and secondary SDKs. NIST indicated that any submitted text would appear verbatim (with typesetting) in draft and final versions of the IREX report and that it would be attributed to the organization. This was optional and NIST put no constraints on the content beyond a 600 word limit, and a statement that anything labelled as confidential or proprietary would be omitted.

The provider of SDK B2, Cogent Systems, elected not to submit any information

On August 17, 2009, NIST invited the IREX participants to submit a description their comments on an draft version of the IREX report. This was intended to allow participants to assist readers in the interpretation of a large and complicated testing effort. NIST indicated that any submitted text would appear verbatim (with typesetting) in the final version of the IREX report and that it would be attributed to the organization. Submission of content was optional and NIST put no constraints on the content beyond a word limit, and a statement that anything labelled as confidential or proprietary would be omitted.

The provider of SDK B2, Cogent Systems, submitted the following to NIST - we make no comment on this information.

When kind 16 instances are involved, the matching performance of Cogent's IREX SDK is affected by a data decoding error. This is discussed in the following comments.

1. The error occurred during the process of decoding kind 48 format data. The decoding was not part of the feature extraction algorithms or matching algorithms.

During IREX testing, iris matching was performed on proprietary templates which were generated from iris data in different formats. In the case when iris data was provided in kind 16 format (unsegmented polar), the NIST test harness converted kind 16 data to kind 48 data (reconstructed rectilinear image). Cogent's template generator took the kind 48 data as input, decoded it get raw image, and performed feature extraction on raw image to produce the proprietary template that would be used for matching.

2. Matching accuracy was affected when one or both templates were generated from kind 16 / kind 48 data.

This includes the following:

- Results reported in Figure 26 (page 70)
 - Results listed under K16 in Table 9 (page 64)
 - Results listed under K16 in Table 10 (page 65)
 - Results listed under K16 in Table 11 (page 66)
 - Results listed under K16 in Table 14 (page 79)
3. Results on kind 1 (K1), kind 3 (K3), and kind 7 (K7) data were not affected.
 4. The kind 16 records generated by Cogent's SDK were not affected.

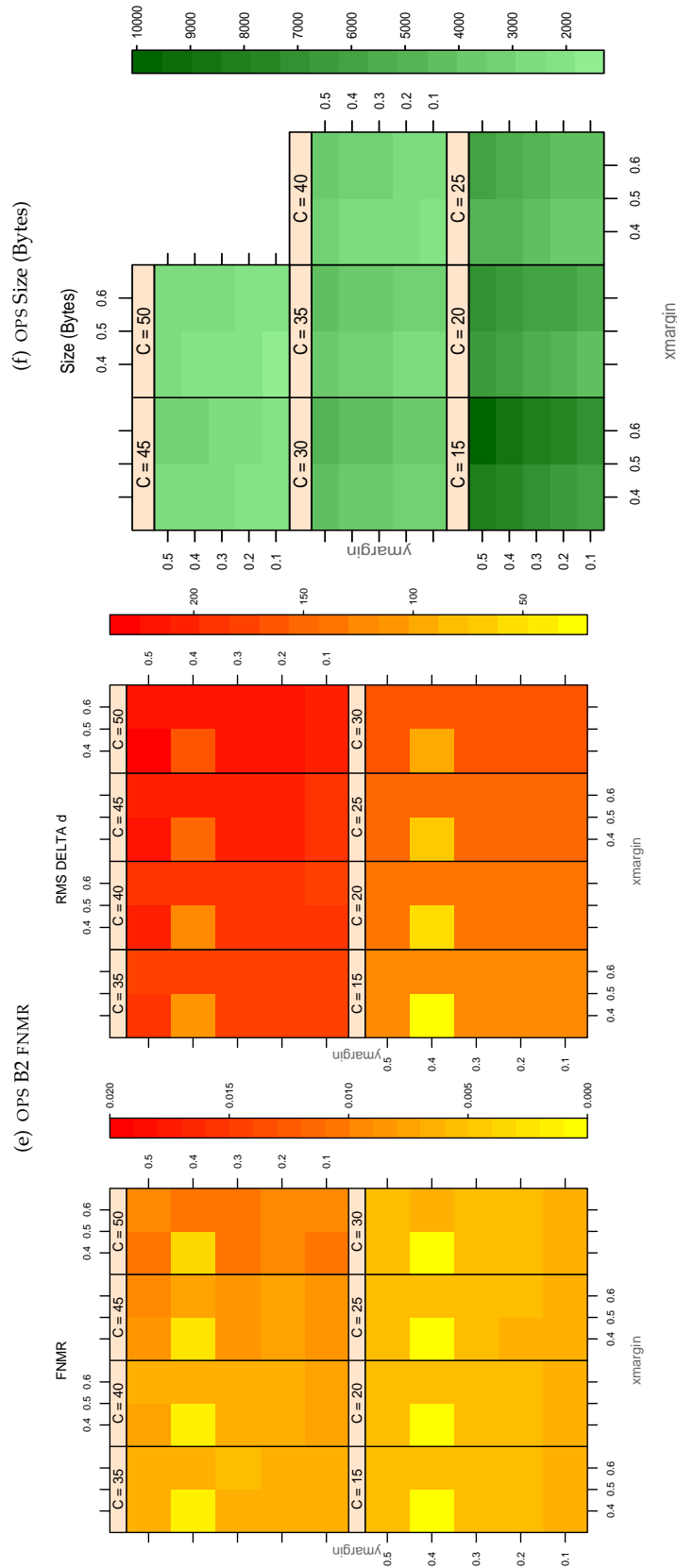


Table 39: For the IREX partition of the OPS database the plots at left show the dependence of cFNMR on the vertical and horizontal iris cropping margins for various compression ratios. This applies only for KIND 3 records. The margins are in units of iris radius. The use of conditional FNMR means that the plots exclude comparisons that were falsely rejected even before any compression was applied. On the **right side** is the rms difference between the crop+compress and the uncompressed comparison scores for each image pair. All computations are driven by the bounding box coordinates reported by the II SDK. The number of bits per pixel is $8/C$, where C is the compression ratio. The iris radius varies and because the cropping margins are fixed multiples of the radius the image size varies. The compressed size, in bytes, is the width times height divided by C . Values of cFNMR greater than 0.02 are shown as 0.02.

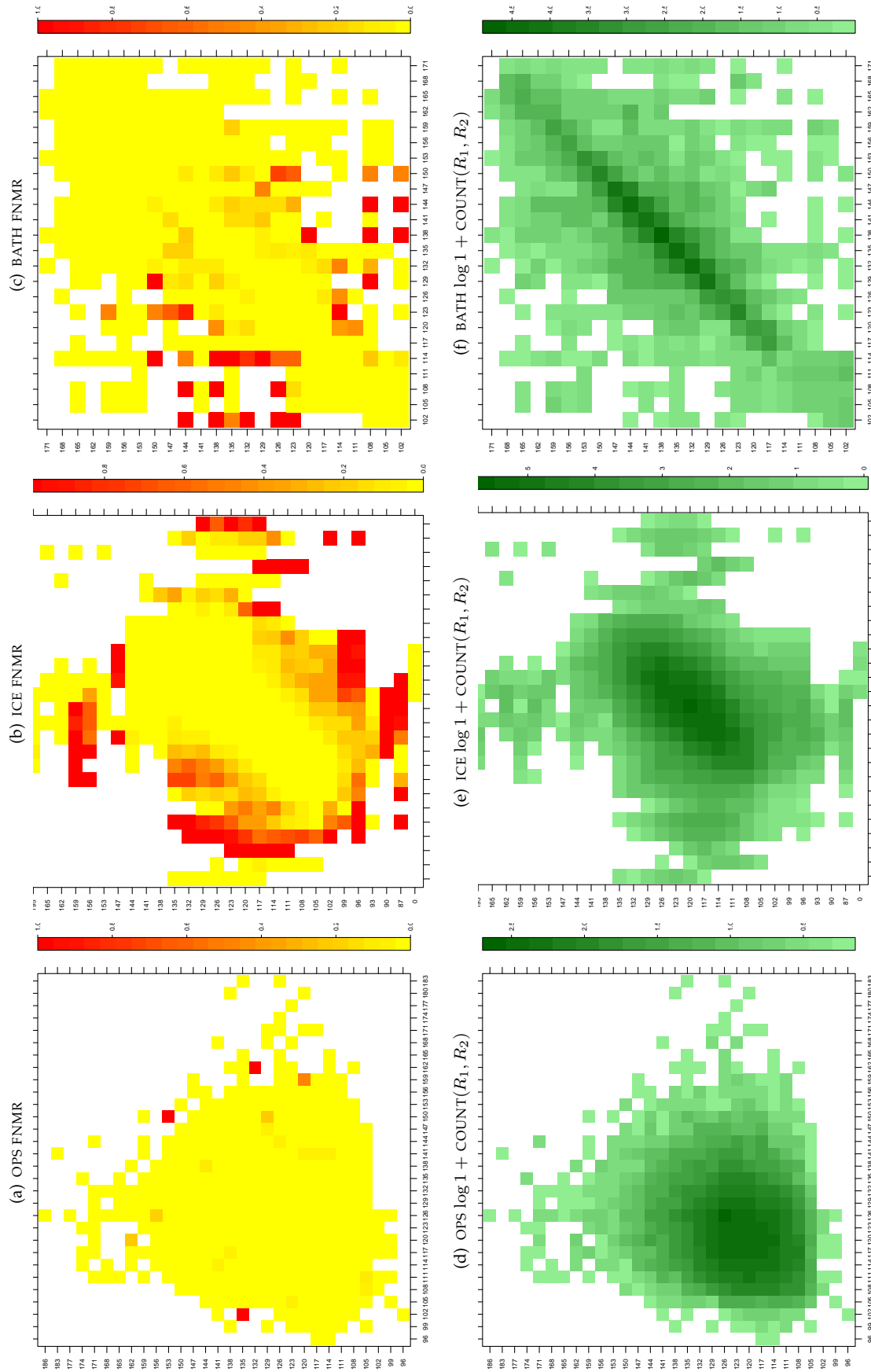


Table 40: For the three IREX databases: In the **top** row the color in each cell represents the occurrence of genuine comparisons with the given pair of radii. The *y*-axis represents enrollment samples with verification samples on the *x*-axis; In the **bottom** row the color scale plots $\log 1 + \text{COUNT}(R_1, R_2)$. The radii are quantized into three-pixel bins. The radii for DOD are on the range $96 \leq r \leq 186$ pixels. The radii for ICE are on the range $87 \leq r \leq 165$ pixels. The radii for BATH are on the range $100 \leq r \leq 170$ pixels.

A = SAGEM	B = COGENT	C = CROSSMATCH	D = CAMBRIDGE	E = L1	$x1$ = PRIMARY
F = RETICA	G = LG	H = HONEYWELL	I = IRITECH	J = NEUROTECHNOLOGY	$x2$ = SECONDARY
KIND 1 = RAW 640x480		KIND 3 = CROP		KIND 7 = CROP+MASK	KIND 16 = CONCENTRIC POLAR

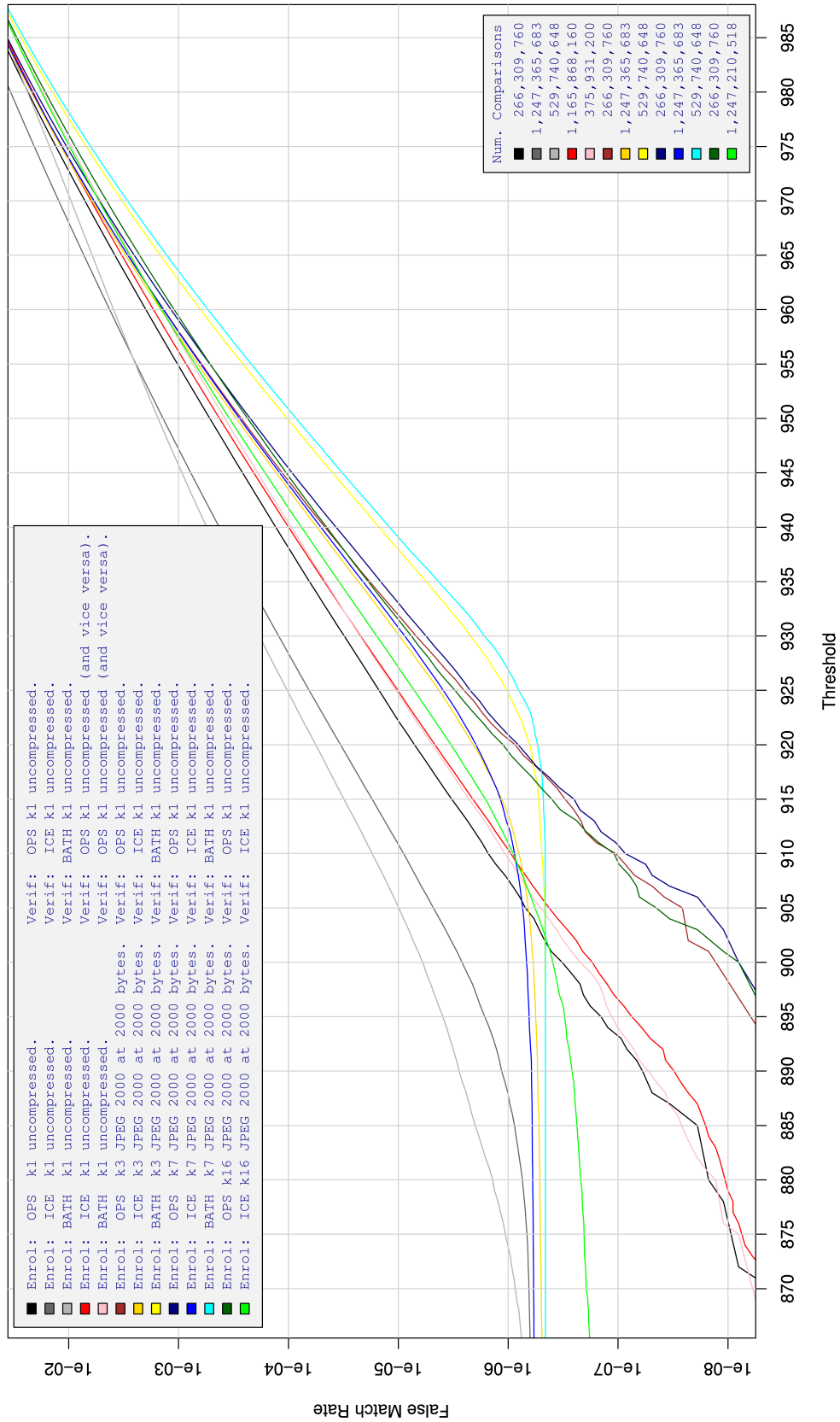


Table 41: For implementation B2, the dependency of FMR on threshold. for various combinations of enrollment and verification dataset, format, and compression.

A = SAGEM	B = COGENT	C = CROSSMATCH	D = CAMBRIDGE	E = L1	x1 = PRIMARY
F = RETICA	G = LG	H = HONEYWELL	I = IRITECH	J = NEUROTECHNOLOGY	x2 = SECONDARY
KIND 1 = RAW 640x480		KIND 3 = CROP		KIND 7 = CROP+MASK	KIND 16 = CONCENTRIC POLAR

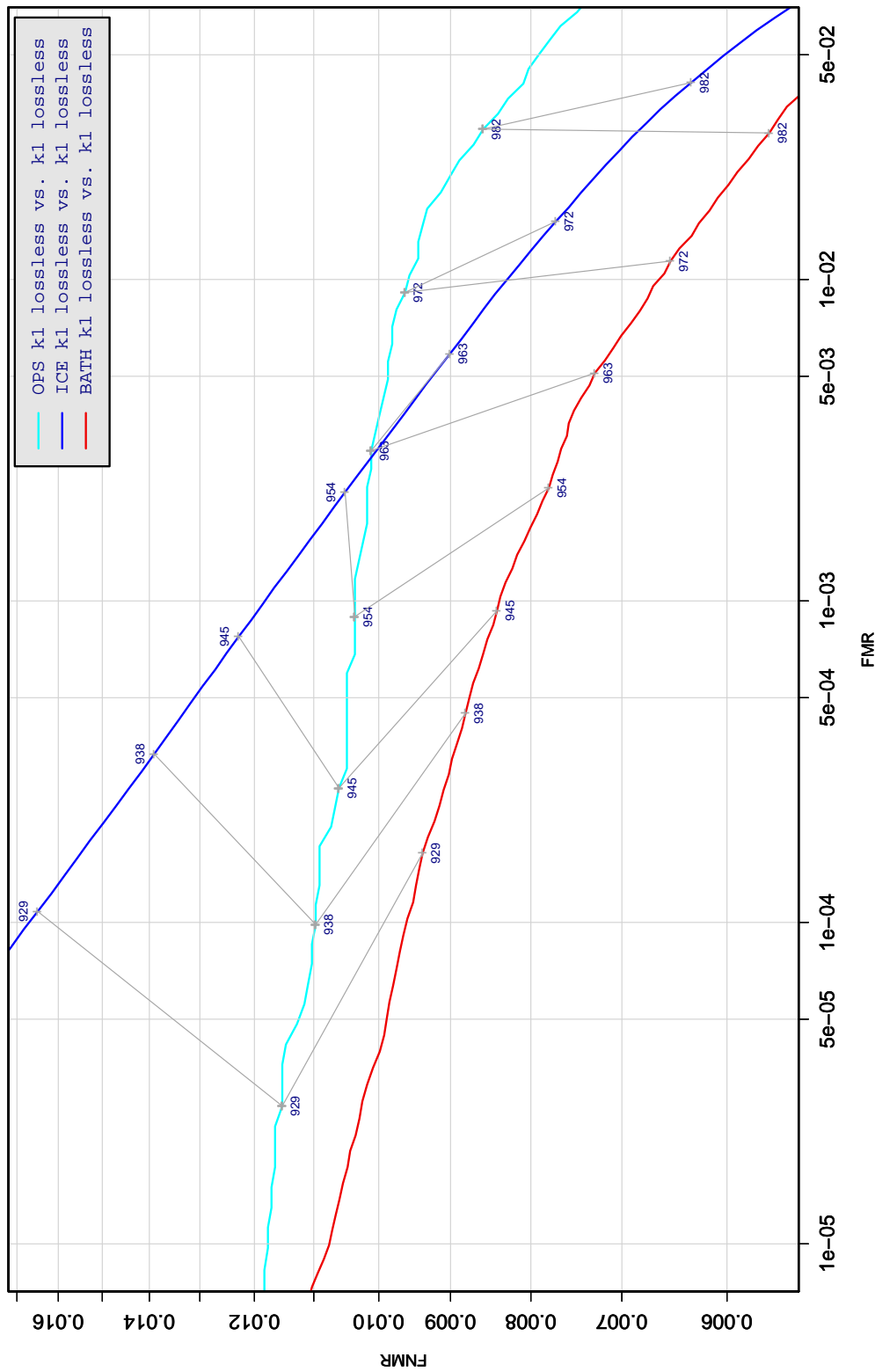


Table 42: DET curve for implementation B2 on three IREX databases. All comparisons are with uncompressed KIND 1 vs. KIND 1 images. The lines join points corresponding to the a fixed threshold. Non-vertical links indicate a change in FMR when the database changes. All results apply to native operation. Failures to produce a template i.e. FTE are ignored because the plots are intended to show *matching* effects, specifically to compare DET slopes and to show the effect of fixing a threshold.

A = SAGEM	B = COGENT	C = CROSSMATCH	D = CAMBRIDGE	E = L1	x1 = PRIMARY
F = RETICA	G = LG	H = HONEYWELL	I = IRITECH	J = NEUROTECHNOLOGY	x2 = SECONDARY
KIND 1 = RAW 640x480		KIND 3 = CROP	KIND 7 = CROP+MASK	KIND 16 = CONCENTRIC POLAR	

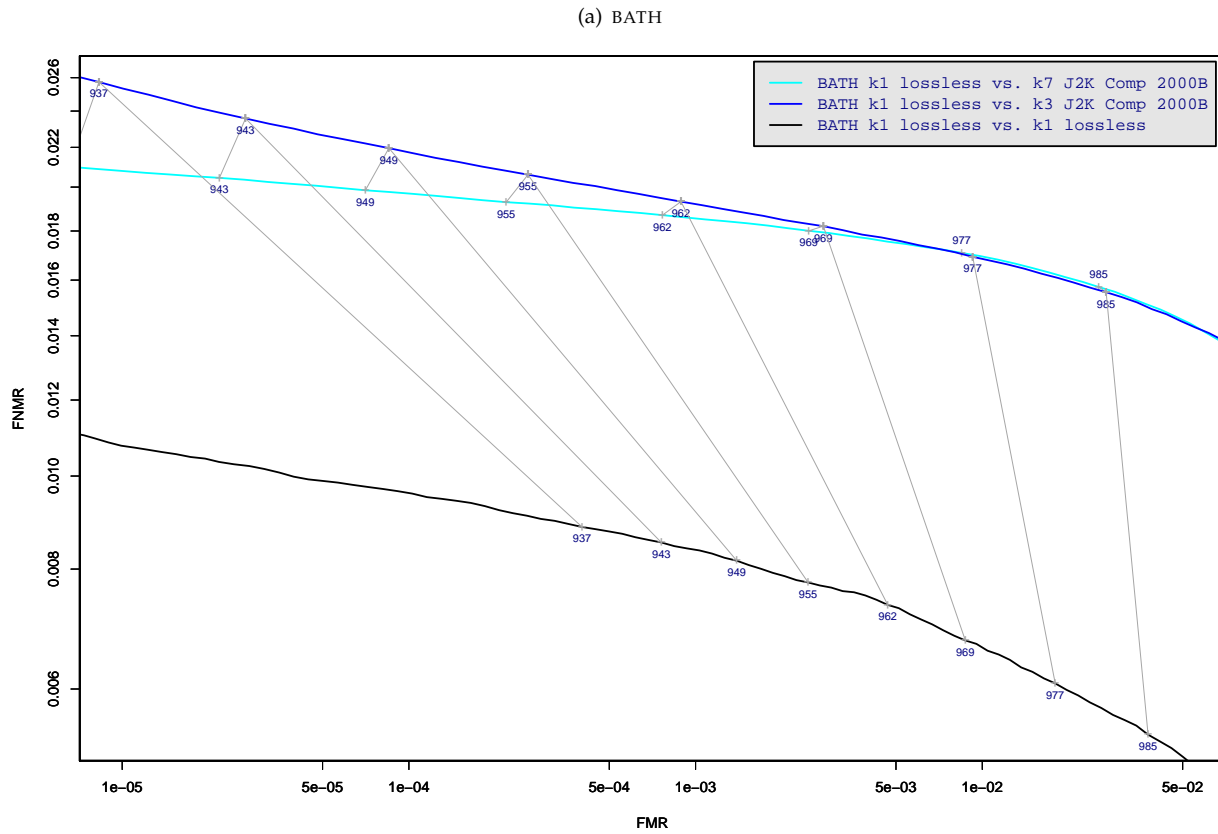


Table 43: DET curve for implementation B2 on the BATH database for the various supported KINDS . The DET characteristics are linked by lines joining points of equal threshold. Non-vertical links indicate a change in false acceptance when the data KIND changes. All results apply to native operation, and the effects of FTE are included.

A = SAGEM	B = COGENT	C = CROSSMATCH	D = CAMBRIDGE	E = L1	x1 = PRIMARY
F = RETICA	G = LG	H = HONEYWELL	I = IRITECH	J = NEUROTECHNOLOGY	x2 = SECONDARY
KIND 1 = RAW 640x480		KIND 3 = CROP		KIND 7 = CROP+MASK	
KIND 16 = CONCENTRIC POLAR					

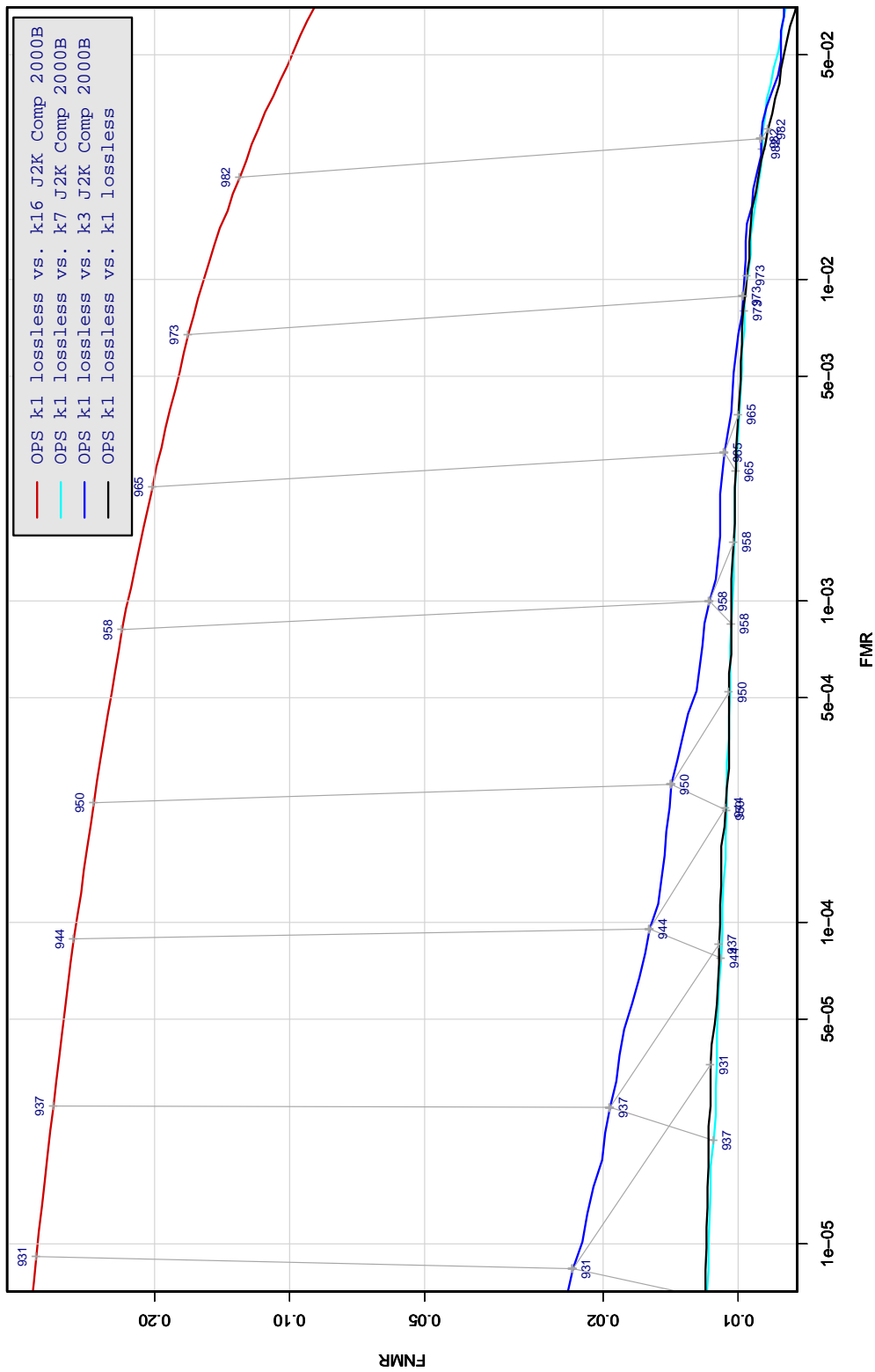


Table 44: DET curve for implementation B2 on the OPS database for the various supported KINDS . The DET characteristics are linked by lines joining points of equal threshold. Non-vertical links indicate a change in false acceptance when the data KIND changes. All results apply to native operation, and the effects of FTE are included.

A = SAGEM	B = COGENT	C = CROSSMATCH	D = CAMBRIDGE	E = L1	x1 = PRIMARY
F = RETICA	G = LG	H = HONEYWELL	I = IRITECH	J = NEUROTECHNOLOGY	x2 = SECONDARY
KIND 1 = RAW 640x480		KIND 3 = CROP		KIND 7 = CROP+MASK	KIND 16 = CONCENTRIC POLAR

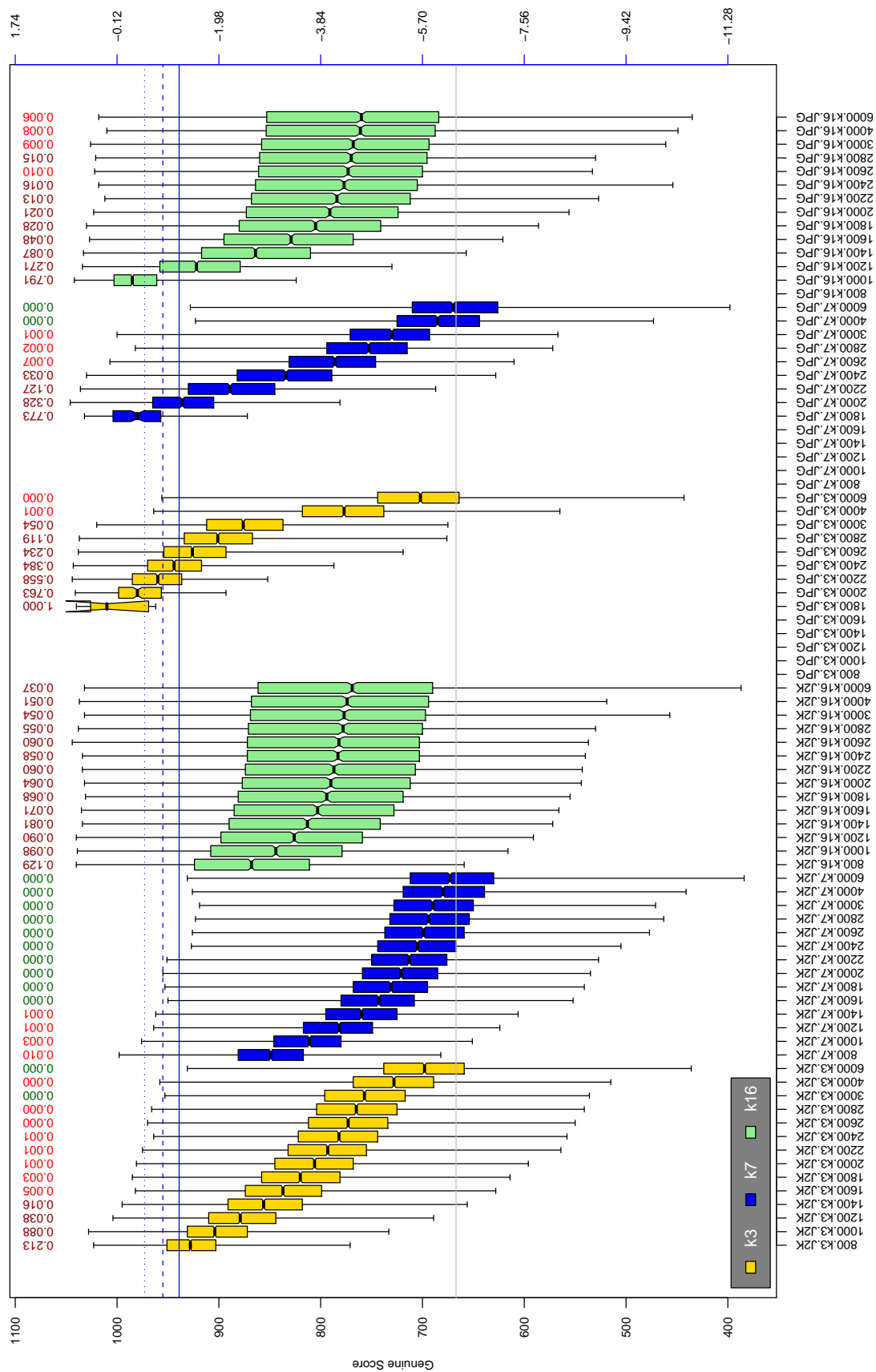


Table 45: The distribution of B2 native genuine comparison scores by size of the compressed image, KIND and the compression algorithm. The images are from the ops dataset. The right axis scale gives the corresponding value for $d' = (s - \mu_I) / \sqrt{0.5(\sigma_I^2 + \sigma_C^2)}$ for genuine score s . The boxplots only include comparison scores if the uncompressed version of the same image was matched below the FMR = 0.001 threshold. Above the boxplots are FNMR values at FMR = 10^{-3} . The three blue lines correspond, from the top, to FMR of $10^{-2}, -3, -4$. The lower grey line refers to the median score obtained from comparison of uncompressed KIND 3 images. Any comparison for which either template had not been generated is excluded. Note that the iris record size on the horizontal axis is not evenly spaced above 3000 bytes.

A = SAGEM	B = COGENT	C = CROSSMATCH	D = CAMBRIDGE	E = L1	$x1$ = PRIMARY
F = RETICA	G = LG	H = HONEYWELL	I = IRITECH	J = NEUROTECHNOLOGY	$x2$ = SECONDARY
KIND 1 = RAW 640x480		KIND 3 = CROP	KIND 7 = CROP+MASK	KIND 16 = CONCENTRIC POLAR	

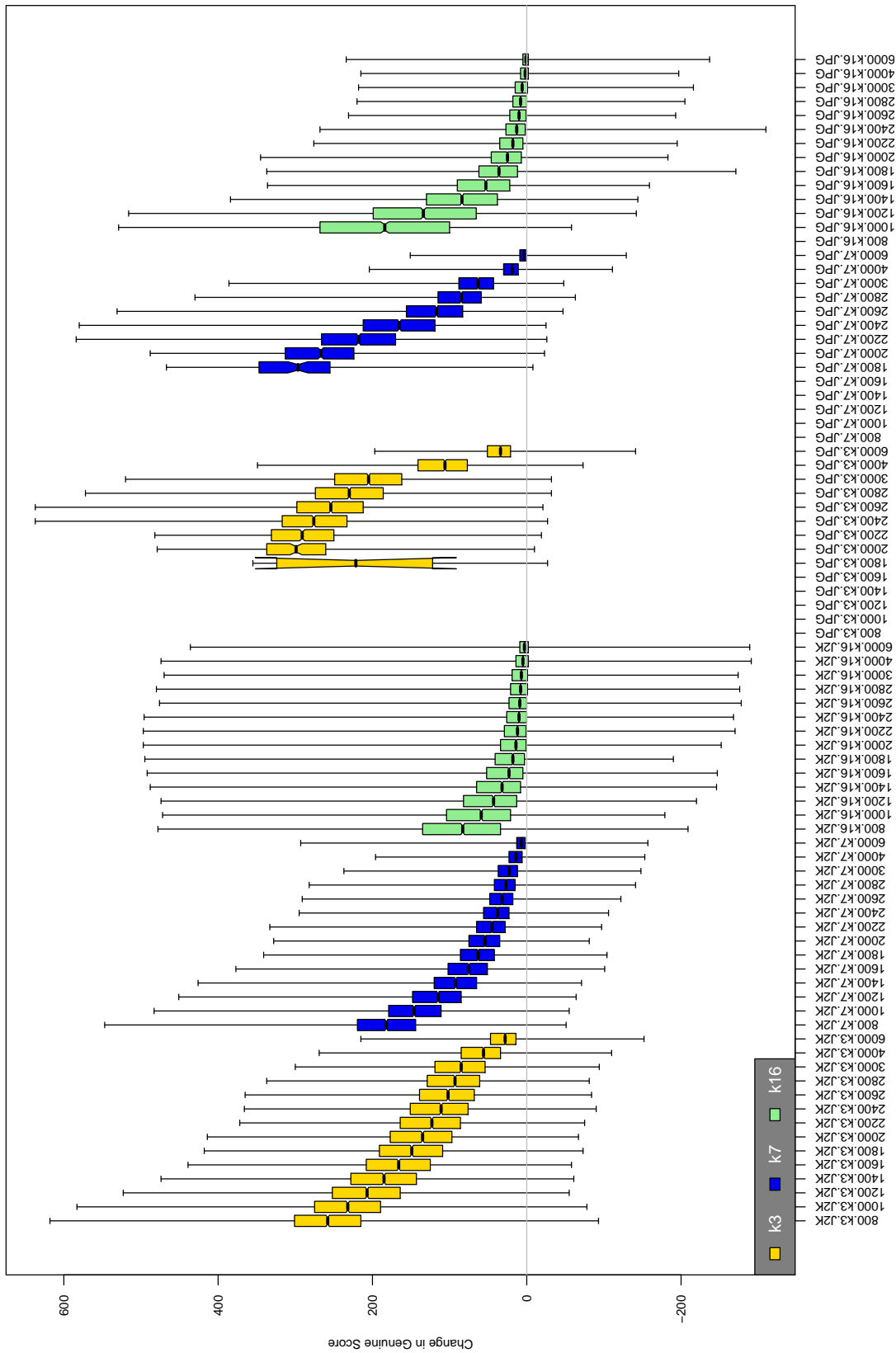


Table 46: The distribution of the *increase* in B2 native genuine comparison scores between the uncompressed “parent” and the compressed image, arranged by size, KIND and the compression algorithm. The images are from the OPS dataset. Any comparison involving a failed template is excluded. Note that the iris record size on the horizontal axis is not evenly spaced above 3000 bytes.

A = SAGEM	B = COGENT	C = CROSSMATCH	D = CAMBRIDGE	E = L1	x1 = PRIMARY
F = RETICA	G = LG	H = HONEYWELL	I = IRITECH	J = NEUROTECHNOLOGY	x2 = SECONDARY
KIND 1 = RAW 640x480		KIND 3 = CROP	KIND 7 = CROP+MASK	KIND 16 = CONCENTRIC POLAR	

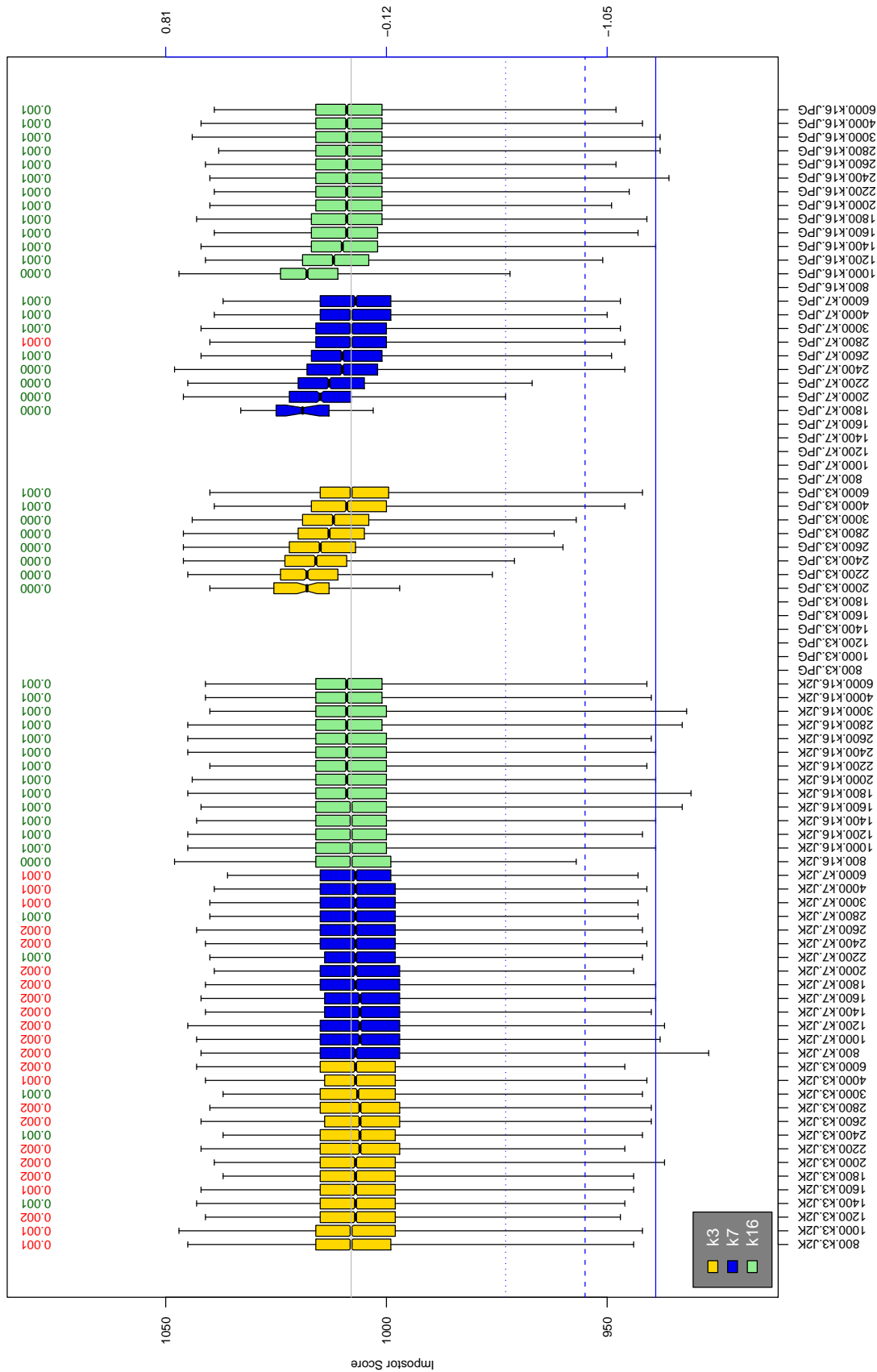


Table 47: The distribution of B2 native impostor comparison scores by size of the compressed image, KIND and the compression algorithm. The right axis scale gives the corresponding value for $d' = (s - \mu_1) / \sqrt{0.5(\sigma_1^2 + \sigma_2^2)}$ for impostor score s . The three blue lines correspond, from the top, to FMR of 10^{-2} , 10^{-3} , and 10^{-4} . The lower grey line refers to the median score obtained from comparison of uncompressed KIND 3 images. Any comparison involving a failed template is excluded. Above the boxplots are FMR values at the threshold that gives FMR = 10^{-3} on uncompressed images. These figures are computed from only 4000 comparisons so the FMR values and the tails of the impostor distribution are poorly characterized. Note that the iris record size on the horizontal axis is not evenly spaced above 3000 bytes.

A = SAGEM	B = COGENT	C = CROSSMATCH	D = CAMBRIDGE	E = L1	$x1$ = PRIMARY
F = RETICA	G = LG	H = HONEYWELL	I = IRITECH	J = NEUROTECHNOLOGY	$x2$ = SECONDARY
KIND 1 = RAW 640x480		KIND 3 = CROP		KIND 7 = CROP+MASK	KIND 16 = CONCENTRIC POLAR

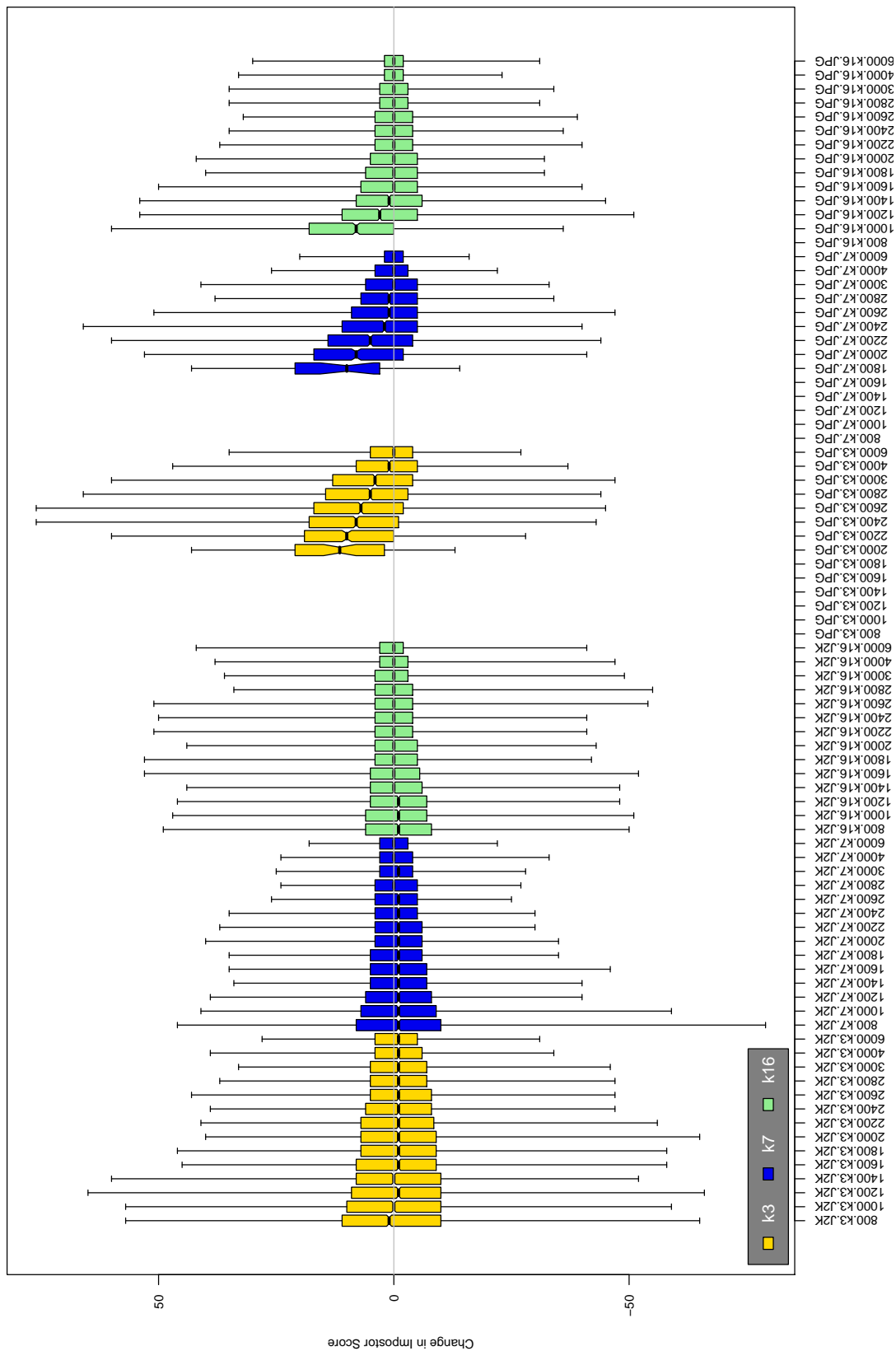


Table 48: The distribution of the increase in B2 native impostor comparison scores between the uncompressed “parent” and the compressed image, arranged by size, KIND and the compression algorithm. The images are from the OPS dataset. Any comparison involving a failed template is excluded. Note that the iris record size on the horizontal axis is not evenly spaced above 3000 bytes.

A = SAGEM	B = COGENT	C = CROSSMATCH	D = CAMBRIDGE	E = L1	x1 = PRIMARY
F = RETICA	G = LG	H = HONEYWELL	I = IRITECH	J = NEUROTECHNOLOGY	x2 = SECONDARY
KIND 1 = RAW 640x480		KIND 3 = CROP	KIND 7 = CROP+MASK	KIND 16 = CONCENTRIC POLAR	

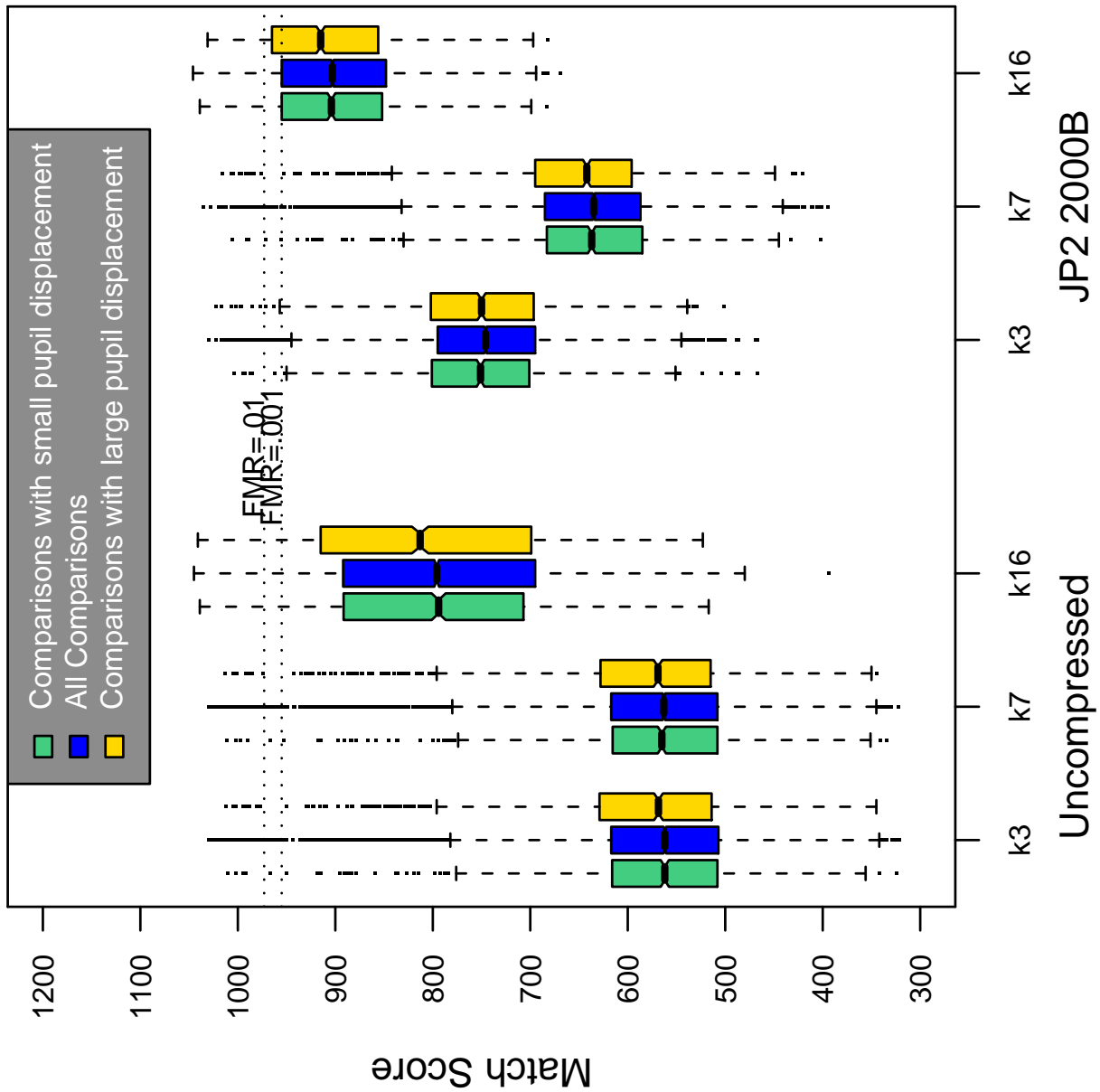


Table 49: Effect of pupil displacement on the genuine score distribution for B2

A = SAGEM	B = COGENT	C = CROSSMATCH	D = CAMBRIDGE	E = L1	x1 = PRIMARY
F = RETICA	G = LG	H = HONEYWELL	I = IRITECH	J = NEUROTECHNOLOGY	x2 = SECONDARY
KIND 1 = RAW 640x480		KIND 3 = CROP	KIND 7 = CROP+MASK	KIND 16 = CONCENTRIC POLAR	

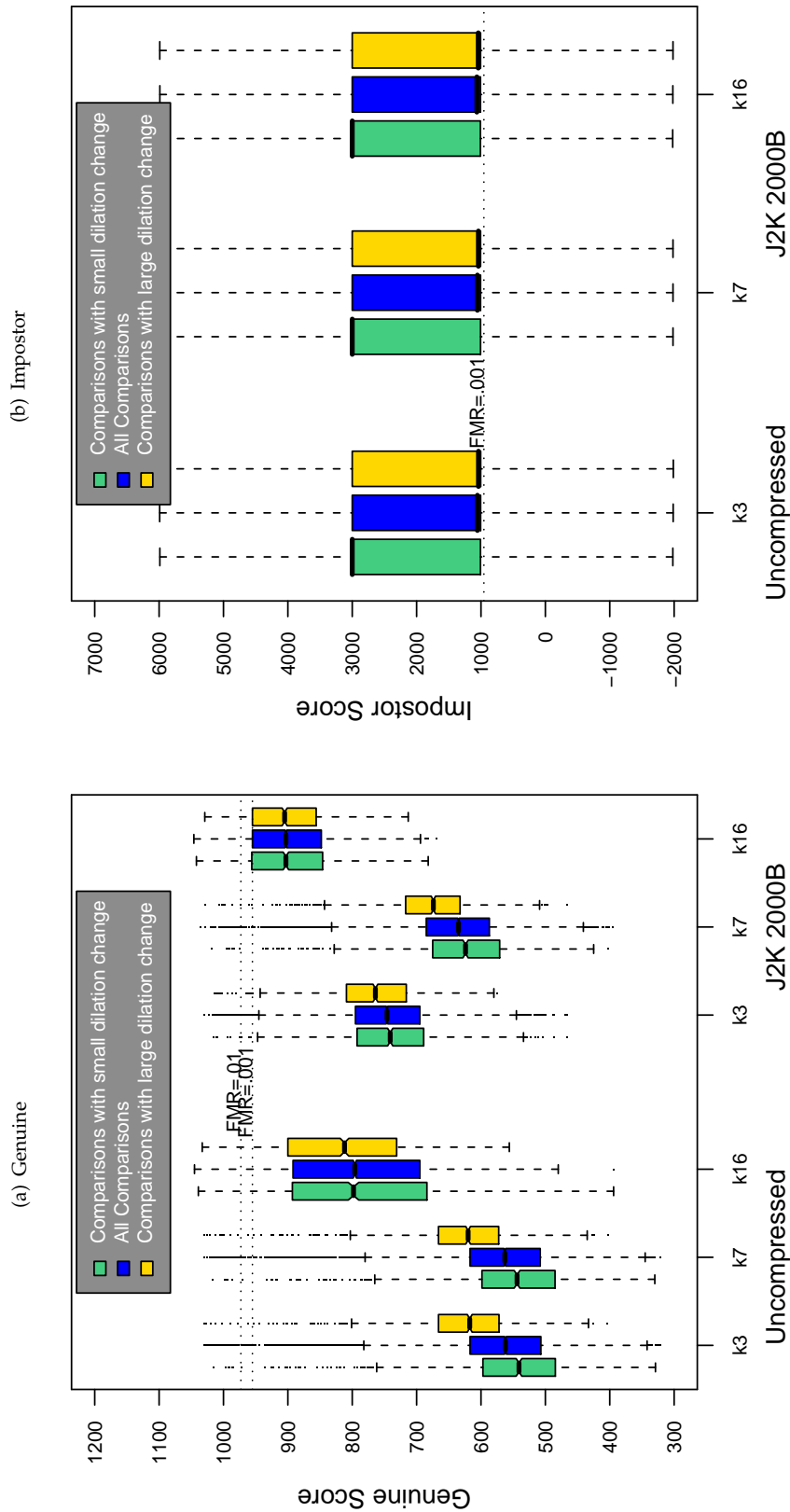


Table 50: The effect of dilation change on the two scores distributions for SDK B2.

A = SAGEM	B = COGENT	C = CROSSMATCH	D = CAMBRIDGE	E = L1	$x1$ = PRIMARY
F = RETICA	G = LG	H = HONEYWELL	I = IRITECH	J = NEUROTECHNOLOGY	$x2$ = SECONDARY
KIND 1 = RAW 640x480		KIND 3 = CROP	KIND 7 = CROP+MASK	KIND 16 = CONCENTRIC POLAR	

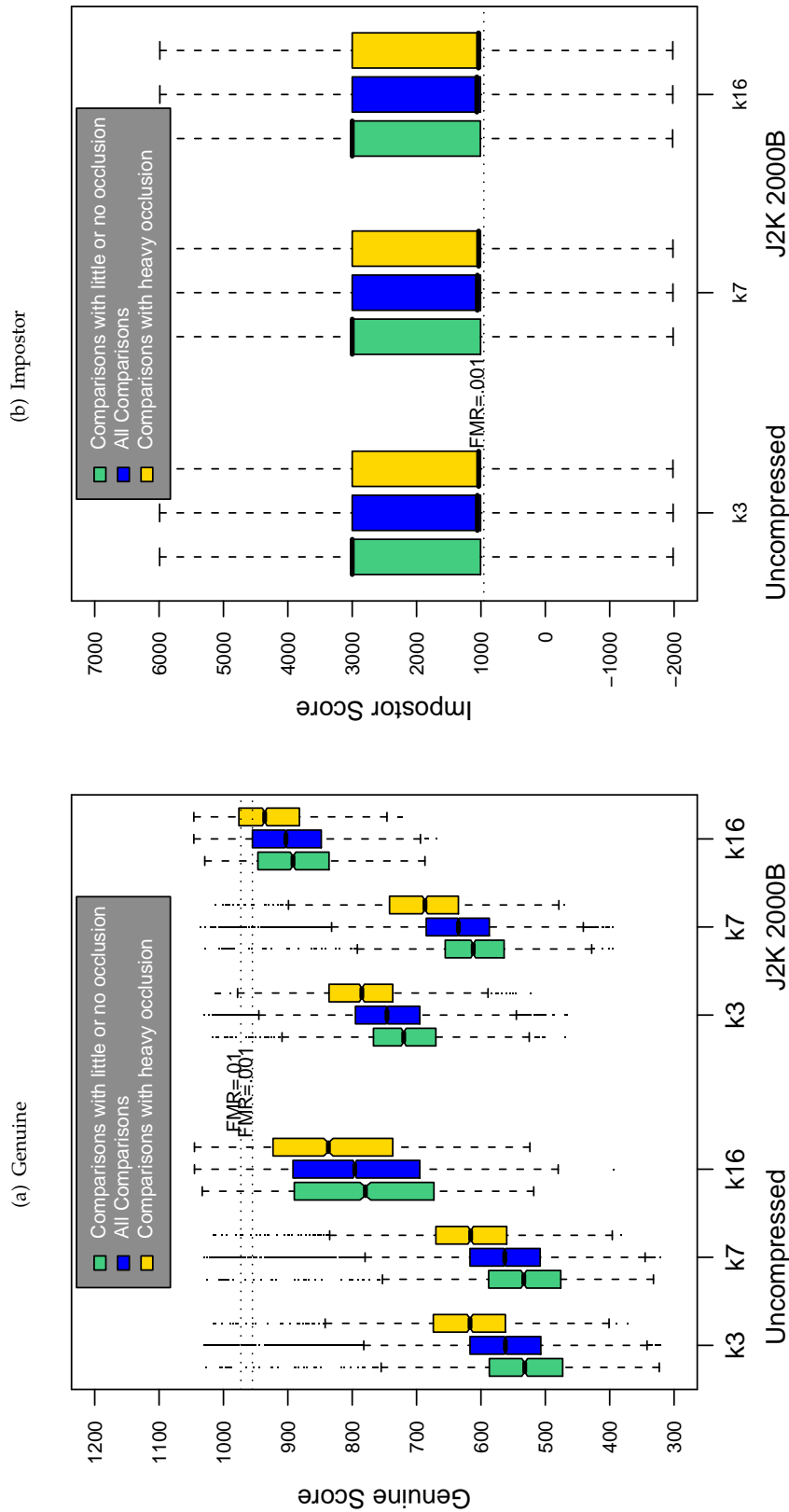
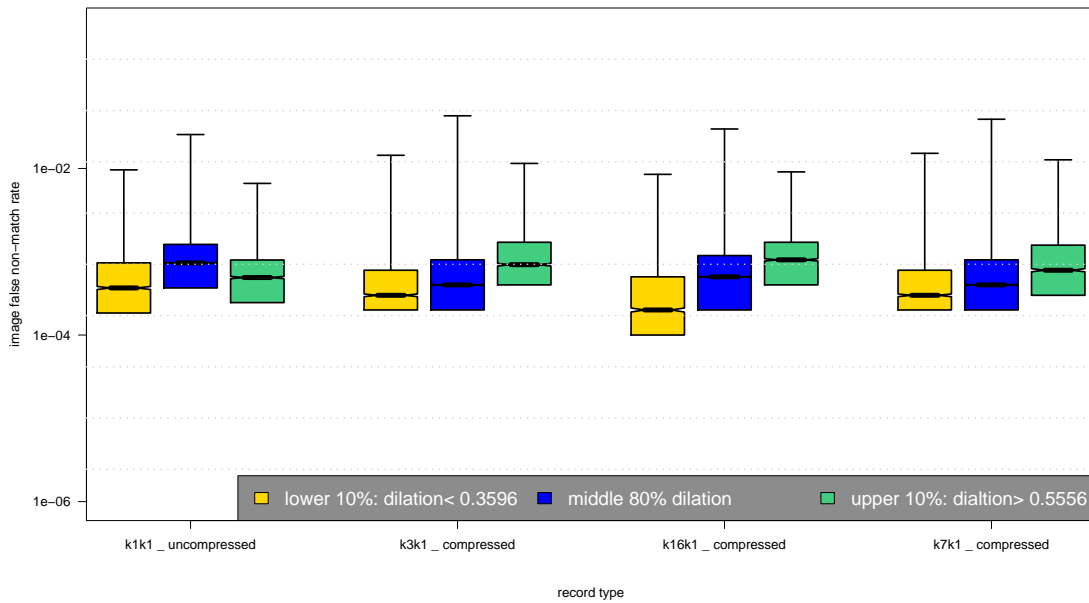
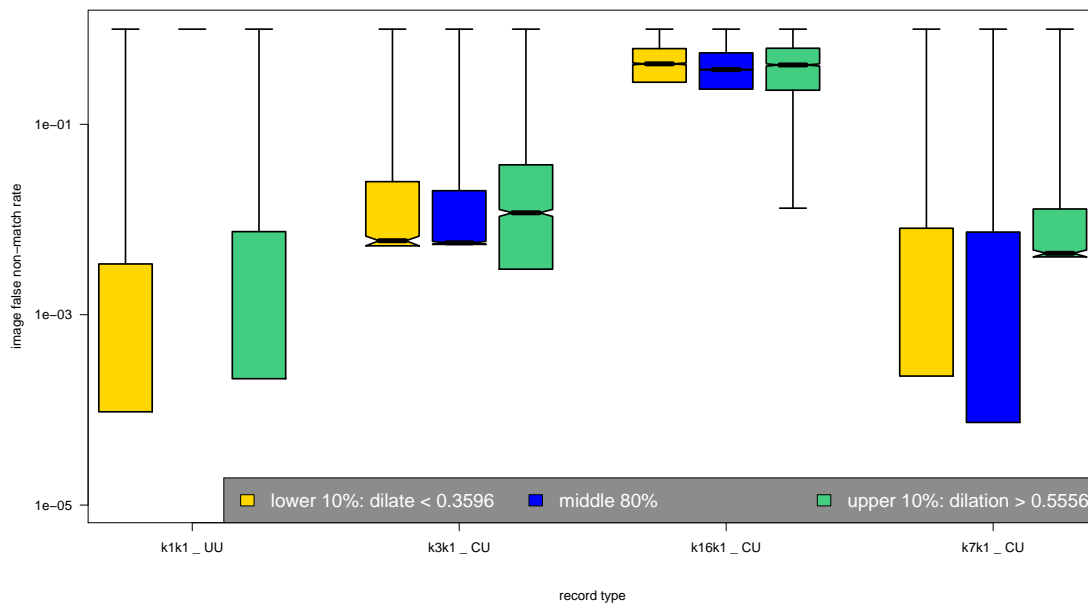


Table 51: The effect of eyelid occlusion on the two scores distributions for SDK B2.

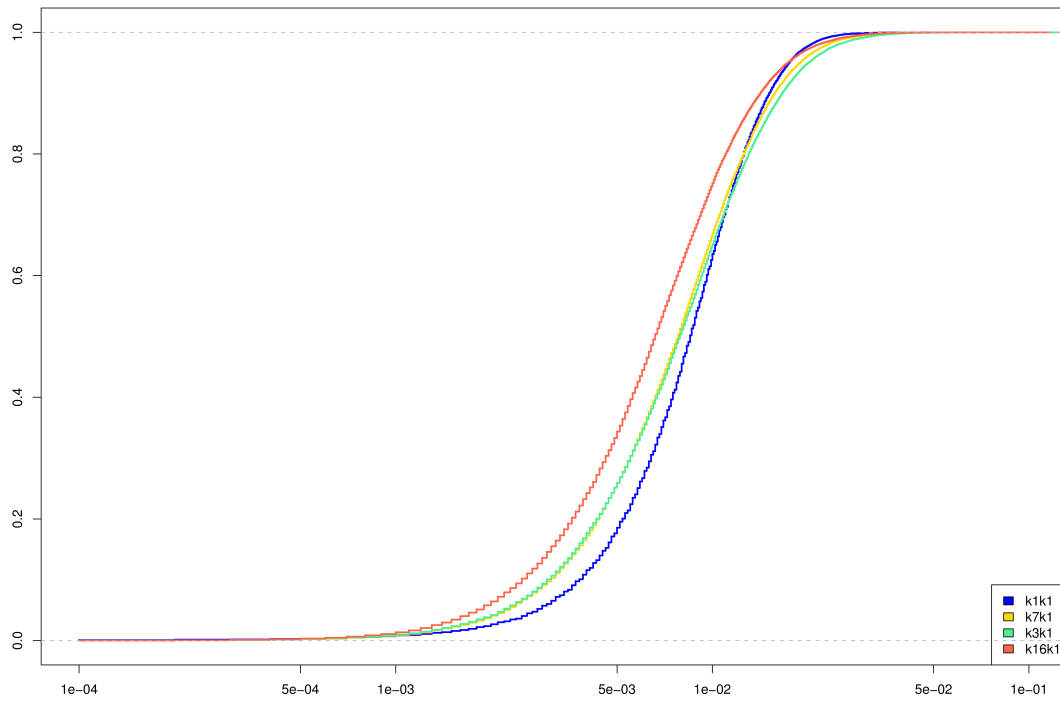
(a) iFMR using A1 dilation estimates



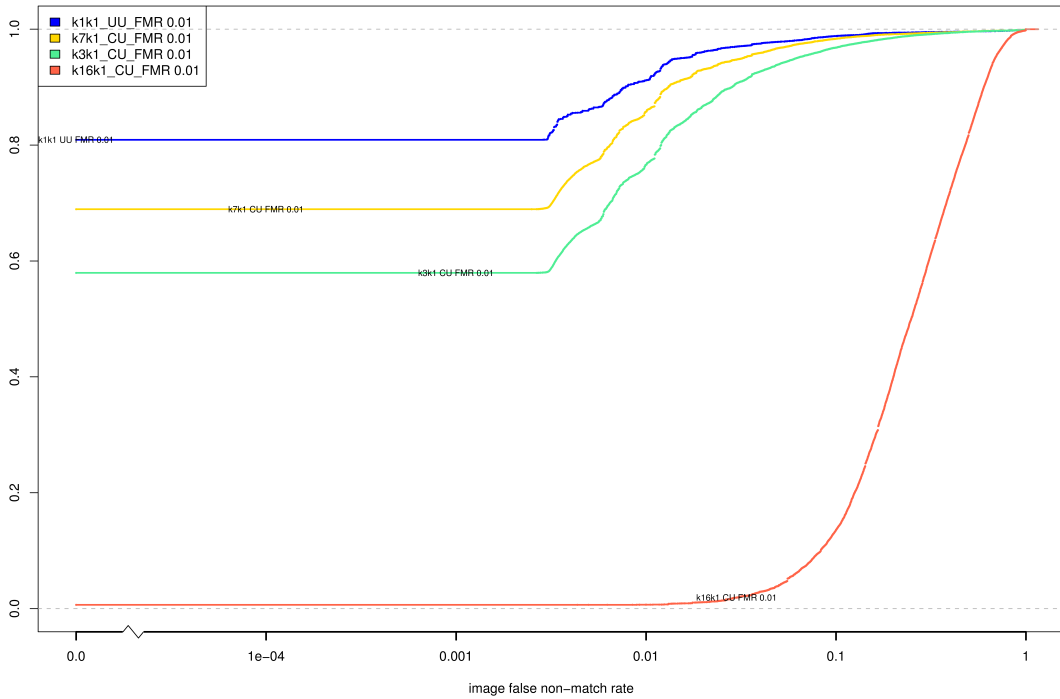
(b) iFNMR using A1 dilation estimates



(c) iFMR CDF



(d) iFNMR CDF



A = SAGEM	B = COGENT	C = CROSSMATCH	D = CAMBRIDGE	E = L1	x1 = PRIMARY		
F = RETICA	G = LG	H = HONEYWELL	I = IRITECH	J = NEUROTECHNOLOGY	x2 = SECONDARY		
KIND 1 = RAW 640x480		KIND 3 = CROP		KIND 7 = CROP+MASK		KIND 16 = CONCENTRIC POLAR	

Compiled Results for Implementation C1

On June 25, 2009, NIST invited the IREX participants to submit a description of the SDKs submitted for the IREX effort. The intent was to allow providers to describe and contrast the feature sets, optimization, operational suitability and availability of the primary and secondary SDKs. NIST indicated that any submitted text would appear verbatim (with typesetting) in draft and final versions of the IREX report and that it would be attributed to the organization. This was optional and NIST put no constraints on the content beyond a 600 word limit, and a statement that anything labelled as confidential or proprietary would be omitted.

The provider of SDK C1, Crossmatch Technologies, submitted the following to NIST - we are unable to validate this information.

Cross Match specializes in the design, development and manufacture of high quality finger and iris imaging devices, platforms and solutions.

Our iris algorithms are optimized to perform extraction and matching using images from our mobile and handheld client devices. These devices offer speed, reduced memory (template size) requirements, and limited on board data base size, usually less than 100,000 people. Based on our image quality and optimized client performance objectives we are confident our algorithm compares favorably with other similar solutions. The algorithm has not been optimized to process poor images or perform matching against large databases at this time.

As a new entrant in the iris recognition field, the company has placed top priority on the performance of its integrated hardware and software solutions. Efforts will be made to enhance performance on images from other sources in accordance with market requirements.

On August 17, 2009, NIST invited the IREX participants to submit a description their comments on an draft version of the IREX report. This was intended to allow participants to assist readers in the interpretation of a large and complicated testing effort. NIST indicated that any submitted text would appear verbatim (with typesetting) in the final version of the IREX report and that it would be attributed to the organization. Submission of content was optional and NIST put no constraints on the content beyond a word limit, and a statement that anything labelled as confidential or proprietary would be omitted.

The provider of SDK C1, Crossmatch Technologies, elected not to submit any information

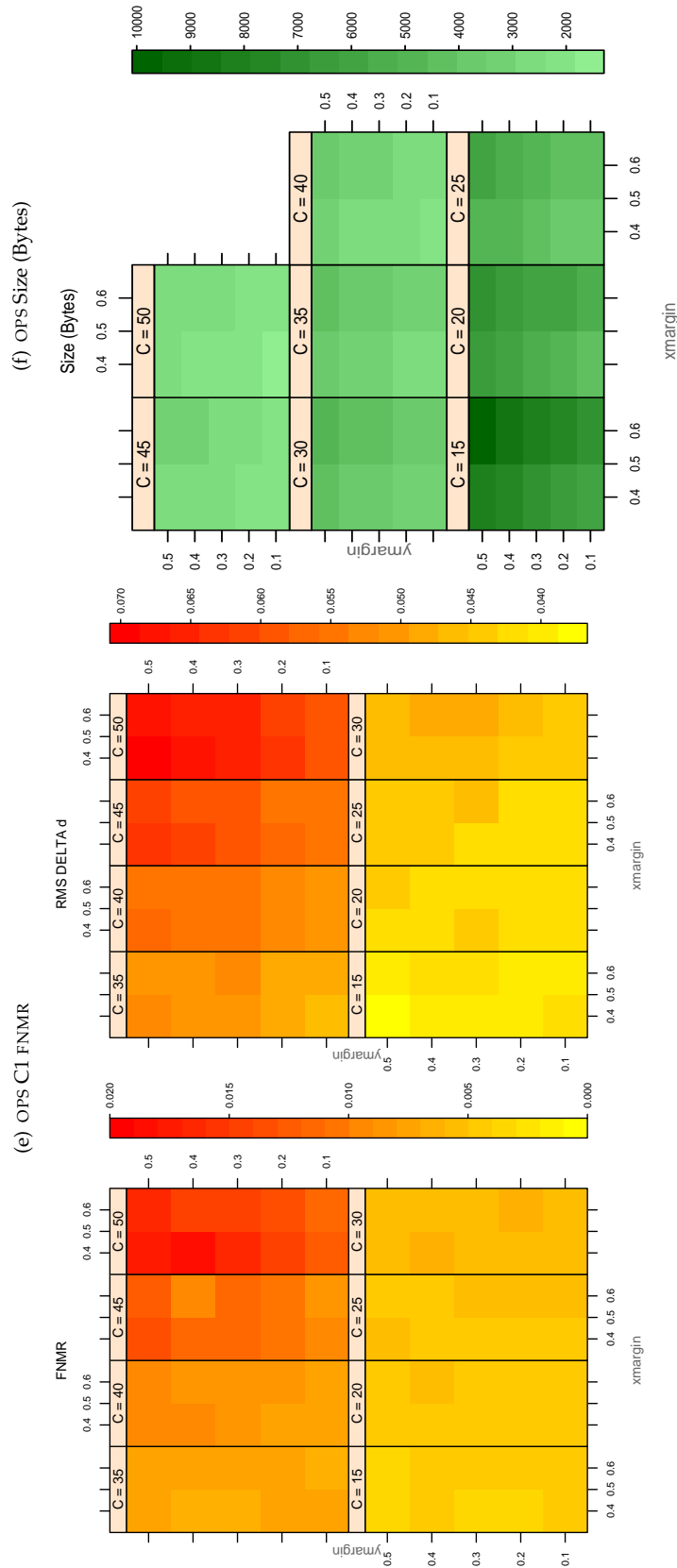


Table 52: For the IREX partition of the OPS database the plots at left show the dependence of cFNMNR on the vertical and horizontal iris cropping margins for various compression ratios. This applies only for KIND 3 records. The margins are in units of iris radius. The use of conditional FNMNR means that the plots exclude comparisons that were falsely rejected even before any compression was applied. On the **right side** is the rms difference between the crop+compress and the uncompressed comparison scores for each image pair. All computations are driven by the bounding box coordinates reported by the II SDK. The number of bits per pixel is $8/C$, where C is the compression ratio. The iris radius varies and because the cropping margins are fixed multiples of the radius the image size varies. The compressed size, in bytes, is the width times height divided by C . Values of cFNMNR greater than 0.02 are shown as 0.02.

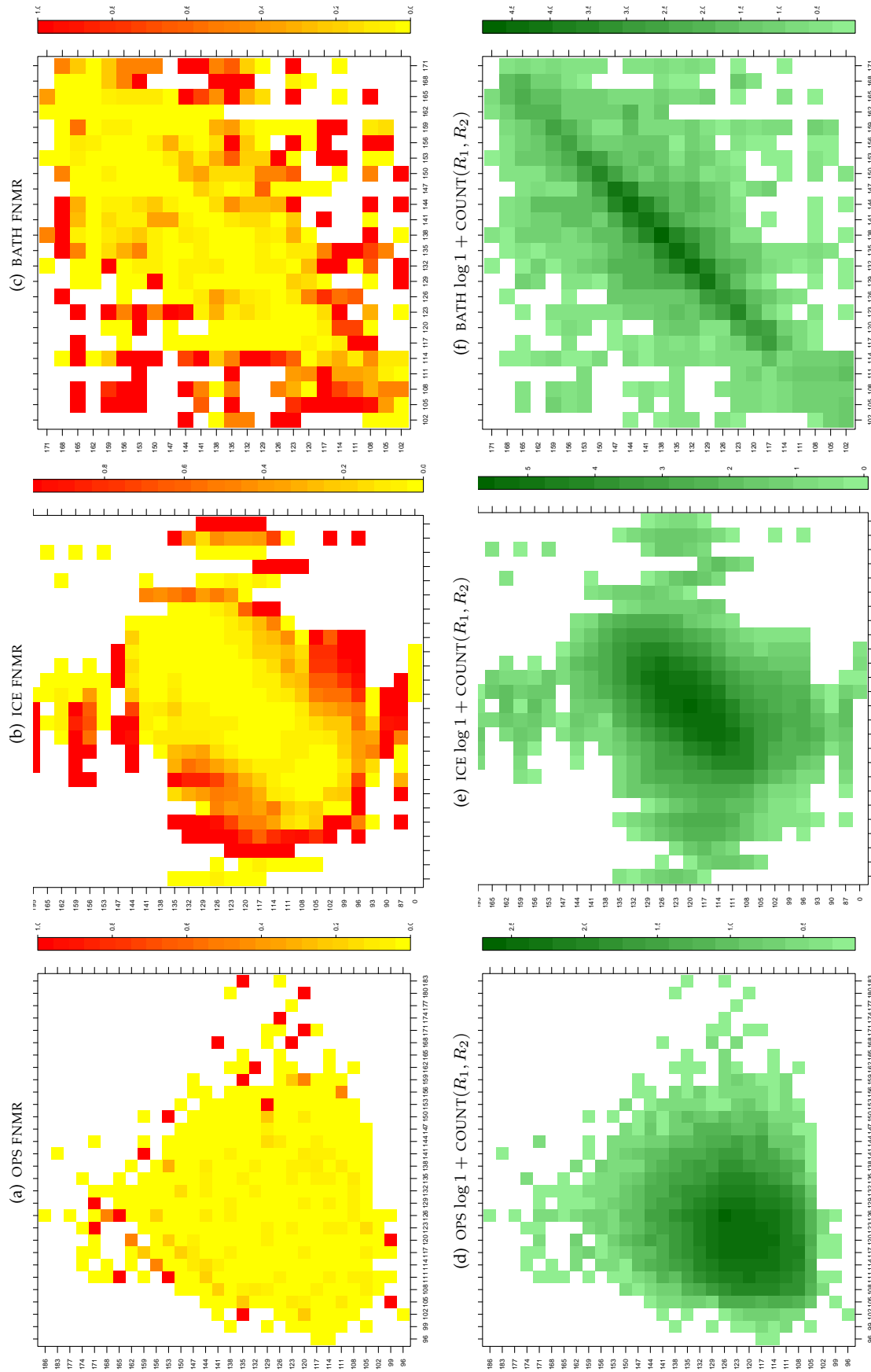


Table 53: For the three IREX databases: In the **top** row the color in each cell represents the occurrence of genuine comparisons with the given pair of radii. The *y*-axis represents enrollment samples with verification samples on the *x*-axis; In the **bottom** row the color scale plots $\log 1 + \text{COUNT}(R_1, R_2)$. The radii are quantized into three-pixel bins. The radii for DOD are on the range $96 \leq r \leq 186$ pixels. The radii for ICE are on the range $87 \leq r \leq 165$ pixels. The radii for BATH are on the range $100 \leq r \leq 170$ pixels.

A = SAGEM	B = COGENT	C = CROSSMATCH	D = CAMBRIDGE	E = L1	$x1$ = PRIMARY
F = RETICA	G = LG	H = HONEYWELL	I = IRITECH	J = NEUROTECHNOLOGY	$x2$ = SECONDARY
KIND 1 = RAW 640x480		KIND 3 = CROP		KIND 7 = CROP+MASK	
KIND 16 = CONCENTRIC POLAR					

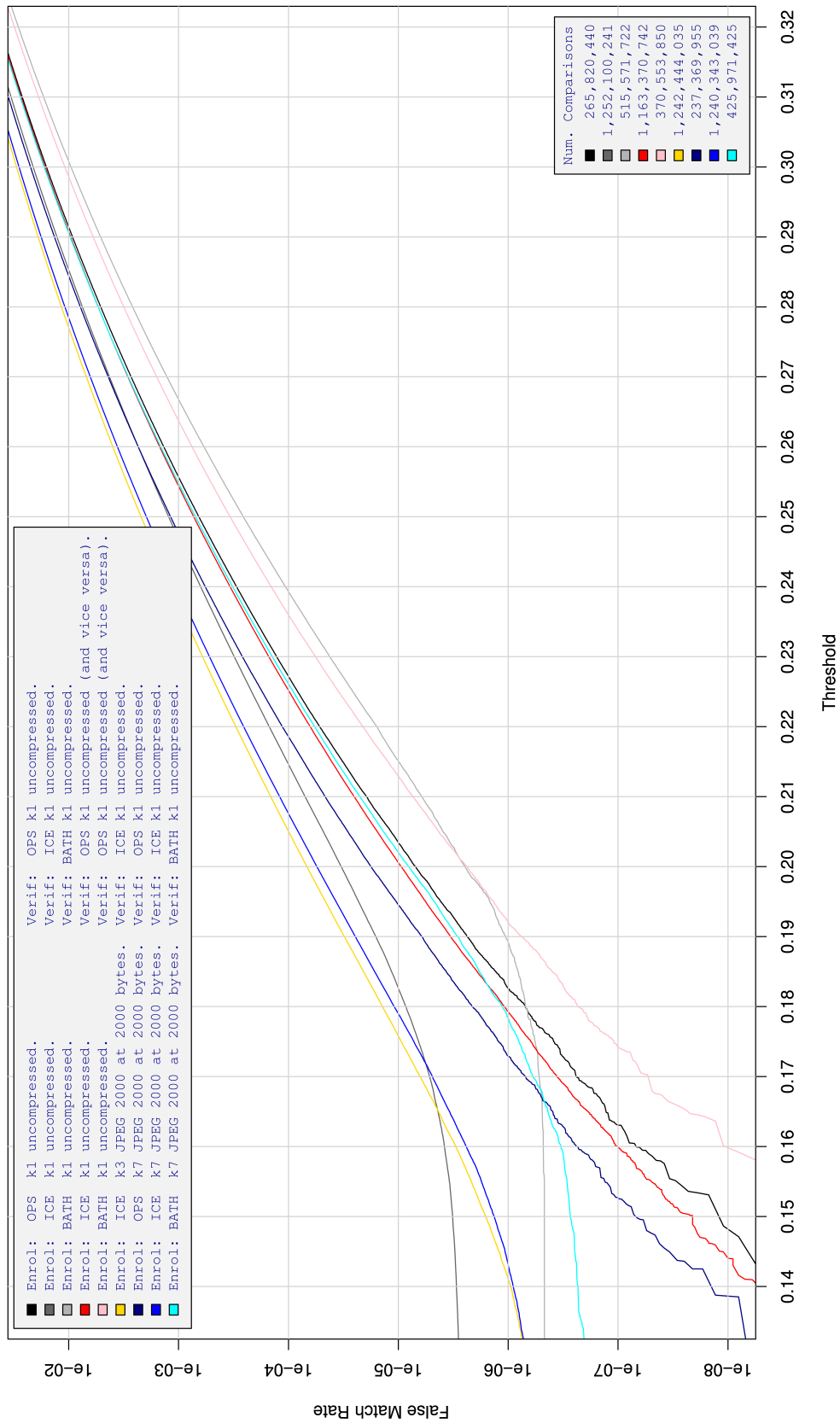


Table 54: For implementation C1, the dependency of FMR on threshold. for various combinations of enrollment and verification dataset, format, and compression.

A = SAGEM	B = COGENT	C = CROSSMATCH	D = CAMBRIDGE	E = L1	x1 = PRIMARY
F = RETICA	G = LG	H = HONEYWELL	I = IRITECH	J = NEUROTECHNOLOGY	x2 = SECONDARY
KIND 1 = RAW 640x480		KIND 3 = CROP	KIND 7 = CROP+MASK	KIND 16 = CONCENTRIC POLAR	

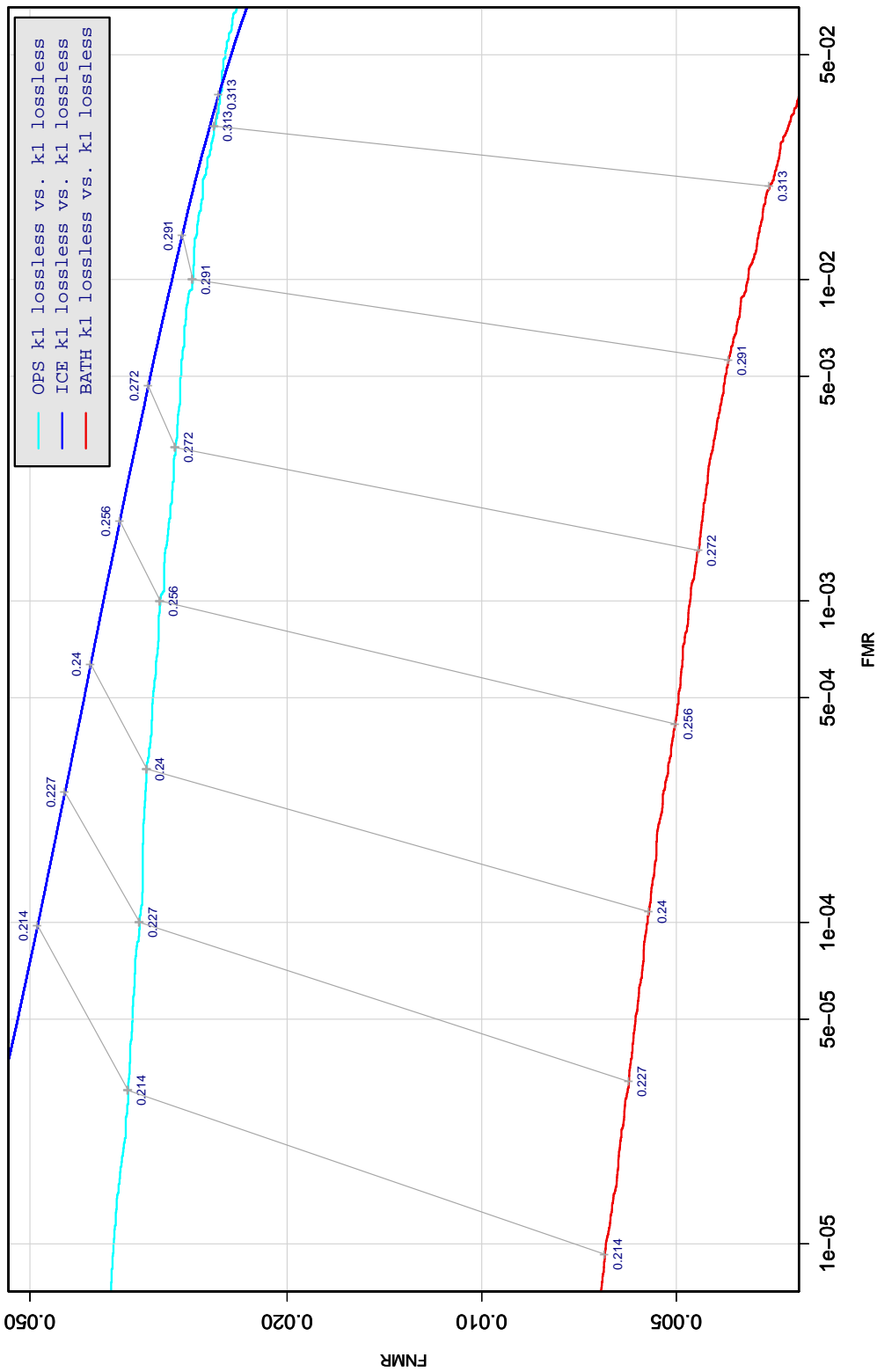


Table 55: DET curve for implementation C1 on three IREX databases. All comparisons are with uncompressed KIND 1 vs. KIND 1 images. The lines join points corresponding to the a fixed threshold. Non-vertical links indicate a change in FMR when the database changes. All results apply to native operation. Failures to produce a template i.e. FTE are ignored because the plots are intended to show *matching* effects, specifically to compare DET slopes and to show the effect of fixing a threshold.

A = SAGEM	B = COGENT	C = CROSSMATCH	D = CAMBRIDGE	E = L1	x1 = PRIMARY
F = RETICA	G = LG	H = HONEYWELL	I = IRITECH	J = NEUROTECHNOLOGY	x2 = SECONDARY
KIND 1 = RAW 640x480		KIND 3 = CROP	KIND 7 = CROP+MASK	KIND 16 = CONCENTRIC POLAR	

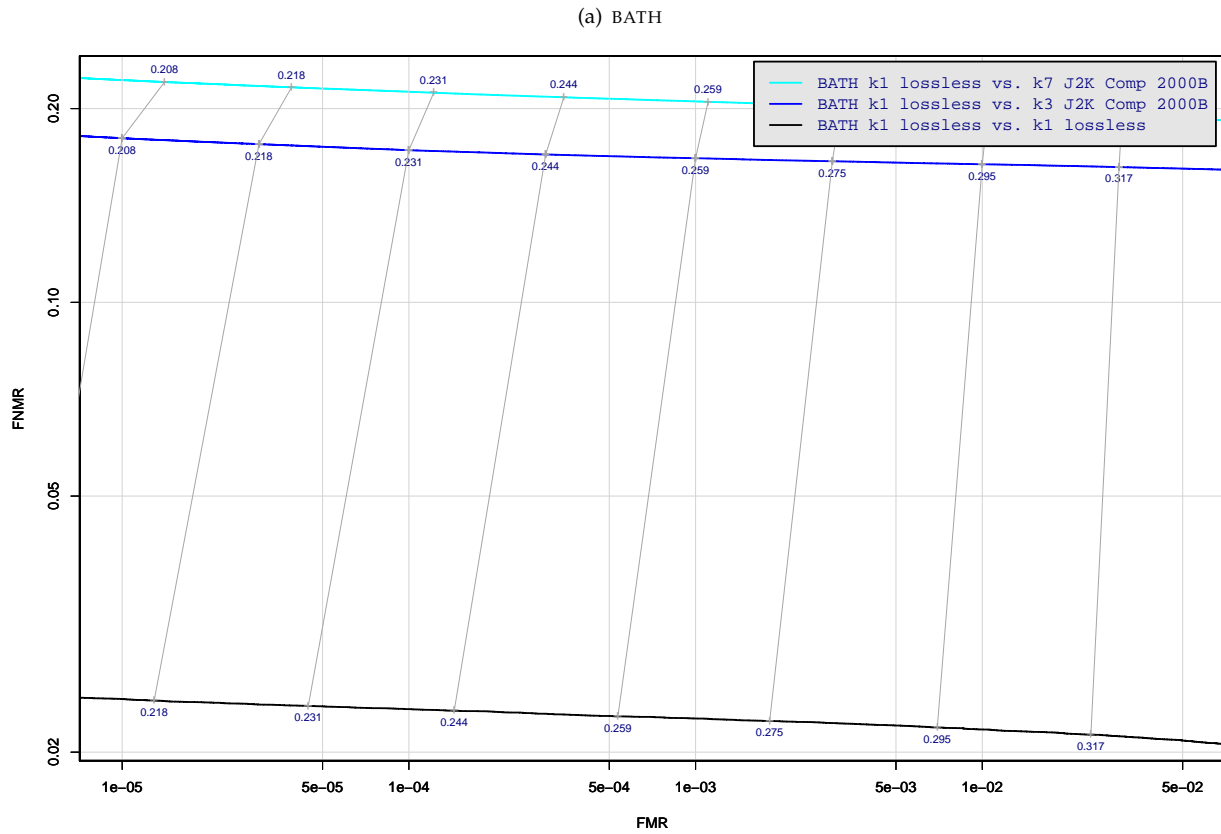


Table 56: DET curve for implementation C1 on the BATH database for the various supported KINDS . The DET characteristics are linked by lines joining points of equal threshold. Non-vertical links indicate a change in false acceptance when the data KIND changes. All results apply to native operation, and the effects of FTE are included.

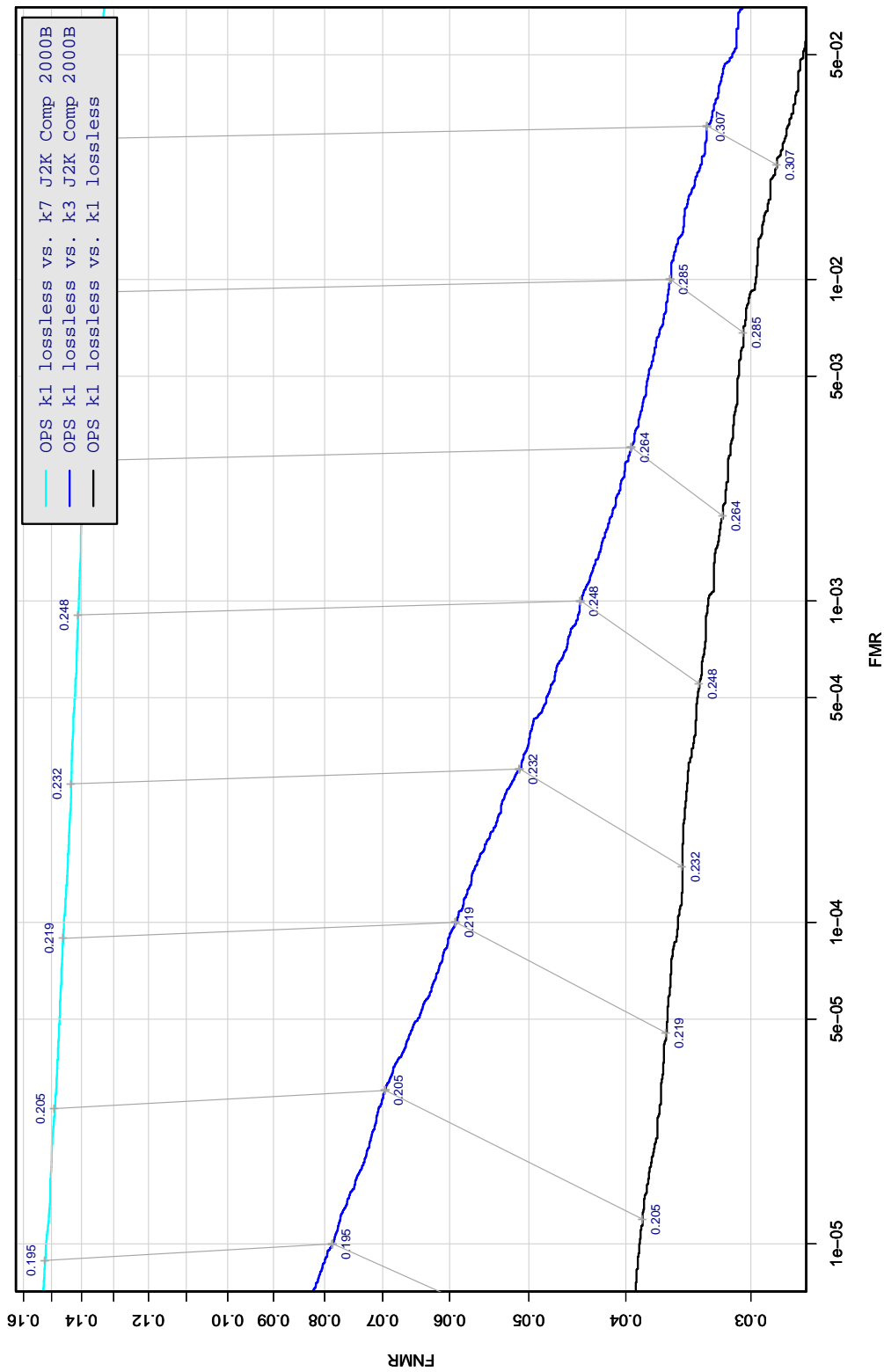


Table 57: DET curve for implementation C1 on the OPS database for the various supported KINDS . The DET characteristics are linked by lines joining points of equal threshold. Non-vertical links indicate a change in false acceptance when the data KIND changes. All results apply to native operation, and the effects of FTE are included.

A = SAGEM	B = COGENT	C = CROSSMATCH	D = CAMBRIDGE	E = L1	x1 = PRIMARY
F = RETICA	G = LG	H = HONEYWELL	I = IRITECH	J = NEUROTECHNOLOGY	x2 = SECONDARY
KIND 1 = RAW 640x480		KIND 3 = CROP		KIND 7 = CROP+MASK	KIND 16 = CONCENTRIC POLAR

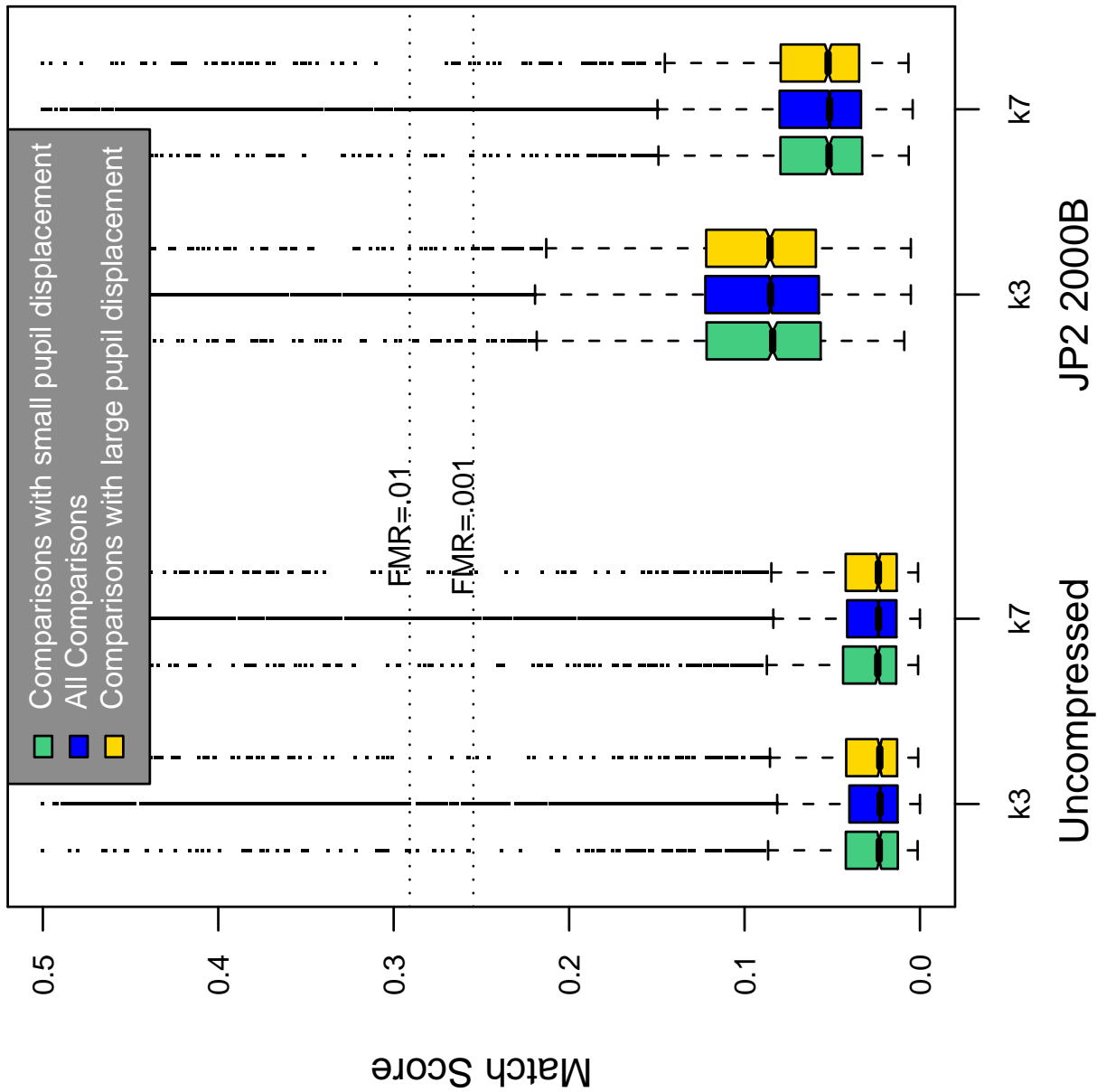


Table 58: Effect of pupil displacement on the genuine score distribution for C1

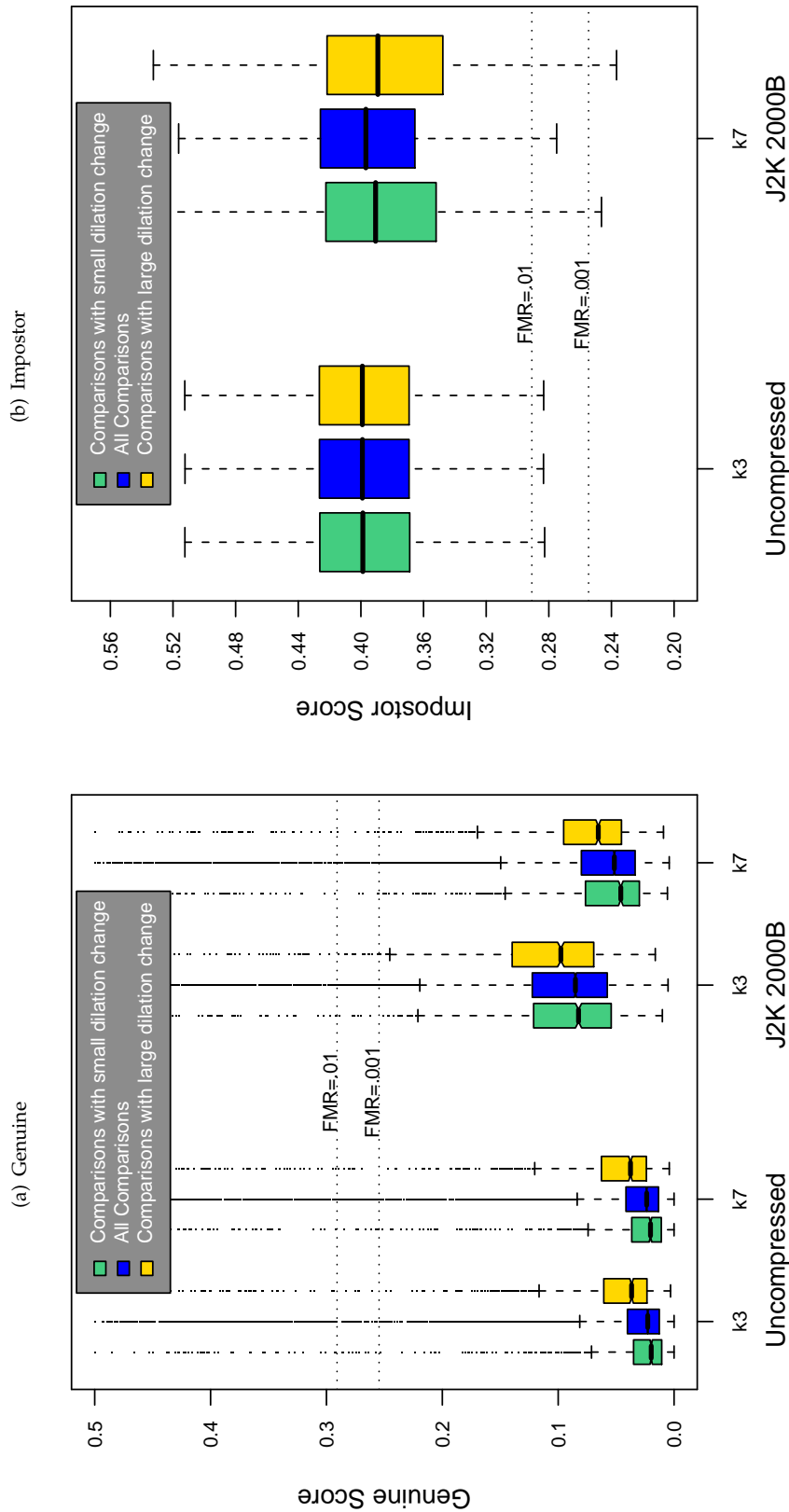


Table 59: The effect of dilation change on the two scores distributions for SDK C1.

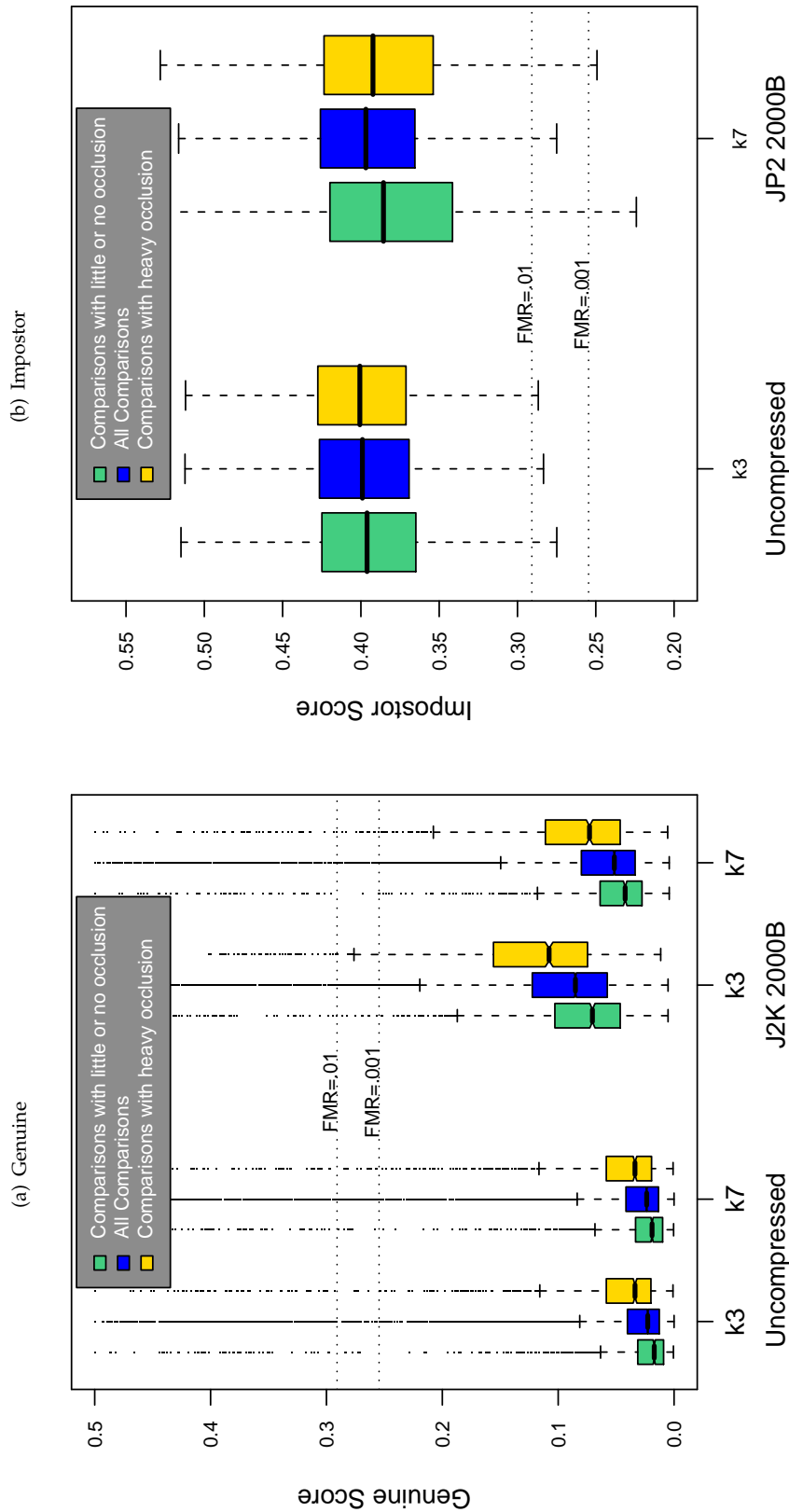
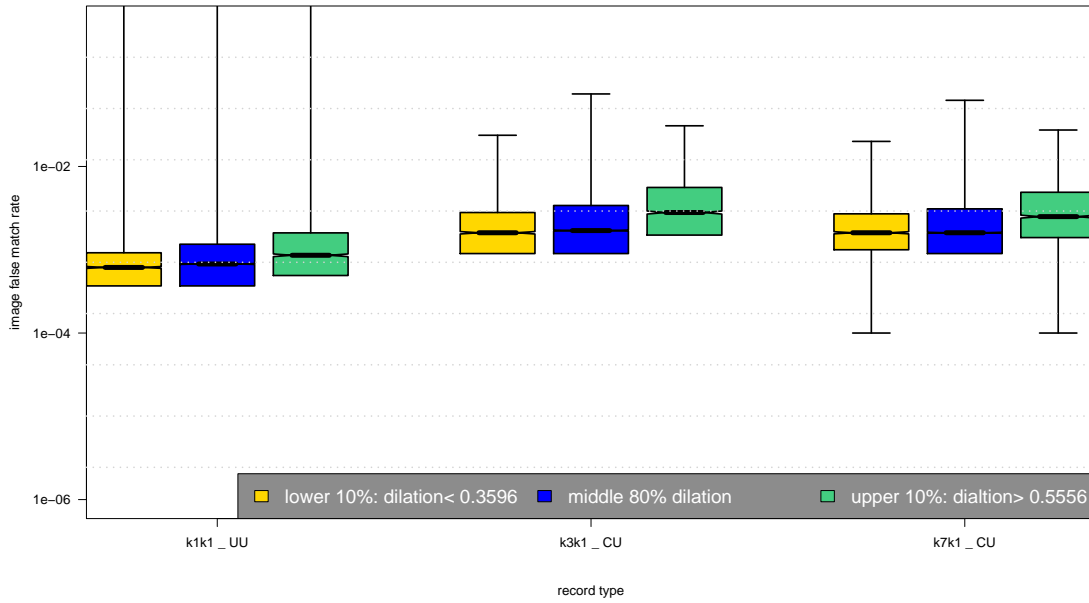
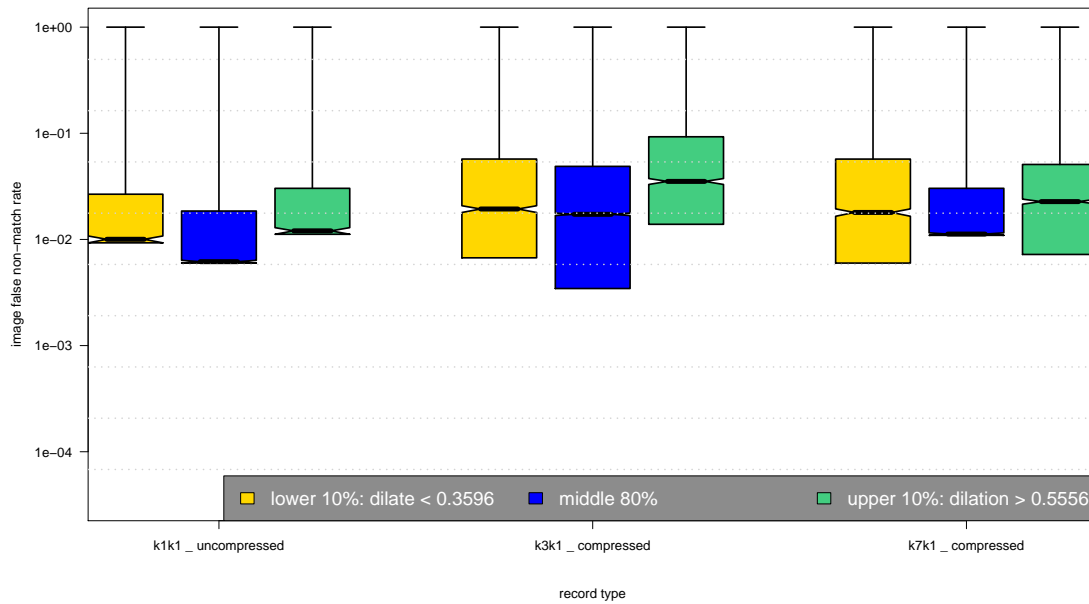


Table 60: The effect of eyelid occlusion on the two scores distributions for SDK C1.

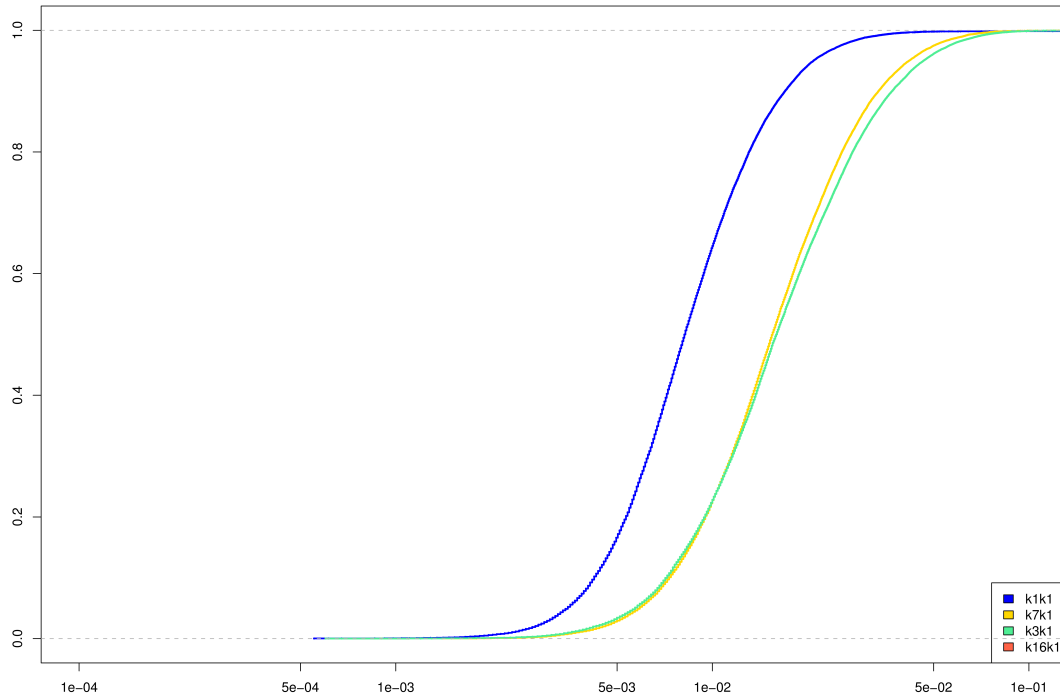
(a) iFMR using A1 dilation estimates



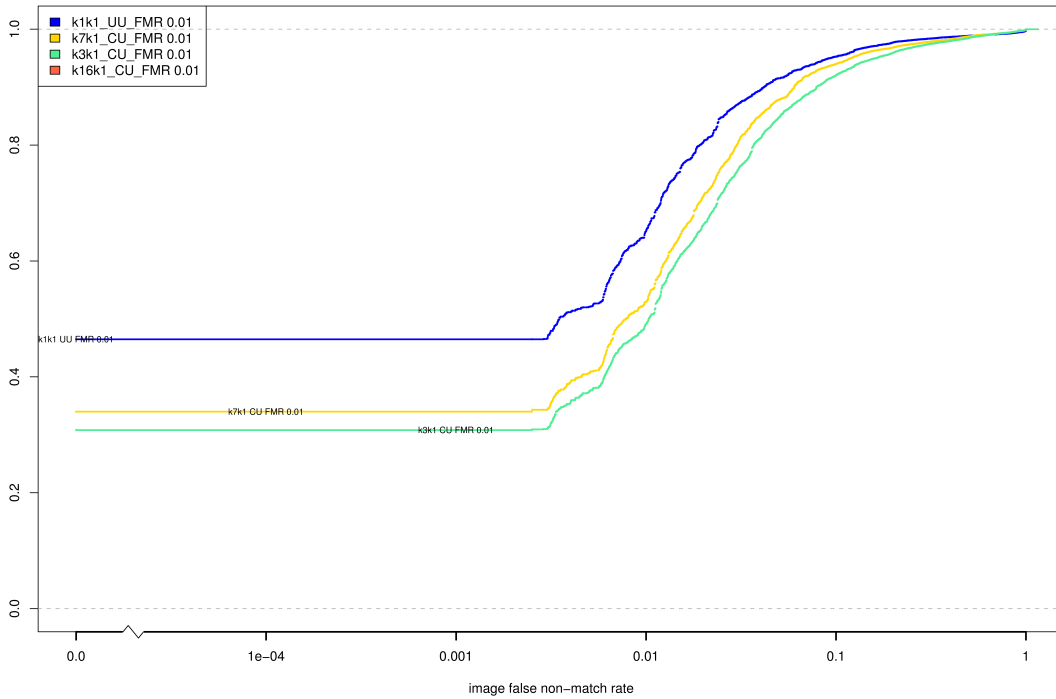
(b) iFNMR using A1 dilation estimates



(c) iFMR CDF



(d) iFNMR CDF



Compiled Results for Implementation C2

On June 25, 2009, NIST invited the IREX participants to submit a description of the SDKs submitted for the IREX effort. The intent was to allow providers to describe and contrast the feature sets, optimization, operational suitability and availability of the primary and secondary SDKs. NIST indicated that any submitted text would appear verbatim (with typesetting) in draft and final versions of the IREX report and that it would be attributed to the organization. This was optional and NIST put no constraints on the content beyond a 600 word limit, and a statement that anything labelled as confidential or proprietary would be omitted.

The provider of SDK C2, Crossmatch Technologies, submitted the following to NIST - we are unable to validate this information.

Cross Match specializes in the design, development and manufacture of high quality finger and iris imaging devices, platforms and solutions.

Our iris algorithms are optimized to perform extraction and matching using images from our mobile and handheld client devices. These devices offer speed, reduced memory (template size) requirements, and limited on board data base size, usually less than 100,000 people. Based on our image quality and optimized client performance objectives we are confident our algorithm compares favorably with other similar solutions. The algorithm has not been optimized to process poor images or perform matching against large databases at this time.

As a new entrant in the iris recognition field, the company has placed top priority on the performance of its integrated hardware and software solutions. Efforts will be made to enhance performance on images from other sources in accordance with market requirements.

On August 17, 2009, NIST invited the IREX participants to submit a description their comments on an draft version of the IREX report. This was intended to allow participants to assist readers in the interpretation of a large and complicated testing effort. NIST indicated that any submitted text would appear verbatim (with typesetting) in the final version of the IREX report and that it would be attributed to the organization. Submission of content was optional and NIST put no constraints on the content beyond a word limit, and a statement that anything labelled as confidential or proprietary would be omitted.

The provider of SDK C2, Crossmatch Technologies, elected not to submit any information

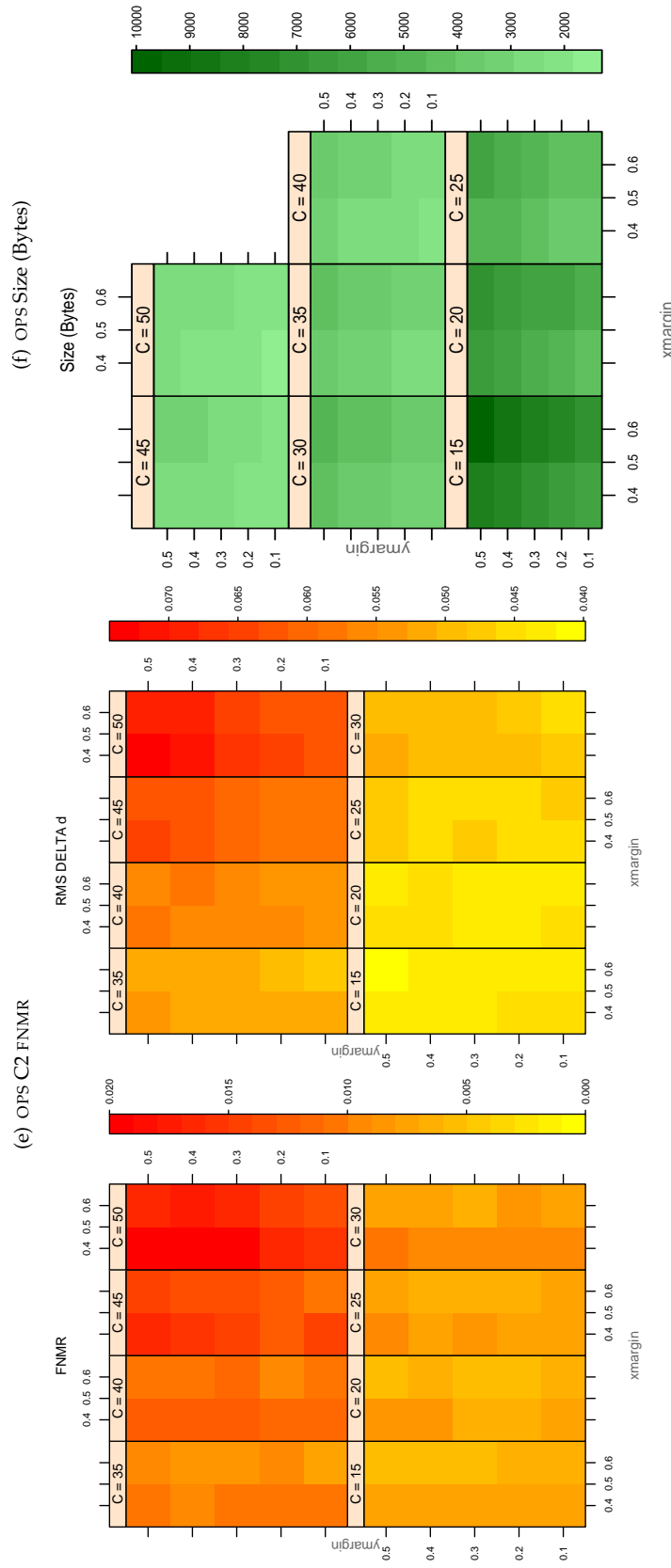


Table 61: For the IREX partition of the OPS database the plots at left show the dependence of cFNMNR on the vertical and horizontal iris cropping margins for various compression ratios. This applies only for KIND 3 records. The margins are in units of iris radius. The use of conditional FNMNR means that the plots exclude comparisons that were falsely rejected even before any compression was applied. On the **right side** is the rms difference between the crop+compress and the uncompressed comparison scores for each image pair. All computations are driven by the bounding box coordinates reported by the II SDK. The number of bits per pixel is $8/C$, where C is the compression ratio. The iris radius varies and because the cropping margins are fixed multiples of the radius the image size varies. The compressed size, in bytes, is the width times height divided by C . Values of cFNMNR greater than 0.02 are shown as 0.02.

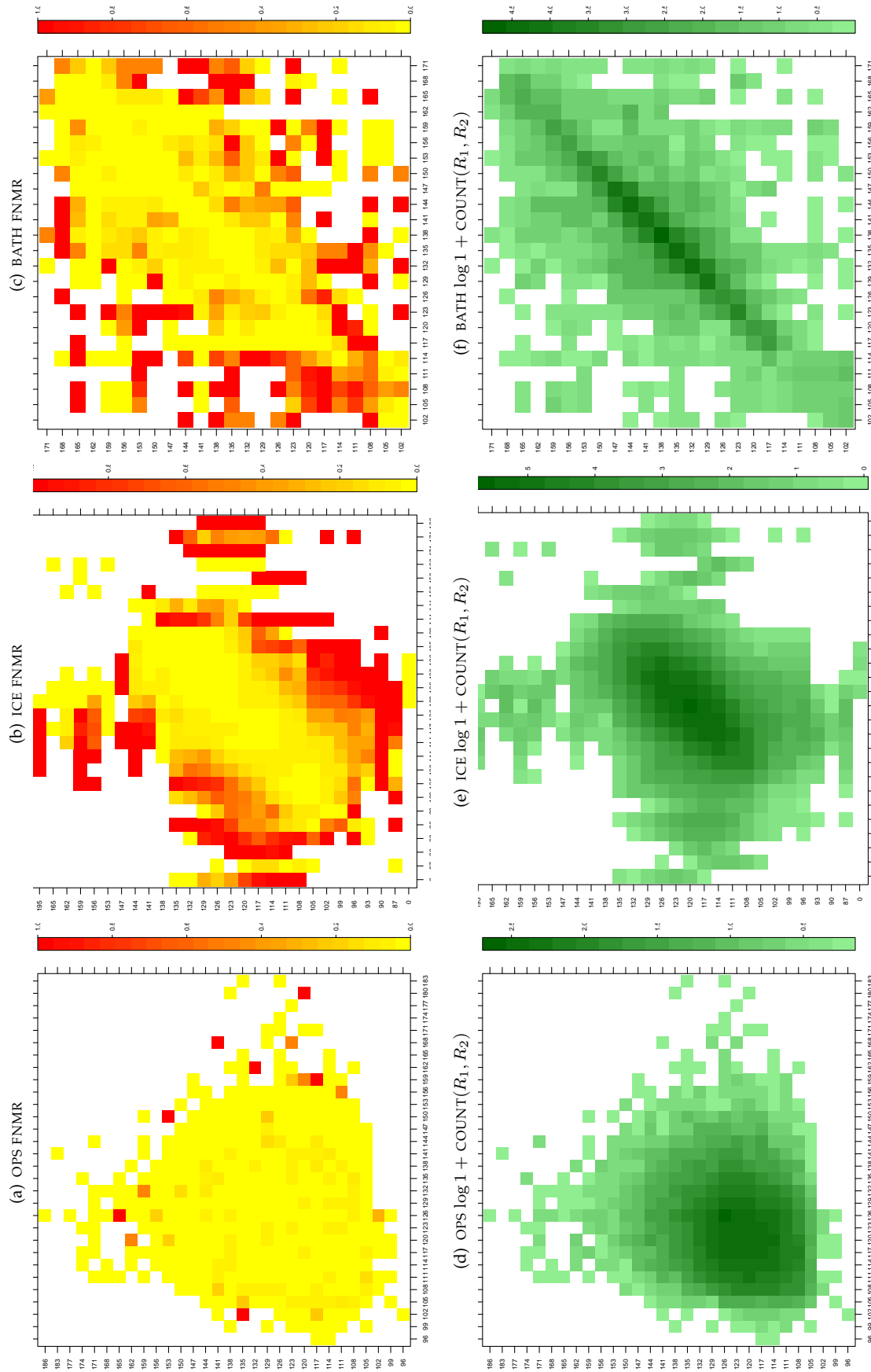


Table 62: For the three IREX databases: In the **top** row the color in each cell represents the occurrence of genuine comparisons with the given pair of radii. The y -axis represents enrollment samples with verification samples on the x -axis; In the **bottom** row the color scale plots $\log 1 + \text{COUNT}(R_1, R_2)$. The radii are quantized into three-pixel bins. The radii for DOD are on the range $96 \leq r \leq 186$ pixels. The radii for ICE are on the range $87 \leq r \leq 165$ pixels. The radii for BATH are on the range $100 \leq r \leq 170$ pixels.

A = SAGEM	B = COGENT	C = CROSSMATCH	D = CAMBRIDGE	E = L1	$x1$ = PRIMARY
F = RETICA	G = LG	H = HONEYWELL	I = IRITECH	J = NEUROTECHNOLOGY	$x2$ = SECONDARY
KIND 1 = RAW 640x480		KIND 3 = CROP	KIND 7 = CROP+MASK	KIND 16 = CONCENTRIC POLAR	

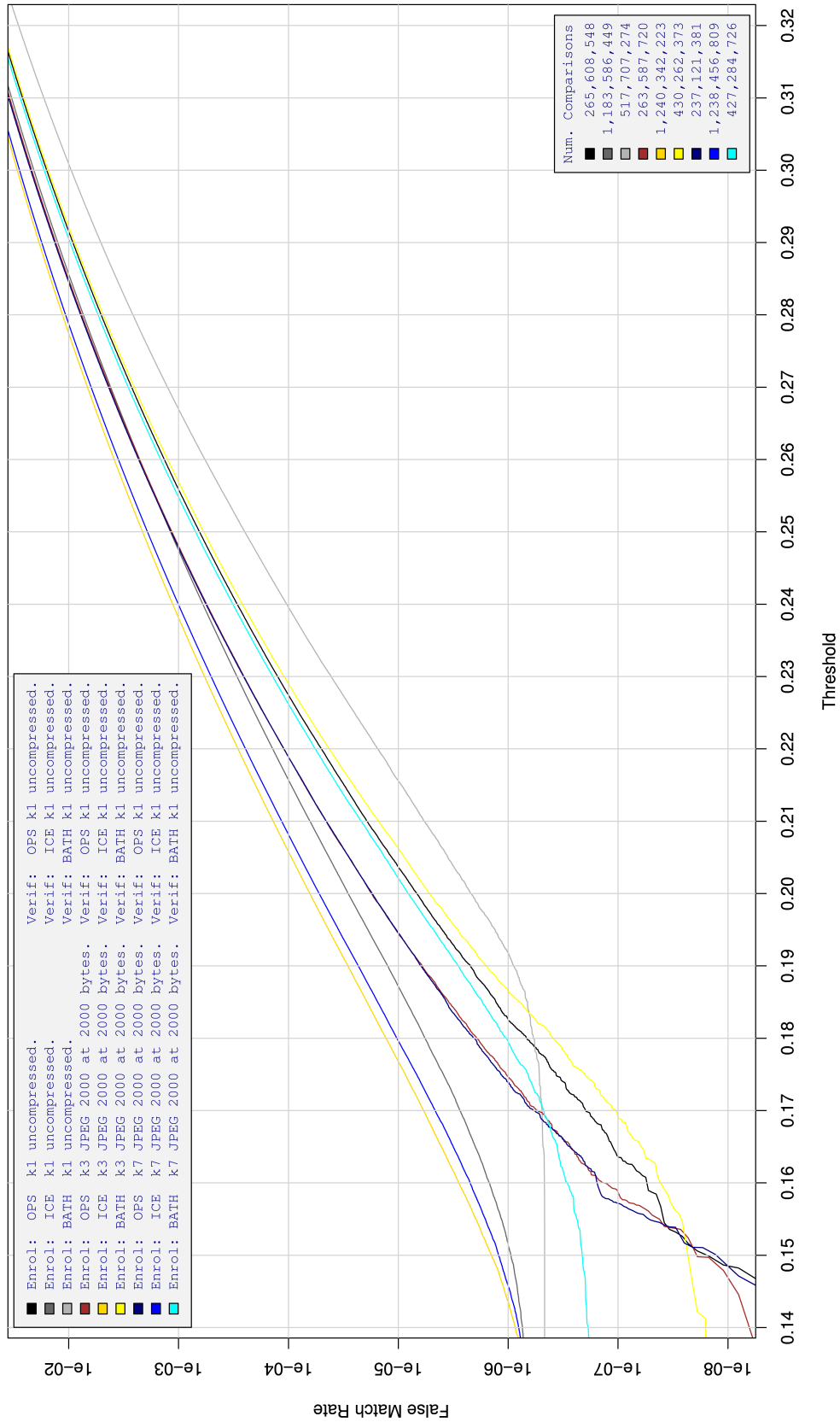


Table 63: For implementation C2, the dependency of FMR on threshold. for various combinations of enrollment and verification dataset, format, and compression.

A = SAGEM	B = COGENT	C = CROSSMATCH	D = CAMBRIDGE	E = L1	x1 = PRIMARY
F = RETICA	G = LG	H = HONEYWELL	I = IRITECH	J = NEUROTECHNOLOGY	x2 = SECONDARY
KIND 1 = RAW 640x480		KIND 3 = CROP	KIND 7 = CROP+MASK	KIND 16 = CONCENTRIC POLAR	

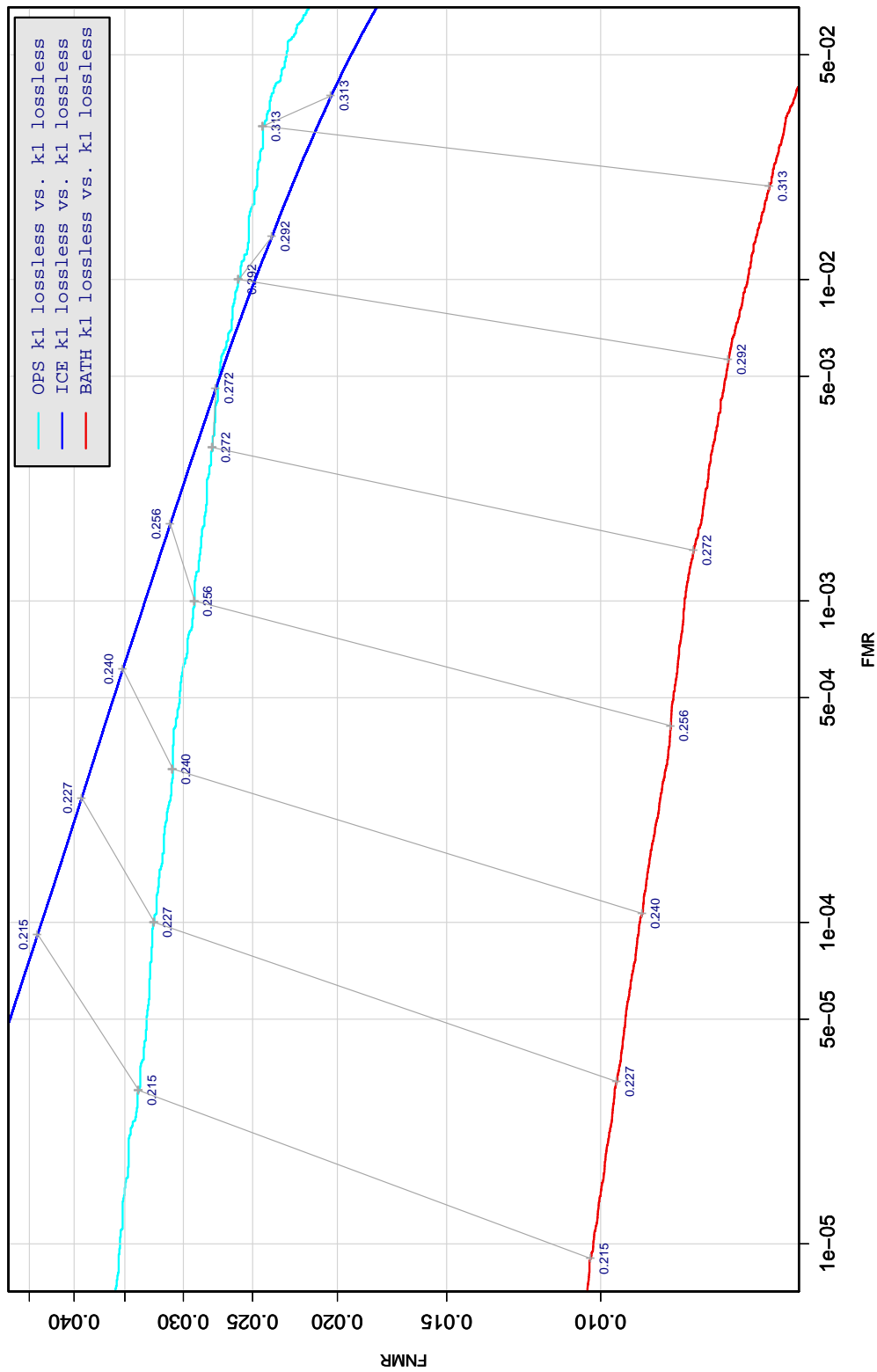


Table 64: DET curve for implementation C2 on three IREX databases. All comparisons are with uncompressed KIND 1 vs. KIND 1 images. The lines join points corresponding to the a fixed threshold. Non-vertical links indicate a change in FMR when the database changes. All results apply to native operation. Failures to produce a template i.e. FTE are ignored because the plots are intended to show *matching* effects, specifically to compare DET slopes and to show the effect of fixing a threshold.

A = SAGEM	B = COGENT	C = CROSSMATCH	D = CAMBRIDGE	E = L1	$x1$ = PRIMARY
F = RETICA	G = LG	H = HONEYWELL	I = IRITECH	J = NEUROTECHNOLOGY	$x2$ = SECONDARY
KIND 1 = RAW 640x480		KIND 3 = CROP	KIND 7 = CROP+MASK	KIND 16 = CONCENTRIC POLAR	

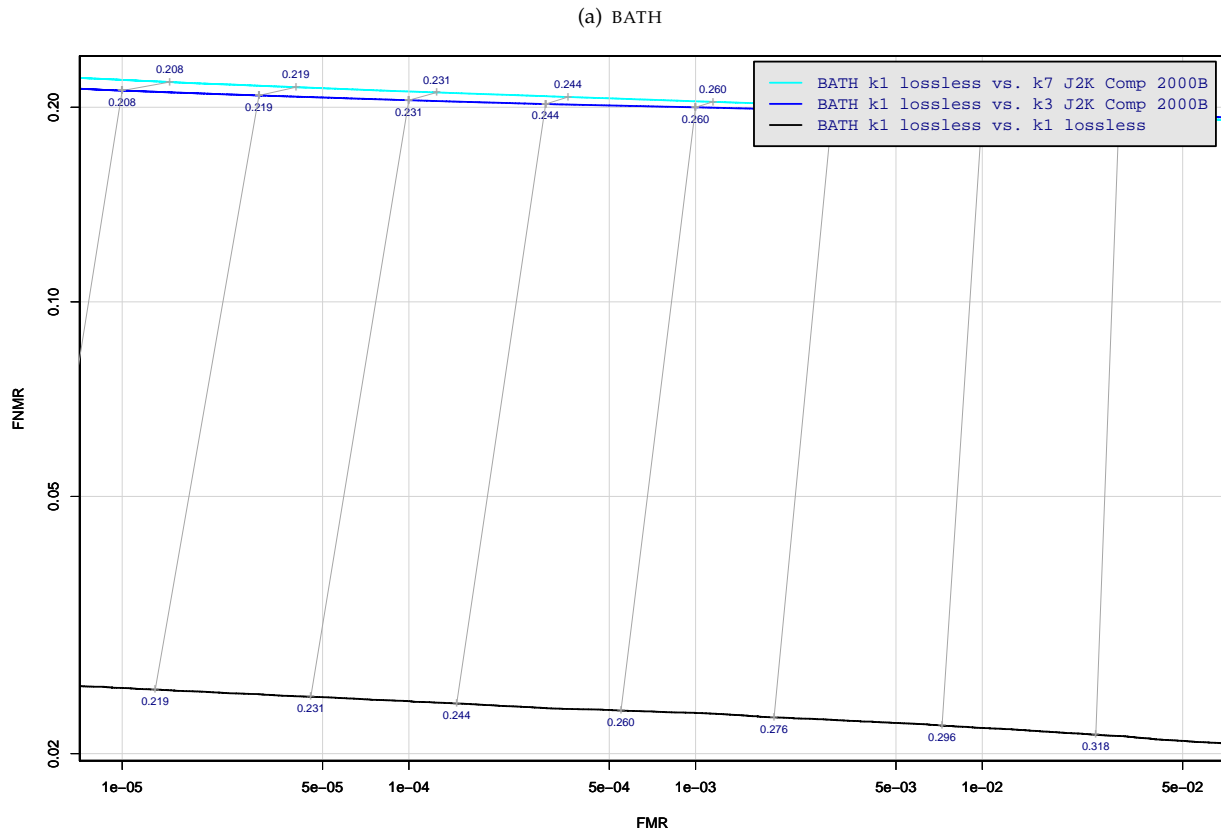


Table 65: DET curve for implementation C2 on the BATH database for the various supported KINDS . The DET characteristics are linked by lines joining points of equal threshold. Non-vertical links indicate a change in false acceptance when the data KIND changes. All results apply to native operation, and the effects of FTE are included.

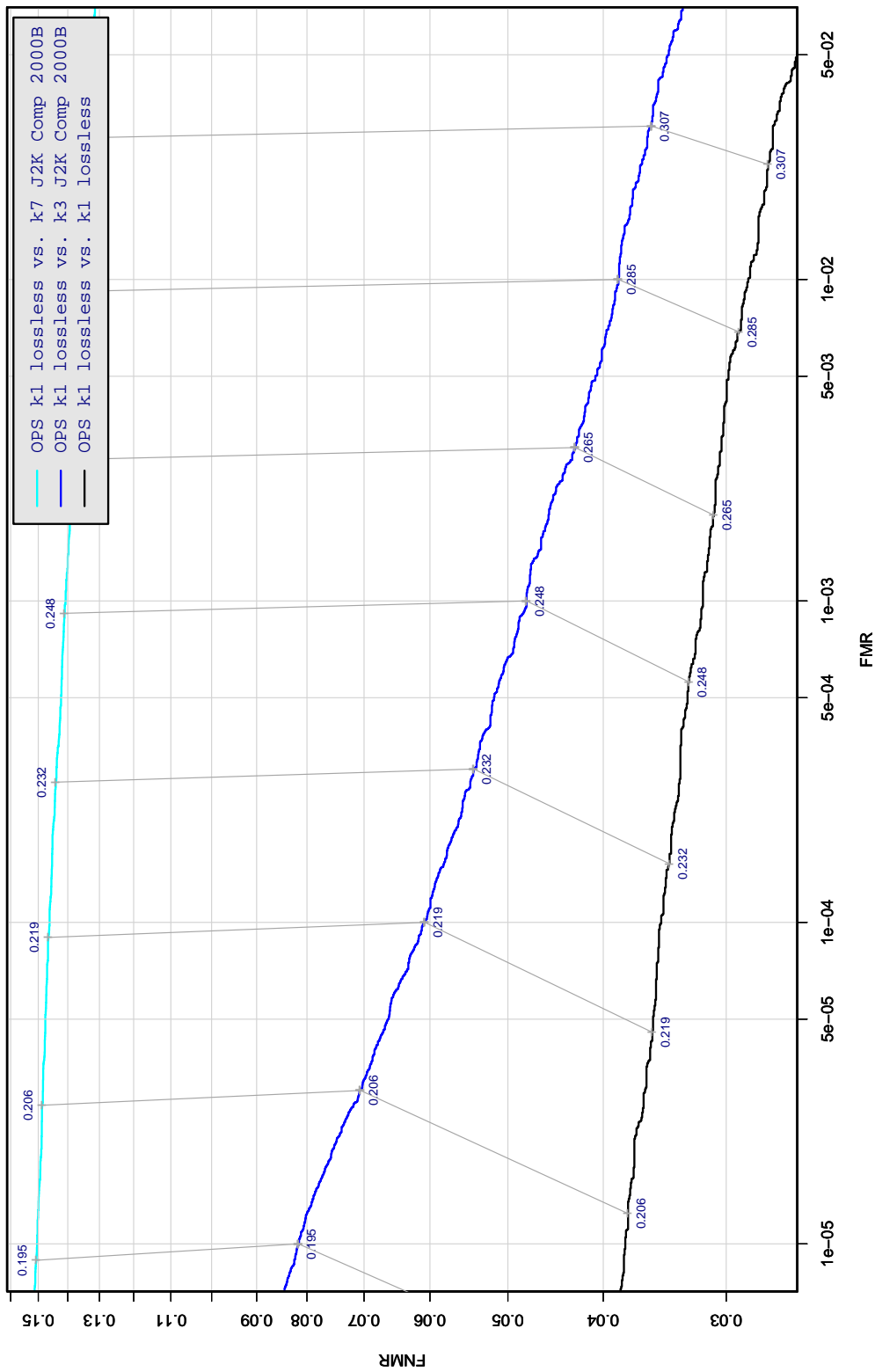


Table 66: DET curve for implementation C2 on the OPS database for the various supported KINDS . The DET characteristics are linked by lines joining points of equal threshold. Non-vertical links indicate a change in false acceptance when the data KIND changes. All results apply to native operation, and the effects of FTE are included.

A = SAGEM	B = COGENT	C = CROSSMATCH	D = CAMBRIDGE	E = L1	x1 = PRIMARY
F = RETICA	G = LG	H = HONEYWELL	I = IRITECH	J = NEUROTECHNOLOGY	x2 = SECONDARY
KIND 1 = RAW 640x480		KIND 3 = CROP		KIND 7 = CROP+MASK	KIND 16 = CONCENTRIC POLAR

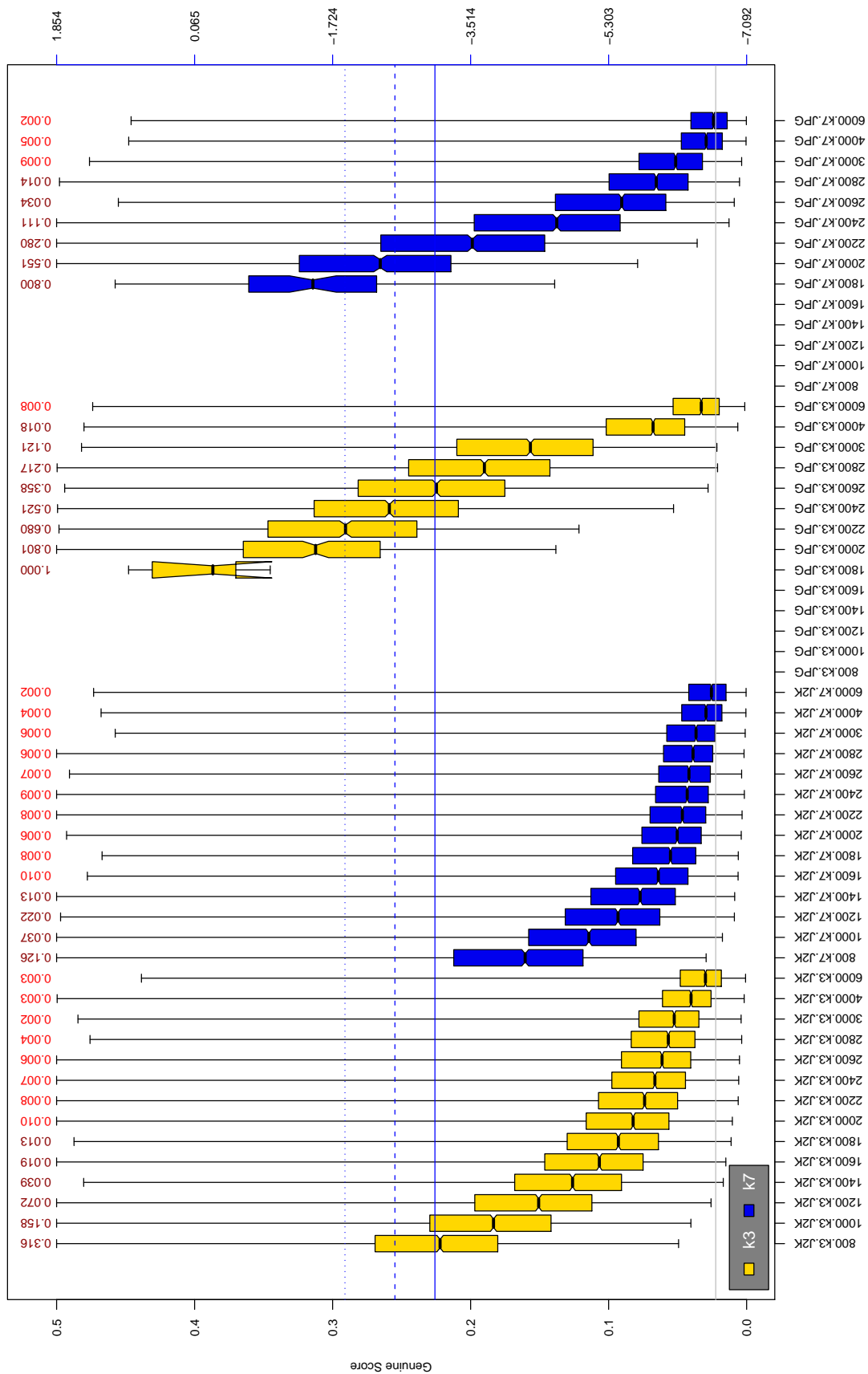


Table 67: The distribution of C2 native genuine comparison scores by size of the compressed image, KIND and the compression algorithm. The images are from the OPS dataset. The right axis scale gives the corresponding value for $d' = (s - \mu_I) / \sqrt{0.5(\sigma_I^2 + \sigma_C^2)}$ for genuine score s . The boxplots only include comparison scores if the uncompressed version of the same image was matched below the FMR = 0.001 threshold. Above the boxplots are FNMR values at FMR = 10⁻³. The three blue lines correspond, from the top, to FMR of 10^[-2,-3,-4]. The lower grey line refers to the median score obtained from comparison of uncompressed KIND 3 images. Any comparison for which either template had not been generated is excluded. Note that the iris record size on the horizontal axis is not evenly spaced above 3000 bytes.

A = SAGEM	B = COGENT	C = CROSSMATCH	D = CAMBRIDGE	E = L1	$x1$ = PRIMARY
F = RETICA	G = LG	H = HONEYWELL	I = IRITECH	J = NEUROTECHNOLOGY	$x2$ = SECONDARY
KIND 1 = RAW 640x480		KIND 3 = CROP	KIND 7 = CROP+MASK	KIND 16 = CONCENTRIC POLAR	

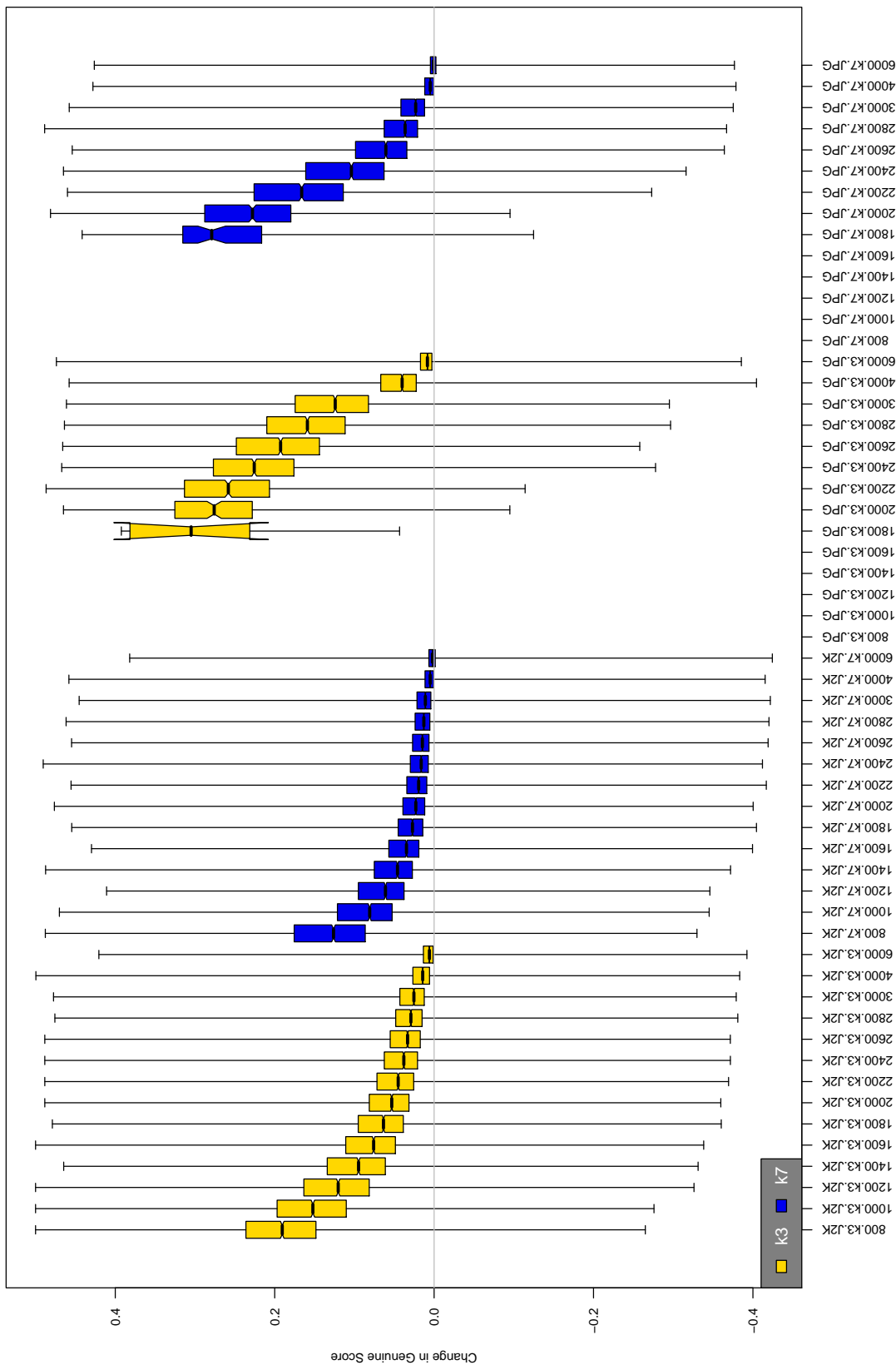


Table 68: The distribution of the *increase* in C2 native genuine comparison scores between the uncompressed “parent” and the compressed image, arranged by size, KIND and the compression algorithm. The images are from the OPS dataset. Any comparison involving a failed template is excluded. Note that the iris record size on the horizontal axis is not evenly spaced above 3000 bytes.

A = SAGEM	B = COGENT	C = CROSSMATCH	D = CAMBRIDGE	E = L1	x1 = PRIMARY
F = RETICA	G = LG	H = HONEYWELL	I = IRITECH	J = NEUROTECHNOLOGY	x2 = SECONDARY
KIND 1 = RAW 640x480		KIND 3 = CROP	KIND 7 = CROP+MASK	KIND 16 = CONCENTRIC POLAR	

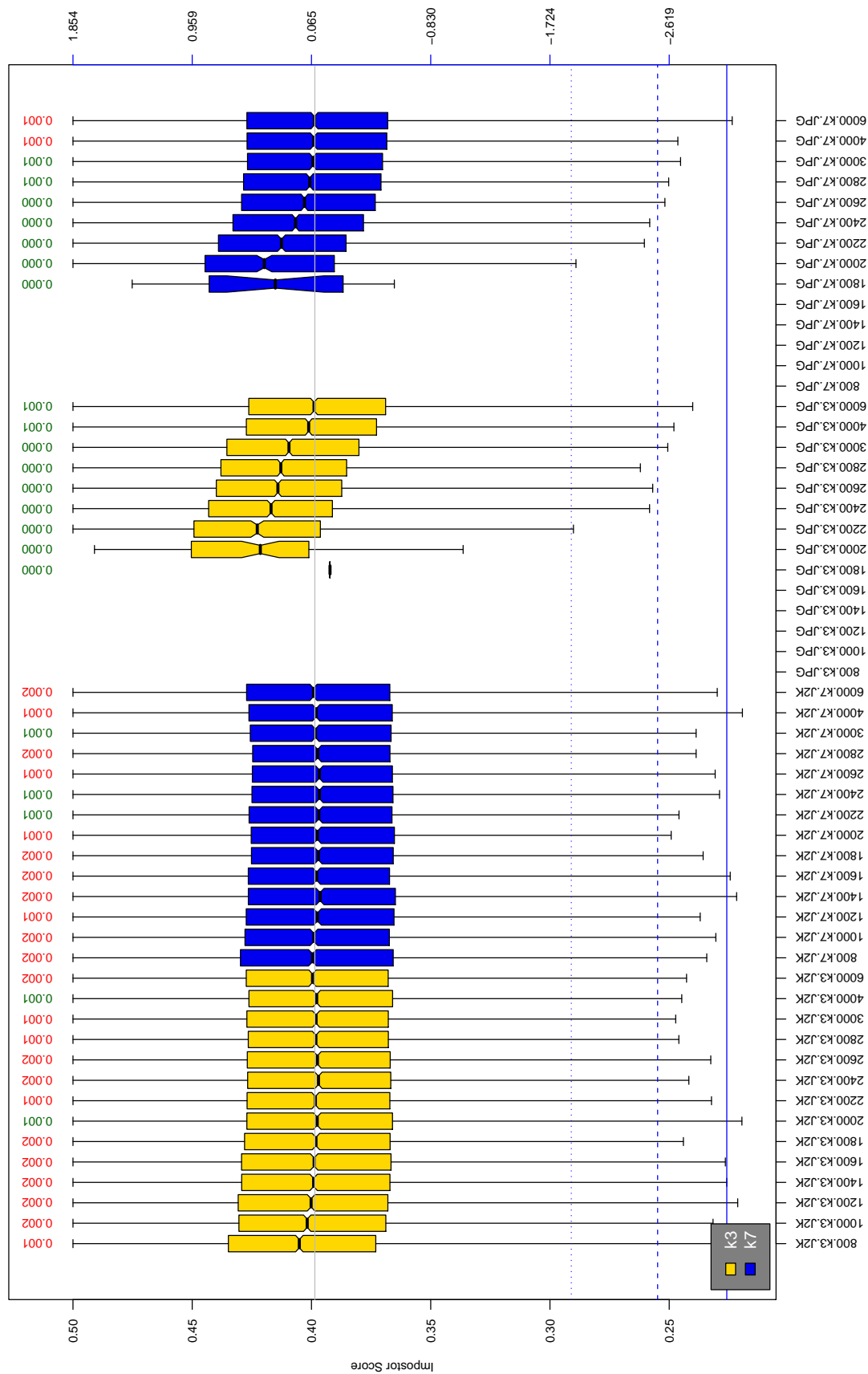


Table 69: The distribution of C2 native impostor comparison scores by size of the compressed image, KIND and the compression algorithm. The right axis scale gives the corresponding value for $d' = (s - \mu_1) / \sqrt{0.5(\sigma_1^2 + \sigma_2^2)}$ for impostor score s . The three blue lines correspond, from the top, to FMR of $10^{-2}, -3, -4$. The lower grey line refers to the median score obtained from comparison of uncompressed KIND 3 images. Any comparison involving a failed template is excluded. Above the boxplots are FMR values at the threshold that gives FMR = 10^{-3} on uncompressed images. These figures are computed from only 4000 comparisons so the FMR values and the tails of the impostor distribution are poorly characterized. Note that the iris record size on the horizontal axis is not evenly spaced above 3000 bytes.

A = SAGEM	B = COGENT	C = CROSSMATCH	D = CAMBRIDGE	E = L1	$x1$ = PRIMARY
F = RETICA	G = LG	H = HONEYWELL	I = IRITECH	J = NEUROTECHNOLOGY	$x2$ = SECONDARY
KIND 1 = RAW 640x480		KIND 3 = CROP		KIND 7 = CROP+MASK	KIND 16 = CONCENTRIC POLAR

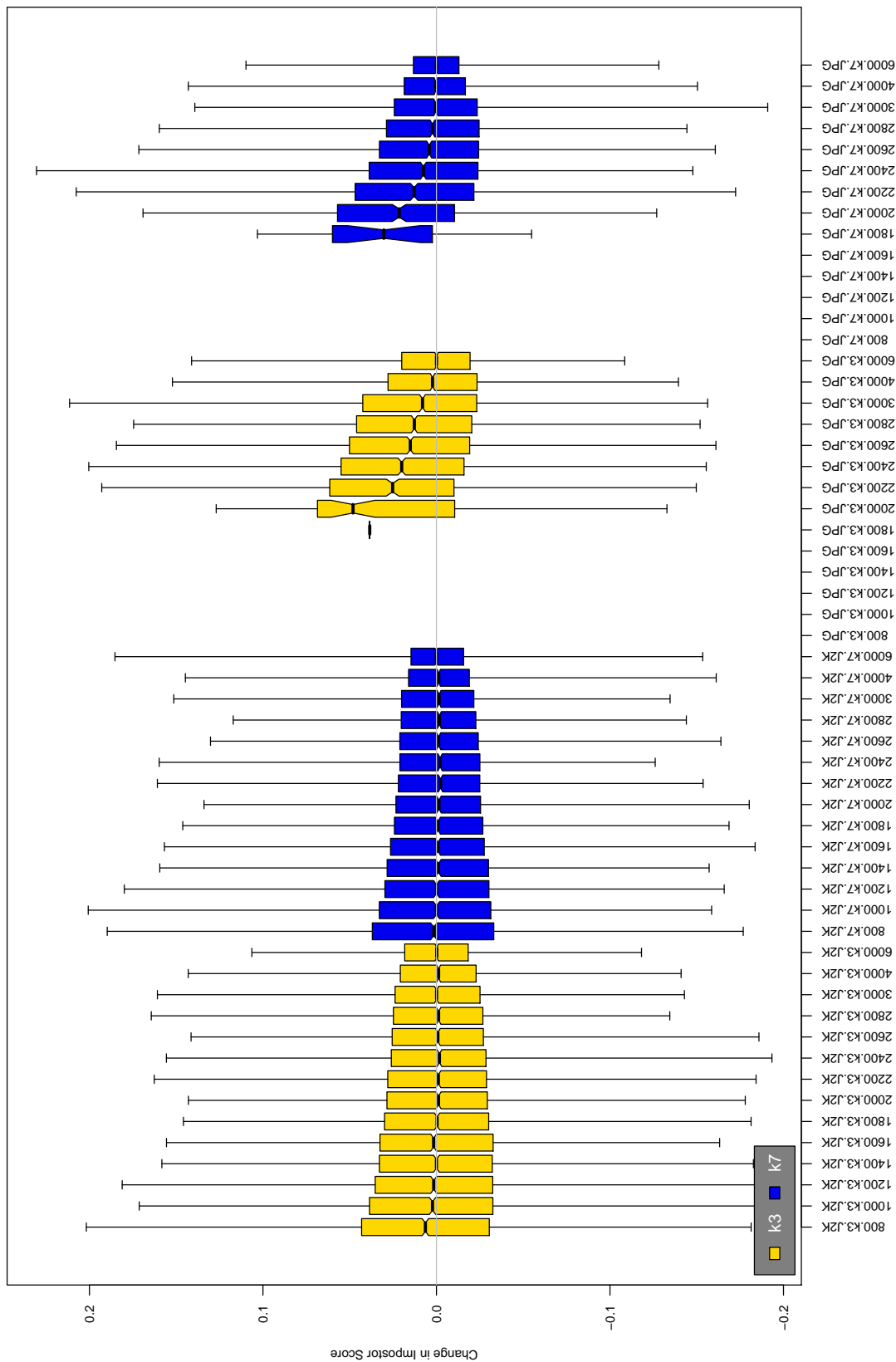


Table 70: The distribution of the increase in C2 native impostor comparison scores between the uncompressed “parent” and the compressed image, arranged by size, KIND and the compression algorithm. The images are from the OPS dataset. Any comparison involving a failed template is excluded. Note that the iris record size on the horizontal axis is not evenly spaced above 3000 bytes.

A = SAGEM	B = COGENT	C = CROSSMATCH	D = CAMBRIDGE	E = L1	x1 = PRIMARY
F = RETICA	G = LG	H = HONEYWELL	I = IRITECH	J = NEUROTECHNOLOGY	x2 = SECONDARY
KIND 1 = RAW 640x480		KIND 3 = CROP	KIND 7 = CROP+MASK	KIND 16 = CONCENTRIC POLAR	

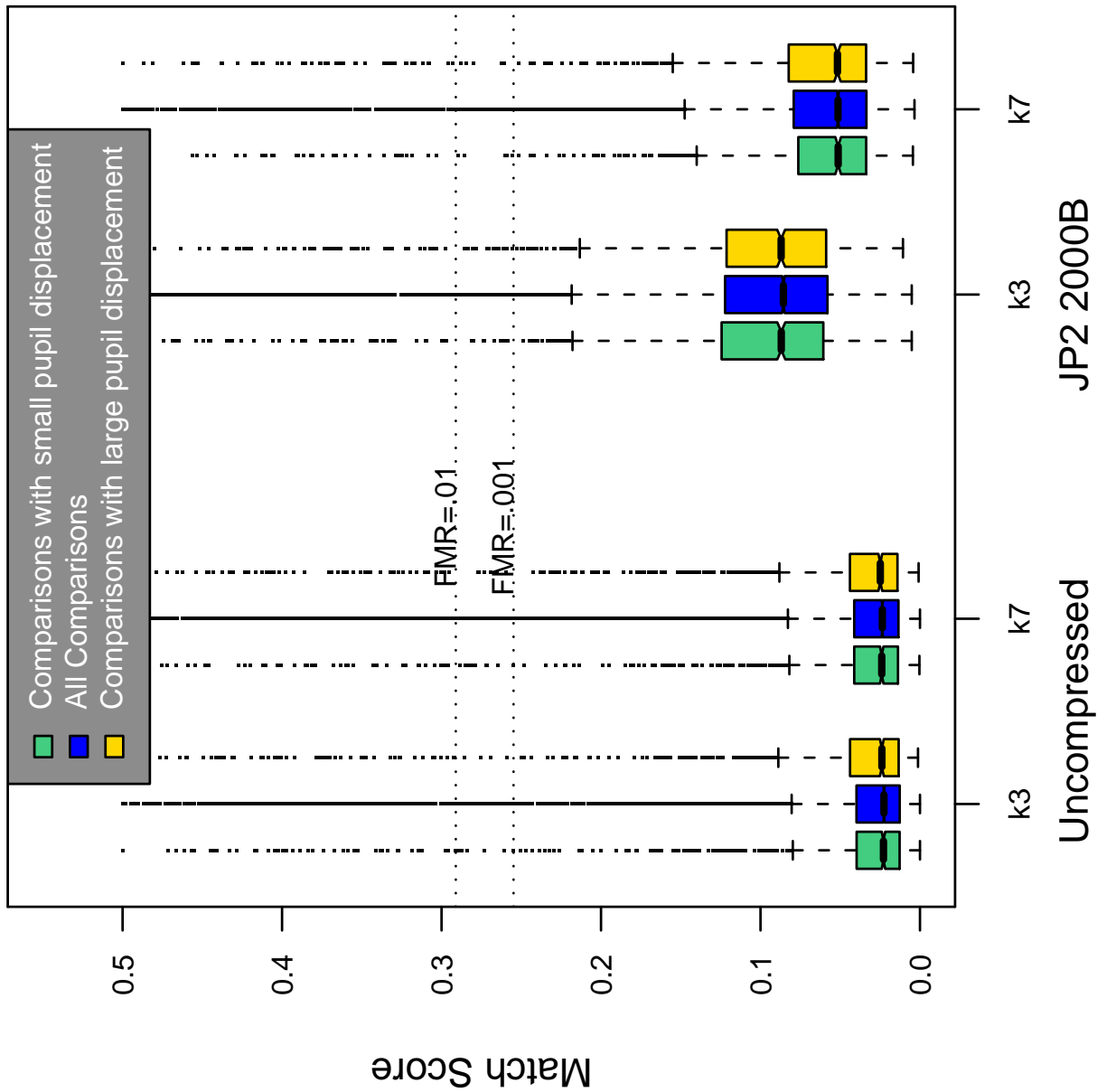


Table 71: Effect of pupil displacement on the genuine score distribution for C2

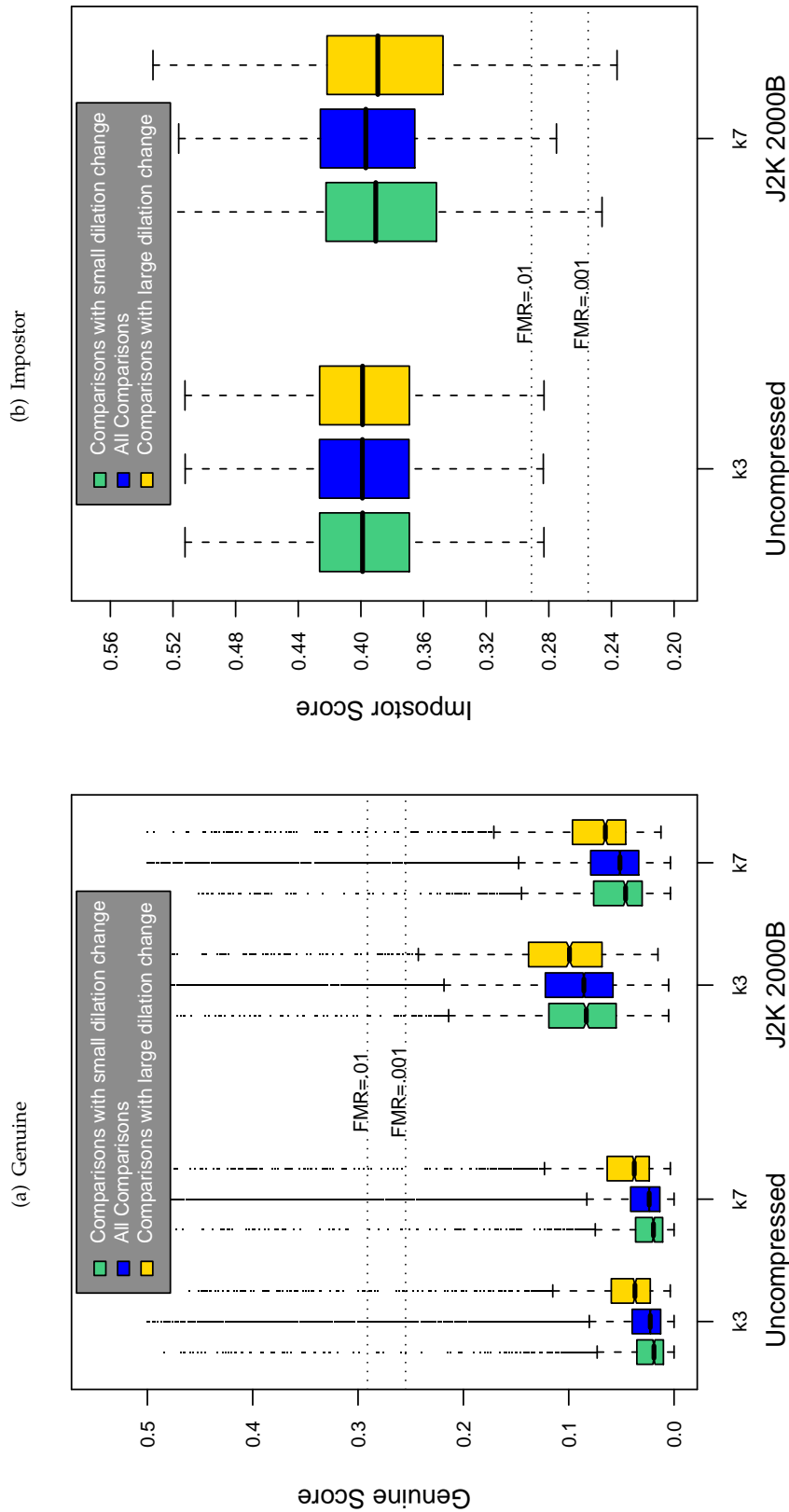


Table 72: The effect of dilation change on the two scores distributions for SDK C2.

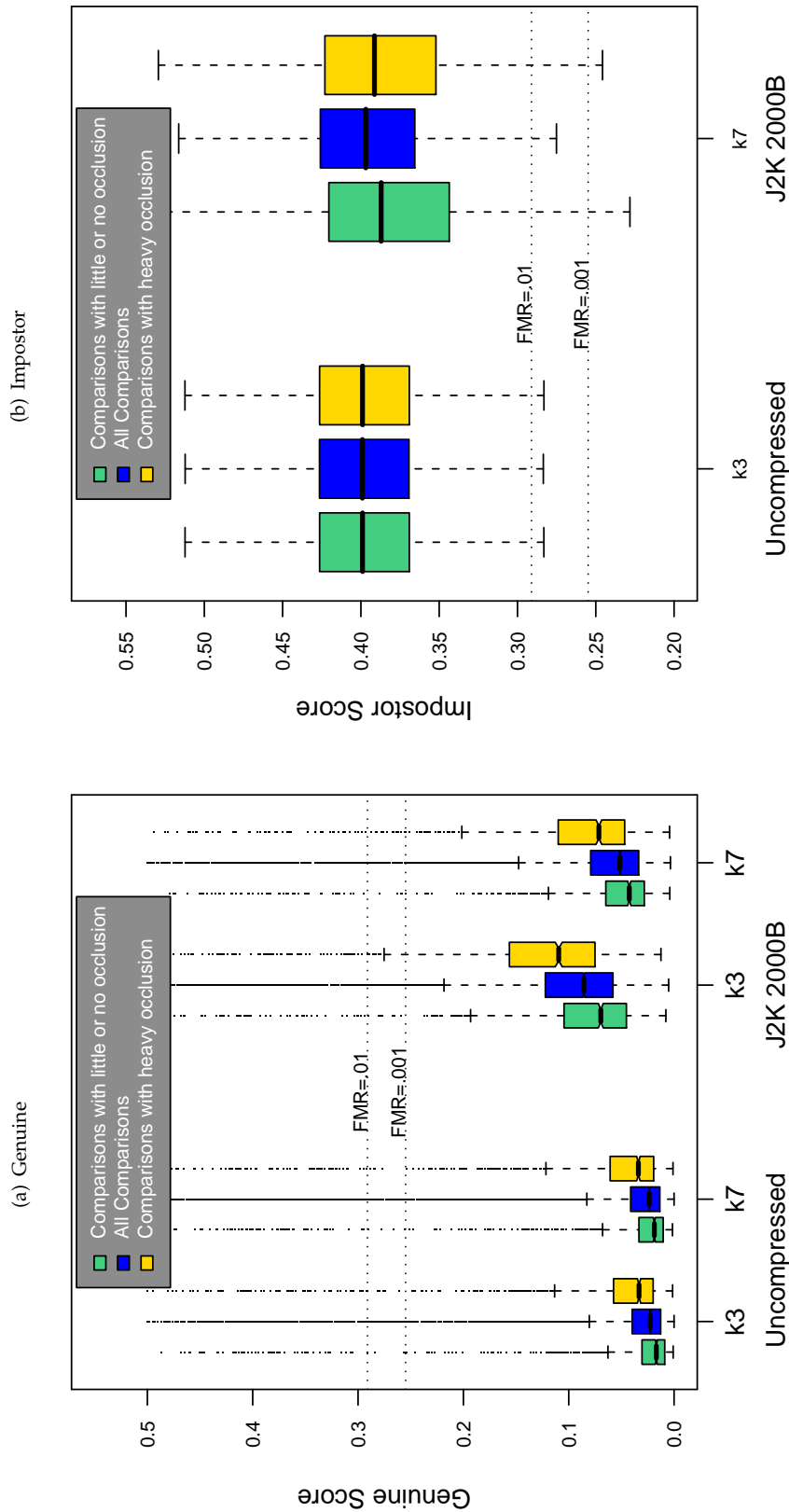
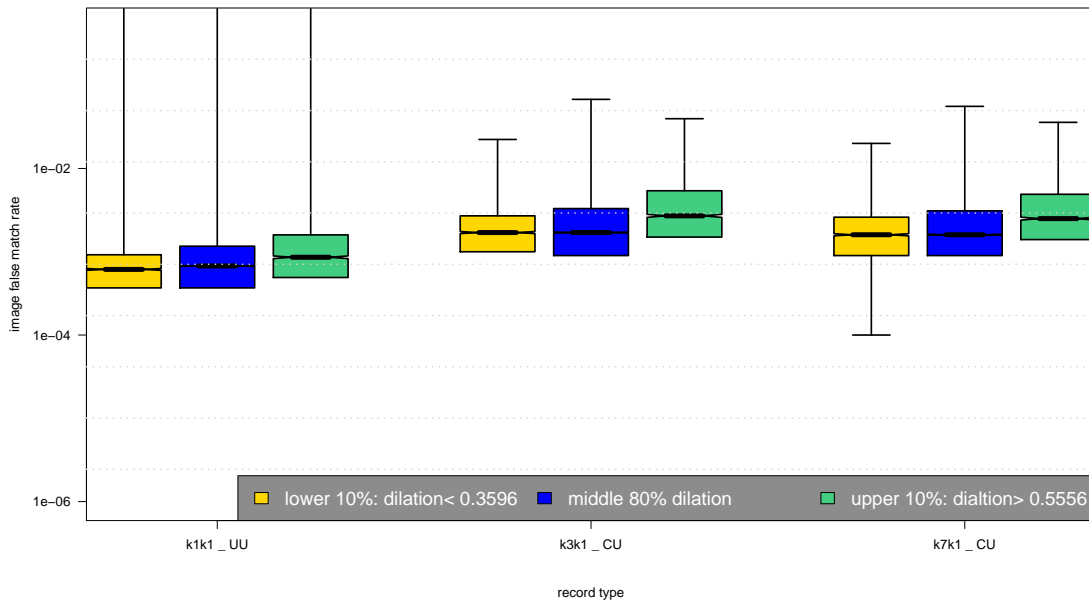
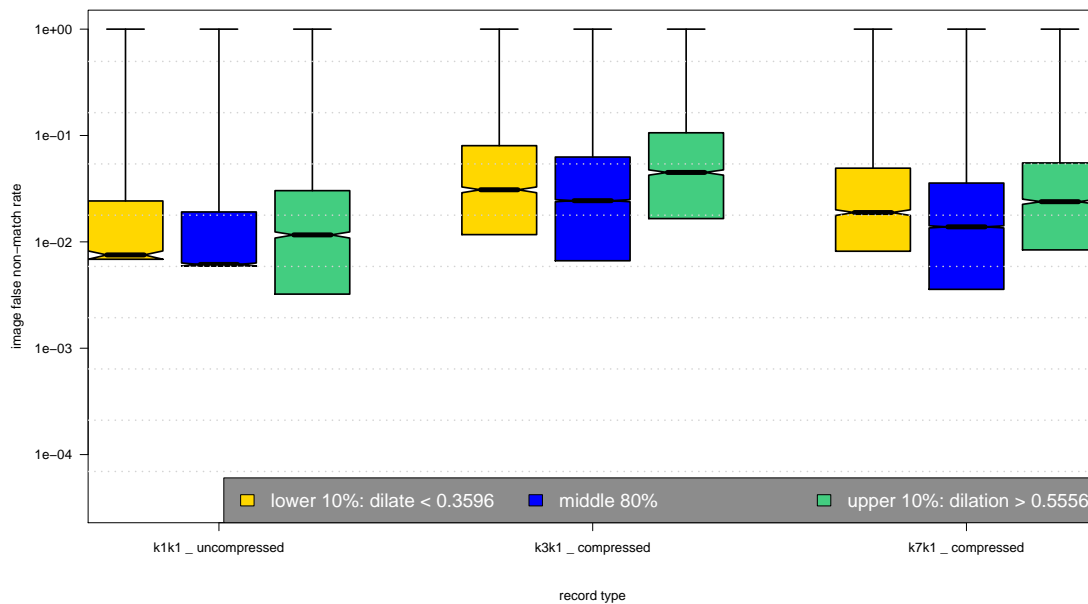


Table 73: The effect of eyelid occlusion on the two scores distributions for SDK C2.

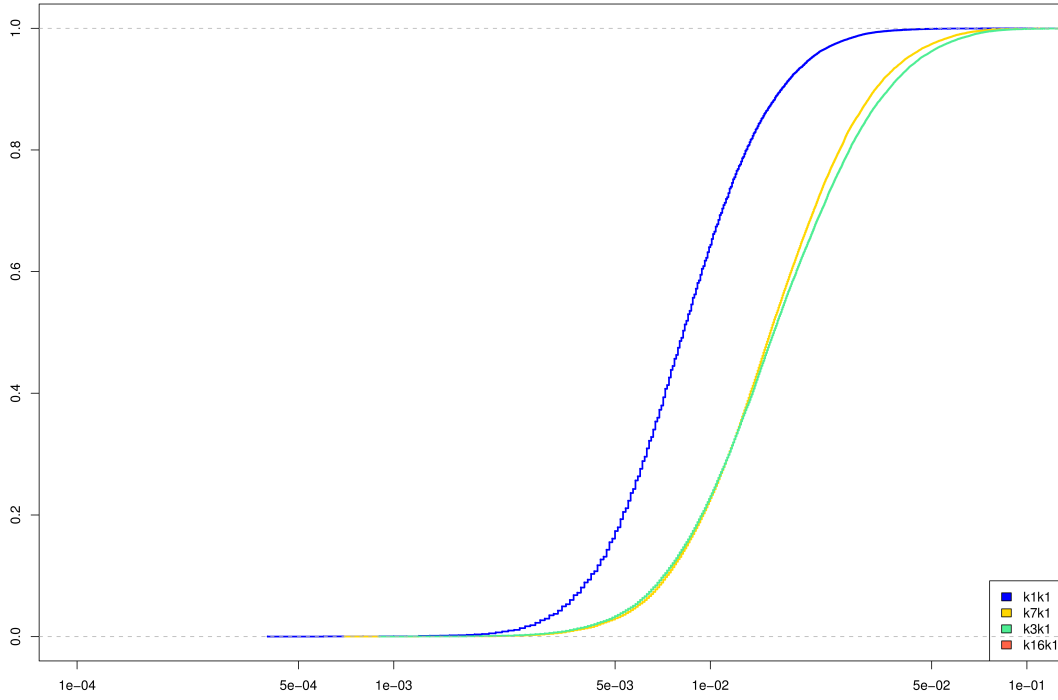
(a) iFMR using A1 dilation estimates



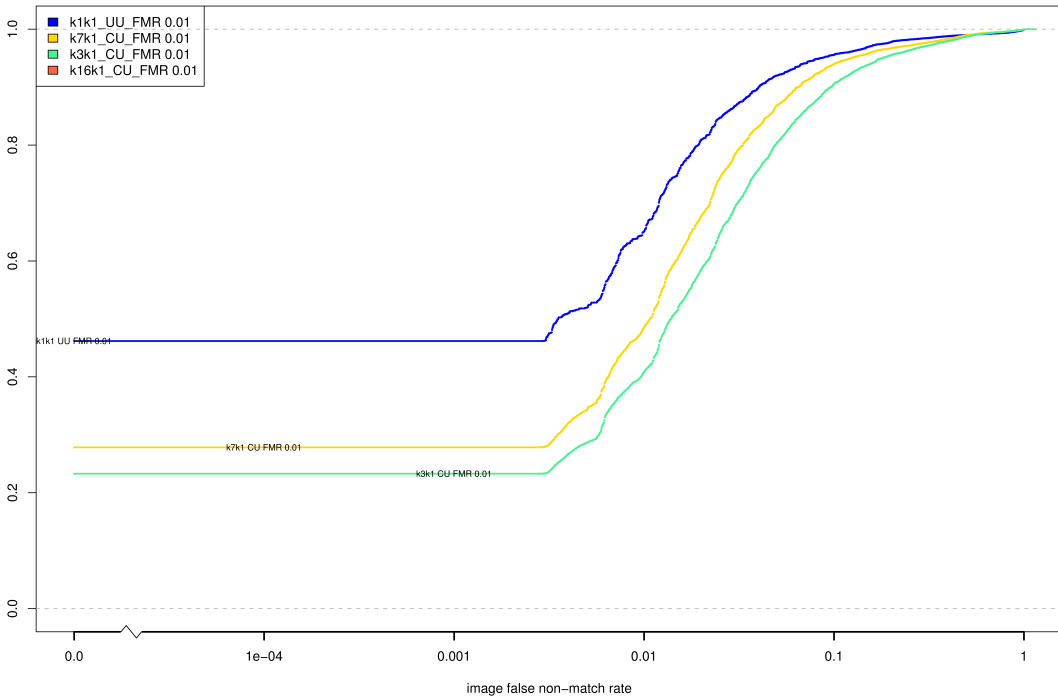
(b) iFNMR using A1 dilation estimates



(c) iFMR CDF



(d) iFNMR CDF



Compiled Results for Implementation D1

On June 25, 2009, NIST invited the IREX participants to submit a description of the SDKs submitted for the IREX effort. The intent was to allow providers to describe and contrast the feature sets, optimization, operational suitability and availability of the primary and secondary SDKs. NIST indicated that any submitted text would appear verbatim (with typesetting) in draft and final versions of the IREX report and that it would be attributed to the organization. This was optional and NIST put no constraints on the content beyond a 600 word limit, and a statement that anything labelled as confidential or proprietary would be omitted.

The provider of SDK D1, Cambridge University, submitted the following to NIST - we are unable to validate this information.

IREX provides a key opportunity to assess, beyond its main focus on image formats and compressibility, the performance of iris recognition at the more demanding False Match Rates in the region of 1 in a million (1.e-6) to 1 in 100 million (1.e-8) for which it was designed and at which it is usually deployed. At least one database in IREX has images from 16,320 different eyes, and so even if only a single image of each eye is used, an Impostors Distribution could be generated comparing 133 million unique pairings of different eyes. If both images of each eye were used, this total would rise to above 500 million. A major shortcoming of ICE was that performance was reported at much less demanding FM rates, since ICE had only 240 Subjects, leading to the bizarre conclusion that iris delivered no better discrimination between persons than face recognition. Cambridge very much hopes that IREX will seize the opportunity to probe and to document the FMR = 1.e-6 to 1.e-8 region of ROC curves, since enough data points are easily available within IREX Impostors Distributions to go that far out along their tails to reach such cumulatives. Otherwise, the distinctive capabilities of iris recognition compared to weaker biometrics may again not be seen.

For the Cambridge SDKs, such demanding FMR regions of ROC curves should correspond to a Hamming Distance threshold in the 0.28 - 0.30 range, where very tiny reductions in threshold yield order-of-magnitude improvements in FMR but at negligible cost to FnMR. Another way to say this is that iris ROC curves (not only those from Cambridge) tend to be very flat: some 3 or 4 orders-of-magnitude are reduced in FMR while the FnMR perhaps only doubles. It is thus misleading to report, as ICE did for example, that iris FnMR in the 0.01 range is achieved at an FMR of 0.001, when the same result can also be cited at an FMR of 1 in a million. All ROC curves must converge into the two corners along the diagonal (in linear coordinates), so if one reports accuracy at undemanding rates like FMR = 0.001 then one should conclude that the length of a Subject's big toe is as good as any other biometric.

The SDKs from Cambridge differed from those used in airports and other large public deployments (as licensed from L-1 to licensees) in two main respects: (1) entropy increase; (2) score normalisation. The flatness of an ROC/DET curve depends on the narrowness of the Impostors Distribution (rapid attenuation of its tail), and this in turn depends on the entropy captured by the code (the number of degrees-of-freedom, or amount of random variation, expressed across a population). Cambridge Primary (PID=60541) encodes 1,536 bytes including mask; corrects for gaze deviation (off-axis capture); explores a narrow range of image tilts; but does not do score normalisation to enforce tail attenuation. When computing Quality Scores, it does not consider aspects of the IrisCode template. Cambridge Secondary (PID=60540) makes a smaller template (1,024 bytes including mask); does consider aspects of the template in assessing Quality (thus expending time for template creation even when only producing an image Record); detects and corrects for deviated gaze; explores a wider range of image tilts; and does perform score normalisation. Both SDKs search for the iris over the entire frame of a raw image, out to its four edges, to allow for the cases seen in ICE of some irises

hanging partly outside of the image frame. Both SDKs employ active contours for deformable iris mappings, and quadrature (complex wavelet) encodings.

On August 17, 2009, NIST invited the IREX participants to submit a description their comments on a draft version of the IREX report. This was intended to allow participants to assist readers in the interpretation of a large and complicated testing effort. NIST indicated that any submitted text would appear verbatim (with typesetting) in the final version of the IREX report and that it would be attributed to the organization. Submission of content was optional and NIST put no constraints on the content beyond a word limit, and a statement that anything labelled as confidential or proprietary would be omitted.

The provider of SDK D1, Cambridge University, submitted the following to NIST - we make no comment on this information.

Cambridge comments (using Table and Figure numbers from 3 July draft): _____

The search for an iris in the image frame (or partly outside it as in some public ICE images), and the segmentation of iris boundaries, by the Cambridge SDKs (D1 D2) covered an iris size search range of from 70 pixels to 140 pixels in radius. This range of 2:1 in size was assumed generous enough and was chosen to accommodate the tendency towards iris cameras with less zoom, or acquiring at a greater distance, with typical iris radius perhaps 100 pixels. This choice of iris size search range matched the public part of the ICE gallery, whose mean iris radius is 119, std_dev 5.3 pixels, and in which the maximum iris radius is only 136 pixels. But our choice was clearly a mistake, as the iris radius in OPS images went up to 186 pixels, and up to 170 pixels in the BATH dataset. Iris sizes in the public ICE gallery are thus not representative of the size ranges tested in IREX. (This is not a criticism of IREX. But whatever percentage of sizes, say 2 percent, are outside the presumed range will become irreducible offsets to FnMR curves for SDKs making such assumptions.) Figure 4d ("heat plots" for FnMR versus iris radius) and Tables 84(a) and 98(a) show that almost all Failures-to-Match by the Cambridge SDKs occurred for iris radius values above 140 pixels, which was the size cut-off of our 2:1 size search range. These could have been avoided if Cambridge had made a better guess about size range than 70 - 140 pixels radius.

Nonetheless it is valuable and gratifying that IREX has confirmed several Cambridge claims published in the academic literature:

1. Astronomic attenuation of False Match Rates from minuscule reductions in Hamming Distance threshold: Table 14 shows that for cross-dataset comparisons (bottom red curve), False Match Rate reaches 1 in 100 million at HD = 0.315 and attenuates at a rate of a further factor of 10 for each additional reduction of 0.01 in the HD threshold, exactly as has been published. See also tabulations in Table 15. Many doubted these claims.
2. Confirmation of great speed in template creation and in matching, although IREX also shows valuably that False nonMatch Rates can be improved when match speed is reduced by two orders-of-magnitude, as may be tolerated in 1-to-1 verification applications.
3. Confirmation of the stability of the distribution of Imposters scores, regardless of almost every image manipulation, including variations in presentation. This was also confirmed for nearly all of the algorithms submitted. This observation is important for the credibility of iris recognition generally, as it allows extrapolation to large-scale database search, and prediction of performance as a function of decision threshold.

4. Confirmation that iris images can be severely compressed to as little as 2,000 bytes with little impact on performance, provided that JP2K is used instead of JPEG compression, and provided that non-iris regions are first masked ("Region-of-Interest" isolation) to avoid wasting the image coding budget on non-iris structures. The ROI format has the further advantage that the same algorithms as run on raw images can be used directly on ROI images with no modifications required.
5. Confirmation that polar image coding schemes are harmful for performance and for interoperability. These recommendations about iris image data formats, confirmed by IREX, were adopted by the ISO working group concerned with biometric data interoperability at its meeting in Moscow in July 2009. Thus IREX has already had great impact, achieving its purpose, and the iris data Standard ISO 19794-6 is now one of the most empirical, evidence-based of the various biometric Standards being revised.

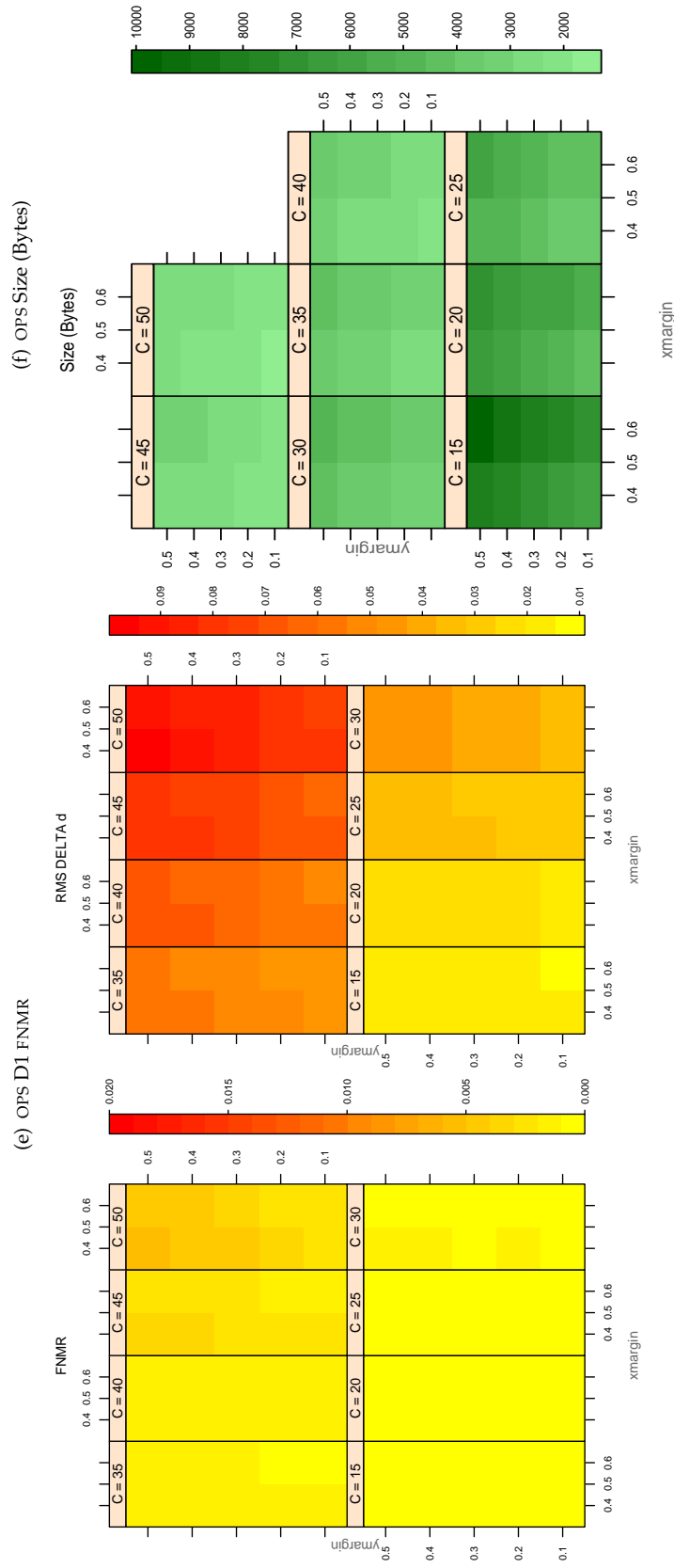


Table 74: For the IREX partition of the OPS database the plots at left show the dependence of cFNMNR on the vertical and horizontal iris cropping margins for various compression ratios. This applies only for KIND 3 records. The margins are in units of iris radius. The use of conditional FNMNR means that the plots exclude comparisons that were falsely rejected even before any compression was applied. On the **right side** is the rms difference between the crop+compress and the uncompressed comparison scores for each image pair. All computations are driven by the bounding box coordinates reported by the II SDK. The number of bits per pixel is $8/C$, where C is the compression ratio. The iris radius varies and because the cropping margins are fixed multiples of the radius the image size varies. The compressed size, in bytes, is the width times height divided by C . Values of cFNMNR greater than 0.02 are shown as 0.02.

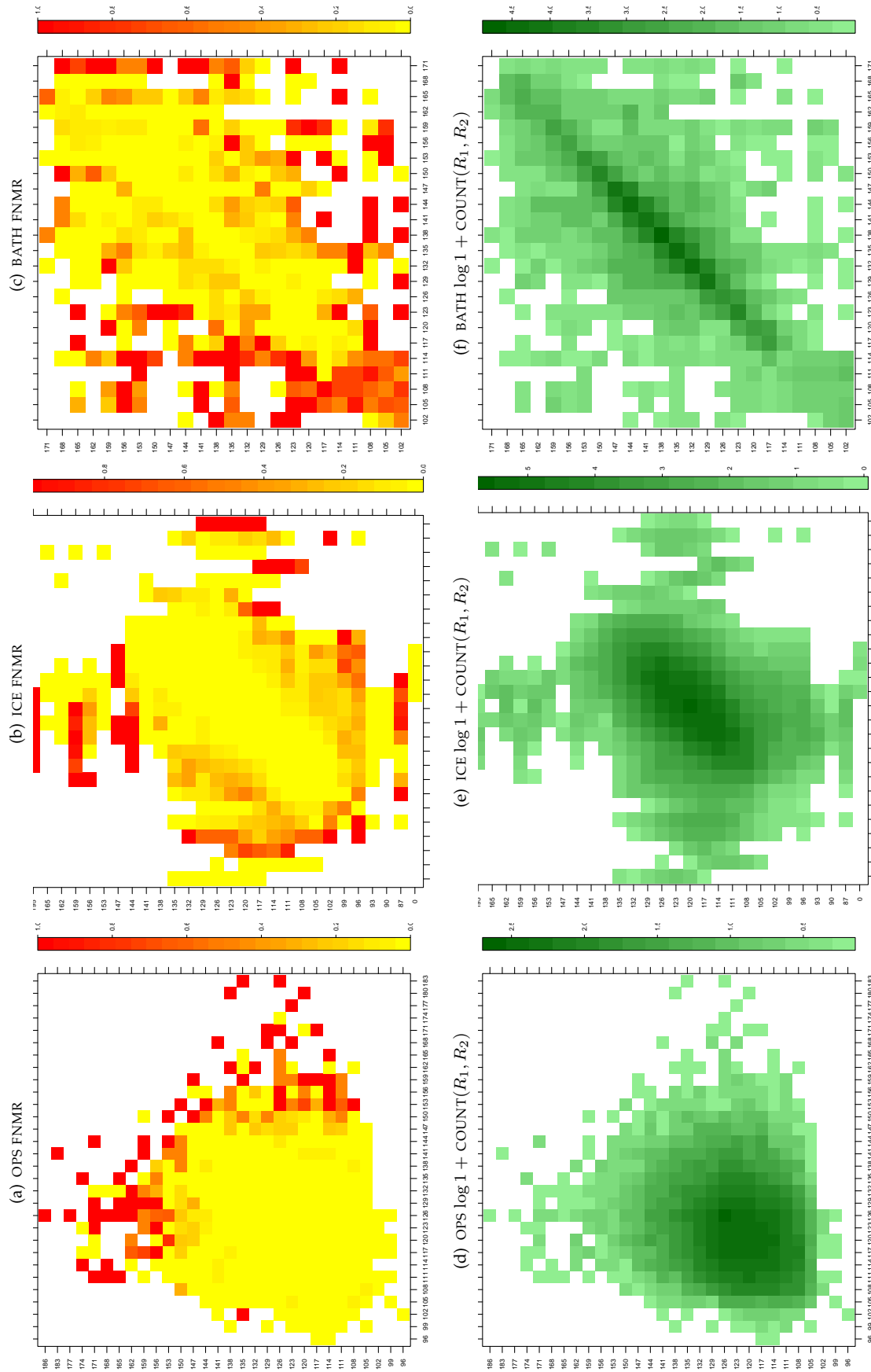


Table 75: For the three IREX databases: In the **top** row the color in each cell represents the occurrence of genuine comparisons with the given pair of radii. The *y*-axis represents enrollment samples with verification samples on the *x*-axis; In the **bottom** row the color scale plots $\log 1 + \text{COUNT}(R_1, R_2)$. The radii are quantized into three-pixel bins. The radii for DOD are on the range $96 \leq r \leq 186$ pixels. The radii for ICE are on the range $87 \leq r \leq 165$ pixels. The radii for BATH are on the range $100 \leq r \leq 170$ pixels.

A = SAGEM	B = COGENT	C = CROSSMATCH	D = CAMBRIDGE	E = L1	$x1$ = PRIMARY
F = RETICA	G = LG	H = HONEYWELL	I = IRITECH	J = NEUROTECHNOLOGY	$x2$ = SECONDARY
KIND 1 = RAW 640x480		KIND 3 = CROP		KIND 7 = CROP+MASK	
KIND 16 = CONCENTRIC POLAR					

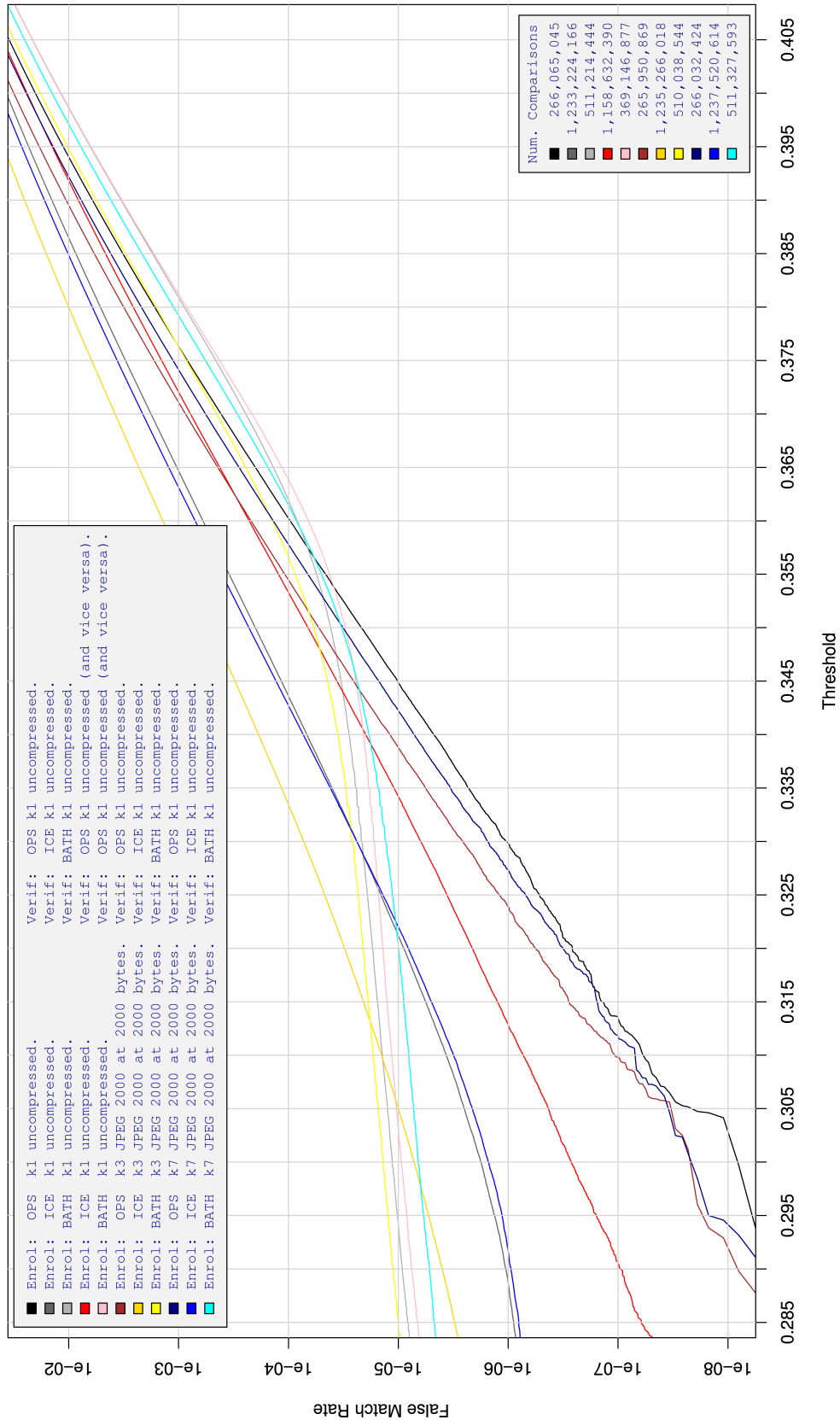


Table 76: For implementation D1, the dependency of FMR on threshold. for various combinations of enrollment and verification dataset, format, and compression.

A = SAGEM	B = COGENT	C = CROSSMATCH	D = CAMBRIDGE	E = L1	x1 = PRIMARY
F = RETICA	G = LG	H = HONEYWELL	I = IRITECH	J = NEUROTECHNOLOGY	x2 = SECONDARY
KIND 1 = RAW 640x480		KIND 3 = CROP	KIND 7 = CROP+MASK	KIND 16 = CONCENTRIC POLAR	

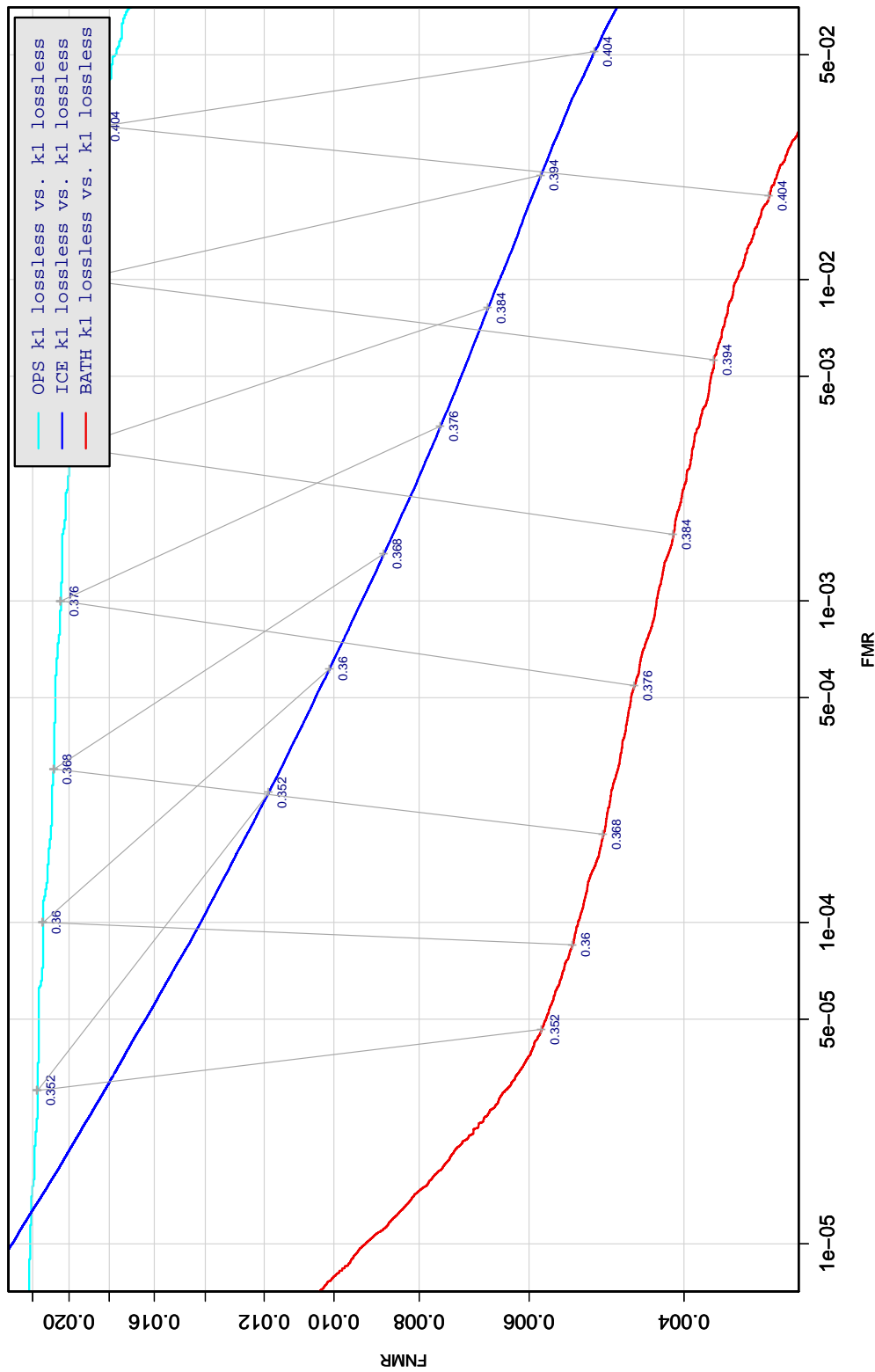


Table 77: DET curve for implementation D1 on three IREX databases. All comparisons are with uncompressed KIND 1 vs. KIND 1 images. The lines join points corresponding to the a fixed threshold. Non-vertical links indicate a change in FMR when the database changes. All results apply to native operation. Failures to produce a template i.e. FTE are ignored because the plots are intended to show *matching* effects, specifically to compare DET slopes and to show the effect of fixing a threshold.

A = SAGEM	B = COGENT	C = CROSSMATCH	D = CAMBRIDGE	E = L1	$x1$ = PRIMARY
F = RETICA	G = LG	H = HONEYWELL	I = IRITECH	J = NEUROTECHNOLOGY	$x2$ = SECONDARY
KIND 1 = RAW 640x480		KIND 3 = CROP	KIND 7 = CROP+MASK	KIND 16 = CONCENTRIC POLAR	

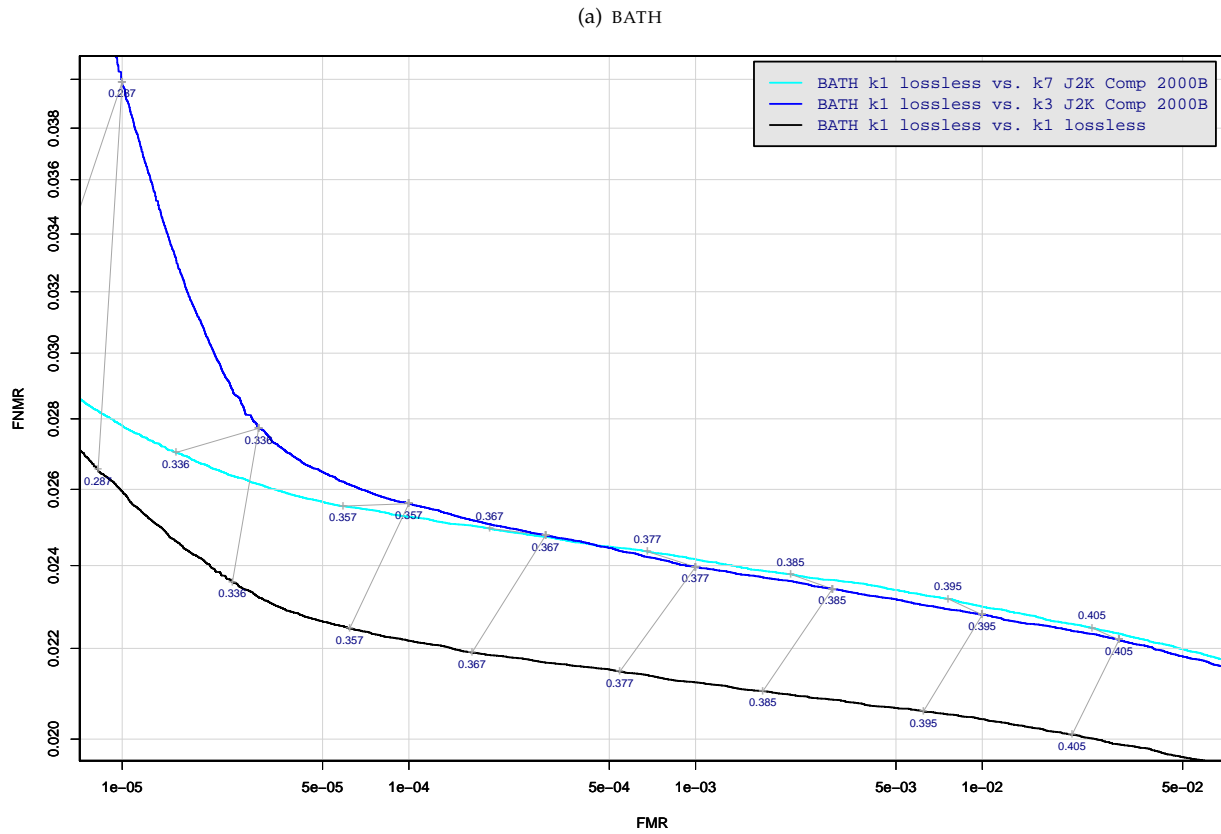


Table 78: DET curve for implementation D1 on the BATH database for the various supported KINDS . The DET characteristics are linked by lines joining points of equal threshold. Non-vertical links indicate a change in false acceptance when the data KIND changes. All results apply to native operation, and the effects of FTE are included.

A = SAGEM	B = COGENT	C = CROSSMATCH	D = CAMBRIDGE	E = L1	x1 = PRIMARY
F = RETICA	G = LG	H = HONEYWELL	I = IRITECH	J = NEUROTECHNOLOGY	x2 = SECONDARY
KIND 1 = RAW 640x480		KIND 3 = CROP		KIND 7 = CROP+MASK	
KIND 16 = CONCENTRIC POLAR					

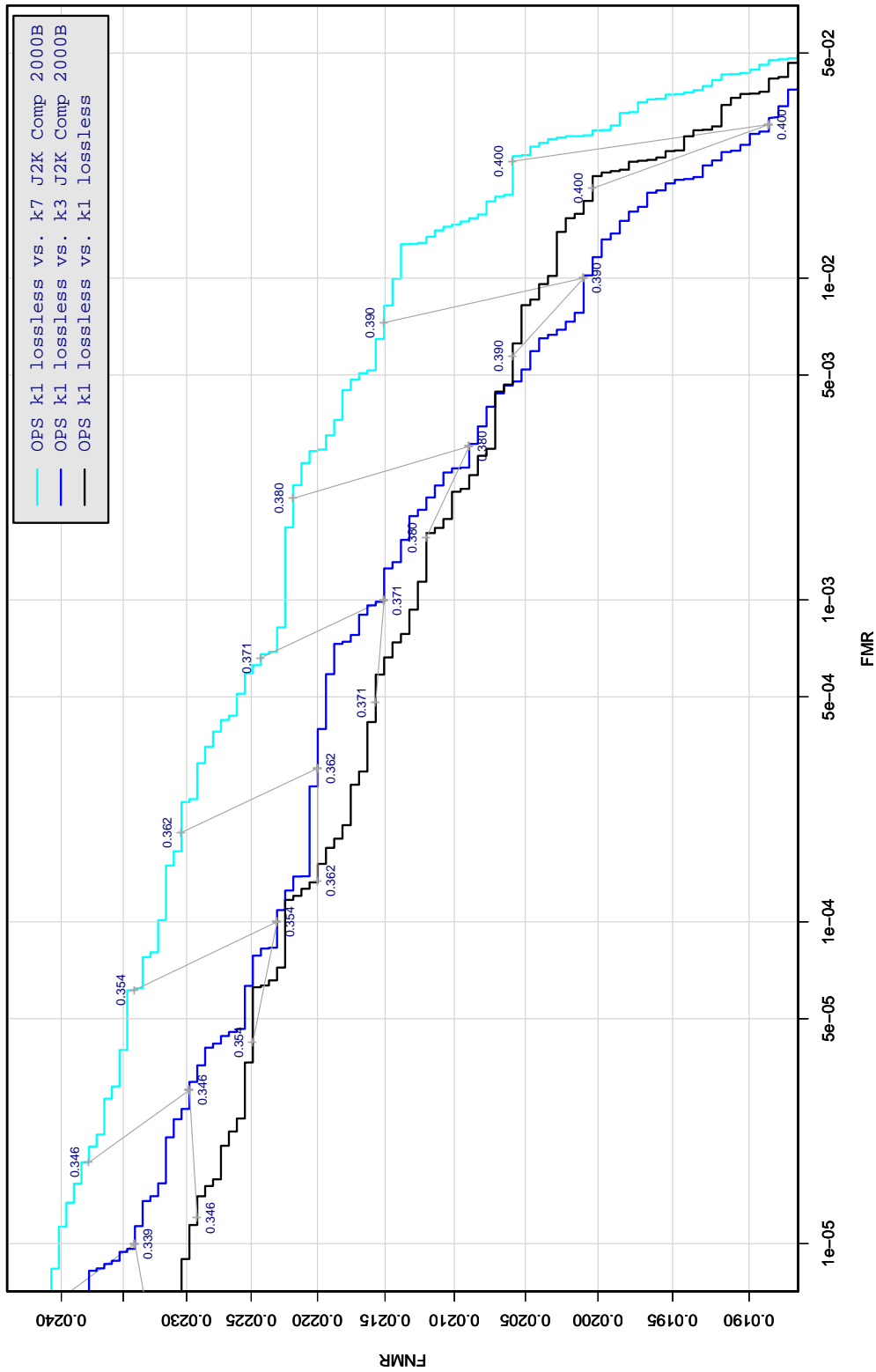


Table 79: DET curve for implementation D1 on the OPS database for the various supported KINDS . The DET characteristics are linked by lines joining points of equal threshold. Non-vertical links indicate a change in false acceptance when the data KIND changes. All results apply to native operation, and the effects of FTE are included.

A = SAGEM	B = COGENT	C = CROSSMATCH	D = CAMBRIDGE	E = L1	x1 = PRIMARY
F = RETICA	G = LG	H = HONEYWELL	I = IRITECH	J = NEUROTECHNOLOGY	x2 = SECONDARY
KIND 1 = RAW 640x480		KIND 3 = CROP	KIND 7 = CROP+MASK	KIND 16 = CONCENTRIC POLAR	

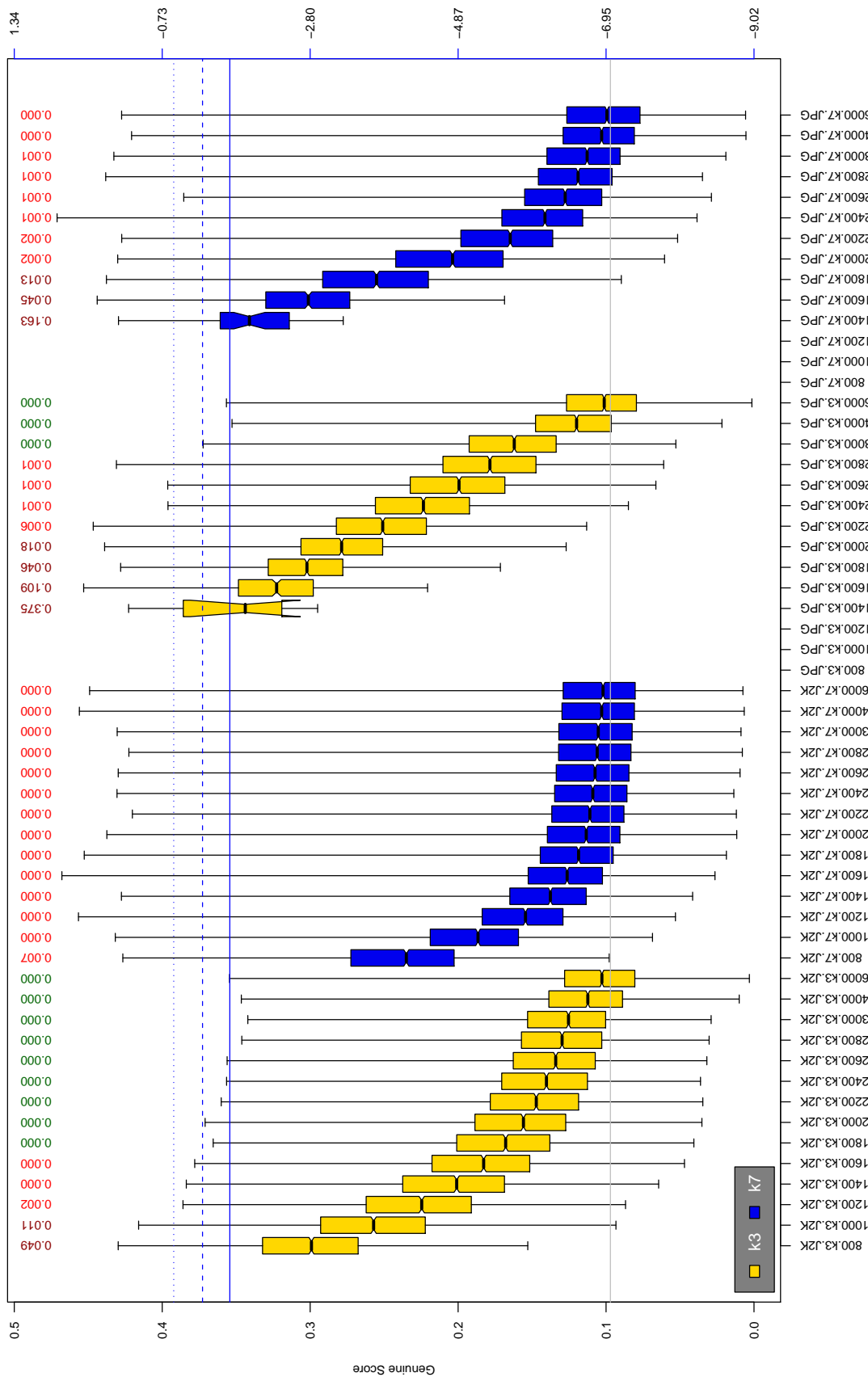


Table 80: The distribution of D1 native genuine comparison scores by size of the compressed image, KIND and the compression algorithm. The images are from the OPS dataset. The right axis scale gives the corresponding value for $d' = (s - \mu_I) / \sqrt{0.5(\sigma_I^2 + \sigma_C^2)}$ for genuine score s . The boxplots only include comparison scores if the uncompressed version of the same image was matched below the FMR = 0.001 threshold. Above the boxplots are FNMR values at FMR = 10^{-3} . The three blue lines correspond, from the top, to FMR of $10^{-2}, -3, -4$. The lower grey line refers to the median score obtained from comparison of uncompressed KIND 3 images. Any comparison for which either template had not been generated is excluded. Note that the iris record size on the horizontal axis is not evenly spaced above 3000 bytes.

A = SAGEM	B = COGENT	C = CROSSMATCH	D = CAMBRIDGE	E = L1	$x1$ = PRIMARY
F = RETICA	G = LG	H = HONEYWELL	I = IRITECH	J = NEUROTECHNOLOGY	$x2$ = SECONDARY
KIND 1 = RAW 640x480		KIND 3 = CROP	KIND 7 = CROP+MASK	KIND 16 = CONCENTRIC POLAR	

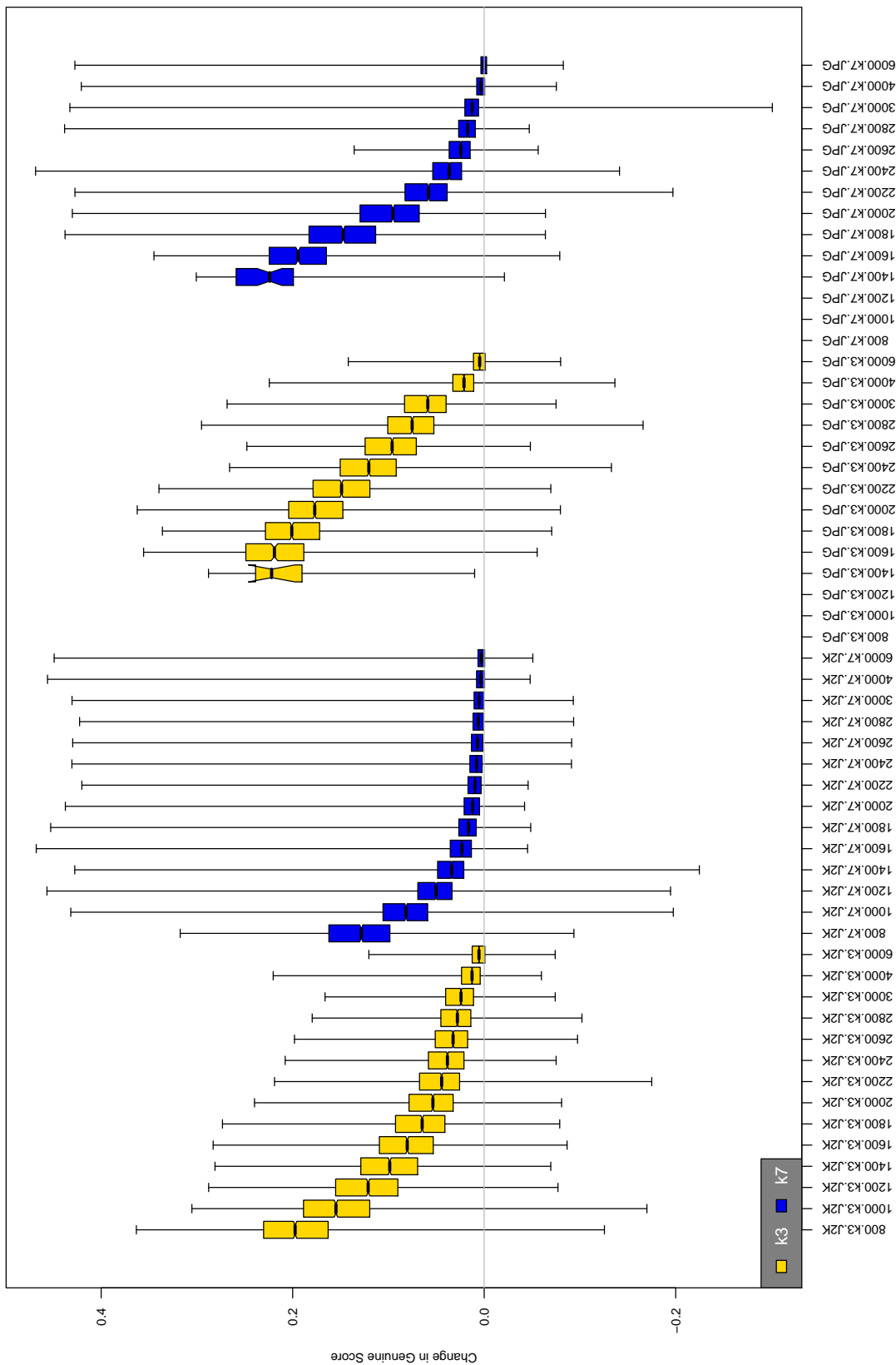


Table 81: The distribution of the *increase* in D1 native genuine comparison scores between the uncompressed “parent” and the compressed image, arranged by size, KIND and the compression algorithm. The images are from the OPS dataset. Any comparison involving a failed template is excluded. Note that the iris record size on the horizontal axis is not evenly spaced above 3000 bytes.

A = SAGEM	B = COGENT	C = CROSSMATCH	D = CAMBRIDGE	E = L1	$x1$ = PRIMARY
F = RETICA	G = LG	H = HONEYWELL	I = IRITECH	J = NEUROTECHNOLOGY	$x2$ = SECONDARY
KIND 1 = RAW 640x480		KIND 3 = CROP	KIND 7 = CROP+MASK	KIND 16 = CONCENTRIC POLAR	

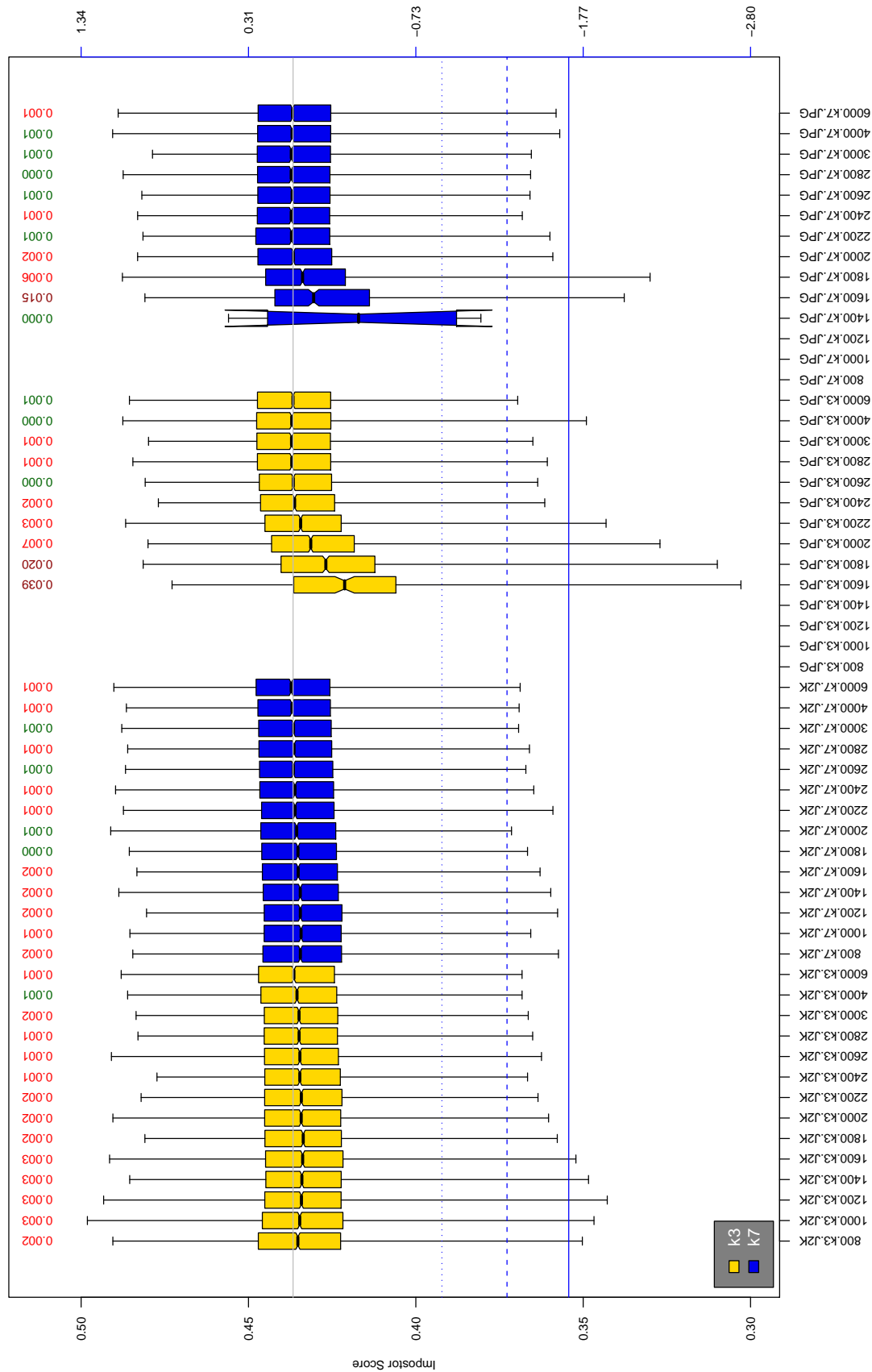


Table 82: The distribution of D1 native impostor comparison scores by size of the compressed image, KIND and the compression algorithm. The right axis scale gives the corresponding value for $d' = (s - \mu_1) / \sqrt{0.5(\sigma_1^2 + \sigma_2^2)}$ for impostor score s . The three blue lines correspond, from the top, to FMR of $10^{-2}, -3, -4$. The lower grey line refers to the median score obtained from comparison of uncompressed KIND 3 images. Any comparison involving a failed template is excluded. Above the boxplots are FMR values at the threshold that gives FMR = 10^{-3} on uncompressed images. These figures are computed from only 4000 comparisons so the FMR values and the tails of the impostor distribution are poorly characterized. Note that the iris record size on the horizontal axis is not evenly spaced above 3000 bytes.

A = SAGEM	B = COGENT	C = CROSSMATCH	D = CAMBRIDGE	E = L1	$x1$ = PRIMARY
F = RETICA	G = LG	H = HONEYWELL	I = IRITECH	J = NEUROTECHNOLOGY	$x2$ = SECONDARY
KIND 1 = RAW 640x480		KIND 3 = CROP	KIND 7 = CROP+MASK	KIND 16 = CONCENTRIC POLAR	

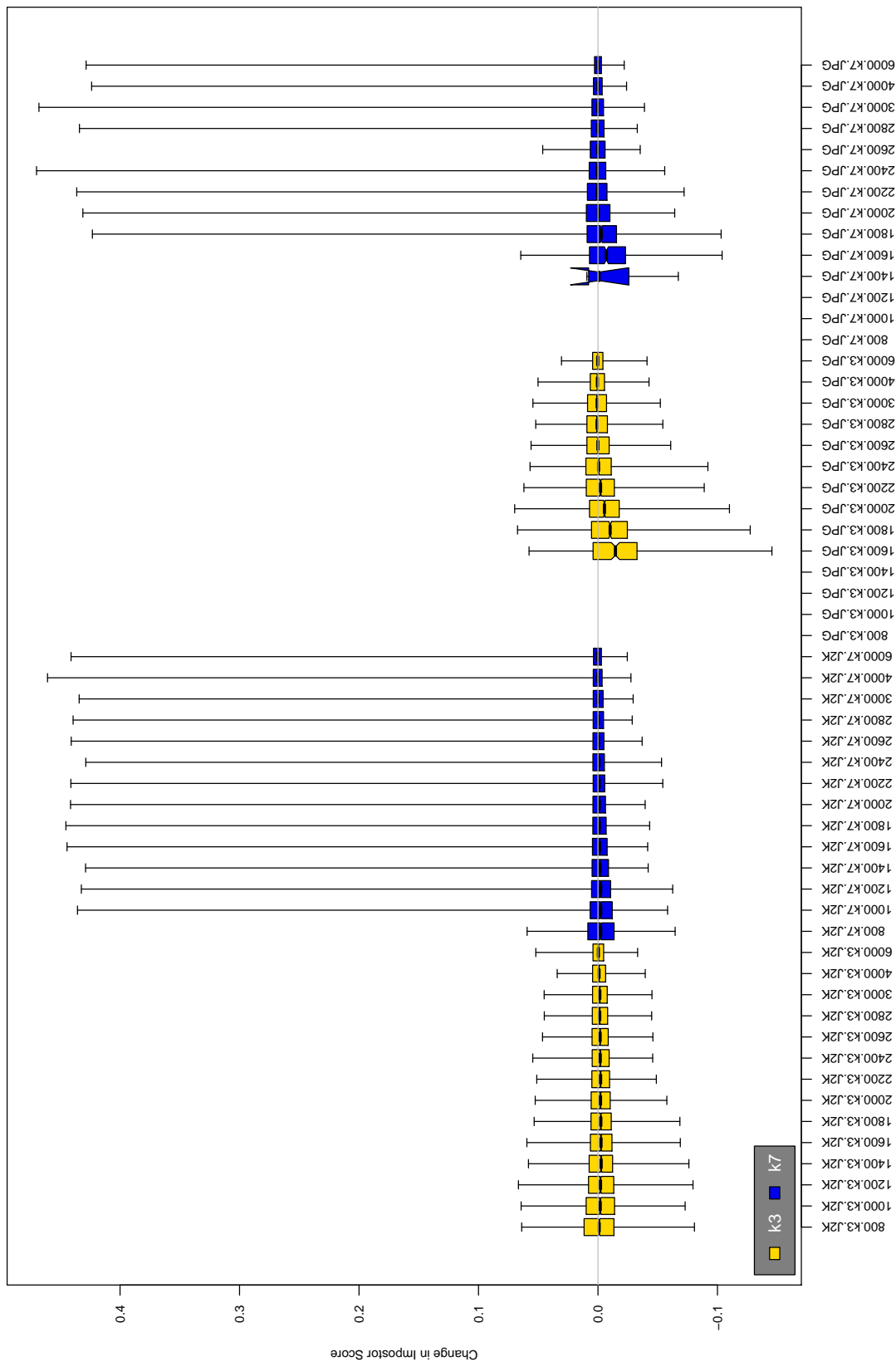


Table 83: The distribution of the increase in D1 native impostor comparison scores between the uncompressed “parent” and the compressed image, arranged by size, KIND and the compression algorithm. The images are from the OPS dataset. Any comparison involving a failed template is excluded. Note that the iris record size on the horizontal axis is not evenly spaced above 3000 bytes.

A = SAGEM	B = COGENT	C = CROSSMATCH	D = CAMBRIDGE	E = L1	x1 = PRIMARY
F = RETICA	G = LG	H = HONEYWELL	I = IRITECH	J = NEUROTECHNOLOGY	x2 = SECONDARY
KIND 1 = RAW 640x480		KIND 3 = CROP	KIND 7 = CROP+MASK	KIND 16 = CONCENTRIC POLAR	

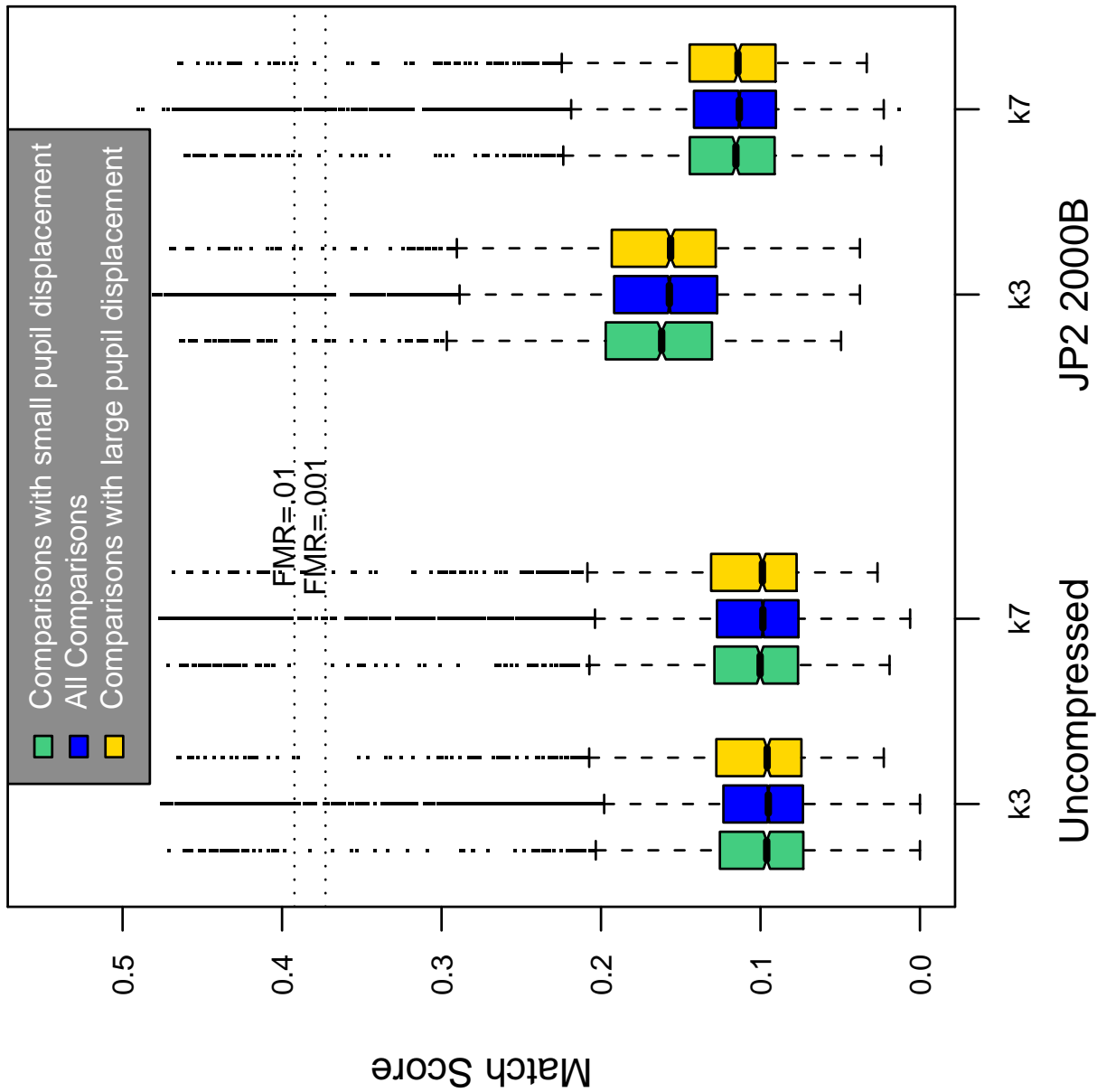


Table 84: Effect of pupil displacement on the genuine score distribution for D1

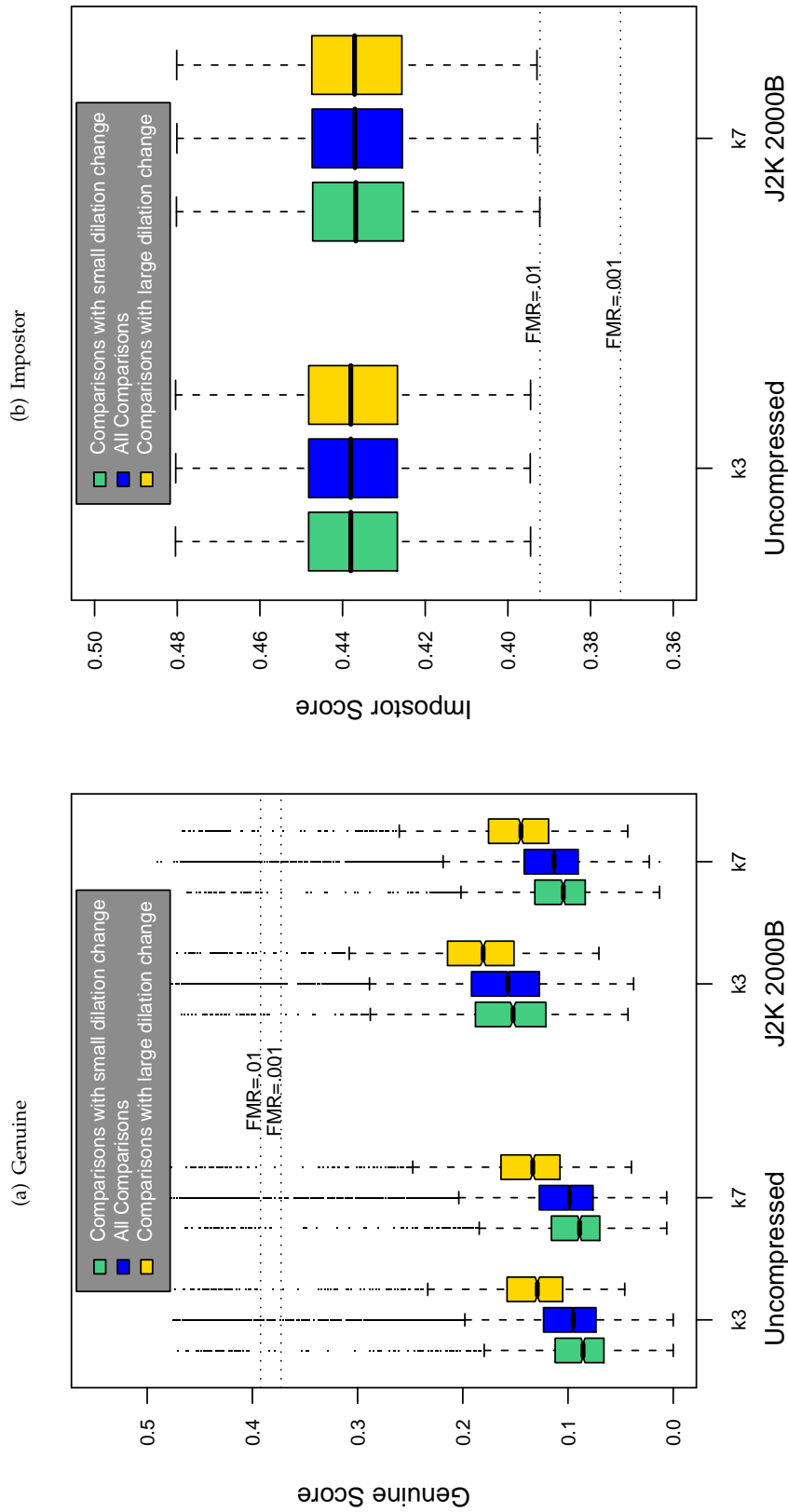


Table 85: The effect of dilation change on the two scores distributions for SDK D1.

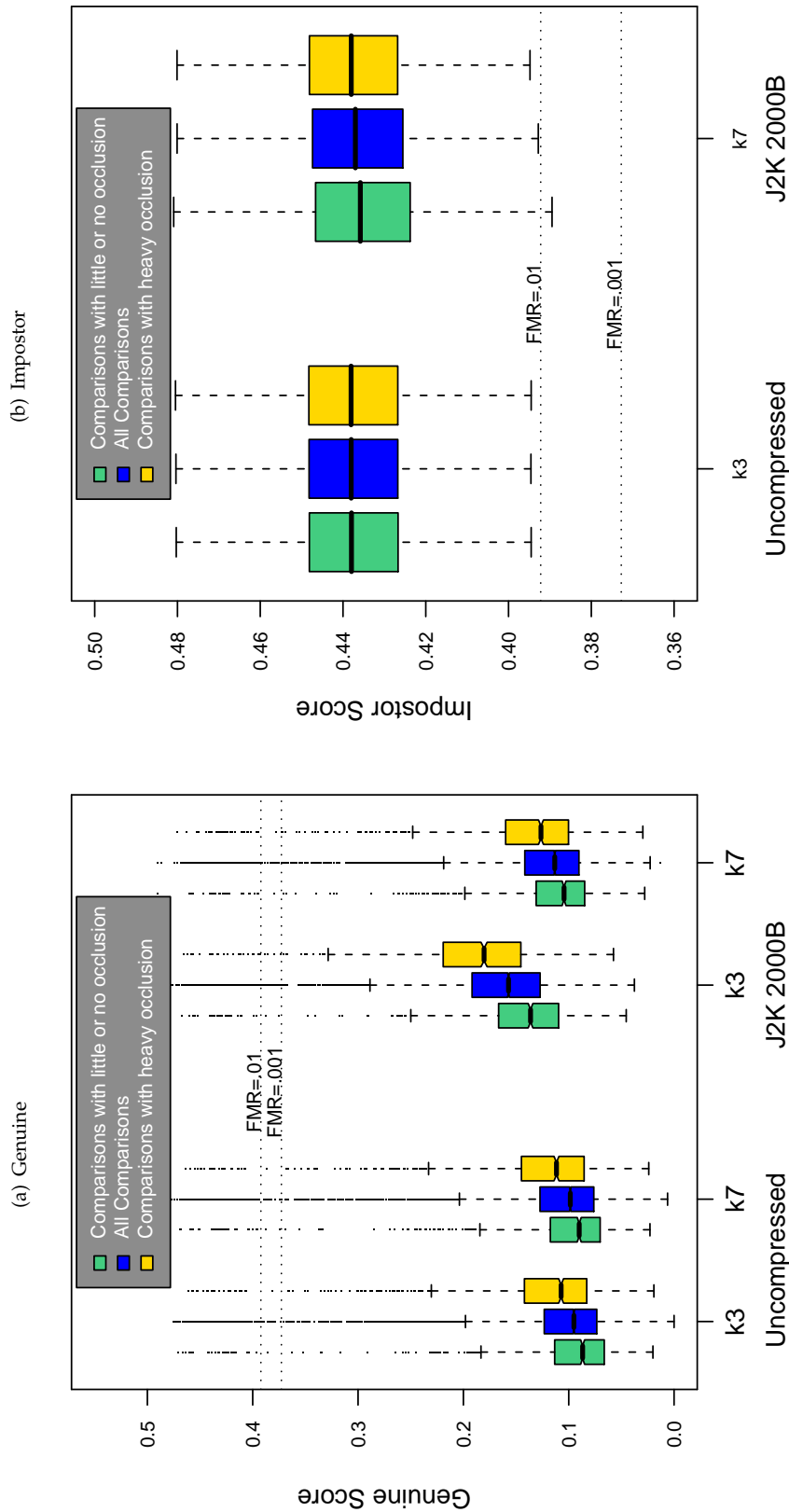
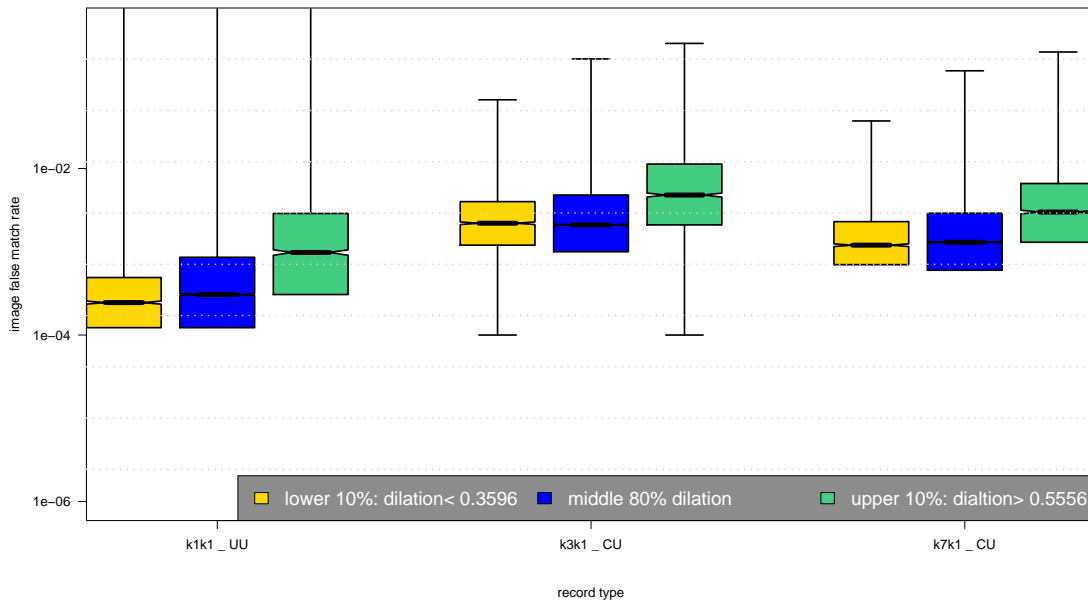
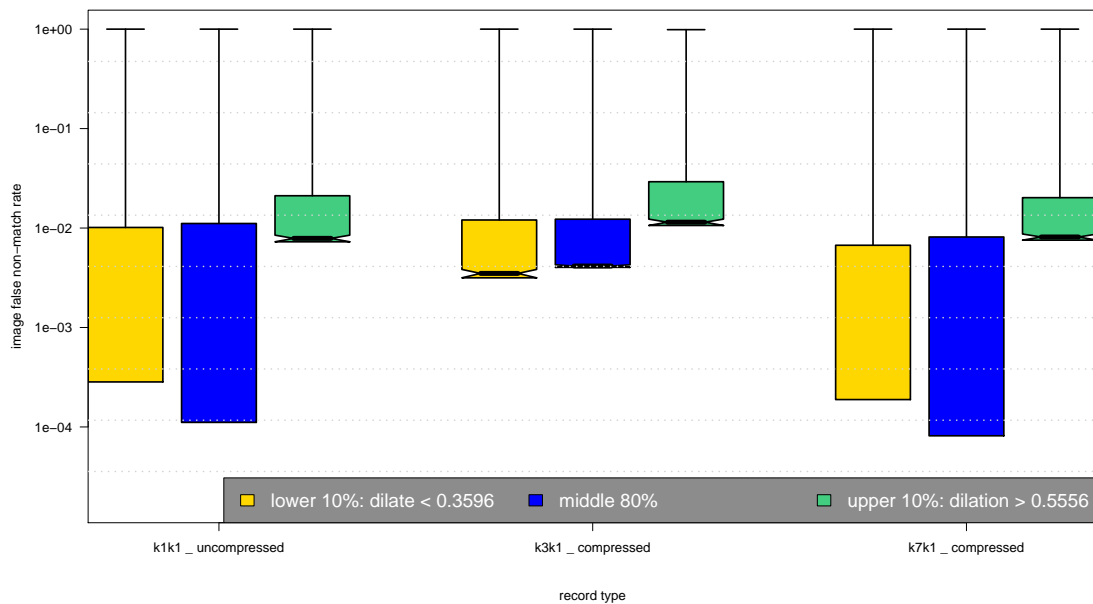


Table 86: The effect of eyelid occlusion on the two scores distributions for SDK D1.

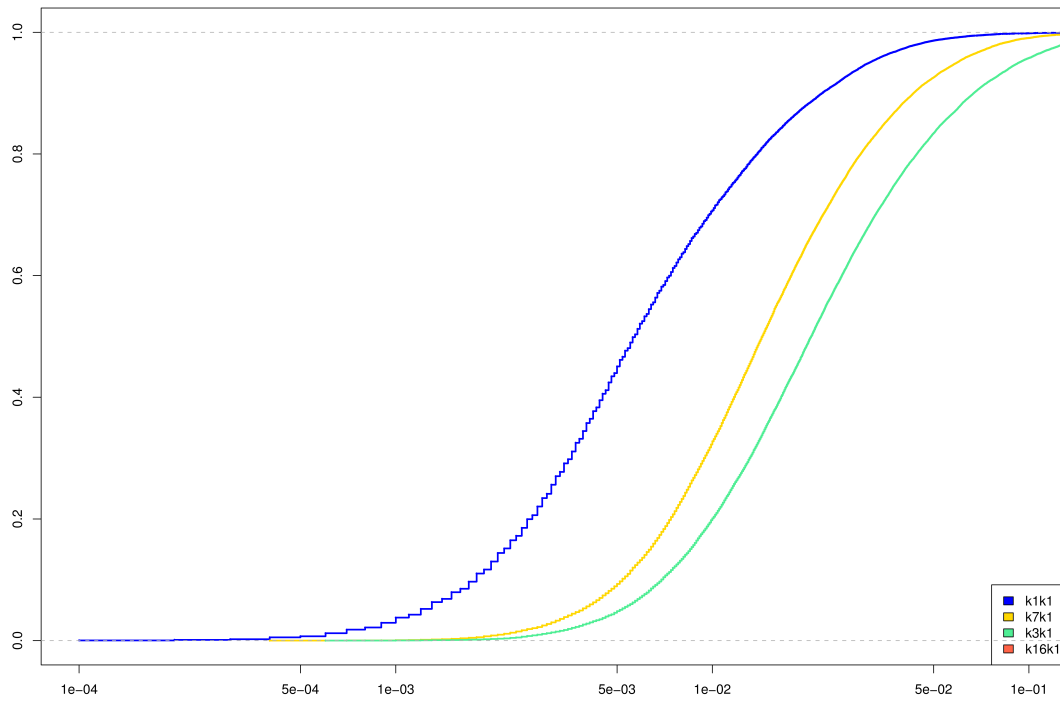
(a) iFMR using A1 dilation estimates



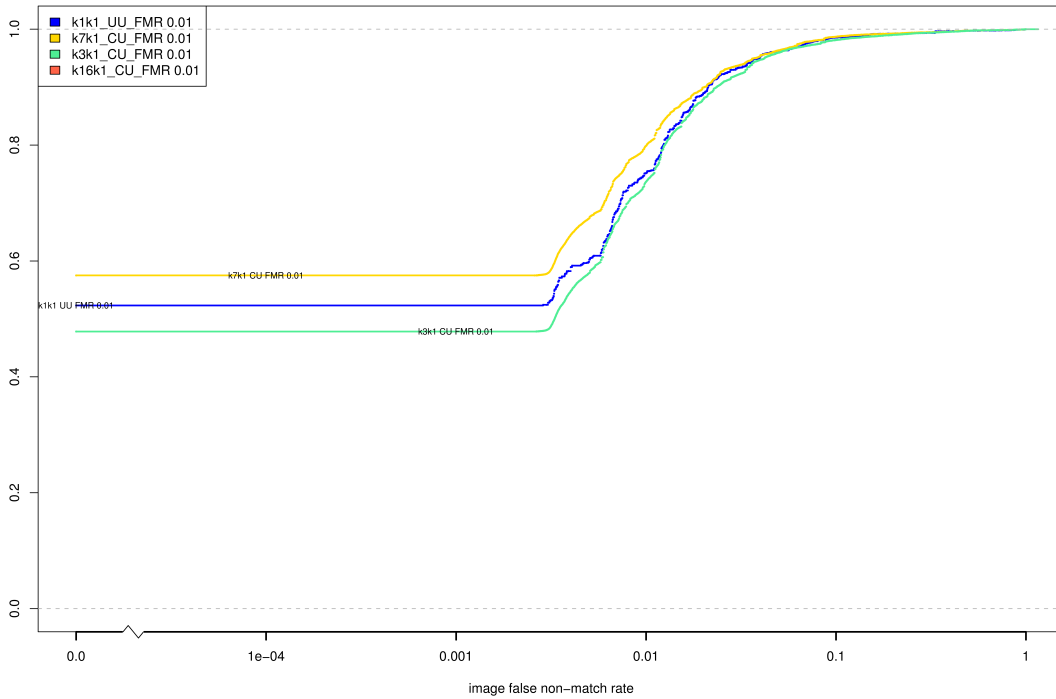
(b) iFNMR using A1 dilation estimates



(c) iFMR CDF



(d) iFNMR CDF



Compiled Results for Implementation D2

On June 25, 2009, NIST invited the IREX participants to submit a description of the SDKs submitted for the IREX effort. The intent was to allow providers to describe and contrast the feature sets, optimization, operational suitability and availability of the primary and secondary SDKs. NIST indicated that any submitted text would appear verbatim (with typesetting) in draft and final versions of the IREX report and that it would be attributed to the organization. This was optional and NIST put no constraints on the content beyond a 600 word limit, and a statement that anything labelled as confidential or proprietary would be omitted.

The provider of SDK D2, Cambridge University, submitted the following to NIST - we are unable to validate this information.

IREX provides a key opportunity to assess, beyond its main focus on image formats and compressibility, the performance of iris recognition at the more demanding False Match Rates in the region of 1 in a million (1.e-6) to 1 in 100 million (1.e-8) for which it was designed and at which it is usually deployed. At least one database in IREX has images from 16,320 different eyes, and so even if only a single image of each eye is used, an Impostors Distribution could be generated comparing 133 million unique pairings of different eyes. If both images of each eye were used, this total would rise to above 500 million. A major shortcoming of ICE was that performance was reported at much less demanding FM rates, since ICE had only 240 Subjects, leading to the bizarre conclusion that iris delivered no better discrimination between persons than face recognition. Cambridge very much hopes that IREX will seize the opportunity to probe and to document the FMR = 1.e-6 to 1.e-8 region of ROC curves, since enough data points are easily available within IREX Impostors Distributions to go that far out along their tails to reach such cumulatives. Otherwise, the distinctive capabilities of iris recognition compared to weaker biometrics may again not be seen.

For the Cambridge SDKs, such demanding FMR regions of ROC curves should correspond to a Hamming Distance threshold in the 0.28 - 0.30 range, where very tiny reductions in threshold yield order-of-magnitude improvements in FMR but at negligible cost to FnMR. Another way to say this is that iris ROC curves (not only those from Cambridge) tend to be very flat: some 3 or 4 orders-of-magnitude are reduced in FMR while the FnMR perhaps only doubles. It is thus misleading to report, as ICE did for example, that iris FnMR in the 0.01 range is achieved at an FMR of 0.001, when the same result can also be cited at an FMR of 1 in a million. All ROC curves must converge into the two corners along the diagonal (in linear coordinates), so if one reports accuracy at undemanding rates like FMR = 0.001 then one should conclude that the length of a Subject's big toe is as good as any other biometric.

The SDKs from Cambridge differed from those used in airports and other large public deployments (as licensed from L-1 to licensees) in two main respects: (1) entropy increase; (2) score normalisation. The flatness of an ROC/DET curve depends on the narrowness of the Impostors Distribution (rapid attenuation of its tail), and this in turn depends on the entropy captured by the code (the number of degrees-of-freedom, or amount of random variation, expressed across a population). Cambridge Primary (PID=60541) encodes 1,536 bytes including mask; corrects for gaze deviation (off-axis capture); explores a narrow range of image tilts; but does not do score normalisation to enforce tail attenuation. When computing Quality Scores, it does not consider aspects of the IrisCode template. Cambridge Secondary (PID=60540) makes a smaller template (1,024 bytes including mask); does consider aspects of the template in assessing Quality (thus expending time for template creation even when only producing an image Record); detects and corrects for deviated gaze; explores a wider range of image tilts; and does perform score normalisation. Both SDKs search for the iris over the entire frame of a raw image, out to its four edges, to allow for the cases seen in ICE of some irises

hanging partly outside of the image frame. Both SDKs employ active contours for deformable iris mappings, and quadrature (complex wavelet) encodings.

On August 17, 2009, NIST invited the IREX participants to submit a description their comments on a draft version of the IREX report. This was intended to allow participants to assist readers in the interpretation of a large and complicated testing effort. NIST indicated that any submitted text would appear verbatim (with typesetting) in the final version of the IREX report and that it would be attributed to the organization. Submission of content was optional and NIST put no constraints on the content beyond a word limit, and a statement that anything labelled as confidential or proprietary would be omitted.

The provider of SDK D2, Cambridge University, submitted the following to NIST - we make no comment on this information.

Cambridge comments (using Table and Figure numbers from 3 July draft): _____

The search for an iris in the image frame (or partly outside it as in some public ICE images), and the segmentation of iris boundaries, by the Cambridge SDKs (D1 D2) covered an iris size search range of from 70 pixels to 140 pixels in radius. This range of 2:1 in size was assumed generous enough and was chosen to accommodate the tendency towards iris cameras with less zoom, or acquiring at a greater distance, with typical iris radius perhaps 100 pixels. This choice of iris size search range matched the public part of the ICE gallery, whose mean iris radius is 119, std_dev 5.3 pixels, and in which the maximum iris radius is only 136 pixels. But our choice was clearly a mistake, as the iris radius in OPS images went up to 186 pixels, and up to 170 pixels in the BATH dataset. Iris sizes in the public ICE gallery are thus not representative of the size ranges tested in IREX. (This is not a criticism of IREX. But whatever percentage of sizes, say 2 percent, are outside the presumed range will become irreducible offsets to FnMR curves for SDKs making such assumptions.) Figure 4d ("heat plots" for FnMR versus iris radius) and Tables 84(a) and 98(a) show that almost all Failures-to-Match by the Cambridge SDKs occurred for iris radius values above 140 pixels, which was the size cut-off of our 2:1 size search range. These could have been avoided if Cambridge had made a better guess about size range than 70 - 140 pixels radius.

Nonetheless it is valuable and gratifying that IREX has confirmed several Cambridge claims published in the academic literature:

1. Astronomic attenuation of False Match Rates from minuscule reductions in Hamming Distance threshold: Table 14 shows that for cross-dataset comparisons (bottom red curve), False Match Rate reaches 1 in 100 million at HD = 0.315 and attenuates at a rate of a further factor of 10 for each additional reduction of 0.01 in the HD threshold, exactly as has been published. See also tabulations in Table 15. Many doubted these claims.
2. Confirmation of great speed in template creation and in matching, although IREX also shows valuably that False nonMatch Rates can be improved when match speed is reduced by two orders-of-magnitude, as may be tolerated in 1-to-1 verification applications.
3. Confirmation of the stability of the distribution of Imposters scores, regardless of almost every image manipulation, including variations in presentation. This was also confirmed for nearly all of the algorithms submitted. This observation is important for the credibility of iris recognition generally, as it allows extrapolation to large-scale database search, and prediction of performance as a function of decision threshold.

4. Confirmation that iris images can be severely compressed to as little as 2,000 bytes with little impact on performance, provided that JP2K is used instead of JPEG compression, and provided that non-iris regions are first masked ("Region-of-Interest" isolation) to avoid wasting the image coding budget on non-iris structures. The ROI format has the further advantage that the same algorithms as run on raw images can be used directly on ROI images with no modifications required.
5. Confirmation that polar image coding schemes are harmful for performance and for interoperability. These recommendations about iris image data formats, confirmed by IREX, were adopted by the ISO working group concerned with biometric data interoperability at its meeting in Moscow in July 2009. Thus IREX has already had great impact, achieving its purpose, and the iris data Standard ISO 19794-6 is now one of the most empirical, evidence-based of the various biometric Standards being revised.

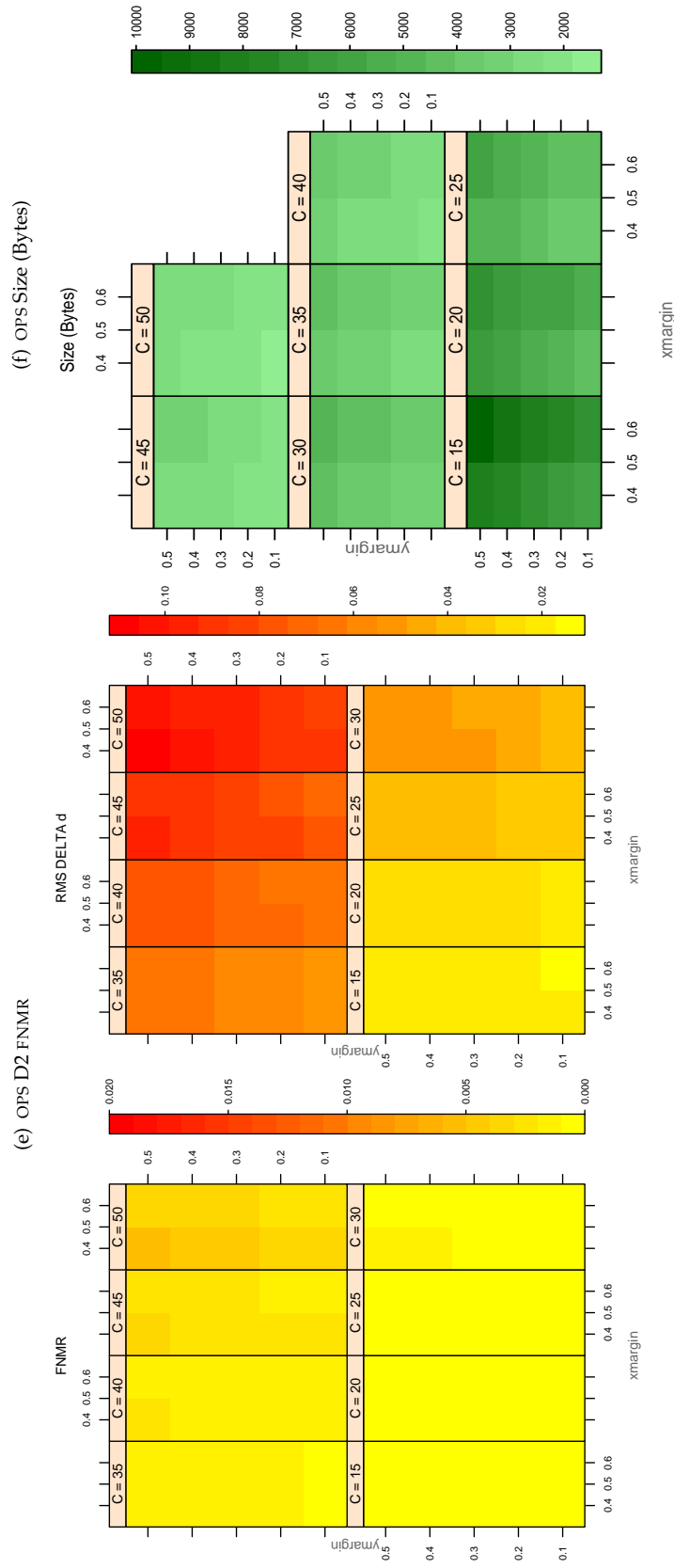


Table 87: For the IREX partition of the OPS database the plots at left show the dependence of cFNMR on the vertical and horizontal iris cropping margins for various compression ratios. This applies only for KIND 3 records. The margins are in units of iris radius. The use of conditional FNMR means that the plots exclude comparisons that were falsely rejected even before any compression was applied. On the **right side** is the rms difference between the crop+compress and the uncompressed comparison scores for each image pair. All computations are driven by the bounding box coordinates reported by the II SDK. The number of bits per pixel is $8/C$, where C is the compression ratio. The iris radius varies and because the cropping margins are fixed multiples of the radius the image size varies. The compressed size, in bytes, is the width times height divided by C . Values of cFNMR greater than 0.02 are shown as 0.02.

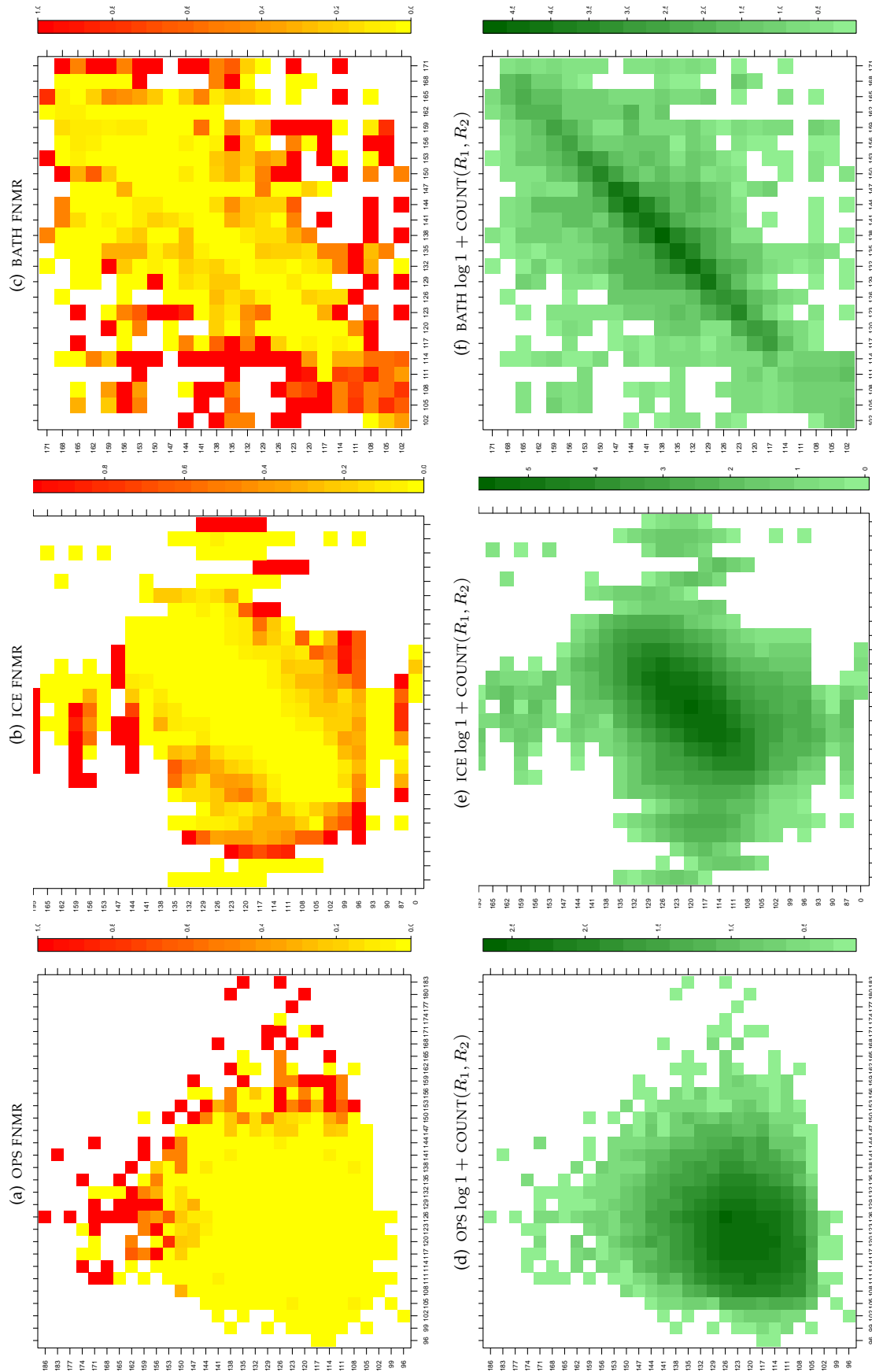


Table 88: For the three IREX databases: In the **top** row the color in each cell represents the occurrence of genuine comparisons with the given pair of radii. The *y*-axis represents enrollment samples with verification samples on the *x*-axis; In the **bottom** row the color scale plots $\log 1 + \text{COUNT}(R_1, R_2)$. The radii are quantized into three-pixel bins. The radii for DOD are on the range $96 \leq r \leq 186$ pixels. The radii for ICE are on the range $87 \leq r \leq 165$ pixels. The radii for BATH are on the range $100 \leq r \leq 170$ pixels.

A = SAGEM	B = COGENT	C = CROSSMATCH	D = CAMBRIDGE	E = L1	$x1 = \text{PRIMARY}$
F = RETICA	G = LG	H = HONEYWELL	I = IRITECH	J = NEUROTECHNOLOGY	$x2 = \text{SECONDARY}$
KIND 1 = RAW 640x480		KIND 3 = CROP	KIND 7 = CROP+MASK	KIND 16 = CONCENTRIC POLAR	

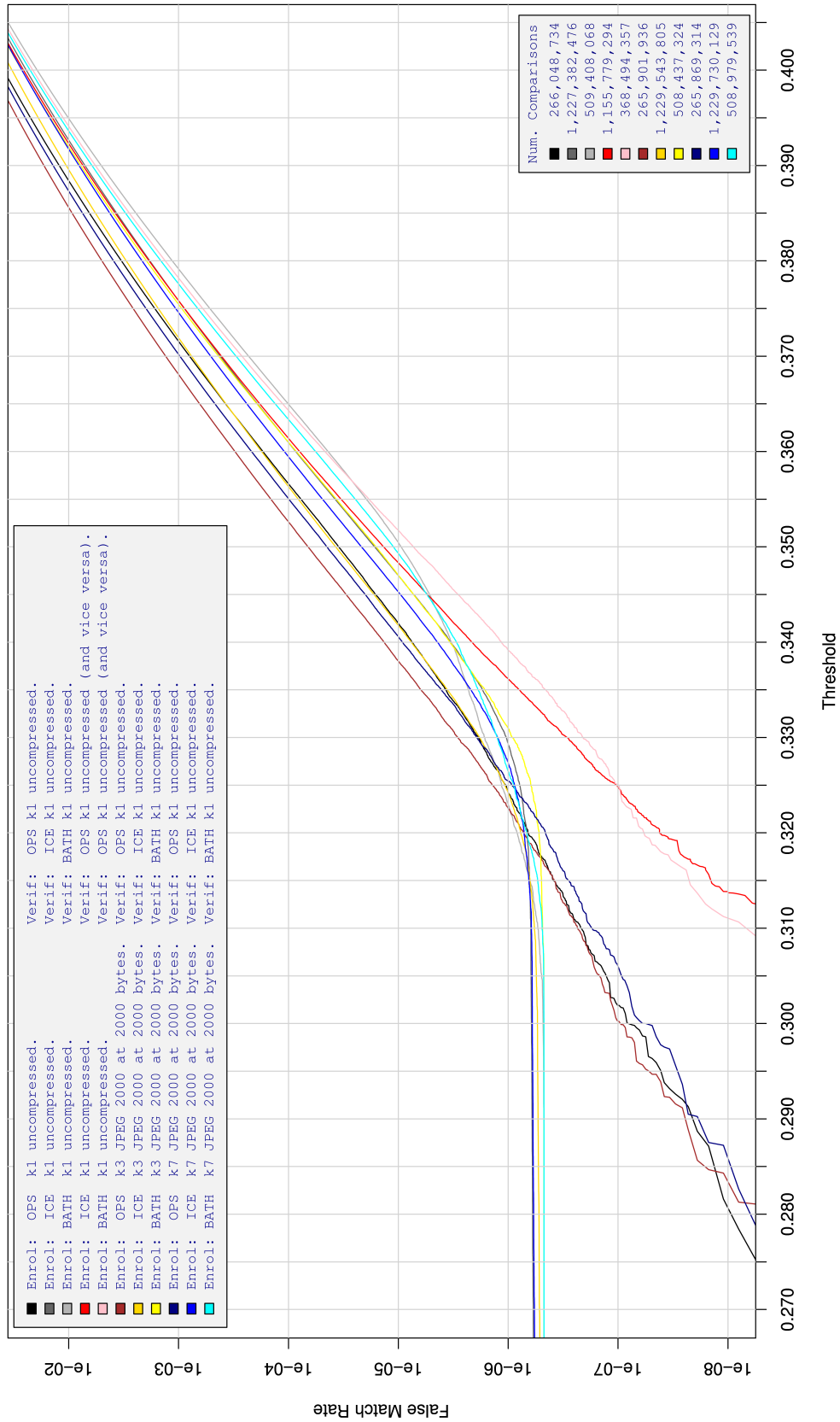


Table 89: For implementation D2, the dependency of FMR on threshold. for various combinations of enrollment and verification dataset, format, and compression.

A = SAGEM	B = COGENT	C = CROSSMATCH	D = CAMBRIDGE	E = L1	x1 = PRIMARY
F = RETICA	G = LG	H = HONEYWELL	I = IRITECH	J = NEUROTECHNOLOGY	x2 = SECONDARY
KIND 1 = RAW 640x480		KIND 3 = CROP	KIND 7 = CROP+MASK	KIND 16 = CONCENTRIC POLAR	

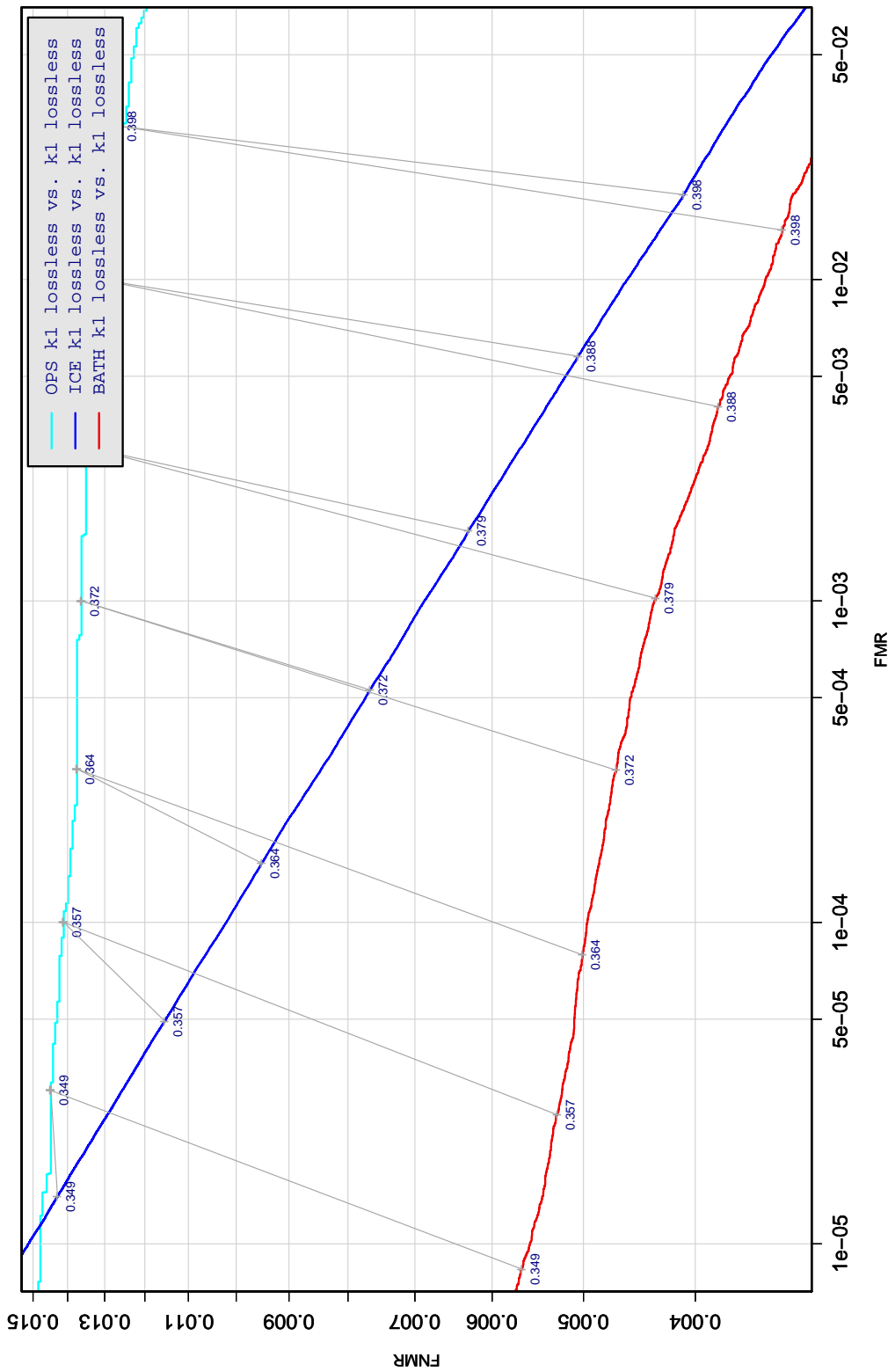


Table 90: DET curve for implementation D2 on three IREX databases. All comparisons are with uncompressed KIND 1 vs. KIND 1 images. The lines join points corresponding to the a fixed threshold. Non-vertical links indicate a change in FMR when the database changes. All results apply to native operation. Failures to produce a template i.e. FTE are ignored because the plots are intended to show *matching* effects, specifically to compare DET slopes and to show the effect of fixing a threshold.

A = SAGEM	B = COGENT	C = CROSSMATCH	D = CAMBRIDGE	E = L1	$x1$ = PRIMARY
F = RETICA	G = LG	H = HONEYWELL	I = IRITECH	J = NEUROTECHNOLOGY	$x2$ = SECONDARY
KIND 1 = RAW 640x480		KIND 3 = CROP	KIND 7 = CROP+MASK	KIND 16 = CONCENTRIC POLAR	

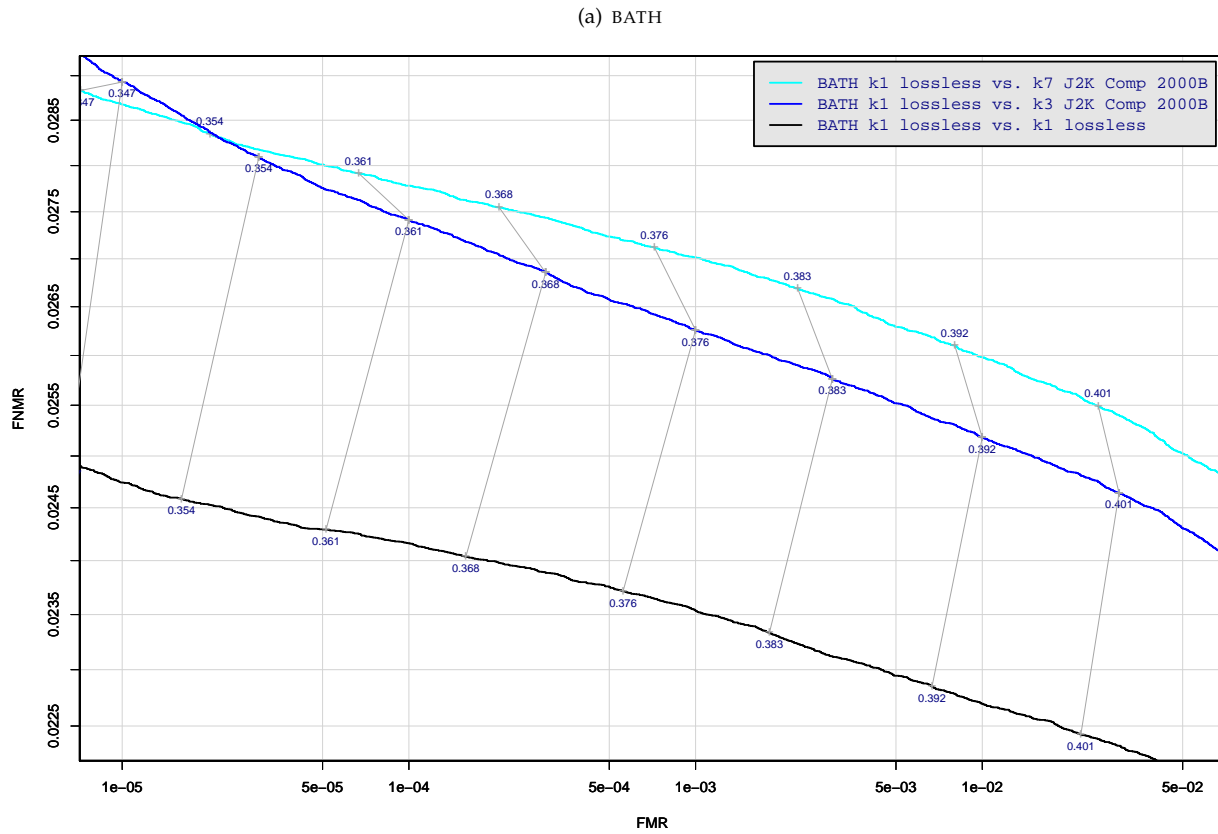


Table 91: DET curve for implementation D2 on the BATH database for the various supported KINDS . The DET characteristics are linked by lines joining points of equal threshold. Non-vertical links indicate a change in false acceptance when the data KIND changes. All results apply to native operation, and the effects of FTE are included.

A = SAGEM	B = COGENT	C = CROSSMATCH	D = CAMBRIDGE	E = L1	x1 = PRIMARY
F = RETICA	G = LG	H = HONEYWELL	I = IRITECH	J = NEUROTECHNOLOGY	x2 = SECONDARY
KIND 1 = RAW 640x480		KIND 3 = CROP	KIND 7 = CROP+MASK	KIND 16 = CONCENTRIC POLAR	

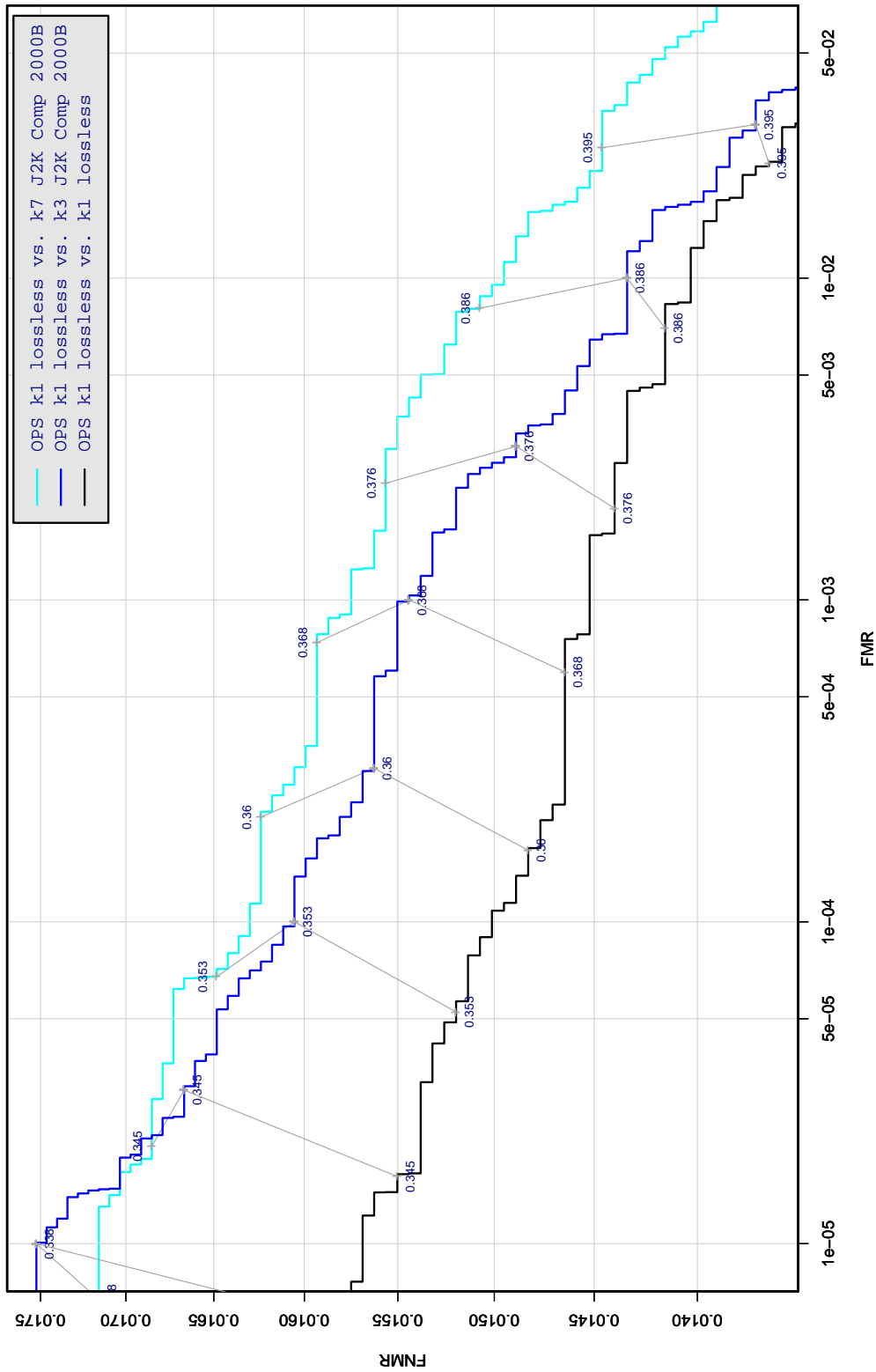


Table 92: DET curve for implementation D2 on the OPS database for the various supported KINDS . The DET characteristics are linked by lines joining points of equal threshold. Non-vertical links indicate a change in false acceptance when the data KIND changes. All results apply to native operation, and the effects of FTE are included.

A = SAGEM	B = COGENT	C = CROSSMATCH	D = CAMBRIDGE	E = L1	$x1$ = PRIMARY
F = RETICA	G = LG	H = HONEYWELL	I = IRITECH	J = NEUROTECHNOLOGY	$x2$ = SECONDARY
KIND 1 = RAW 640x480		KIND 3 = CROP	KIND 7 = CROP+MASK	KIND 16 = CONCENTRIC POLAR	

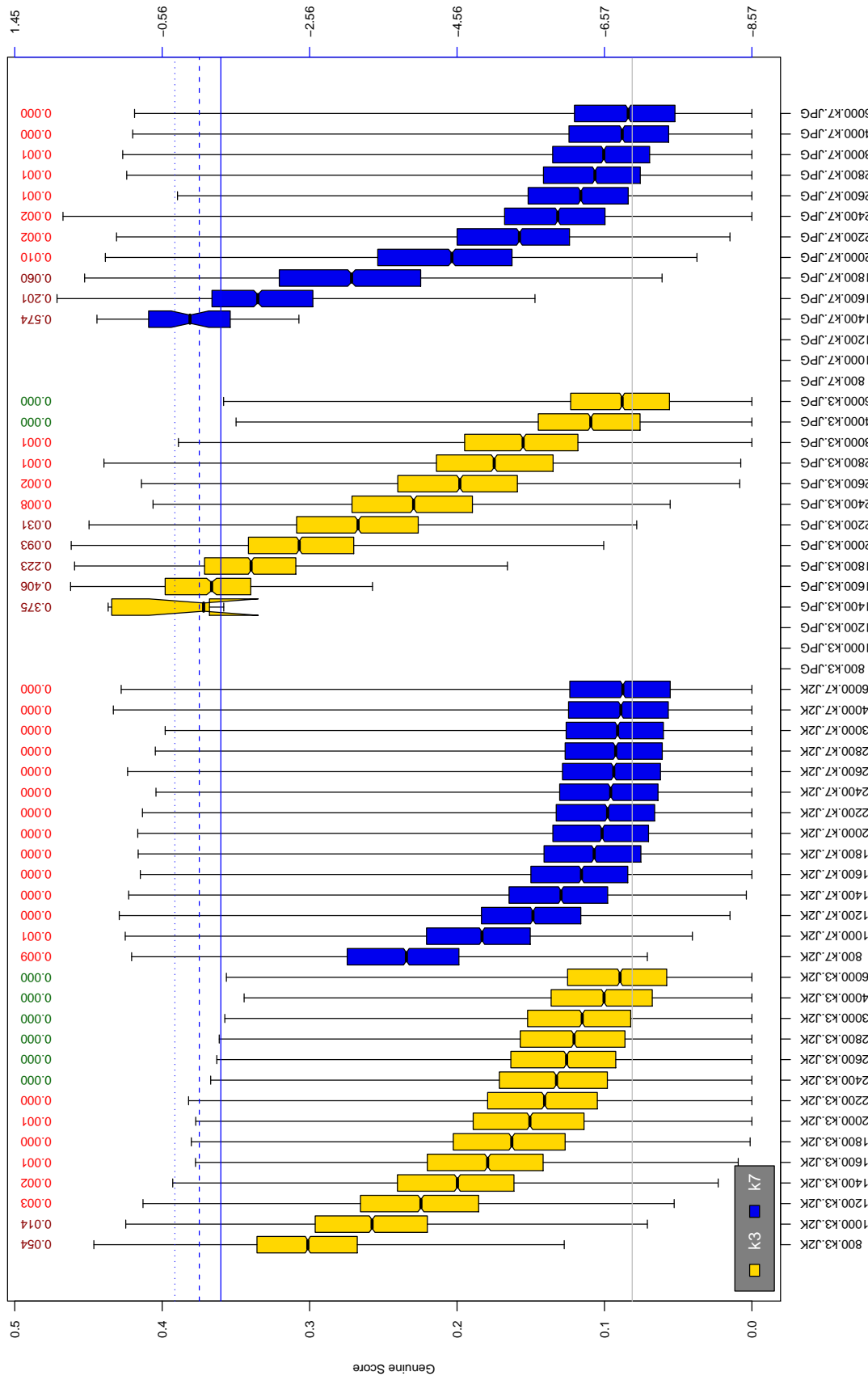


Table 93: The distribution of D2 native genuine comparison scores by size of the compressed image, KIND and the compression algorithm. The images are from the OPS dataset. The right axis scale gives the corresponding value for $d' = (s - \mu_I) / \sqrt{0.5(\sigma_I^2 + \sigma_C^2)}$ for genuine score s . The boxplots only include comparison scores if the uncompressed version of the same image was matched below the FMR = 0.001 threshold. Above the boxplots are FNMR values at FMR = 10^{-3} . The three blue lines correspond, from the top, to FMR of 10^{-2} , 10^{-3} , 10^{-4} . The lower grey line refers to the median score obtained from comparison of uncompressed KIND 3 images. Any comparison for which either template had not been generated is excluded. Note that the iris record size on the horizontal axis is not evenly spaced above 3000 bytes.

A = SAGEM	B = COGENT	C = CROSSMATCH	D = CAMBRIDGE	E = L1	$x1$ = PRIMARY
F = RETICA	G = LG	H = HONEYWELL	I = IRITECH	J = NEUROTECHNOLOGY	$x2$ = SECONDARY
KIND 1 = RAW 640x480		KIND 3 = CROP	KIND 7 = CROP+MASK	KIND 16 = CONCENTRIC POLAR	

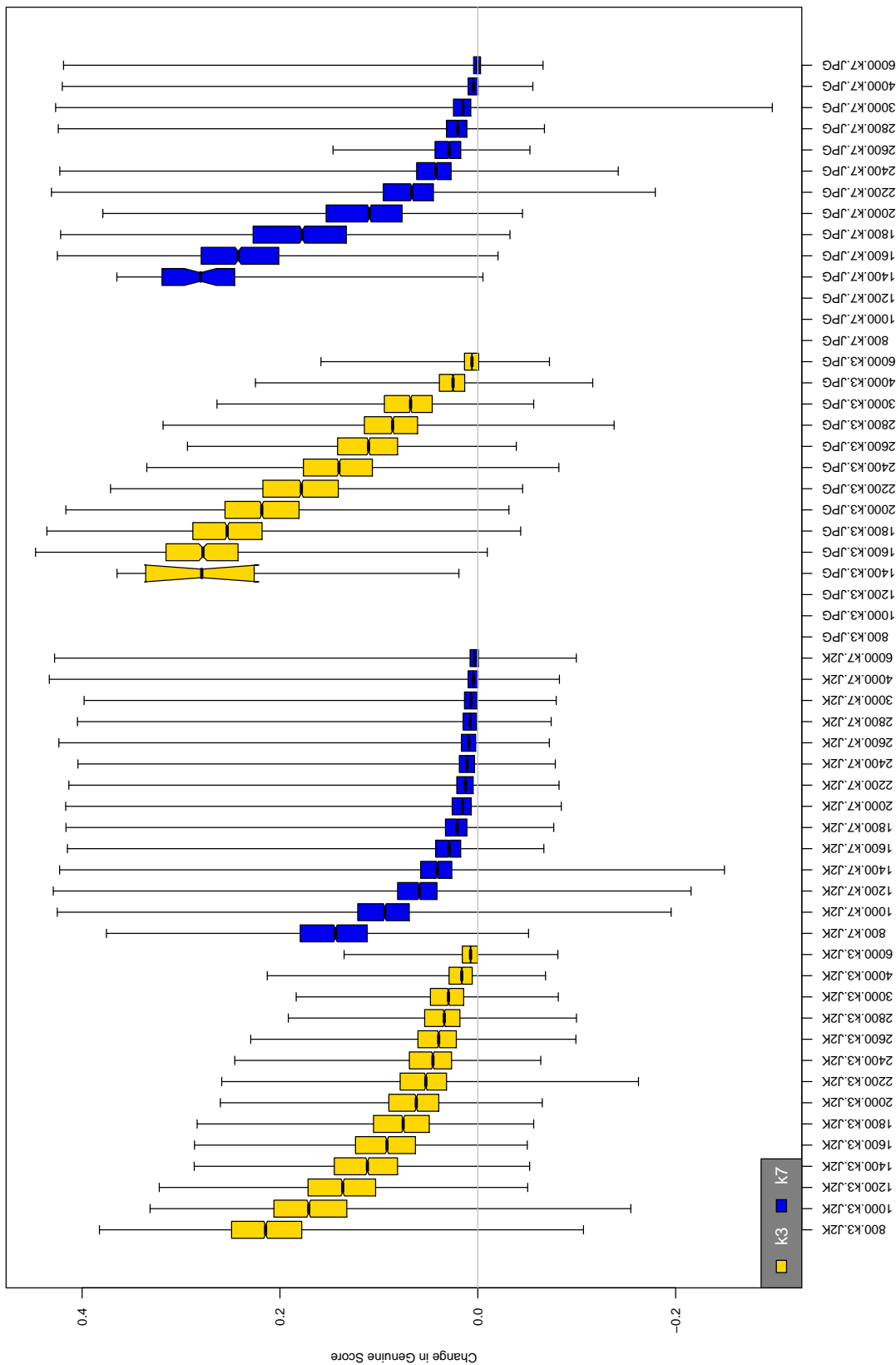


Table 94: The distribution of the *increase* in D2 native genuine comparison scores between the uncompressed “parent” and the compressed image, arranged by size, KIND and the compression algorithm. The images are from the OPS dataset. Any comparison involving a failed template is excluded. Note that the iris record size on the horizontal axis is not evenly spaced above 3000 bytes.

A = SAGEM	B = COGENT	C = CROSSMATCH	D = CAMBRIDGE	E = L1	$x1$ = PRIMARY
F = RETICA	G = LG	H = HONEYWELL	I = IRITECH	J = NEUROTECHNOLOGY	$x2$ = SECONDARY
KIND 1 = RAW 640x480		KIND 3 = CROP	KIND 7 = CROP+MASK	KIND 16 = CONCENTRIC POLAR	

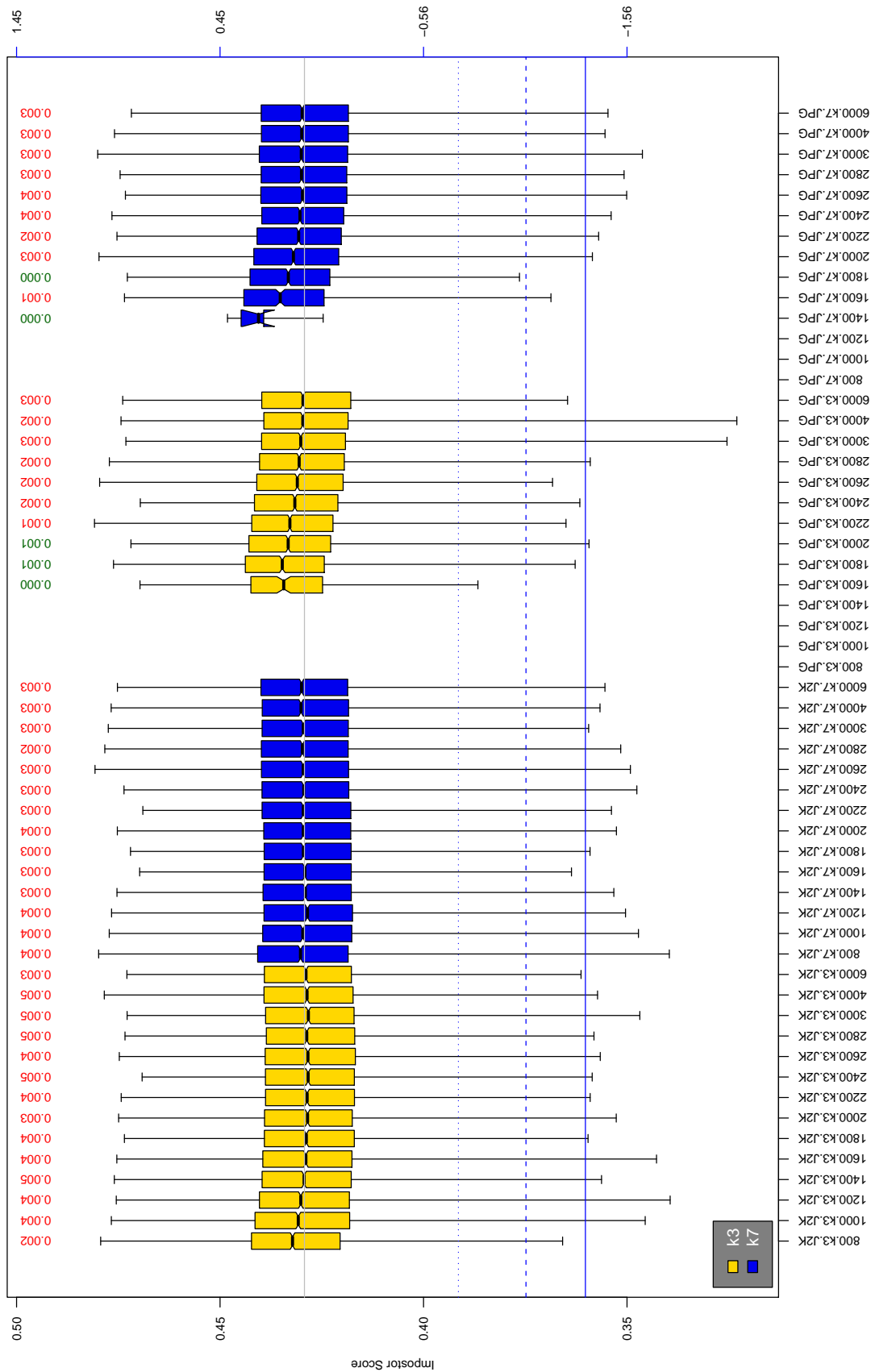


Table 95: The distribution of D2 native impostor comparison scores by size of the compressed image, KIND and the compression algorithm. The right axis scale gives the corresponding value for $d' = (s - \mu_1) / \sqrt{0.5(\sigma_1^2 + \sigma_2^2)}$ for impostor score s . The three blue lines correspond, from the top, to FMR of 10^{-2} , 10^{-3} , and 10^{-4} . The lower grey line refers to the median score obtained from comparison of uncompressed KIND 3 images. Any comparison involving a failed template is excluded. Above the boxplots are FMR values at the threshold that gives FMR = 10^{-3} on uncompressed images. These figures are computed from only 4000 comparisons so the FMR values and the tails of the impostor distribution are poorly characterized. Note that the iris record size on the horizontal axis is not evenly spaced above 3000 bytes.

A = SAGEM	B = COGENT	C = CROSSMATCH	D = CAMBRIDGE	E = L1	$x1$ = PRIMARY
F = RETICA	G = LG	H = HONEYWELL	I = IRITECH	J = NEUROTECHNOLOGY	$x2$ = SECONDARY
KIND 1 = RAW 640x480		KIND 3 = CROP	KIND 7 = CROP+MASK	KIND 16 = CONCENTRIC POLAR	

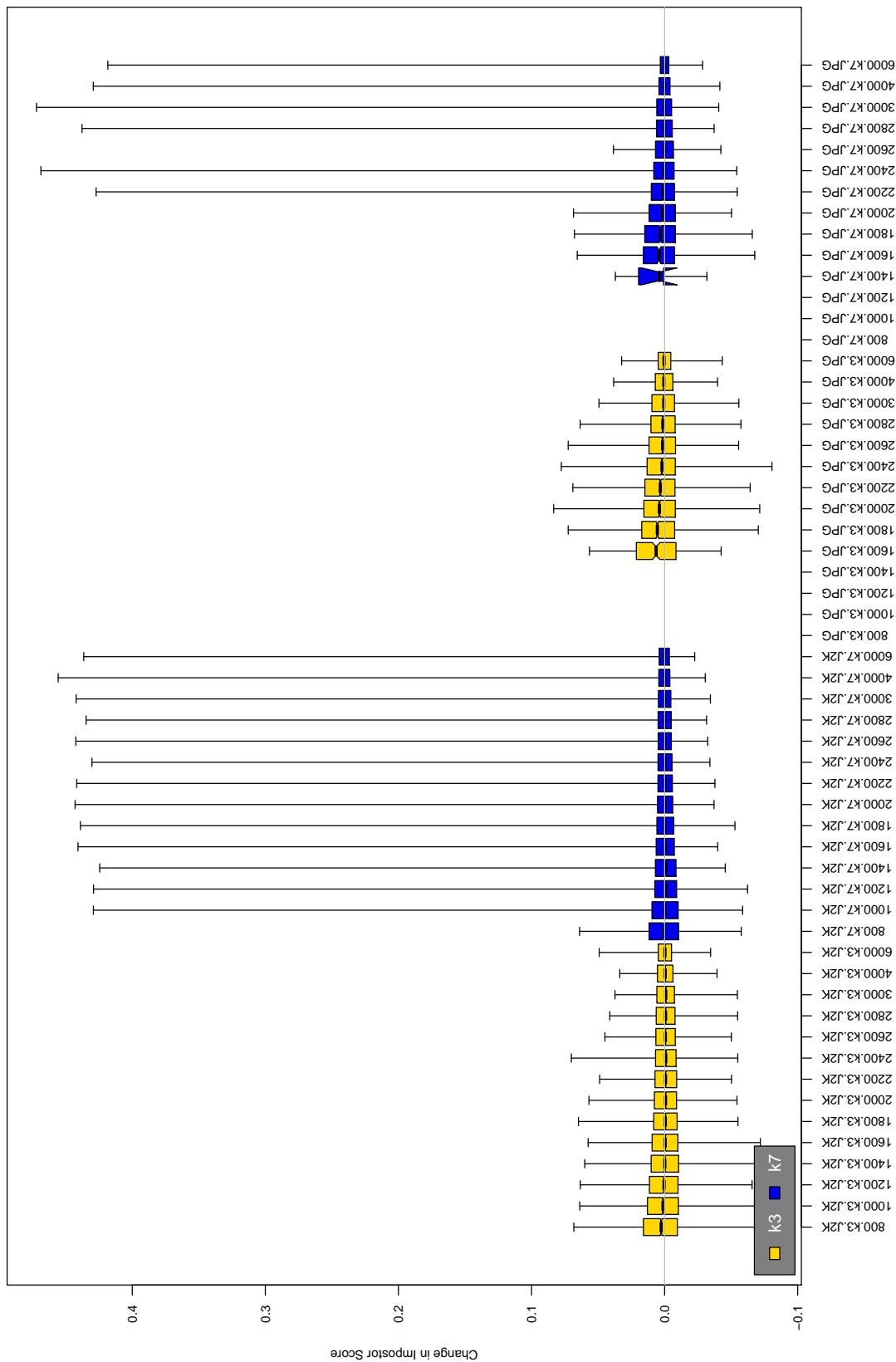


Table 96: The distribution of the increase in D2 native impostor comparison scores between the uncompressed “parent” and the compressed image, arranged by size, KIND and the compression algorithm. The images are from the OPS dataset. Any comparison involving a failed template is excluded. Note that the iris record size on the horizontal axis is not evenly spaced above 3000 bytes.

A = SAGEM	B = COGENT	C = CROSSMATCH	D = CAMBRIDGE	E = L1	x1 = PRIMARY
F = RETICA	G = LG	H = HONEYWELL	I = IRITECH	J = NEUROTECHNOLOGY	x2 = SECONDARY
KIND 1 = RAW 640x480		KIND 3 = CROP	KIND 7 = CROP+MASK	KIND 16 = CONCENTRIC POLAR	

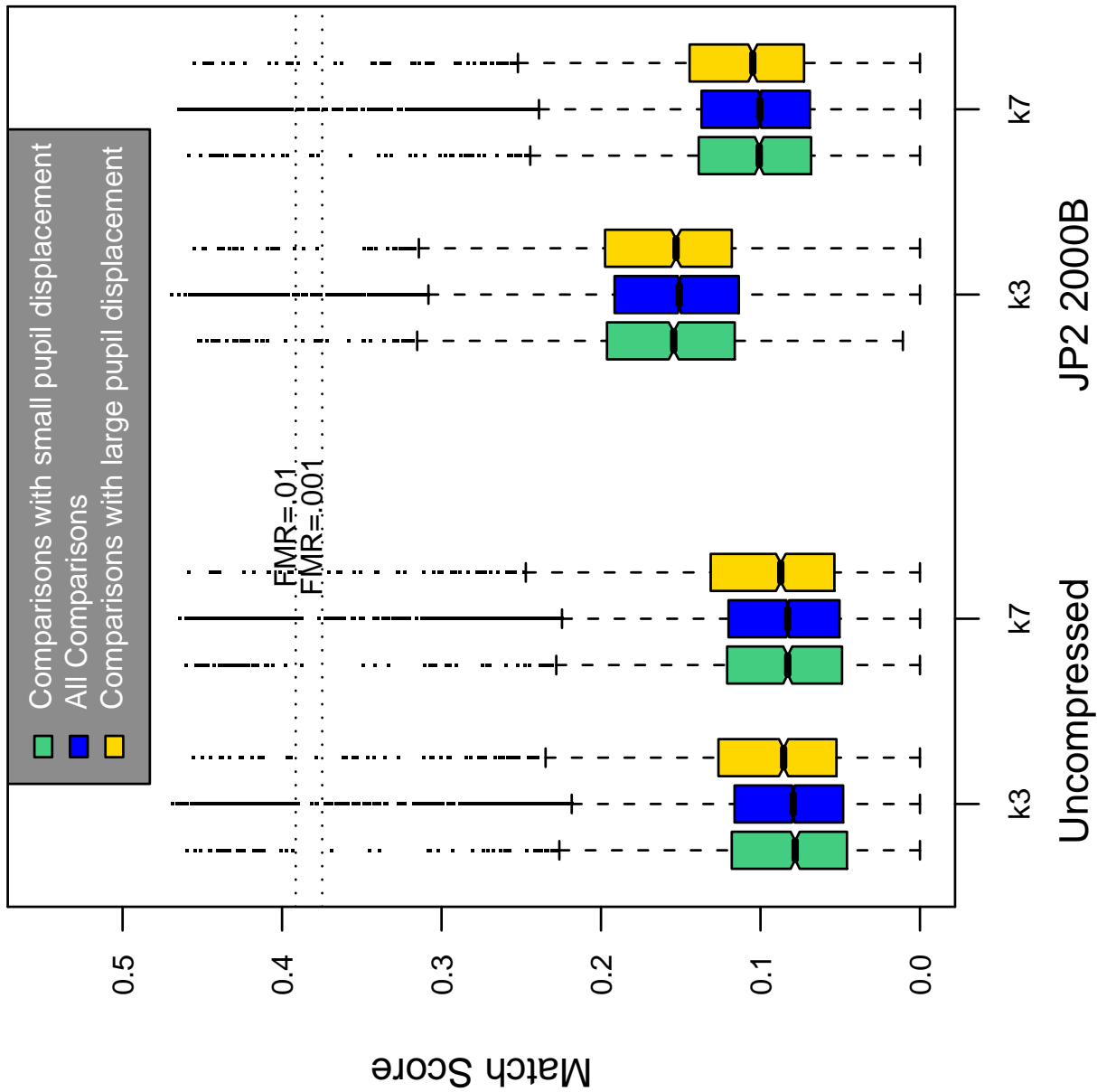


Table 97: Effect of pupil displacement on the genuine score distribution for D2

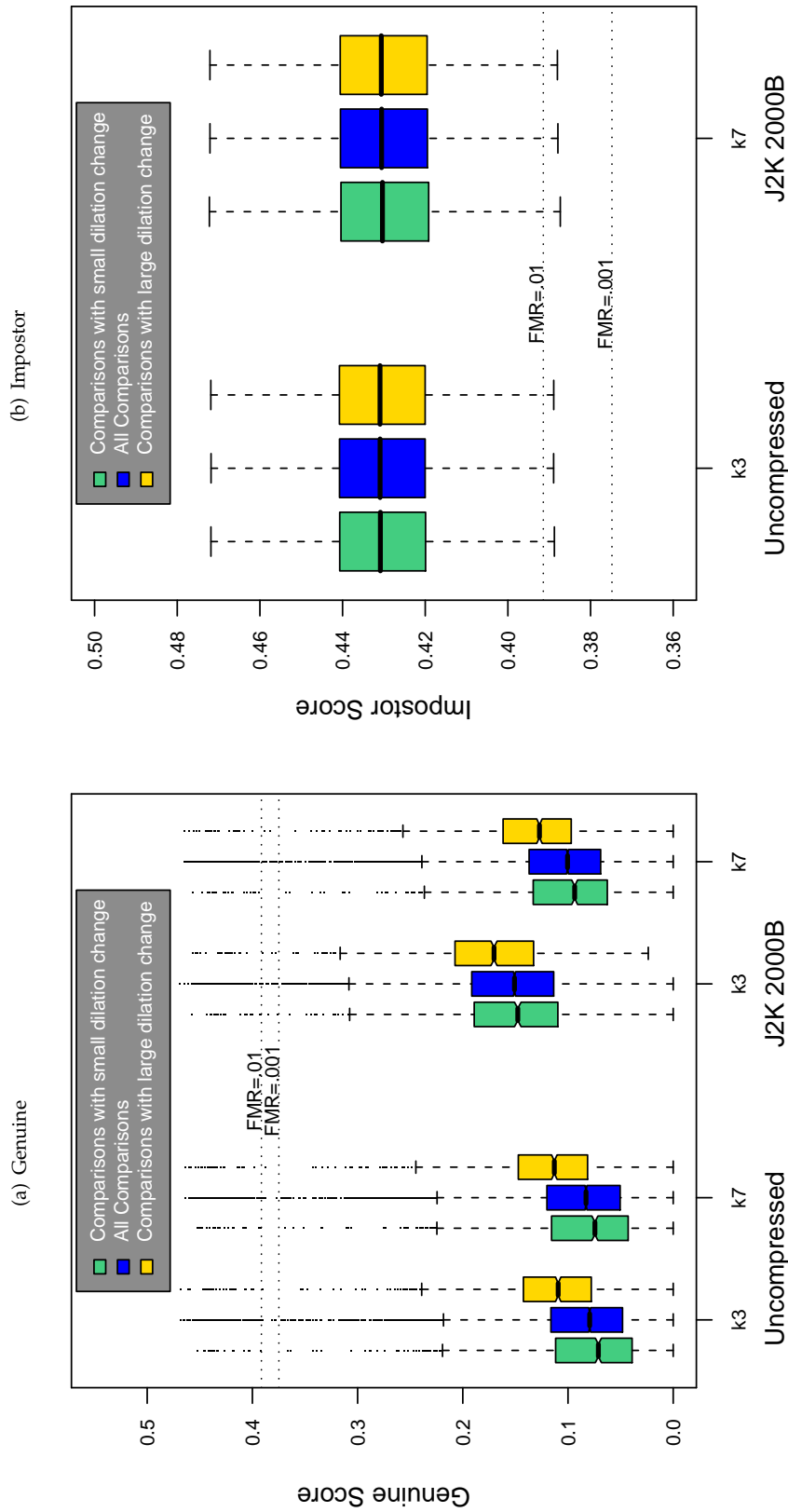


Table 98: The effect of dilation change on the two scores distributions for SDK D2.

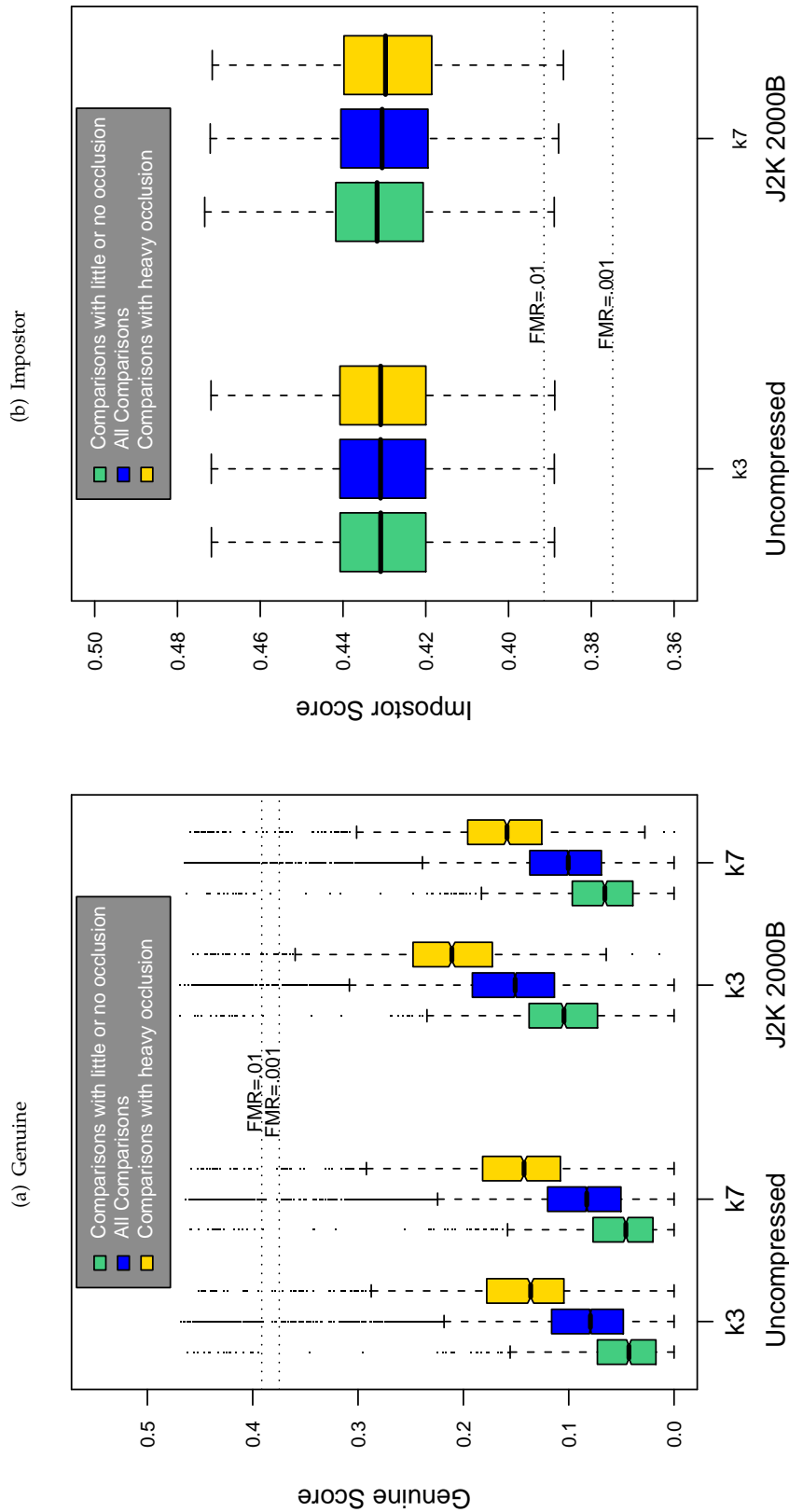
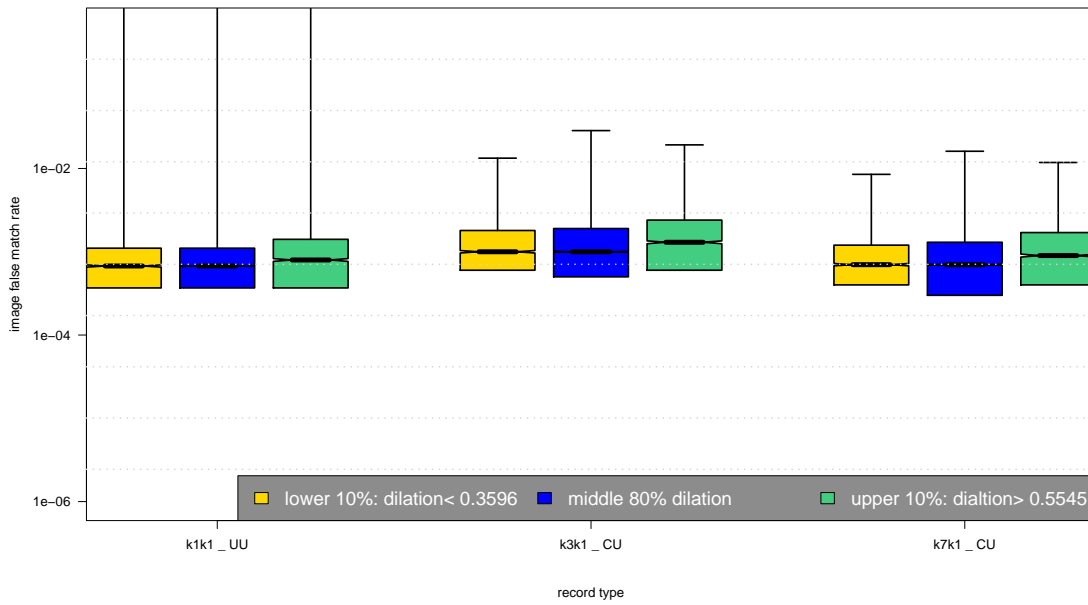
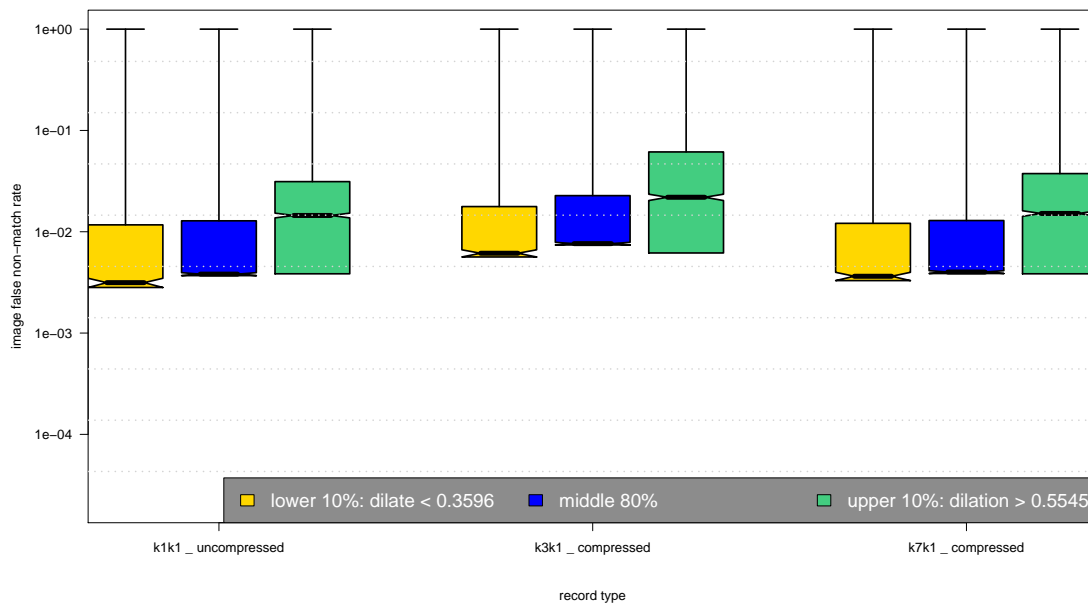


Table 99: The effect of eyelid occlusion on the two scores distributions for SDK D2.

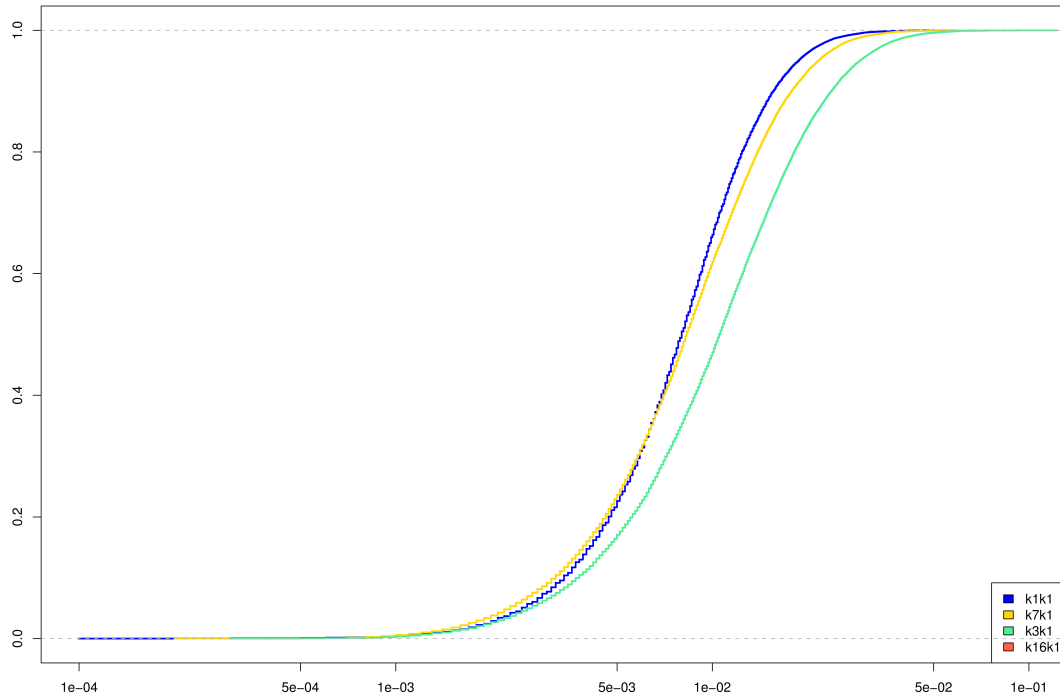
(a) iFMR using A1 dilation estimates



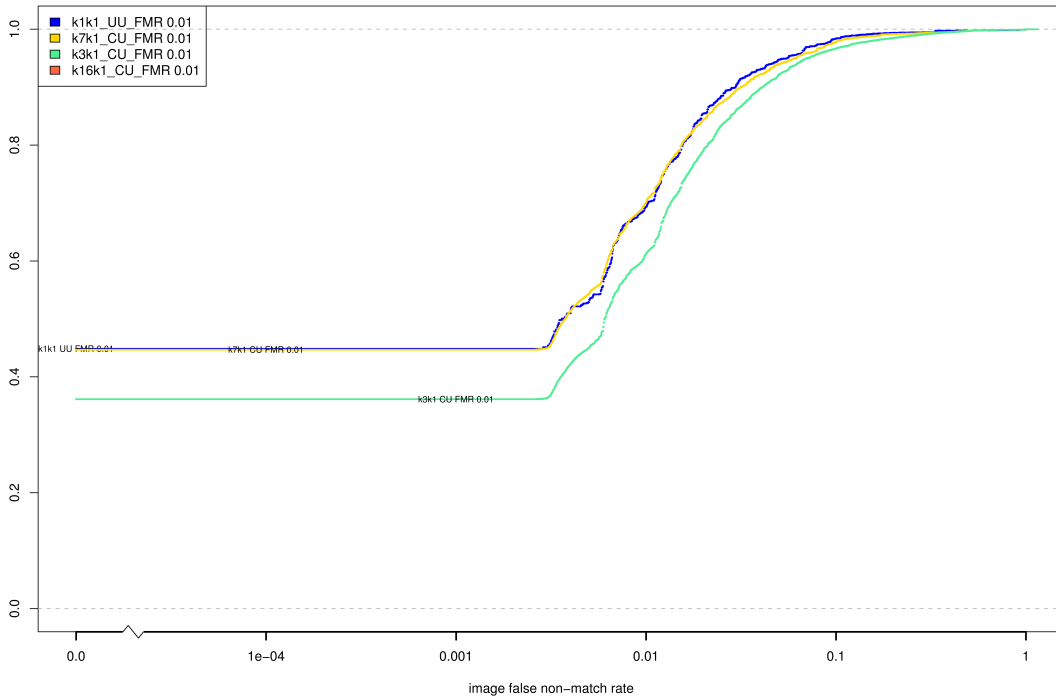
(b) iFNMR using A1 dilation estimates



(c) iFMR CDF



(d) iFNMR CDF



Compiled Results for Implementation E1

On June 25, 2009, NIST invited the IREX participants to submit a description of the SDKs submitted for the IREX effort. The intent was to allow providers to describe and contrast the feature sets, optimization, operational suitability and availability of the primary and secondary SDKs. NIST indicated that any submitted text would appear verbatim (with typesetting) in draft and final versions of the IREX report and that it would be attributed to the organization. This was optional and NIST put no constraints on the content beyond a 600 word limit, and a statement that anything labelled as confidential or proprietary would be omitted.

The provider of SDK E1, L1 Identity Solutions, submitted the following to NIST - we are unable to validate this information.

We would first like to thank NIST for taking on the responsibility of testing the interoperability and compressibility of the various proposed iris image formats. We are pleased to learn that our recommendation to discontinue the use of the polar format and JPEG compression in ISO 19794-6 is supported by the test results.

Both of the L-1 submissions were based on the Daugman algorithm, which has been designed for scalable performance with small templates and fast enrollment and match speeds. Our submission was born from our product experience and was tuned for a balance between stability, scalability and accuracy. Our first submission aimed to stabilize performance under compression by avoiding any dependency on very-high resolution information. As a result, its performance upheld its high levels on images compressed down to almost 2000 bytes¹. Our secondary submission was purely experimental and aimed to exploit higher-resolution iris texture.

A notable aspect of our submission was that it enforced a quality criterion on each sample, thus causing a Failure-To-Enroll (FTE) event whenever the quality of a sample was insufficient for very accurate matching. Quality-based filtering is a widely practiced in commercial live-capture cameras and has proven instrumental in protecting the recognition accuracy against the detrimental effects of eyelid occlusions and camera-eye misalignment. Typically, the camera captures several images in a session and then selects the single best sample for enrollment or verification. FTEs only occur in the rare case that even the best sample does not meet the quality criterion. IREX, by contrast, reflects the case if any of the samples fail to meet the criterion. This counting method overestimates the FTE rate with respect to operational scenarios on data such as BATH and ICE (see table 6). Though our quality criterion may have been too restrictive with respect to iris diameter, it showed the expected effectiveness in reducing the False-Rejects and producing excellent match accuracy as documented for ICE in fig. 12b.

Second, we point out that our algorithm has been designed to control False-Accept-Rates (FAR) to lower than 1 in a million by means of a tightly controlled and stable imposter score distribution. This ensures that databases of several millions of enrollments can be searched exhaustively without generating False Matches. The benefits of this fundamental feature, which are evidenced in our flat DET curves, are critical for success in real-world deployments, but less visible in tests like IREX which focus on relatively undemanding FARs. The stability of our scoring over different databases, however, was visible and specifically pointed out in IREX.

L-1 Identity Solutions patented Daugman algorithm has consistently been a top-tier technology in testing and the results here show the technology to be accurate, stable over different data sets, and highly scalable compared to other SDKs. It is currently the only commercially available technology with a field-proven

¹Graph in initial IREX report

capability to cope with database sizes and throughputs needed for national ID projects. It is deployed in numerous scenarios, including military systems, jail systems, deportation systems, and registered traveler programs. The Daugman algorithm powers iris recognition in L-1 Identity Solutions ABIS multi-biometric search system, the SIRIS search engine, and in the HIIDE and PIER mobile devices. In the end, the L-1 Identity Solutions iris product suite will undoubtedly benefit from the lessons learned in IREX as it will influence our product requirements and algorithmic research goals for the next generation of iris technology. We again thank NIST and their sponsors for providing new insights and validating our old ones with this IREX testing effort.

On August 17, 2009, NIST invited the IREX participants to submit a description their comments on a draft version of the IREX report. This was intended to allow participants to assist readers in the interpretation of a large and complicated testing effort. NIST indicated that any submitted text would appear verbatim (with typesetting) in the final version of the IREX report and that it would be attributed to the organization. Submission of content was optional and NIST put no constraints on the content beyond a word limit, and a statement that anything labelled as confidential or proprietary would be omitted.

The provider of SDK E1, L1 Identity Solutions, elected not to submit any information

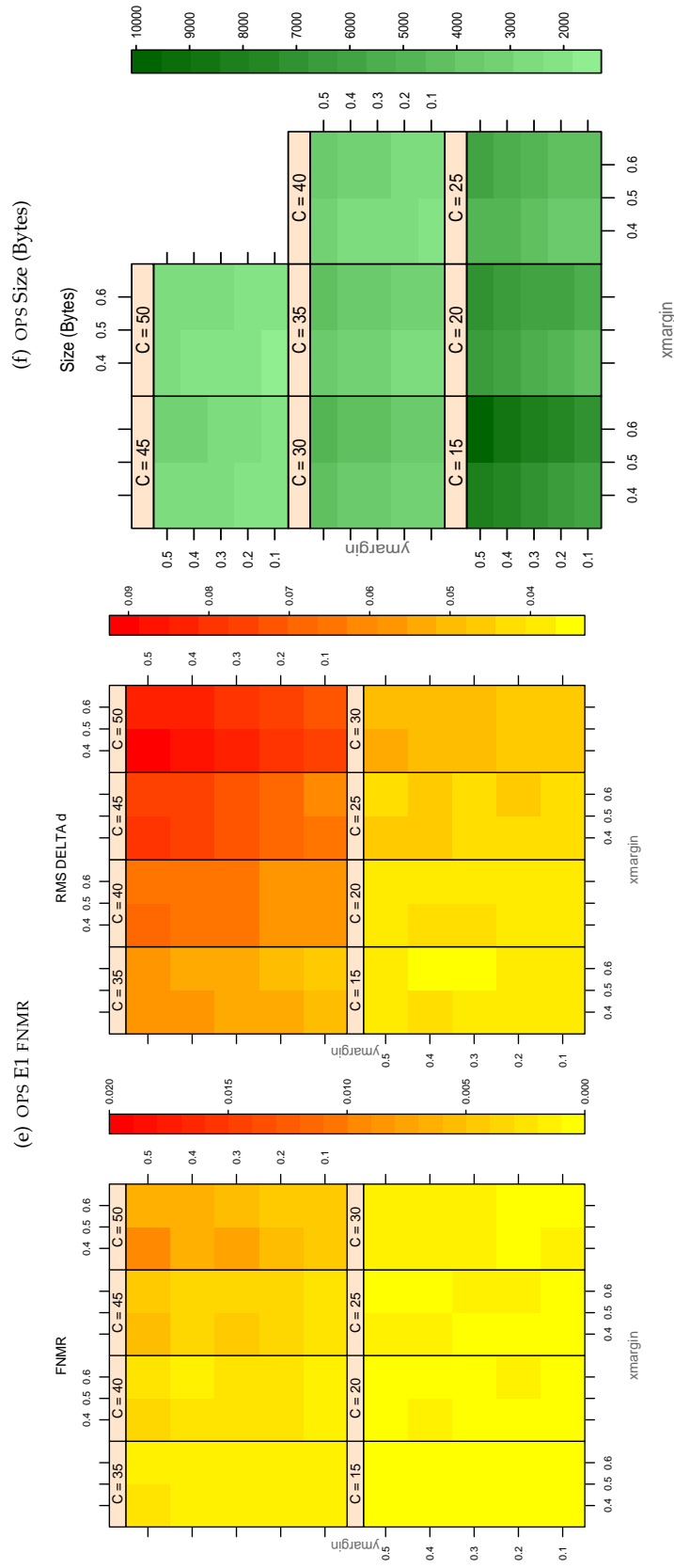


Table 100: For the IREX partition of the OPS database the plots at left show the dependence of cFNMR on the vertical and horizontal iris cropping margins for various compression ratios. This applies only for KIND 3 records. The margins are in units of iris radius. The use of conditional FNMR means that the plots exclude comparisons that were falsely rejected even before any compression was applied. On the **right side** is the rms difference between the crop+compress and the uncompressed comparison scores for each image pair. All computations are driven by the bounding box coordinates reported by the II SDK . The number of bits per pixel is $8/C$, where C is the compression ratio. The iris radius varies and because the cropping margins are fixed multiples of the radius the image size varies. The compressed size, in bytes, is the width times height divided by C . Values of cFNMR greater than 0.02 are shown as 0.02.

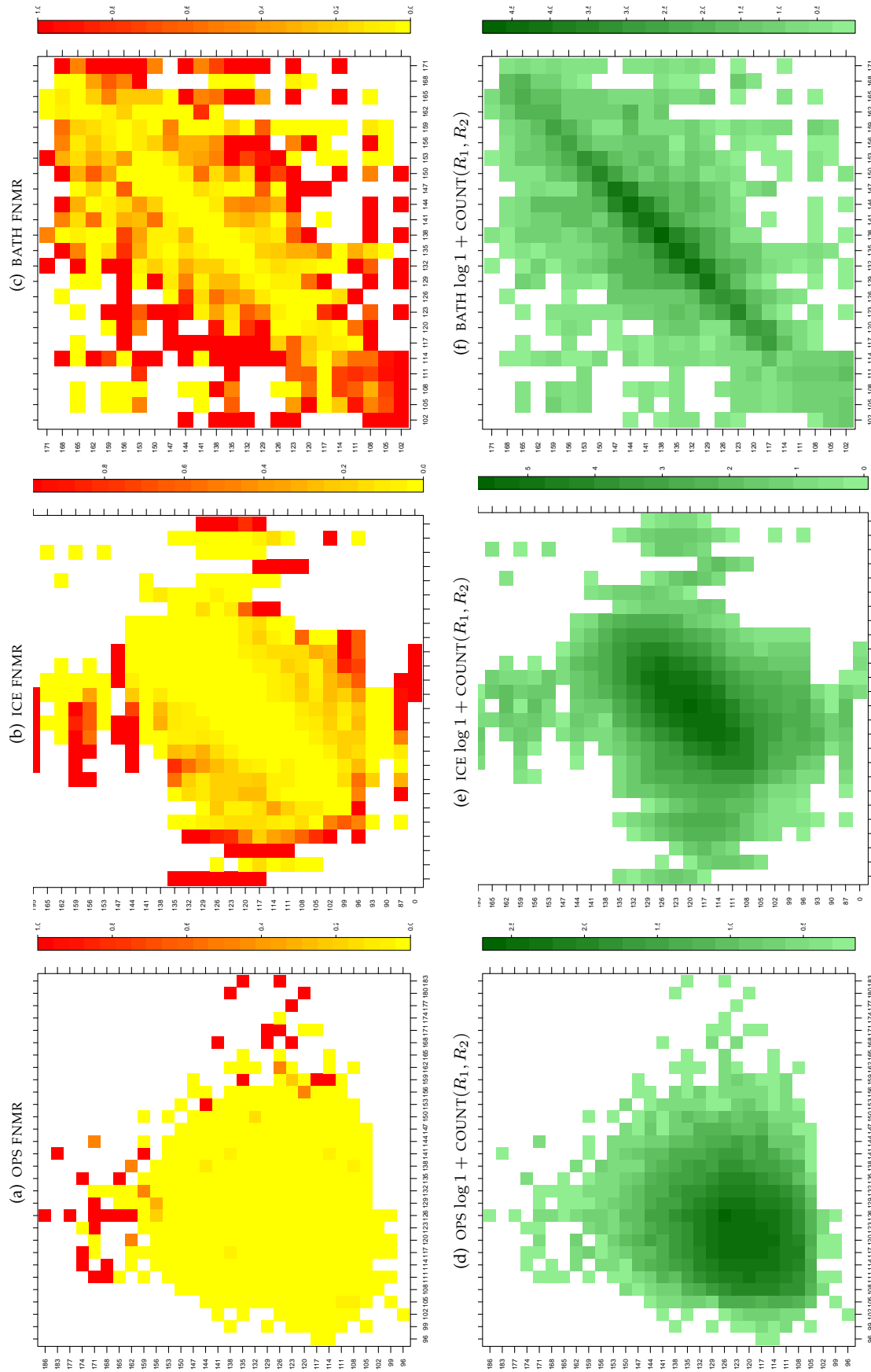


Table 101: For the three IREX databases: In the **top** row the color in each cell represents the occurrence of genuine comparisons with the given pair of radii. The *y*-axis represents enrollment samples with verification samples on the *x*-axis; In the **bottom** row the color scale plots $\log 1 + \text{COUNT}(R_1, R_2)$. The radii are quantized into three-pixel bins. The radii for DOD are on the range $96 \leq r \leq 186$ pixels. The radii for ICE are on the range $87 \leq r \leq 165$ pixels. The radii for BATH are on the range $100 \leq r \leq 170$ pixels.

A = SAGEM	B = COGENT	C = CROSSMATCH	D = CAMBRIDGE	E = L1	$x1$ = PRIMARY
F = RETICA	G = LG	H = HONEYWELL	I = IRITECH	J = NEUROTECHNOLOGY	$x2$ = SECONDARY
KIND 1 = RAW 640x480		KIND 3 = CROP		KIND 7 = CROP+MASK	
KIND 16 = CONCENTRIC POLAR					

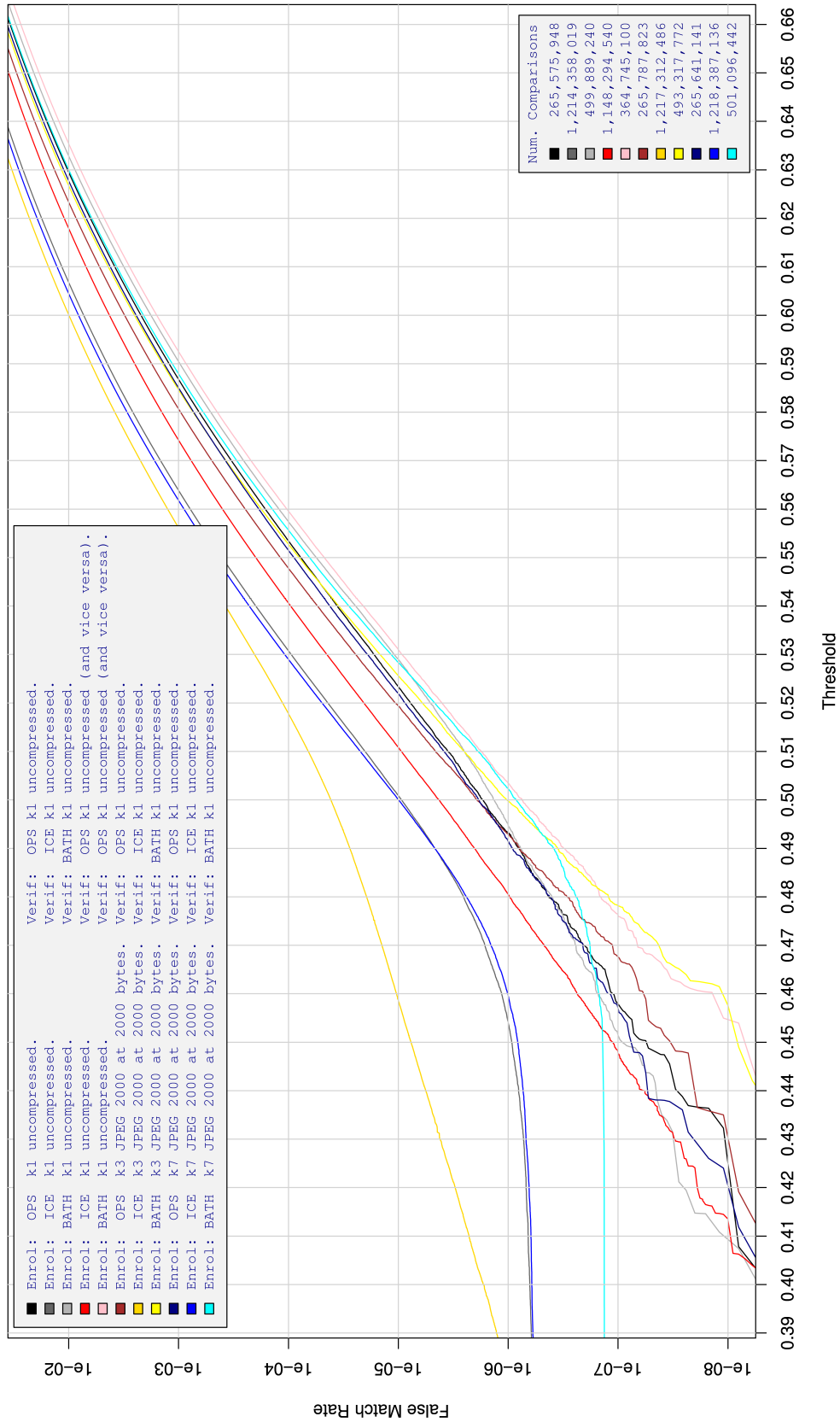


Table 102: For implementation E1, the dependency of FMR on threshold. for various combinations of enrollment and verification dataset, format, and compression.

A = SAGEM	B = COGENT	C = CROSSMATCH	D = CAMBRIDGE	E = L1	x1 = PRIMARY
F = RETICA	G = LG	H = HONEYWELL	I = IRITECH	J = NEUROTECHNOLOGY	x2 = SECONDARY
KIND 1 = RAW 640x480		KIND 3 = CROP	KIND 7 = CROP+MASK	KIND 16 = CONCENTRIC POLAR	

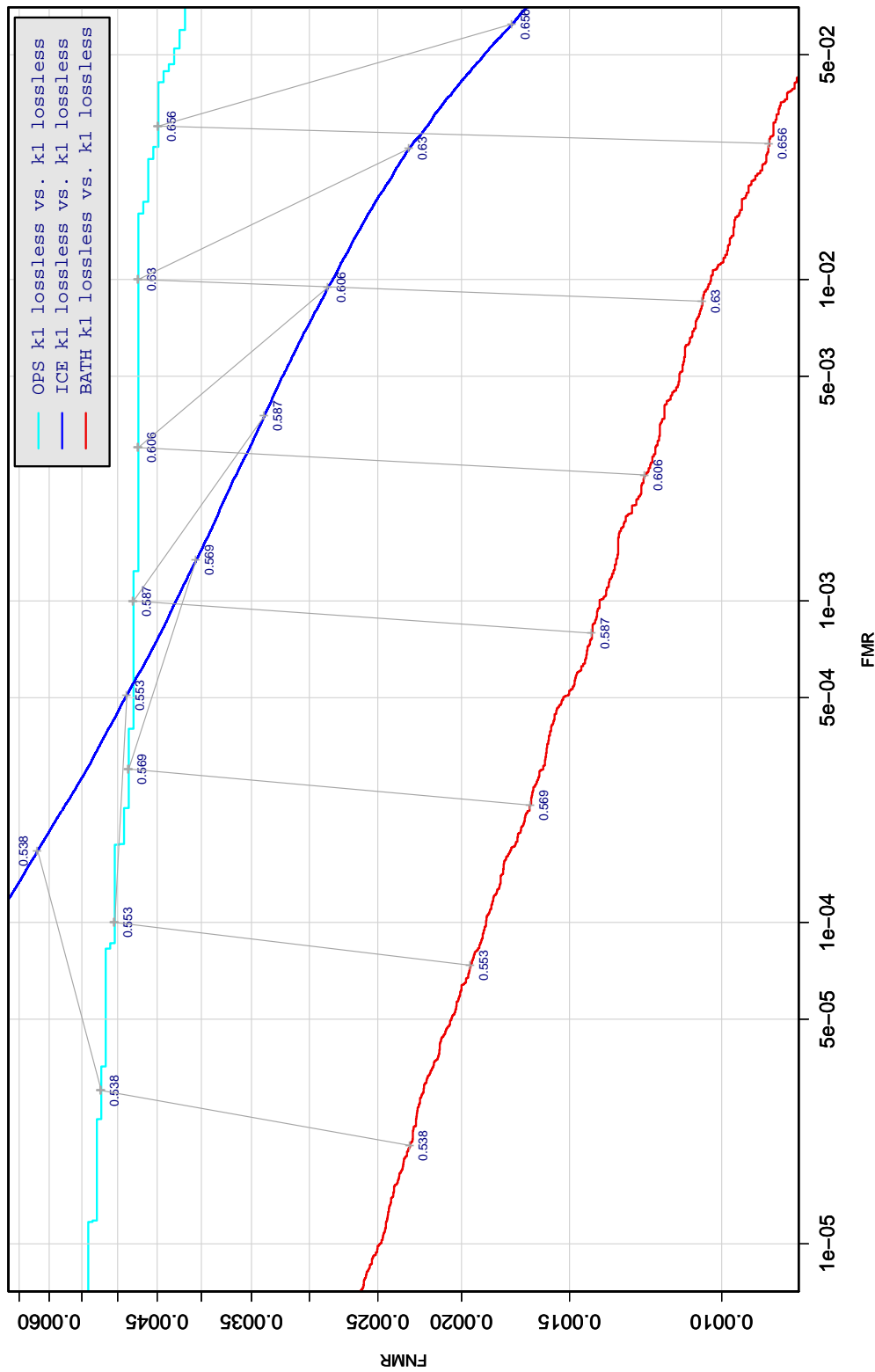


Table 103: DET curve for implementation E1 on three IREX databases. All comparisons are with uncompressed KIND 1 vs. KIND 1 images. The lines join points corresponding to the a fixed threshold. Non-vertical links indicate a change in FMR when the database changes. All results apply to native operation. Failures to produce a template i.e. FTE are ignored because the plots are intended to show *matching* effects, specifically to compare DET slopes and to show the effect of fixing a threshold.

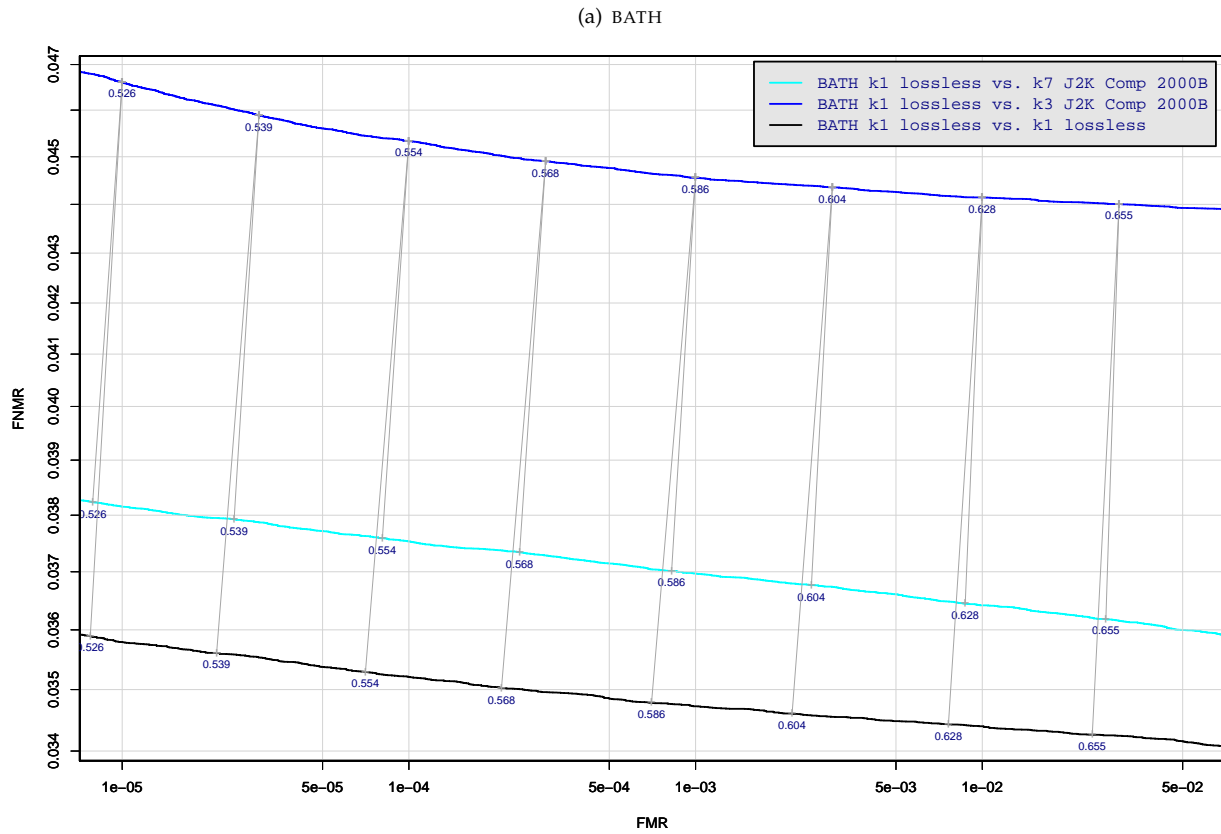


Table 104: DET curve for implementation E1 on the BATH database for the various supported KINDS . The DET characteristics are linked by lines joining points of equal threshold. Non-vertical links indicate a change in false acceptance when the data KIND changes. All results apply to native operation, and the effects of FTE are included.

A = SAGEM	B = COGENT	C = CROSSMATCH	D = CAMBRIDGE	E = L1	x1 = PRIMARY
F = RETICA	G = LG	H = HONEYWELL	I = IRITECH	J = NEUROTECHNOLOGY	x2 = SECONDARY
KIND 1 = RAW 640x480		KIND 3 = CROP		KIND 7 = CROP+MASK	
				KIND 16 = CONCENTRIC POLAR	

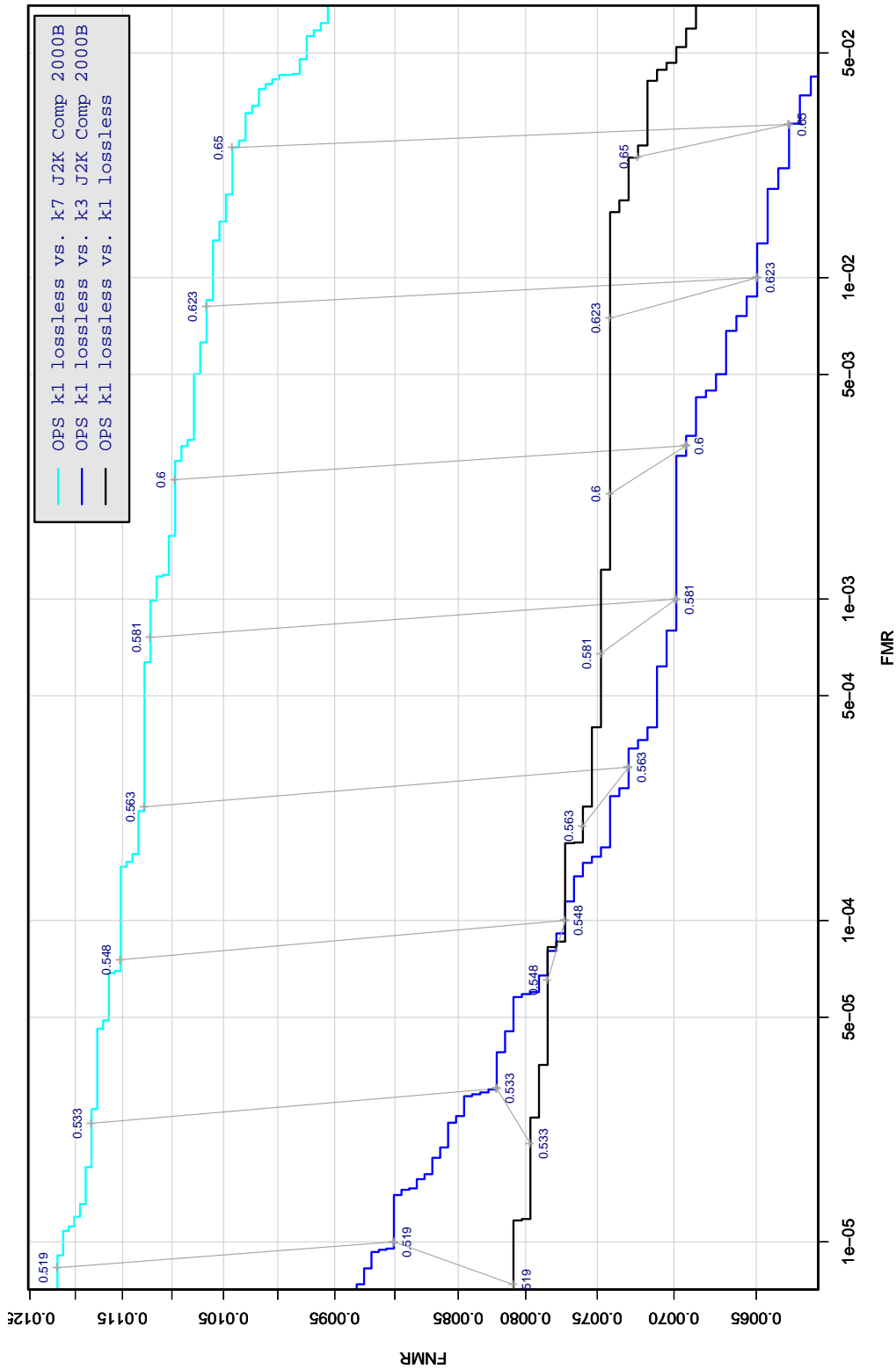


Table 105: DET curve for implementation E1 on the OPS database for the various supported KINDS . The DET characteristics are linked by lines joining points of equal threshold. Non-vertical links indicate a change in false acceptance when the data KIND changes. All results apply to native operation, and the effects of FTE are included.

A = SAGEM	B = COGENT	C = CROSSMATCH	D = CAMBRIDGE	E = L1	x1 = PRIMARY
F = RETICA	G = LG	H = HONEYWELL	I = IRITECH	J = NEUROTECHNOLOGY	x2 = SECONDARY
KIND 1 = RAW 640x480		KIND 3 = CROP	KIND 7 = CROP+MASK	KIND 16 = CONCENTRIC POLAR	

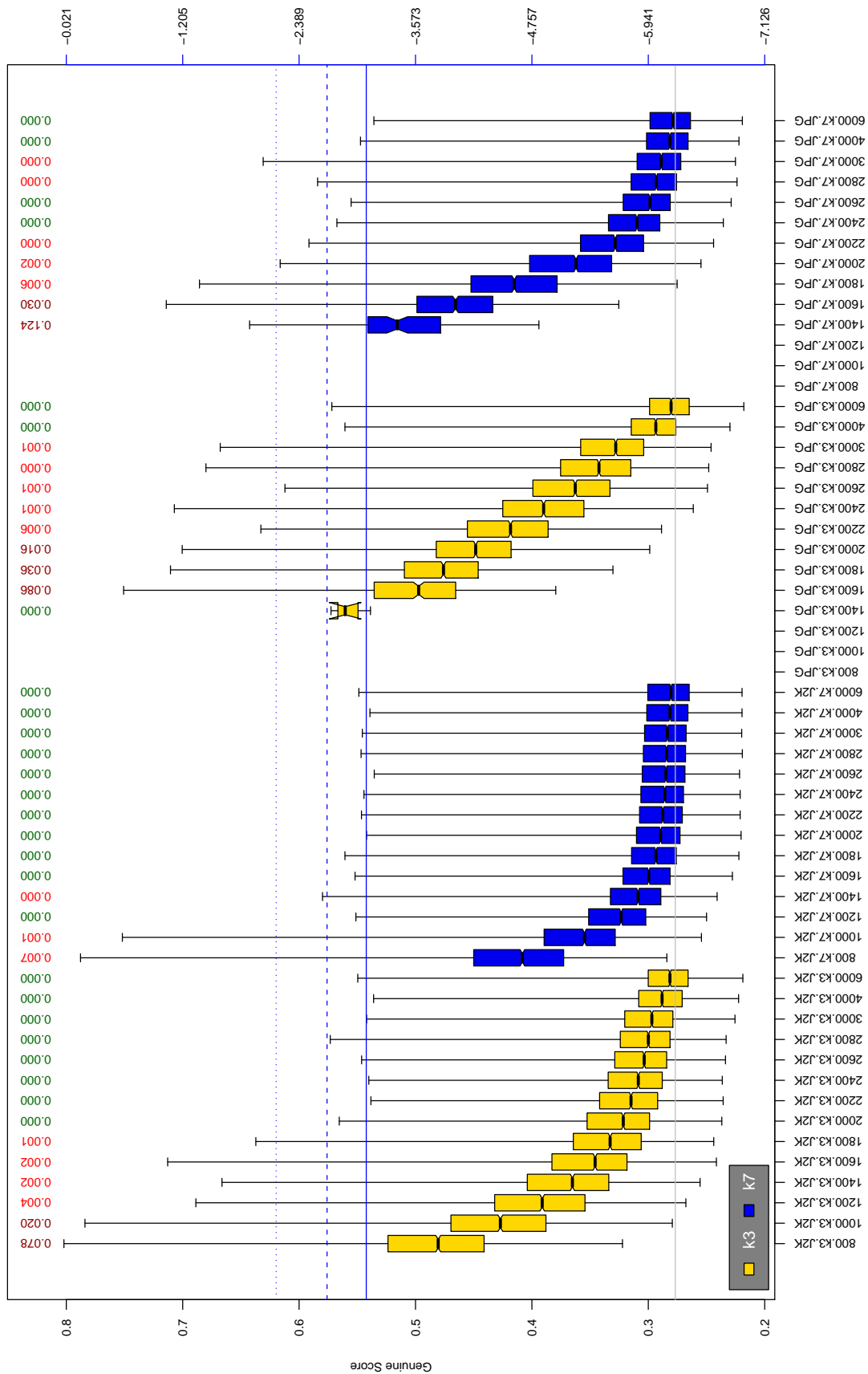


Table 106: The distribution of E1 native genuine comparison scores by size of the compressed image, KIND and the compression algorithm. The images are from the OPS dataset. The right axis scale gives the corresponding value for $d' = (s - \mu_I) / \sqrt{0.5(\sigma_I^2 + \sigma_C^2)}$ for genuine score s . The boxplots only include comparison scores if the uncompressed version of the same image was matched below the FMR = 0.001 threshold. Above the boxplots are FNMR values at FMR = 10^{-3} . The three blue lines correspond, from the top, to FMR of $10^{(-2, -3, -4)}$. The lower grey line refers to the median score obtained from comparison of uncompressed KIND 3 images. Any comparison for which either template had not been generated is excluded. Note that the iris record size on the horizontal axis is not evenly spaced above 3000 bytes.

A = SAGEM	B = COGENT	C = CROSSMATCH	D = CAMBRIDGE	E = L1	$x1$ = PRIMARY
F = RETICA	G = LG	H = HONEYWELL	I = IRITECH	J = NEUROTECHNOLOGY	$x2$ = SECONDARY
KIND 1 = RAW 640x480		KIND 3 = CROP	KIND 7 = CROP+MASK	KIND 16 = CONCENTRIC POLAR	

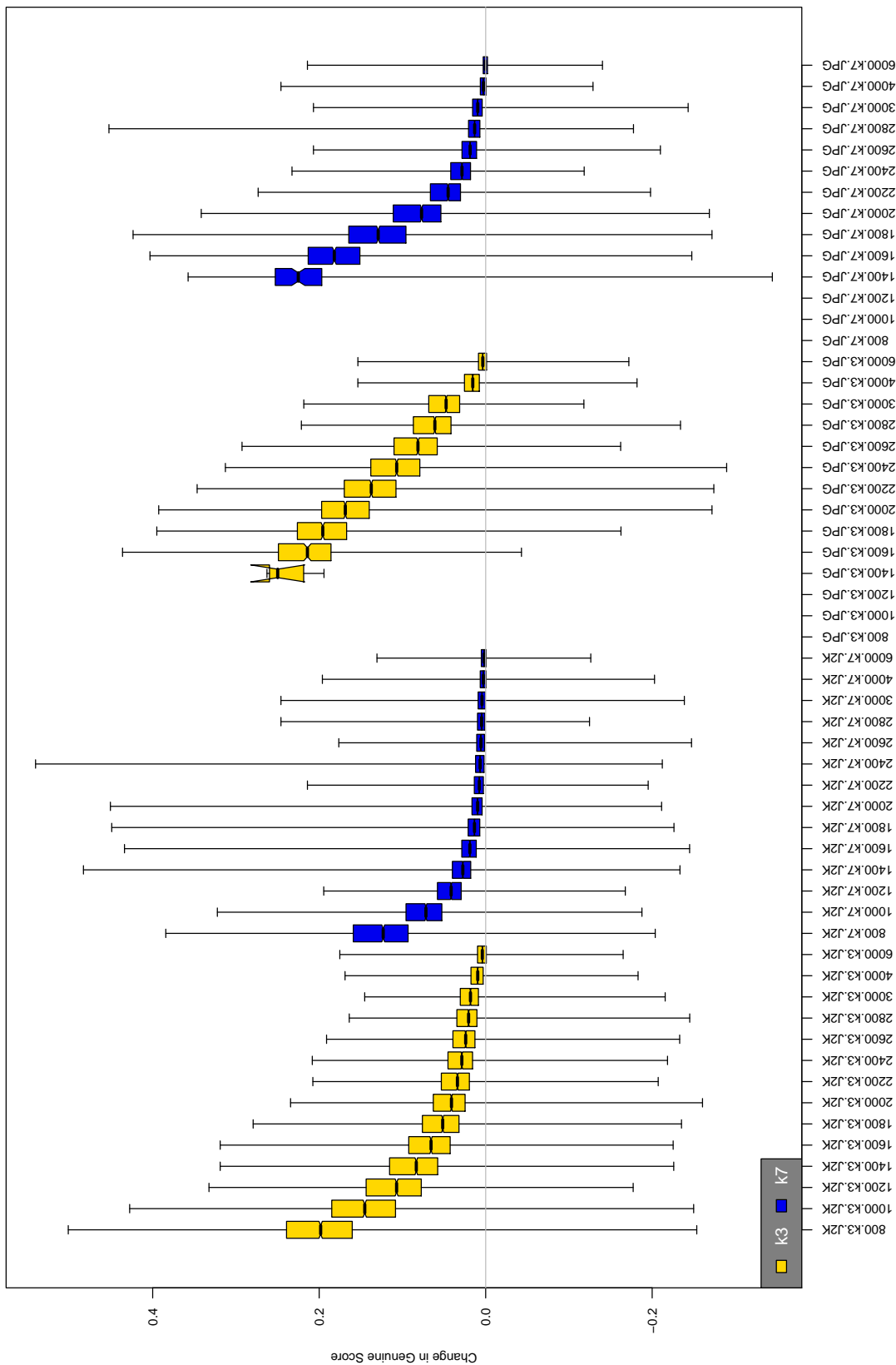


Table 107: The distribution of the *increase* in E1 native genuine comparison scores between the uncompressed “parent” and the compressed image, arranged by size, KIND and the compression algorithm. The images are from the OPS dataset. Any comparison involving a failed template is excluded. Note that the iris record size on the horizontal axis is not evenly spaced above 3000 bytes.

A = SAGEM	B = COGENT	C = CROSSMATCH	D = CAMBRIDGE	E = L1	$x1$ = PRIMARY
F = RETICA	G = LG	H = HONEYWELL	I = IRITECH	J = NEUROTECHNOLOGY	$x2$ = SECONDARY
KIND 1 = RAW 640x480		KIND 3 = CROP	KIND 7 = CROP+MASK	KIND 16 = CONCENTRIC POLAR	

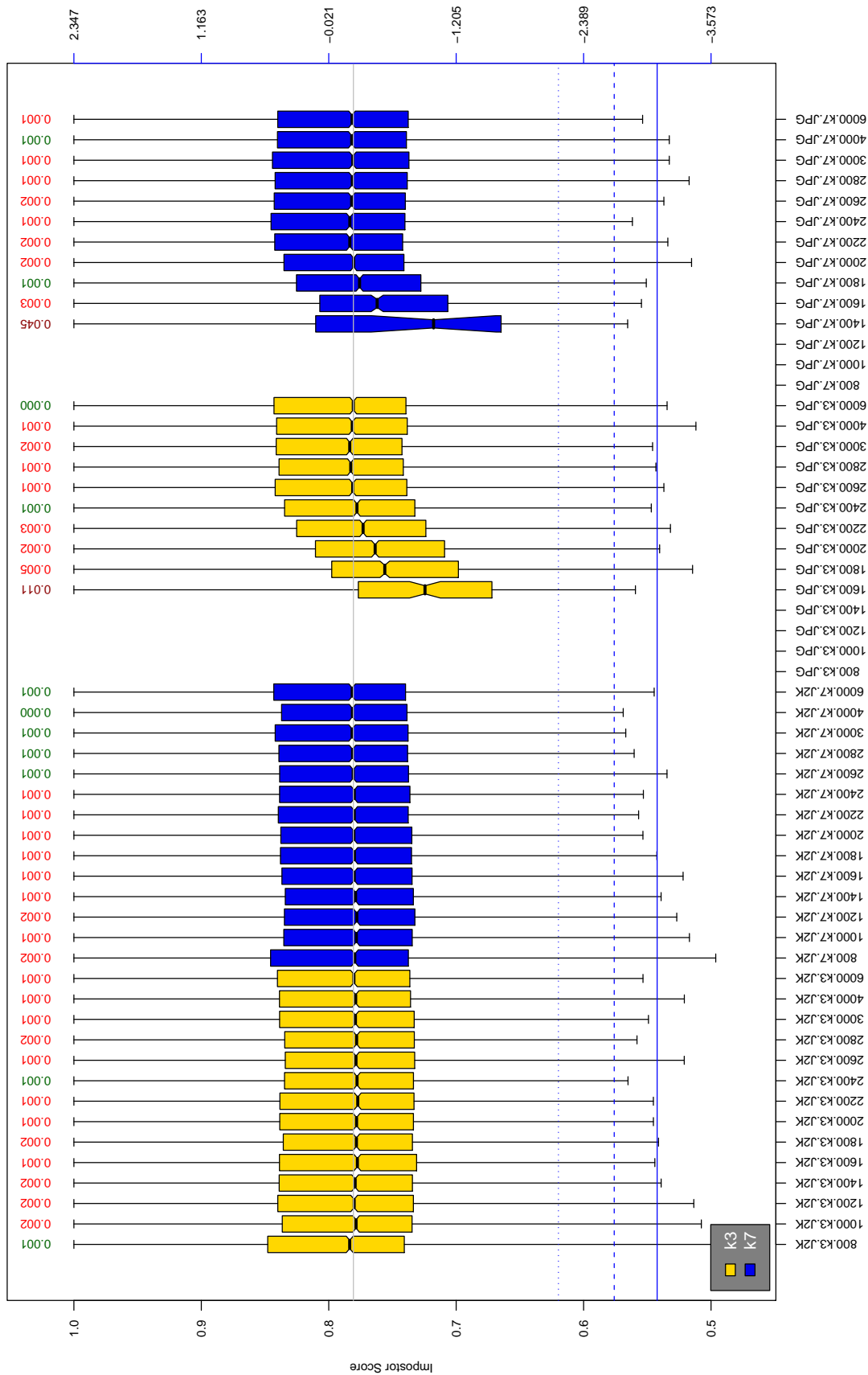


Table 108: The distribution of E1 native impostor comparison scores by size of the compressed image, KIND and the compression algorithm. The right axis gives the corresponding value for $d' = (s - \mu_1) / \sqrt{0.5(\sigma_1^2 + \sigma_2^2)}$ for impostor score s . The three blue lines correspond, from the top, to FMR of $10^{-2}, -3, -4$. The lower grey line refers to the median score obtained from comparison of uncompressed KIND 3 images. Any comparison involving a failed template is excluded. Above the boxplots are FMR values at the threshold that gives FMR = 10^{-3} on uncompressed images. These figures are computed from only 4000 comparisons so the FMR values and the tails of the impostor distribution are poorly characterized. Note that the iris record size on the horizontal axis is not evenly spaced above 3000 bytes.

A = SAGEM	B = COGENT	C = CROSSMATCH	D = CAMBRIDGE	E = L1	$x1$ = PRIMARY
F = RETICA	G = LG	H = HONEYWELL	I = IRITECH	J = NEUROTECHNOLOGY	$x2$ = SECONDARY
KIND 1 = RAW 640x480		KIND 3 = CROP		KIND 7 = CROP+MASK	KIND 16 = CONCENTRIC POLAR

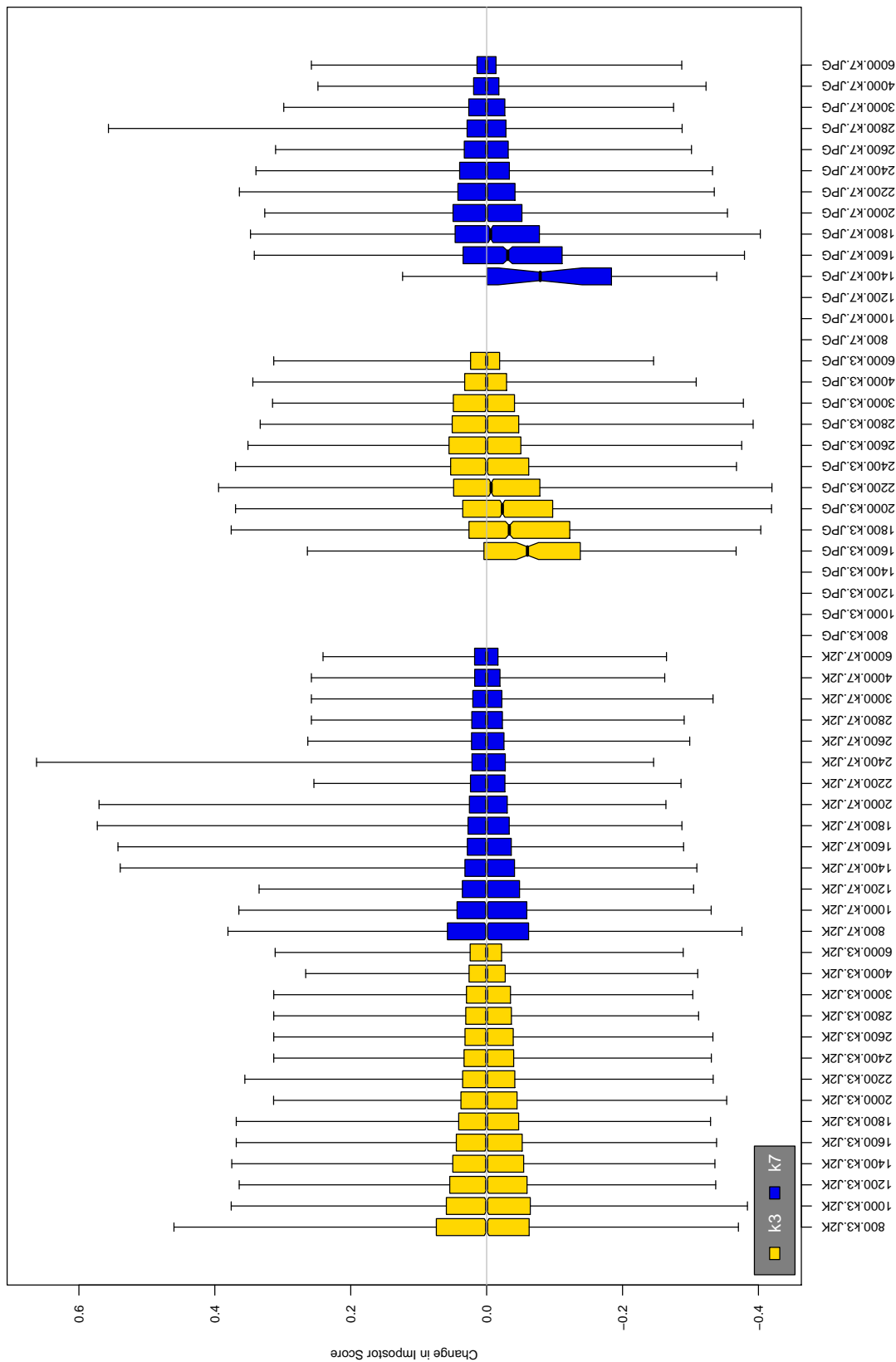


Table 109: The distribution of the increase in E1 native impostor comparison scores between the uncompressed “parent” and the compressed image, arranged by size, KIND and the compression algorithm. The images are from the OPS dataset. Any comparison involving a failed template is excluded. Note that the iris record size on the horizontal axis is not evenly spaced above 3000 bytes.

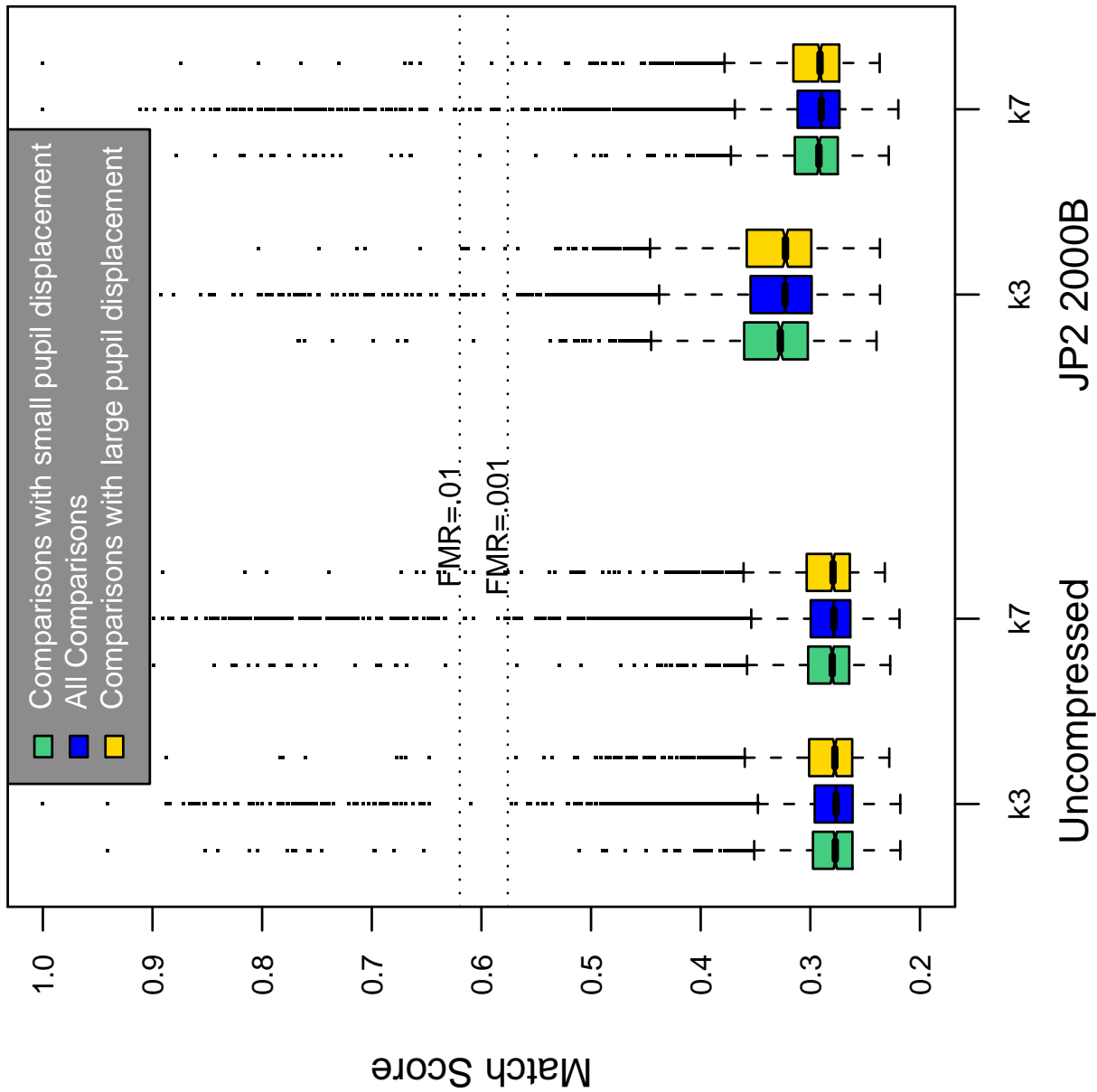


Table 110: Effect of pupil displacement on the genuine score distribution for E1

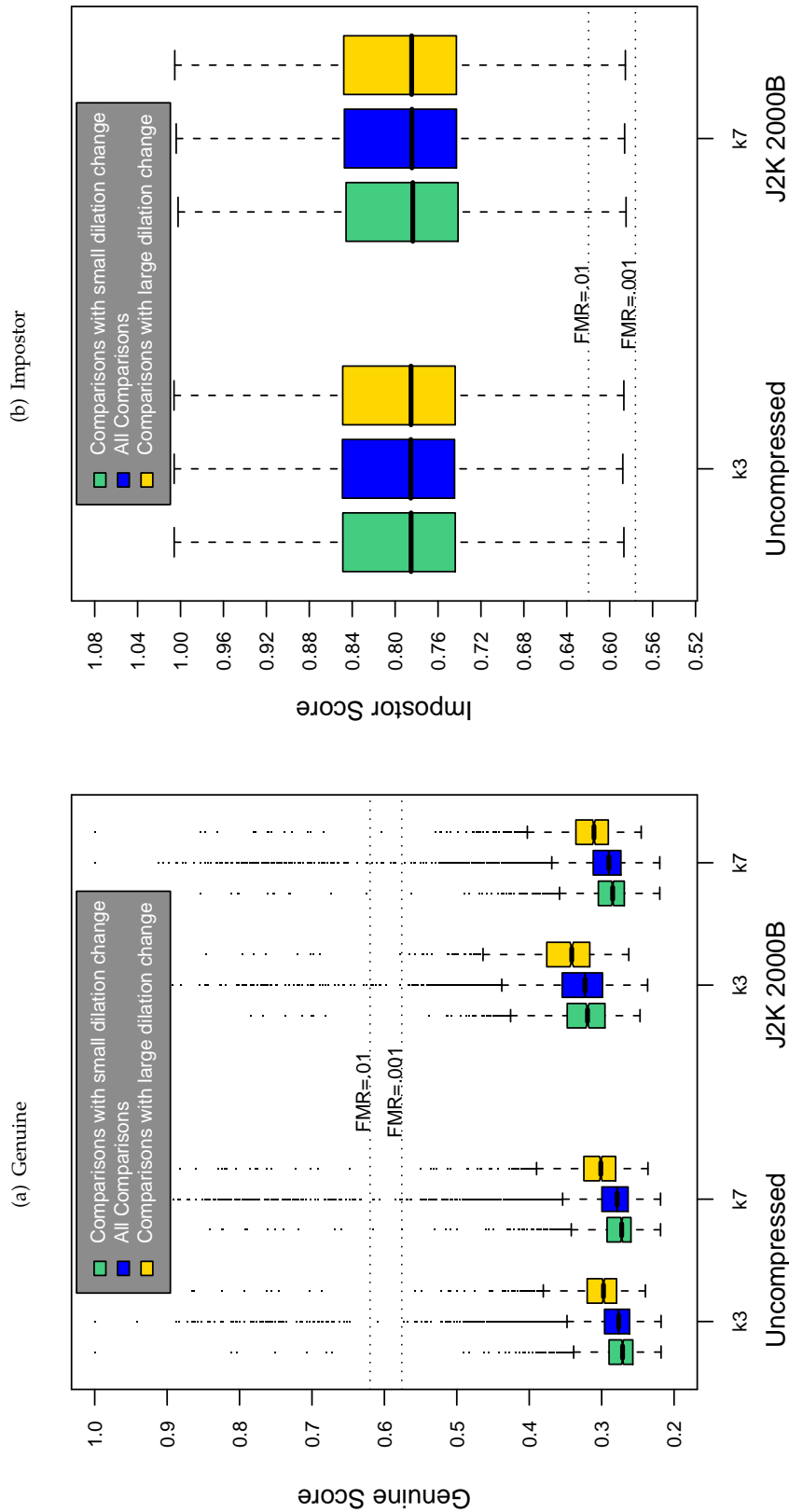


Table 111: The effect of dilation change on the two scores distributions for SDK E1.

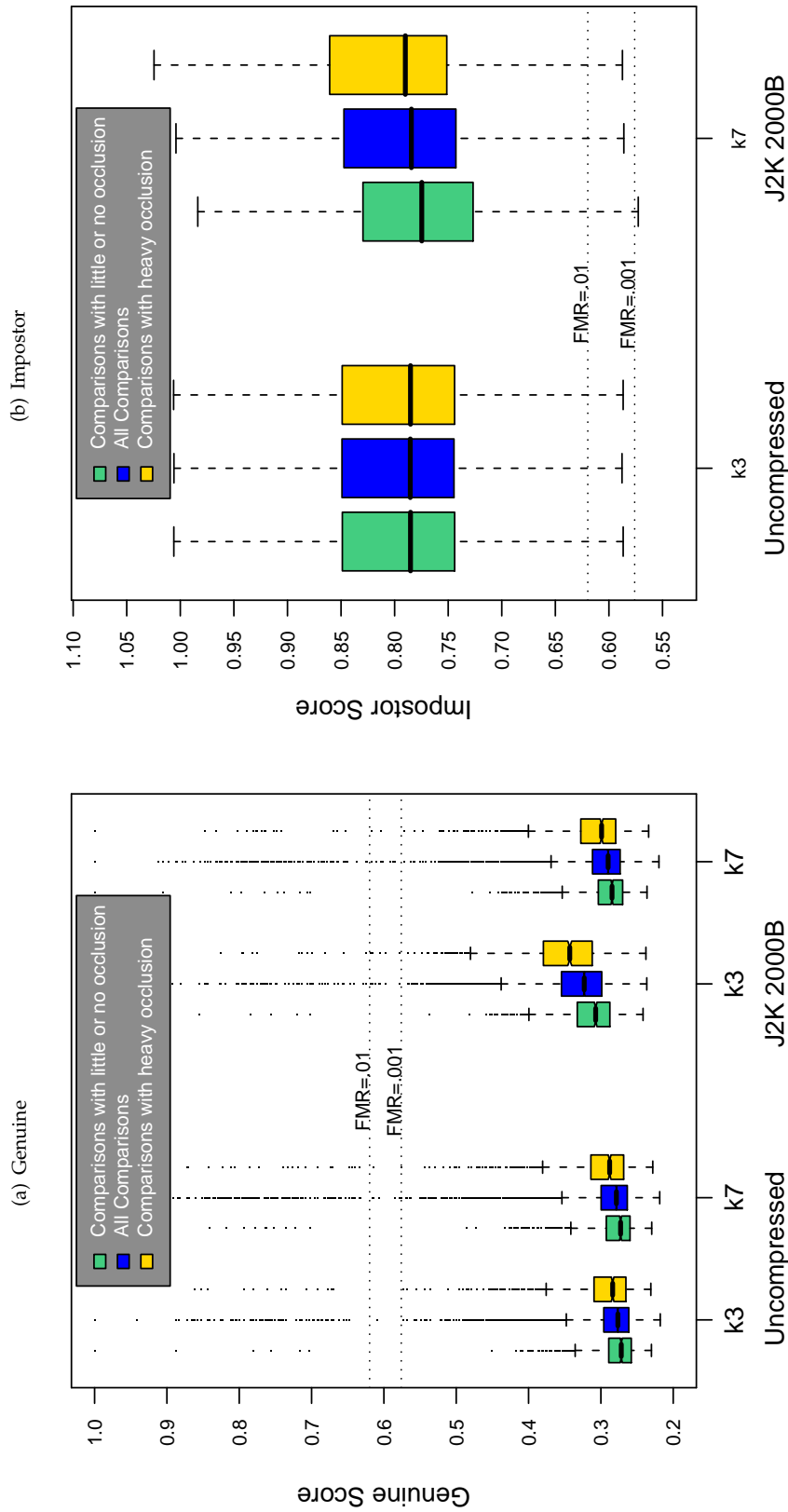
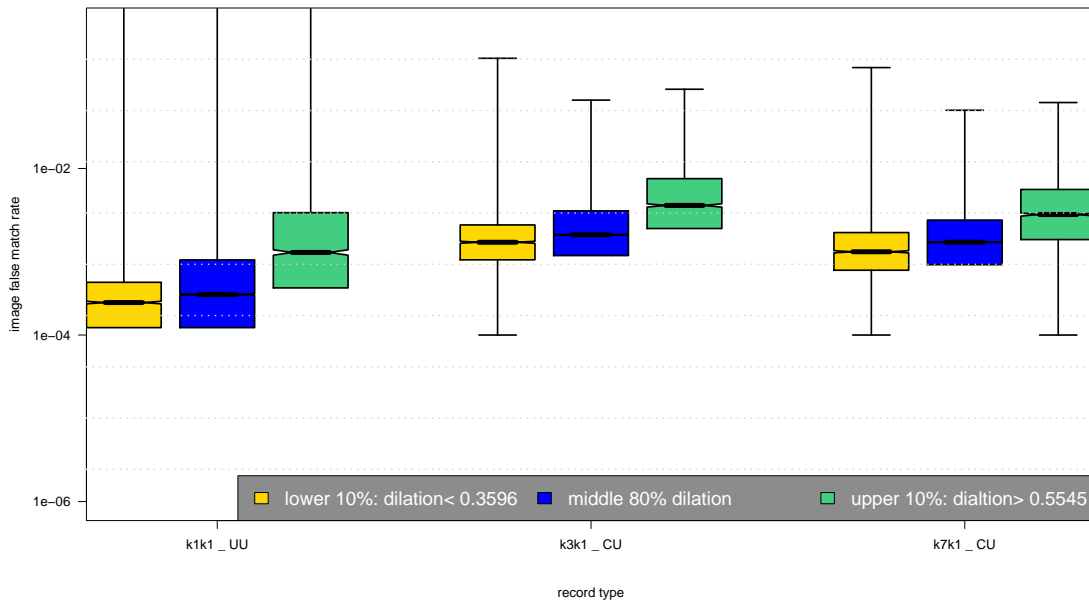
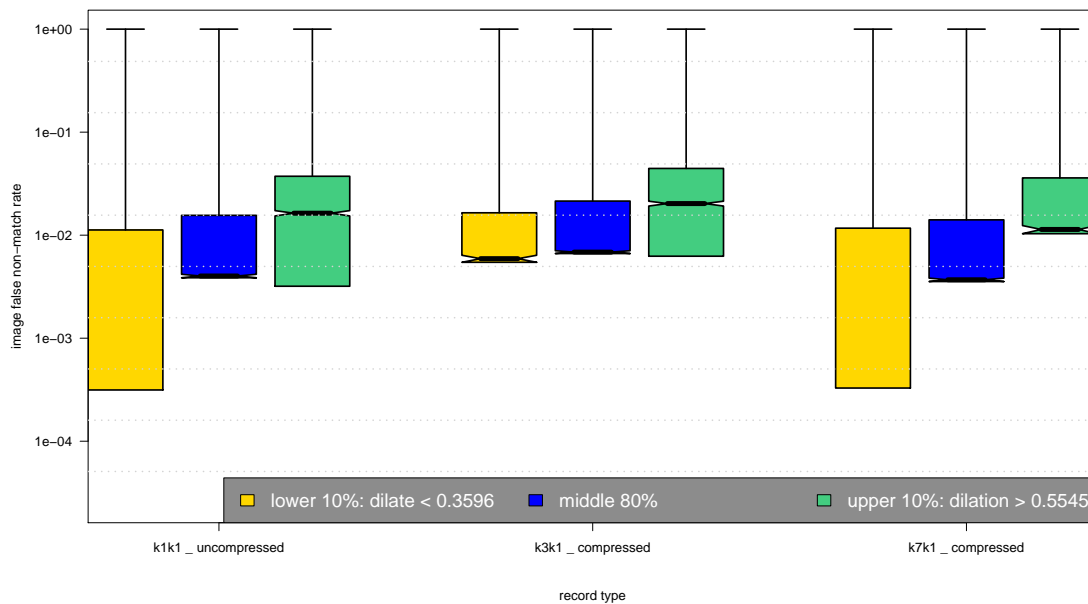


Table 112: The effect of eyelid occlusion on the two scores distributions for SDK E1.

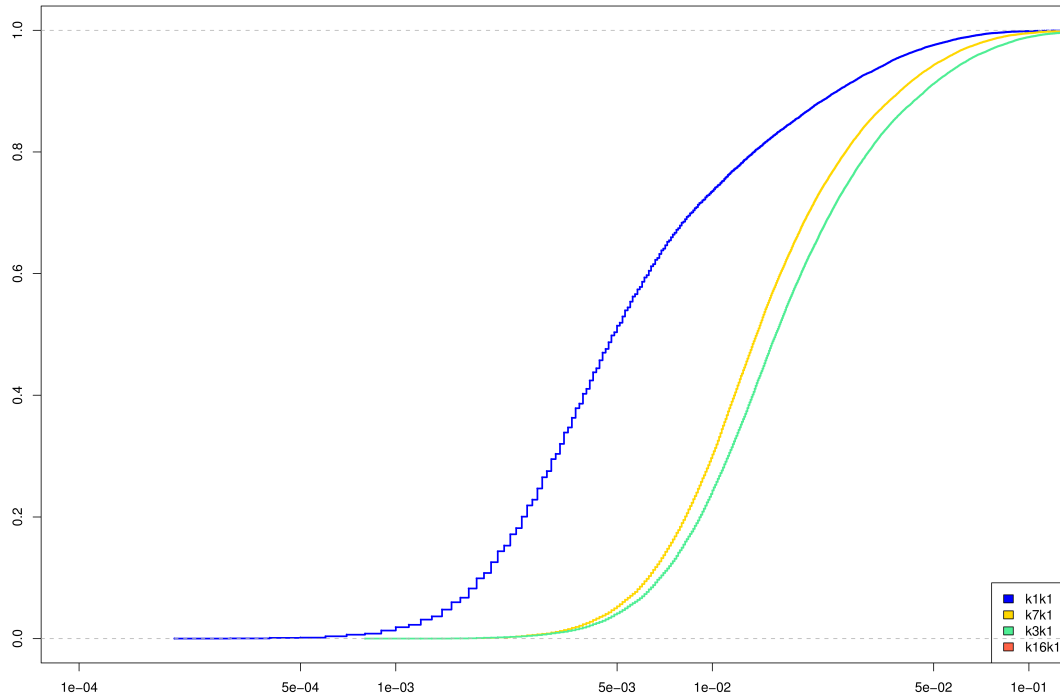
(a) iFMR using A1 dilation estimates



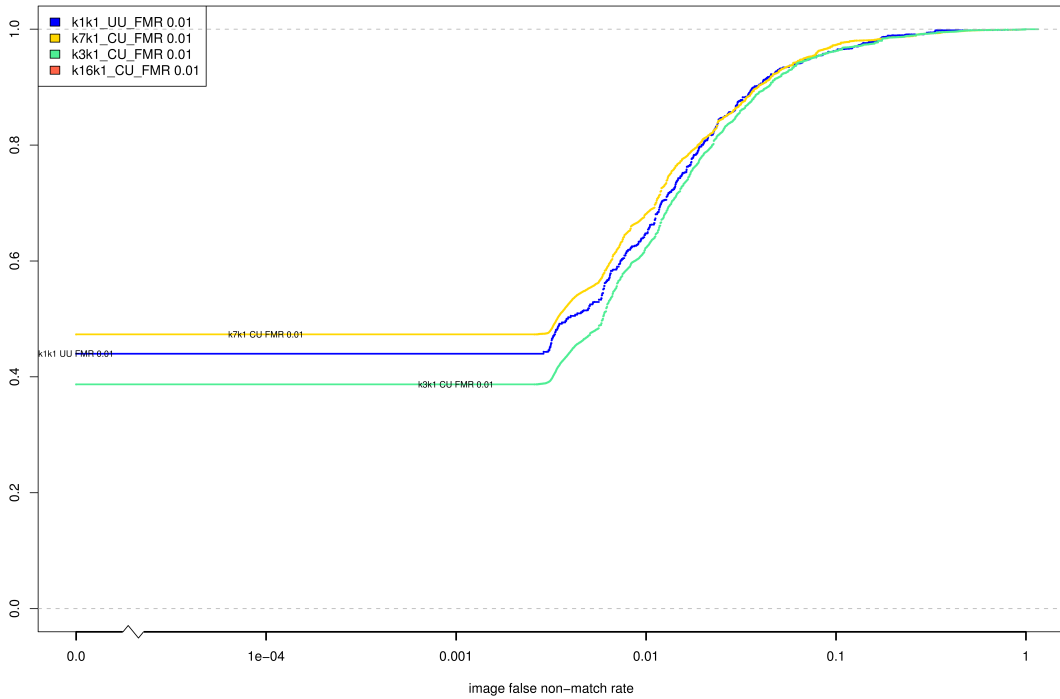
(b) iFNMR using A1 dilation estimates



(c) iFMR CDF



(d) iFNMR CDF



Compiled Results for Implementation E2

On June 25, 2009, NIST invited the IREX participants to submit a description of the SDKs submitted for the IREX effort. The intent was to allow providers to describe and contrast the feature sets, optimization, operational suitability and availability of the primary and secondary SDKs. NIST indicated that any submitted text would appear verbatim (with typesetting) in draft and final versions of the IREX report and that it would be attributed to the organization. This was optional and NIST put no constraints on the content beyond a 600 word limit, and a statement that anything labelled as confidential or proprietary would be omitted.

The provider of SDK E2, L1 Identity Solutions, submitted the following to NIST - we are unable to validate this information.

We would first like to thank NIST for taking on the responsibility of testing the interoperability and compressibility of the various proposed iris image formats. We are pleased to learn that our recommendation to discontinue the use of the polar format and JPEG compression in ISO 19794-6 is supported by the test results.

Both of the L-1 submissions were based on the Daugman algorithm, which has been designed for scalable performance with small templates and fast enrollment and match speeds. Our submission was born from our product experience and was tuned for a balance between stability, scalability and accuracy. Our first submission aimed to stabilize performance under compression by avoiding any dependency on very-high resolution information. As a result, its performance upheld its high levels on images compressed down to almost 2000 bytes². Our secondary submission was purely experimental and aimed to exploit higher-resolution iris texture.

A notable aspect of our submission was that it enforced a quality criterion on each sample, thus causing a Failure-To-Enroll (FTE) event whenever the quality of a sample was insufficient for very accurate matching. Quality-based filtering is a widely practiced in commercial live-capture cameras and has proven instrumental in protecting the recognition accuracy against the detrimental effects of eyelid occlusions and camera-eye misalignment. Typically, the camera captures several images in a session and then selects the single best sample for enrollment or verification. FTEs only occur in the rare case that even the best sample does not meet the quality criterion. IREX, by contrast, reflects the case if any of the samples fail to meet the criterion. This counting method overestimates the FTE rate with respect to operational scenarios on data such as BATH and ICE (see table 6). Though our quality criterion may have been too restrictive with respect to iris diameter, it showed the expected effectiveness in reducing the False-Rejects and producing excellent match accuracy as documented for ICE in fig. 12b.

Second, we point out that our algorithm has been designed to control False-Accept-Rates (FAR) to lower than 1 in a million by means of a tightly controlled and stable imposter score distribution. This ensures that databases of several millions of enrollments can be searched exhaustively without generating False Matches. The benefits of this fundamental feature, which are evidenced in our flat DET curves, are critical for success in real-world deployments, but less visible in tests like IREX which focus on relatively undemanding FARs. The stability of our scoring over different databases, however, was visible and specifically pointed out in IREX.

L-1 Identity Solutions patented Daugman algorithm has consistently been a top-tier technology in testing and the results here show the technology to be accurate, stable over different data sets, and highly scalable compared to other SDKs. It is currently the only commercially available technology with a field-proven

²Graph in initial IREX report

capability to cope with database sizes and throughputs needed for national ID projects. It is deployed in numerous scenarios, including military systems, jail systems, deportation systems, and registered traveler programs. The Daugman algorithm powers iris recognition in L-1 Identity Solutions ABIS multi-biometric search system, the SIRIS search engine, and in the HIIDE and PIER mobile devices. In the end, the L-1 Identity Solutions iris product suite will undoubtedly benefit from the lessons learned in IREX as it will influence our product requirements and algorithmic research goals for the next generation of iris technology. We again thank NIST and their sponsors for providing new insights and validating our old ones with this IREX testing effort.

On August 17, 2009, NIST invited the IREX participants to submit a description their comments on a draft version of the IREX report. This was intended to allow participants to assist readers in the interpretation of a large and complicated testing effort. NIST indicated that any submitted text would appear verbatim (with typesetting) in the final version of the IREX report and that it would be attributed to the organization. Submission of content was optional and NIST put no constraints on the content beyond a word limit, and a statement that anything labelled as confidential or proprietary would be omitted.

The provider of SDK E2, L1 Identity Solutions, elected not to submit any information

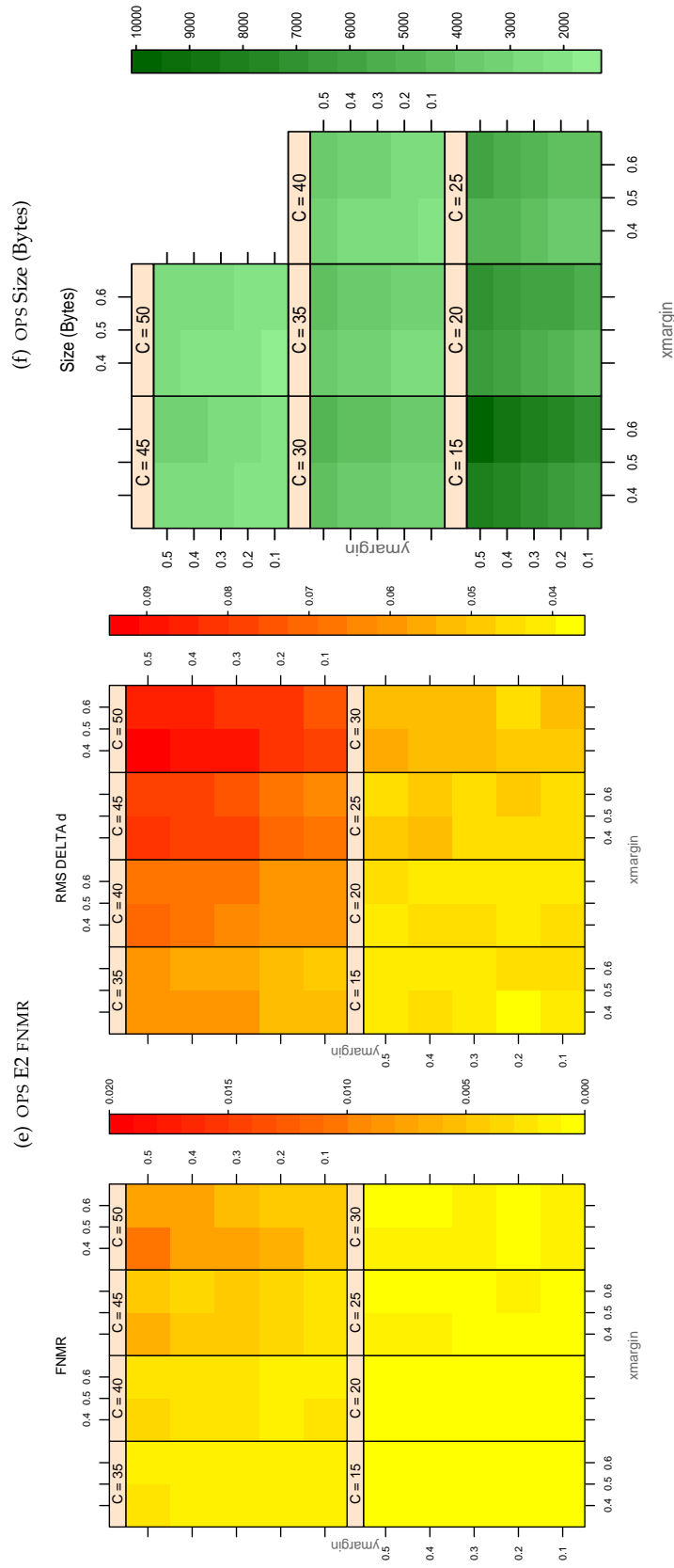


Table 113: For the IREX partition of the OPS database the plots at left show the dependence of cFNMNR on the vertical and horizontal iris cropping margins for various compression ratios. This applies only for KIND 3 records. The margins are in units of iris radius. The use of conditional FNMNR means that the plots exclude comparisons that were falsely rejected even before any compression was applied. On the **right side** is the rms difference between the crop+compress and the uncompressed comparison scores for each image pair. All computations are driven by the bounding box coordinates reported by the II SDK. The number of bits per pixel is $8/C$, where C is the compression ratio. The iris radius varies and because the cropping margins are fixed multiples of the radius the image size varies. The compressed size, in bytes, is the width times height divided by C . Values of cFNMNR greater than 0.02 are shown as 0.02.

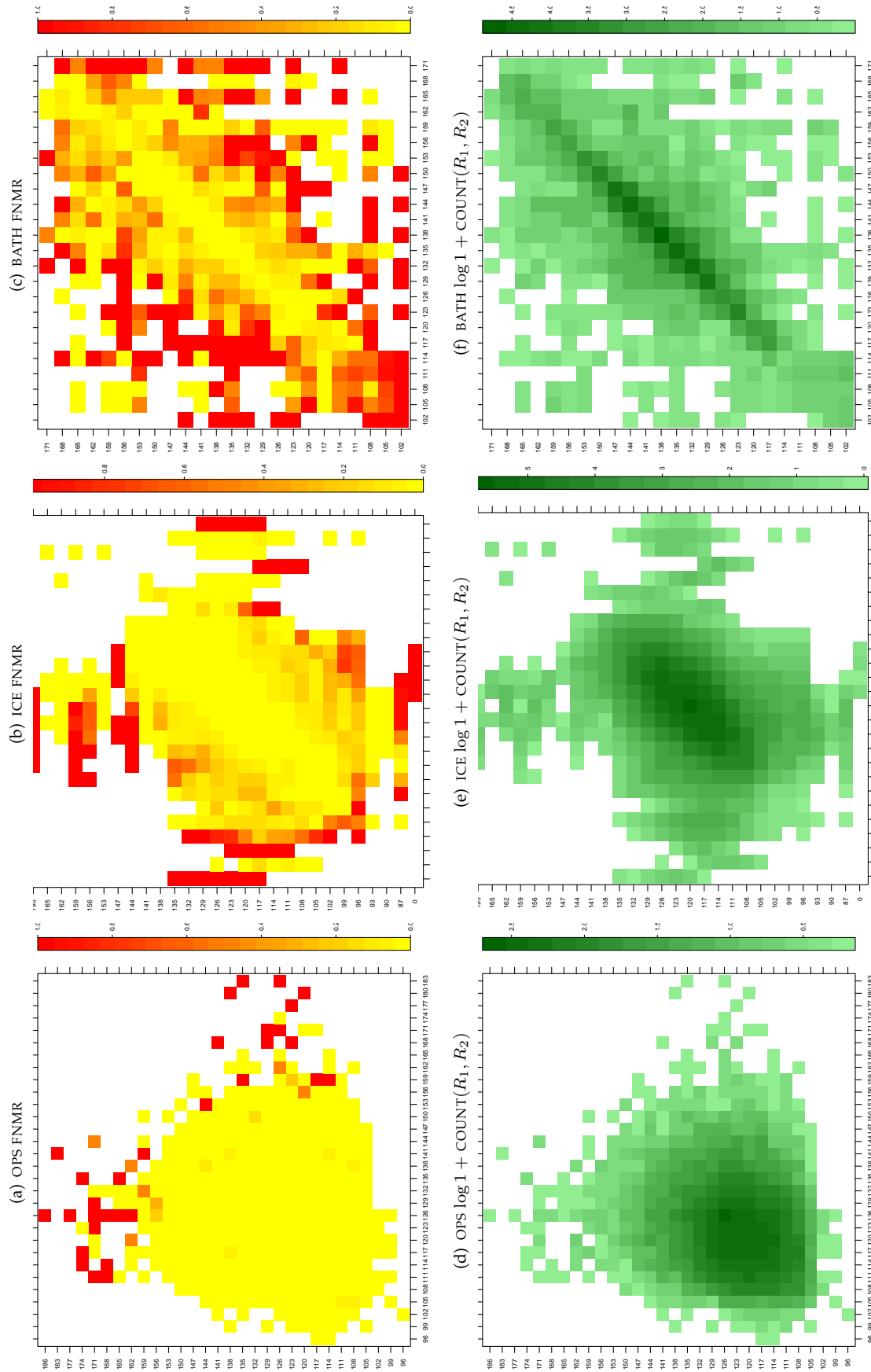


Table 114: For the three IREX databases: In the **top** row the color in each cell represents the occurrence of genuine comparisons with the given pair of radii. The *y*-axis represents enrollment samples with verification samples on the *x*-axis; In the **bottom** row the color scale plots $\log 1 + \text{COUNT}(R_1, R_2)$. The radii are quantized into three-pixel bins. The radii for DOD are on the range $96 \leq r \leq 186$ pixels. The radii for ICE are on the range $87 \leq r \leq 165$ pixels. The radii for BATH are on the range $100 \leq r \leq 170$ pixels.

A = SAGEM	B = COGENT	C = CROSSMATCH	D = CAMBRIDGE	E = L1	$x1$ = PRIMARY
F = RETICA	G = LG	H = HONEYWELL	I = IRITECH	J = NEUROTECHNOLOGY	$x2$ = SECONDARY
KIND 1 = RAW 640x480		KIND 3 = CROP		KIND 7 = CROP+MASK	
KIND 16 = CONCENTRIC POLAR					

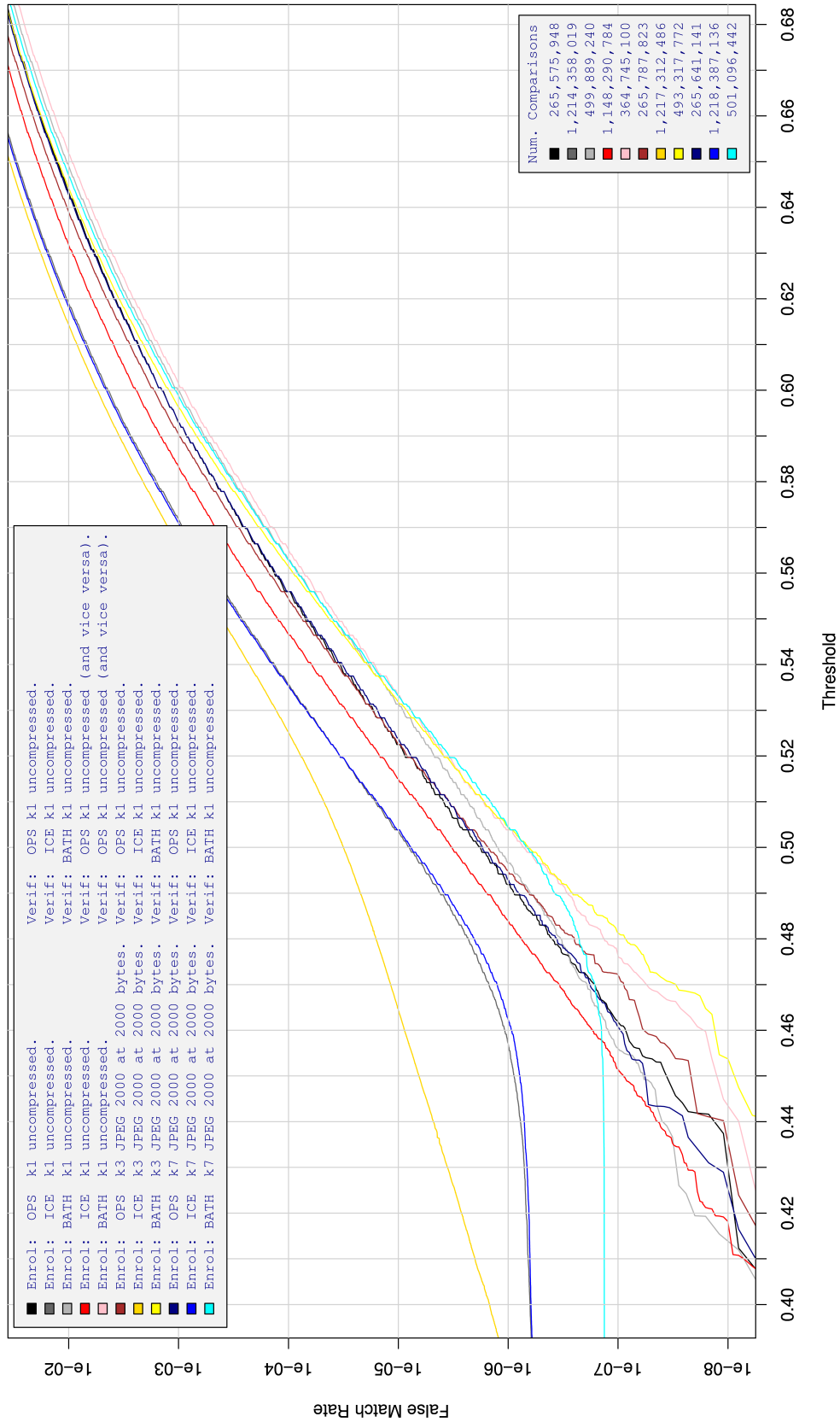


Table 115: For implementation E2, the dependency of FMR on threshold. for various combinations of enrollment and verification dataset, format, and compression.

A = SAGEM	B = COGENT	C = CROSSMATCH	D = CAMBRIDGE	E = L1	x1 = PRIMARY
F = RETICA	G = LG	H = HONEYWELL	I = IRITECH	J = NEUROTECHNOLOGY	x2 = SECONDARY
KIND 1 = RAW 640x480		KIND 3 = CROP	KIND 7 = CROP+MASK	KIND 16 = CONCENTRIC POLAR	

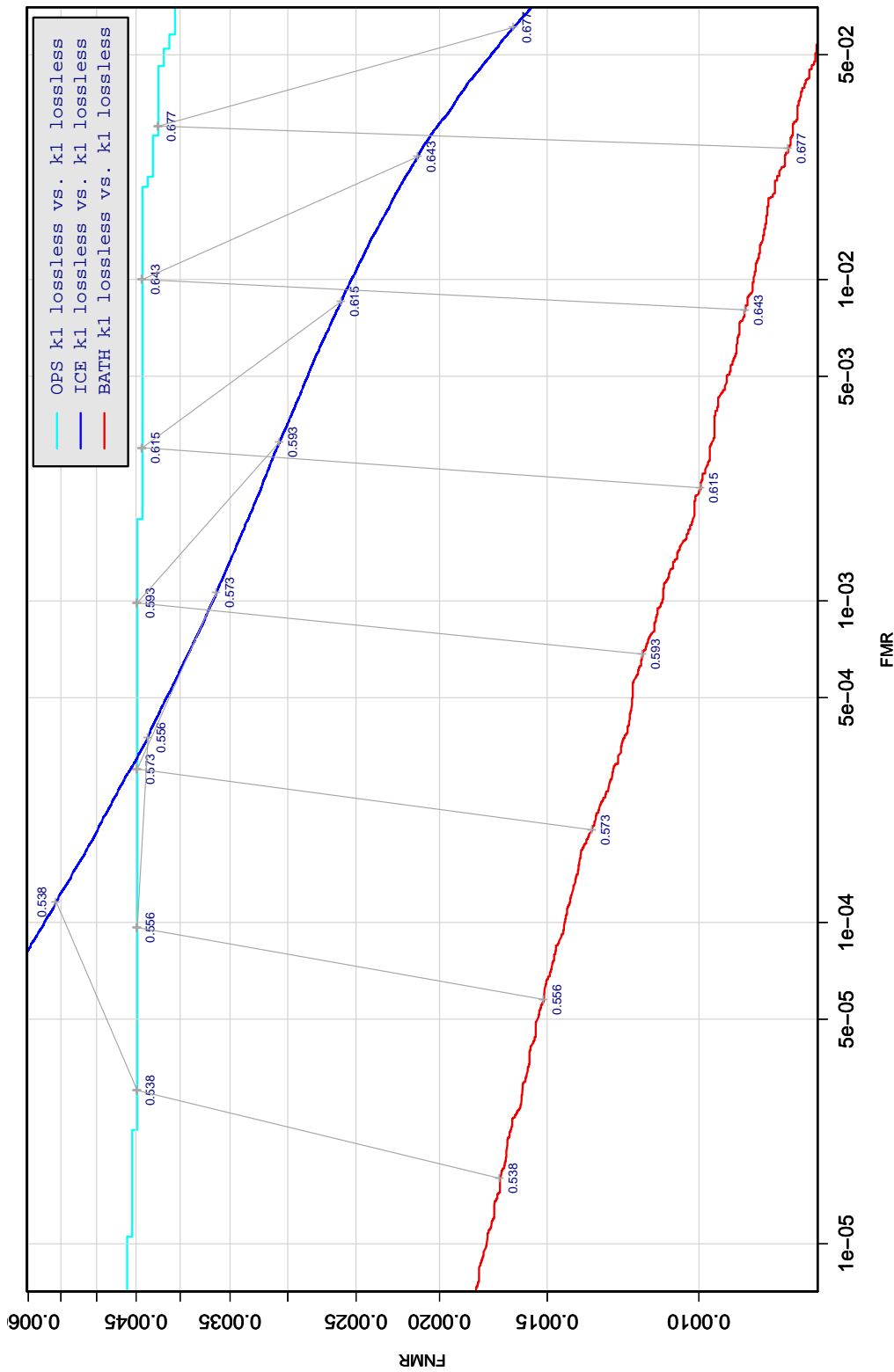


Table 116: DET curve for implementation E2 on three IREX databases. All comparisons are with uncompressed KIND 1 vs. KIND 1 images. The lines join points corresponding to the a fixed threshold. Non-vertical links indicate a change in FMR when the database changes. All results apply to native operation. Failures to produce a template i.e. FTE are ignored because the plots are intended to show *matching* effects, specifically to compare DET slopes and to show the effect of fixing a threshold.

A = SAGEM	B = COGENT	C = CROSSMATCH	D = CAMBRIDGE	E = L1	x1 = PRIMARY
F = RETICA	G = LG	H = HONEYWELL	I = IRITECH	J = NEUROTECHNOLOGY	x2 = SECONDARY
KIND 1 = RAW 640x480		KIND 3 = CROP	KIND 7 = CROP+MASK	KIND 16 = CONCENTRIC POLAR	

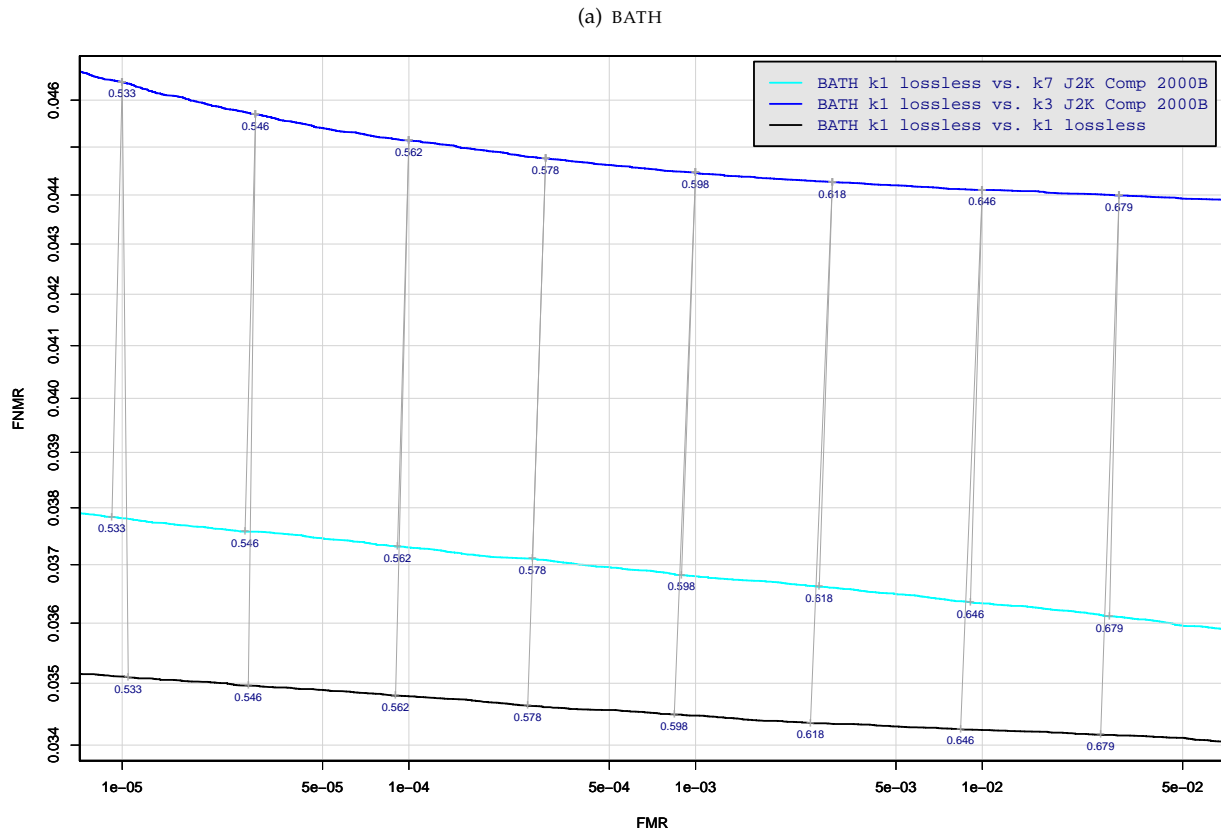


Table 117: DET curve for implementation E2 on the BATH database for the various supported KINDS . The DET characteristics are linked by lines joining points of equal threshold. Non-vertical links indicate a change in false acceptance when the data KIND changes. All results apply to native operation, and the effects of FTE are included.

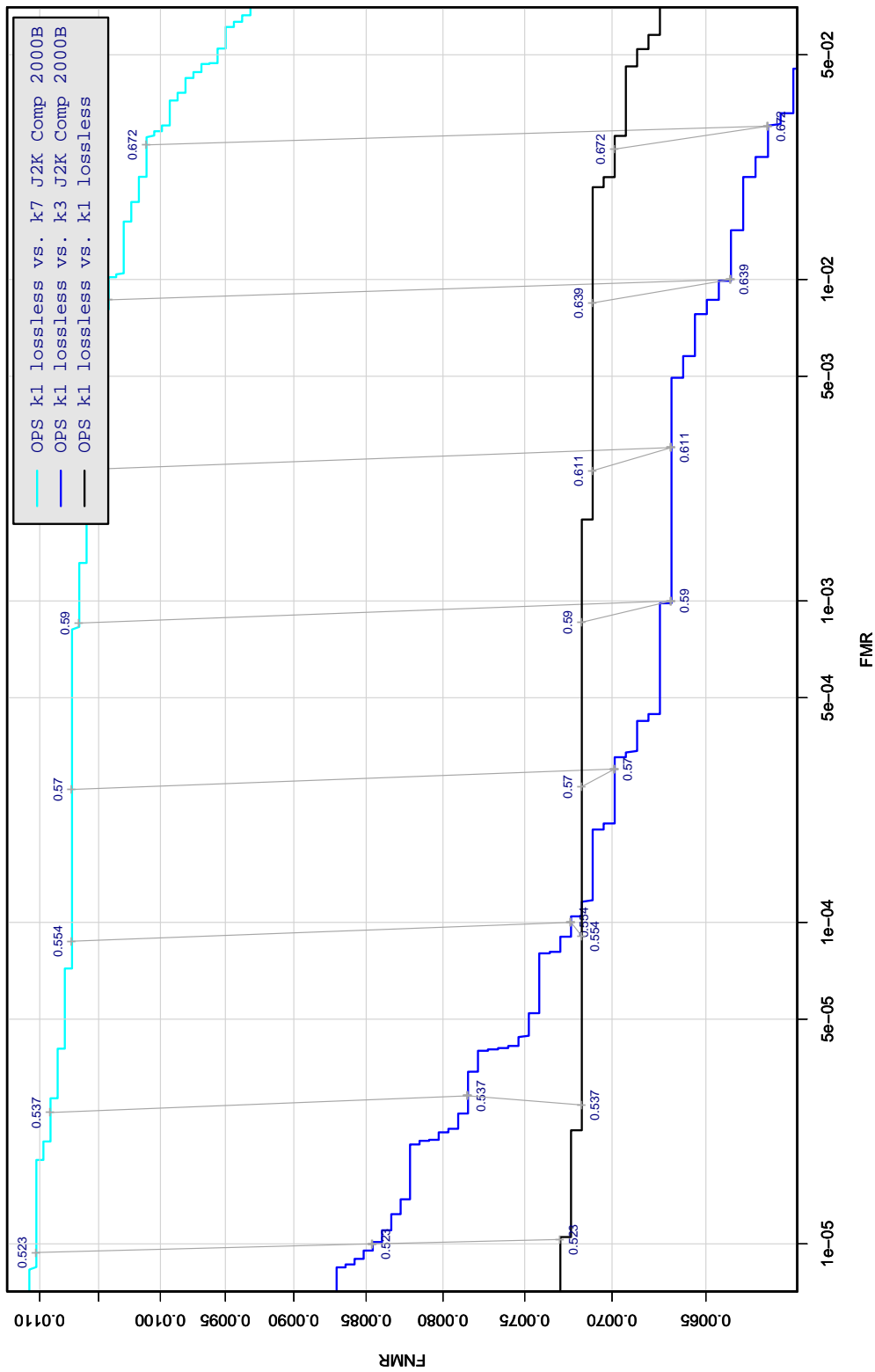


Table 118: DET curve for implementation E2 on the OPS database for the various supported KINDS . The DET characteristics are linked by lines joining points of equal threshold. Non-vertical links indicate a change in false acceptance when the data KIND changes. All results apply to native operation, and the effects of FTE are included.

A = SAGEM	B = COGENT	C = CROSSMATCH	D = CAMBRIDGE	E = L1	x1 = PRIMARY
F = RETICA	G = LG	H = HONEYWELL	I = IRITECH	J = NEUROTECHNOLOGY	x2 = SECONDARY
KIND 1 = RAW 640x480		KIND 3 = CROP		KIND 7 = CROP+MASK	KIND 16 = CONCENTRIC POLAR

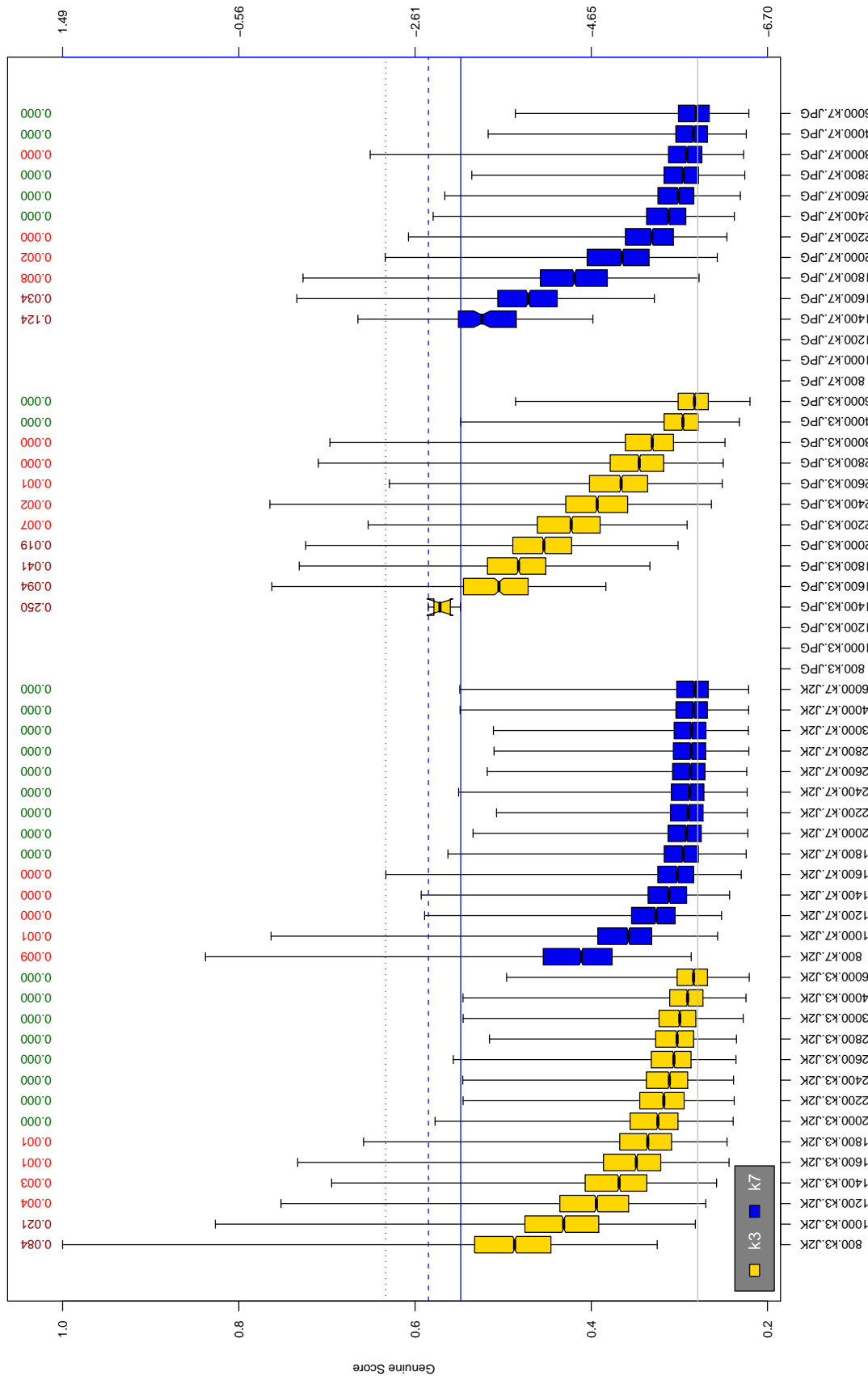


Table 119: The distribution of E2 native genuine comparison scores by size of the compressed image, KIND and the compression algorithm. The images are from the OPS dataset. The right axis scale gives the corresponding value for $d' = (s - \mu_I) / \sqrt{0.5(\sigma_I^2 + \sigma_G^2)}$ for genuine score s . The boxplots only include comparison scores if the uncompressed version of the same image was matched below the FMR = 0.001 threshold. Above the boxplots are FNMR values at FMR = 10^{-3} . The three blue lines correspond, from the top, to FMR of $10^{-2}, -3, -4$. The lower grey line refers to the median score obtained from comparison of uncompressed KIND 3 images. Any comparison for which either template had not been generated is excluded. Note that the iris record size on the horizontal axis is not evenly spaced above 3000 bytes.

A = SAGEM	B = COGENT	C = CROSSMATCH	D = CAMBRIDGE	E = L1	$x1$ = PRIMARY
F = RETICA	G = LG	H = HONEYWELL	I = IRITECH	J = NEUROTECHNOLOGY	$x2$ = SECONDARY
KIND 1 = RAW 640x480		KIND 3 = CROP	KIND 7 = CROP+MASK	KIND 16 = CONCENTRIC POLAR	

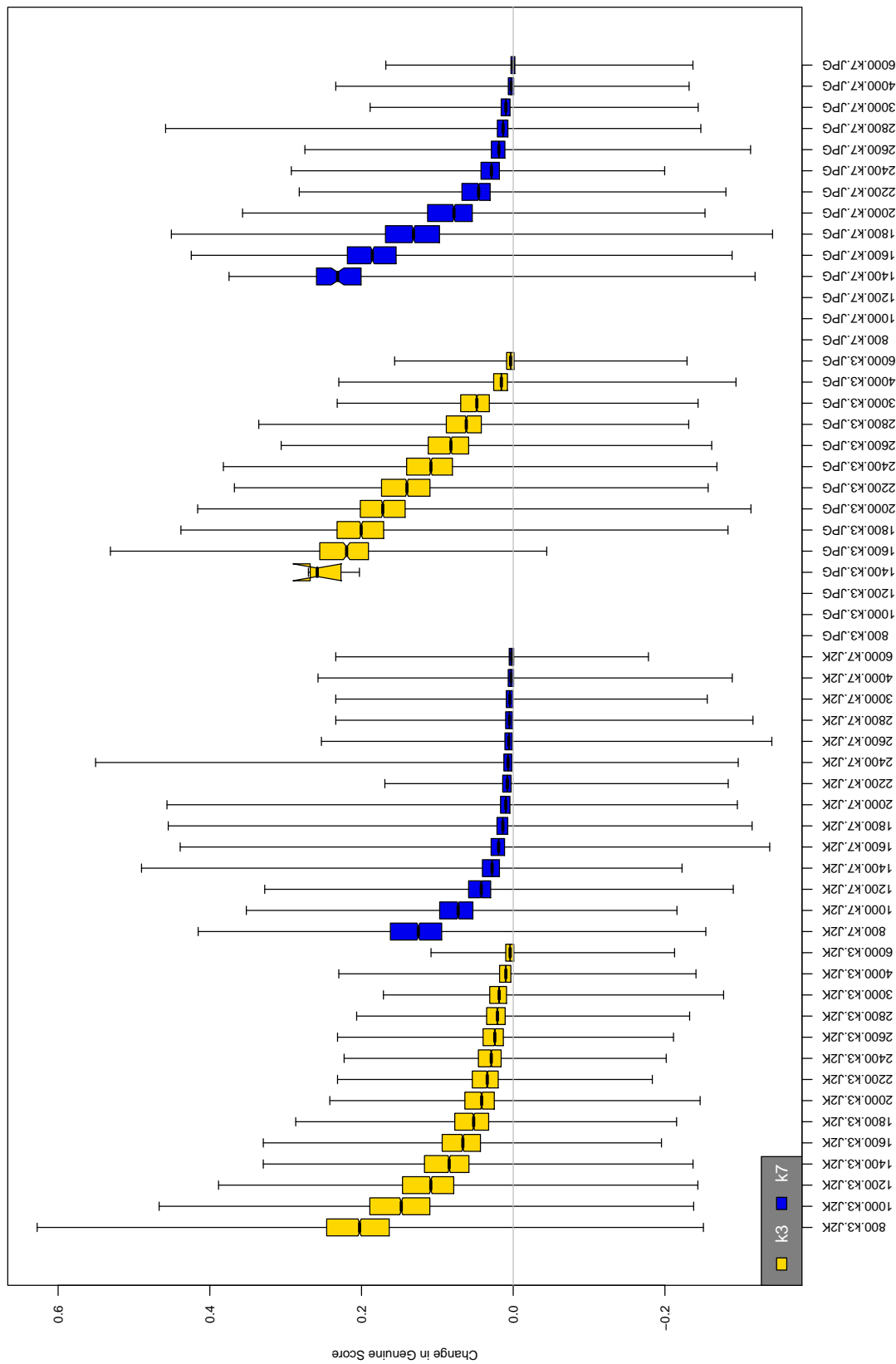


Table 120: The distribution of the *increase* in E2 native genuine comparison scores between the uncompressed “parent” and the compressed image, arranged by size, KIND and the compression algorithm. The images are from the OPS dataset. Any comparison involving a failed template is excluded. Note that the iris record size on the horizontal axis is not evenly spaced above 3000 bytes.

A = SAGEM	B = COGENT	C = CROSSMATCH	D = CAMBRIDGE	E = L1	$x1$ = PRIMARY
F = RETICA	G = LG	H = HONEYWELL	I = IRITECH	J = NEUROTECHNOLOGY	$x2$ = SECONDARY
KIND 1 = RAW 640x480		KIND 3 = CROP	KIND 7 = CROP+MASK	KIND 16 = CONCENTRIC POLAR	

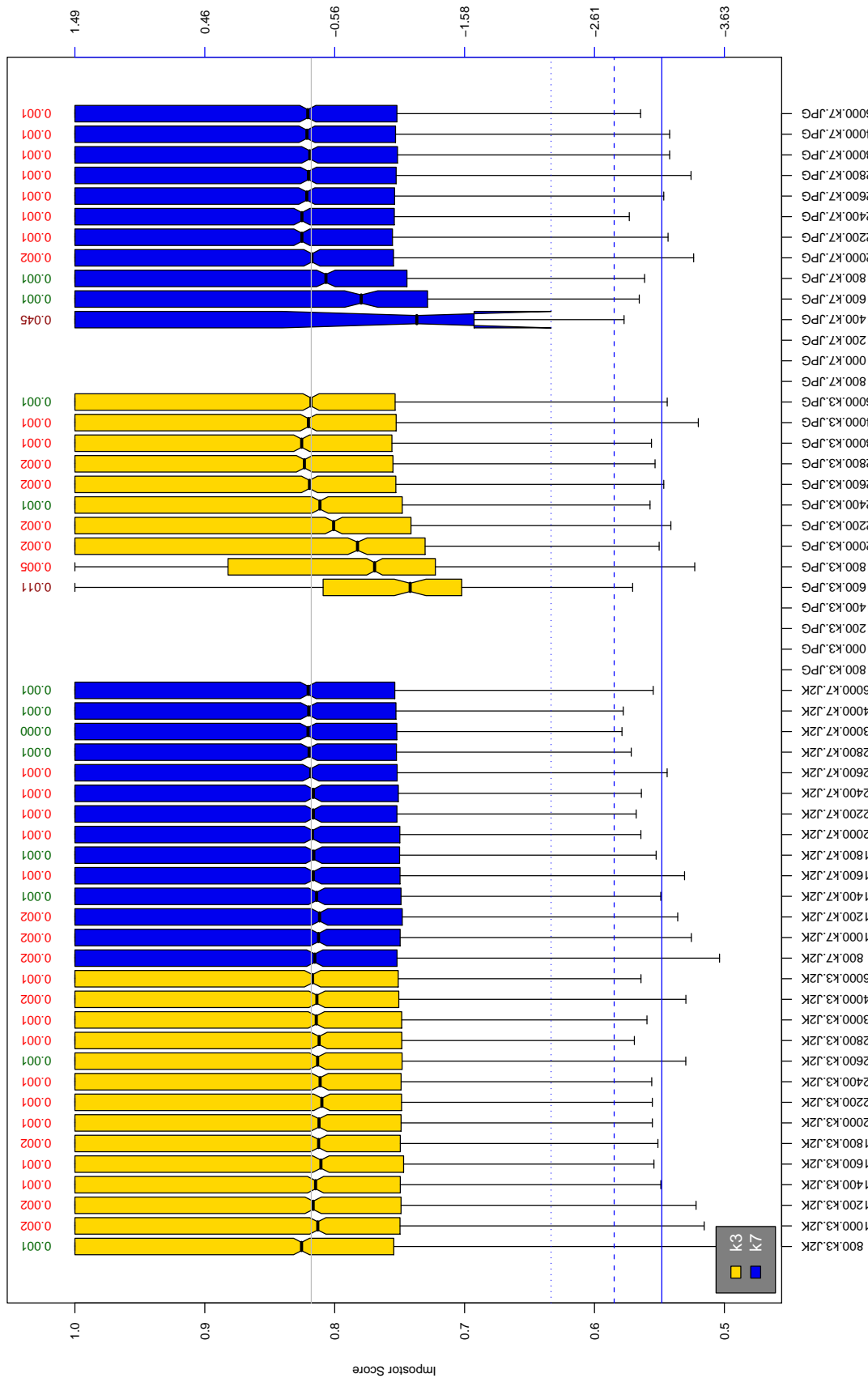


Table 121: The distribution of E2 native impostor comparison scores by size of the compressed image, KIND and the compression algorithm. The right axis gives the corresponding value for $d' = (s - \mu_1) / \sqrt{0.5(\sigma_1^2 + \sigma_2^2)}$ for impostor score s . The three blue lines correspond, from the top, to FMR of 10^{-2} , 10^{-3} , and 10^{-4} . The lower grey line refers to the median score obtained from comparison of uncompressed KIND 3 images. Any comparison involving a failed template is excluded. Above the boxplots are FMR values at the threshold that gives FMR = 10^{-3} on uncompressed images. These figures are computed from only 4000 comparisons so the FMR values and the tails of the impostor distribution are poorly characterized. Note that the iris record size on the horizontal axis is not evenly spaced above 3000 bytes.

A = SAGEM	B = COGENT	C = CROSSMATCH	D = CAMBRIDGE	E = L1	$x1$ = PRIMARY
F = RETICA	G = LG	H = HONEYWELL	I = IRITECH	J = NEUROTECHNOLOGY	$x2$ = SECONDARY
KIND 1 = RAW 640x480		KIND 3 = CROP	KIND 7 = CROP+MASK	KIND 16 = CONCENTRIC POLAR	

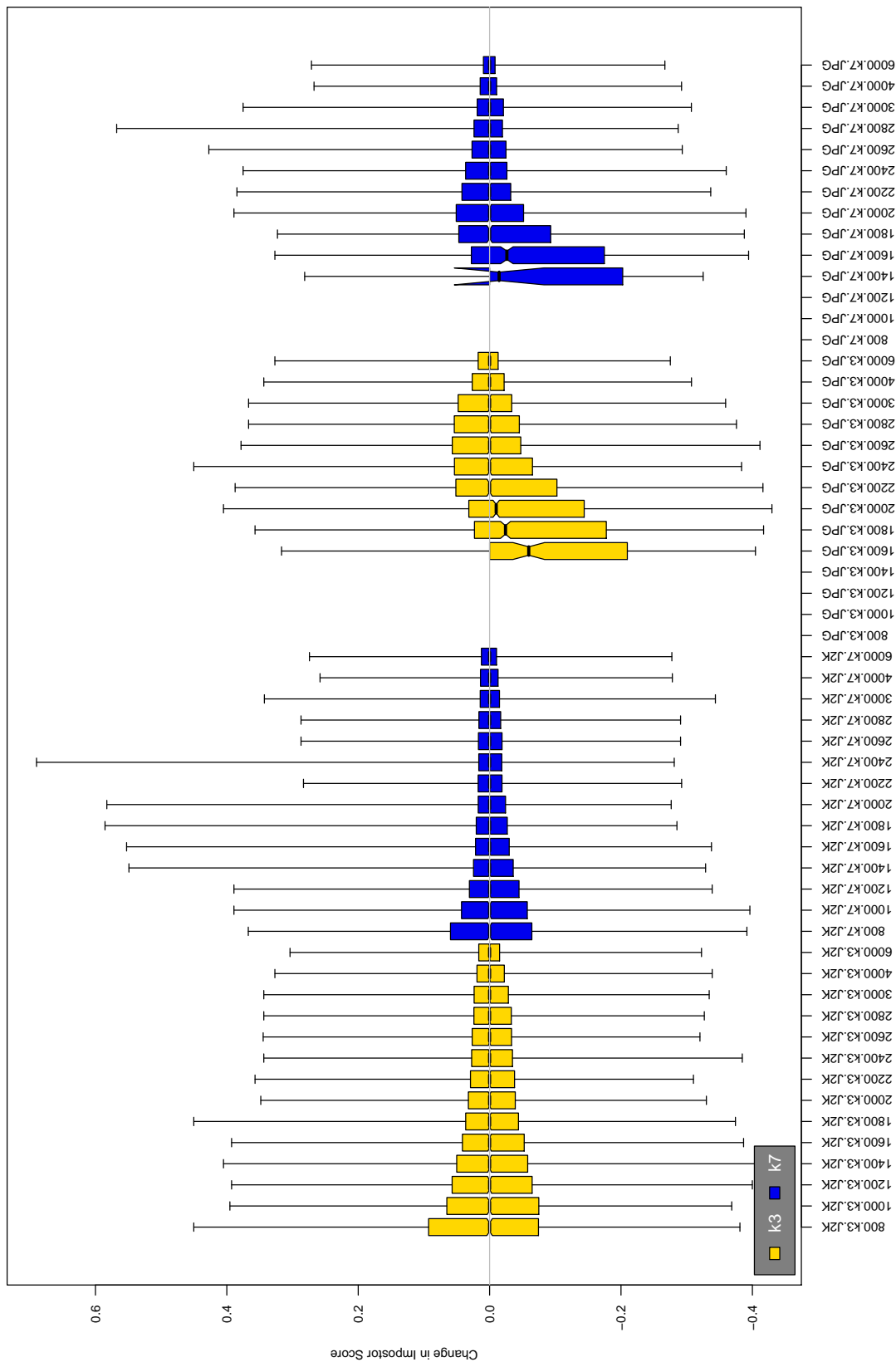


Table 122: The distribution of the increase in E2 native impostor comparison scores between the uncompressed “parent” and the compressed image, arranged by size, KIND and the compression algorithm. The images are from the OPS dataset. Any comparison involving a failed template is excluded. Note that the iris record size on the horizontal axis is not evenly spaced above 3000 bytes.

A = SAGEM	B = COGENT	C = CROSSMATCH	D = CAMBRIDGE	E = L1	x1 = PRIMARY
F = RETICA	G = LG	H = HONEYWELL	I = IRITECH	J = NEUROTECHNOLOGY	x2 = SECONDARY
KIND 1 = RAW 640x480		KIND 3 = CROP	KIND 7 = CROP+MASK	KIND 16 = CONCENTRIC POLAR	

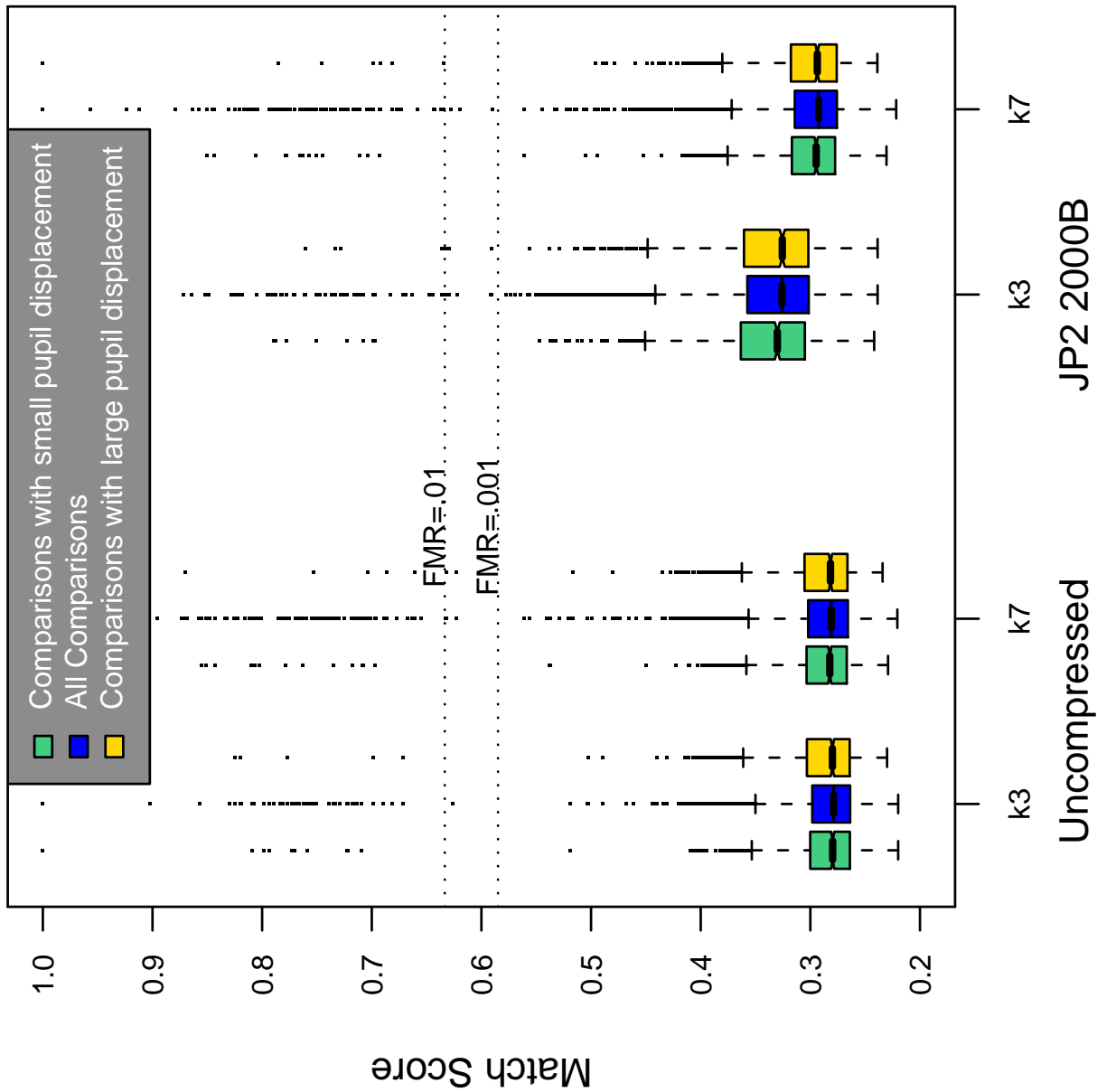


Table 123: Effect of pupil displacement on the genuine score distribution for E2

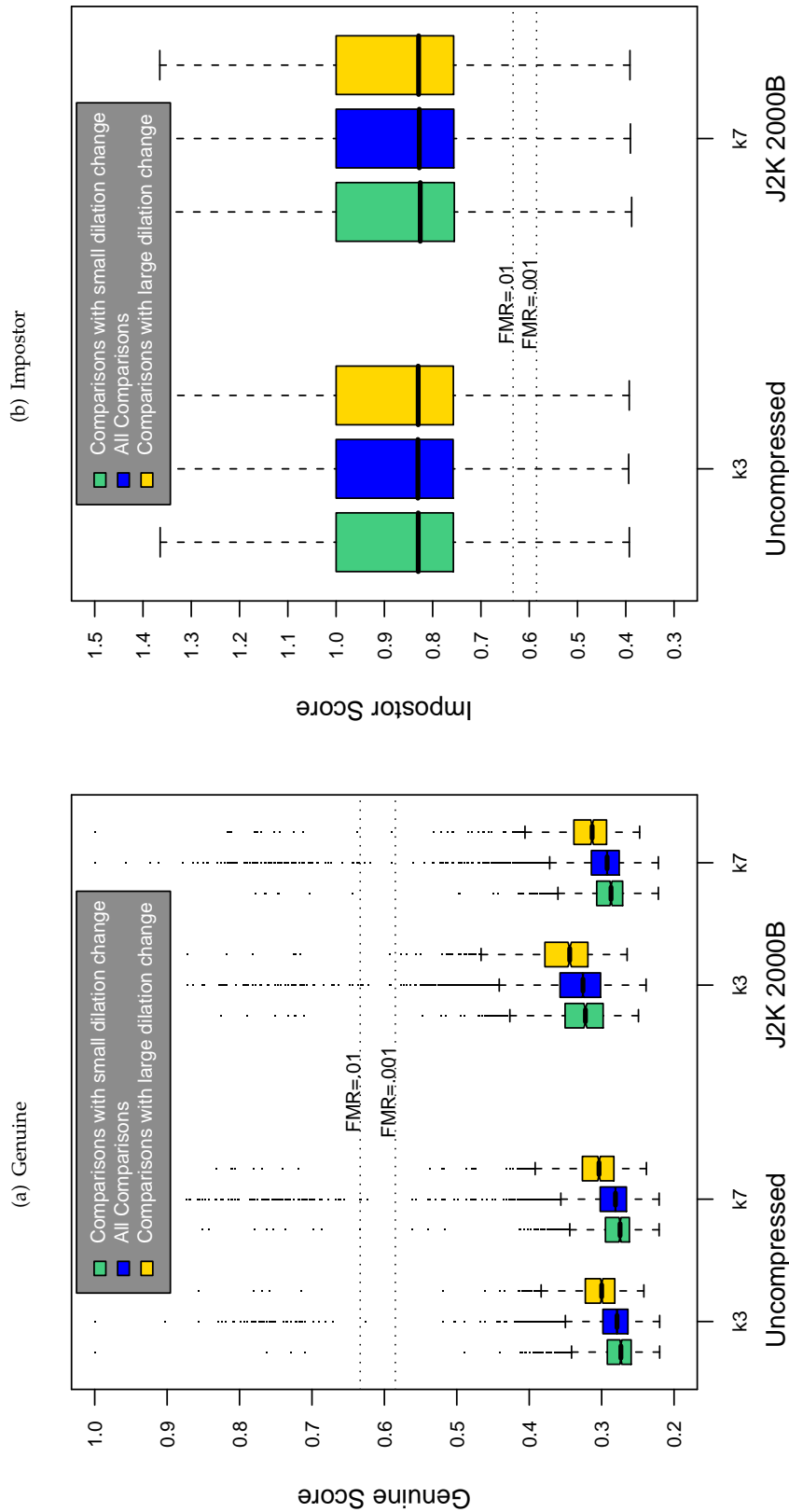


Table 124: The effect of dilation change on the two scores distributions for SDK E2.

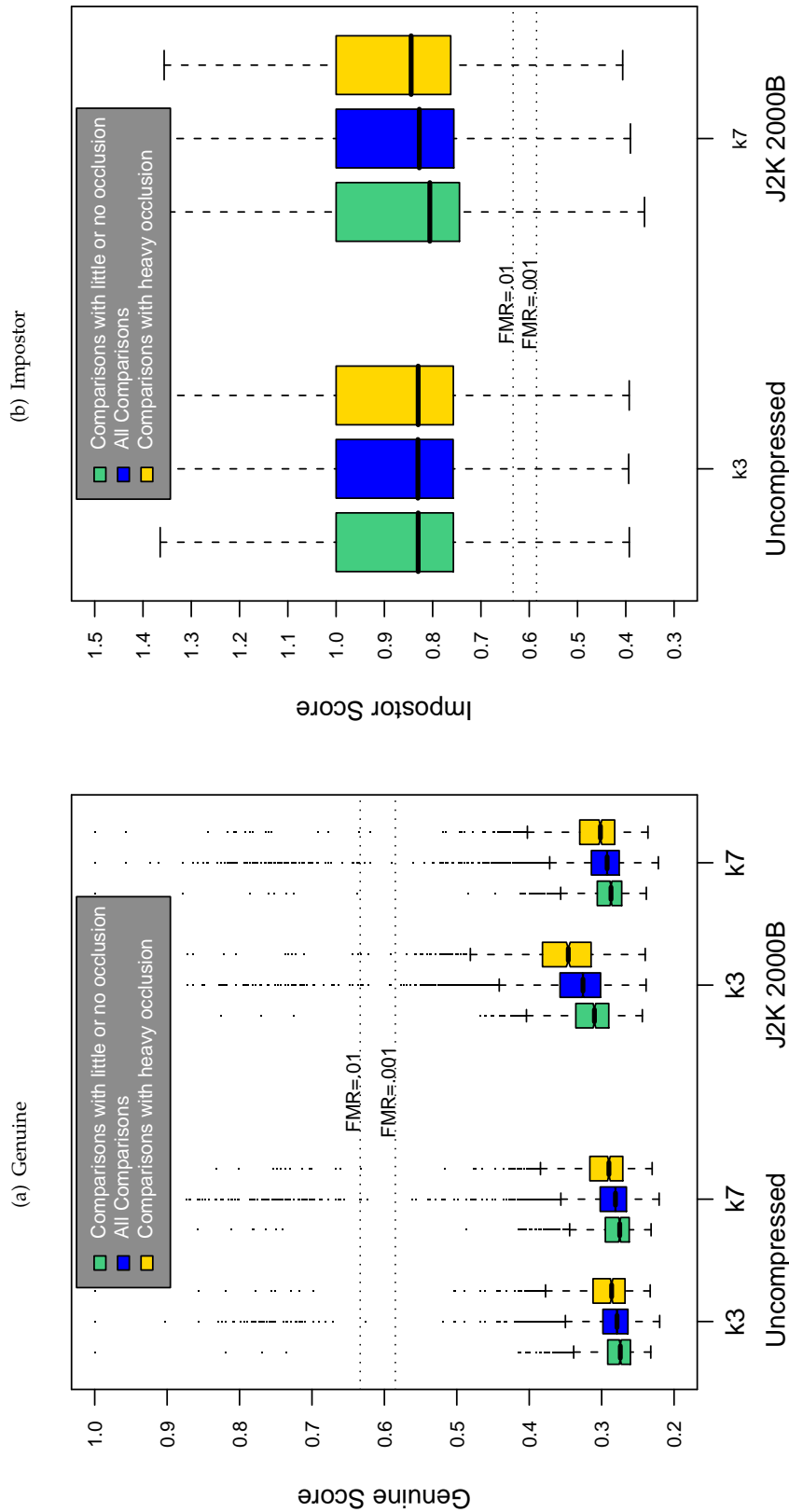
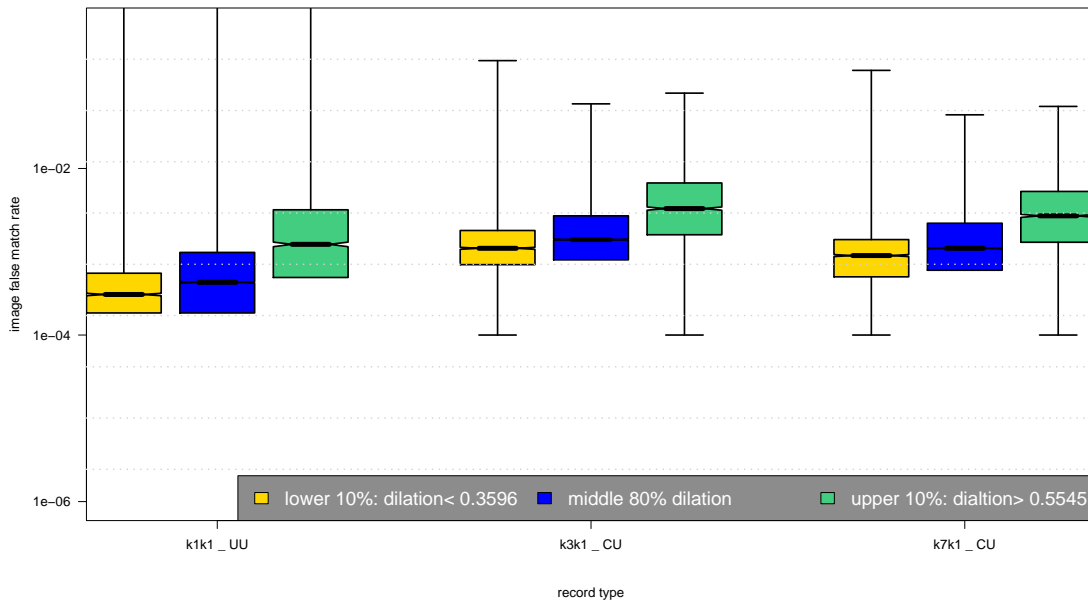
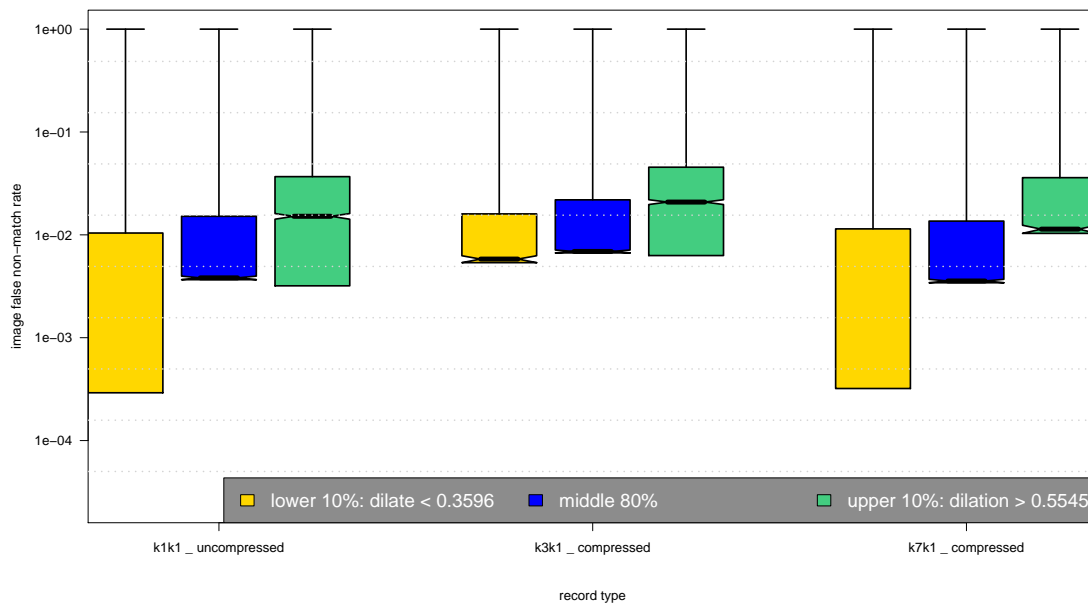


Table 125: The effect of eyelid occlusion on the two scores distributions for SDK E2.

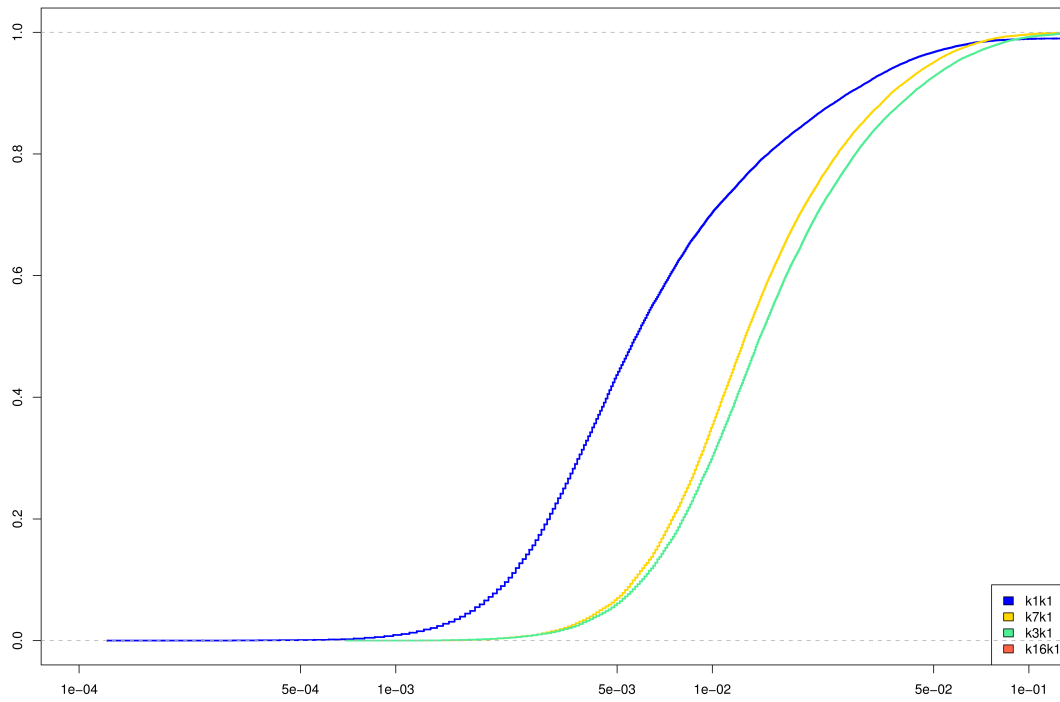
(a) iFMR using A1 dilation estimates



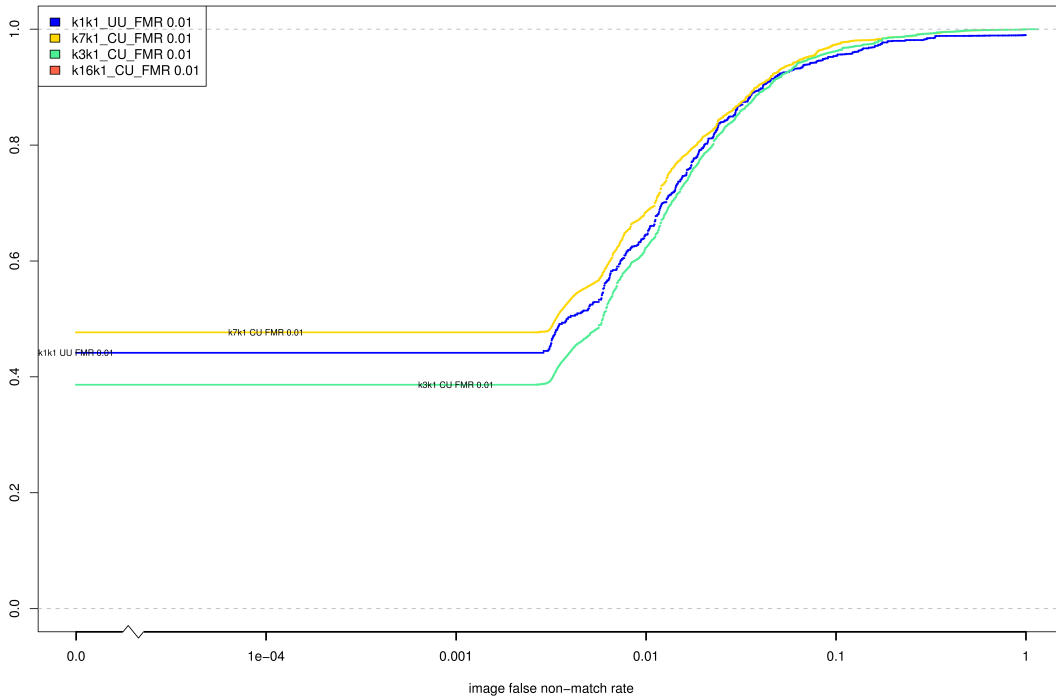
(b) iFNMR using A1 dilation estimates



(c) iFMR CDF



(d) iFNMR CDF



Compiled Results for Implementation F1

On June 25, 2009, NIST invited the IREX participants to submit a description of the SDKs submitted for the IREX effort. The intent was to allow providers to describe and contrast the feature sets, optimization, operational suitability and availability of the primary and secondary SDKs. NIST indicated that any submitted text would appear verbatim (with typesetting) in draft and final versions of the IREX report and that it would be attributed to the organization. This was optional and NIST put no constraints on the content beyond a 600 word limit, and a statement that anything labelled as confidential or proprietary would be omitted.

The provider of SDK F1, Retica Systems, submitted the following to NIST - we are unable to validate this information.

Dear Patrick, 6-26-2009

We greatly appreciate your having conducted this very important study. The results give great guidance on what formats and kinds of compression should be used to satisfy escalating size constraints from 307kb down to 2kb.

As scientists and researchers in biometrics we would strongly suggest that vendors and researchers try and resist the use of any kind of cropping or lossy compression. We would encourage convincing their customers to keep as much information as is economically possible for enrollment databases. Cropped or compressed data should only be used when dictated by application specific constraints and not used broadly within the industry.

We have only begun to scratch at the surface of biometrics. We believe tomorrow's technology will be multimodal and that other anatomical structures will be incorporated into future technologies. We also believe a past practice of adulteration of images severely hampered and continues to hamper our industries growth because of outdated legacy databases. Capturing raw unadulterated images will encourage customers to invest in this technology without the specter of being locked into a particular vendor and allow their investment to take full advantage of future technological advancements. A free market encourages innovation, reduces costs and will only strengthen our industry.

Retica Systems, Inc.

On August 17, 2009, NIST invited the IREX participants to submit a description their comments on an draft version of the IREX report. This was intended to allow participants to assist readers in the interpretation of a large and complicated testing effort. NIST indicated that any submitted text would appear verbatim (with typesetting) in the final version of the IREX report and that it would be attributed to the organization. Submission of content was optional and NIST put no constraints on the content beyond a word limit, and a statement that anything labelled as confidential or proprietary would be omitted.

The provider of SDK F1, Retica Systems, elected not to submit any information

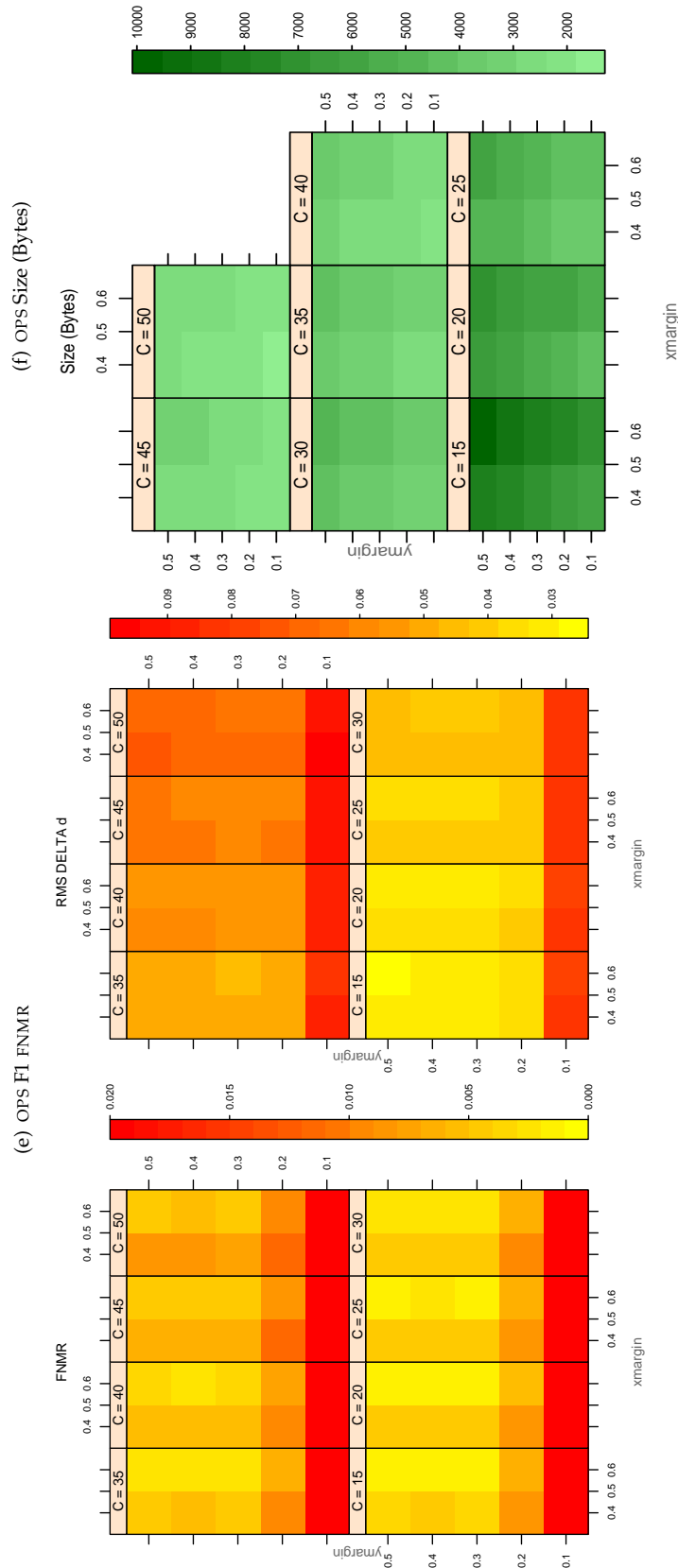


Table 126: For the IREX partition of the OPS database the plots at left show the dependence of cFNMR on the vertical and horizontal iris cropping margins for various compression ratios. This applies only for KIND 3 records. The margins are in units of iris radius. The use of conditional FNMR means that the plots exclude comparisons that were falsely rejected even before any compression was applied. On the **right side** is the rms difference between the crop+compress and the uncompressed comparison scores for each image pair. All computations are driven by the bounding box coordinates reported by the II SDK. The number of bits per pixel is $8/C$, where C is the compression ratio. The iris radius varies and because the cropping margins are fixed multiples of the radius the image size varies. The compressed size, in bytes, is the width times height divided by C . Values of cFNMR greater than 0.02 are shown as 0.02.

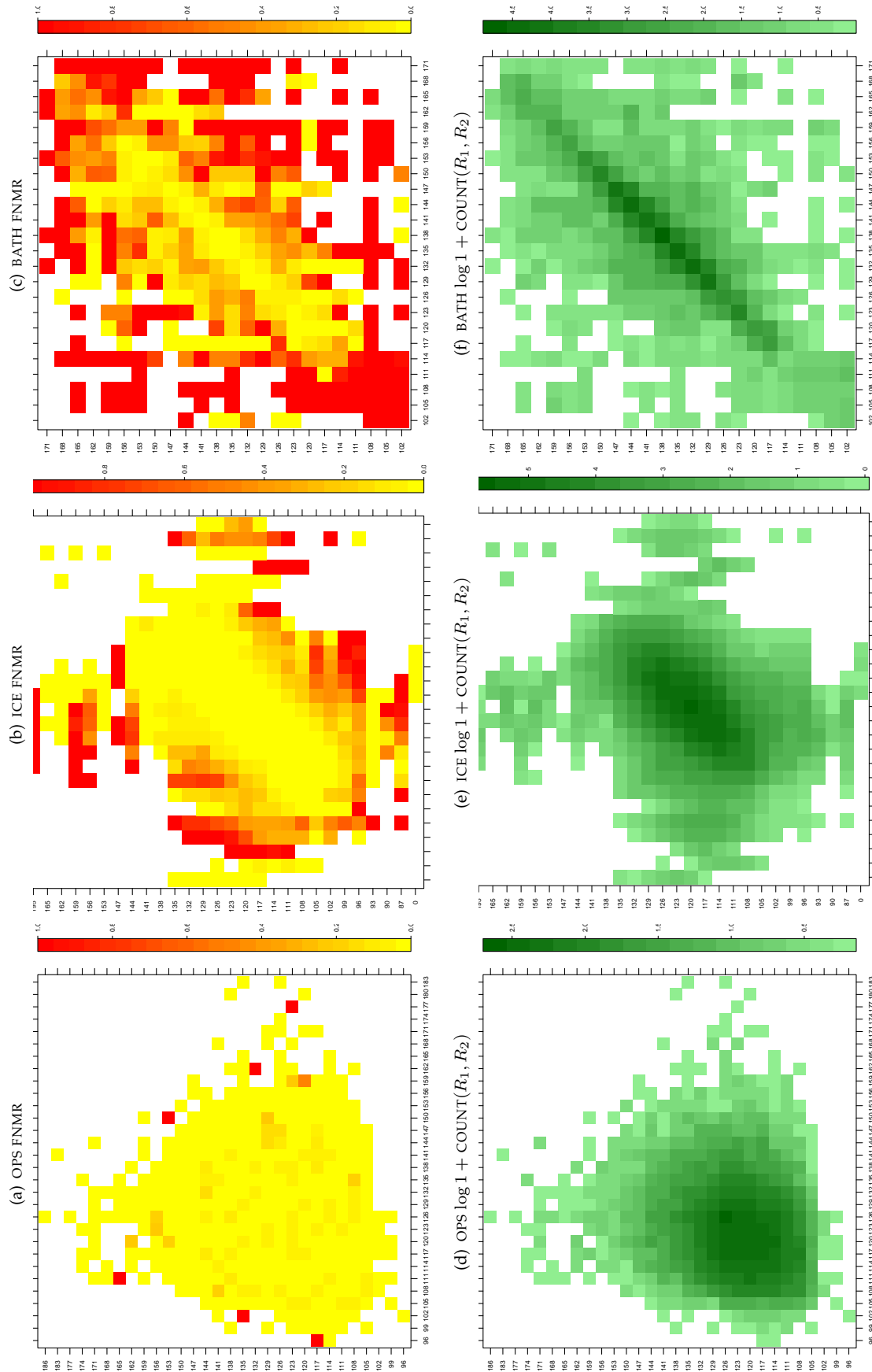


Table 127: For the three IREX databases: In the **top** row the color in each cell represents the occurrence of genuine comparisons with the given pair of radii. The *y*-axis represents enrollment samples with verification samples on the *x*-axis; In the **bottom** row the color scale plots $\log 1 + \text{COUNT}(R_1, R_2)$. The radii are quantized into three-pixel bins. The radii for DOD are on the range $96 \leq r \leq 186$ pixels. The radii for ICE are on the range $87 \leq r \leq 165$ pixels. The radii for BATH are on the range $100 \leq r \leq 170$ pixels.

A = SAGEM	B = COGENT	C = CROSSMATCH	D = CAMBRIDGE	E = L1	$x1$ = PRIMARY
F = RETICA	G = LG	H = HONEYWELL	I = IRITECH	J = NEUROTECHNOLOGY	$x2$ = SECONDARY
KIND 1 = RAW 640x480		KIND 3 = CROP		KIND 7 = CROP+MASK	
KIND 16 = CONCENTRIC POLAR					

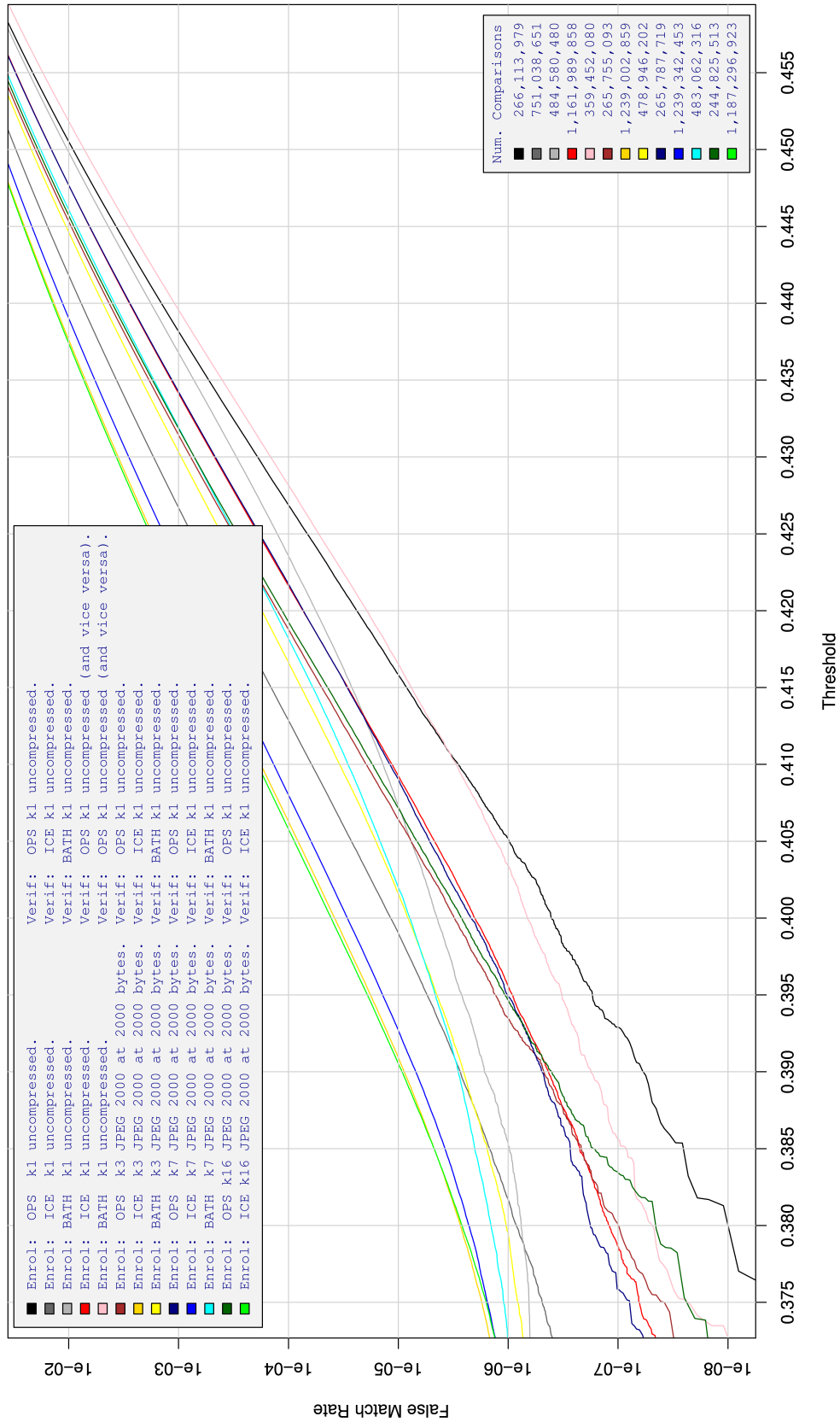


Table 128: For implementation F1, the dependency of FMR on threshold, for various combinations of enrollment and verification dataset, format, and compression.

A = SAGEM	B = COGENT	C = CROSSMATCH	D = CAMBRIDGE	E = L1	x1 = PRIMARY
F = RETICA	G = LG	H = HONEYWELL	I = IRITECH	J = NEUROTECHNOLOGY	x2 = SECONDARY
KIND 1 = RAW 640x480		KIND 3 = CROP		KIND 7 = CROP+MASK	KIND 16 = CONCENTRIC POLAR

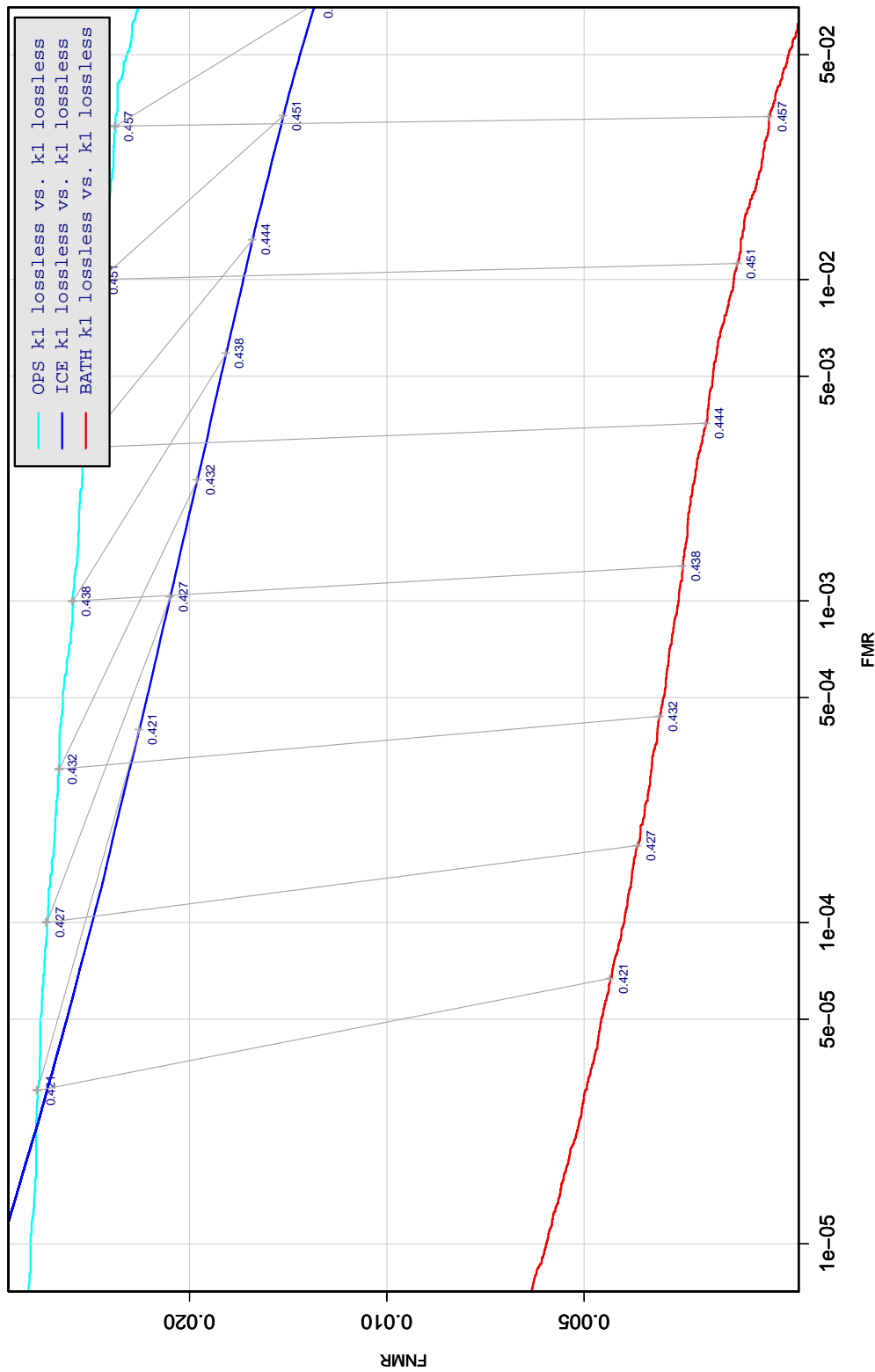


Table 129: DET curve for implementation F1 on three IREX databases. All comparisons are with uncompressed KIND 1 vs. KIND 1 images. The lines join points corresponding to the a fixed threshold. Non-vertical links indicate a change in FMR when the database changes. All results apply to native operation. Failures to produce a template i.e. FTE are ignored because the plots are intended to show *matching* effects, specifically to compare DET slopes and to show the effect of fixing a threshold.

A = SAGEM	B = COGENT	C = CROSSMATCH	D = CAMBRIDGE	E = L1	x1 = PRIMARY
F = RETICA	G = LG	H = HONEYWELL	I = IRITECH	J = NEUROTECHNOLOGY	x2 = SECONDARY
KIND 1 = RAW 640x480		KIND 3 = CROP	KIND 7 = CROP+MASK	KIND 16 = CONCENTRIC POLAR	

(a) BATH

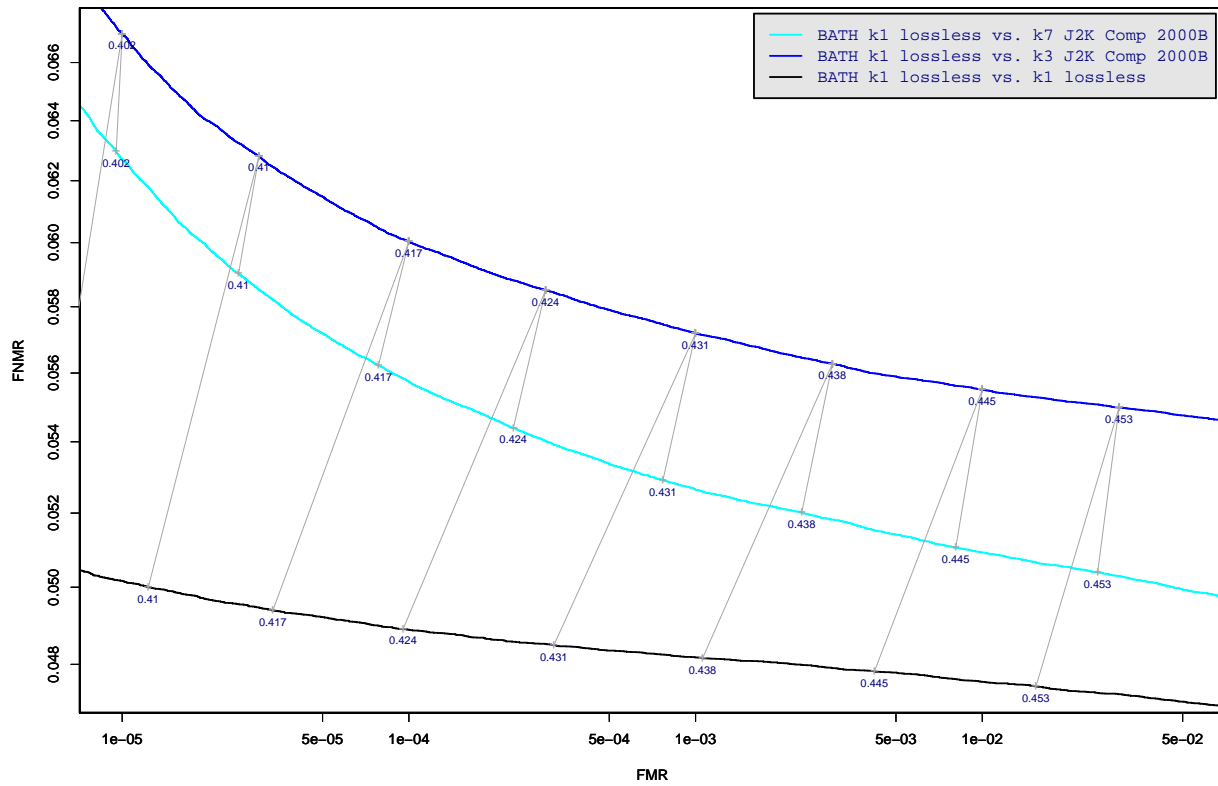


Table 130: DET curve for implementation F1 on the BATH database for the various supported KINDS . The DET characteristics are linked by lines joining points of equal threshold. Non-vertical links indicate a change in false acceptance when the data KIND changes. All results apply to native operation, and the effects of FTE are included.

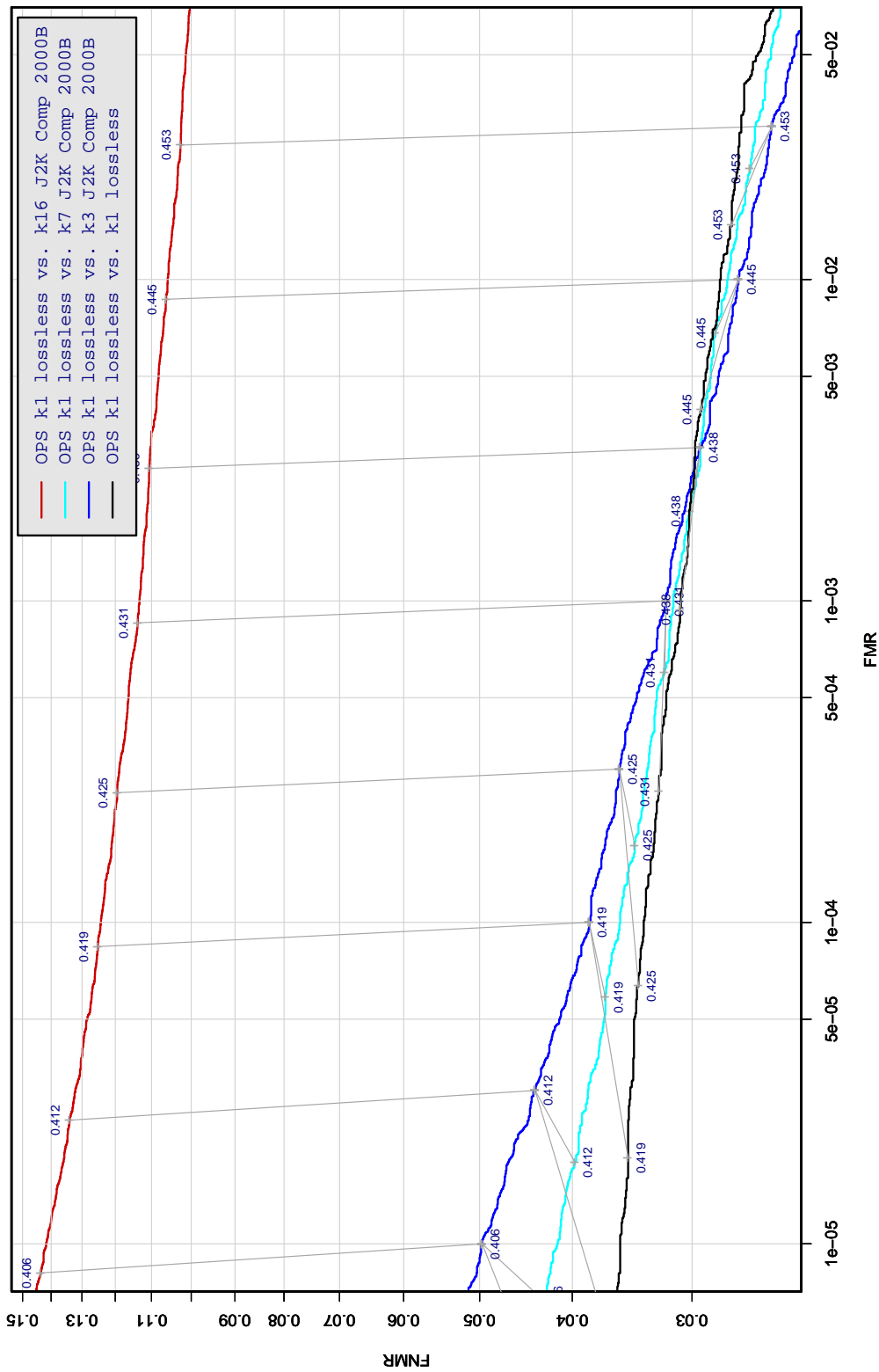


Table 131: DET curve for implementation F1 on the OPS database for the various supported KINDS . The DET characteristics are linked by lines joining points of equal threshold. Non-vertical links indicate a change in false acceptance when the data KIND changes. All results apply to native operation, and the effects of FTE are included.

A = SAGEM	B = COGENT	C = CROSSMATCH	D = CAMBRIDGE	E = L1	x1 = PRIMARY
F = RETICA	G = LG	H = HONEYWELL	I = IRITECH	J = NEUROTECHNOLOGY	x2 = SECONDARY
KIND 1 = RAW 640x480		KIND 3 = CROP		KIND 7 = CROP+MASK	KIND 16 = CONCENTRIC POLAR

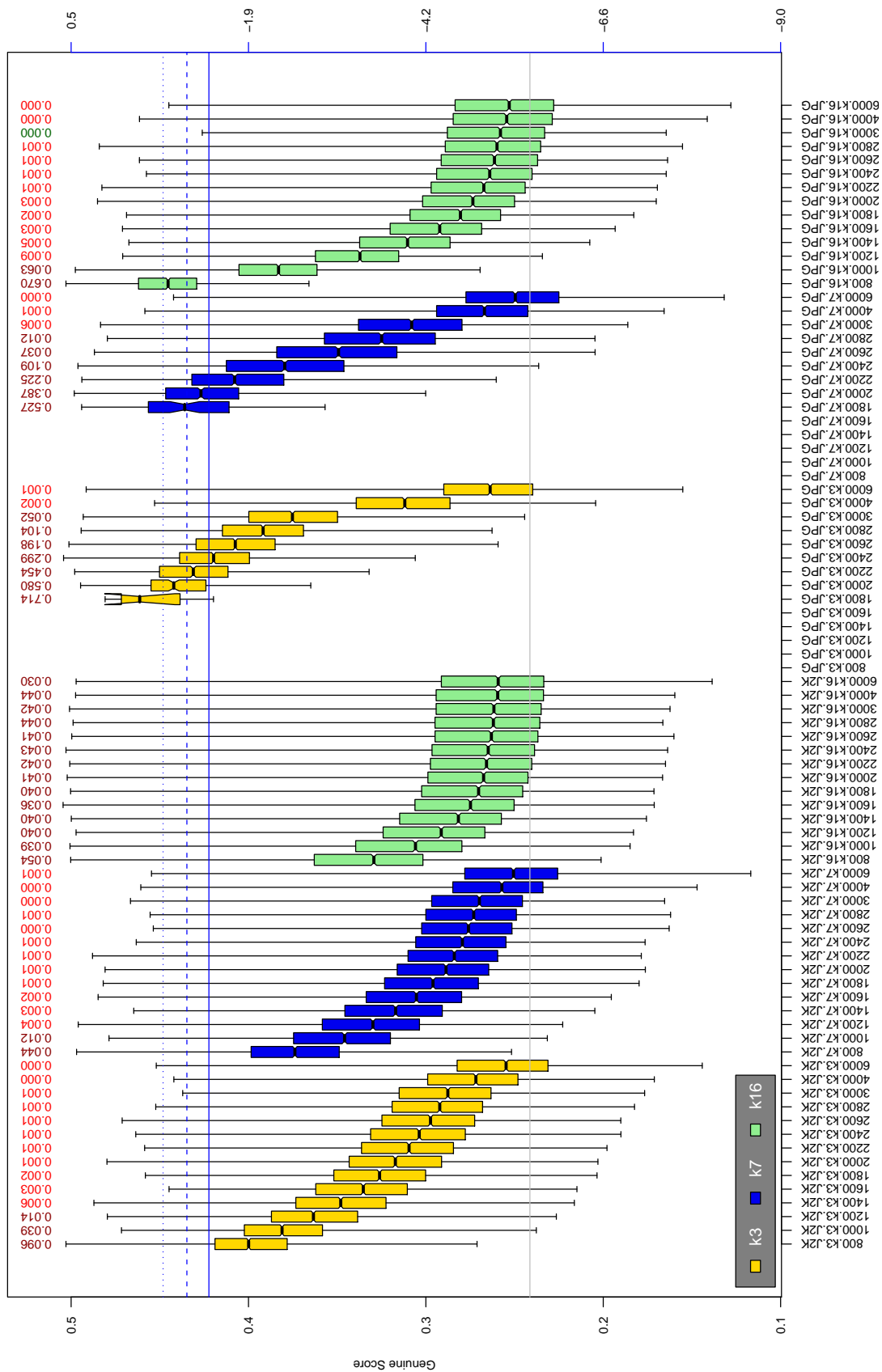


Table 132: The distribution of F1 native genuine comparison scores by size of the compressed image, KIND and the compression algorithm. The images are from the OPS dataset. The right axis scale gives the corresponding value for $d' = (s - \mu_I) / \sqrt{0.5(\sigma_I^2 + \sigma_C^2)}$ for genuine score s . The boxplots only include comparison scores if the uncompressed version of the same image was matched below the FMR = 0.001 threshold. Above the boxplots are FNMR values at FMR = 10^{-3} . The three blue lines correspond, from the top, to FMR of 10^{-2} , 10^{-3} , 10^{-4} . The lower grey line refers to the median score obtained from comparison of uncompressed KIND 3 images. Any comparison for which either template had not been generated is excluded. Note that the iris record size on the horizontal axis is not evenly spaced above 3000 bytes.

A = SAGEM	B = COGENT	C = CROSSMATCH	D = CAMBRIDGE	E = L1	$x1$ = PRIMARY
F = RETICA	G = LG	H = HONEYWELL	I = IRITECH	J = NEUROTECHNOLOGY	$x2$ = SECONDARY
KIND 1 = RAW 640x480		KIND 3 = CROP	KIND 7 = CROP+MASK	KIND 16 = CONCENTRIC POLAR	

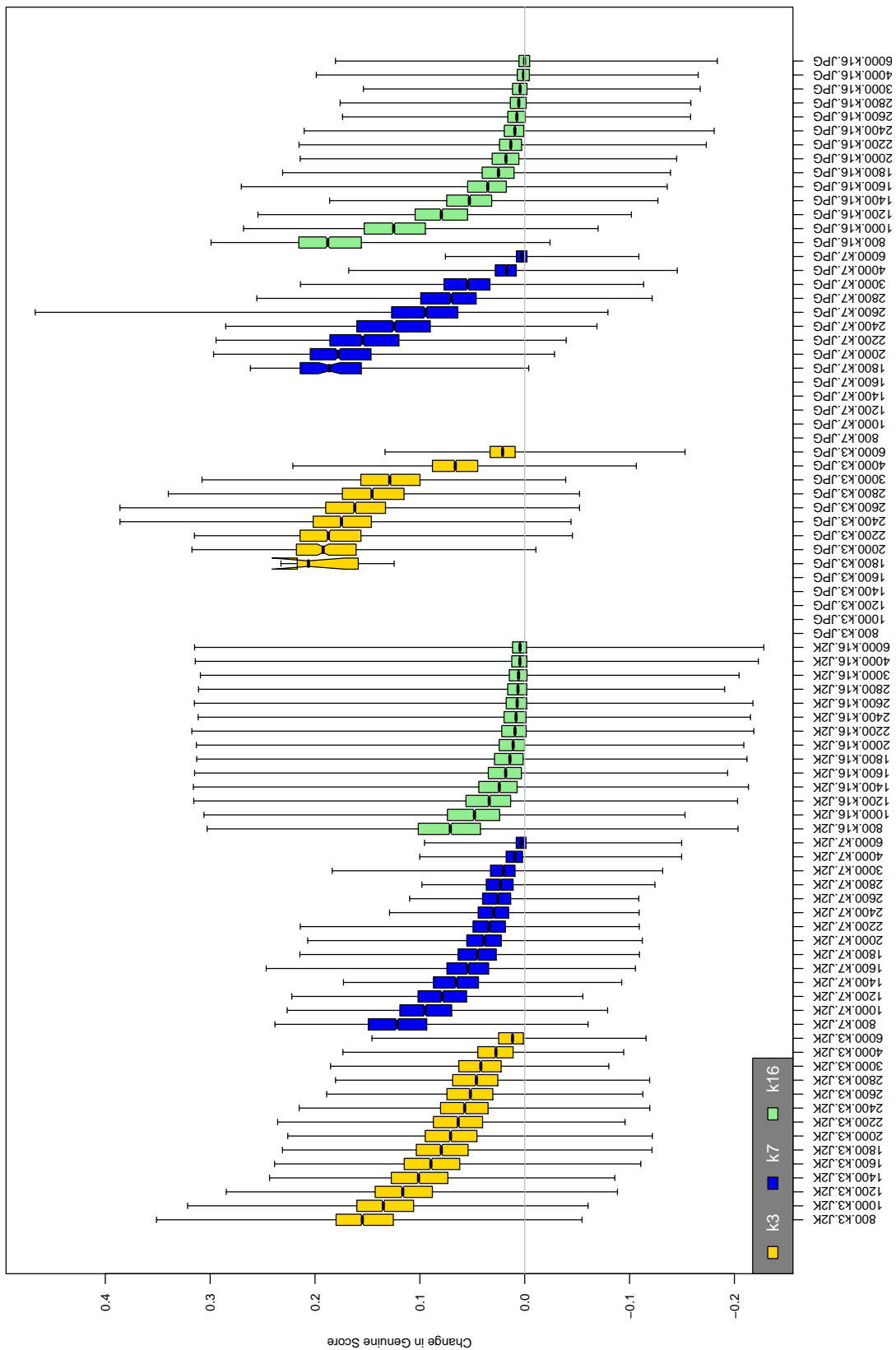


Table 133: The distribution of the *increase* in F1 native genuine comparison scores between the uncompressed “parent” and the compressed image, arranged by size, KIND and the compression algorithm. The images are from the OPS dataset. Any comparison involving a failed template is excluded. Note that the iris record size on the horizontal axis is not evenly spaced above 3000 bytes.

A = SAGEM	B = COGENT	C = CROSSMATCH	D = CAMBRIDGE	E = L1	x1 = PRIMARY
F = RETICA	G = LG	H = HONEYWELL	I = IRITECH	J = NEUROTECHNOLOGY	x2 = SECONDARY
KIND 1 = RAW 640x480		KIND 3 = CROP	KIND 7 = CROP+MASK	KIND 16 = CONCENTRIC POLAR	

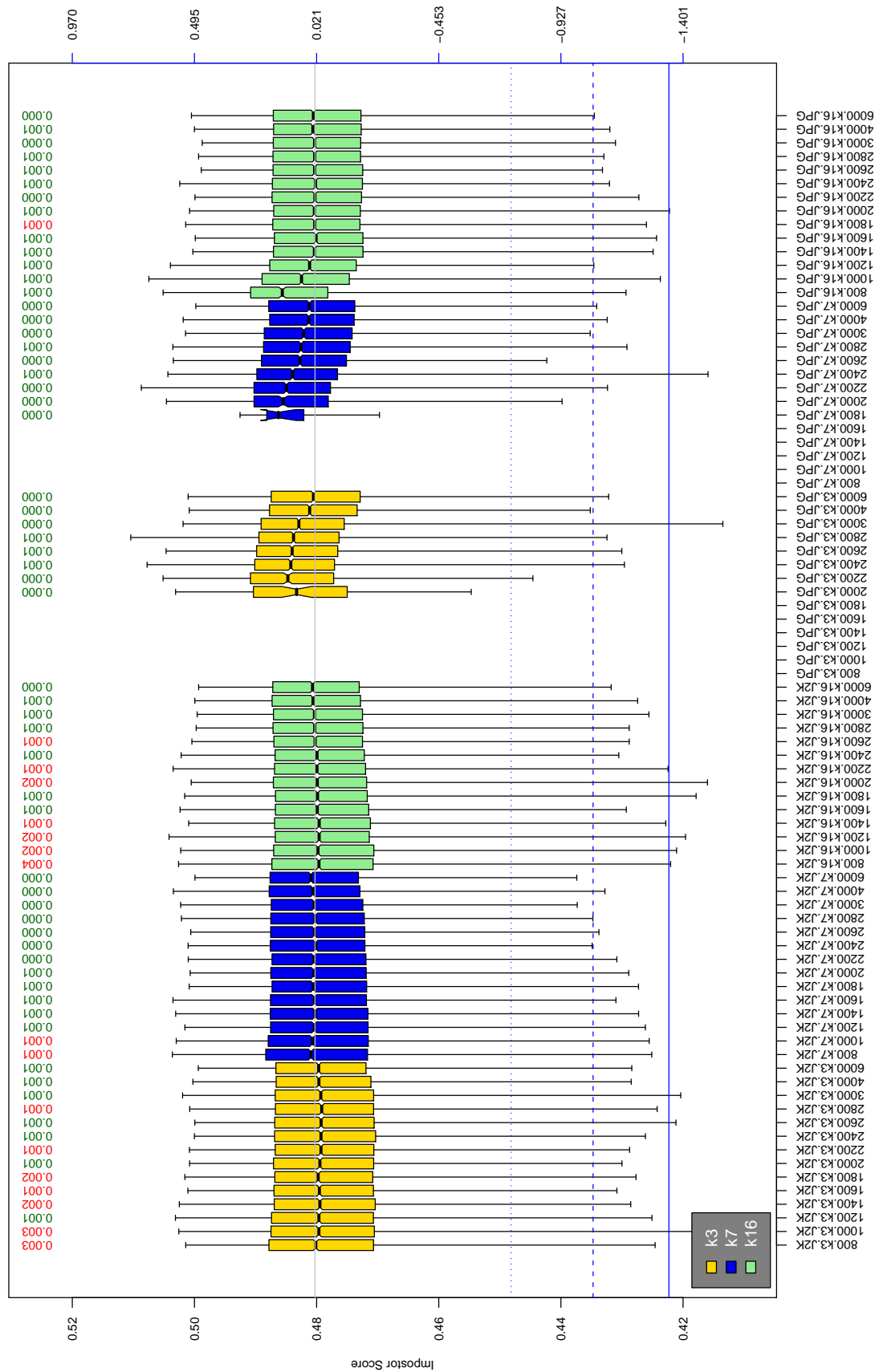


Table 134: The distribution of F1 native impostor comparison scores by size of the compressed image, KIND and the compression algorithm. The right axis scale gives the corresponding value for $d' = (s - \mu_1) / \sqrt{0.5(\sigma_1^2 + \sigma_2^2)}$ for impostor score s . The three blue lines correspond, from the top, to FMR of $10^{-2}, -3, -4$. The lower grey line refers to the median score obtained from comparison of uncompressed KIND 3 images. Any comparison involving a failed template is excluded. Above the boxplots are FMR values at the threshold that gives FMR = 10^{-3} on uncompressed images. These figures are computed from only 4000 comparisons so the FMR values and the tails of the impostor distribution are poorly characterized. Note that the iris record size on the horizontal axis is not evenly spaced above 3000 bytes.

A = SAGEM	B = COGENT	C = CROSSMATCH	D = CAMBRIDGE	E = L1	$x1$ = PRIMARY
F = RETICA	G = LG	H = HONEYWELL	I = IRITECH	J = NEUROTECHNOLOGY	$x2$ = SECONDARY
KIND 1 = RAW 640x480		KIND 3 = CROP		KIND 7 = CROP+MASK	KIND 16 = CONCENTRIC POLAR

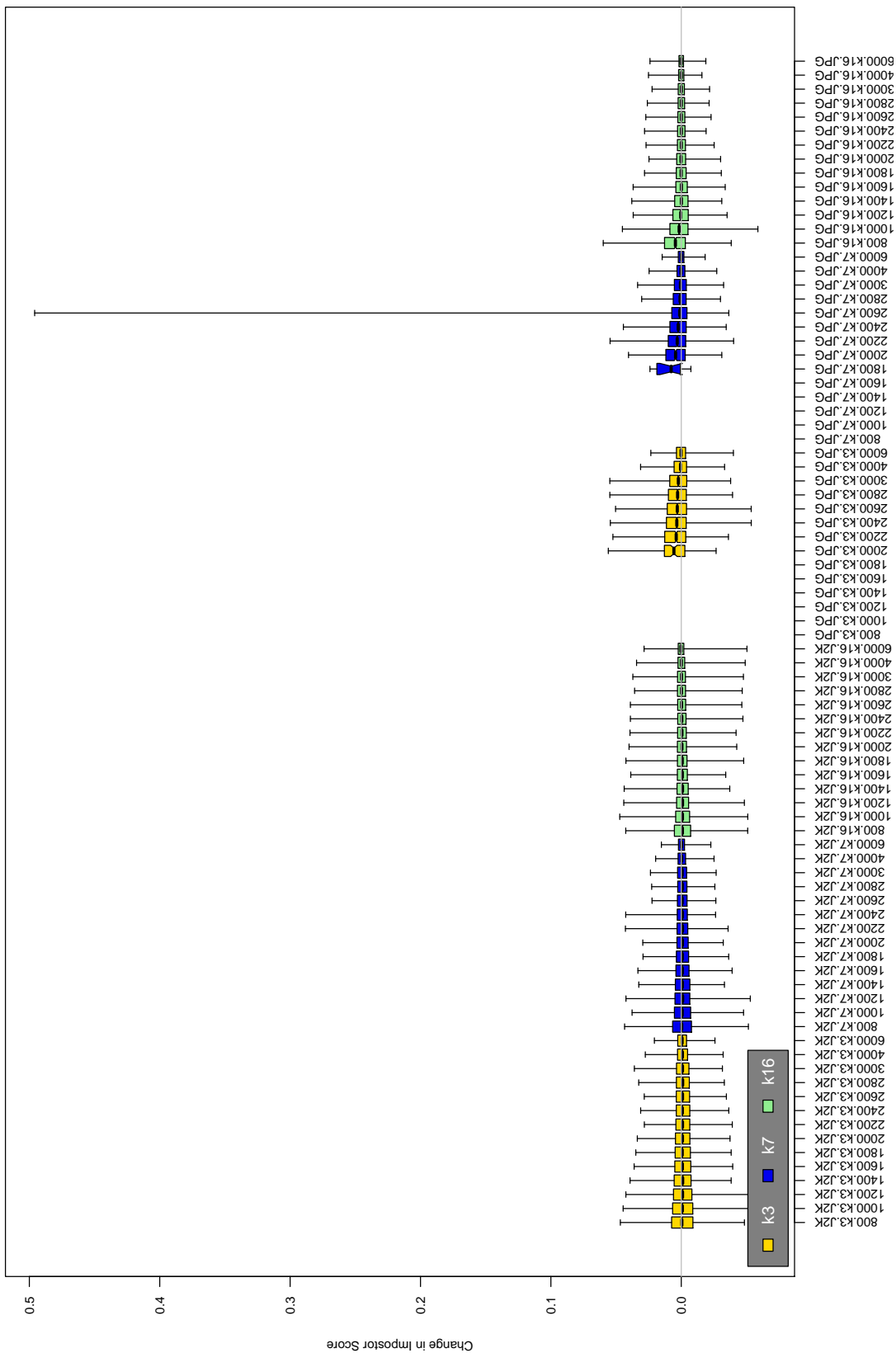


Table 135: The distribution of the increase in F1 native impostor comparison scores between the uncompressed “parent” and the compressed image, arranged by size, KIND and the compression algorithm. The images are from the OPS dataset. Any comparison involving a failed template is excluded. Note that the iris record size on the horizontal axis is not evenly spaced above 3000 bytes.

A = SAGEM	B = COGENT	C = CROSSMATCH	D = CAMBRIDGE	E = L1	x1 = PRIMARY
F = RETICA	G = LG	H = HONEYWELL	I = IRITECH	J = NEUROTECHNOLOGY	x2 = SECONDARY
KIND 1 = RAW 640x480		KIND 3 = CROP	KIND 7 = CROP+MASK	KIND 16 = CONCENTRIC POLAR	

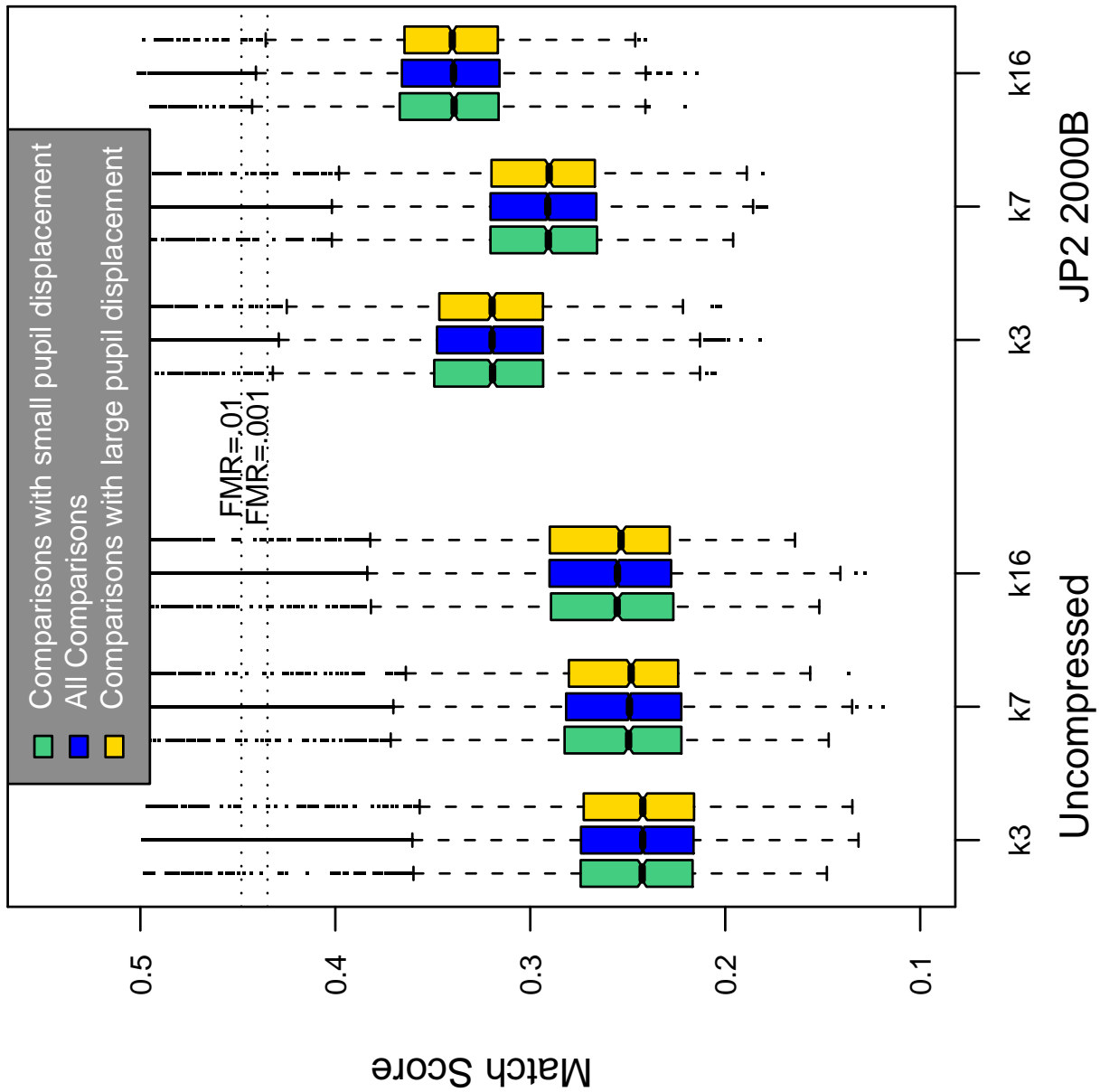


Table 136: Effect of pupil displacement on the genuine score distribution for F1

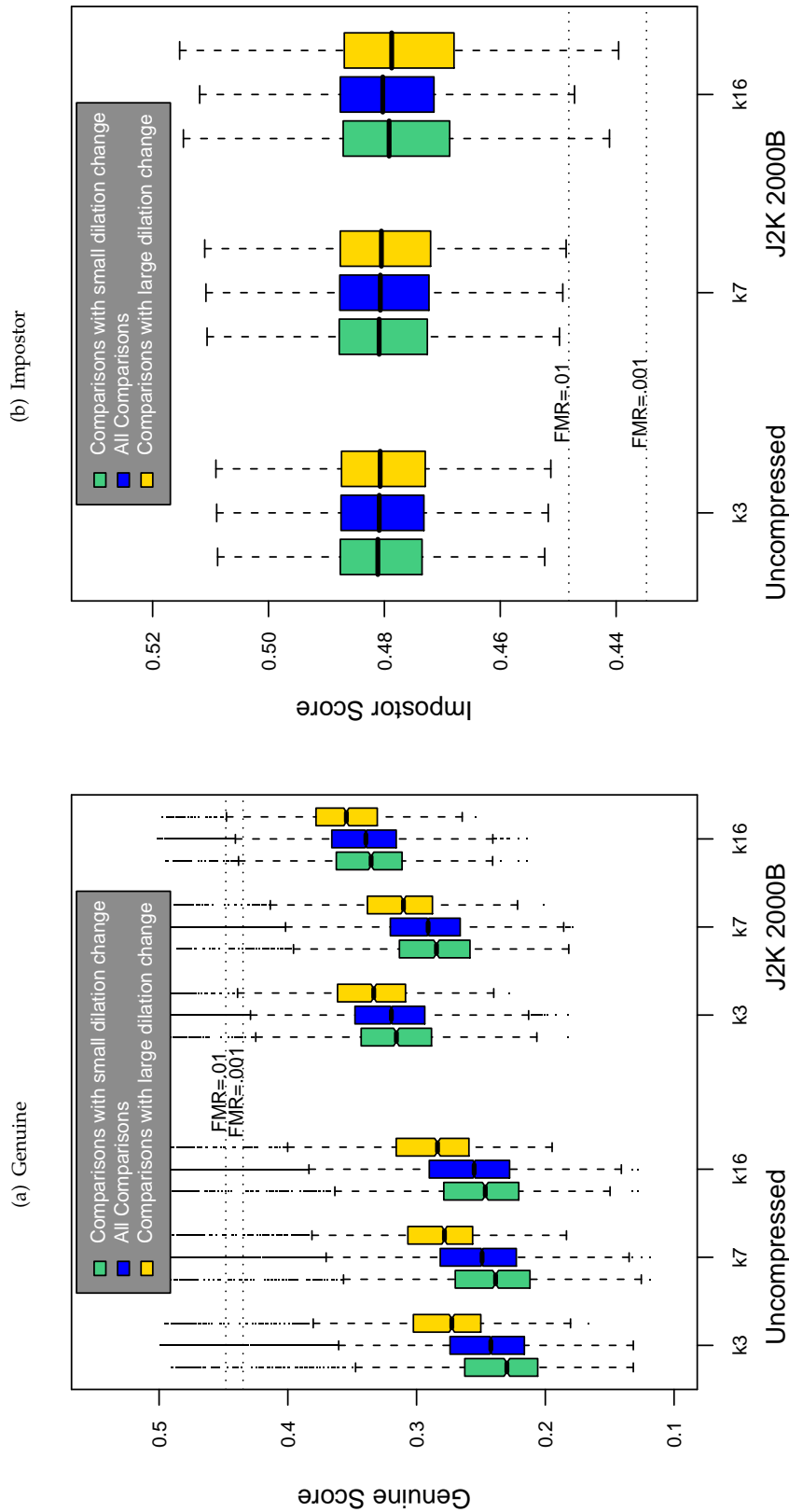


Table 137: The effect of dilation change on the two scores distributions for SDK FL.

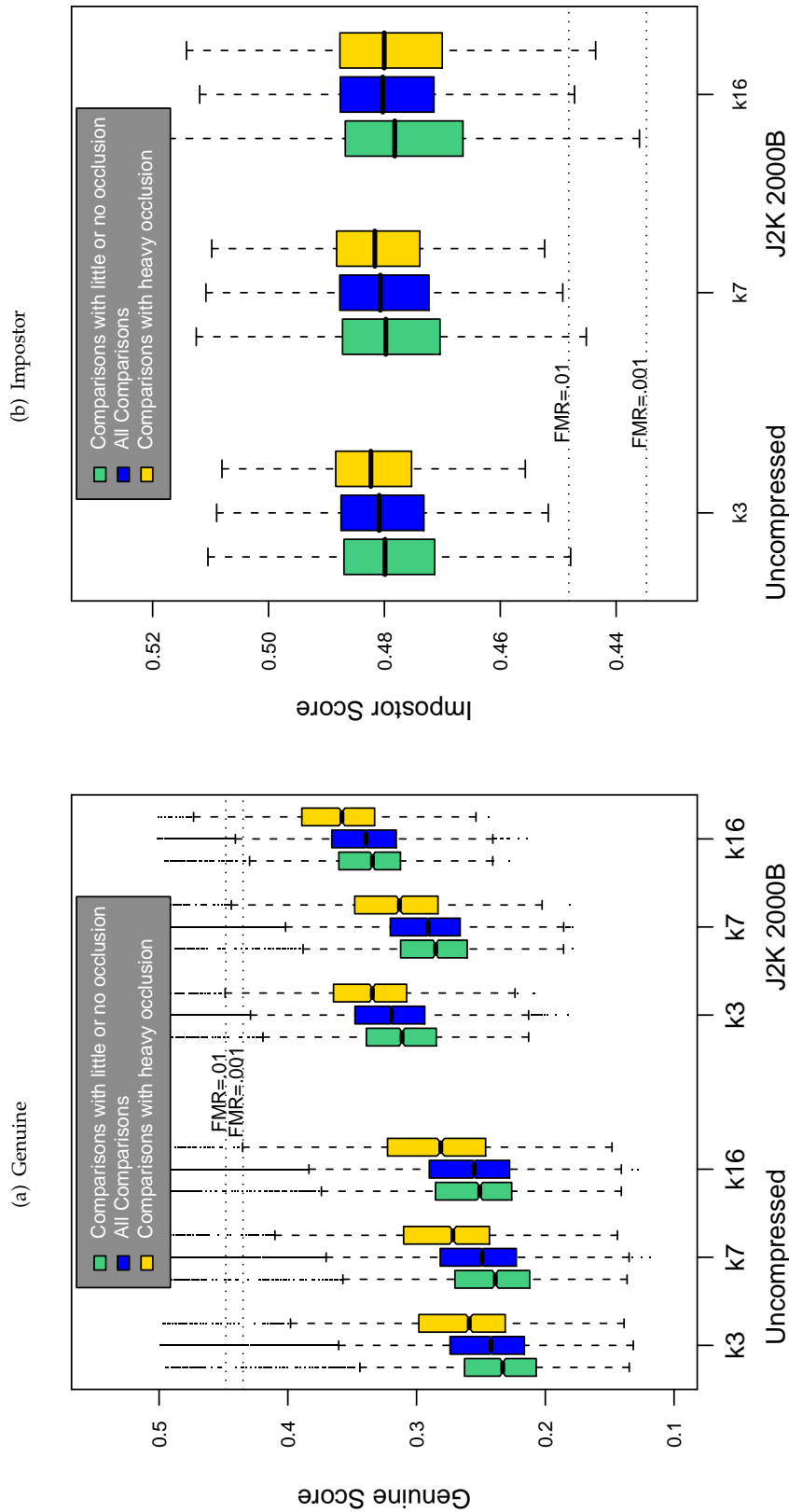
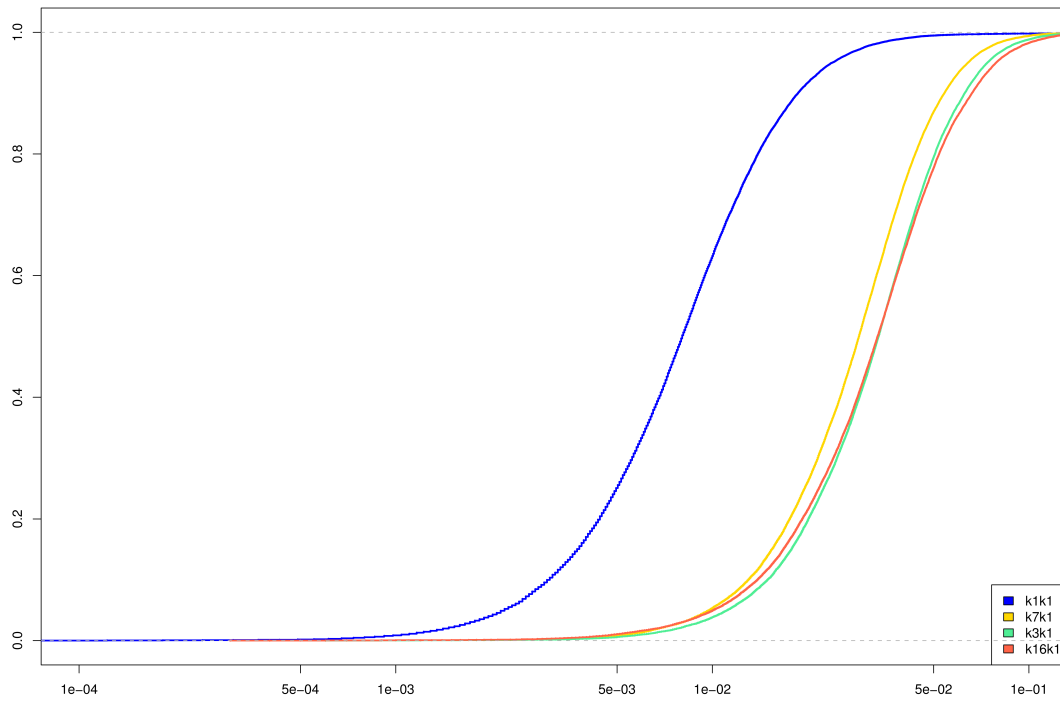
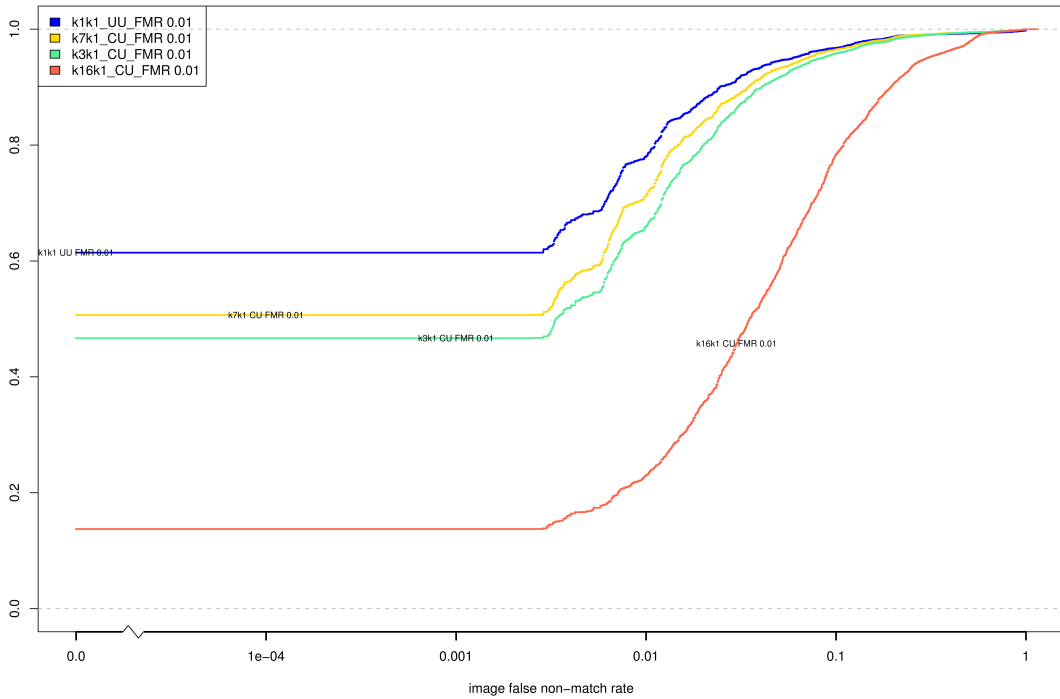


Table 138: The effect of eyelid occlusion on the two scores distributions for SDK F1.

(a) iFMR CDF



(b) iFNMR CDF



Compiled Results for Implementation G1

On June 25, 2009, NIST invited the IREX participants to submit a description of the SDKs submitted for the IREX effort. The intent was to allow providers to describe and contrast the feature sets, optimization, operational suitability and availability of the primary and secondary SDKs. NIST indicated that any submitted text would appear verbatim (with typesetting) in draft and final versions of the IREX report and that it would be attributed to the organization. This was optional and NIST put no constraints on the content beyond a 600 word limit, and a statement that anything labelled as confidential or proprietary would be omitted.

The provider of SDK G1, LG, elected not to submit any information

On August 17, 2009, NIST invited the IREX participants to submit a description their comments on an draft version of the IREX report. This was intended to allow participants to assist readers in the interpretation of a large and complicated testing effort. NIST indicated that any submitted text would appear verbatim (with typesetting) in the final version of the IREX report and that it would be attributed to the organization. Submission of content was optional and NIST put no constraints on the content beyond a word limit, and a statement that anything labelled as confidential or proprietary would be omitted.

The provider of SDK G1, LG, elected not to submit any information

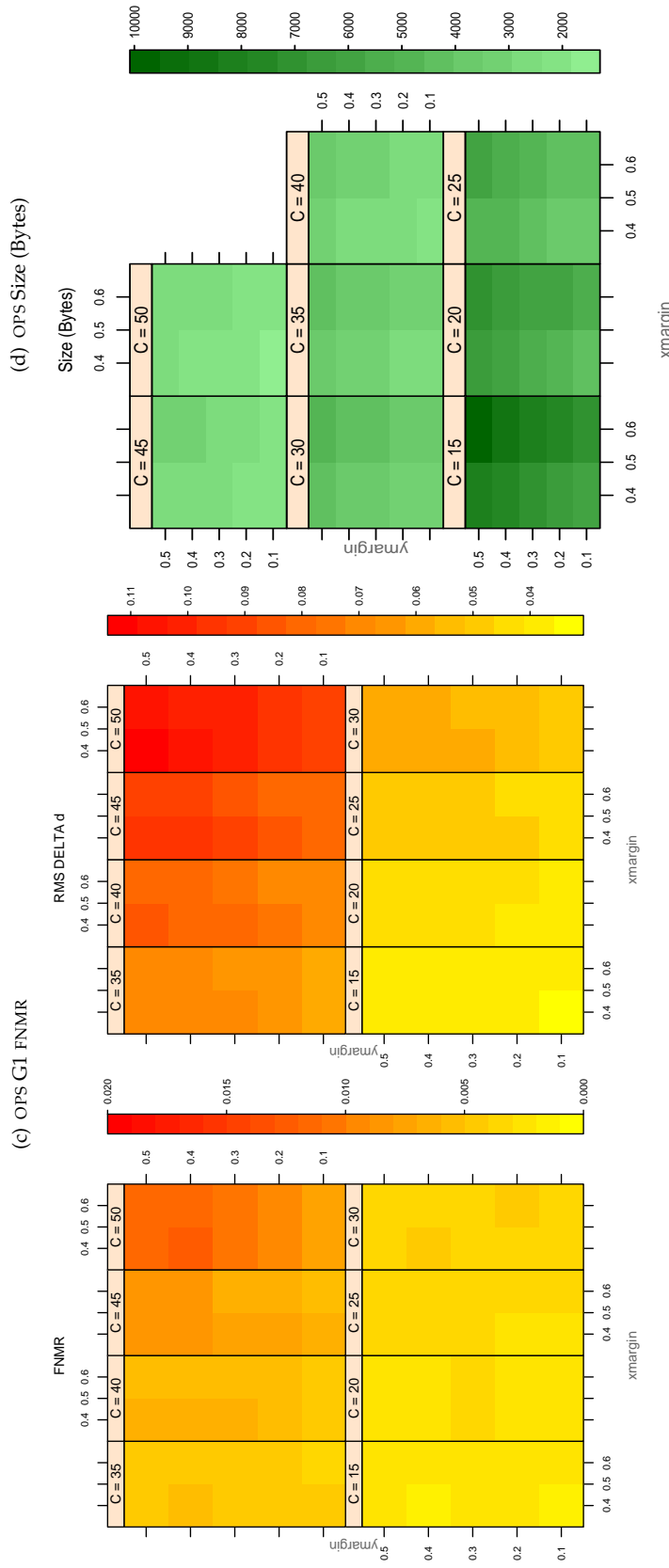


Table 139: For the IREX partition of the OPS database the plots at left show the dependence of cFNMR on the vertical and horizontal iris cropping margins for various compression ratios. This applies only for KIND 3 records. The margins are in units of iris radius. The use of conditional FNMR means that the plots exclude comparisons that were falsely rejected even before any compression was applied. On the **right side** is the rms difference between the crop+compress and the uncompressed comparison scores for each image pair. All computations are driven by the bounding box coordinates reported by the II SDK. The number of bits per pixel is $8/C$, where C is the compression ratio. The iris radius varies and because the cropping margins are fixed multiples of the radius the image size varies. The compressed size, in bytes, is the width times height divided by C . Values of cFNMR greater than 0.02 are shown as 0.02.

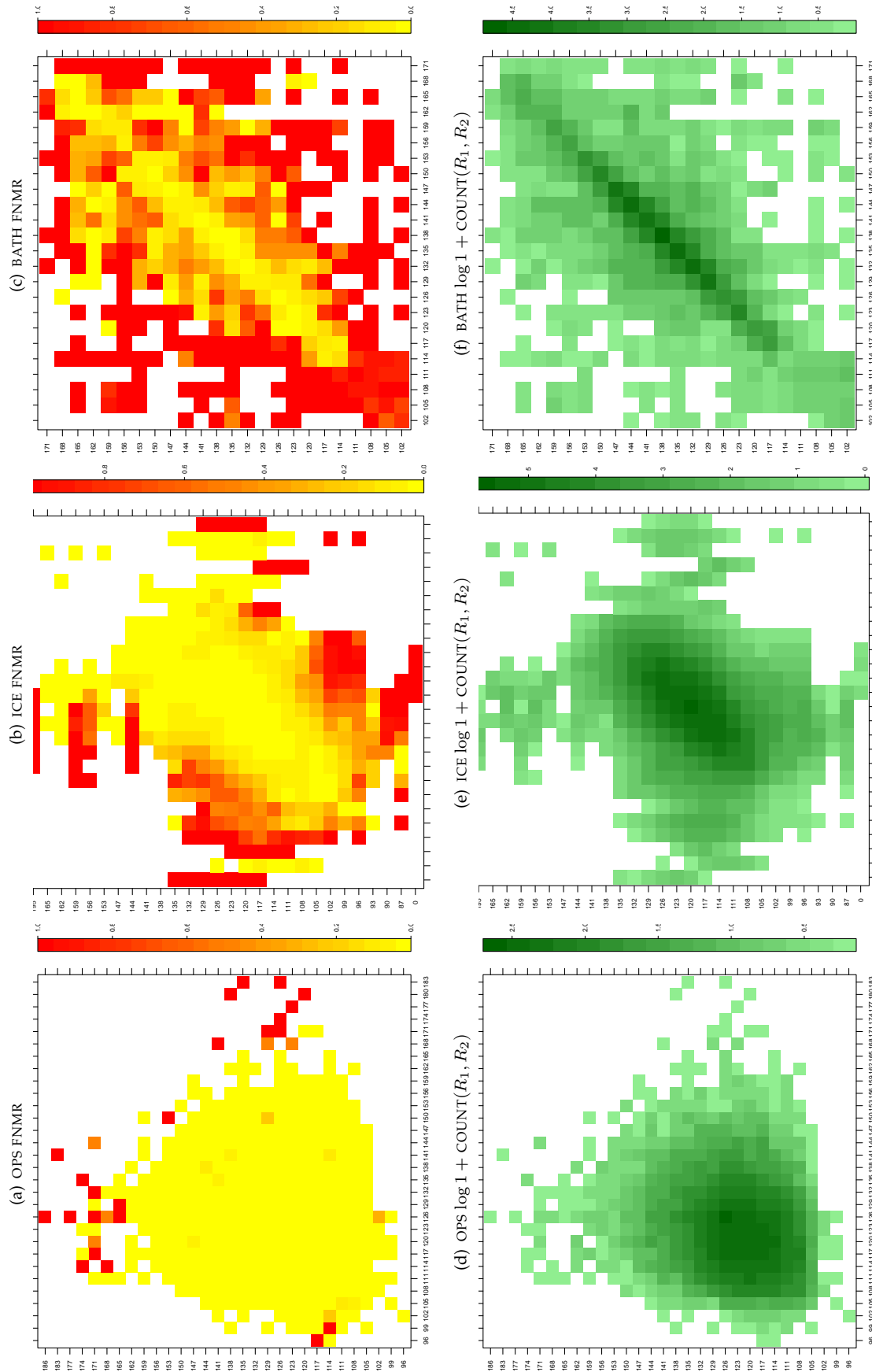


Table 140: For the three IREX databases: In the **top** row the color in each cell represents the occurrence of genuine comparisons with the given pair of radii. The *y*-axis represents enrollment samples with verification samples on the *x*-axis; In the **bottom** row the color scale plots $\log 1 + \text{COUNT}(R_1, R_2)$. The radii are quantized into three-pixel bins. The radii for DOD are on the range $96 \leq r \leq 186$ pixels. The radii for ICE are on the range $87 \leq r \leq 165$ pixels. The radii for BATH are on the range $100 \leq r \leq 170$ pixels.

A = SAGEM	B = COGENT	C = CROSSMATCH	D = CAMBRIDGE	E = L1	$x1$ = PRIMARY
F = RETICA	G = LG	H = HONEYWELL	I = IRITECH	J = NEUROTECHNOLOGY	$x2$ = SECONDARY
KIND 1 = RAW 640x480		KIND 3 = CROP	KIND 7 = CROP+MASK	KIND 16 = CONCENTRIC POLAR	

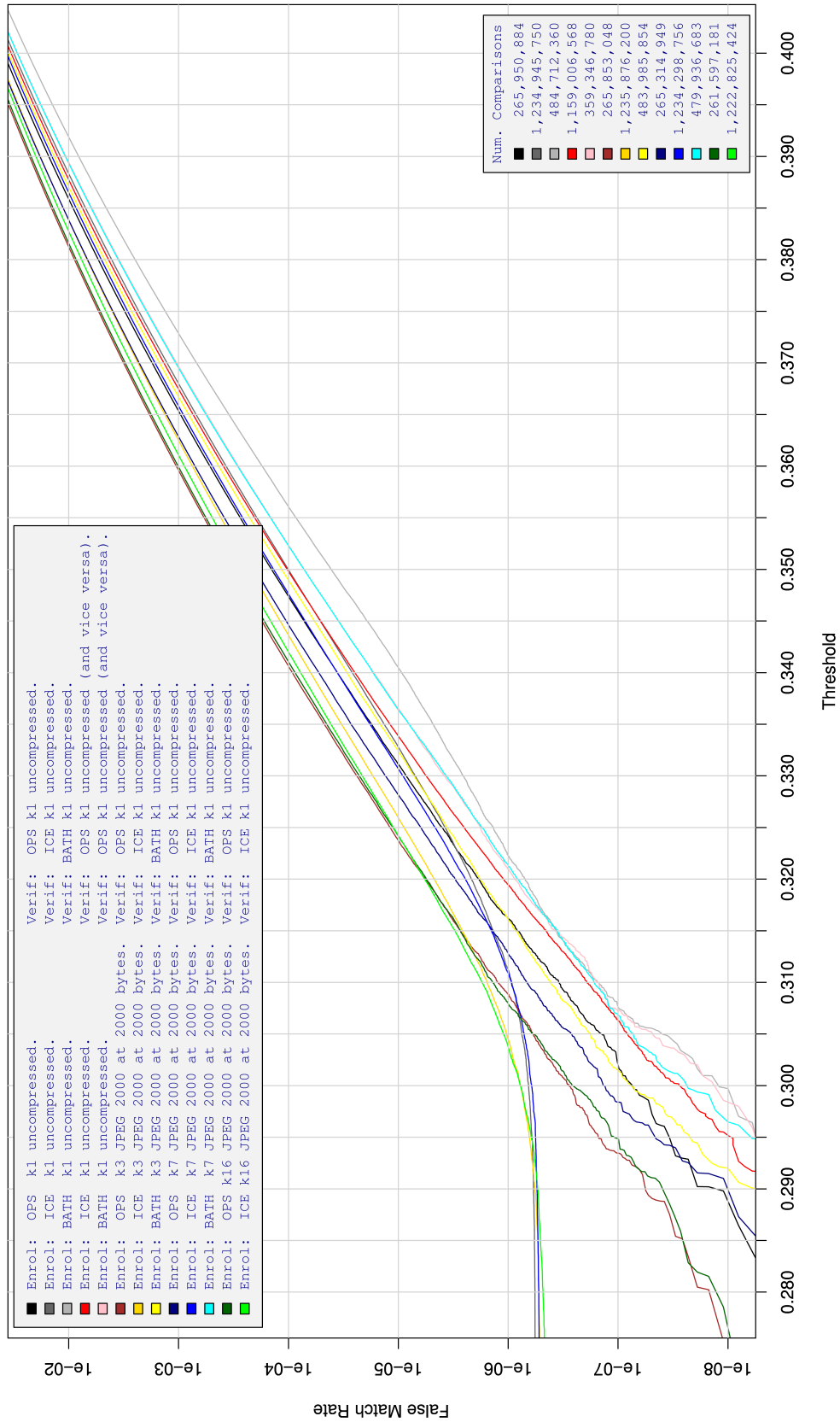


Table 141: For implementation G1, the dependency of FMR on threshold. for various combinations of enrollment and verification dataset, format, and compression.

A = SAGEM	B = COGENT	C = CROSSMATCH	D = CAMBRIDGE	E = L1	x1 = PRIMARY
F = RETICA	G = LG	H = HONEYWELL	I = IRITECH	J = NEUROTECHNOLOGY	x2 = SECONDARY
KIND 1 = RAW 640x480		KIND 3 = CROP		KIND 7 = CROP+MASK	KIND 16 = CONCENTRIC POLAR

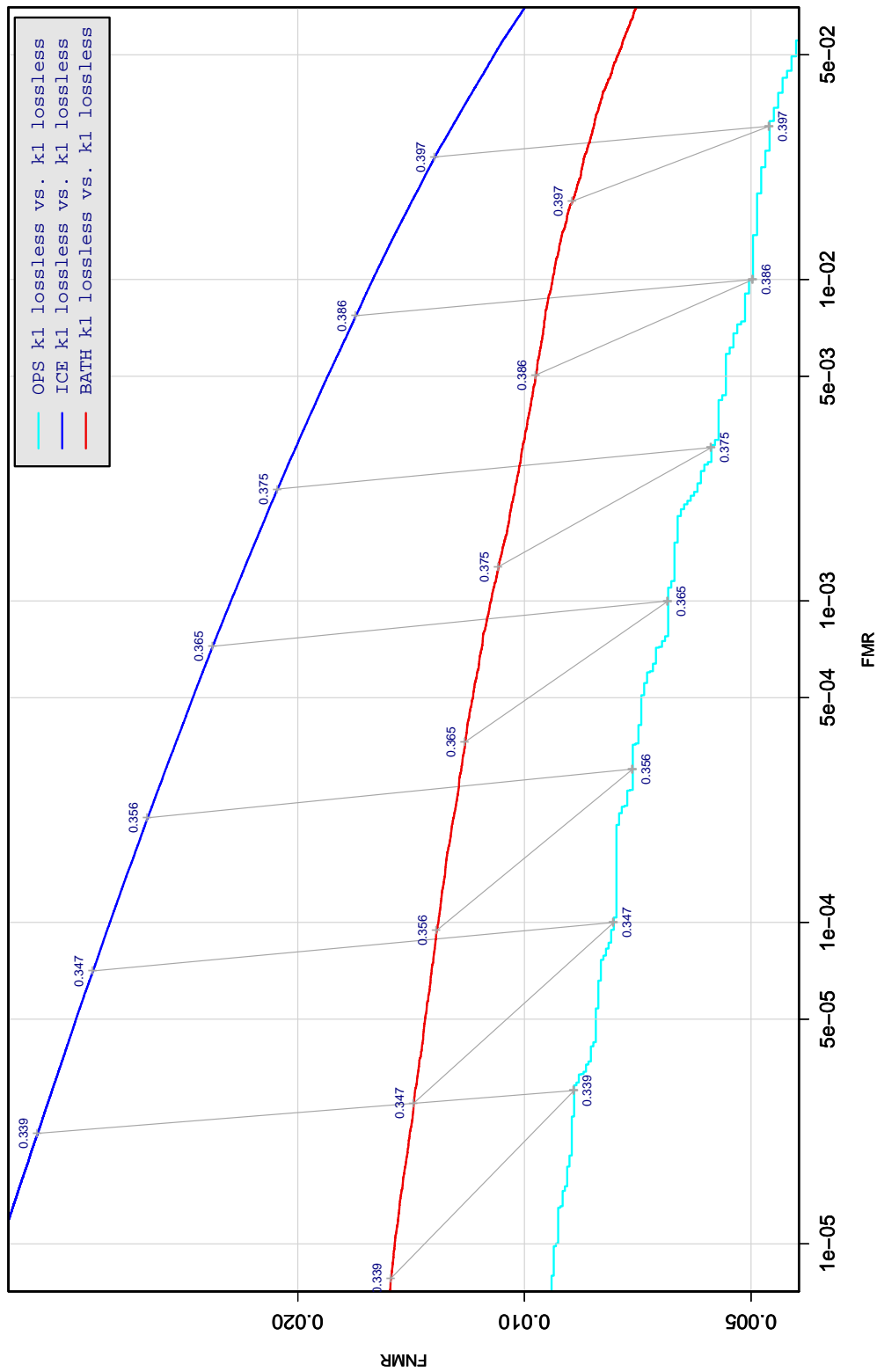


Table 142: DET curve for implementation G1 on three IREX databases. All comparisons are with uncompressed KIND 1 vs. KIND 1 images. The lines join points corresponding to the a fixed threshold. Non-vertical links indicate a change in FMR when the database changes. All results apply to native operation. Failures to produce a template i.e. FTE are ignored because the plots are intended to show *matching* effects, specifically to compare DET slopes and to show the effect of fixing a threshold.

A = SAGEM	B = COGENT	C = CROSSMATCH	D = CAMBRIDGE	E = L1	x1 = PRIMARY
F = RETICA	G = LG	H = HONEYWELL	I = IRITECH	J = NEUROTECHNOLOGY	x2 = SECONDARY
KIND 1 = RAW 640x480		KIND 3 = CROP	KIND 7 = CROP+MASK	KIND 16 = CONCENTRIC POLAR	

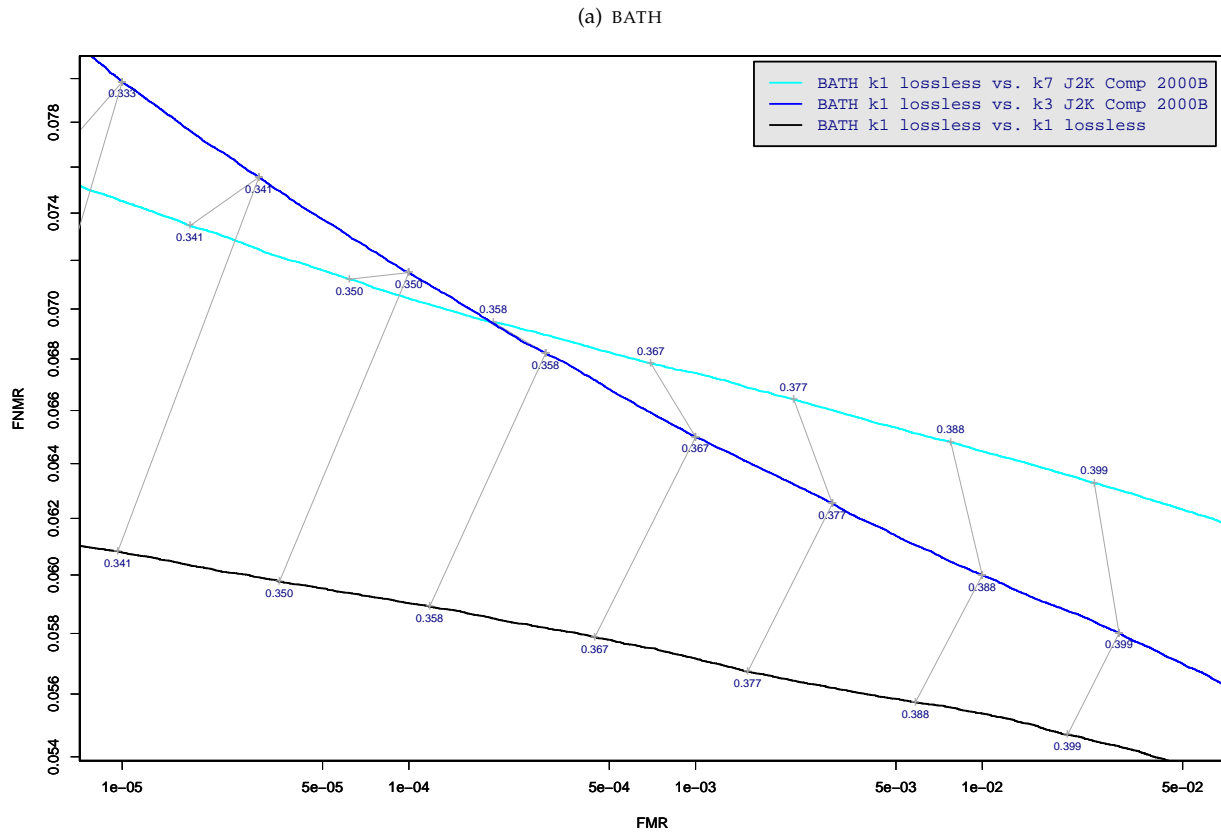


Table 143: DET curve for implementation G1 on the BATH database for the various supported KINDS . The DET characteristics are linked by lines joining points of equal threshold. Non-vertical links indicate a change in false acceptance when the data KIND changes. All results apply to native operation, and the effects of FTE are included.

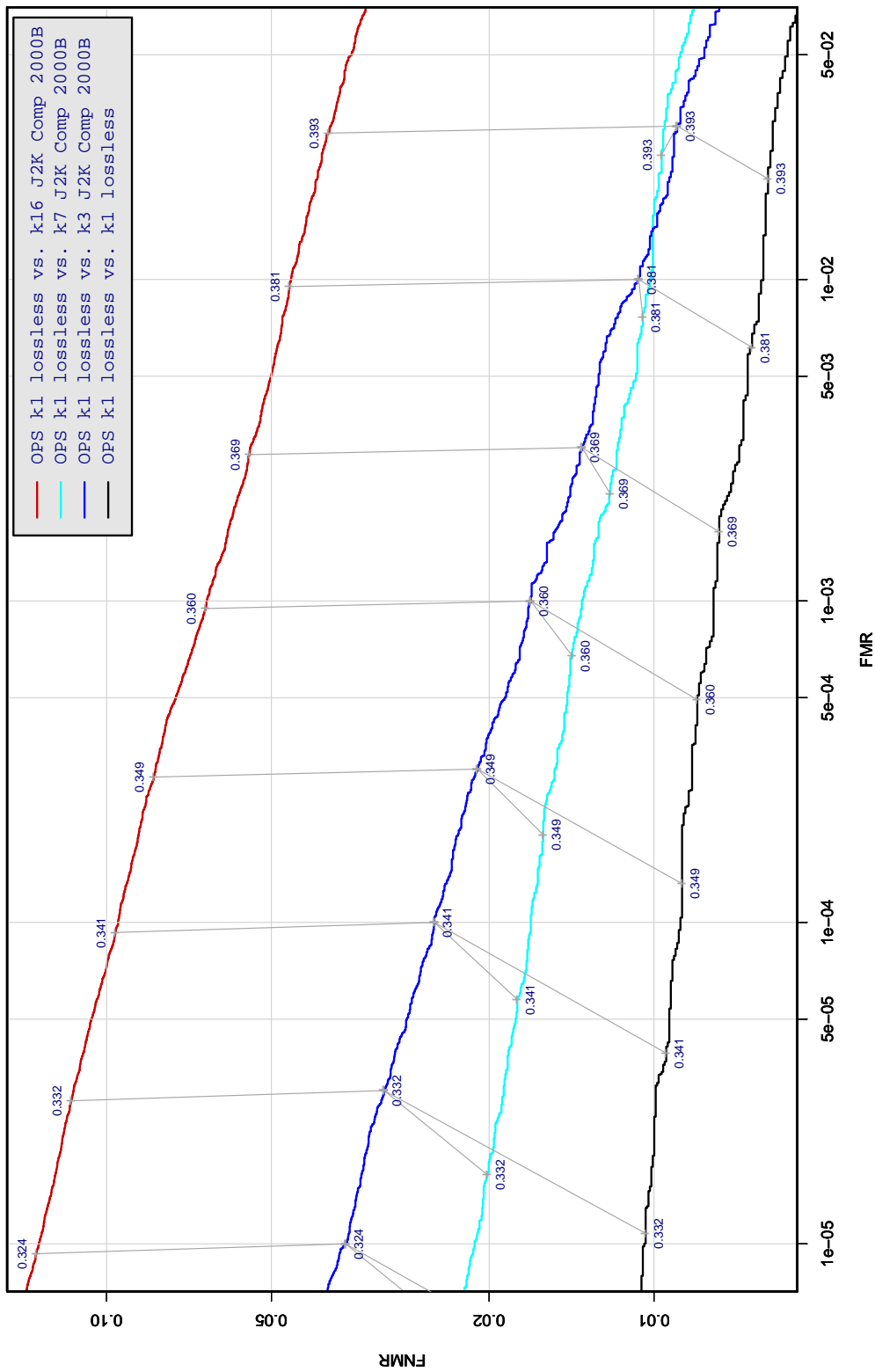


Table 144: DET curve for implementation G1 on the OPS database for the various supported KINDS . The DET characteristics are linked by lines joining points of equal threshold. Non-vertical links indicate a change in false acceptance when the data KIND changes. All results apply to native operation, and the effects of FTE are included.

A = SAGEM	B = COGENT	C = CROSSMATCH	D = CAMBRIDGE	E = L1	x1 = PRIMARY
F = RETICA	G = LG	H = HONEYWELL	I = IRITECH	J = NEUROTECHNOLOGY	x2 = SECONDARY
KIND 1 = RAW 640x480		KIND 3 = CROP	KIND 7 = CROP+MASK	KIND 16 = CONCENTRIC POLAR	

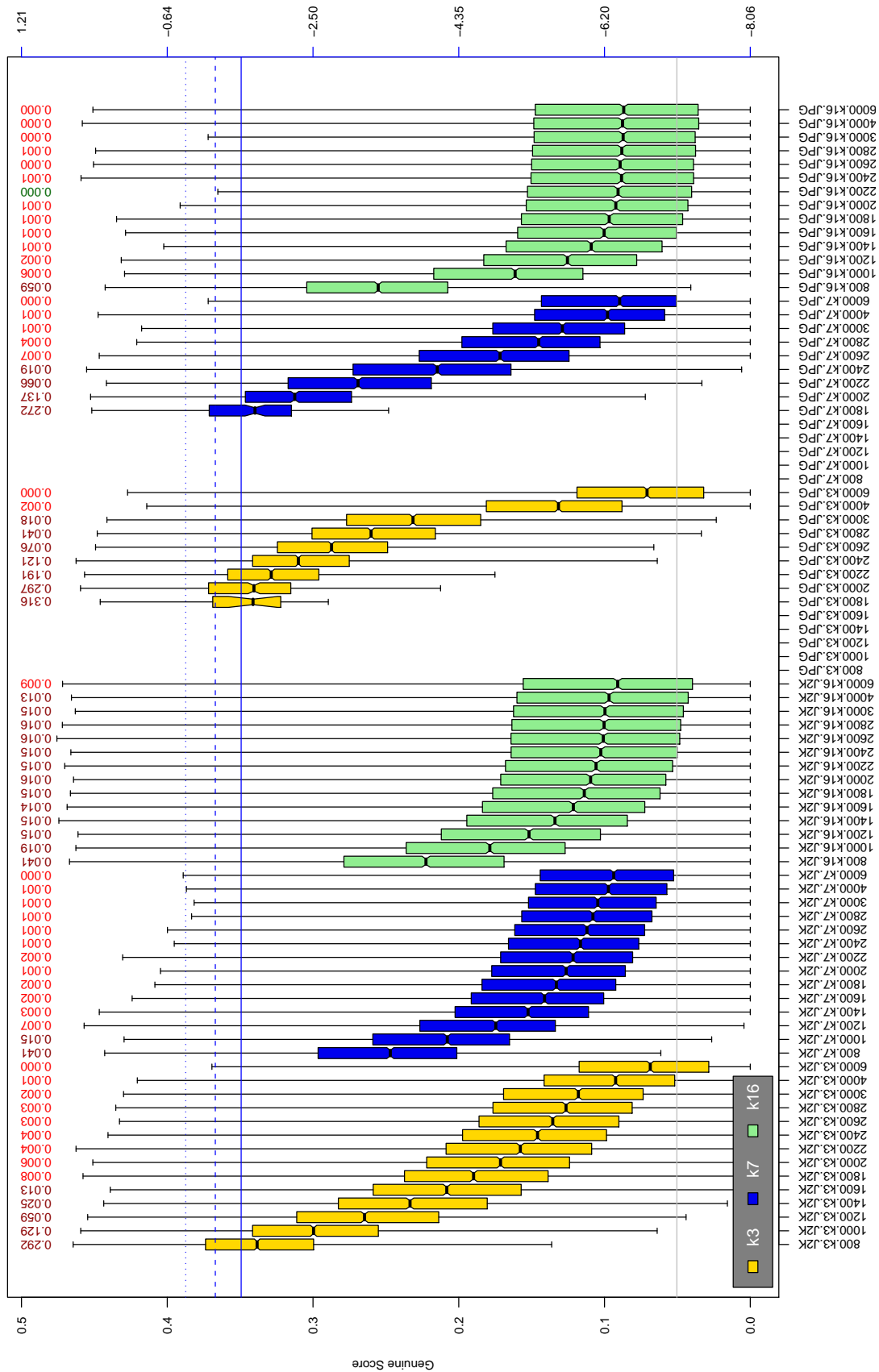


Table 145: The distribution of G1 native genuine comparison scores by size of the compressed image, KIND and the compression algorithm. The images are from the OPS dataset. The right axis scale gives the corresponding value for $d' = (s - \mu_I) / \sqrt{0.5(\sigma_I^2 + \sigma_G^2)}$ for genuine score s . The boxplots only include comparison scores if the uncompressed version of the same image was matched below the FMR = 0.001 threshold. Above the boxplots are FNMR values at FMR = 10^{-3} . The three blue lines correspond, from the top, to FMR of $10^{(-2, -3, -4)}$. The lower grey line refers to the median score obtained from comparison of uncompressed KIND 3 images. Any comparison for which either template had not been generated is excluded. Note that the iris record size on the horizontal axis is not evenly spaced above 3000 bytes.

A = SAGEM	B = COGENT	C = CROSSMATCH	D = CAMBRIDGE	E = L1	$x1$ = PRIMARY
F = RETICA	G = LG	H = HONEYWELL	I = IRITECH	J = NEUROTECHNOLOGY	$x2$ = SECONDARY
KIND 1 = RAW 640x480		KIND 3 = CROP	KIND 7 = CROP+MASK	KIND 16 = CONCENTRIC POLAR	

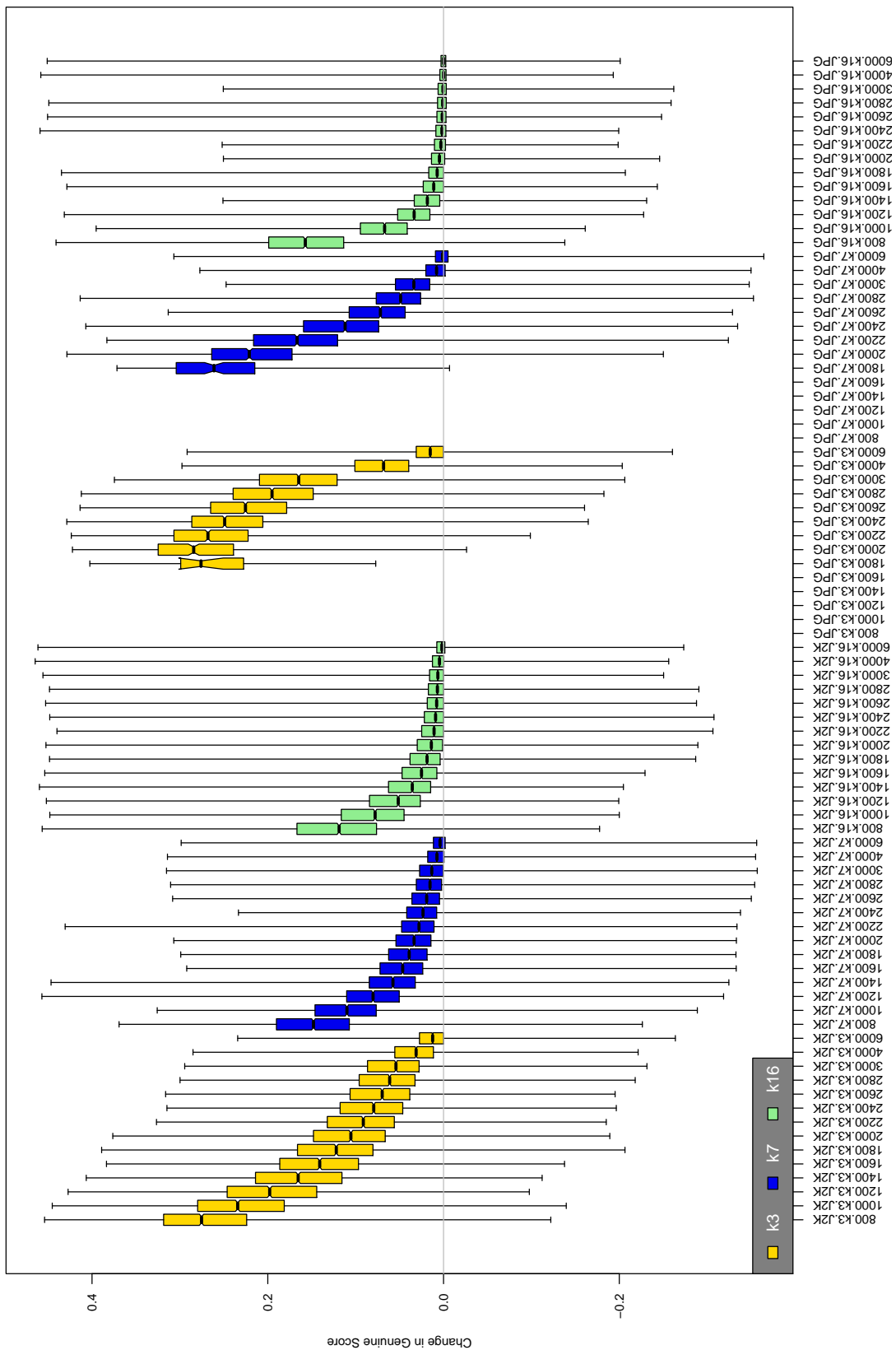


Table 146: The distribution of the *increase* in G1 native genuine comparison scores between the uncompressed “parent” and the compressed image, arranged by size, KIND and the compression algorithm. The images are from the OPS dataset. Any comparison involving a failed template is excluded. Note that the iris record size on the horizontal axis is not evenly spaced above 3000 bytes.

A = SAGEM	B = COGENT	C = CROSSMATCH	D = CAMBRIDGE	E = L1	x1 = PRIMARY
F = RETICA	G = LG	H = HONEYWELL	I = IRITECH	J = NEUROTECHNOLOGY	x2 = SECONDARY
KIND 1 = RAW 640x480		KIND 3 = CROP	KIND 7 = CROP+MASK	KIND 16 = CONCENTRIC POLAR	

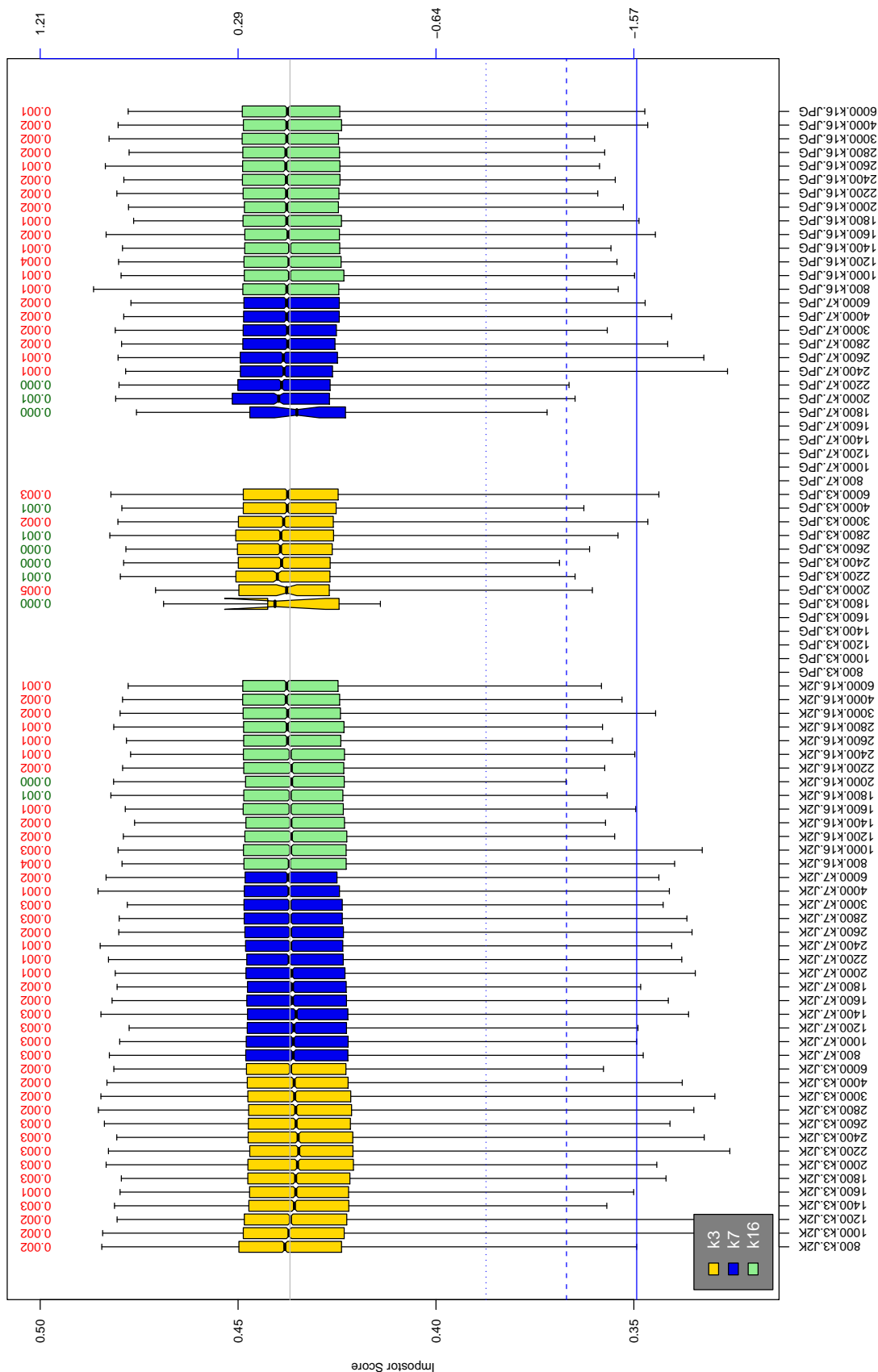


Table 147: The distribution of C1 native impostor comparison scores by size of the compressed image, KIND and the compression algorithm. The right axis scale gives the corresponding value for $d' = (s - \mu_1) / \sqrt{0.5(\sigma_1^2 + \sigma_2^2)}$ for impostor score s . The three blue lines correspond, from the top, to FMR of 10^{-2} , 10^{-3} , and 10^{-4} . The lower grey line refers to the median score obtained from comparison of uncompressed KIND 3 images. Any comparison involving a failed template is excluded. Above the boxplots are FMR values at the threshold that gives FMR = 10^{-3} on uncompressed images. These figures are computed from only 4000 comparisons so the FMR values and the tails of the impostor distribution are poorly characterized. Note that the iris record size on the horizontal axis is not evenly spaced above 3000 bytes.

A = SAGEM	B = COGENT	C = CROSSMATCH	D = CAMBRIDGE	E = L1	$x1$ = PRIMARY
F = RETICA	G = LG	H = HONEYWELL	I = IRITECH	J = NEUROTECHNOLOGY	$x2$ = SECONDARY
KIND 1 = RAW 640x480		KIND 3 = CROP	KIND 7 = CROP+MASK	KIND 16 = CONCENTRIC POLAR	

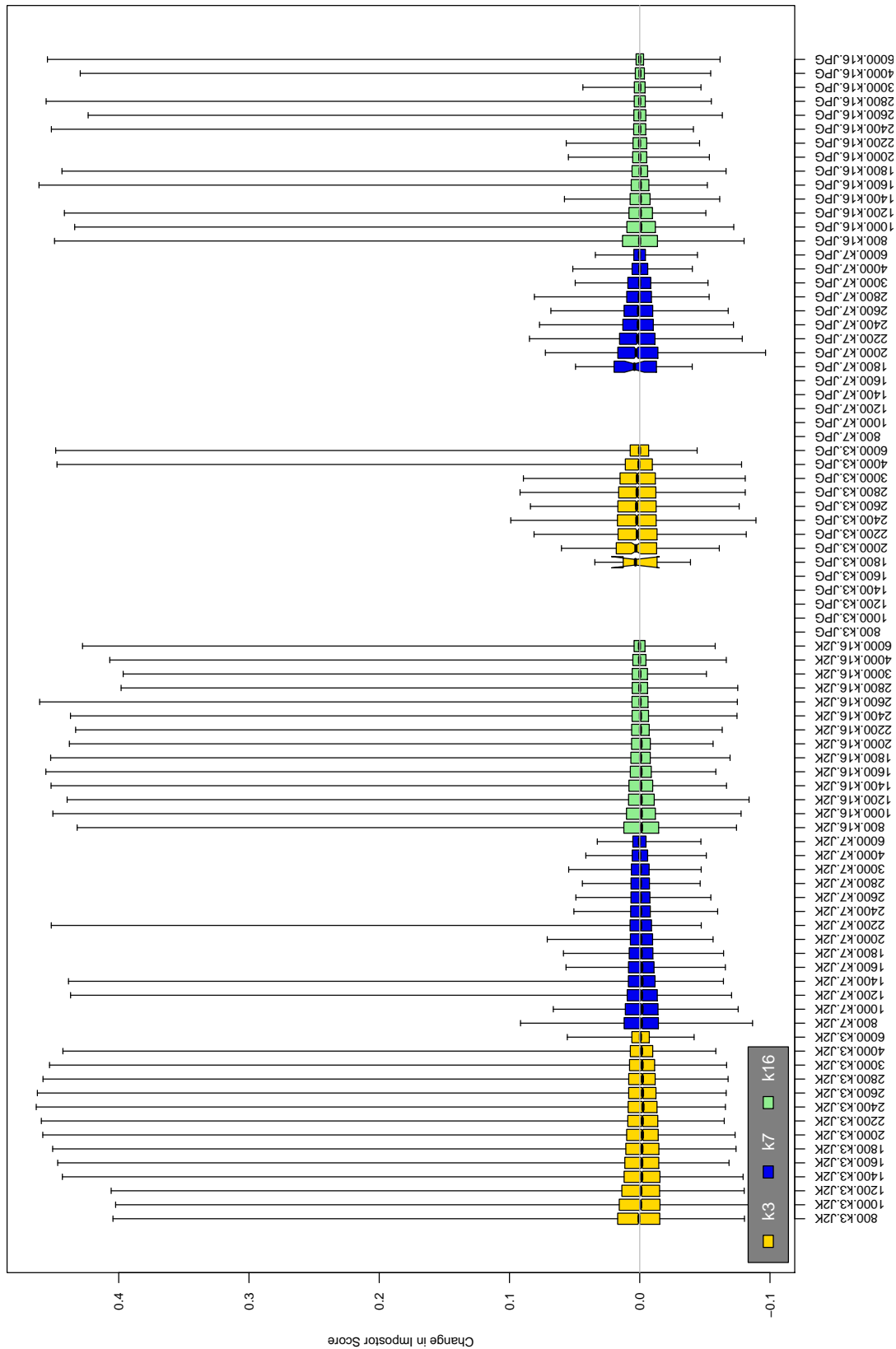


Table 148: The distribution of the increase in G1 native impostor comparison scores between the uncompressed “parent” and the compressed image, arranged by size, KIND and the compression algorithm. The images are from the OPS dataset. Any comparison involving a failed template is excluded. Note that the iris record size on the horizontal axis is not evenly spaced above 3000 bytes.

A = SAGEM	B = COGENT	C = CROSSMATCH	D = CAMBRIDGE	E = L1	x1 = PRIMARY
F = RETICA	G = LG	H = HONEYWELL	I = IRITECH	J = NEUROTECHNOLOGY	x2 = SECONDARY
KIND 1 = RAW 640x480		KIND 3 = CROP	KIND 7 = CROP+MASK	KIND 16 = CONCENTRIC POLAR	

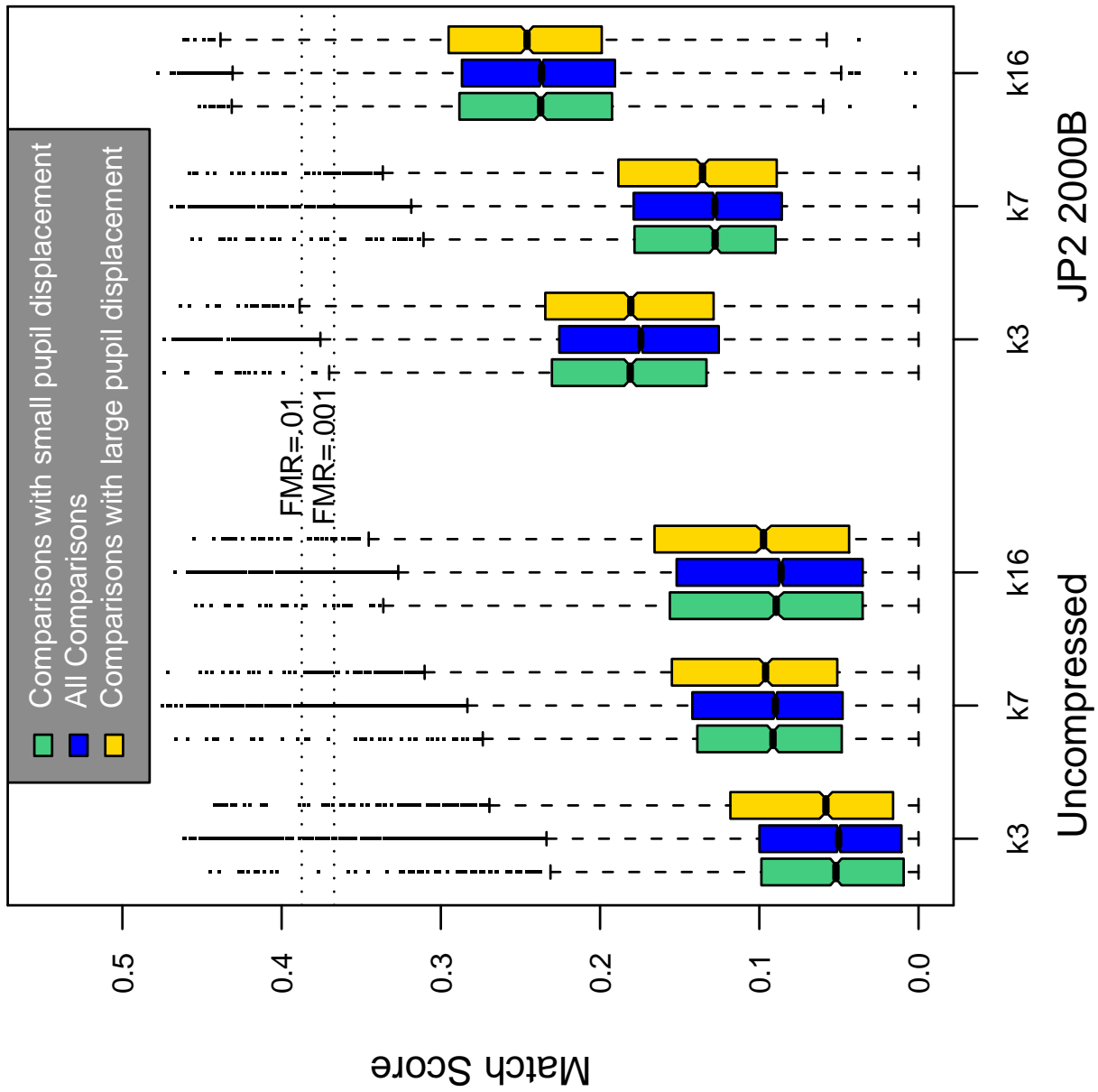


Table 149: Effect of pupil displacement on the genuine score distribution for G1

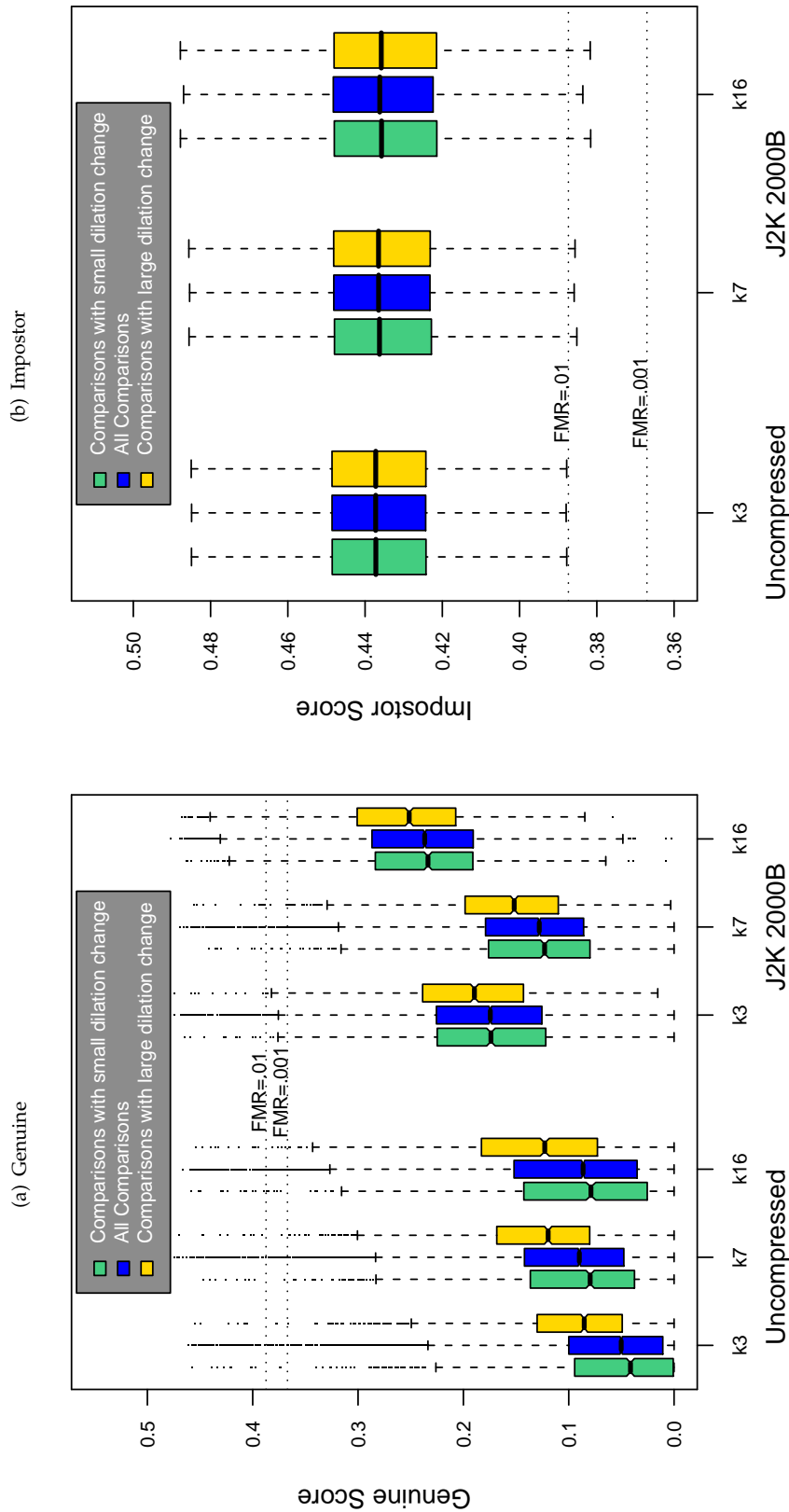


Table 150: The effect of dilation change on the two scores distributions for SDK G1.

A = SAGEM	B = COGENT	C = CROSSMATCH	D = CAMBRIDGE	E = L1	x1 = PRIMARY
F = RETICA	G = LG	H = HONEYWELL	I = IRITECH	J = NEUROTECHNOLOGY	x2 = SECONDARY
KIND 1 = RAW 640x480		KIND 3 = CROP	KIND 7 = CROP+MASK	KIND 16 = CONCENTRIC POLAR	

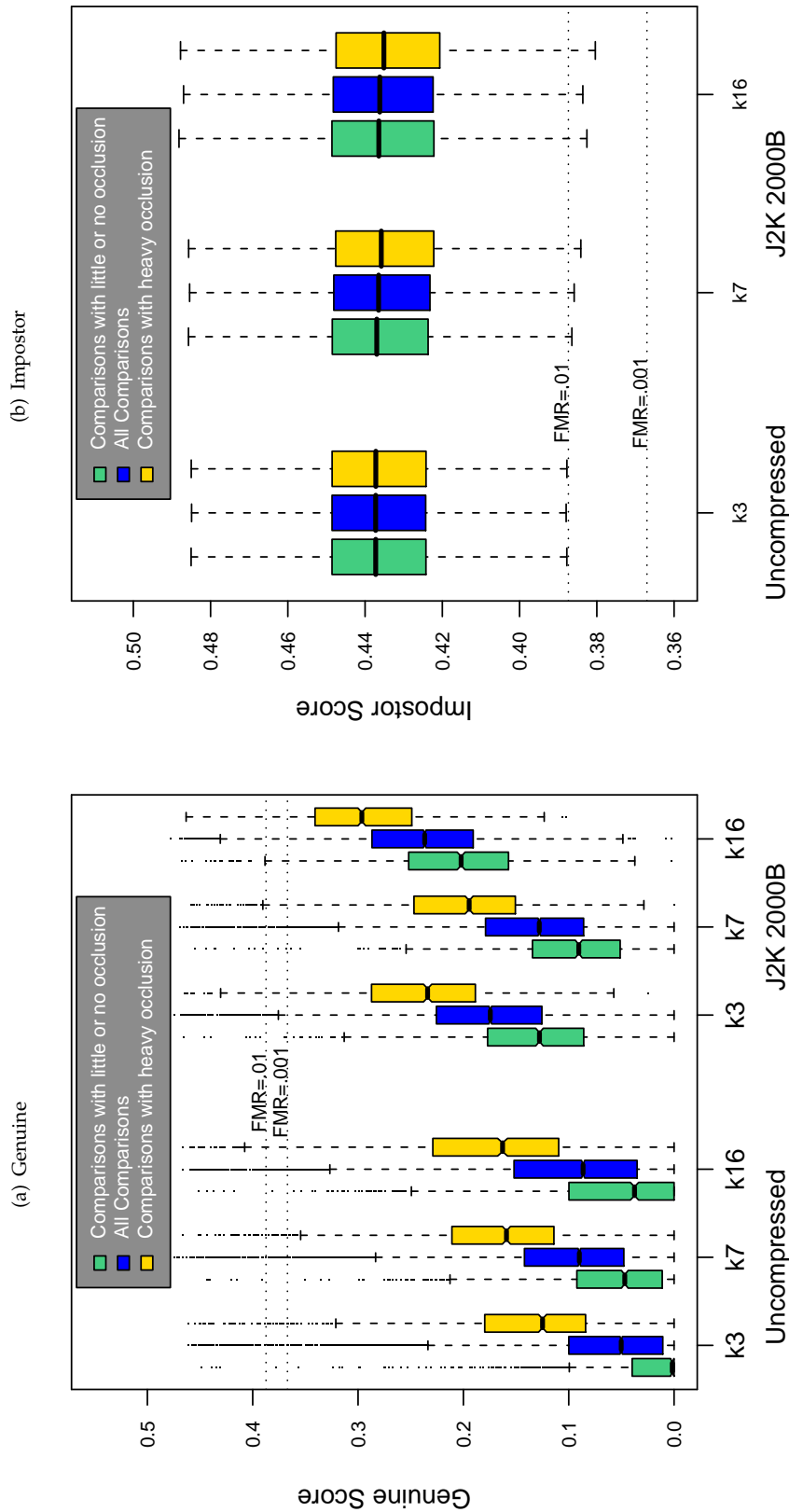
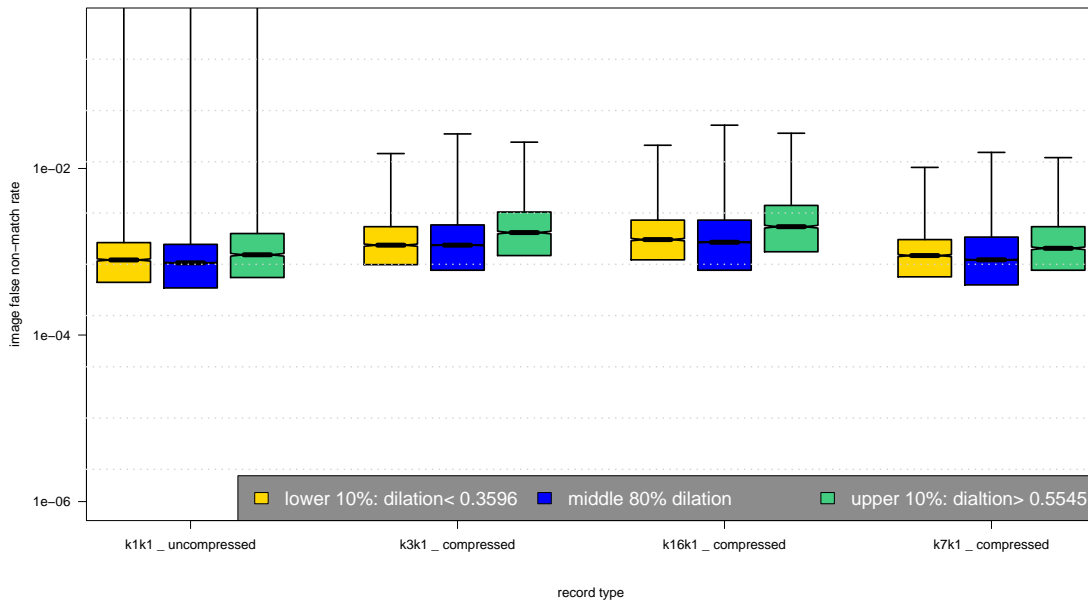
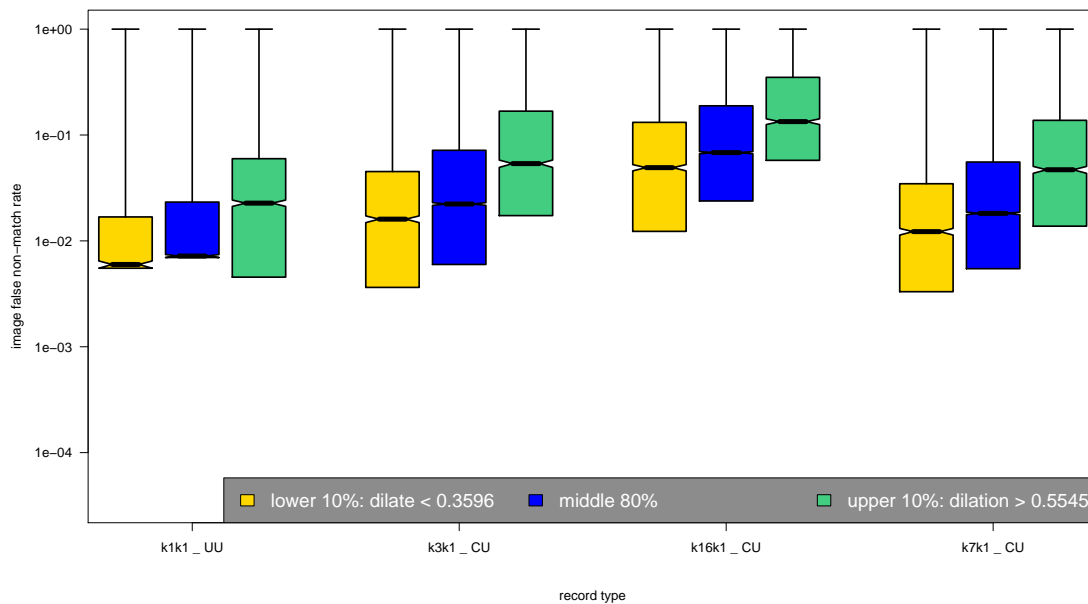


Table 151: The effect of eyelid occlusion on the two scores distributions for SDK G1.

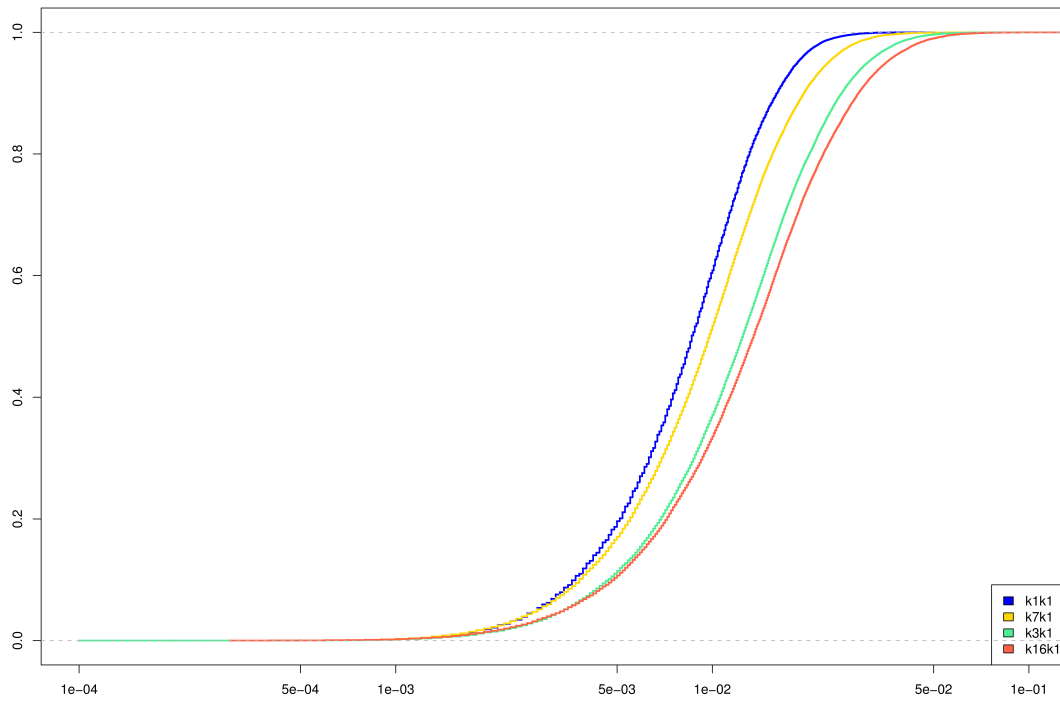
(a) iFMR using A1 dilation estimates



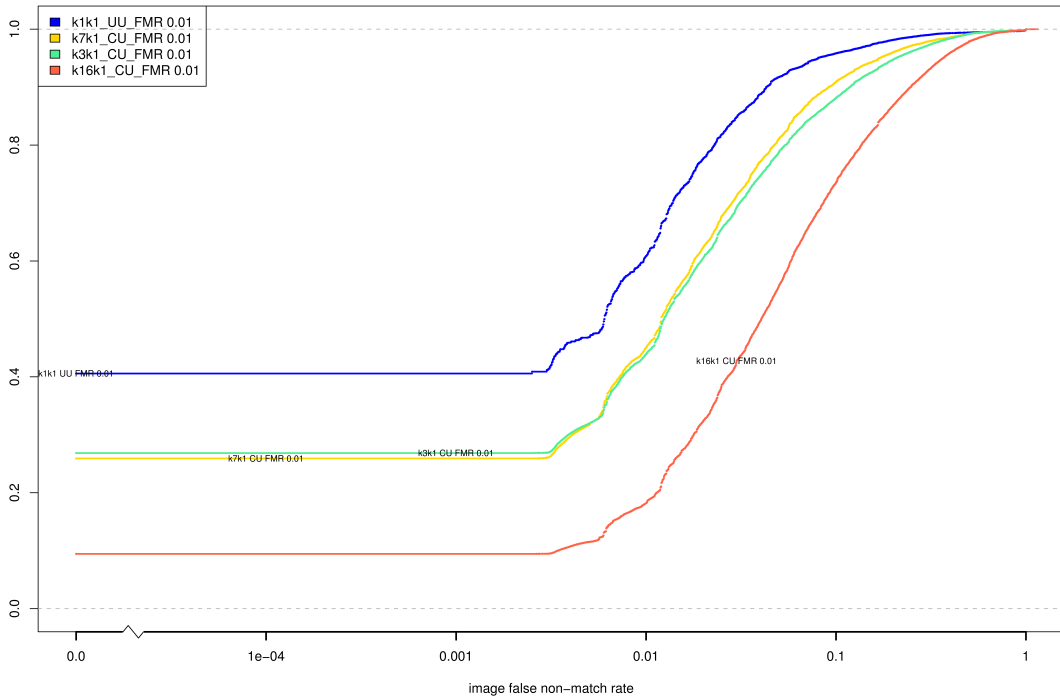
(b) iFNMR using A1 dilation estimates



(c) iFMR CDF



(d) iFNMR CDF



Compiled Results for Implementation G2

On June 25, 2009, NIST invited the IREX participants to submit a description of the SDKs submitted for the IREX effort. The intent was to allow providers to describe and contrast the feature sets, optimization, operational suitability and availability of the primary and secondary SDKs. NIST indicated that any submitted text would appear verbatim (with typesetting) in draft and final versions of the IREX report and that it would be attributed to the organization. This was optional and NIST put no constraints on the content beyond a 600 word limit, and a statement that anything labelled as confidential or proprietary would be omitted.

The provider of SDK G2, LG, elected not to submit any information

On August 17, 2009, NIST invited the IREX participants to submit a description their comments on an draft version of the IREX report. This was intended to allow participants to assist readers in the interpretation of a large and complicated testing effort. NIST indicated that any submitted text would appear verbatim (with typesetting) in the final version of the IREX report and that it would be attributed to the organization. Submission of content was optional and NIST put no constraints on the content beyond a word limit, and a statement that anything labelled as confidential or proprietary would be omitted.

The provider of SDK G2, LG, elected not to submit any information

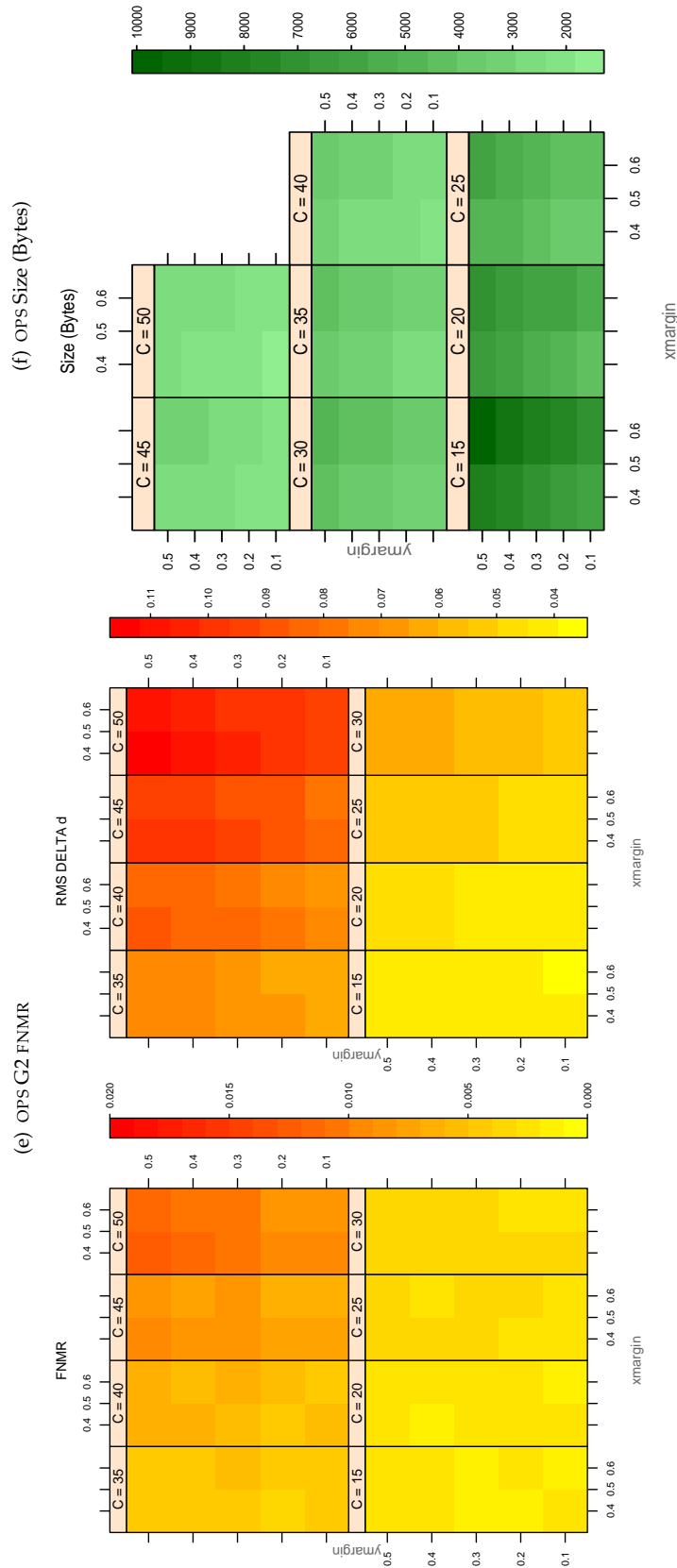


Table 152: For the IREX partition of the OPS database the plots at left show the dependence of cFNMR on the vertical and horizontal iris cropping margins for various compression ratios. This applies only for KIND 3 records. The margins are in units of iris radius. The use of conditional FNMR means that the plots exclude comparisons that were falsely rejected even before any compression was applied. On the **right side** is the rms difference between the crop+compress and the uncompressed comparison scores for each image pair. All computations are driven by the bounding box coordinates reported by the II SDK. The number of bits per pixel is $8/C$, where C is the compression ratio. The iris radius varies and because the cropping margins are fixed multiples of the radius the image size varies. The compressed size, in bytes, is the width times height divided by C . Values of cFNMR greater than 0.02 are shown as 0.02.

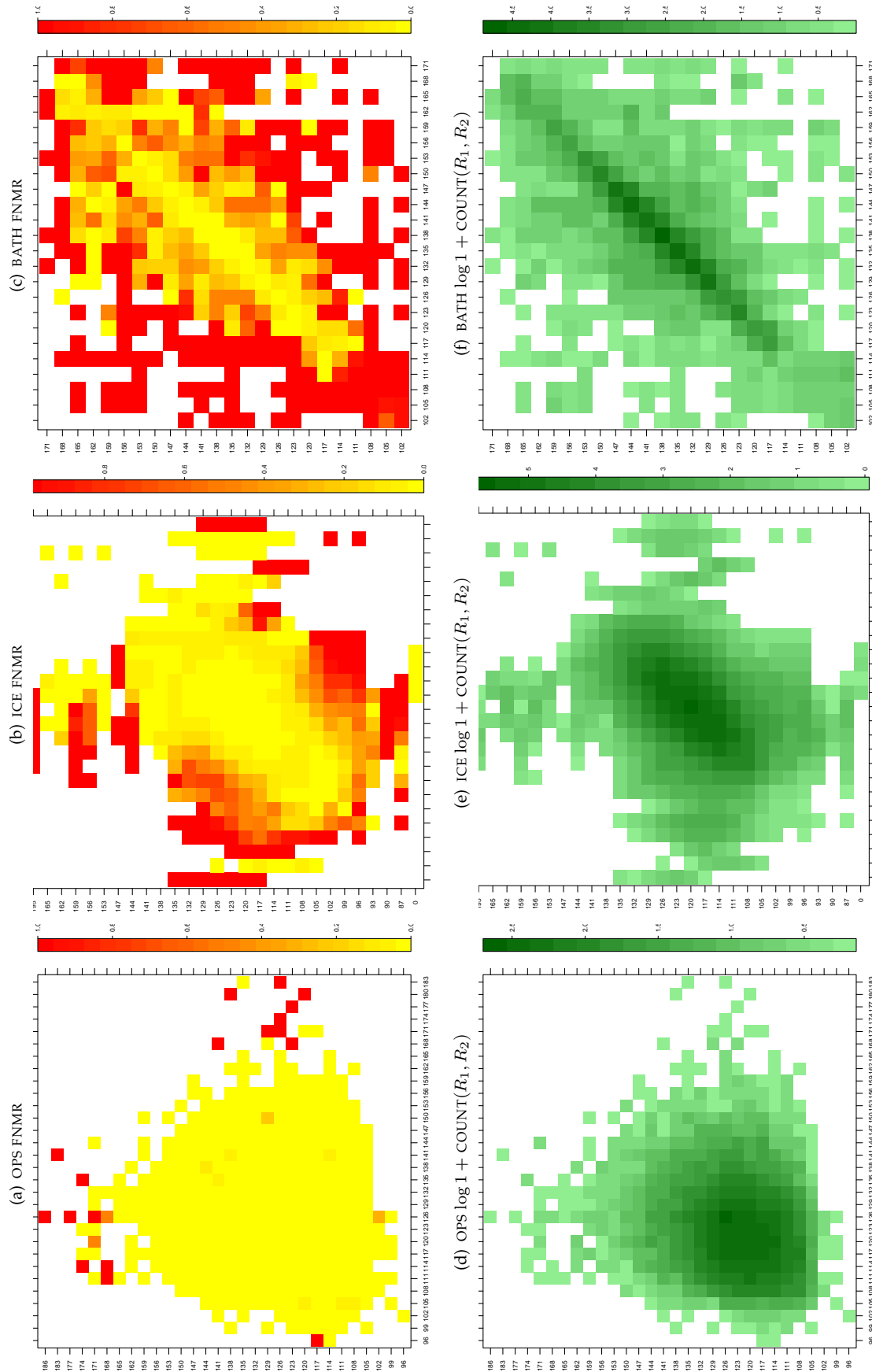


Table 153: For the three IREX databases: In the **top** row the color in each cell represents the occurrence of genuine comparisons with the given pair of radii. The *y*-axis represents enrollment samples with verification samples on the *x*-axis; In the **bottom** row the color scale plots $\log 1 + \text{COUNT}(R_1, R_2)$. The radii are quantized into three-pixel bins. The radii for DOD are on the range $96 \leq r \leq 186$ pixels. The radii for ICE are on the range $87 \leq r \leq 165$ pixels. The radii for BATH are on the range $100 \leq r \leq 170$ pixels.

A = SAGEM	B = COGENT	C = CROSSMATCH	D = CAMBRIDGE	E = L1	$x1$ = PRIMARY
F = RETICA	G = LG	H = HONEYWELL	I = IRITECH	J = NEUROTECHNOLOGY	$x2$ = SECONDARY
KIND 1 = RAW 640x480		KIND 3 = CROP		KIND 7 = CROP+MASK	
KIND 16 = CONCENTRIC POLAR					

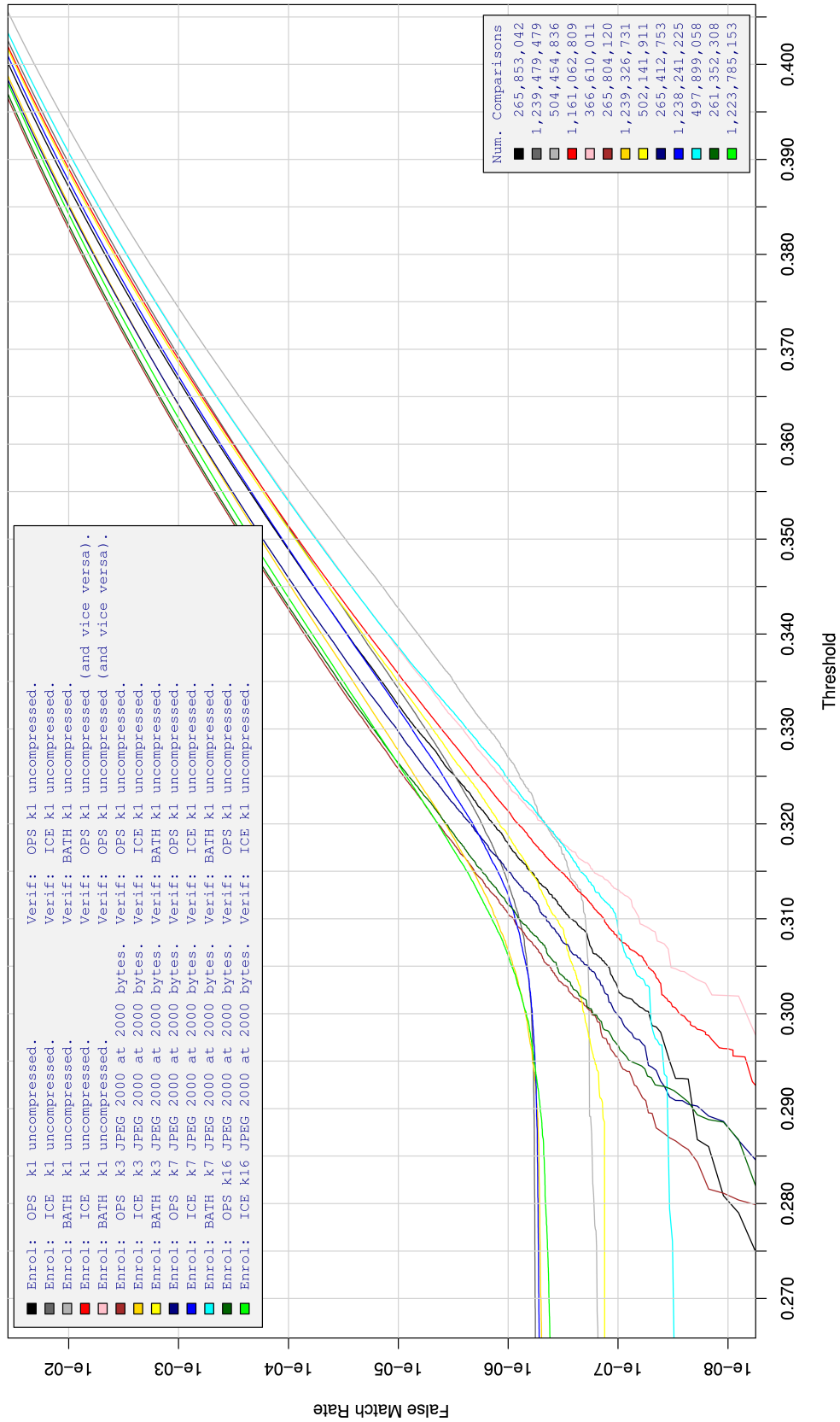


Table 154: For implementation G2, the dependency of FMR on threshold. for various combinations of enrollment and verification dataset, format, and compression.

A = SAGEM	B = COGENT	C = CROSSMATCH	D = CAMBRIDGE	E = L1	x1 = PRIMARY
F = RETICA	G = LG	H = HONEYWELL	I = IRITECH	J = NEUROTECHNOLOGY	x2 = SECONDARY
KIND 1 = RAW 640x480		KIND 3 = CROP		KIND 7 = CROP+MASK	KIND 16 = CONCENTRIC POLAR

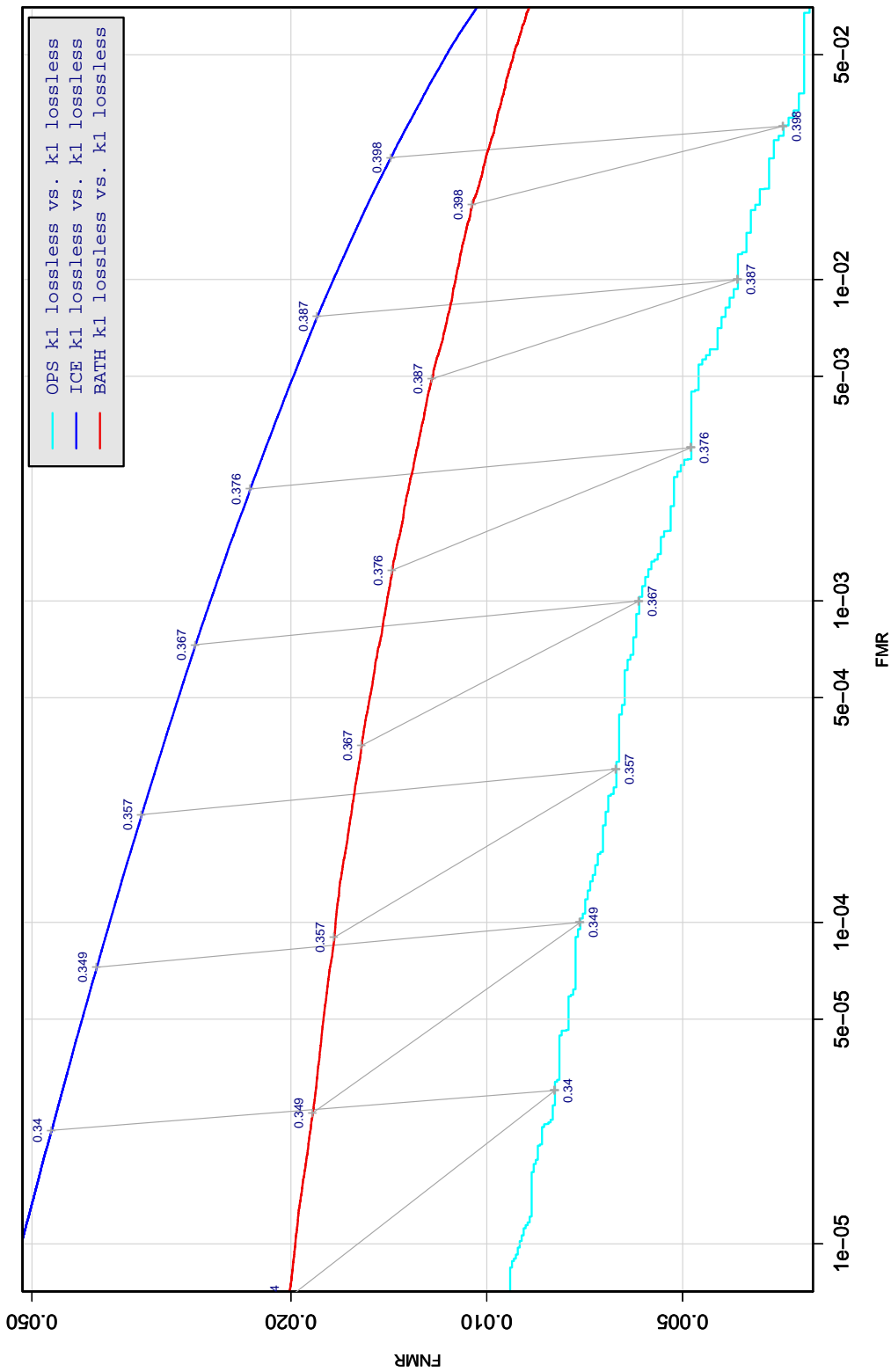


Table 155: DET curve for implementation G2 on three IREX databases. All comparisons are with uncompressed KIND 1 vs. KIND 1 images. The lines join points corresponding to the a fixed threshold. Non-vertical links indicate a change in FMR when the database changes. All results apply to native operation. Failures to produce a template i.e. FTE are ignored because the plots are intended to show *matching* effects, specifically to compare DET slopes and to show the effect of fixing a threshold.

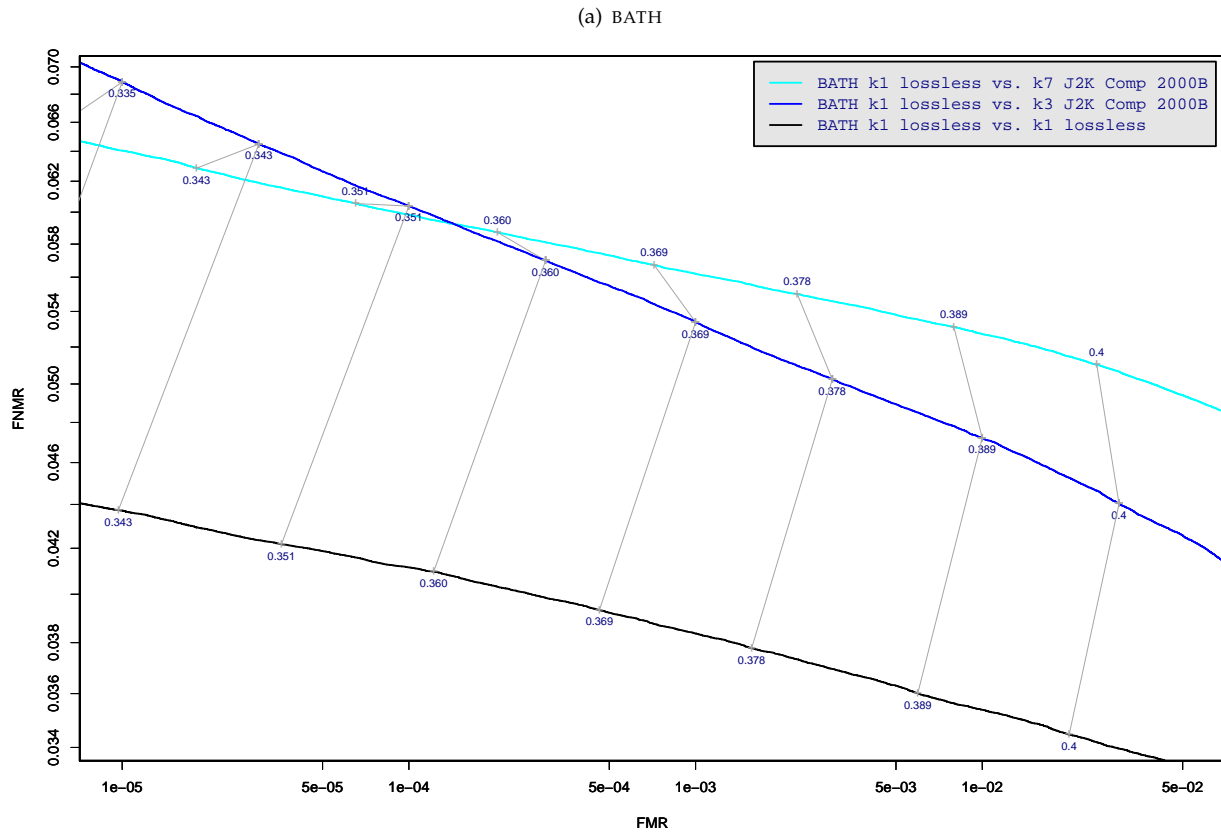


Table 156: DET curve for implementation G2 on the BATH database for the various supported KINDS . The DET characteristics are linked by lines joining points of equal threshold. Non-vertical links indicate a change in false acceptance when the data KIND changes. All results apply to native operation, and the effects of FTE are included.

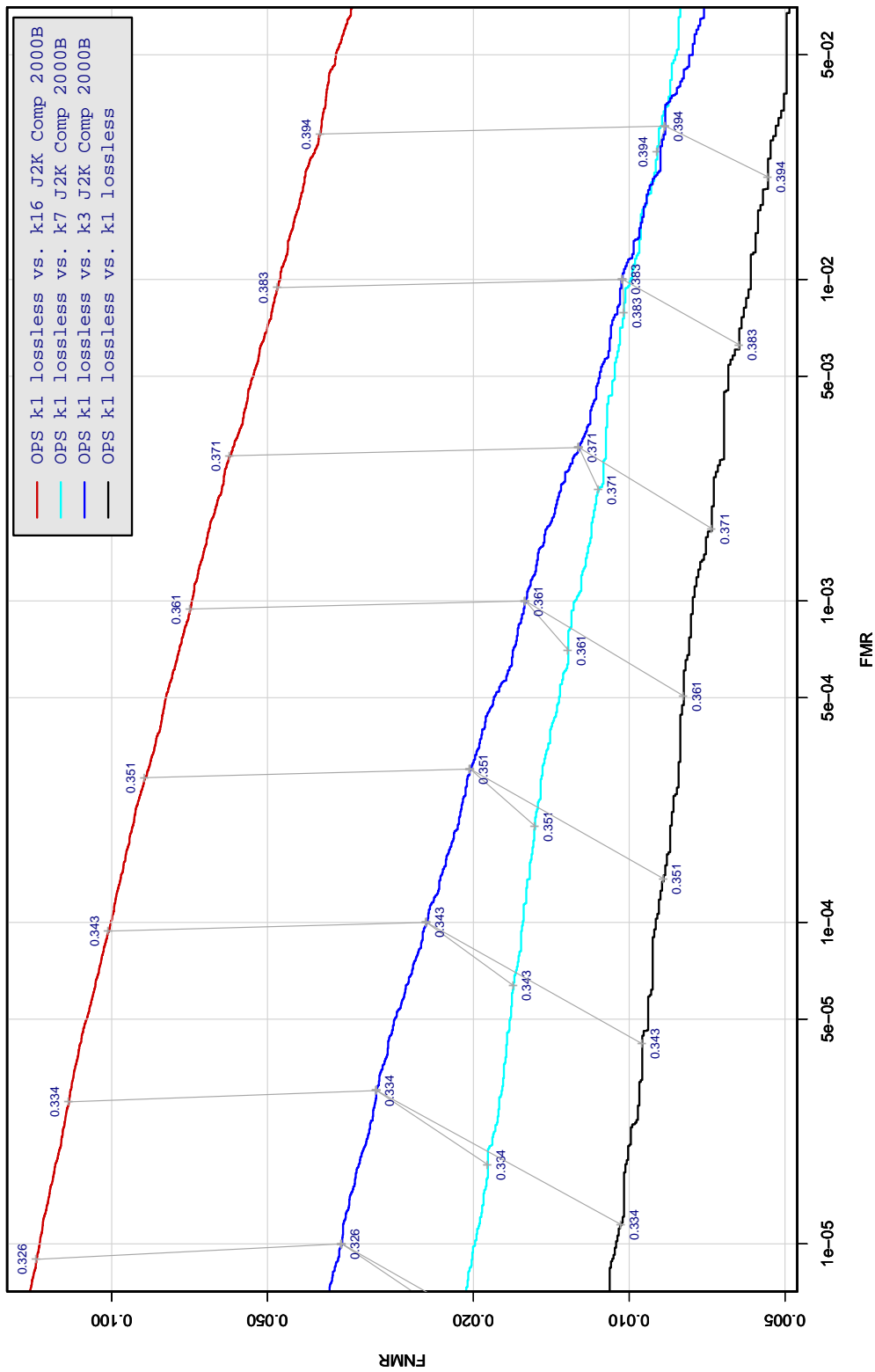


Table 157: DET curve for implementation G2 on the OPS database for the various supported KINDS . The DET characteristics are linked by lines joining points of equal threshold. Non-vertical links indicate a change in false acceptance when the data KIND changes. All results apply to native operation, and the effects of FTE are included.

A = SAGEM	B = COGENT	C = CROSSMATCH	D = CAMBRIDGE	E = L1	x1 = PRIMARY
F = RETICA	G = LG	H = HONEYWELL	I = IRITECH	J = NEUROTECHNOLOGY	x2 = SECONDARY
KIND 1 = RAW 640x480		KIND 3 = CROP		KIND 7 = CROP+MASK	KIND 16 = CONCENTRIC POLAR

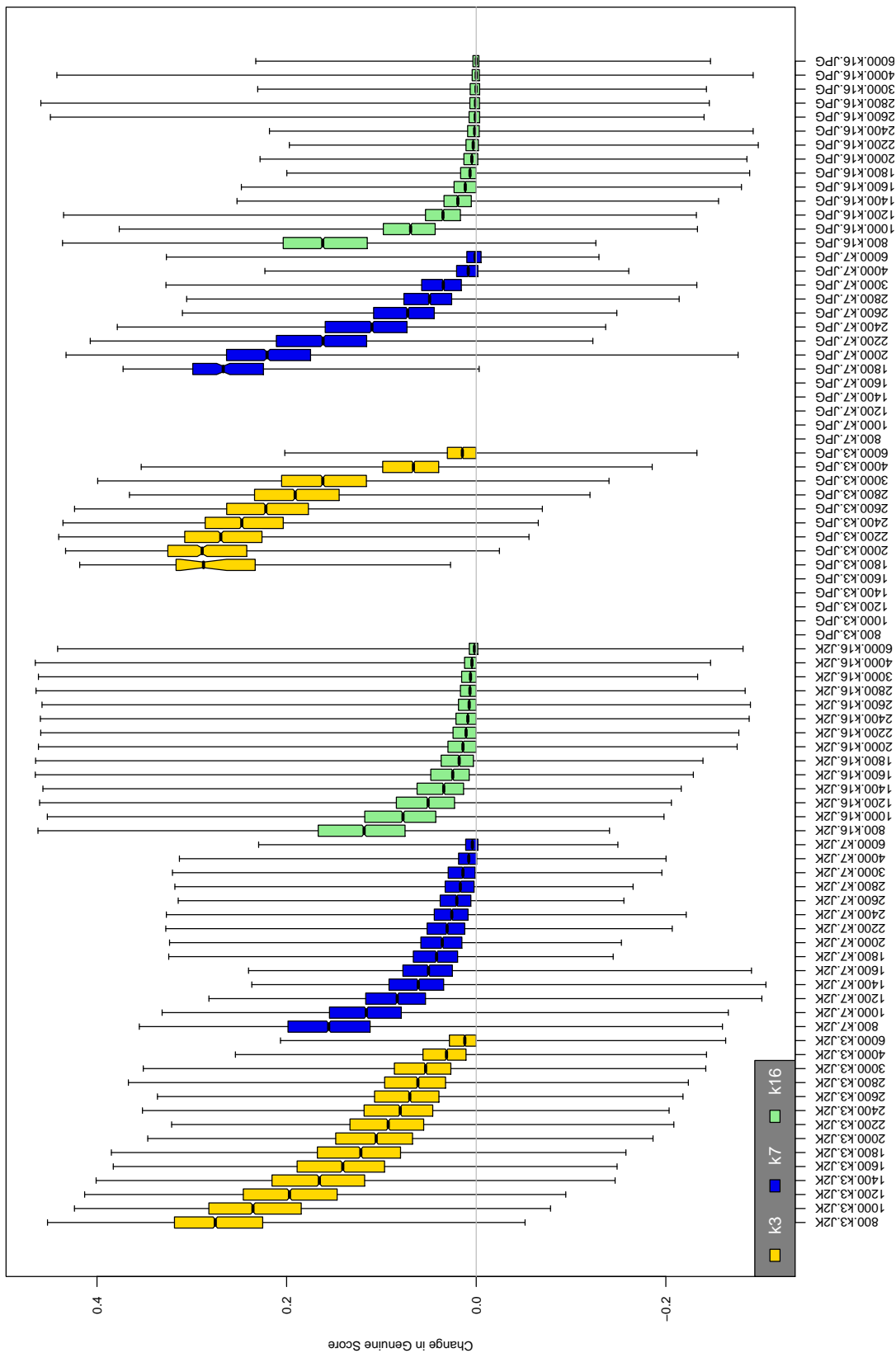


Table 159: The distribution of the *increase* in G2 native genuine comparison scores between the uncompressed “parent” and the compressed image, arranged by size, KIND and the compression algorithm. The images are from the OPS dataset. Any comparison involving a failed template is excluded. Note that the iris record size on the horizontal axis is not evenly spaced above 3000 bytes.

A = SAGEM	B = COGENT	C = CROSSMATCH	D = CAMBRIDGE	E = L1	x1 = PRIMARY
F = RETICA	G = LG	H = HONEYWELL	I = IRITECH	J = NEUROTECHNOLOGY	x2 = SECONDARY
KIND 1 = RAW 640x480		KIND 3 = CROP		KIND 7 = CROP+MASK	
				KIND 16 = CONCENTRIC POLAR	

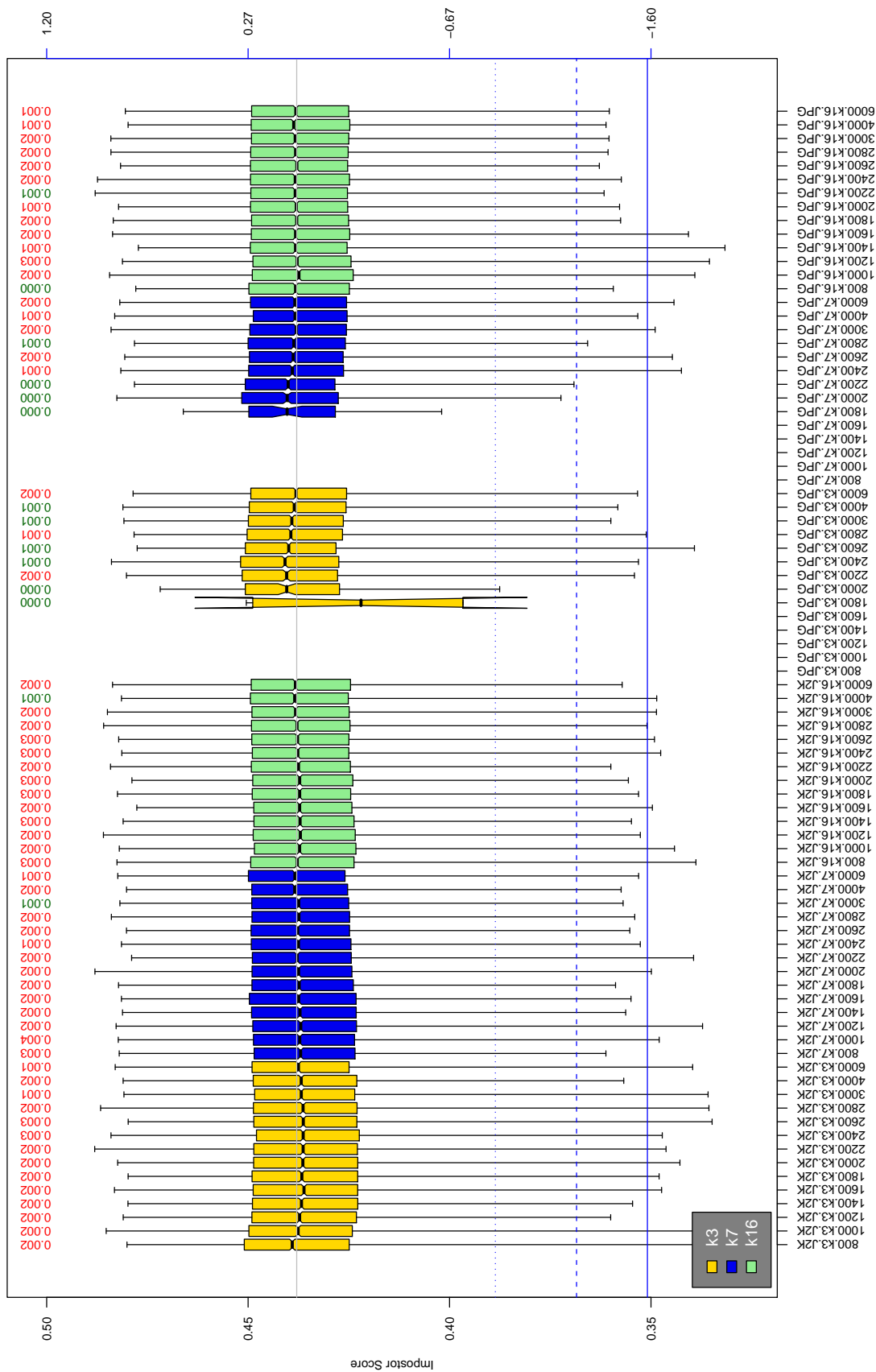


Table 160: The distribution of G2 native impostor comparison scores by size of the compressed image, KIND and the compression algorithm. The right axis scale gives the corresponding value for $d' = (s - \mu_1) / \sqrt{0.5(\sigma_1^2 + \sigma_2^2)}$ for impostor score s . The three blue lines correspond, from the top, to FMR of $10^{-2}, -3, -4$. The lower grey line refers to the median score obtained from comparison of uncompressed KIND 3 images. Any comparison involving a failed template is excluded. Above the boxplots are FMR values at the threshold that gives FMR = 10^{-3} on uncompressed images. These figures are computed from only 4000 comparisons so the FMR values and the tails of the impostor distribution are poorly characterized. Note that the iris record size on the horizontal axis is not evenly spaced above 3000 bytes.

A = SAGEM	B = COGENT	C = CROSSMATCH	D = CAMBRIDGE	E = L1	$x1$ = PRIMARY
F = RETICA	G = LG	H = HONEYWELL	I = IRITECH	J = NEUROTECHNOLOGY	$x2$ = SECONDARY
KIND 1 = RAW 640x480		KIND 3 = CROP	KIND 7 = CROP+MASK	KIND 16 = CONCENTRIC POLAR	

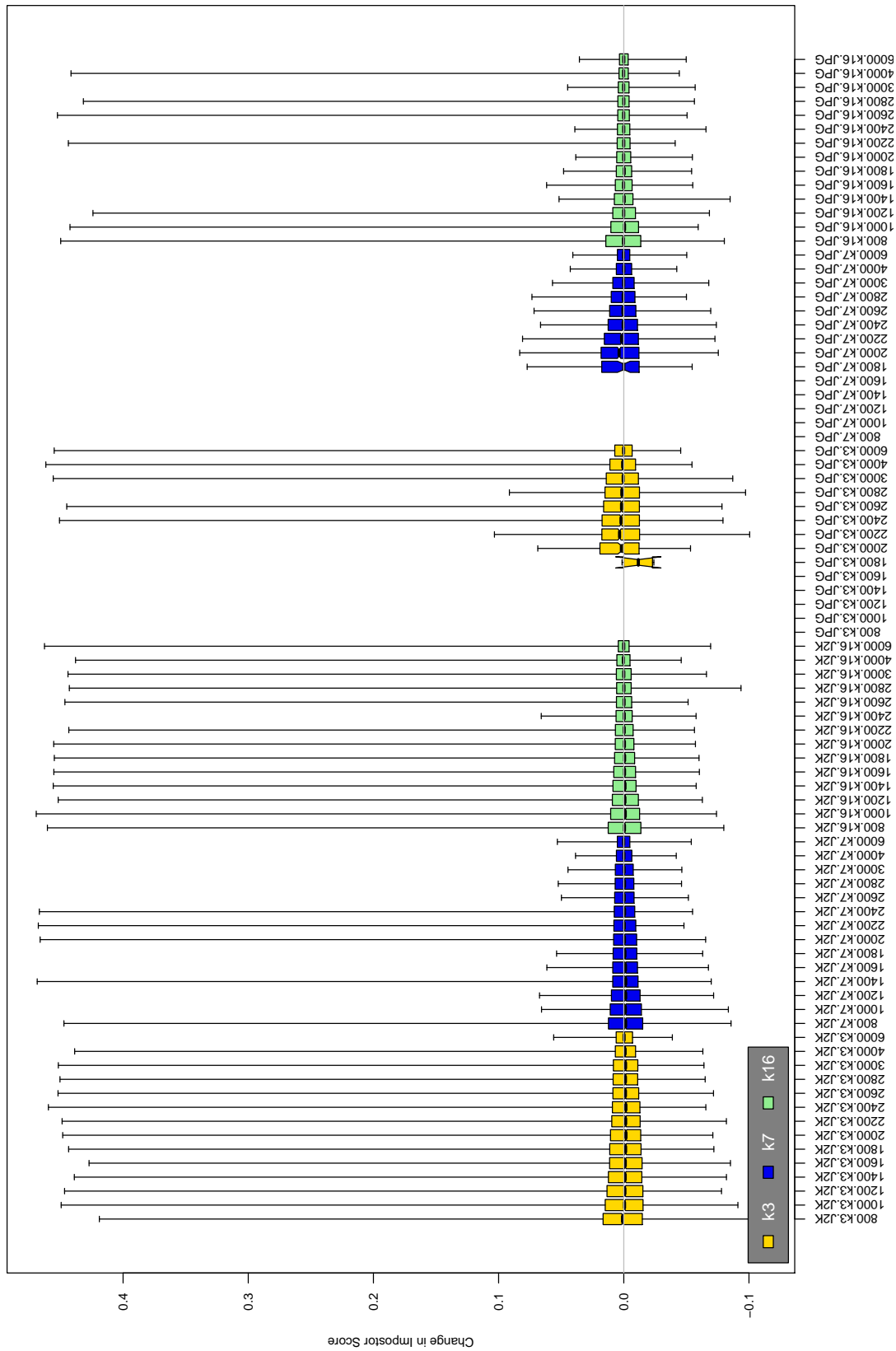


Table 161: The distribution of the increase in G2 native impostor comparison scores between the uncompressed “parent” and the compressed image, arranged by size, KIND and the compression algorithm. The images are from the OPS dataset. Any comparison involving a failed template is excluded. Note that the iris record size on the horizontal axis is not evenly spaced above 3000 bytes.

A = SAGEM	B = COGENT	C = CROSSMATCH	D = CAMBRIDGE	E = L1	x1 = PRIMARY
F = RETICA	G = LG	H = HONEYWELL	I = IRITECH	J = NEUROTECHNOLOGY	x2 = SECONDARY
KIND 1 = RAW 640x480		KIND 3 = CROP		KIND 7 = CROP+MASK	KIND 16 = CONCENTRIC POLAR

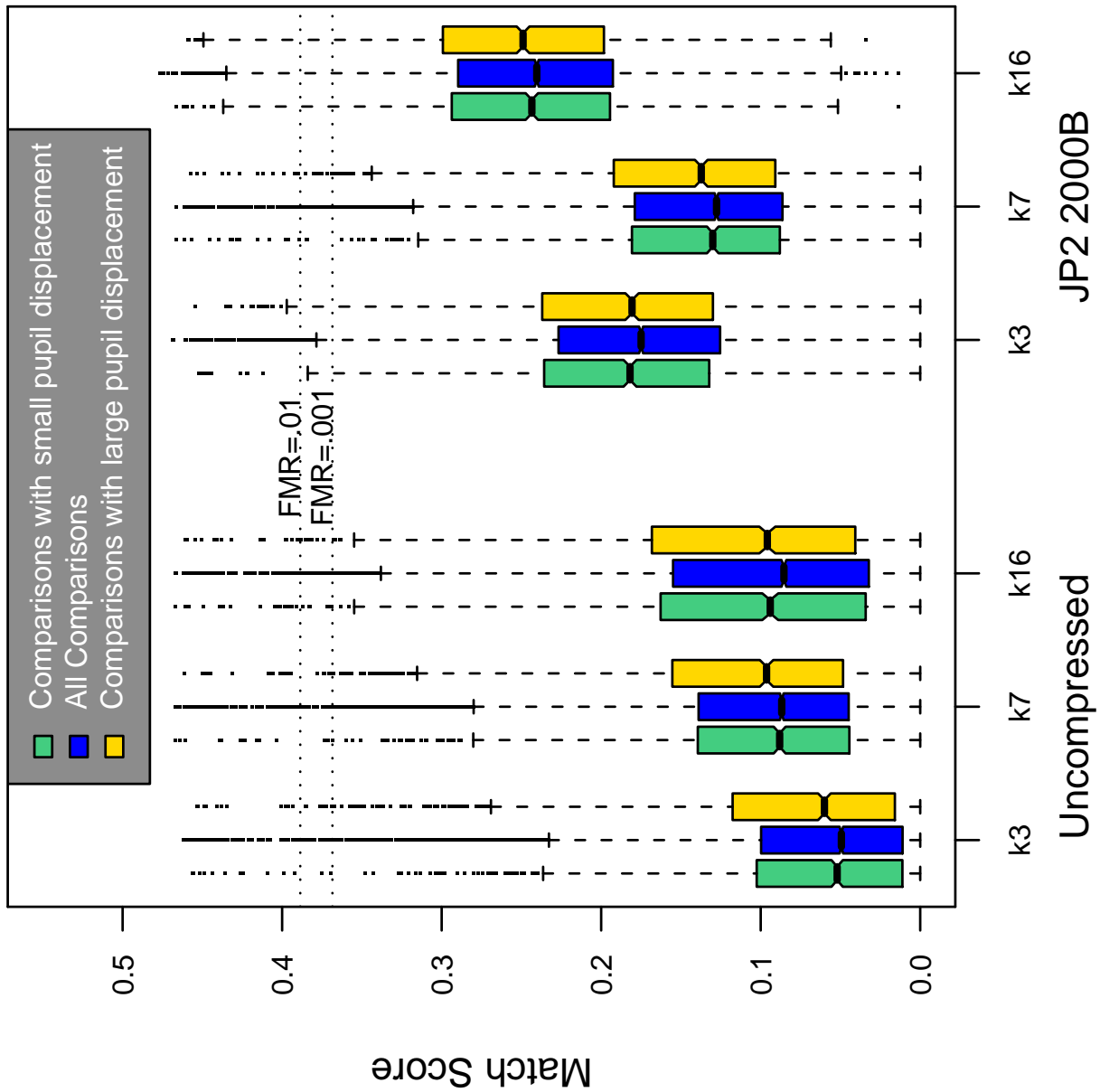


Table 162: Effect of pupil displacement on the genuine score distribution for G2

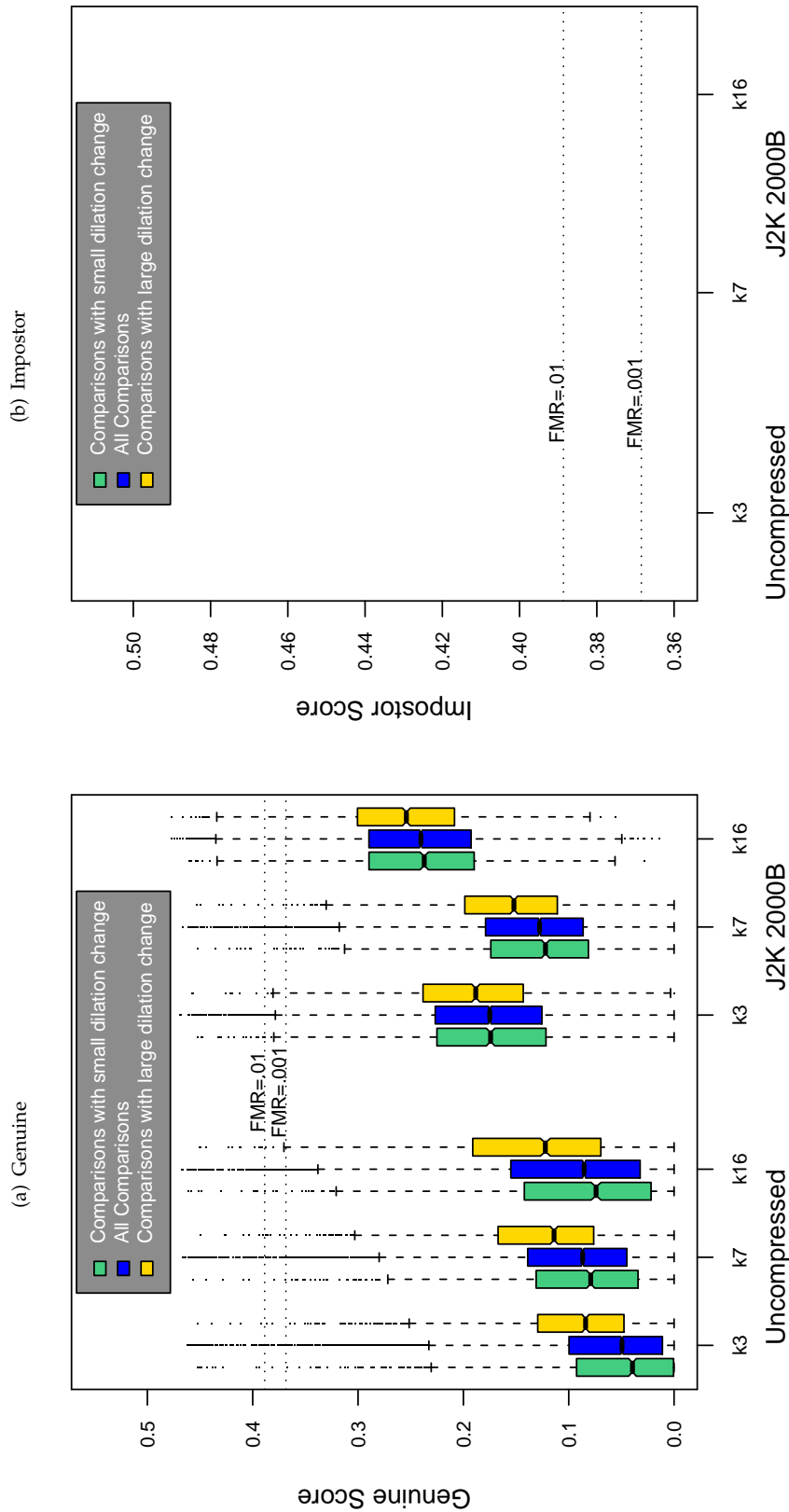


Table 163: The effect of dilation change on the two scores distributions for SDK G2.

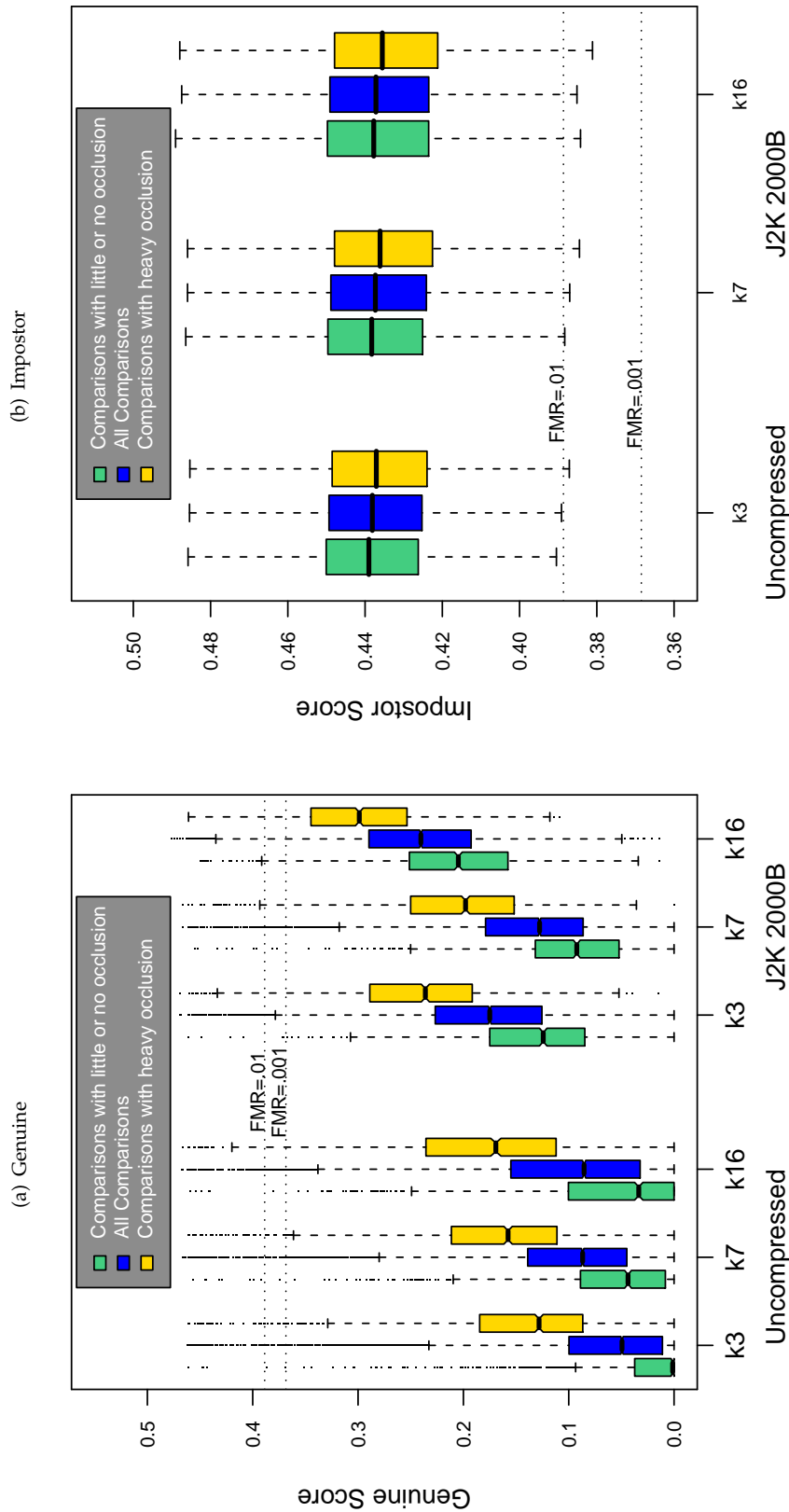
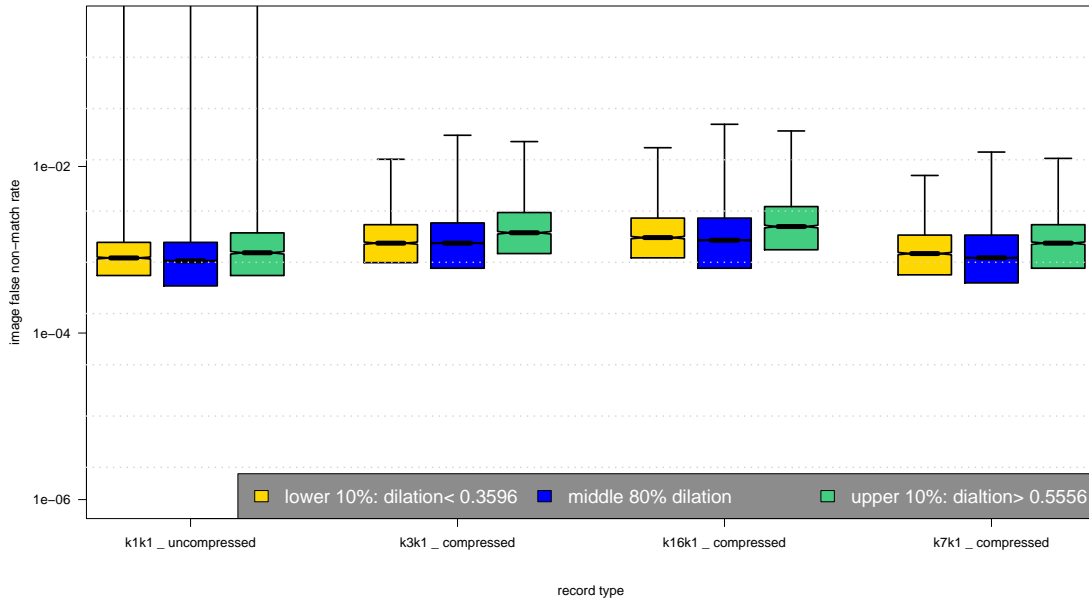
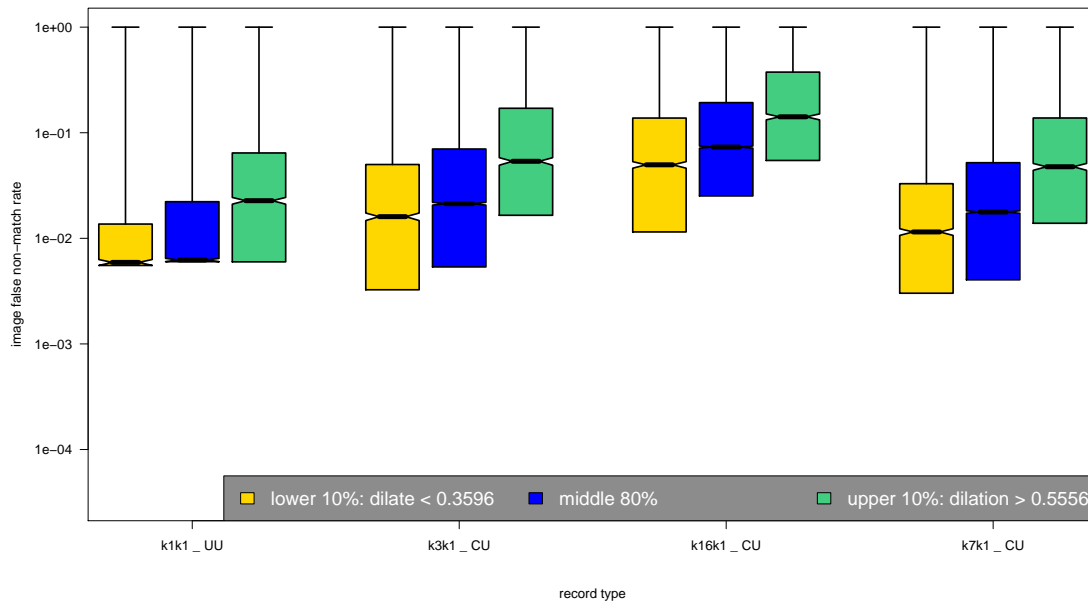


Table 164: The effect of eyelid occlusion on the two scores distributions for SDK G2.

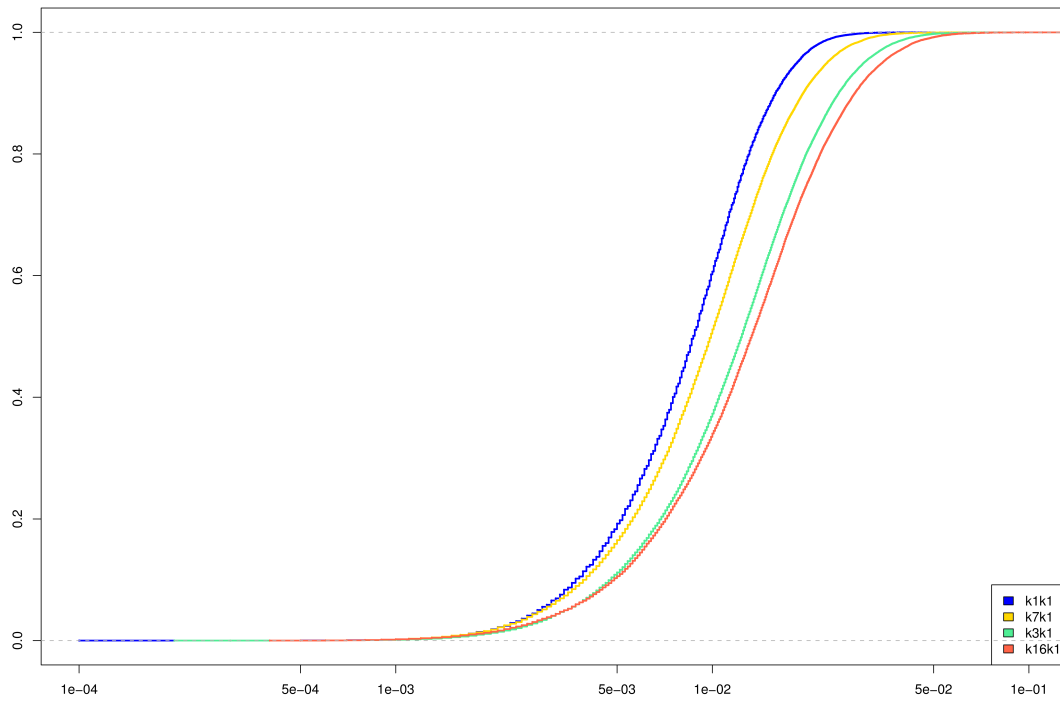
(a) iFMR using A1 dilation estimates



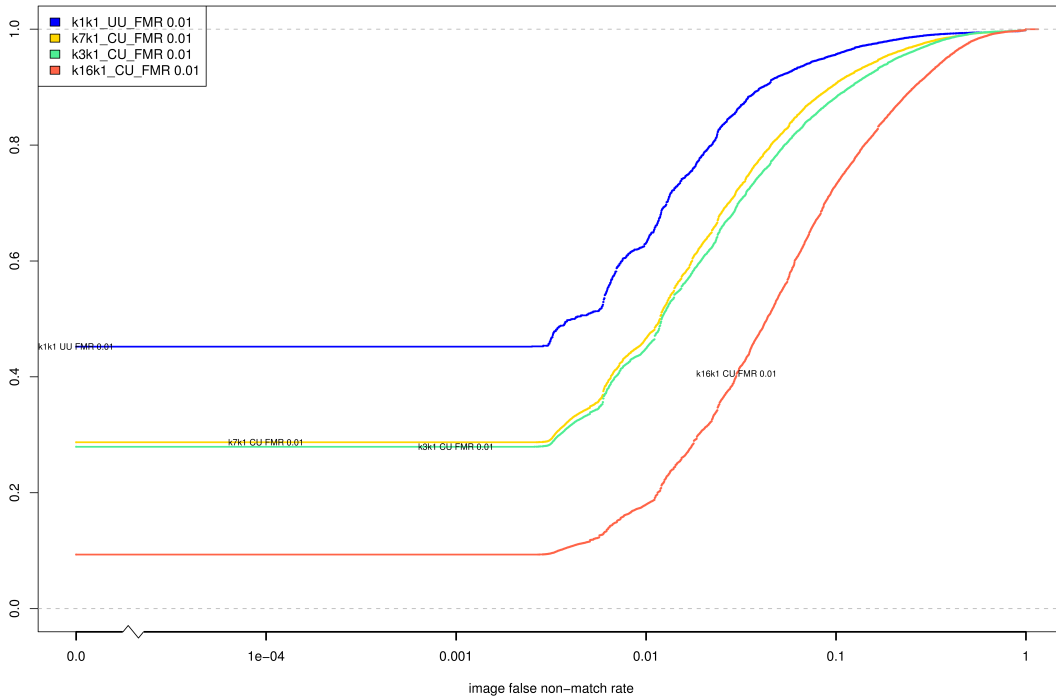
(b) iFNMR using A1 dilation estimates



(c) iFMR CDF



(d) iFNMR CDF



Compiled Results for Implementation H1

On June 25, 2009, NIST invited the IREX participants to submit a description of the SDKs submitted for the IREX effort. The intent was to allow providers to describe and contrast the feature sets, optimization, operational suitability and availability of the primary and secondary SDKs. NIST indicated that any submitted text would appear verbatim (with typesetting) in draft and final versions of the IREX report and that it would be attributed to the organization. This was optional and NIST put no constraints on the content beyond a 600 word limit, and a statement that anything labelled as confidential or proprietary would be omitted.

The provider of SDK H1, Honeywell, elected not to submit any information

On August 17, 2009, NIST invited the IREX participants to submit a description their comments on an draft version of the IREX report. This was intended to allow participants to assist readers in the interpretation of a large and complicated testing effort. NIST indicated that any submitted text would appear verbatim (with typesetting) in the final version of the IREX report and that it would be attributed to the organization. Submission of content was optional and NIST put no constraints on the content beyond a word limit, and a statement that anything labelled as confidential or proprietary would be omitted.

The provider of SDK H1, Honeywell, submitted the following to NIST - we make no comment on this information.

The Honeywell algorithms were developed for standoff iris recognition systems to identify non-cooperative subjects. The algorithmic approach was developed to cope with larger margin of variations than are present in the IREX dataset. Both algorithms were implemented to tolerate a wide range of acquisition and non-constrained environmenta key advantage of the recently developed Honeywell CFAIRS system (combined face and iris recognition system) to identify iris on the move at distances that can extend up to 4m.

The Honeywell technique uses a novel iris segmentation scheme that takes the analysis of edges into the polar domain at an earlier stage. Mapping the segmentation analysis to polar domain permits the detection of any irregular shapes of irises. This is a key advantage of Honeywell proposed segmentation technique that is well suited for unconstrained standoff iris acquisition where non-frontal irregular shapes are captured at various gazed angles. The approach has proven its efficiency and robustness by allowing iris recognition under suboptimal image acquisition conditions. The results in this IREX report confirm this claim as both Honeywell techniques were more competitive on the suboptimal images (ICE, BATH) than on the frontal dataset (OPS). The competitive advantage of a reliable segmentation approach is undermined when applied only to frontal images. The results do not reflect the true Honeywell algorithm advantages for the following reasons:

- Both Honeywell algorithms were calibrated to handle ICE like dataset. However, the comparison was mostly evaluated on OPS. OPS and BATH are significantly different data than ICE-2005. Honeywell algorithms were purposely designed to handle larger variations to accurately segment non-cooperative subjects that can be calibrated to different ranges of zooming acquisitions. Both Honeywell algorithms use non-iterative polar differential operator to locate the inner and outer borders of the iris. These ranges are specified a priori in the calibration of the algorithm. However, no such calibration was performed on the results reported in this IREX report. .
- The Honeywell algorithms are more amenable to poor quality iris samples. The robustness of the Honeywell standoff iris recognition approach relies heavily on accurate iris segmentation. The IREX evaluation probes the uniqueness and richness of iris patterns even when deployed to a large populationa

requirement that must be met to deploy the technology as a true biometric tool. These are very encouraging results however a significant amount of the evaluation was biased by the sensors used for collecting the images used in this report. It is hard to reflect from the evaluation how these developed techniques address the true nature of iris irregularity in iris segmentation.

- The Honeywell algorithms were set for a non-cooperative calibration mode in this evaluation (rather than a frontal operational mode) to handle more irregular iris images. Because of this mode setting, Honeywell algorithm performed significantly better than others in segmenting and creating non-failed template records per table 5. This mode of operation is effective in tolerating more gazed eyes at the expense of loss of overall matching accuracy. These advantages are not reflected on high quality samples such as the OPS dataset. In addition, the exclusion of failed templates on poor quality images aided others by preventing poor quality images from being considered in the matching accuracy, and thus prevented fair comparison of algorithms (refer to table 11 and 12).
- Inconsistency in computational requirements in extracting an iris signature prevents a fair comparison among algorithms. In Honeywell algorithms, some processes related to iris quality measures (IQM) were turned off to reduce the computational load.

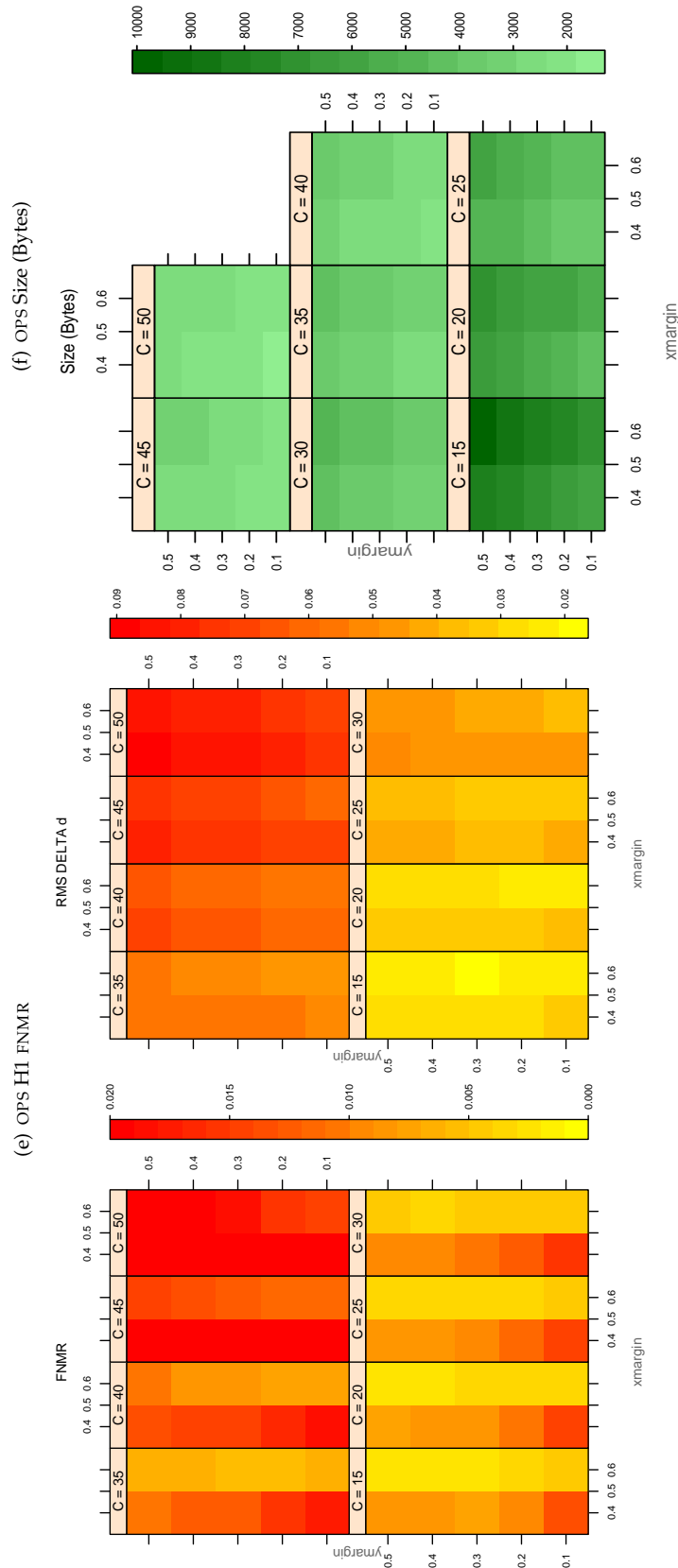


Table 165: For the IREX partition of the OPS database the plots at left show the dependence of cFNMR on the vertical and horizontal iris cropping margins for various compression ratios. This applies only for KIND 3 records. The margins are in units of iris radius. The use of conditional FNMR means that the plots exclude comparisons that were falsely rejected even before any compression was applied. On the **right side** is the rms difference between the crop+compress and the uncompressed comparison scores for each image pair. All computations are driven by the bounding box coordinates reported by the II SDK. The number of bits per pixel is $8/C$, where C is the compression ratio. The iris radius varies and because the cropping margins are fixed multiples of the radius the image size varies. The compressed size, in bytes, is the width times height divided by C . Values of cFNMR greater than 0.02 are shown as 0.02.

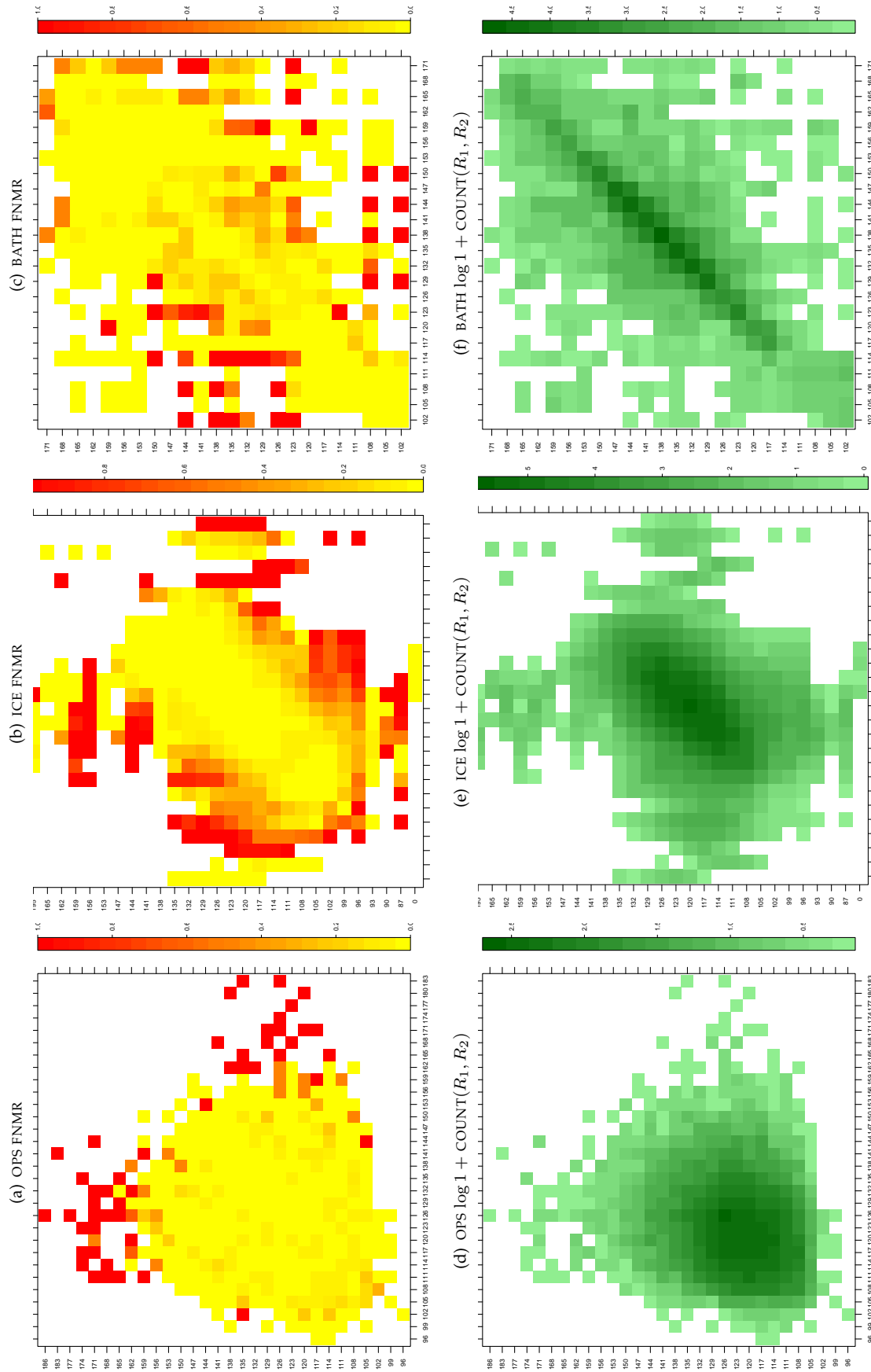


Table 166: For the three IREX databases: In the **top** row the color in each cell represents the occurrence of genuine comparisons with the given pair of radii. The *y*-axis represents enrollment samples with verification samples on the *x*-axis; In the **bottom** row the color scale plots $\log 1 + \text{COUNT}(R_1, R_2)$. The radii are quantized into three-pixel bins. The radii for DOD are on the range $96 \leq r \leq 186$ pixels. The radii for ICE are on the range $87 \leq r \leq 165$ pixels. The radii for BATH are on the range $100 \leq r \leq 170$ pixels.

A = SAGEM	B = COGENT	C = CROSSMATCH	D = CAMBRIDGE	E = L1	$x1$ = PRIMARY
F = RETICA	G = LG	H = HONEYWELL	I = IRITECH	J = NEUROTECHNOLOGY	$x2$ = SECONDARY
KIND 1 = RAW 640x480		KIND 3 = CROP	KIND 7 = CROP+MASK	KIND 16 = CONCENTRIC POLAR	

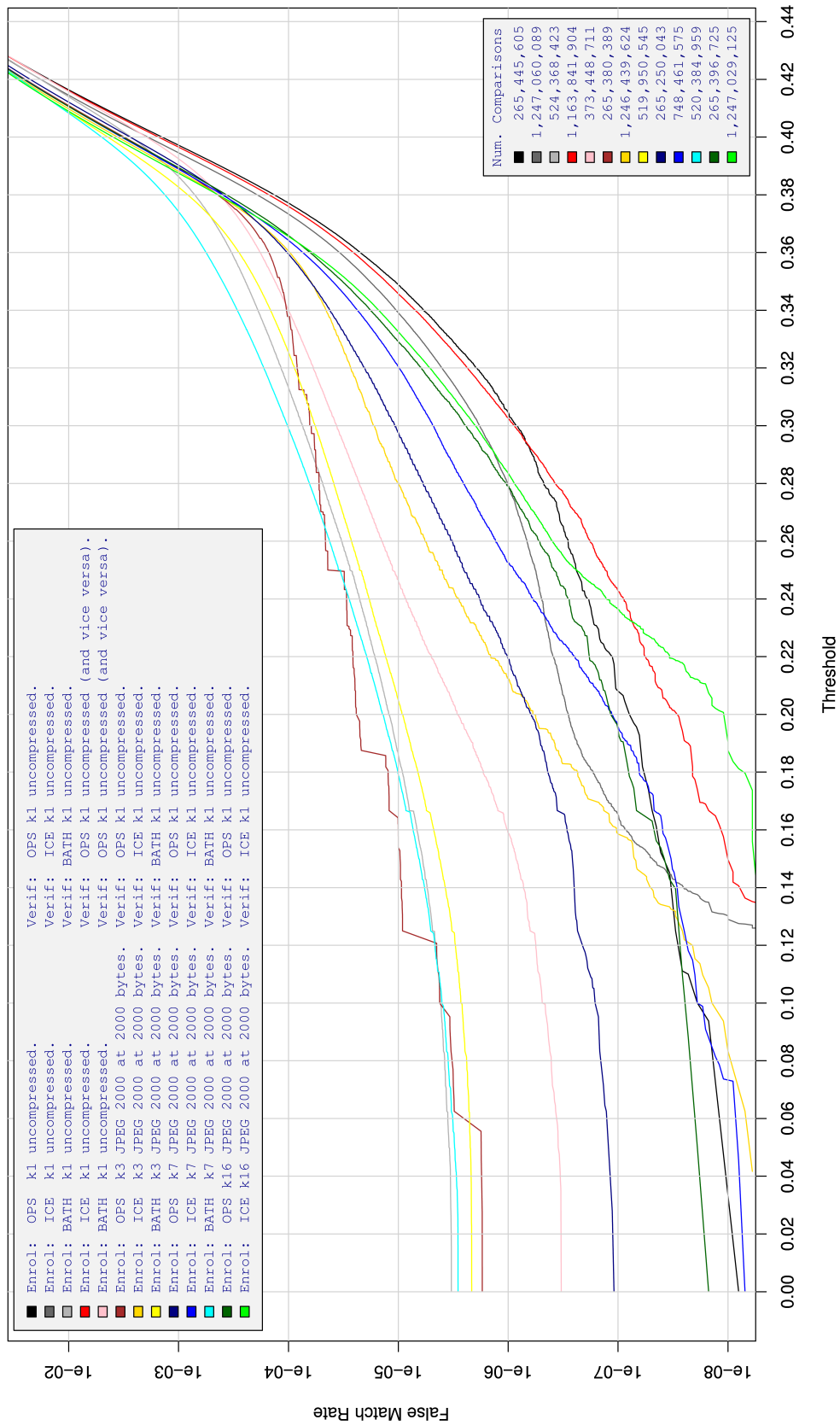


Table 167: For implementation H1, the dependency of FMR on threshold, for various combinations of enrollment and verification dataset, format, and compression.

A = SAGEM	B = COGENT	C = CROSSMATCH	D = CAMBRIDGE	E = L1	x1 = PRIMARY
F = RETICA	G = LG	H = HONEYWELL	I = IRITECH	J = NEUROTECHNOLOGY	x2 = SECONDARY
KIND 1 = RAW 640x480		KIND 3 = CROP		KIND 7 = CROP+MASK	
				KIND 16 = CONCENTRIC POLAR	

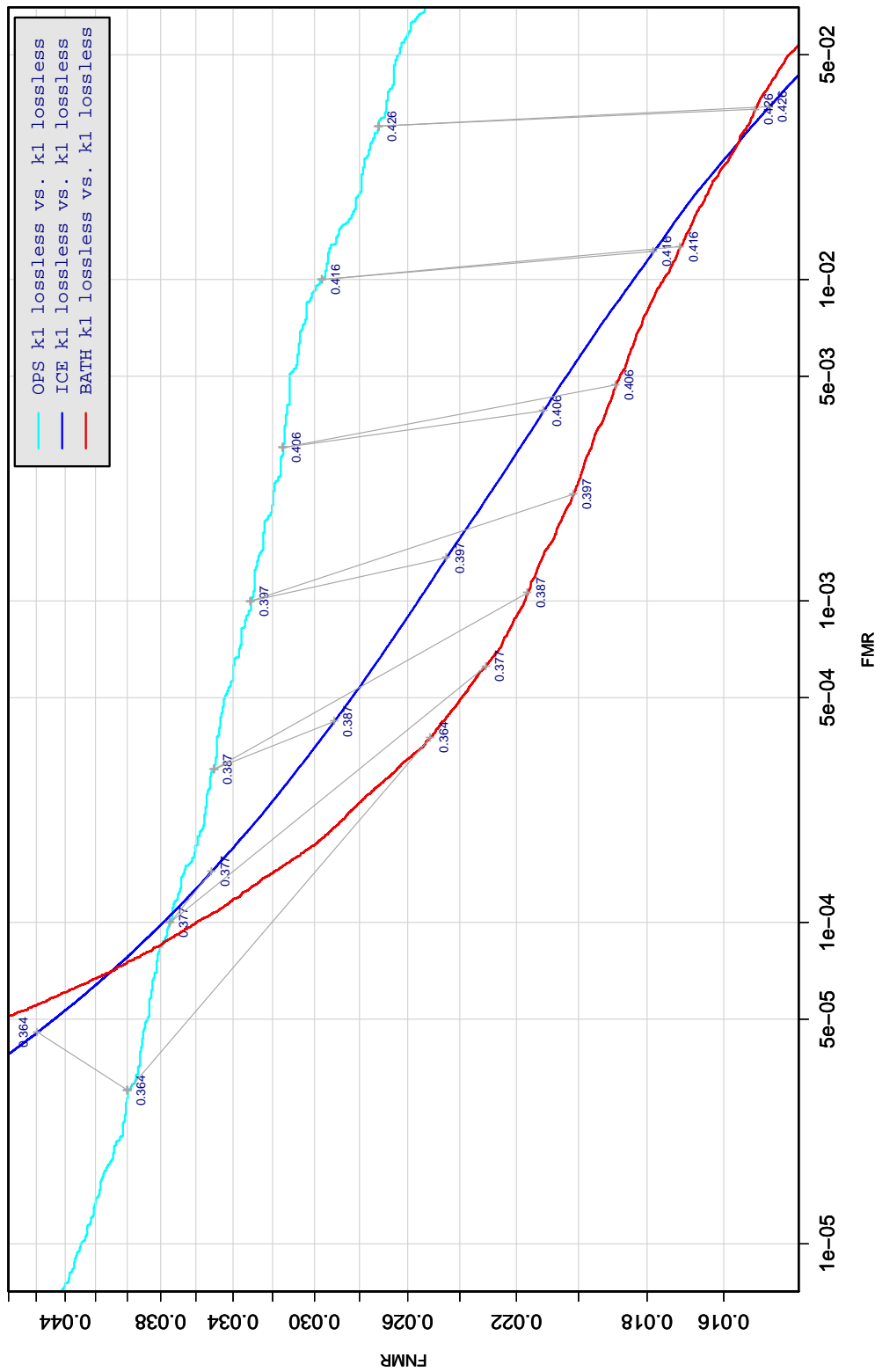


Table 168: DET curve for implementation H1 on three IREX databases. All comparisons are with uncompressed KIND 1 vs. KIND 1 images. The lines join points corresponding to the a fixed threshold. Non-vertical links indicate a change in FMR when the database changes. All results apply to native operation. Failures to produce a template i.e. FTE are ignored because the plots are intended to show *matching* effects, specifically to compare DET slopes and to show the effect of fixing a threshold.

A = SAGEM	B = COGENT	C = CROSSMATCH	D = CAMBRIDGE	E = L1	$x1$ = PRIMARY
F = RETICA	G = LG	H = HONEYWELL	I = IRITECH	J = NEUROTECHNOLOGY	$x2$ = SECONDARY
KIND 1 = RAW 640x480		KIND 3 = CROP	KIND 7 = CROP+MASK	KIND 16 = CONCENTRIC POLAR	

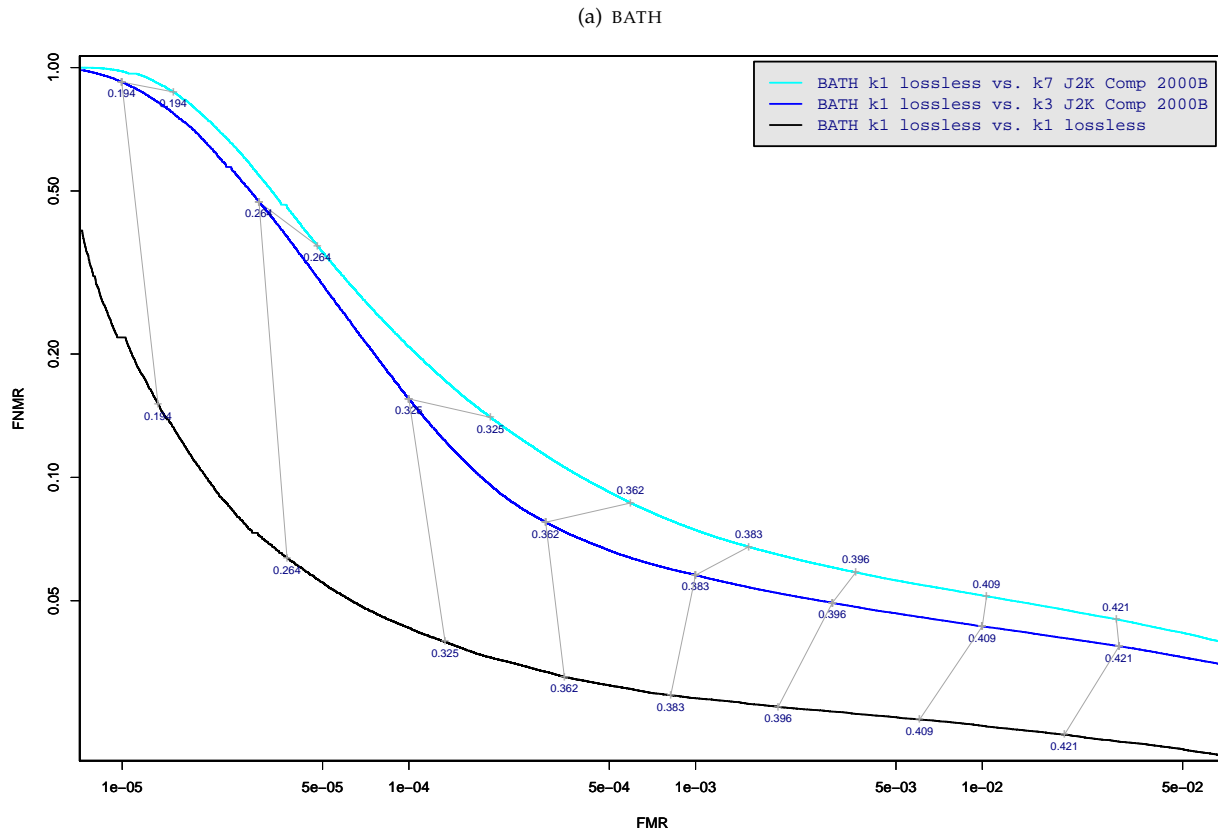


Table 169: DET curve for implementation H1 on the BATH database for the various supported KINDS . The DET characteristics are linked by lines joining points of equal threshold. Non-vertical links indicate a change in false acceptance when the data KIND changes. All results apply to native operation, and the effects of FTE are included.

A = SAGEM	B = COGENT	C = CROSSMATCH	D = CAMBRIDGE	E = L1	$x1$ = PRIMARY
F = RETICA	G = LG	H = HONEYWELL	I = IRITECH	J = NEUROTECHNOLOGY	$x2$ = SECONDARY
KIND 1 = RAW 640x480		KIND 3 = CROP		KIND 7 = CROP+MASK	KIND 16 = CONCENTRIC POLAR

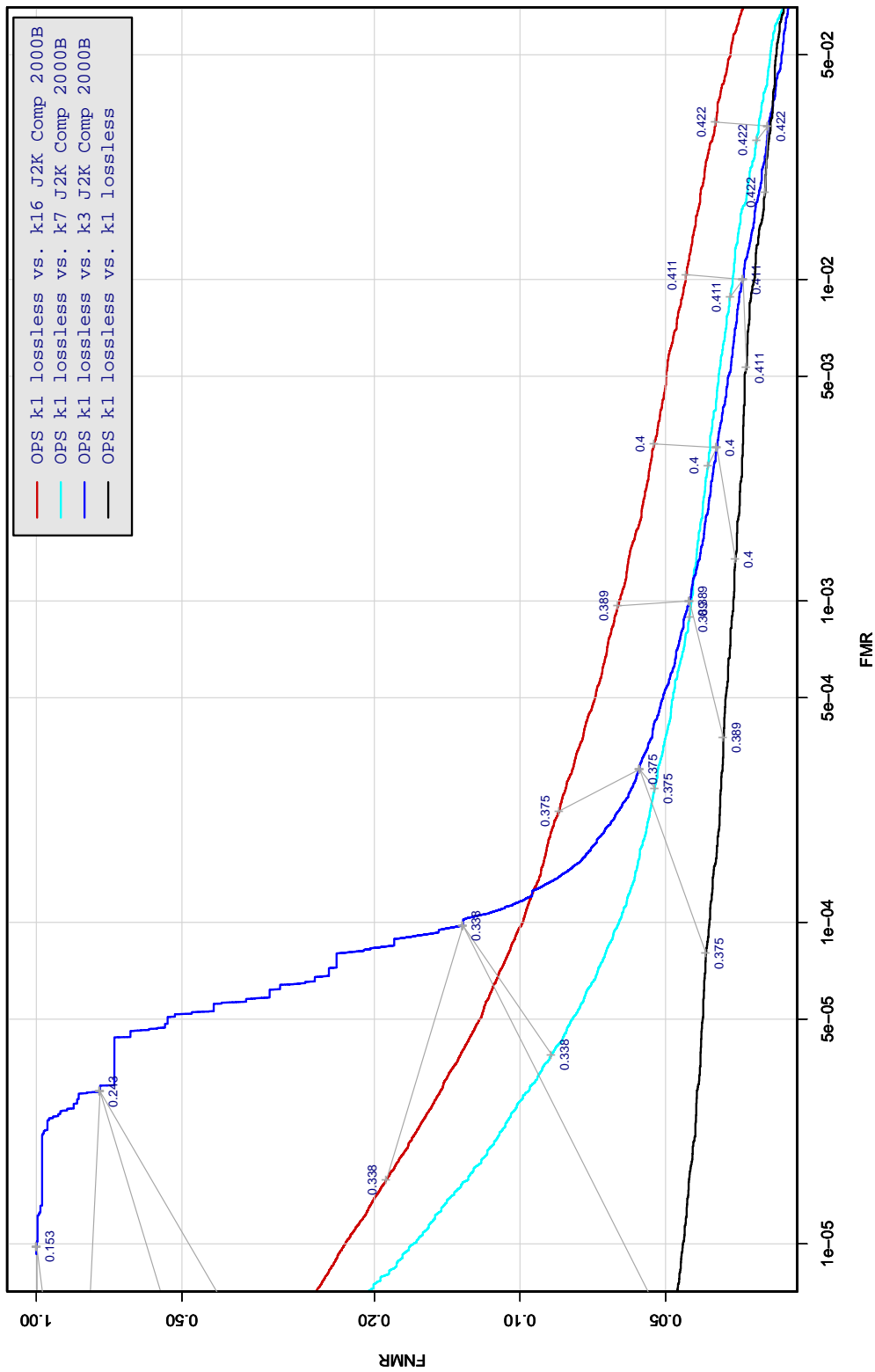


Table 170: DET curve for implementation H1 on the OPS database for the various supported KINDS . The DET characteristics are linked by lines joining points of equal threshold. Non-vertical links indicate a change in false acceptance when the data KIND changes. All results apply to native operation, and the effects of FTE are included.

A = SAGEM	B = COGENT	C = CROSSMATCH	D = CAMBRIDGE	E = L1	x1 = PRIMARY
F = RETICA	G = LG	H = HONEYWELL	I = IRITECH	J = NEUROTECHNOLOGY	x2 = SECONDARY
KIND 1 = RAW 640x480		KIND 3 = CROP		KIND 7 = CROP+MASK	KIND 16 = CONCENTRIC POLAR

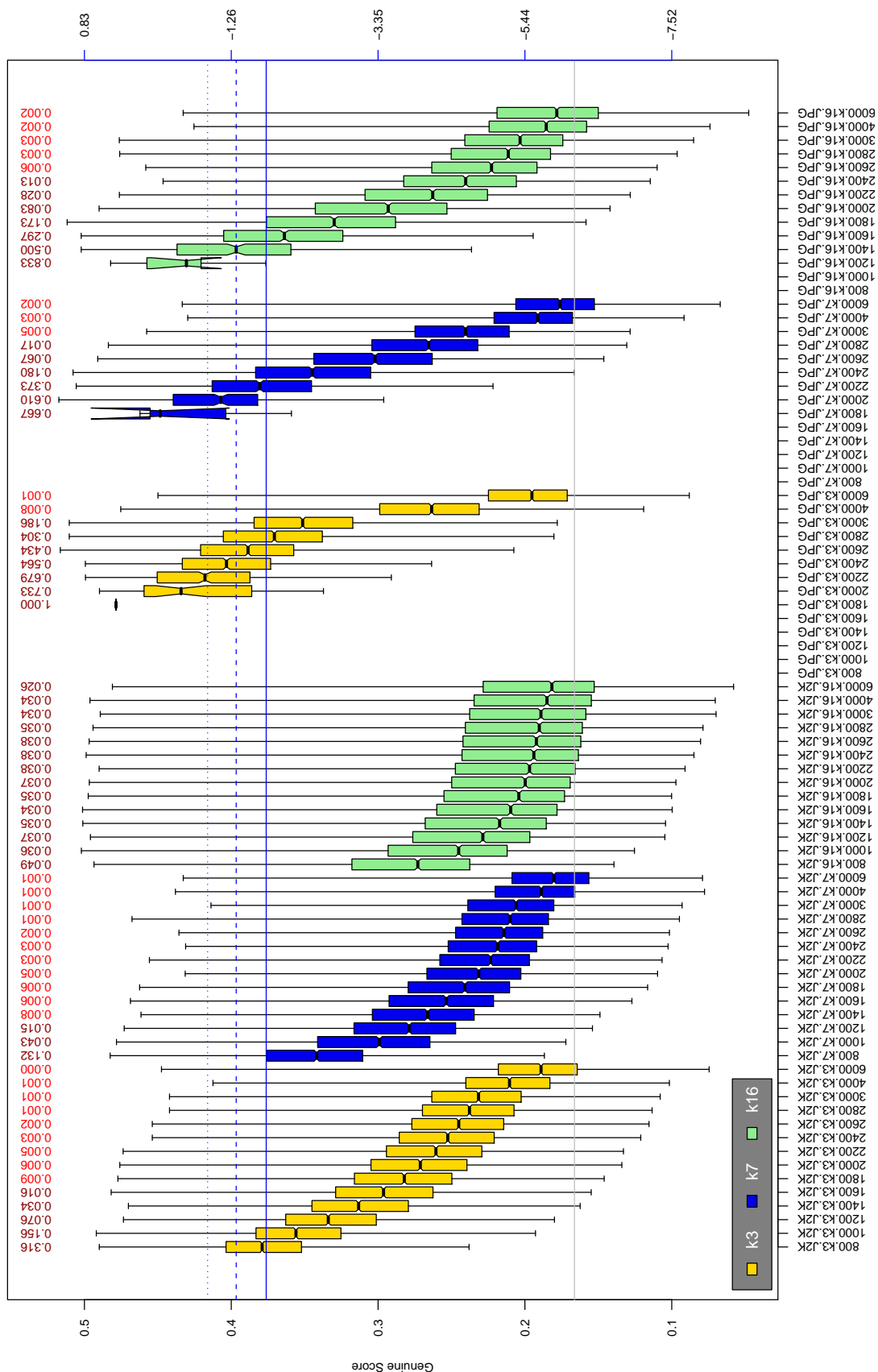


Table 171: The distribution of H1 native genuine comparison scores by size of the compressed image, KIND and the compression algorithm. The images are from the OPS dataset. The right axis scale gives the corresponding value for $d' = (s - \mu_I) / \sqrt{0.5(\sigma_I^2 + \sigma_C^2)}$ for genuine score s . The boxplots only include comparison scores if the uncompressed version of the same image was matched below the FMR = 0.001 threshold. Above the boxplots are FNMR values at FMR = 10^{-3} . The three blue lines correspond, from the top, to FMR of $10^{-2}, -3, -4$. The lower grey line refers to the median score obtained from comparison of uncompressed KIND 3 images. Any comparison for which either template had not been generated is excluded. Note that the iris record size on the horizontal axis is not evenly spaced above 3000 bytes.

A = SAGEM	B = COGENT	C = CROSSMATCH	D = CAMBRIDGE	E = L1	$x1$ = PRIMARY
F = RETICA	G = LG	H = HONEYWELL	I = IRITECH	J = NEUROTECHNOLOGY	$x2$ = SECONDARY
KIND 1 = RAW 640x480		KIND 3 = CROP	KIND 7 = CROP+MASK	KIND 16 = CONCENTRIC POLAR	

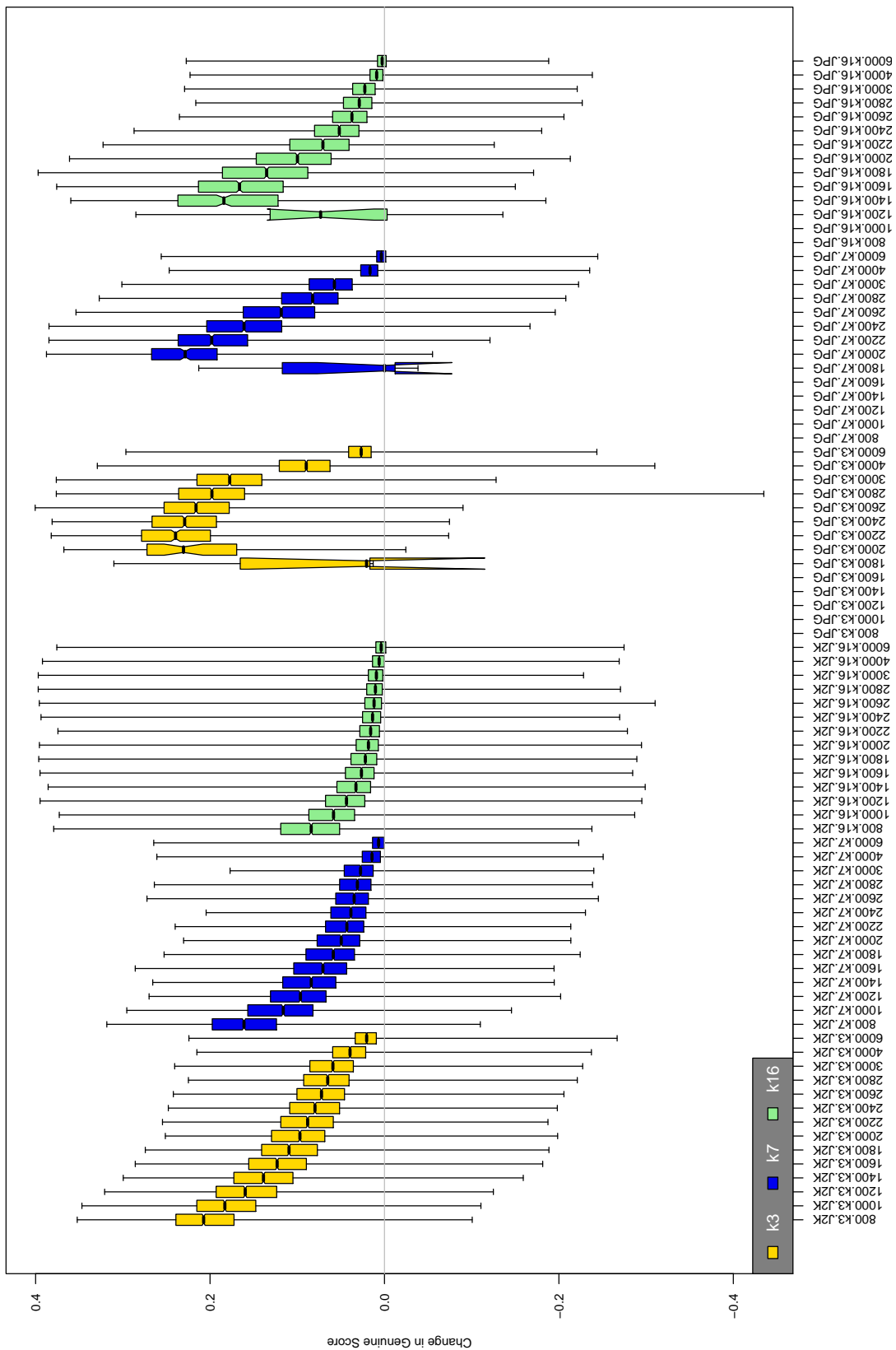


Table 172: The distribution of the *increase* in H1 native genuine comparison scores between the uncompressed “parent” and the compressed image, arranged by size, KIND and the compression algorithm. The images are from the OPS dataset. Any comparison involving a failed template is excluded. Note that the iris record size on the horizontal axis is not evenly spaced above 3000 bytes.

A = SAGEM	B = COGENT	C = CROSSMATCH	D = CAMBRIDGE	E = L1	x1 = PRIMARY
F = RETICA	G = LG	H = HONEYWELL	I = IRITECH	J = NEUROTECHNOLOGY	x2 = SECONDARY
KIND 1 = RAW 640x480		KIND 3 = CROP	KIND 7 = CROP+MASK	KIND 16 = CONCENTRIC POLAR	

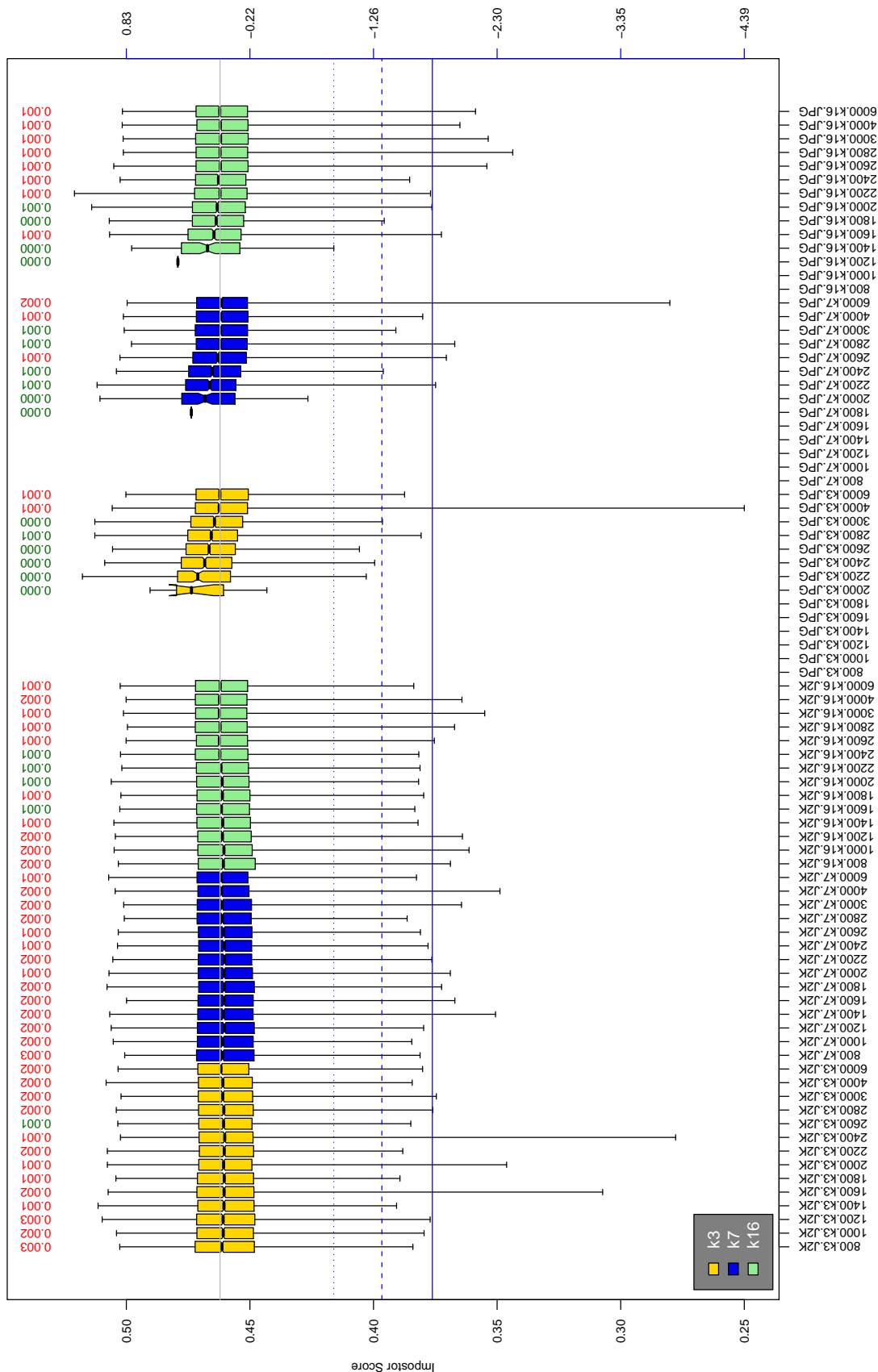


Table 173: The distribution of H1 native impostor comparison scores by size of the compressed image, KIND and the compression algorithm. The right axis scale gives the corresponding value for $d' = (s - \mu_1) / \sqrt{0.5(\sigma_1^2 + \sigma_2^2)}$ for impostor score s . The three blue lines correspond, from the top, to FMR of $10^{-2}, -3, -4$. The lower grey line refers to the median score obtained from comparison of uncompressed KIND 3 images. Any comparison involving a failed template is excluded. Above the boxplots are FMR values at the threshold that gives FMR = 10^{-3} on uncompressed images. These figures are computed from only 4000 comparisons so the FMR values and the tails of the impostor distribution are poorly characterized. Note that the iris record size on the horizontal axis is not evenly spaced above 3000 bytes.

A = SAGEM	B = COGENT	C = CROSSMATCH	D = CAMBRIDGE	E = L1	x_1 = PRIMARY
F = RETICA	G = LG	H = HONEYWELL	I = IRITECH	J = NEUROTECHNOLOGY	x_2 = SECONDARY
KIND 1 = RAW 640x480		KIND 3 = CROP	KIND 7 = CROP+MASK	KIND 16 = CONCENTRIC POLAR	

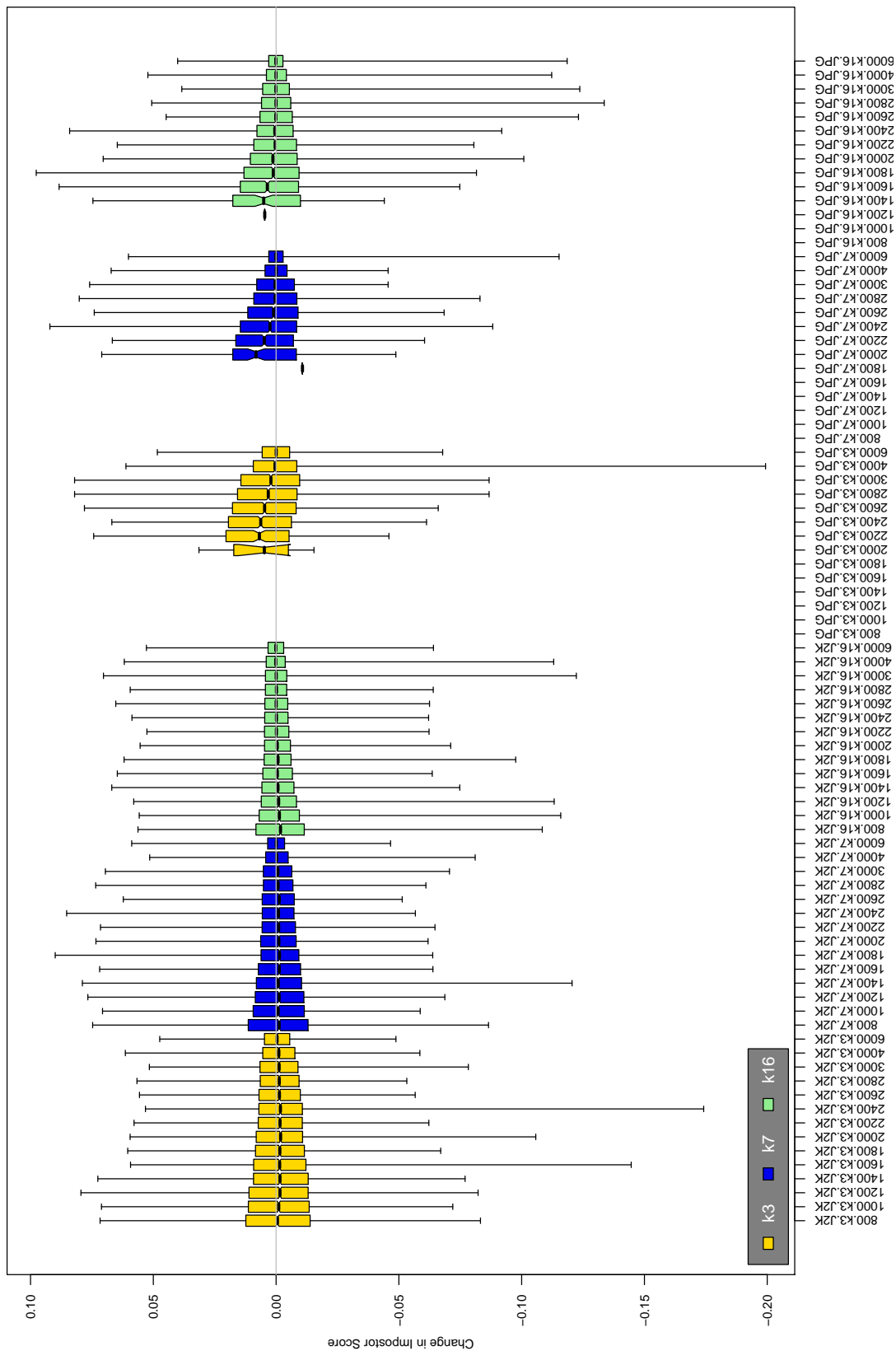


Table 174: The distribution of the increase in H1 native impostor comparison scores between the uncompressed “parent” and the compressed image, arranged by size, KIND and the compression algorithm. The images are from the OPS dataset. Any comparison involving a failed template is excluded. Note that the iris record size on the horizontal axis is not evenly spaced above 3000 bytes.

A = SAGEM	B = COGENT	C = CROSSMATCH	D = CAMBRIDGE	E = L1	x1 = PRIMARY
F = RETICA	G = LG	H = HONEYWELL	I = IRITECH	J = NEUROTECHNOLOGY	x2 = SECONDARY
KIND 1 = RAW 640x480		KIND 3 = CROP		KIND 7 = CROP+MASK	KIND 16 = CONCENTRIC POLAR

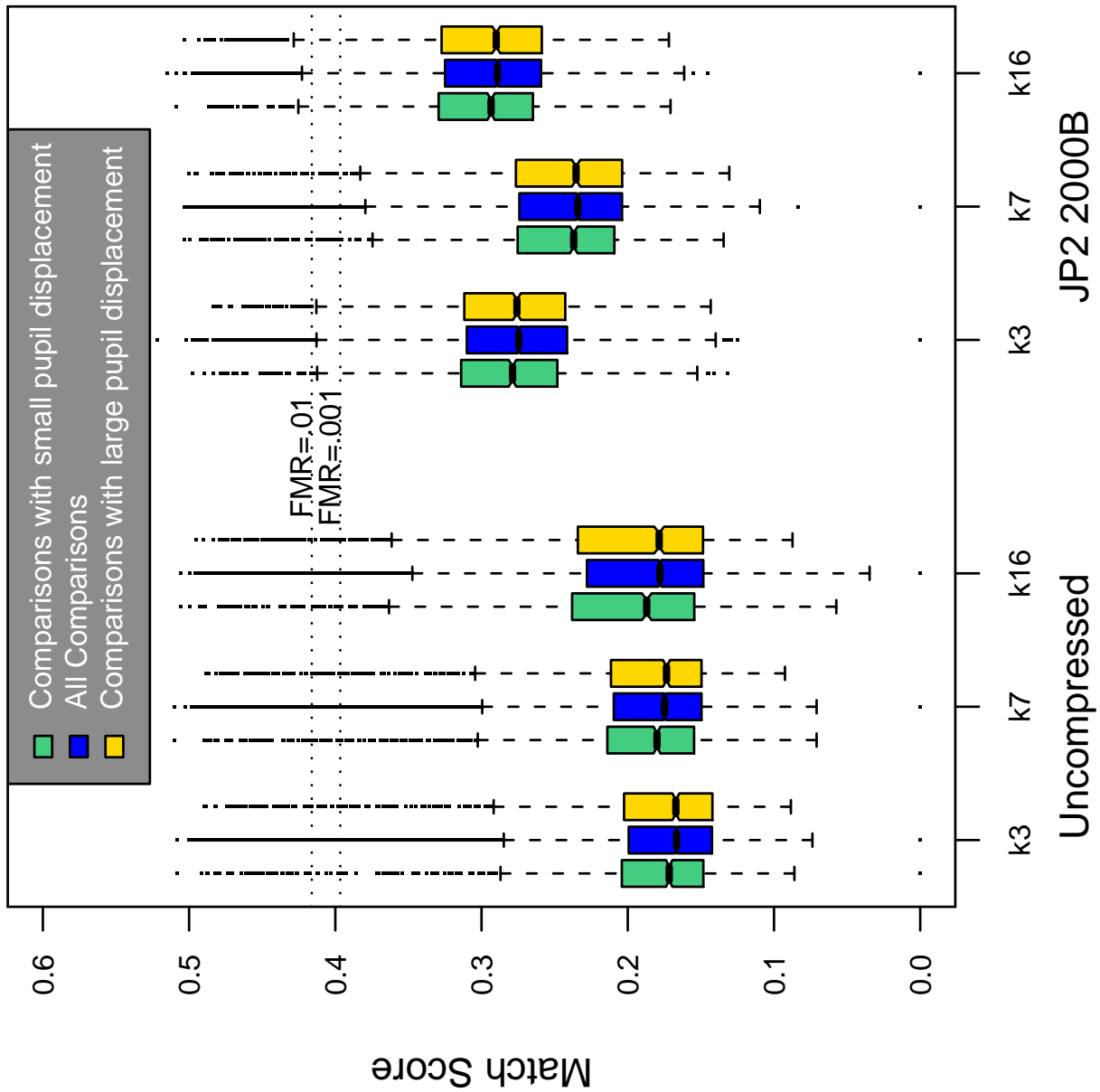


Table 175: Effect of pupil displacement on the genuine score distribution for H1

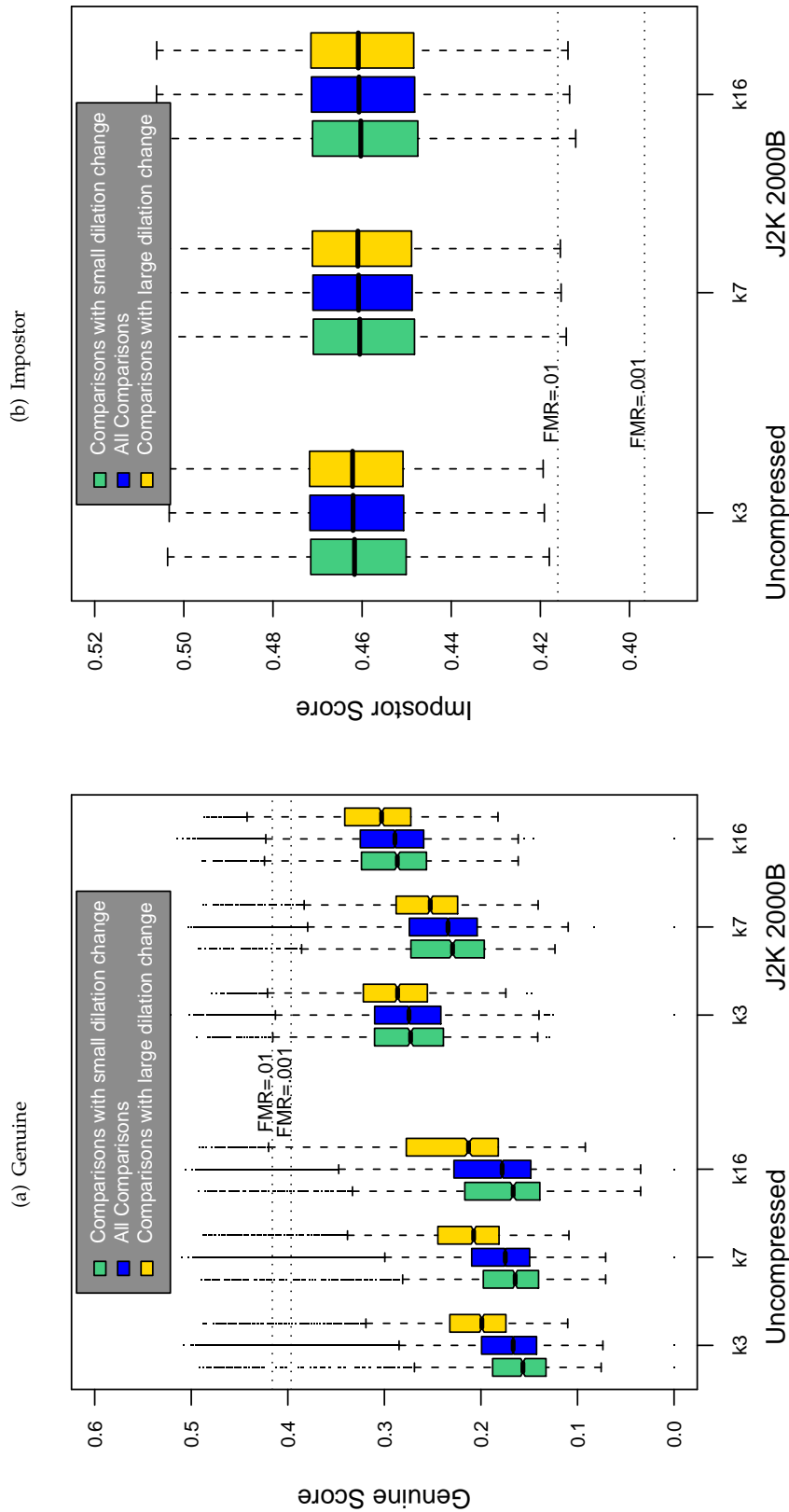


Table 176: The effect of dilation change on the two scores distributions for SDK HI.

A = SAGEM	B = COGENT	C = CROSSMATCH	D = CAMBRIDGE	E = L1	x_1 = PRIMARY
F = RETICA	G = LG	H = HONEYWELL	I = IRITECH	J = NEUROTECHNOLOGY	x_2 = SECONDARY
KIND 1 = RAW 640x480		KIND 3 = CROP	KIND 7 = CROP+MASK	KIND 16 = CONCENTRIC POLAR	

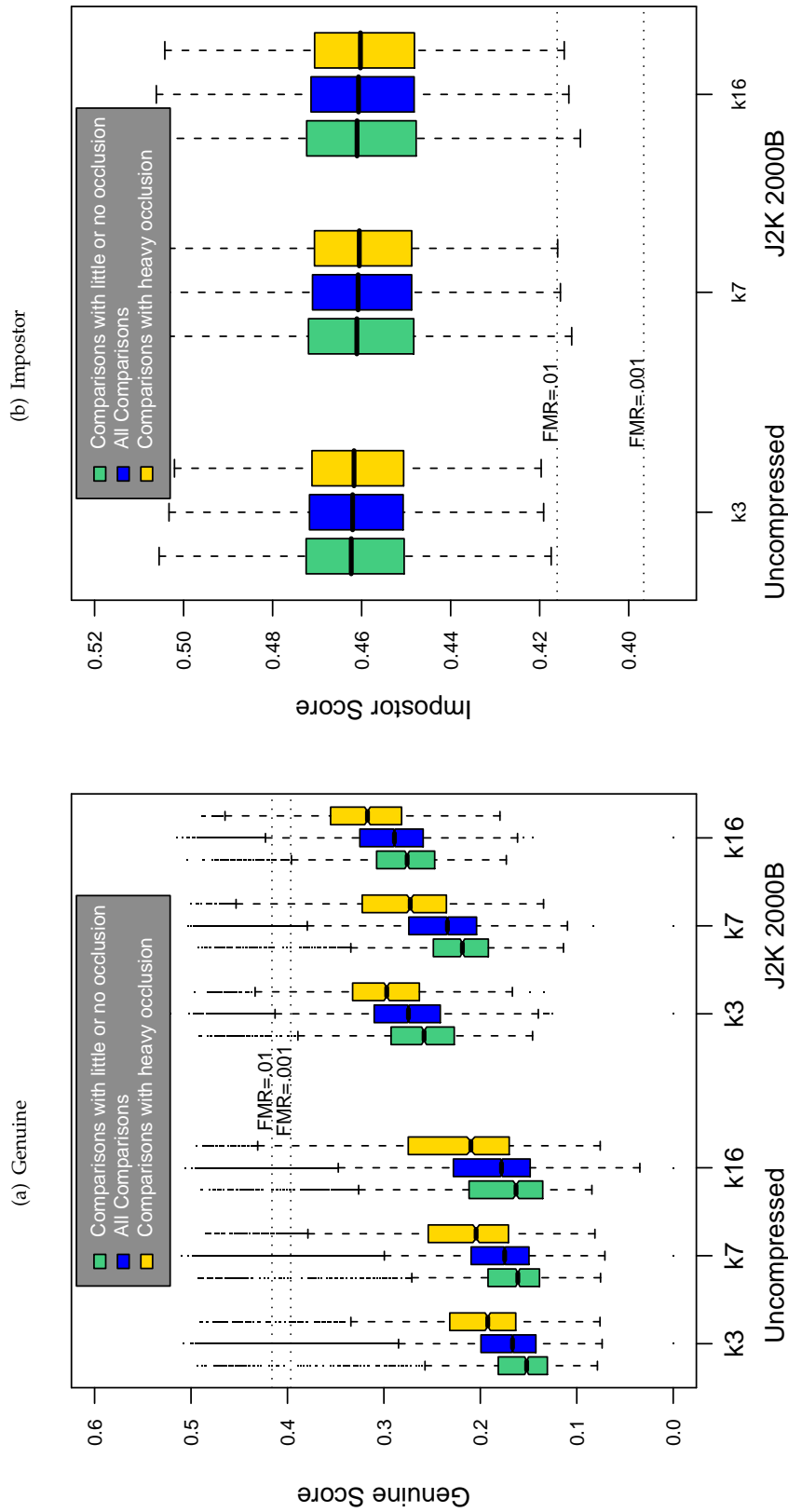
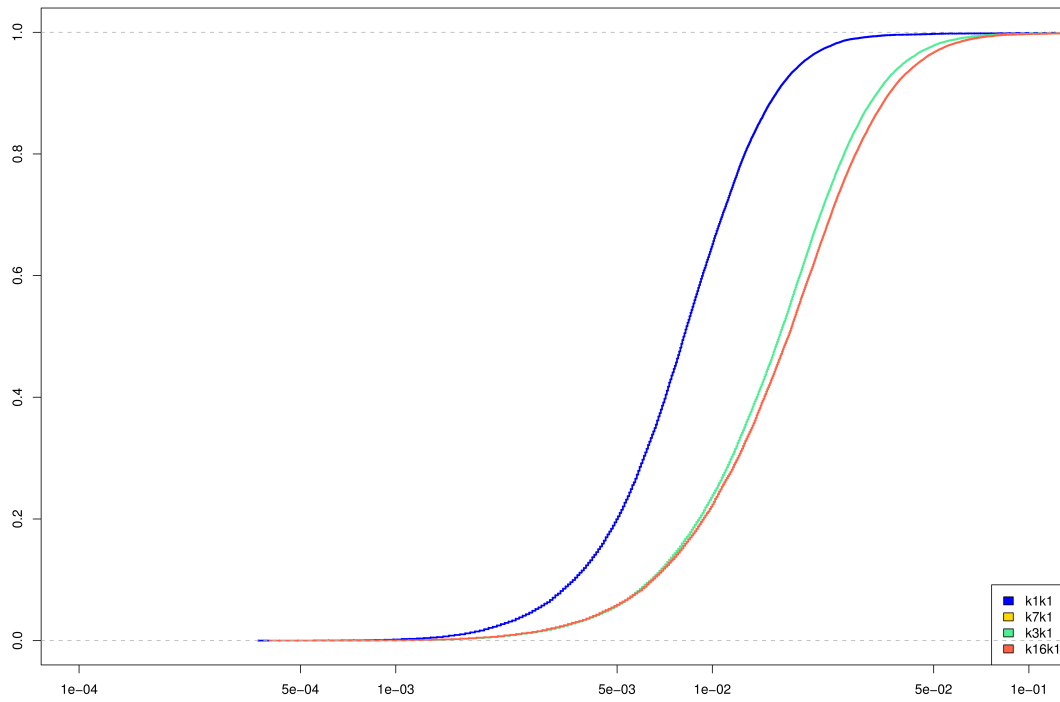
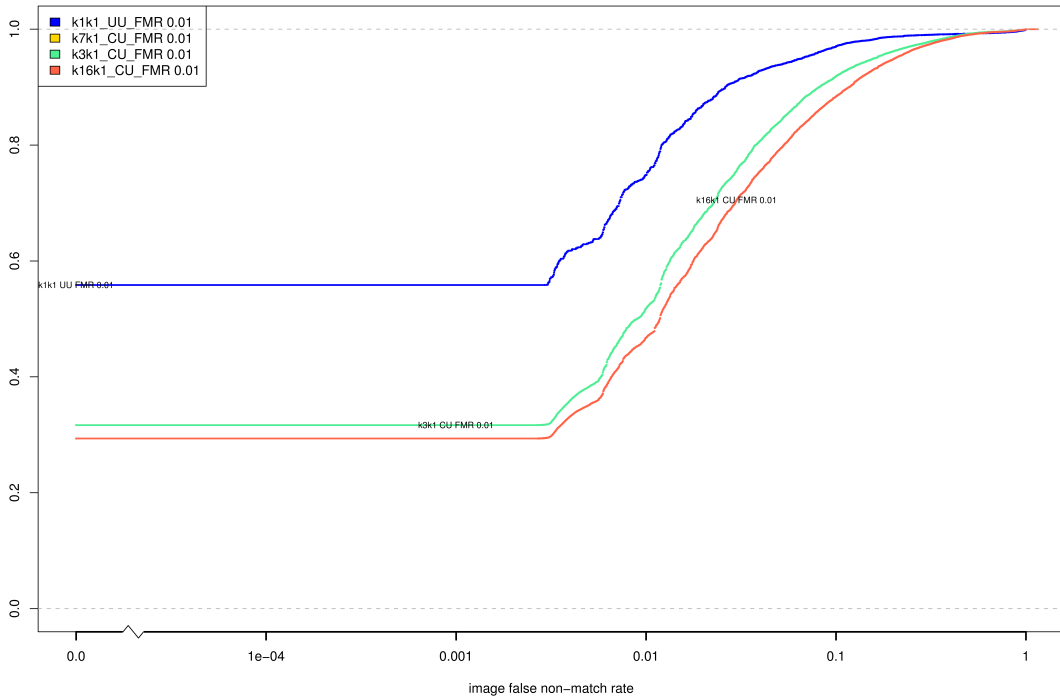


Table 177: The effect of eyelid occlusion on the two scores distributions for SDK H1.

(a) iFMR CDF



(b) iFNMR CDF



Compiled Results for Implementation H2

On June 25, 2009, NIST invited the IREX participants to submit a description of the SDKs submitted for the IREX effort. The intent was to allow providers to describe and contrast the feature sets, optimization, operational suitability and availability of the primary and secondary SDKs. NIST indicated that any submitted text would appear verbatim (with typesetting) in draft and final versions of the IREX report and that it would be attributed to the organization. This was optional and NIST put no constraints on the content beyond a 600 word limit, and a statement that anything labelled as confidential or proprietary would be omitted.

The provider of SDK H2, Honeywell, elected not to submit any information

On August 17, 2009, NIST invited the IREX participants to submit a description their comments on an draft version of the IREX report. This was intended to allow participants to assist readers in the interpretation of a large and complicated testing effort. NIST indicated that any submitted text would appear verbatim (with typesetting) in the final version of the IREX report and that it would be attributed to the organization. Submission of content was optional and NIST put no constraints on the content beyond a word limit, and a statement that anything labelled as confidential or proprietary would be omitted.

The provider of SDK H2, Honeywell, submitted the following to NIST - we make no comment on this information.

The Honeywell algorithms were developed for standoff iris recognition systems to identify non-cooperative subjects. The algorithmic approach was developed to cope with larger margin of variations than are present in the IREX dataset. Both algorithms were implemented to tolerate a wide range of acquisition and non-constrained environmenta key advantage of the recently developed Honeywell CFAIRS system (combined face and iris recognition system) to identify iris on the move at distances that can extend up to 4m.

The Honeywell technique uses a novel iris segmentation scheme that takes the analysis of edges into the polar domain at an earlier stage. Mapping the segmentation analysis to polar domain permits the detection of any irregular shapes of irises. This is a key advantage of Honeywell proposed segmentation technique that is well suited for unconstrained standoff iris acquisition where non-frontal irregular shapes are captured at various gazed angles. The approach has proven its efficiency and robustness by allowing iris recognition under suboptimal image acquisition conditions. The results in this IREX report confirm this claim as both Honeywell techniques were more competitive on the suboptimal images (ICE, BATH) than on the frontal dataset (OPS). The competitive advantage of a reliable segmentation approach is undermined when applied only to frontal images. The results do not reflect the true Honeywell algorithm advantages for the following reasons:

- Both Honeywell algorithms were calibrated to handle ICE like dataset. However, the comparison was mostly evaluated on OPS. OPS and BATH are significantly different data than ICE-2005. Honeywell algorithms were purposely designed to handle larger variations to accurately segment non-cooperative subjects that can be calibrated to different ranges of zooming acquisitions. Both Honeywell algorithms use non-iterative polar differential operator to locate the inner and outer borders of the iris. These ranges are specified a priori in the calibration of the algorithm. However, no such calibration was performed on the results reported in this IREX report. .
- The Honeywell algorithms are more amenable to poor quality iris samples. The robustness of the Honeywell standoff iris recognition approach relies heavily on accurate iris segmentation. The IREX evaluation probes the uniqueness and richness of iris patterns even when deployed to a large populationa

requirement that must be met to deploy the technology as a true biometric tool. These are very encouraging results however a significant amount of the evaluation was biased by the sensors used for collecting the images used in this report. It is hard to reflect from the evaluation how these developed techniques address the true nature of iris irregularity in iris segmentation.

- The Honeywell algorithms were set for a non-cooperative calibration mode in this evaluation (rather than a frontal operational mode) to handle more irregular iris images. Because of this mode setting, Honeywell algorithm performed significantly better than others in segmenting and creating non-failed template records per table 5. This mode of operation is effective in tolerating more gazed eyes at the expense of loss of overall matching accuracy. These advantages are not reflected on high quality samples such as the OPS dataset. In addition, the exclusion of failed templates on poor quality images aided others by preventing poor quality images from being considered in the matching accuracy, and thus prevented fair comparison of algorithms (refer to table 11 and 12).
- Inconsistency in computational requirements in extracting an iris signature prevents a fair comparison among algorithms. In Honeywell algorithms, some processes related to iris quality measures (IQM) were turned off to reduce the computational load.

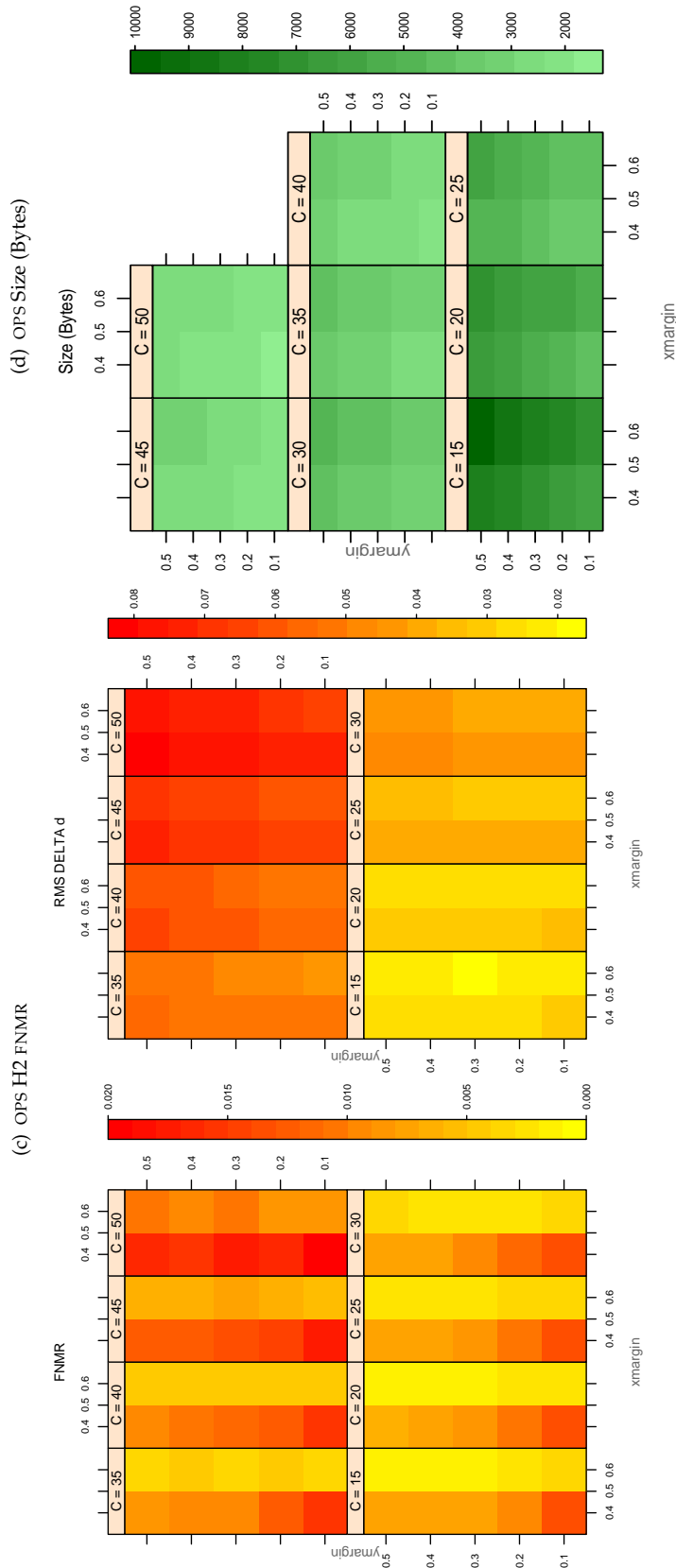


Table 178: For the IREX partition of the OPS database the plots at left show the dependence of cFNMR on the vertical and horizontal iris cropping margins for various compression ratios. This applies only for KIND 3 records. The margins are in units of iris radius. The use of conditional FNMR means that the plots exclude comparisons that were falsely rejected even before any compression was applied. On the **right side** is the rms difference between the crop+compress and the uncompressed comparison scores for each image pair. All computations are driven by the bounding box coordinates reported by the II SDK. The number of bits per pixel is $8/C$, where C is the compression ratio. The iris radius varies and because the cropping margins are fixed multiples of the radius the image size varies. The compressed size, in bytes, is the width times height divided by C . Values of cFNMR greater than 0.02 are shown as 0.02.

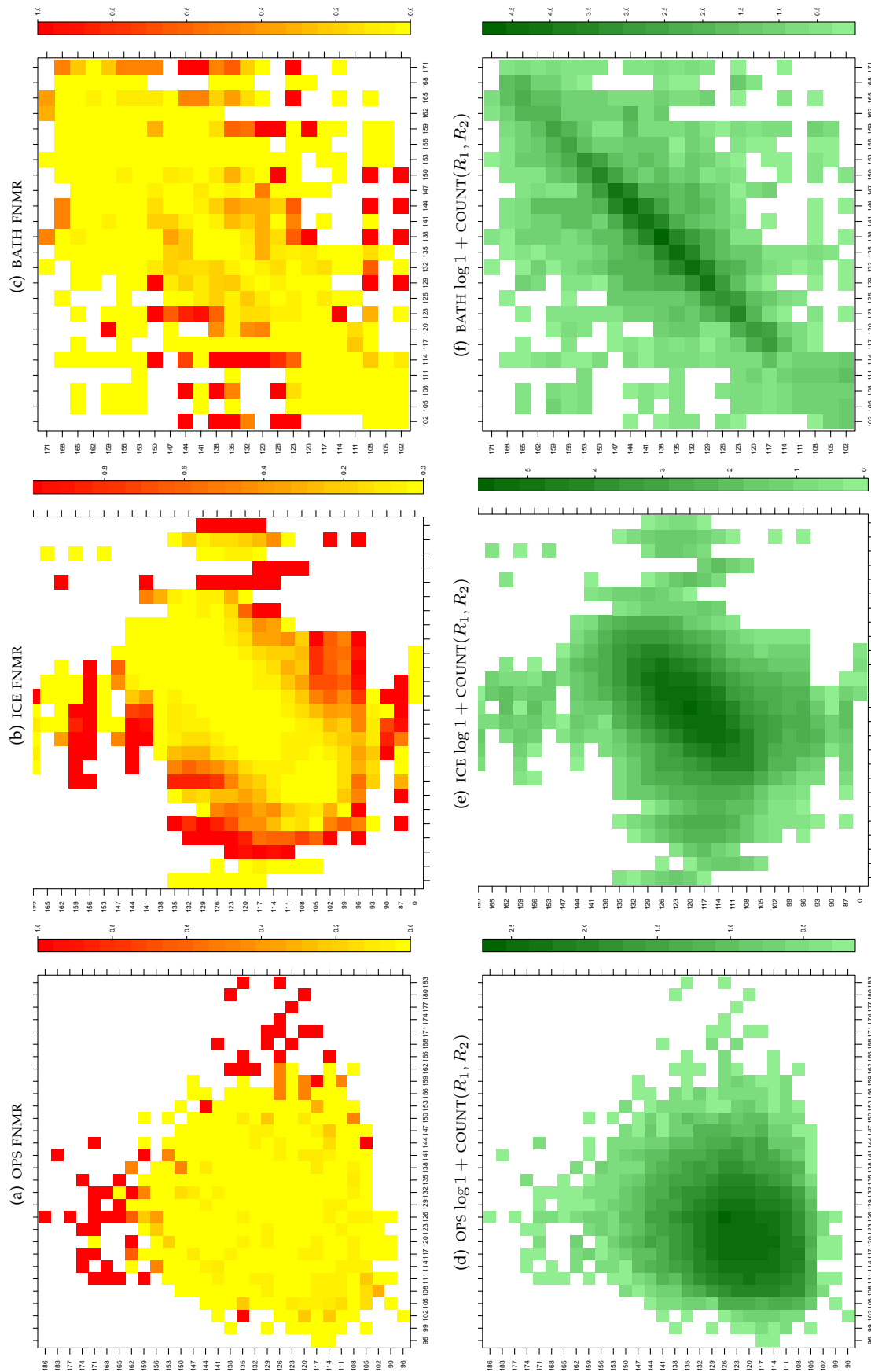


Table 179: For the three IREX databases: In the top row the color in each cell represents the occurrence of genuine comparisons with the given pair of radii. The y-axis represents enrollment samples with verification samples on the x-axis; In the bottom row the color scale plots $\log 1 + \text{COUNT}(R_1, R_2)$. The radii are quantized into three-pixel bins. The radii for DOD are on the range $96 \leq r \leq 186$ pixels. The radii for ICE are on the range $87 \leq r \leq 165$ pixels. The radii for BATH are on the range $100 \leq r \leq 170$ pixels.

A = SAGEM	B = COGENT	C = CROSSMATCH	D = CAMBRIDGE	E = L1	x1 = PRIMARY
F = RETICA	G = LG	H = HONEYWELL	I = IRITECH	J = NEUROTECHNOLOGY	x2 = SECONDARY
KIND 1 = RAW 640x480		KIND 3 = CROP		KIND 7 = CROP+MASK	
				KIND 16 = CONCENTRIC POLAR	

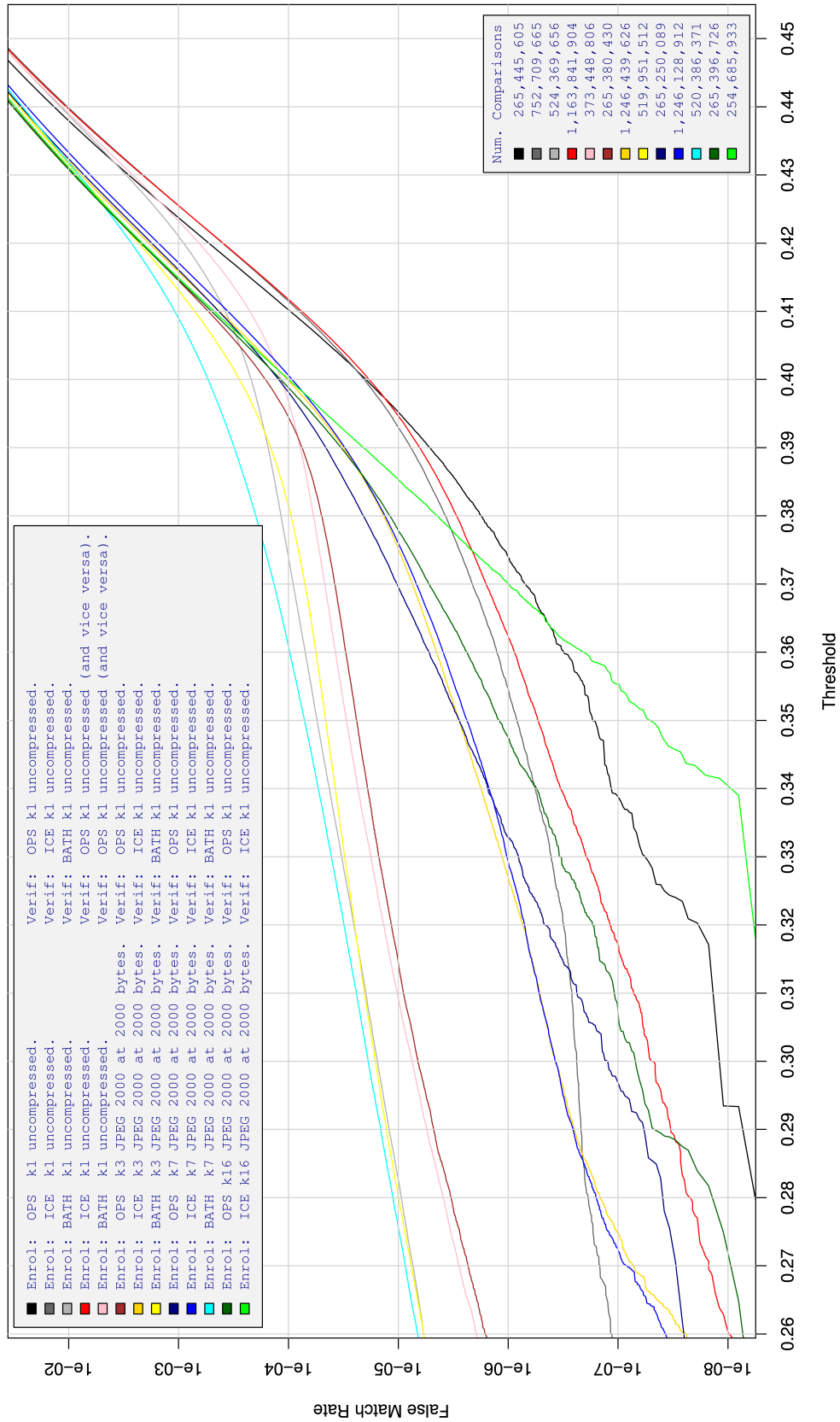


Table 180: For implementation H2, the dependency of FMR on threshold. for various combinations of enrollment and verification dataset, format, and compression.

A = SAGEM	B = COGENT	C = CROSSMATCH	D = CAMBRIDGE	E = L1	x1 = PRIMARY
F = RETICA	G = LG	H = HONEYWELL	I = IRITECH	J = NEUROTECHNOLOGY	x2 = SECONDARY
KIND 1 = RAW 640x480		KIND 3 = CROP		KIND 7 = CROP+MASK	KIND 16 = CONCENTRIC POLAR

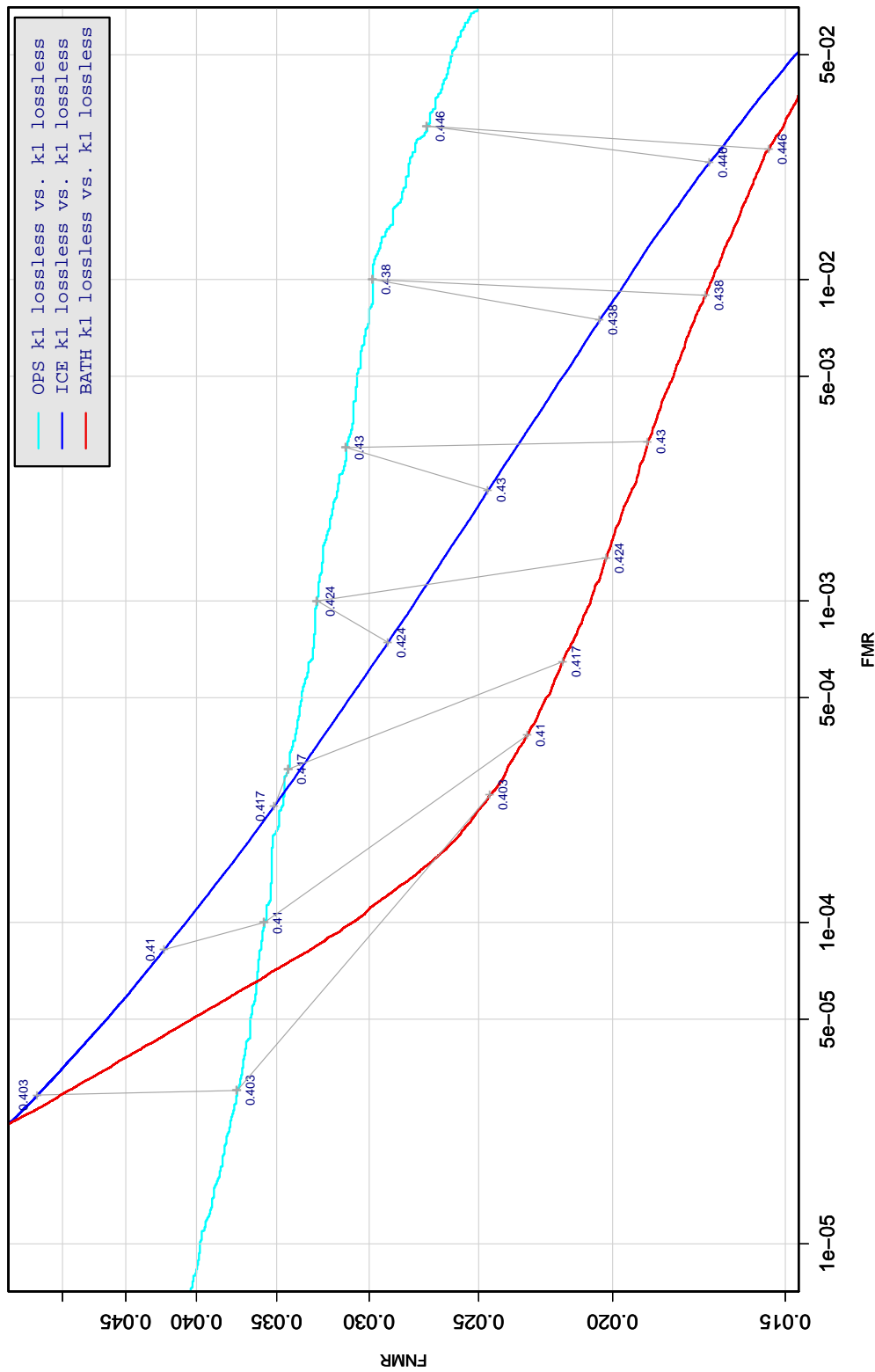


Table 181: DET curve for implementation H2 on three IREX databases. All comparisons are with uncompressed KIND 1 vs. KIND 1 images. The lines join points corresponding to the a fixed threshold. Non-vertical links indicate a change in FMR when the database changes. All results apply to native operation. Failures to produce a template i.e. FTE are ignored because the plots are intended to show *matching* effects, specifically to compare DET slopes and to show the effect of fixing a threshold.

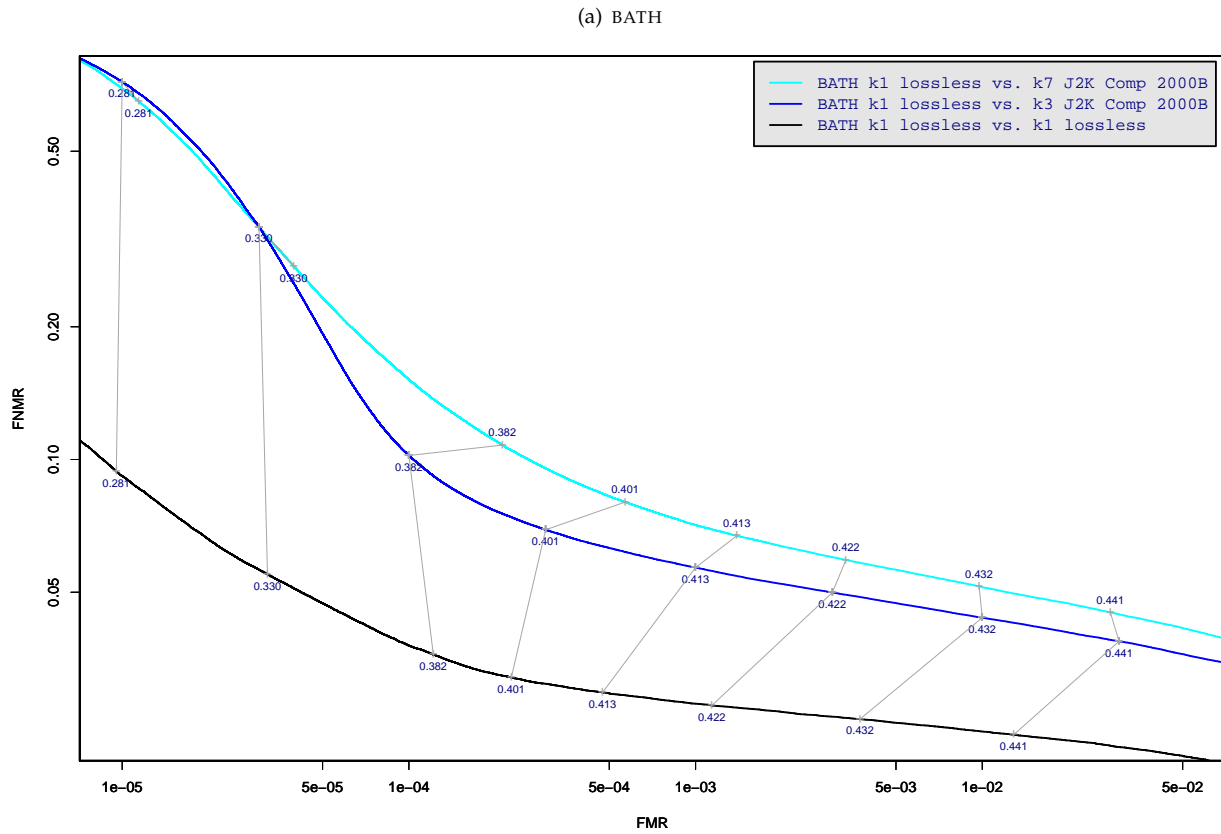


Table 182: DET curve for implementation H2 on the BATH database for the various supported KINDS . The DET characteristics are linked by lines joining points of equal threshold. Non-vertical links indicate a change in false acceptance when the data KIND changes. All results apply to native operation, and the effects of FTE are included.

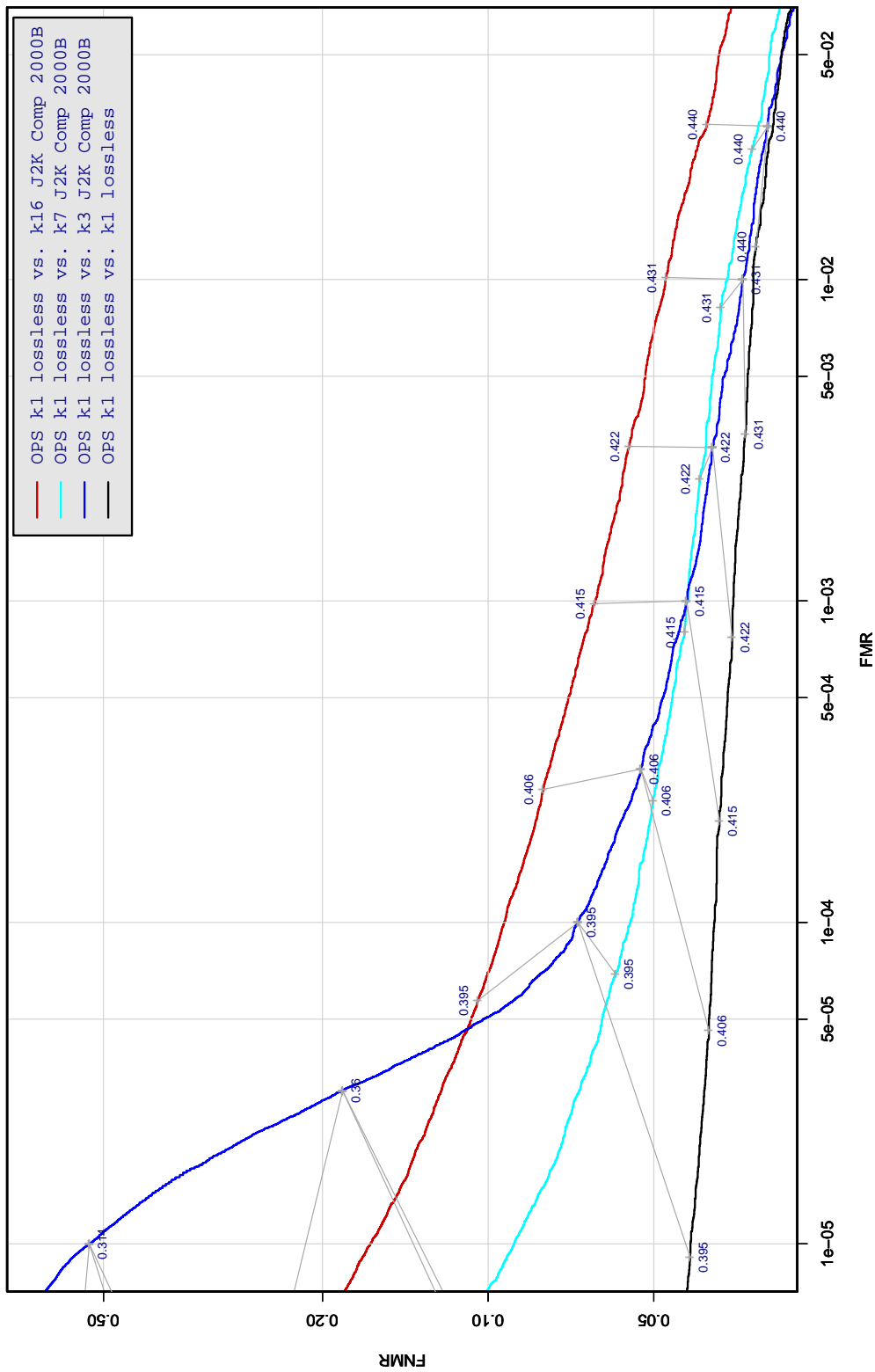


Table 183: DET curve for implementation H2 on the OPS database for the various supported KINDS . The DET characteristics are linked by lines joining points of equal threshold. Non-vertical links indicate a change in false acceptance when the data KIND changes. All results apply to native operation, and the effects of FTE are included.

A = SAGEM	B = COGENT	C = CROSSMATCH	D = CAMBRIDGE	E = L1	x1 = PRIMARY
F = RETICA	G = LG	H = HONEYWELL	I = IRITECH	J = NEUROTECHNOLOGY	x2 = SECONDARY
KIND 1 = RAW 640x480		KIND 3 = CROP		KIND 7 = CROP+MASK	KIND 16 = CONCENTRIC POLAR

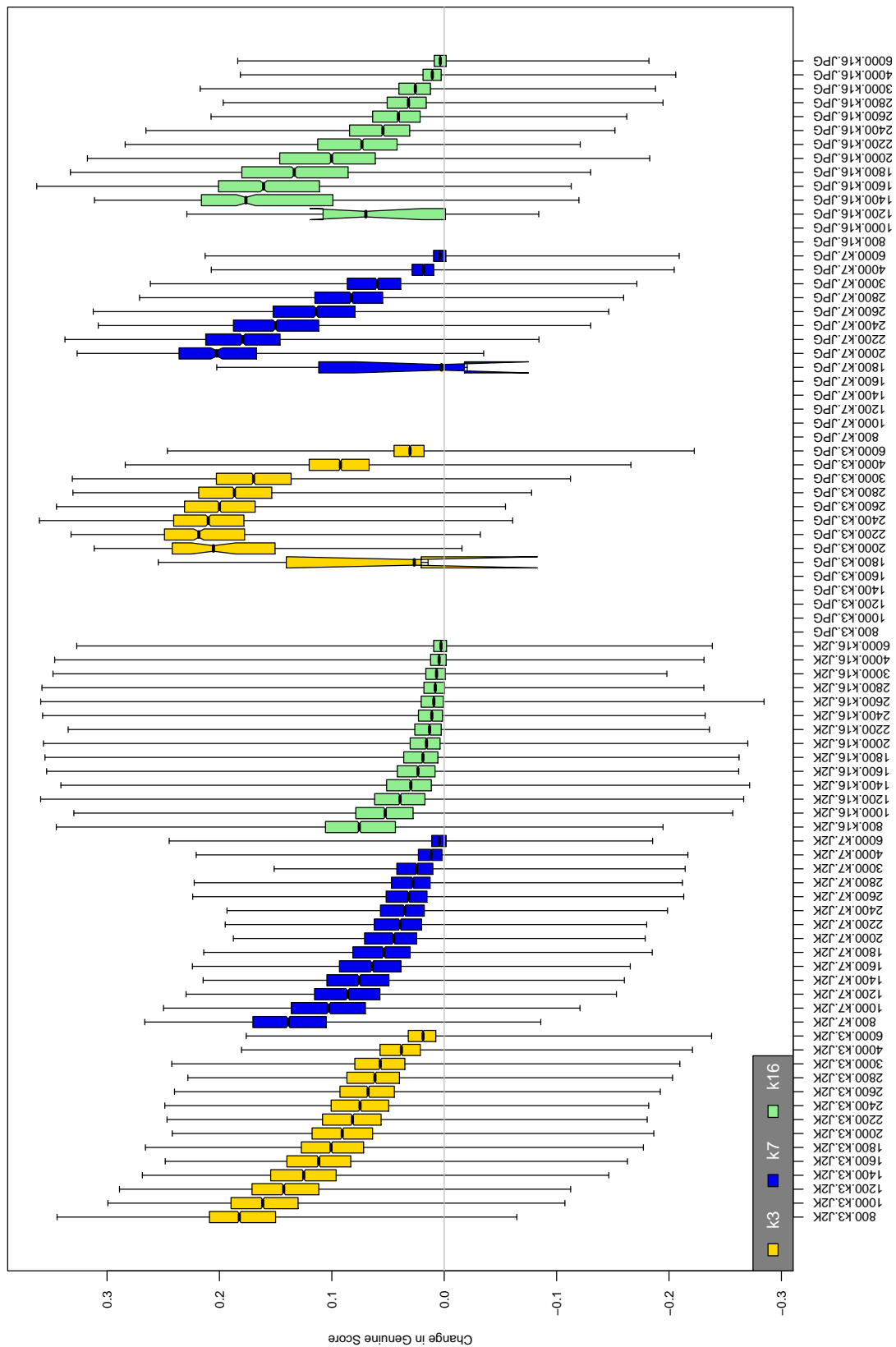


Table 185: The distribution of the *increase* in H2 native genuine comparison scores between the uncompressed “parent” and the compressed image, arranged by size, KIND and the compression algorithm. The images are from the OPS dataset. Any comparison involving a failed template is excluded. Note that the iris record size on the horizontal axis is not evenly spaced above 3000 bytes.

A = SAGEM	B = COGENT	C = CROSSMATCH	D = CAMBRIDGE	E = L1	x1 = PRIMARY
F = RETICA	G = LG	H = HONEYWELL	I = IRITECH	J = NEUROTECHNOLOGY	x2 = SECONDARY
KIND 1 = RAW 640x480		KIND 3 = CROP	KIND 7 = CROP+MASK	KIND 16 = CONCENTRIC POLAR	

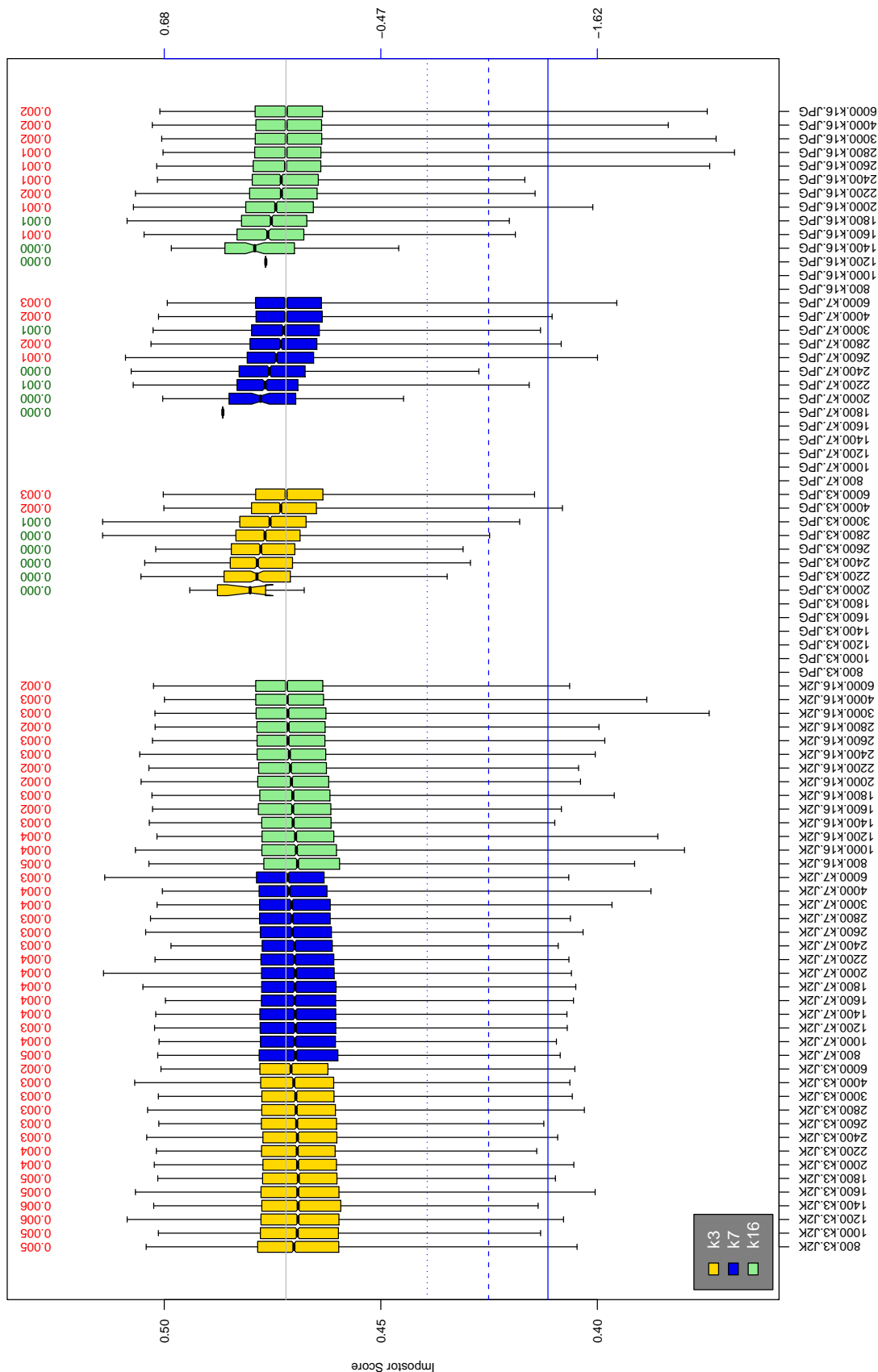


Table 186: The distribution of H2 native impostor comparison scores by size of the compressed image, KIND and the compression algorithm. The right axis scale gives the corresponding value for $d' = (s - \mu_1) / \sqrt{0.5(\sigma_1^2 + \sigma_2^2)}$ for impostor score s . The three blue lines correspond, from the top, to FMR of 10^{-2} , 10^{-3} , and 10^{-4} . The lower grey line refers to the median score obtained from comparison of uncompressed KIND 3 images. Any comparison involving a failed template is excluded. Above the boxplots are FMR values at the threshold that gives FMR = 10^{-3} on uncompressed images. These figures are computed from only 4000 comparisons so the FMR values and the tails of the impostor distribution are poorly characterized. Note that the iris record size on the horizontal axis is not evenly spaced above 3000 bytes.

A = SAGEM	B = COGENT	C = CROSSMATCH	D = CAMBRIDGE	E = L1	$x1$ = PRIMARY
F = RETICA	G = LG	H = HONEYWELL	I = IRITECH	J = NEUROTECHNOLOGY	$x2$ = SECONDARY
KIND 1 = RAW 640x480		KIND 3 = CROP		KIND 7 = CROP+MASK	
				KIND 16 = CONCENTRIC POLAR	

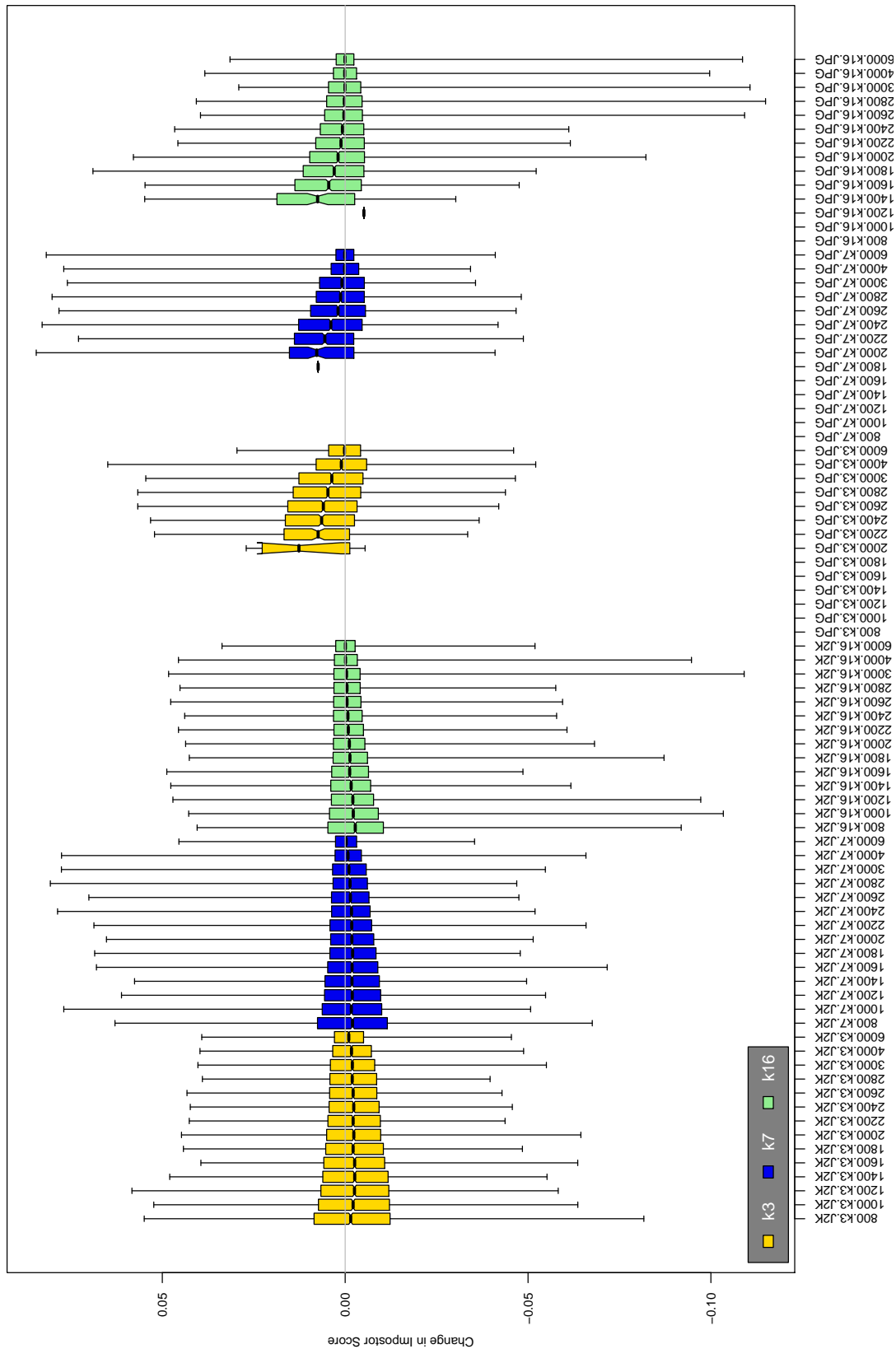


Table 187: The distribution of the increase in H2 native impostor comparison scores between the uncompressed “parent” and the compressed image, arranged by size, KIND and the compression algorithm. The images are from the OPS dataset. Any comparison involving a failed template is excluded. Note that the iris record size on the horizontal axis is not evenly spaced above 3000 bytes.

A = SAGEM	B = COGENT	C = CROSSMATCH	D = CAMBRIDGE	E = L1	x1 = PRIMARY
F = RETICA	G = LG	H = HONEYWELL	I = IRITECH	J = NEUROTECHNOLOGY	x2 = SECONDARY
KIND 1 = RAW 640x480		KIND 3 = CROP		KIND 7 = CROP+MASK	
KIND 16 = CONCENTRIC POLAR					

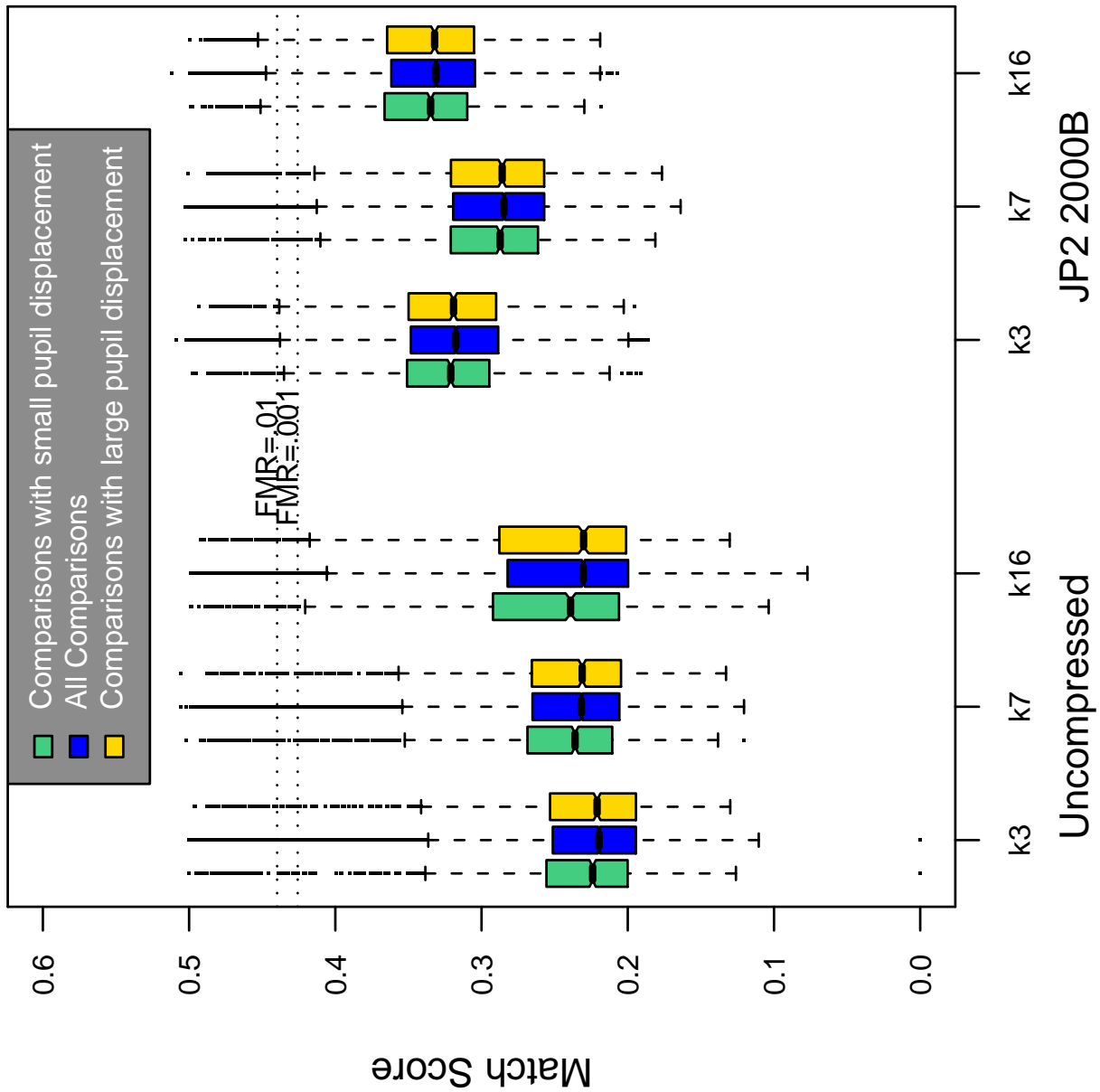


Table 188: Effect of pupil displacement on the genuine score distribution for H2

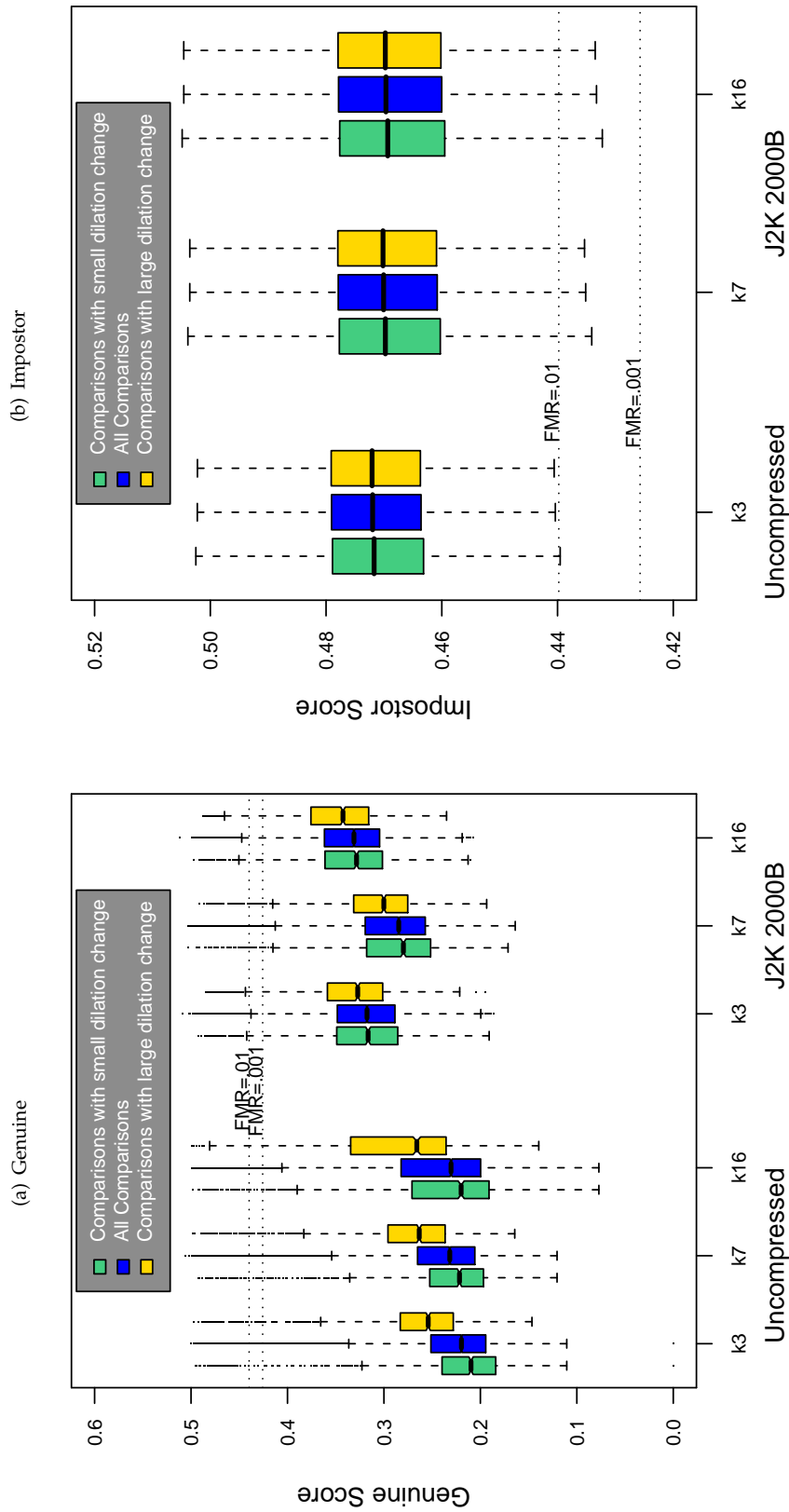


Table 189: The effect of dilation change on the two scores distributions for SDK H2.

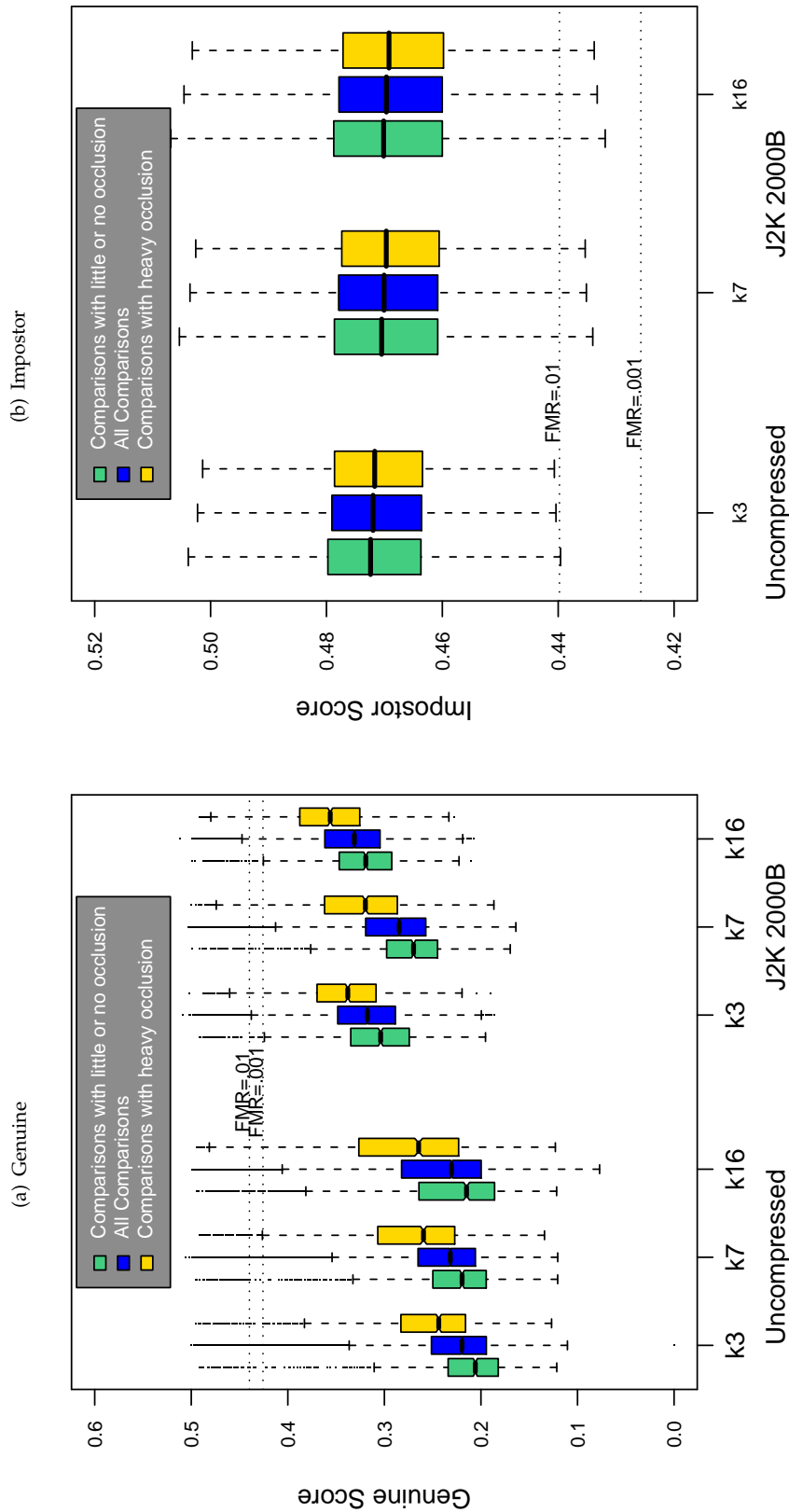
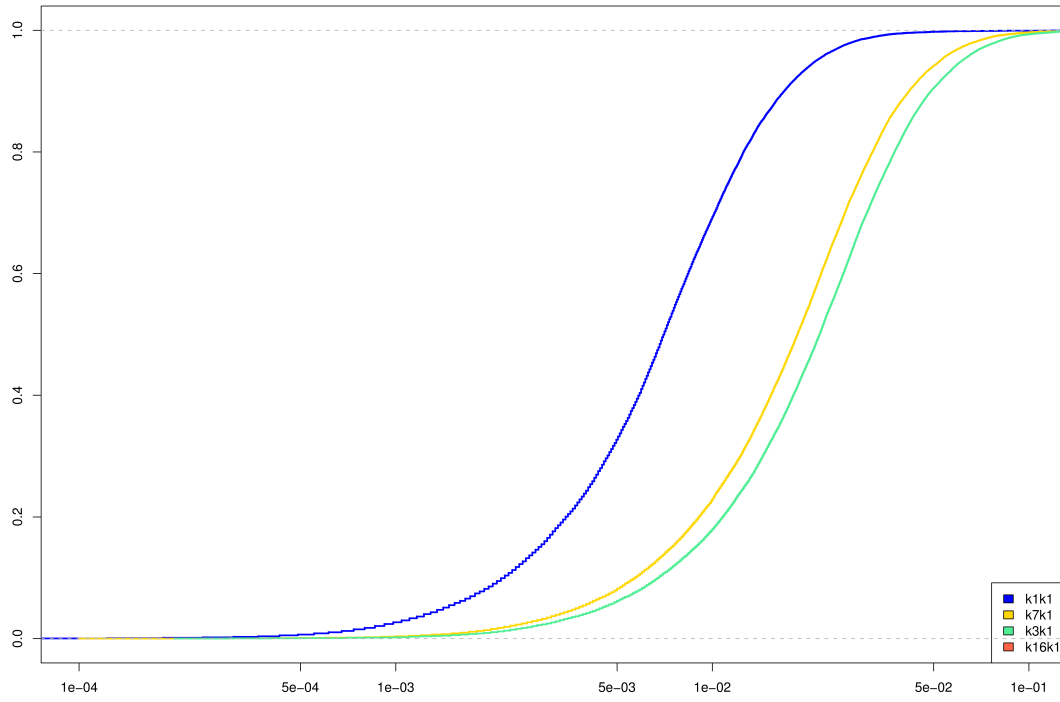
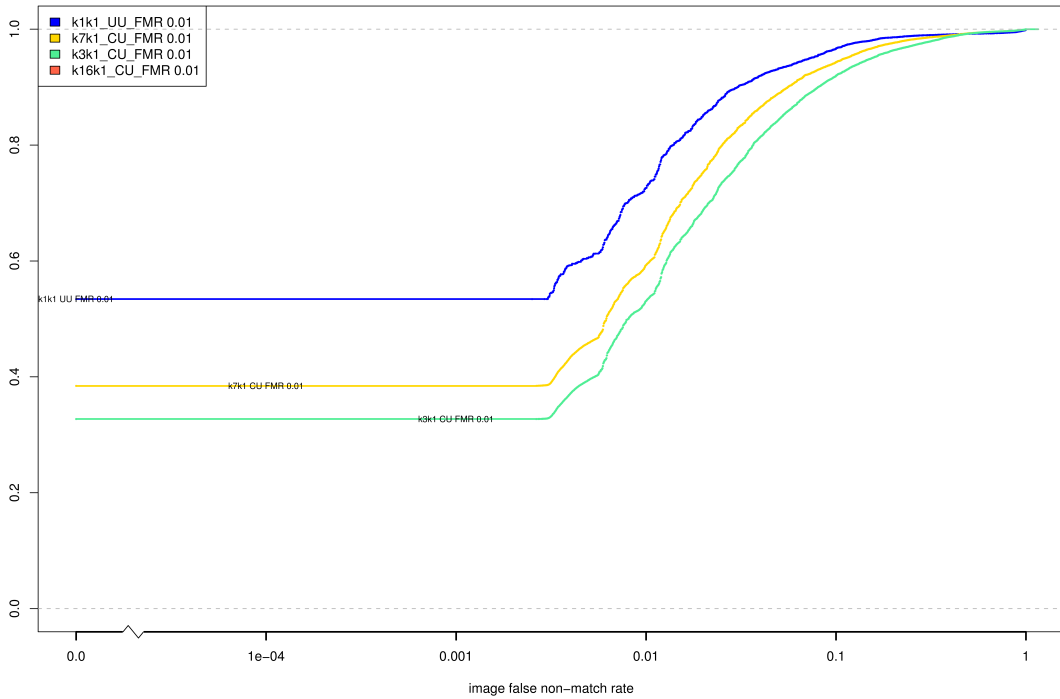


Table 190: The effect of eyelid occlusion on the two scores distributions for SDK H2.

(a) iFMR CDF



(b) iFNMR CDF



Compiled Results for Implementation I1

On June 25, 2009, NIST invited the IREX participants to submit a description of the SDKs submitted for the IREX effort. The intent was to allow providers to describe and contrast the feature sets, optimization, operational suitability and availability of the primary and secondary SDKs. NIST indicated that any submitted text would appear verbatim (with typesetting) in draft and final versions of the IREX report and that it would be attributed to the organization. This was optional and NIST put no constraints on the content beyond a 600 word limit, and a statement that anything labelled as confidential or proprietary would be omitted.

The provider of SDK I1, Iritech, submitted the following to NIST - we are unable to validate this information.

Prior knowledge of the characteristics of the images to be tested is the most important determining factor in the parameter tuning of iris recognition library. Due to the blind nature of IREX test, some extra—but unnecessary under normal circumstances—precautions were taken for the versions of IriTech’s SDKs submitted to NIST, which has adversely affected the SDKs’ performance in terms of the speed of execution and the sizes of the SDKs and the templates they generate. If the nature of images is known, say, if the camera with which the images were taken is known a priori, IriTech’s SDKs would have worked much faster and their sizes would have been a lot smaller.

On August 17, 2009, NIST invited the IREX participants to submit a description their comments on an draft version of the IREX report. This was intended to allow participants to assist readers in the interpretation of a large and complicated testing effort. NIST indicated that any submitted text would appear verbatim (with typesetting) in the final version of the IREX report and that it would be attributed to the organization. Submission of content was optional and NIST put no constraints on the content beyond a word limit, and a statement that anything labelled as confidential or proprietary would be omitted.

The provider of SDK I1, Iritech, submitted the following to NIST - we make no comment on this information.

Prior knowledge of the characteristics of the images to be tested is the most important determining factor in the parameter tuning of iris recognition library. Due to the blind nature of IREX test, some extra—but unnecessary under normal circumstances—precautions were taken for the versions of IriTech’s SDKs submitted to NIST, which has adversely affected IriTech’s SDKs’ performance in terms of the speed of execution and the size of the templates they generate. If the nature of images were known a priori, say, if the camera with which the images were taken were known, IriTech’s SDKs could have easily forgone such extra precautions, thereby resulting in far faster speed of execution and sizable template size reduction.

IriTechs performance in Tables 15, 16 and 17 should be interpreted correctly as follows: Since IriTechs SDKs are extremely accurate in the uncompressed K1-K1 comparison, its FMR = 0.0001 threshold is shifted to the too far right, which of course is quite desirable. But as the IREX records are significantly compressed in the K1-K3, K1-K7, K1-K16 comparisons and as compressed images lose a certain amount of information, the accuracy in these cases cannot be as great, which means that the corresponding thresholds cannot move to the right as much. These are the reason for the seemingly less stellar performance. Remediating it is simple: Instead of fixing the FMR = 0.0001 threshold from the uncompressed K1-K1 comparison, one can set it to be the lesser of the FMR = 0.0001 thresholds coming from compressed K1-K3 or K1-K3 comparisons.

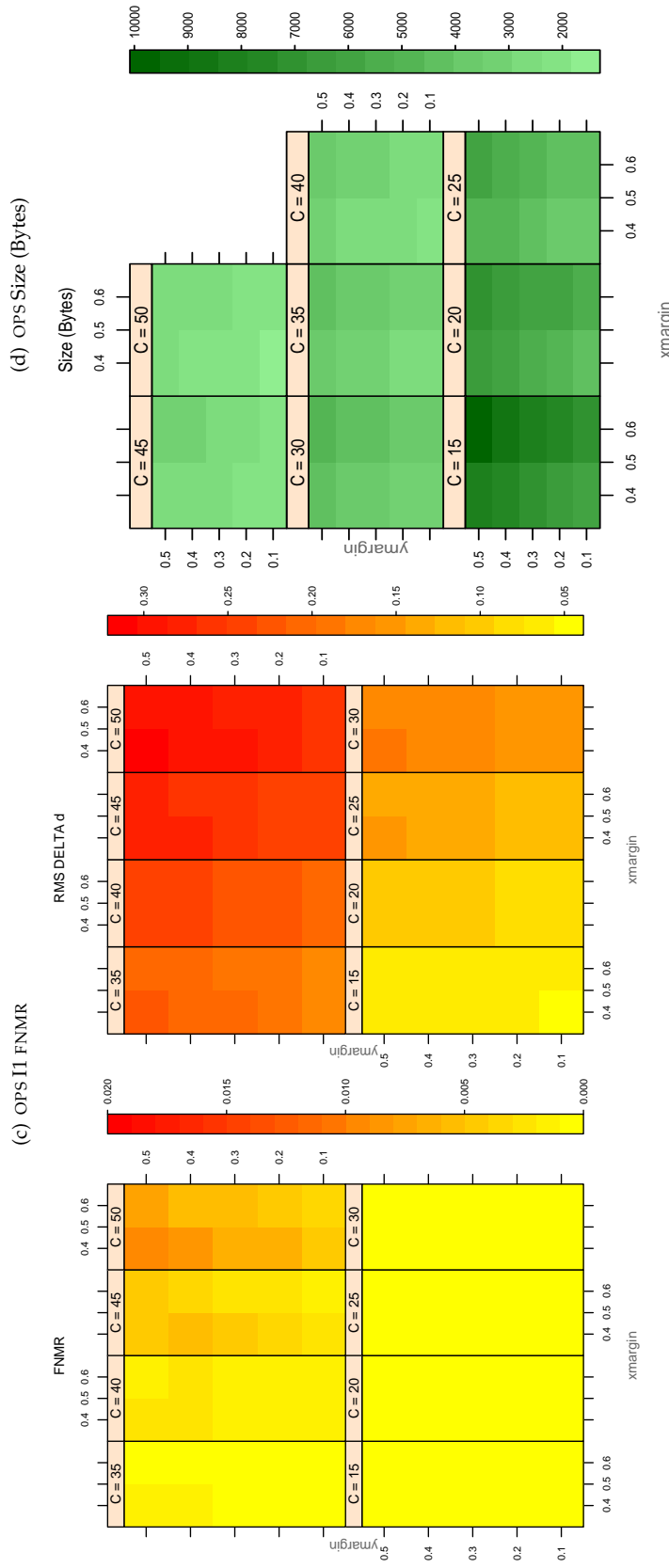


Table 191: For the IREX partition of the OPS database the plots at left show the dependence of cFNMR on the vertical and horizontal iris cropping margins for various compression ratios. This applies only for KIND 3 records. The margins are in units of iris radius. The use of conditional FNMR means that the plots exclude comparisons that were falsely rejected even before any compression was applied. On the **right side** is the rms difference between the crop+compress and the uncompressed comparison scores for each image pair. All computations are driven by the bounding box coordinates reported by the II SDK. The number of bits per pixel is $8/C$, where C is the compression ratio. The iris radius varies and because the cropping margins are fixed multiples of the radius the image size varies. The compressed size, in bytes, is the width times height divided by C . Values of cFNMR greater than 0.02 are shown as 0.02.

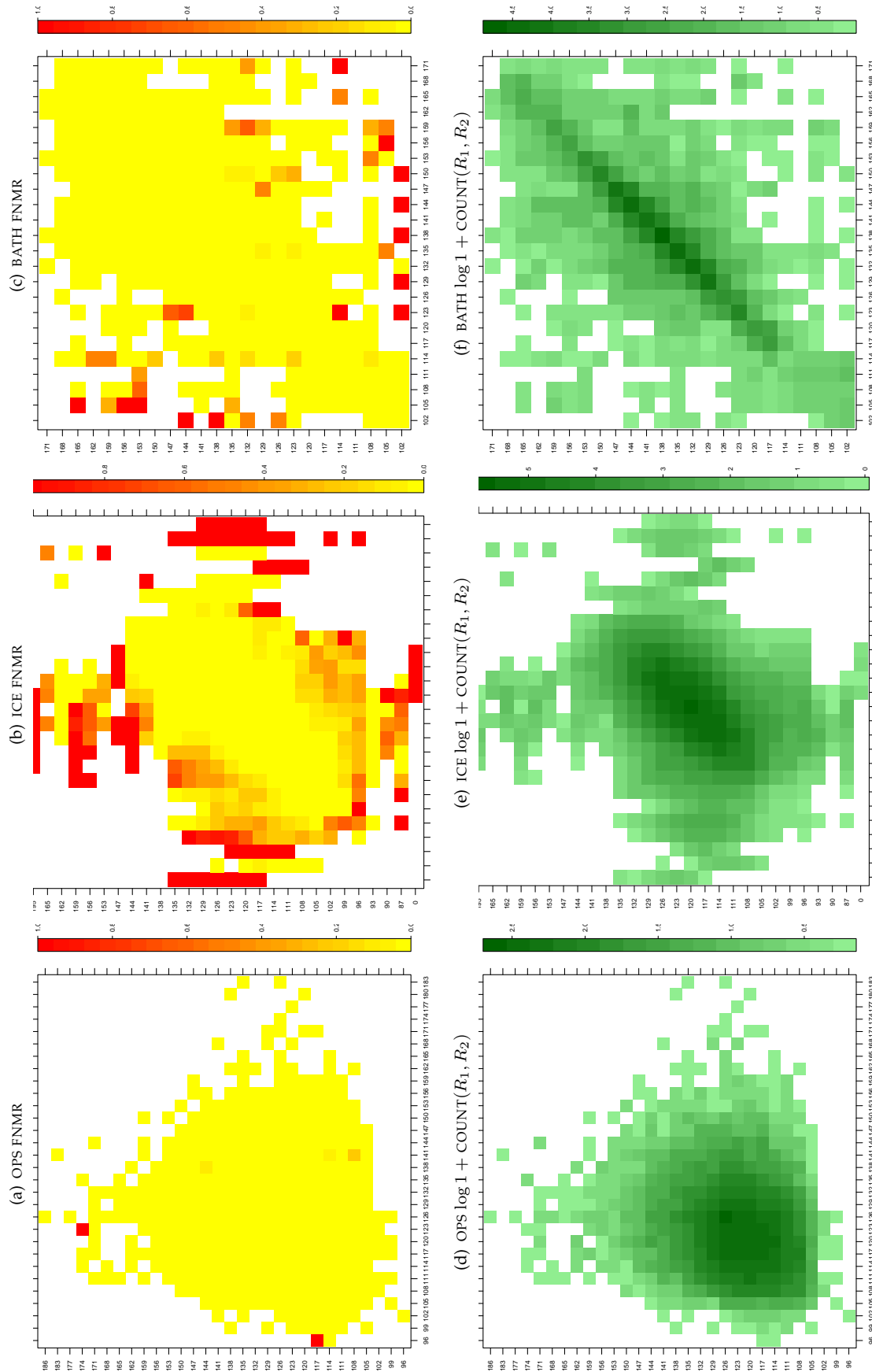


Table 192: For the three IREX databases: In the **top** row the color in each cell represents the occurrence of genuine comparisons with the given pair of radii. The *y*-axis represents enrollment samples with verification samples on the *x*-axis; In the **bottom** row the color scale plots $\log 1 + \text{COUNT}(R_1, R_2)$. The radii are quantized into three-pixel bins. The radii for DOD are on the range $96 \leq r \leq 186$ pixels. The radii for ICE are on the range $87 \leq r \leq 165$ pixels. The radii for BATH are on the range $100 \leq r \leq 170$ pixels.

A = SAGEM	B = COGENT	C = CROSSMATCH	D = CAMBRIDGE	E = L1	$x1$ = PRIMARY
F = RETICA	G = LG	H = HONEYWELL	I = IRITECH	J = NEUROTECHNOLOGY	$x2$ = SECONDARY
KIND 1 = RAW 640x480		KIND 3 = CROP		KIND 7 = CROP+MASK	
KIND 16 = CONCENTRIC POLAR					

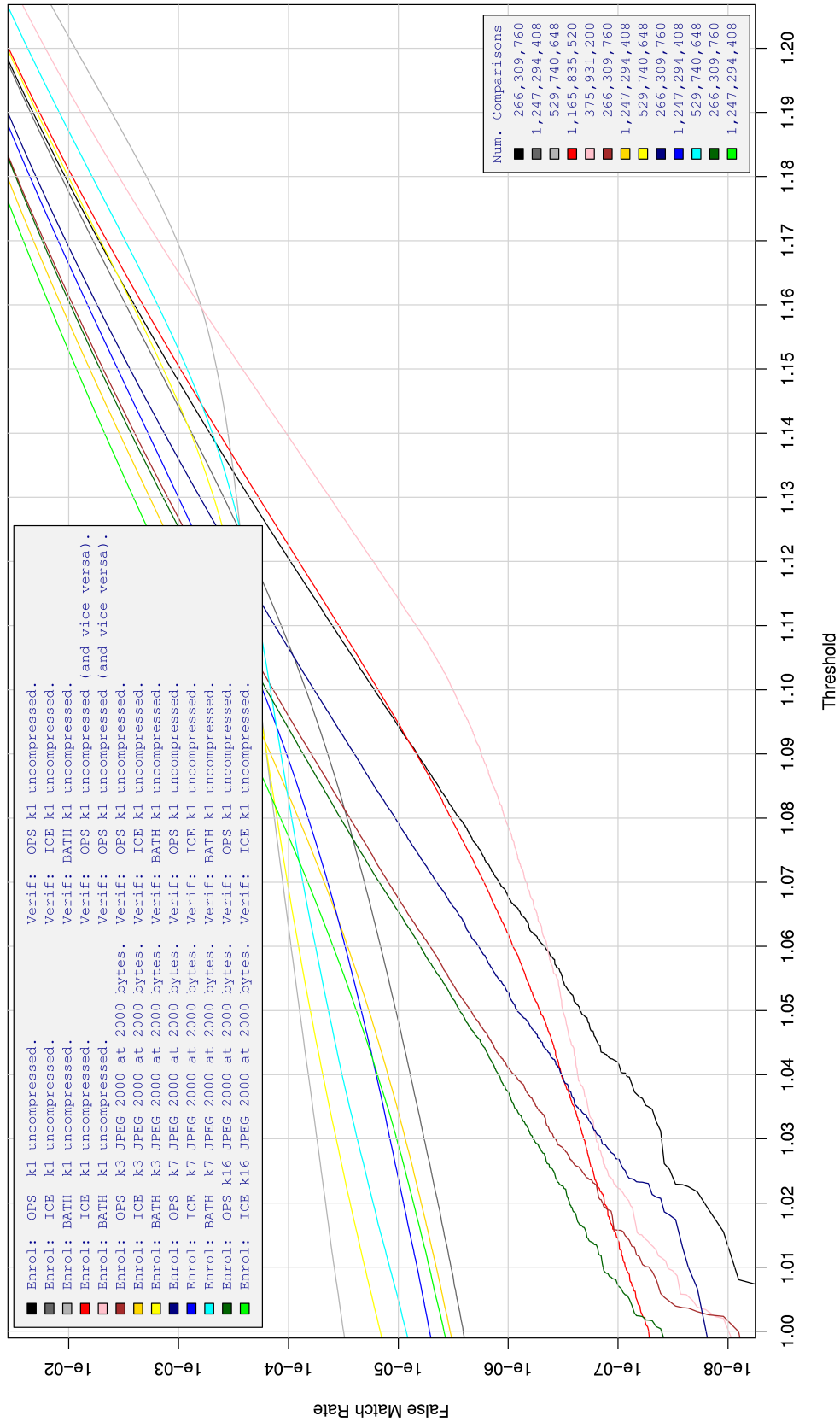


Table 193: For implementation I1, the dependency of FMR on threshold. for various combinations of enrollment and verification dataset, format, and compression.

A = SAGEM	B = COGENT	C = CROSSMATCH	D = CAMBRIDGE	E = L1	x1 = PRIMARY
F = RETICA	G = LG	H = HONEYWELL	I = IRITECH	J = NEUROTECHNOLOGY	x2 = SECONDARY
KIND 1 = RAW 640x480		KIND 3 = CROP		KIND 7 = CROP+MASK	KIND 16 = CONCENTRIC POLAR

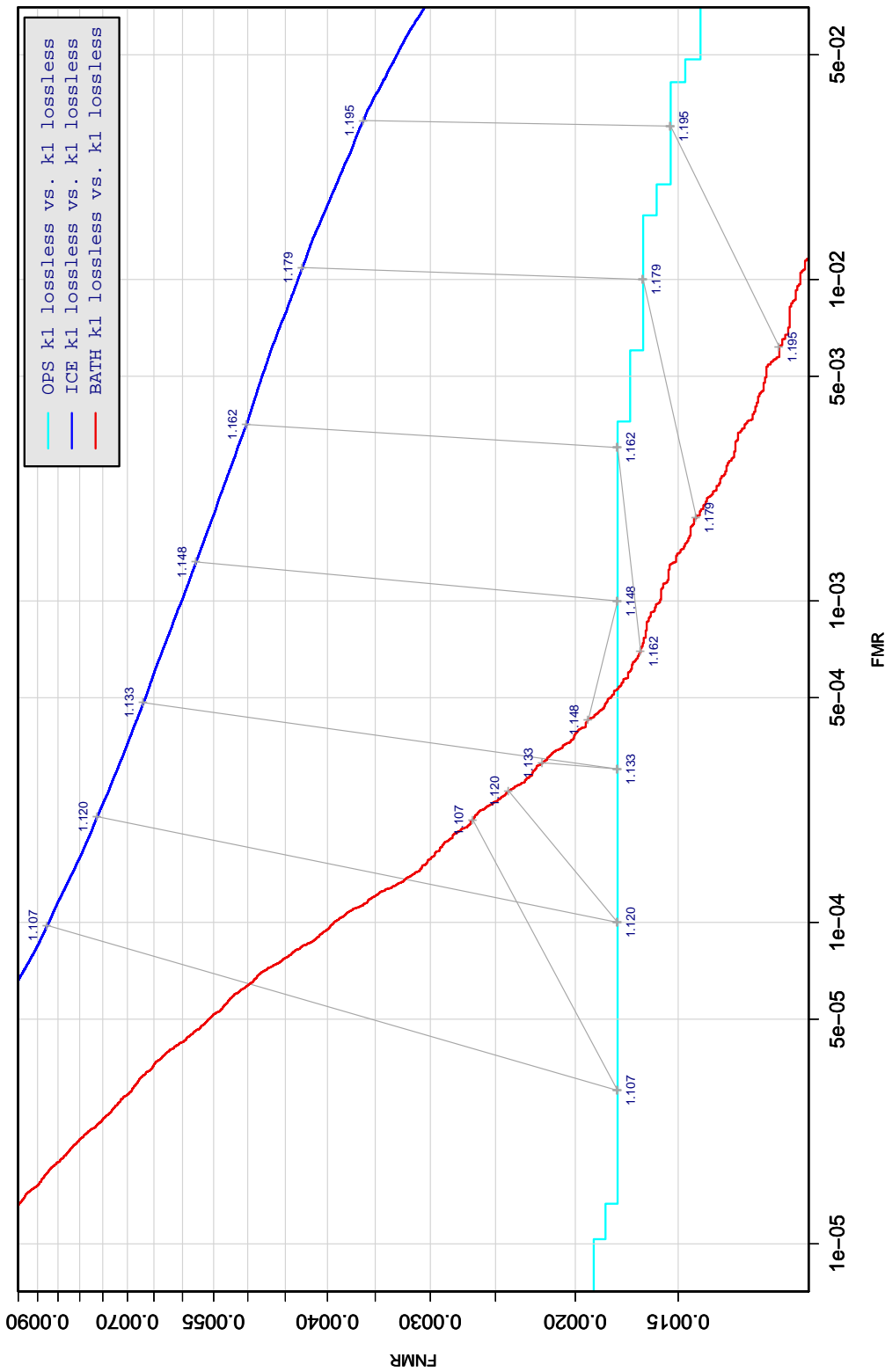


Table 194: DET curve for implementation I1 on three IREX databases. All comparisons are with uncompressed KIND 1 vs. KIND 1 images. The lines join points corresponding to the a fixed threshold. Non-vertical links indicate a change in FMR when the database changes. All results apply to native operation. Failures to produce a template i.e. FTE are ignored because the plots are intended to show *matching* effects, specifically to compare DET slopes and to show the effect of fixing a threshold.

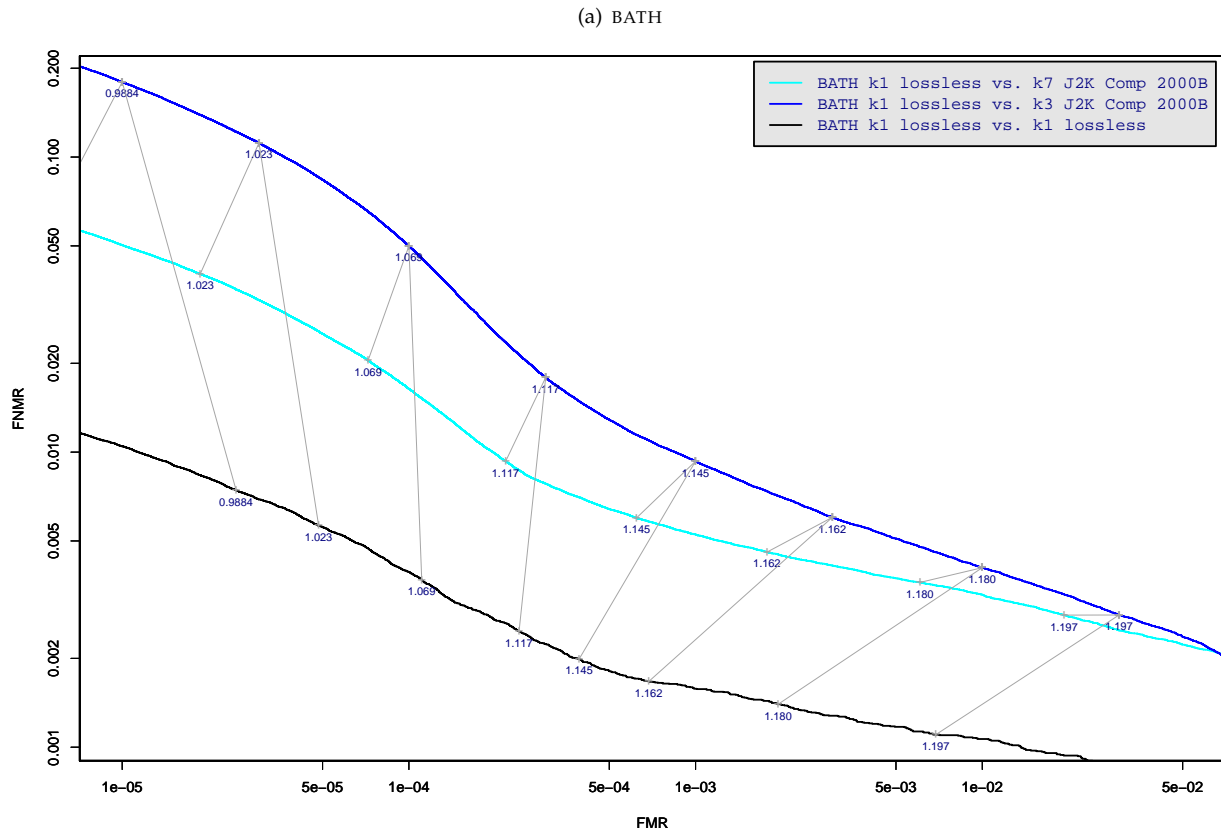


Table 195: DET curve for implementation I1 on the BATH database for the various supported KINDS . The DET characteristics are linked by lines joining points of equal threshold. Non-vertical links indicate a change in false acceptance when the data KIND changes. All results apply to native operation, and the effects of FTE are included.

A = SAGEM	B = COGENT	C = CROSSMATCH	D = CAMBRIDGE	E = L1	x1 = PRIMARY
F = RETICA	G = LG	H = HONEYWELL	I = IRITECH	J = NEUROTECHNOLOGY	x2 = SECONDARY
KIND 1 = RAW 640x480		KIND 3 = CROP	KIND 7 = CROP+MASK	KIND 16 = CONCENTRIC POLAR	

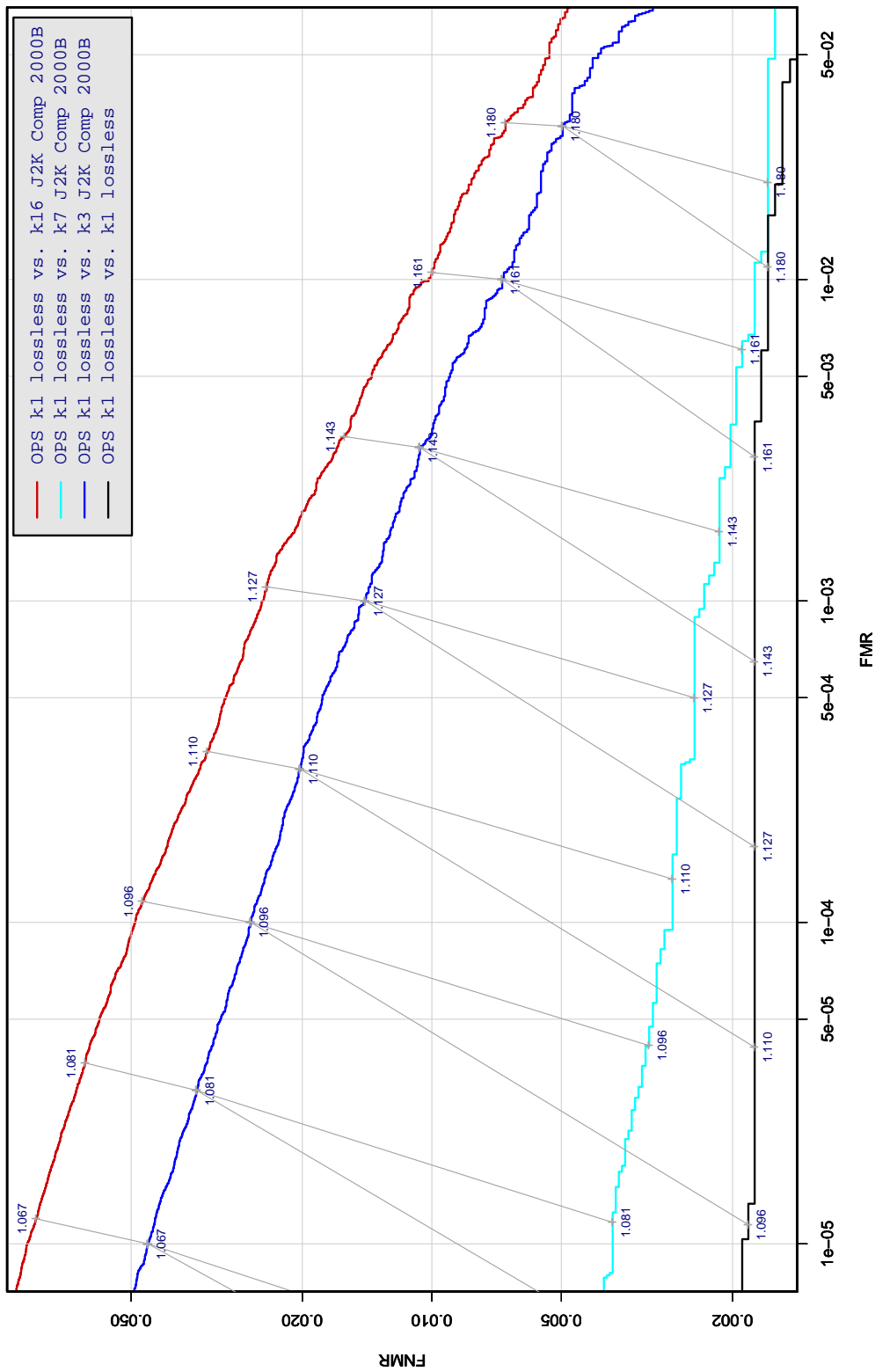


Table 196: DET curve for implementation I1 on the OPS database for the various supported KINDS . The DET characteristics are linked by lines joining points of equal threshold. Non-vertical links indicate a change in false acceptance when the data KIND changes. All results apply to native operation, and the effects of FTE are included.

A = SAGEM	B = COGENT	C = CROSSMATCH	D = CAMBRIDGE	E = L1	x1 = PRIMARY
F = RETICA	G = LG	H = HONEYWELL	I = IRITECH	J = NEUROTECHNOLOGY	x2 = SECONDARY
KIND 1 = RAW 640x480		KIND 3 = CROP		KIND 7 = CROP+MASK	
				KIND 16 = CONCENTRIC POLAR	

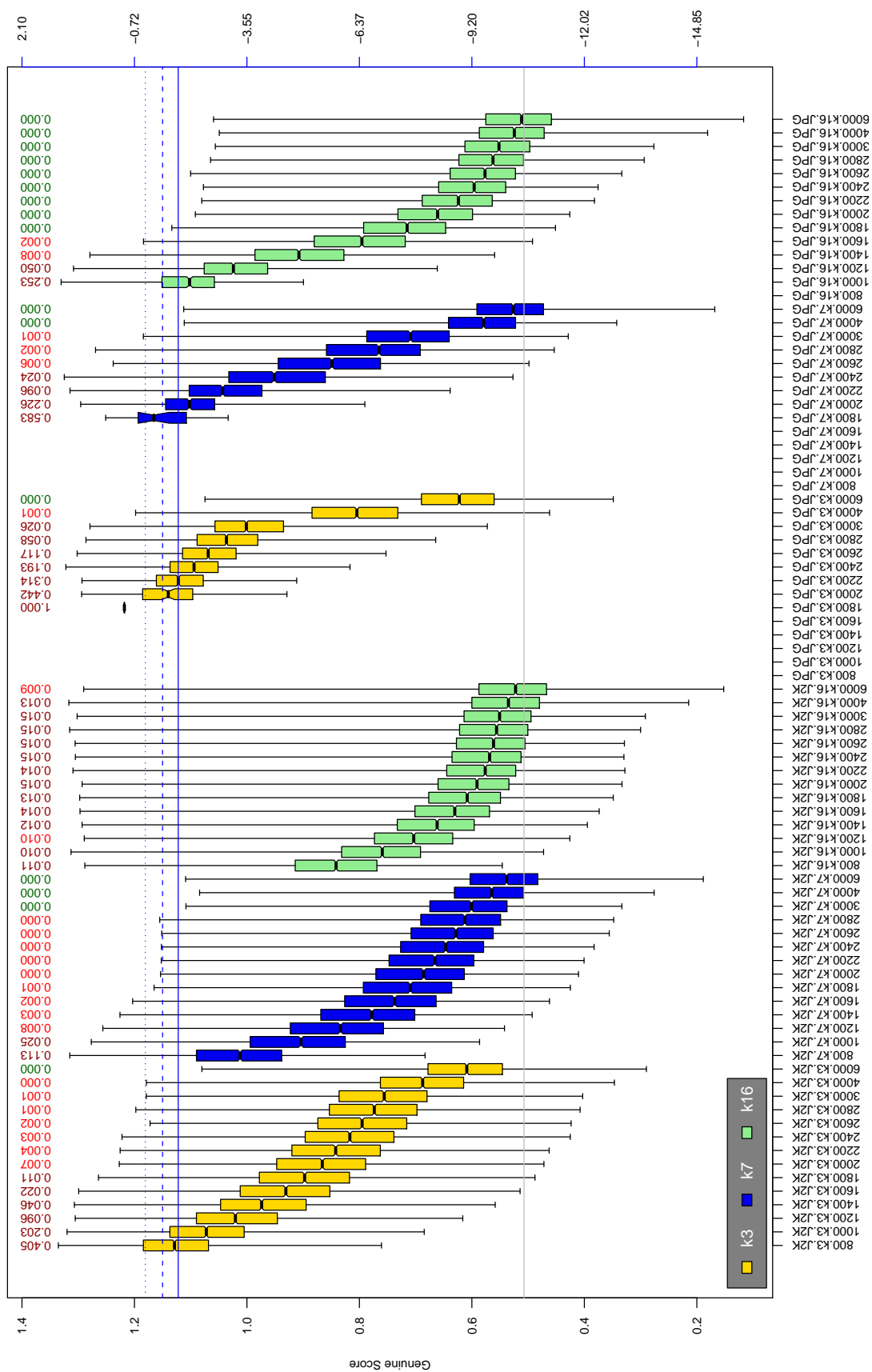


Table 197: The distribution of I1 native genuine comparison scores by size of the compressed image, KIND and the compression algorithm. The images are from the OPS dataset. The right axis scale gives the corresponding value for $d' = (s - \mu_I) / \sqrt{0.5(\sigma_I^2 + \sigma_C^2)}$ for genuine score s . The boxplots only include comparison scores if the uncompressed version of the same image was matched below the FMR = 0.001 threshold. Above the boxplots are FNMR values at FMR = 10⁻³. The three blue lines correspond, from the top, to FMR of 10^[-2,-3,-4]. The lower grey line refers to the median score obtained from comparison of uncompressed KIND 3 images. Any comparison for which either template had not been generated is excluded. Note that the iris record size on the horizontal axis is not evenly spaced above 3000 bytes.

A = SAGEM	B = COGENT	C = CROSSMATCH	D = CAMBRIDGE	E = L1	x1 = PRIMARY
F = RETICA	G = LG	H = HONEYWELL	I = IRITECH	J = NEUROTECHNOLOGY	x2 = SECONDARY
KIND 1 = RAW 640x480		KIND 3 = CROP	KIND 7 = CROP+MASK	KIND 16 = CONCENTRIC POLAR	

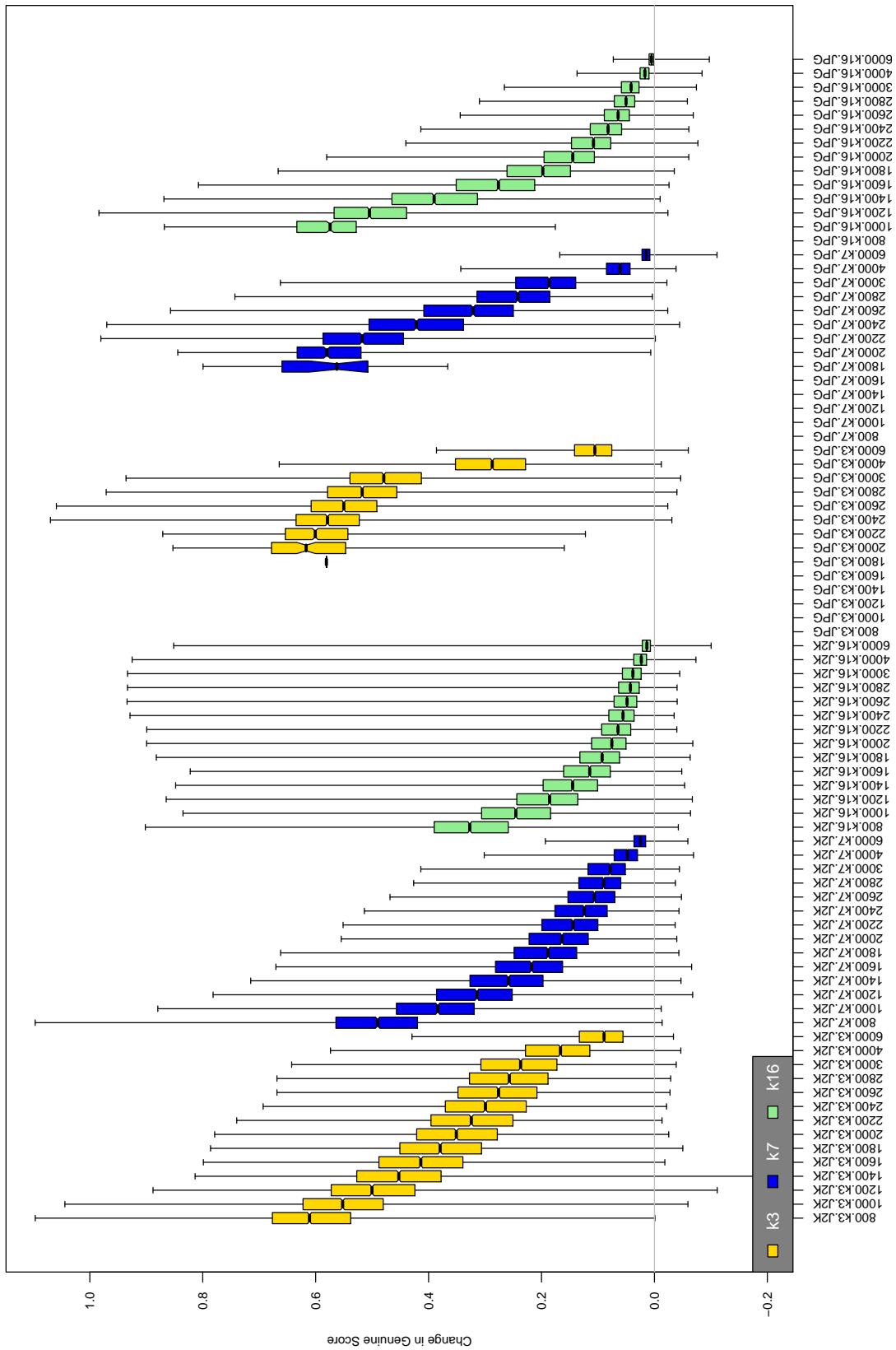


Table 198: The distribution of the *increase* in I1 native genuine comparison scores between the uncompressed “parent” and the compressed image, arranged by size, KIND and the compression algorithm. The images are from the OPS dataset. Any comparison involving a failed template is excluded. Note that the iris record size on the horizontal axis is not evenly spaced above 3000 bytes.

A = SAGEM	B = COGENT	C = CROSSMATCH	D = CAMBRIDGE	E = L1	x1 = PRIMARY
F = RETICA	G = LG	H = HONEYWELL	I = IRITECH	J = NEUROTECHNOLOGY	x2 = SECONDARY
KIND 1 = RAW 640x480		KIND 3 = CROP	KIND 7 = CROP+MASK	KIND 16 = CONCENTRIC POLAR	

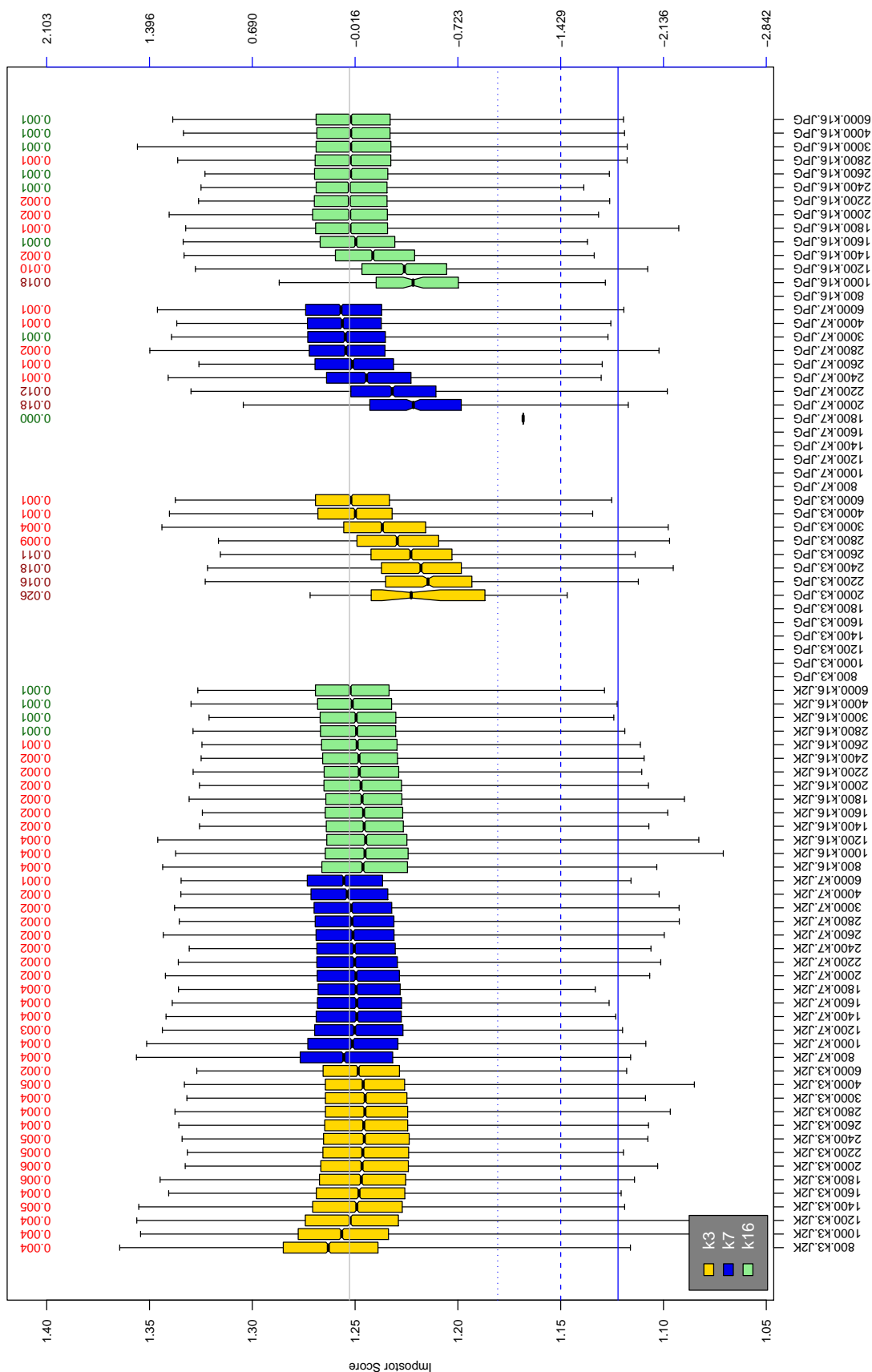


Table 199: The distribution of Π native impostor comparison scores by size of the compressed image, KIND and the compression algorithm. The right axis scale gives the corresponding value for $d' = (s - \mu_1) / \sqrt{0.5(\sigma_1^2 + \sigma_2^2)}$ for impostor score s . The three blue lines correspond, from the top, to FMR of 10^{-2} , 10^{-3} , and 10^{-4} . The lower grey line refers to the median score obtained from comparison of uncompressed KIND 3 images. Any comparison involving a failed template is excluded. Above the boxplots are FMR values at the threshold that gives FMR = 10^{-3} on uncompressed images. These figures are computed from only 4000 comparisons so the FMR values and the tails of the impostor distribution are poorly characterized. Note that the iris record size on the horizontal axis is not evenly spaced above 3000 bytes.

A = SAGEM	B = COGENT	C = CROSSMATCH	D = CAMBRIDGE	E = L1	$x1$ = PRIMARY
F = RETICA	G = LG	H = HONEYWELL	I = IRITECH	J = NEUROTECHNOLOGY	$x2$ = SECONDARY
KIND 1 = RAW 640x480		KIND 3 = CROP	KIND 7 = CROP+MASK	KIND 16 = CONCENTRIC POLAR	

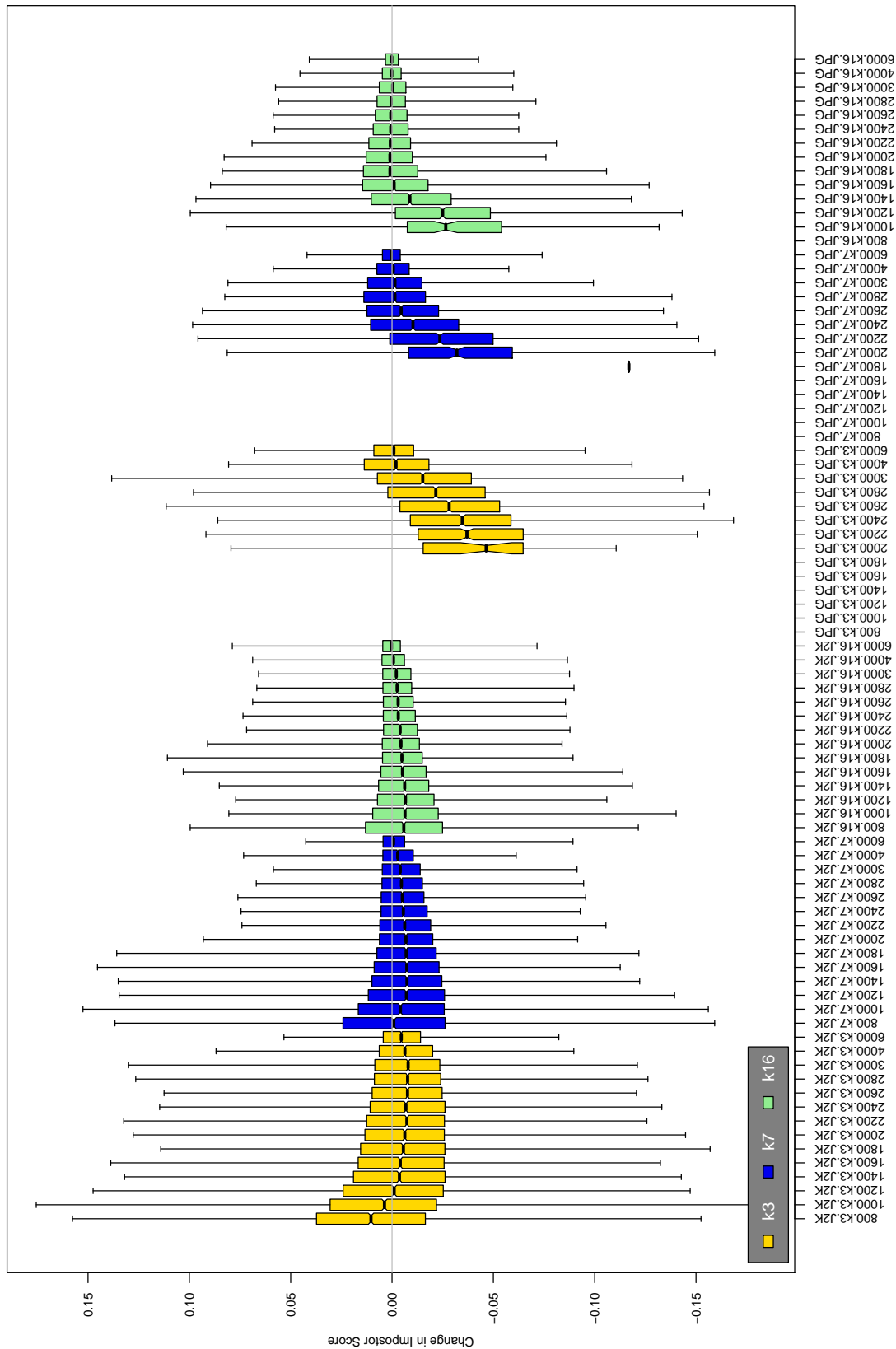


Table 200: The distribution of the increase in I1 native impostor comparison scores between the uncompressed “parent” and the compressed image, arranged by size, KIND and the compression algorithm. The images are from the OPS dataset. Any comparison involving a failed template is excluded. Note that the iris record size on the horizontal axis is not evenly spaced above 3000 bytes.

A = SAGEM	B = COGENT	C = CROSSMATCH	D = CAMBRIDGE	E = L1	x1 = PRIMARY
F = RETICA	G = LG	H = HONEYWELL	I = IRITECH	J = NEUROTECHNOLOGY	x2 = SECONDARY
KIND 1 = RAW 640x480		KIND 3 = CROP		KIND 7 = CROP+MASK	KIND 16 = CONCENTRIC POLAR

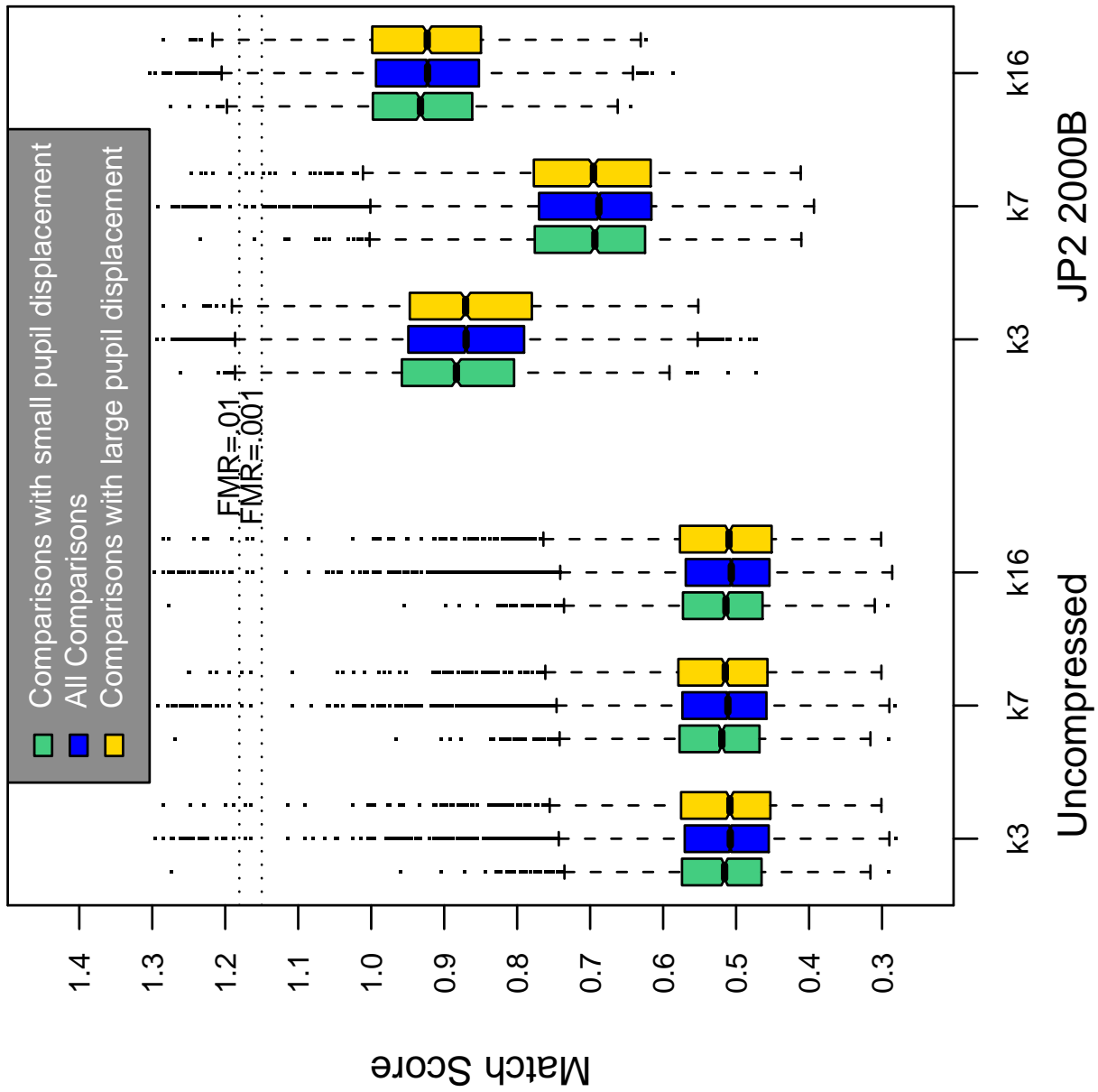


Table 201: Effect of pupil displacement on the genuine score distribution for I1

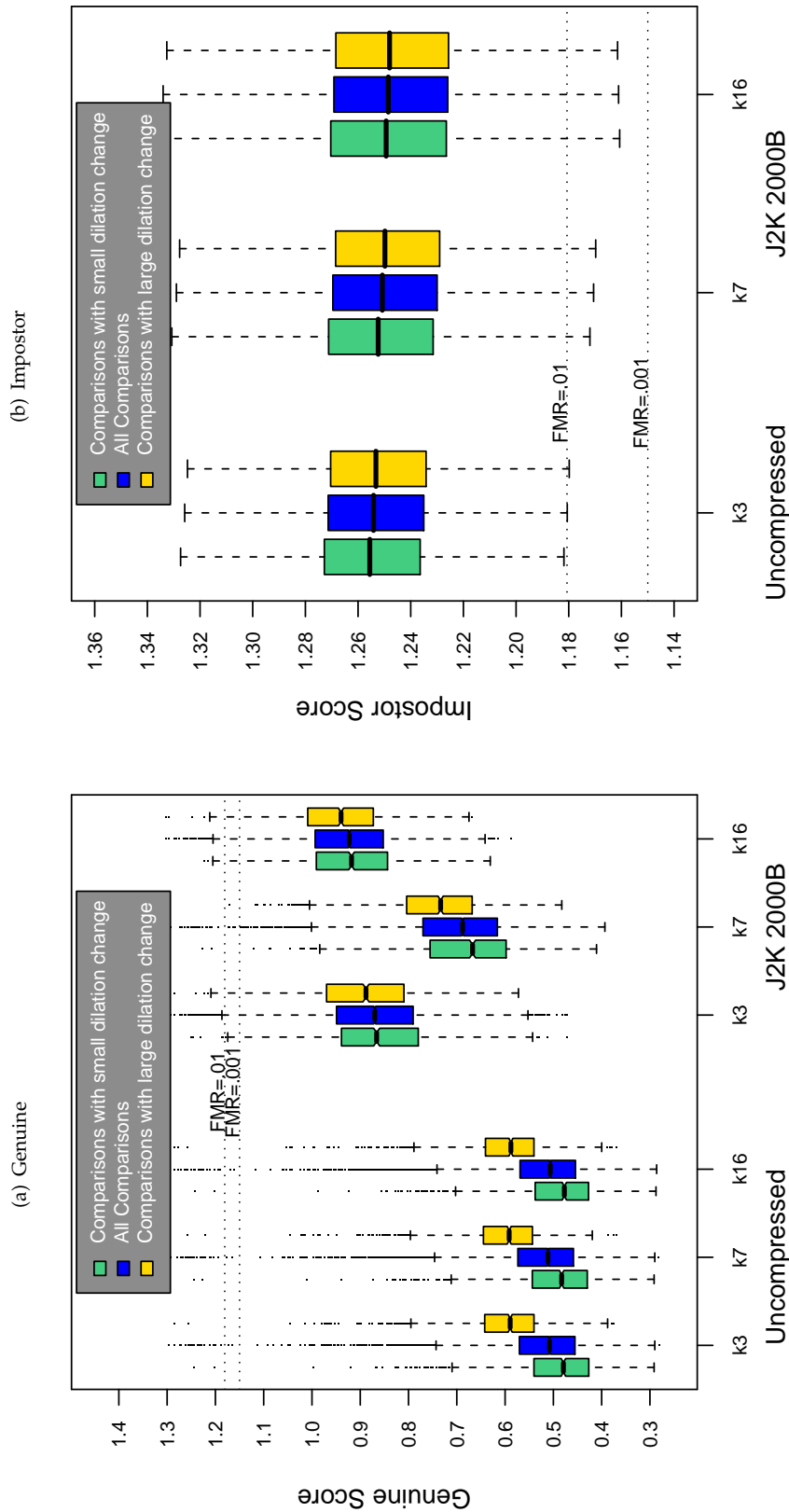


Table 202: The effect of dilation change on the two scores distributions for SDK II.

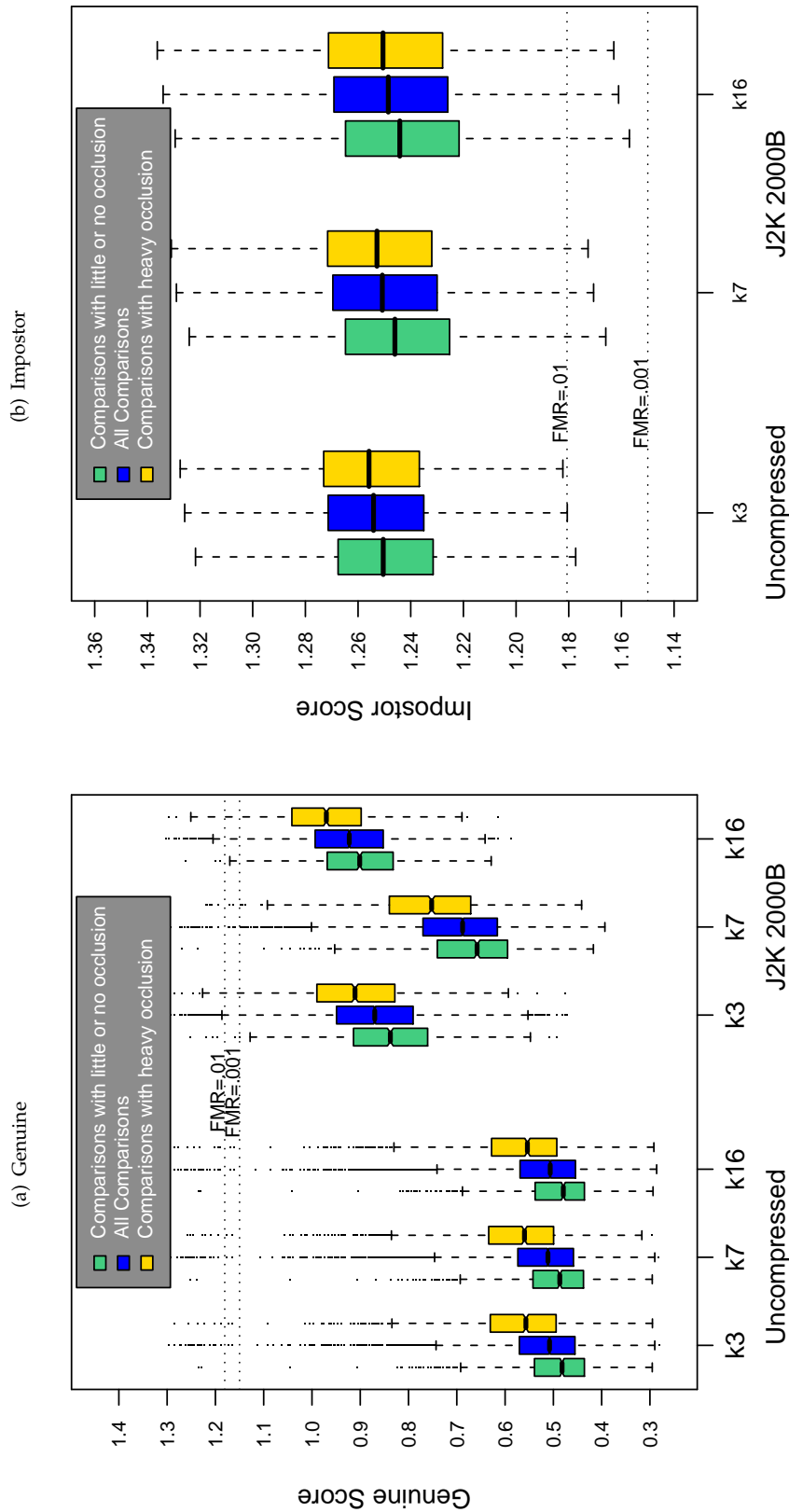
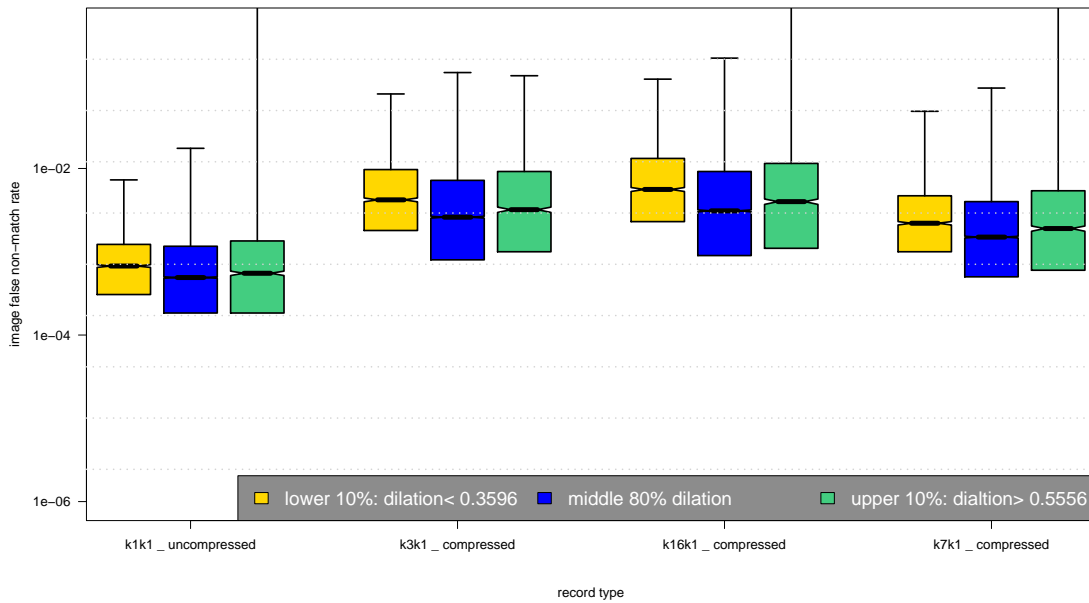
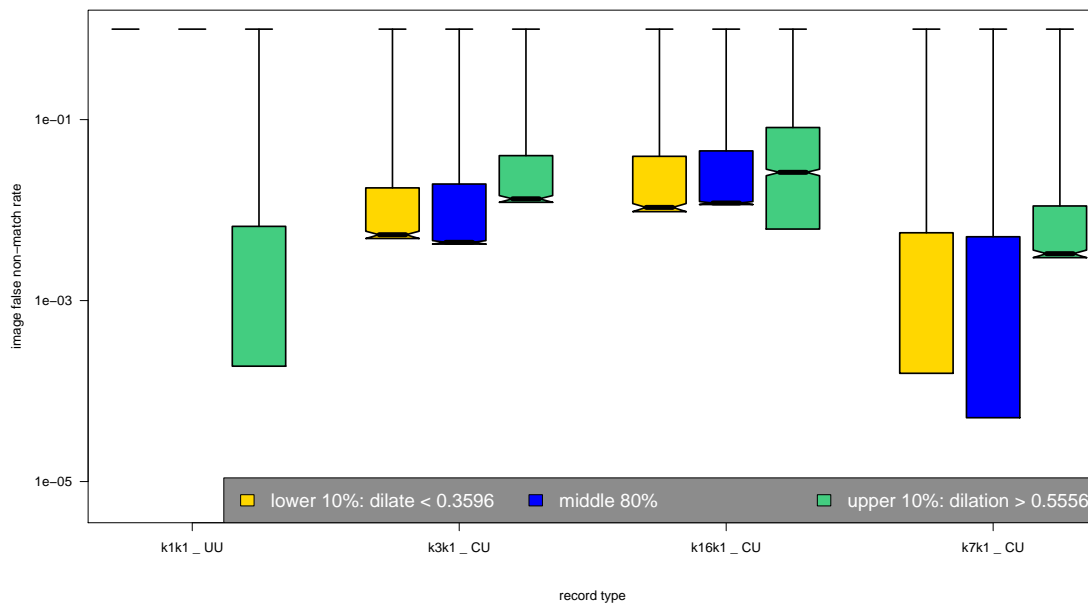


Table 203: The effect of eyelid occlusion on the two scores distributions for SDK II.

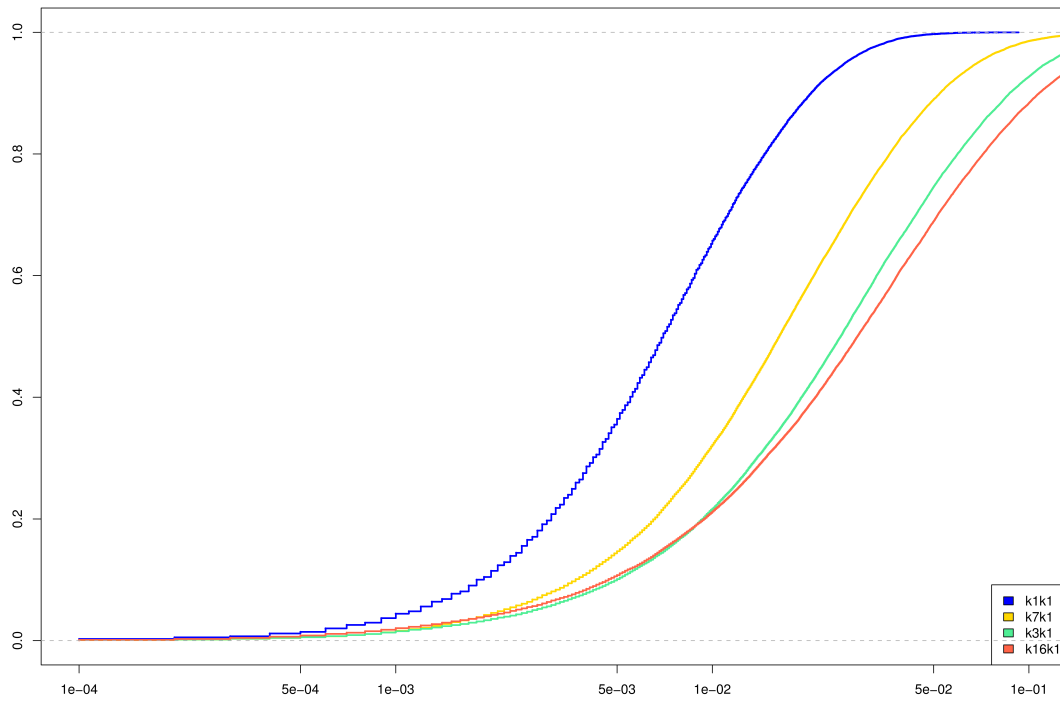
(a) iFMR using A1 dilation estimates



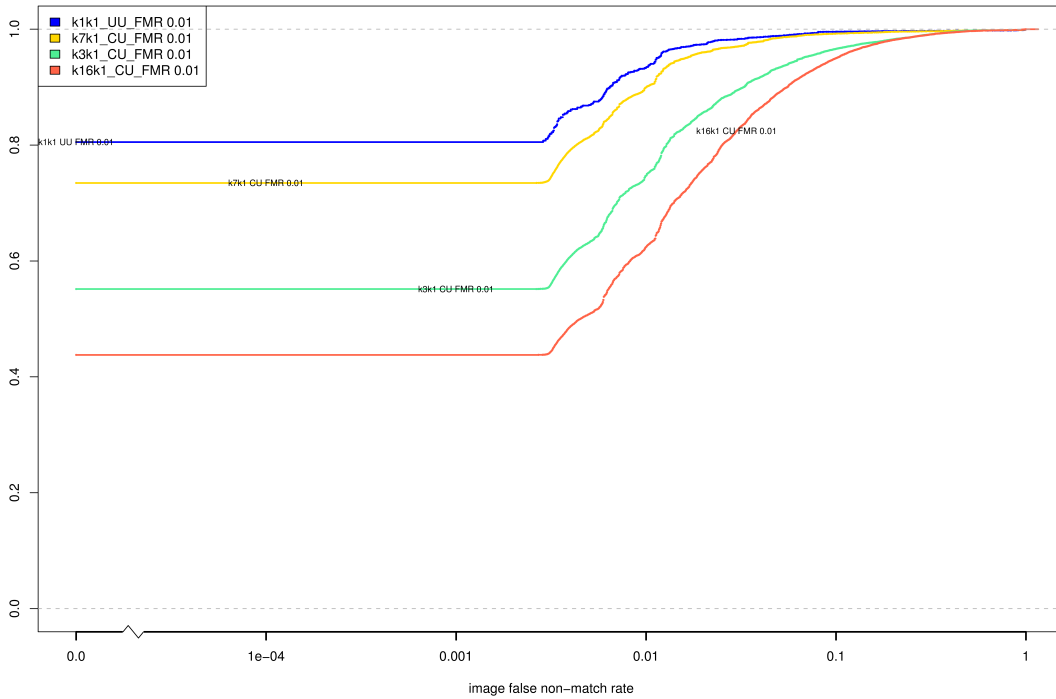
(b) iFNMR using A1 dilation estimates



(c) iFMR CDF



(d) iFNMR CDF



Compiled Results for Implementation I2

On June 25, 2009, NIST invited the IREX participants to submit a description of the SDKs submitted for the IREX effort. The intent was to allow providers to describe and contrast the feature sets, optimization, operational suitability and availability of the primary and secondary SDKs. NIST indicated that any submitted text would appear verbatim (with typesetting) in draft and final versions of the IREX report and that it would be attributed to the organization. This was optional and NIST put no constraints on the content beyond a 600 word limit, and a statement that anything labelled as confidential or proprietary would be omitted.

The provider of SDK I2, Iritech, submitted the following to NIST - we are unable to validate this information.

Prior knowledge of the characteristics of the images to be tested is the most important determining factor in the parameter tuning of iris recognition library. Due to the blind nature of IREX test, some extra—but unnecessary under normal circumstances—precautions were taken for the versions of IriTech’s SDKs submitted to NIST, which has adversely affected the SDKs’ performance in terms of the speed of execution and the sizes of the SDKs and the templates they generate. If the nature of images is known, say, if the camera with which the images were taken is known a priori, IriTech’s SDKs would have worked much faster and their sizes would have been a lot smaller.

On August 17, 2009, NIST invited the IREX participants to submit a description their comments on an draft version of the IREX report. This was intended to allow participants to assist readers in the interpretation of a large and complicated testing effort. NIST indicated that any submitted text would appear verbatim (with typesetting) in the final version of the IREX report and that it would be attributed to the organization. Submission of content was optional and NIST put no constraints on the content beyond a word limit, and a statement that anything labelled as confidential or proprietary would be omitted.

The provider of SDK I2, Iritech, submitted the following to NIST - we make no comment on this information.

Prior knowledge of the characteristics of the images to be tested is the most important determining factor in the parameter tuning of iris recognition library. Due to the blind nature of IREX test, some extra—but unnecessary under normal circumstances—precautions were taken for the versions of IriTech’s SDKs submitted to NIST, which has adversely affected IriTech’s SDKs’ performance in terms of the speed of execution and the size of the templates they generate. If the nature of images were known a priori, say, if the camera with which the images were taken were known, IriTech’s SDKs could have easily forgone such extra precautions, thereby resulting in far faster speed of execution and sizable template size reduction.

IriTechs performance in Tables 15, 16 and 17 should be interpreted correctly as follows: Since IriTechs SDKs are extremely accurate in the uncompressed K1-K1 comparison, its FMR = 0.0001 threshold is shifted to the too far right, which of course is quite desirable. But as the IREX records are significantly compressed in the K1-K3, K1-K7, K1-K16 comparisons and as compressed images lose a certain amount of information, the accuracy in these cases cannot be as great, which means that the corresponding thresholds cannot move to the right as much. These are the reason for the seemingly less stellar performance. Remediating it is simple: Instead of fixing the FMR = 0.0001 threshold from the uncompressed K1-K1 comparison, one can set it to be the lesser of the FMR = 0.0001 thresholds coming from compressed K1-K3 or K1-K3 comparisons.

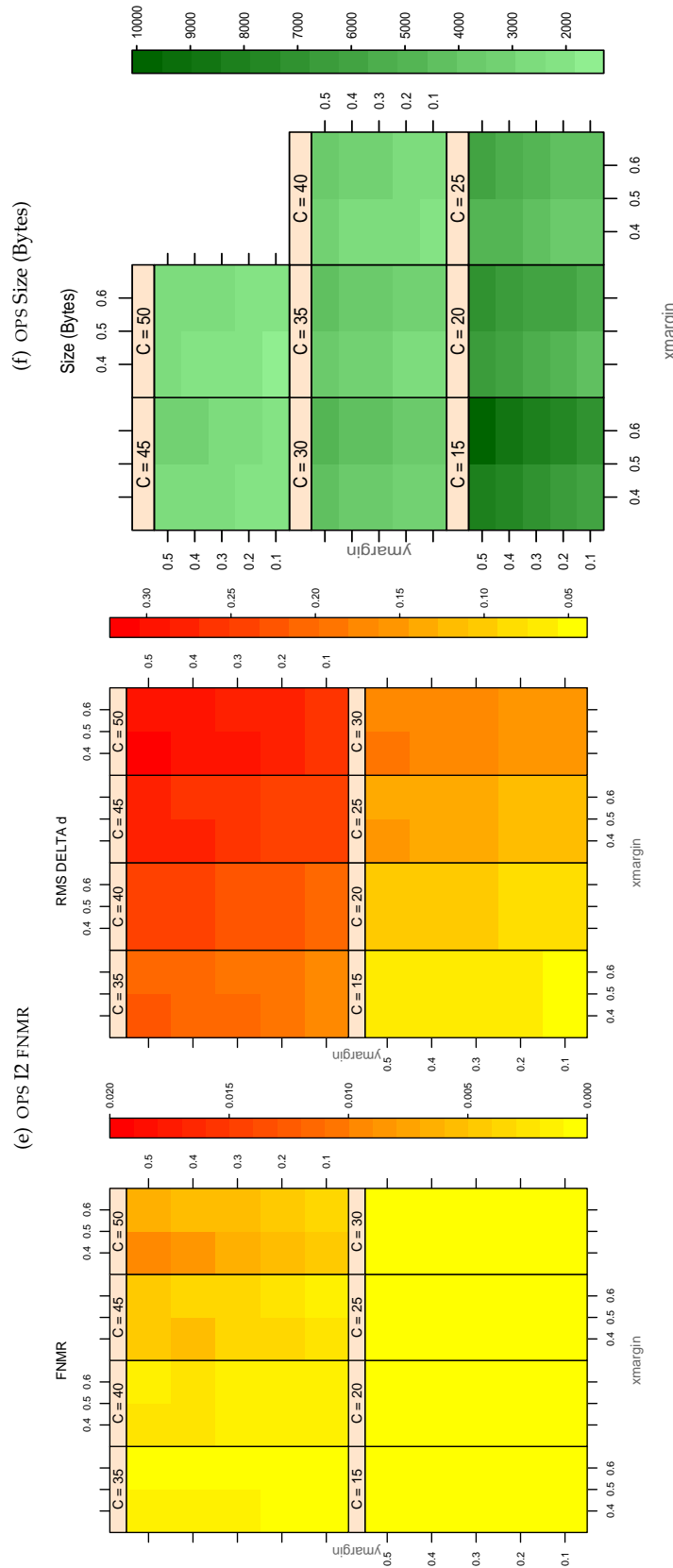


Table 204: For the IREX partition of the OPS database the plots at left show the dependence of cFNMNR on the vertical and horizontal iris cropping margins for various compression ratios. This applies only for KIND 3 records. The margins are in units of iris radius. The use of conditional FNMNR means that the plots exclude comparisons that were falsely rejected even before any compression was applied. On the **right side** is the rms difference between the crop+compress and the uncompressed comparison scores for each image pair. All computations are driven by the bounding box coordinates reported by the II SDK. The number of bits per pixel is $8/C$, where C is the compression ratio. The iris radius varies and because the cropping margins are fixed multiples of the radius the image size varies. The compressed size, in bytes, is the width times height divided by C . Values of cFNMNR greater than 0.02 are shown as 0.02.

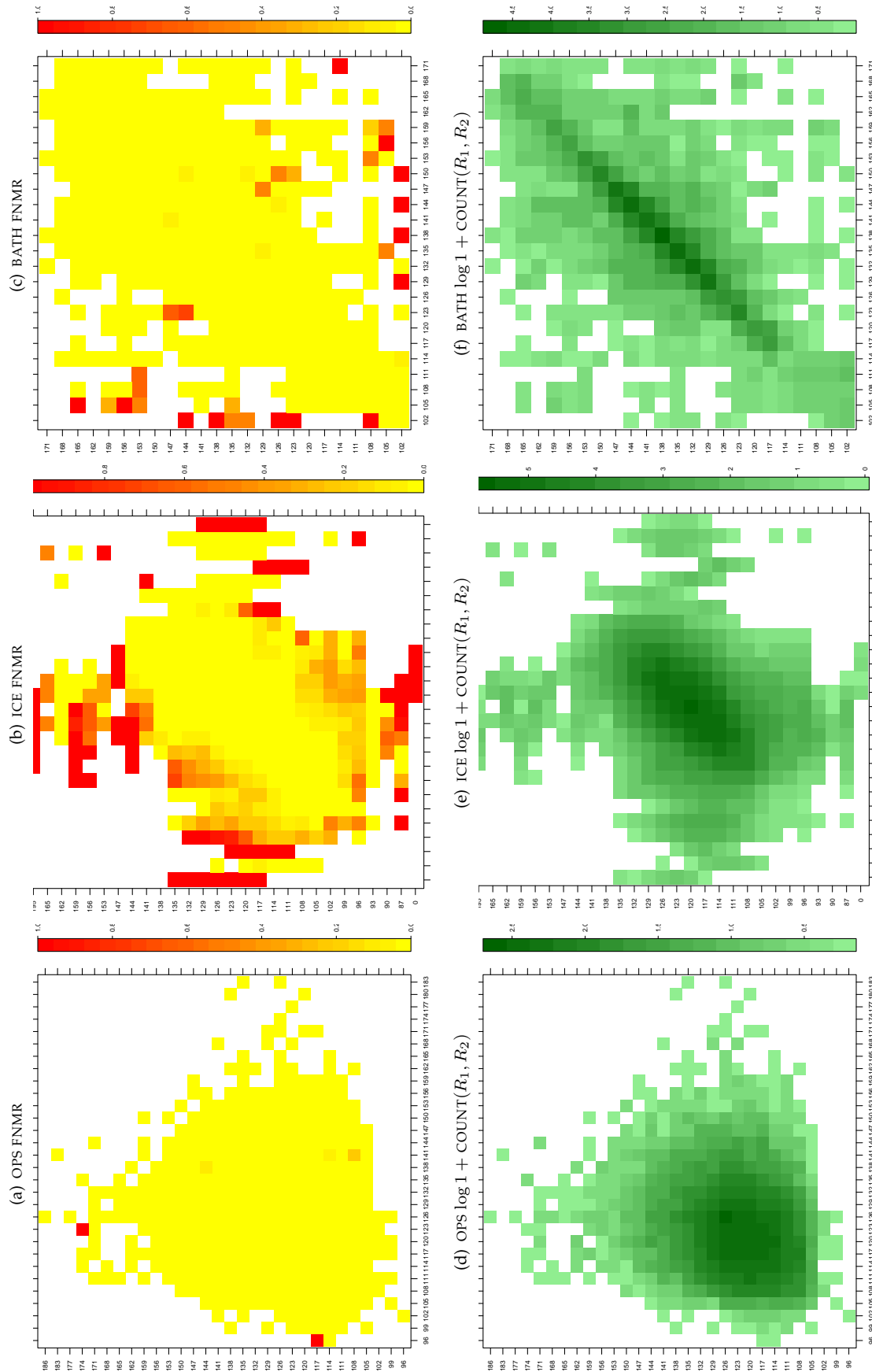


Table 205: For the three IREX databases: In the **top** row the color in each cell represents the occurrence of genuine comparisons with the given pair of radii. The *y*-axis represents enrollment samples with verification samples on the *x*-axis; In the **bottom** row the color scale plots $\log 1 + \text{COUNT}(R_1, R_2)$. The radii are quantized into three-pixel bins. The radii for DOD are on the range $96 \leq r \leq 186$ pixels. The radii for ICE are on the range $87 \leq r \leq 165$ pixels. The radii for BATH are on the range $100 \leq r \leq 170$ pixels.

A = SAGEM	B = COGENT	C = CROSSMATCH	D = CAMBRIDGE	E = L1	$x1$ = PRIMARY
F = RETICA	G = LG	H = HONEYWELL	I = IRITECH	J = NEUROTECHNOLOGY	$x2$ = SECONDARY
KIND 1 = RAW 640x480		KIND 3 = CROP		KIND 7 = CROP+MASK	
KIND 16 = CONCENTRIC POLAR					

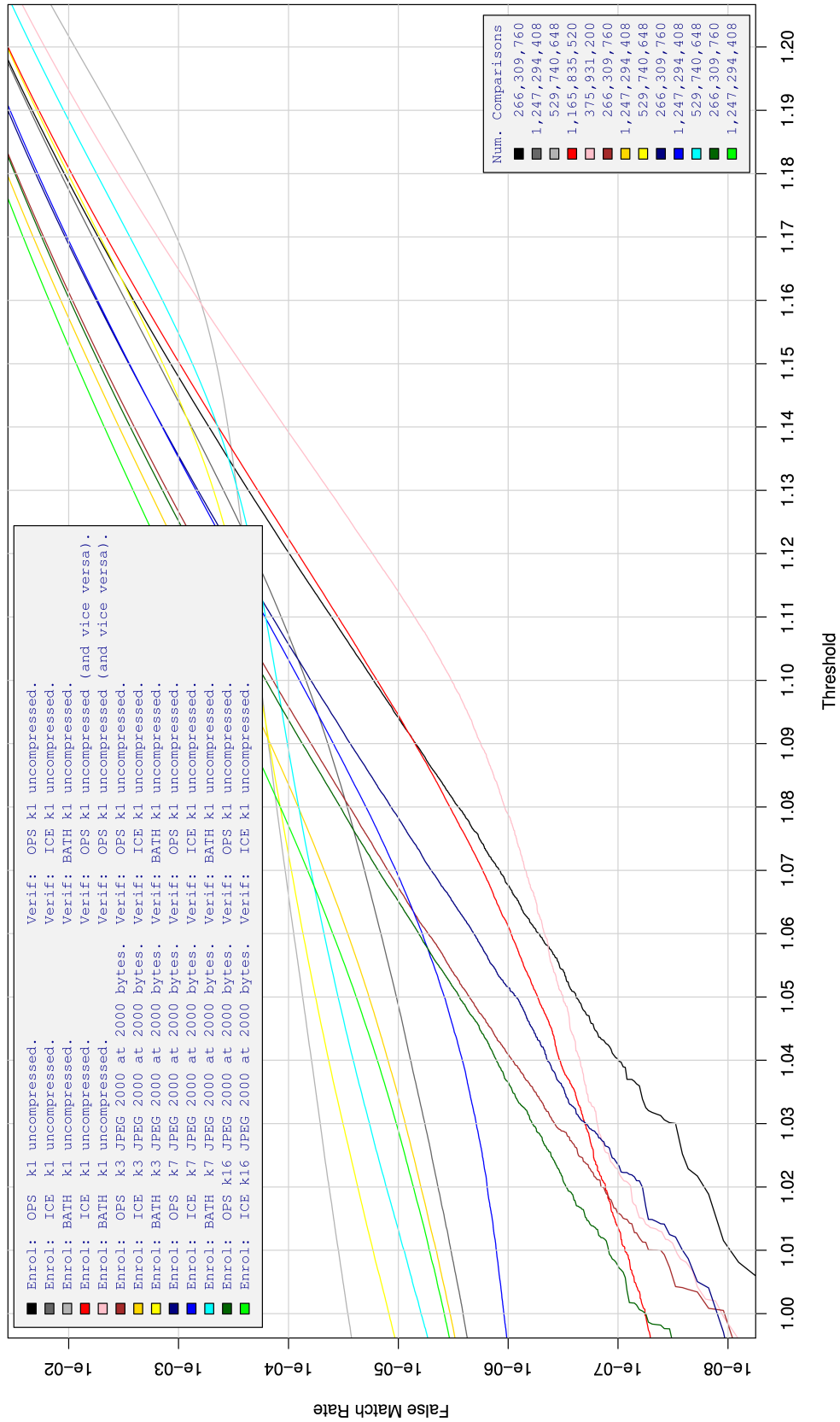


Table 206: For implementation I2, the dependency of FMR on threshold. for various combinations of enrollment and verification dataset, format, and compression.

A = SAGEM	B = COGENT	C = CROSSMATCH	D = CAMBRIDGE	E = L1	x1 = PRIMARY
F = RETICA	G = LG	H = HONEYWELL	I = IRITECH	J = NEUROTECHNOLOGY	x2 = SECONDARY
KIND 1 = RAW 640x480		KIND 3 = CROP		KIND 7 = CROP+MASK	
KIND 16 = CONCENTRIC POLAR					

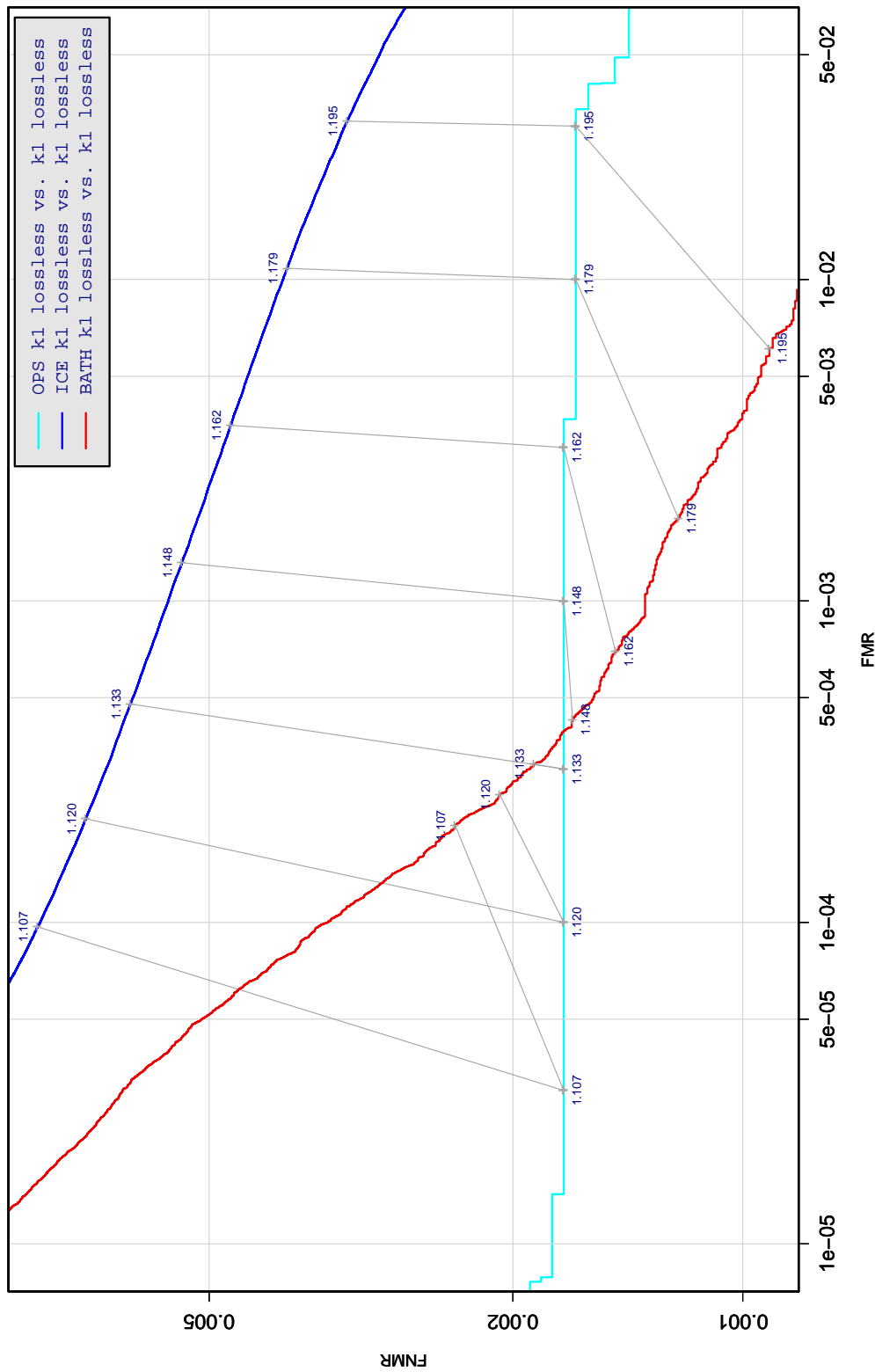


Table 207: DET curve for implementation I2 on three IREX databases. All comparisons are with uncompressed KIND 1 vs. KIND 1 images. The lines join points corresponding to the a fixed threshold. Non-vertical links indicate a change in FMR when the database changes. All results apply to native operation. Failures to produce a template i.e. FTE are ignored because the plots are intended to show *matching* effects, specifically to compare DET slopes and to show the effect of fixing a threshold.

A = SAGEM	B = COGENT	C = CROSSMATCH	D = CAMBRIDGE	E = L1	x1 = PRIMARY
F = RETICA	G = LG	H = HONEYWELL	I = IRITECH	J = NEUROTECHNOLOGY	x2 = SECONDARY
KIND 1 = RAW 640x480		KIND 3 = CROP	KIND 7 = CROP+MASK	KIND 16 = CONCENTRIC POLAR	

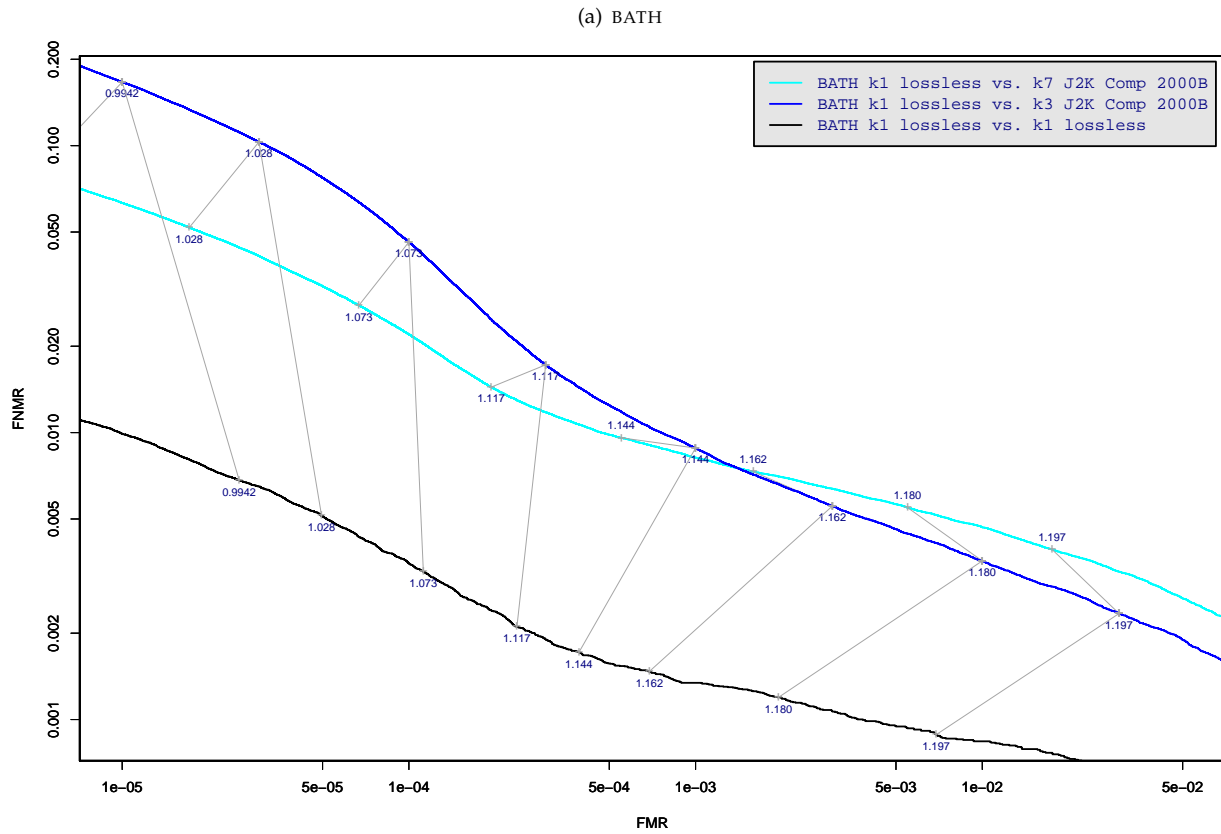


Table 208: DET curve for implementation I2 on the BATH database for the various supported KINDS . The DET characteristics are linked by lines joining points of equal threshold. Non-vertical links indicate a change in false acceptance when the data KIND changes. All results apply to native operation, and the effects of FTE are included.

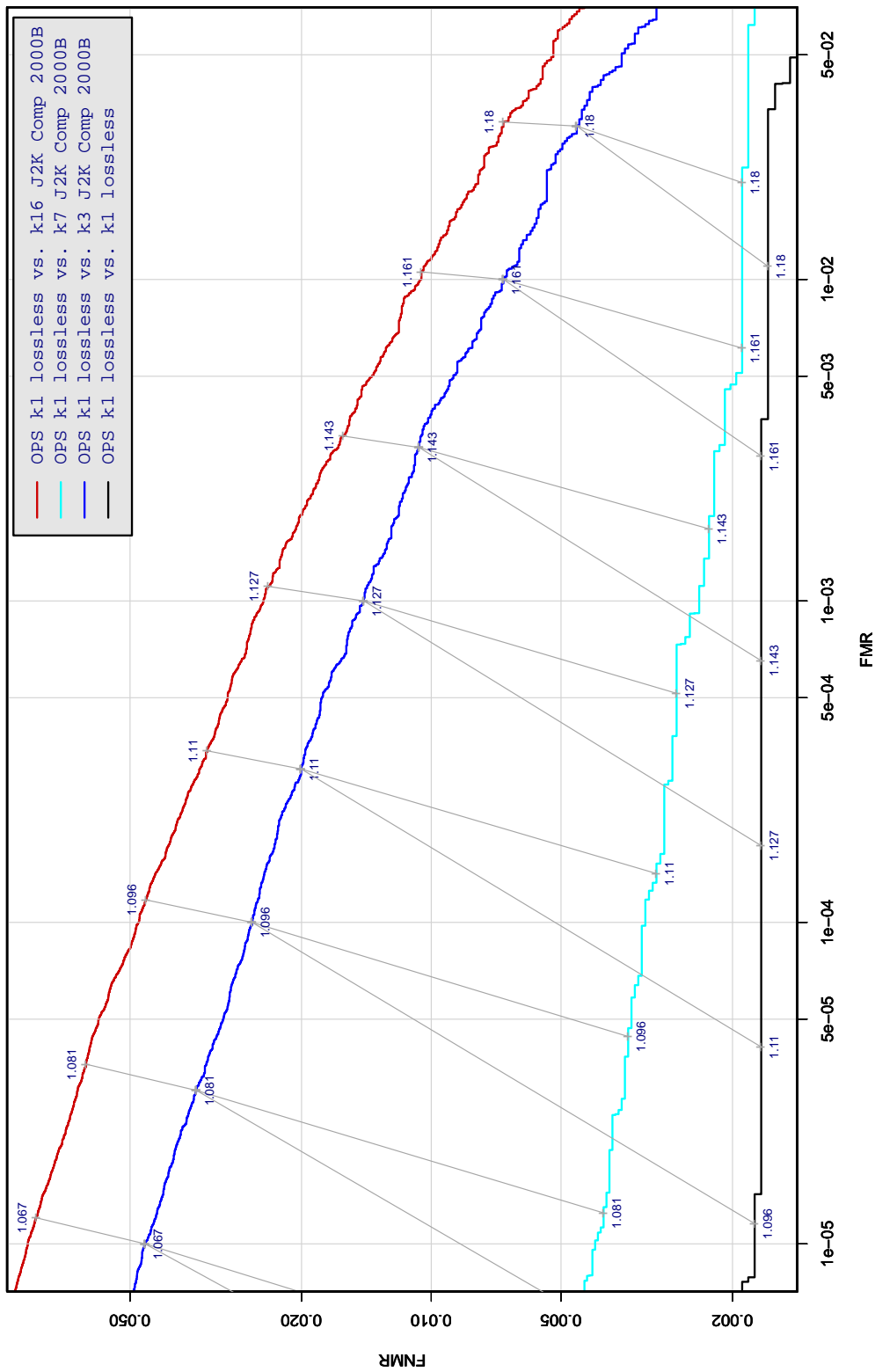


Table 209: DET curve for implementation I2 on the OPS database for the various supported KINDS . The DET characteristics are linked by lines joining points of equal threshold. Non-vertical links indicate a change in false acceptance when the data KIND changes. All results apply to native operation, and the effects of FTE are included.

A = SAGEM	B = COGENT	C = CROSSMATCH	D = CAMBRIDGE	E = L1	x1 = PRIMARY
F = RETICA	G = LG	H = HONEYWELL	I = IRITECH	J = NEUROTECHNOLOGY	x2 = SECONDARY
KIND 1 = RAW 640x480		KIND 3 = CROP	KIND 7 = CROP+MASK	KIND 16 = CONCENTRIC POLAR	

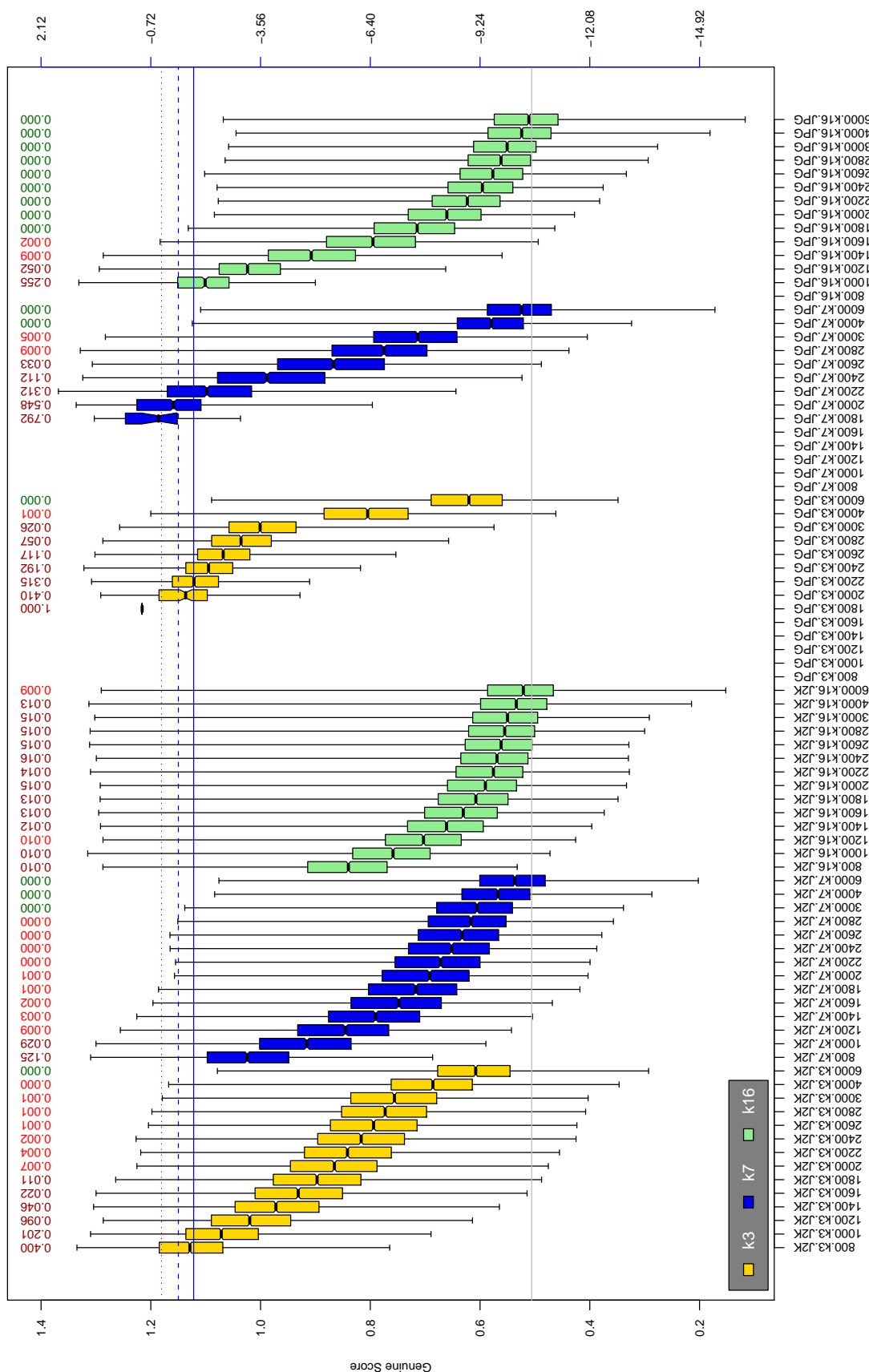


Table 210: The distribution of 12 native genuine comparison scores by size of the compressed image, KIND and the compression algorithm. The images are from the OPS dataset. The right axis scale gives the corresponding value for $d' = (s - \mu_I) / \sqrt{0.5(\sigma_I^2 + \sigma_C^2)}$ for genuine score s . The boxplots only include comparison scores if the uncompressed version of the same image was matched below the FMR = 0.001 threshold. Above the boxplots are FNMR values at FMR = 10^{-3} . The three blue lines correspond, from the top, to FMR of 10^{-2} , 10^{-3} , 10^{-4} . The lower grey line refers to the median score obtained from comparison of uncompressed KIND 3 images. Any comparison for which either template had not been generated is excluded. Note that the iris record size on the horizontal axis is not evenly spaced above 3000 bytes.

A = SAGEM	B = COGENT	C = CROSSMATCH	D = CAMBRIDGE	E = L1	$x1$ = PRIMARY
F = RETICA	G = LG	H = HONEYWELL	I = IRITECH	J = NEUROTECHNOLOGY	$x2$ = SECONDARY
KIND 1 = RAW 640x480		KIND 3 = CROP	KIND 7 = CROP+MASK	KIND 16 = CONCENTRIC POLAR	

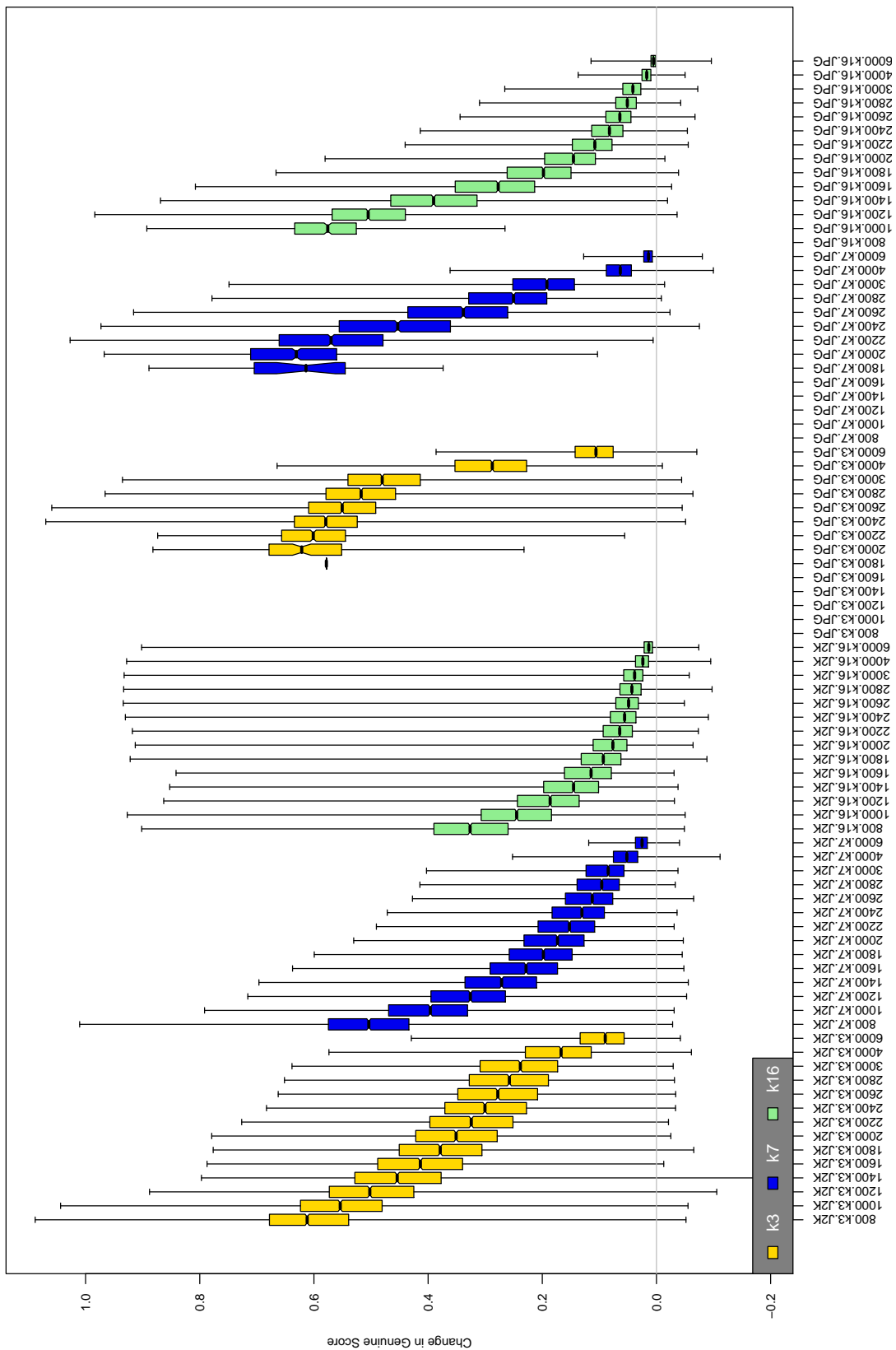


Table 211: The distribution of the *increase* in 12 native genuine comparison scores between the uncompressed “parent” and the compressed image, arranged by size, KIND and the compression algorithm. The images are from the OPS dataset. Any comparison involving a failed template is excluded. Note that the iris record size on the horizontal axis is not evenly spaced above 3000 bytes.

A = SAGEM	B = COGENT	C = CROSSMATCH	D = CAMBRIDGE	E = L1	x1 = PRIMARY
F = RETICA	G = LG	H = HONEYWELL	I = IRITECH	J = NEUROTECHNOLOGY	x2 = SECONDARY
KIND 1 = RAW 640x480		KIND 3 = CROP		KIND 7 = CROP+MASK	KIND 16 = CONCENTRIC POLAR

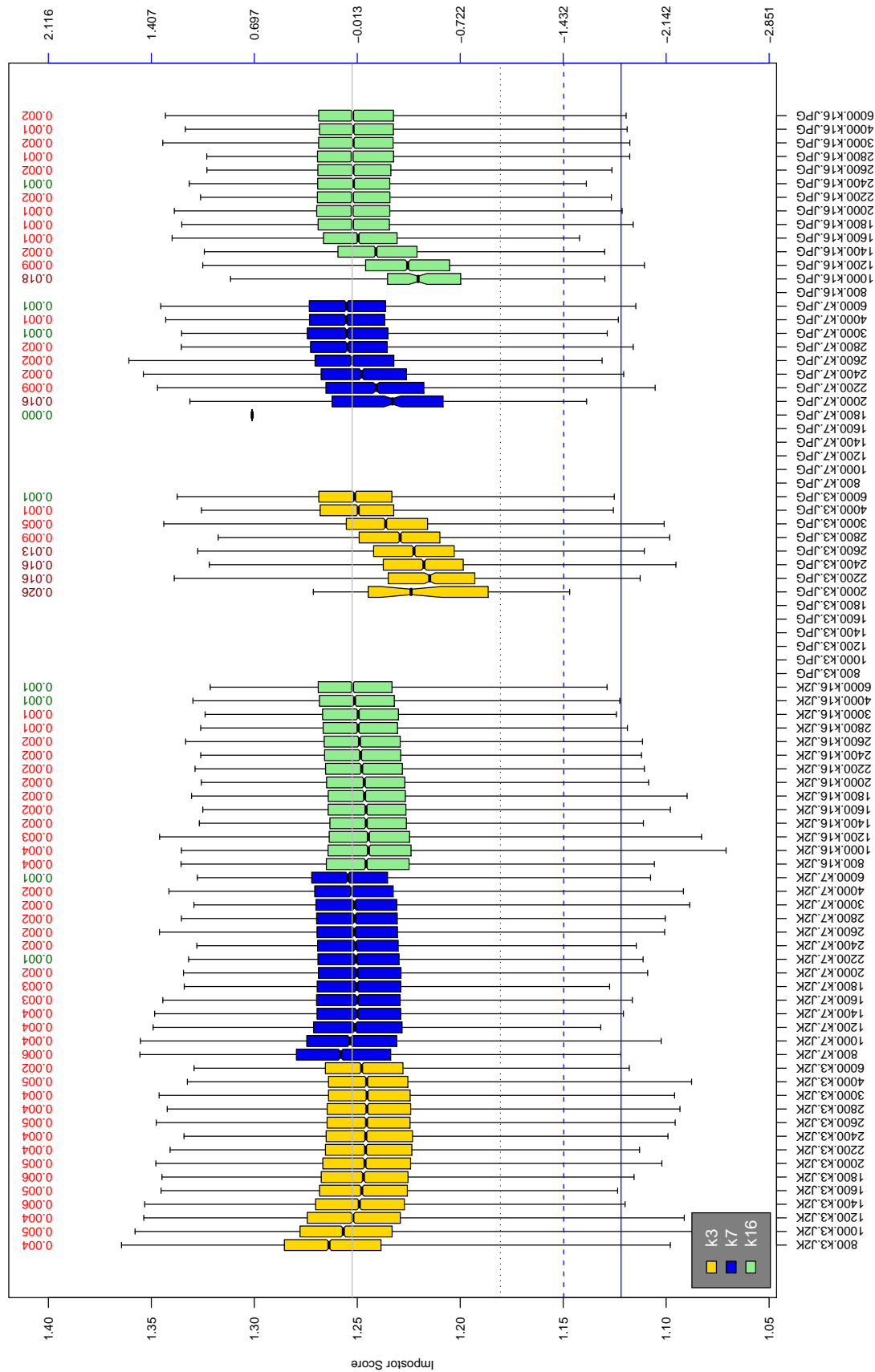


Table 212: The distribution of 12 native impostor comparison scores by size of the compressed image, KIND and the compression algorithm. The right axis scale gives the corresponding value for $d' = (s - \mu_1) / \sqrt{0.5(\sigma_1^2 + \sigma_2^2)}$ for impostor score s . The three blue lines correspond, from the top, to FMR of $10^{-2}, -3, -4$. The lower grey line refers to the median score obtained from comparison of uncompressed KIND 3 images. Any comparison involving a failed template is excluded. Above the boxplots are FMR values at the threshold that gives FMR = 10^{-3} on uncompressed images. These figures are computed from only 4000 comparisons so the FMR values and the tails of the impostor distribution are poorly characterized. Note that the iris record size on the horizontal axis is not evenly spaced above 3000 bytes.

A = SAGEM	B = COGENT	C = CROSSMATCH	D = CAMBRIDGE	E = L1	x_1 = PRIMARY
F = RETICA	G = LG	H = HONEYWELL	I = IRITECH	J = NEUROTECHNOLOGY	x_2 = SECONDARY
KIND 1 = RAW 640x480		KIND 3 = CROP	KIND 7 = CROP+MASK	KIND 16 = CONCENTRIC POLAR	

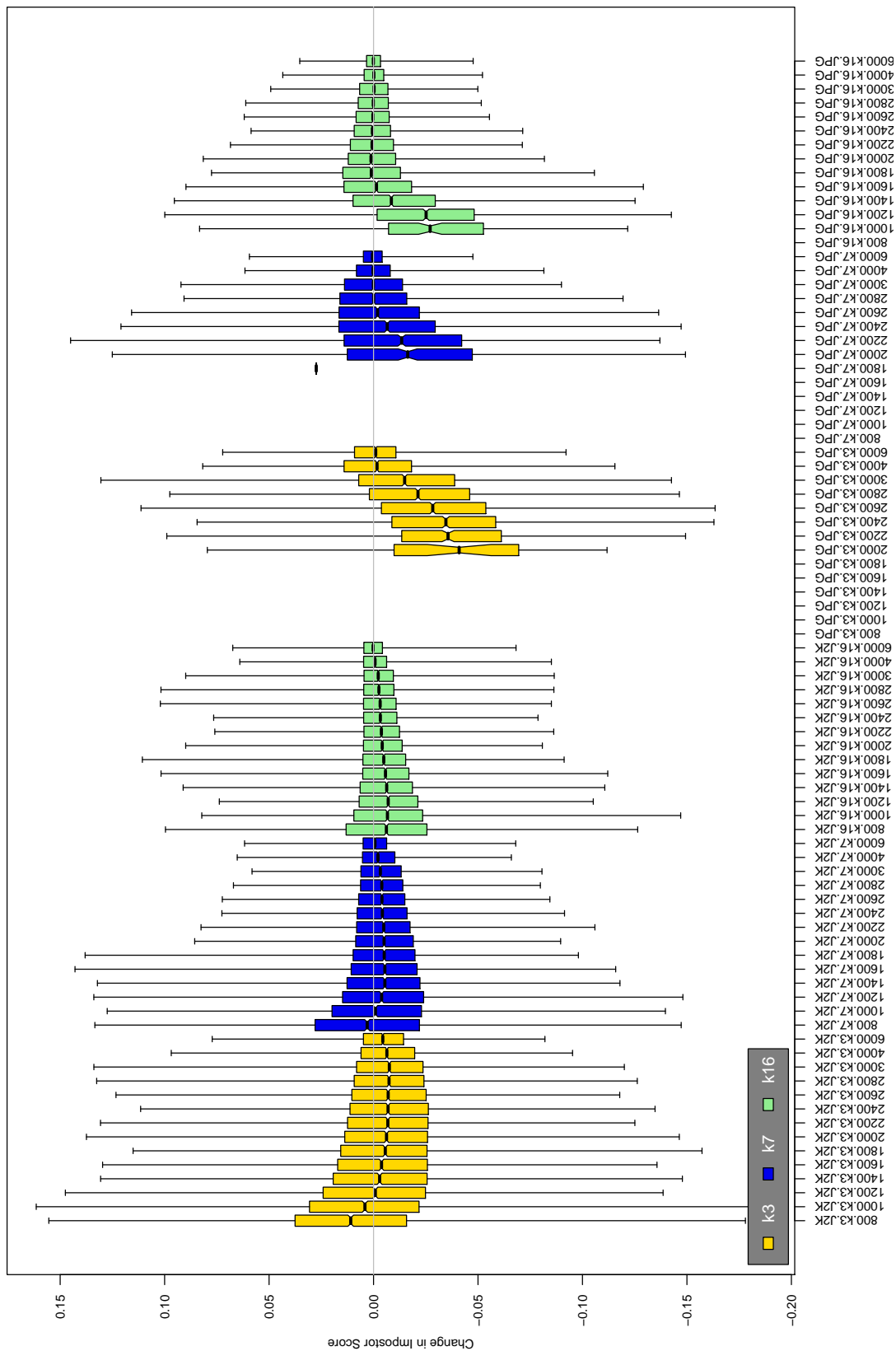


Table 213: The distribution of the increase in 12 native impostor comparison scores between the uncompressed “parent” and the compressed image, arranged by size, KIND and the compression algorithm. The images are from the OPS dataset. Any comparison involving a failed template is excluded. Note that the iris record size on the horizontal axis is not evenly spaced above 3000 bytes.

A = SAGEM	B = COGENT	C = CROSSMATCH	D = CAMBRIDGE	E = L1	x1 = PRIMARY
F = RETICA	G = LG	H = HONEYWELL	I = IRITECH	J = NEUROTECHNOLOGY	x2 = SECONDARY
KIND 1 = RAW 640x480		KIND 3 = CROP		KIND 7 = CROP+MASK	KIND 16 = CONCENTRIC POLAR

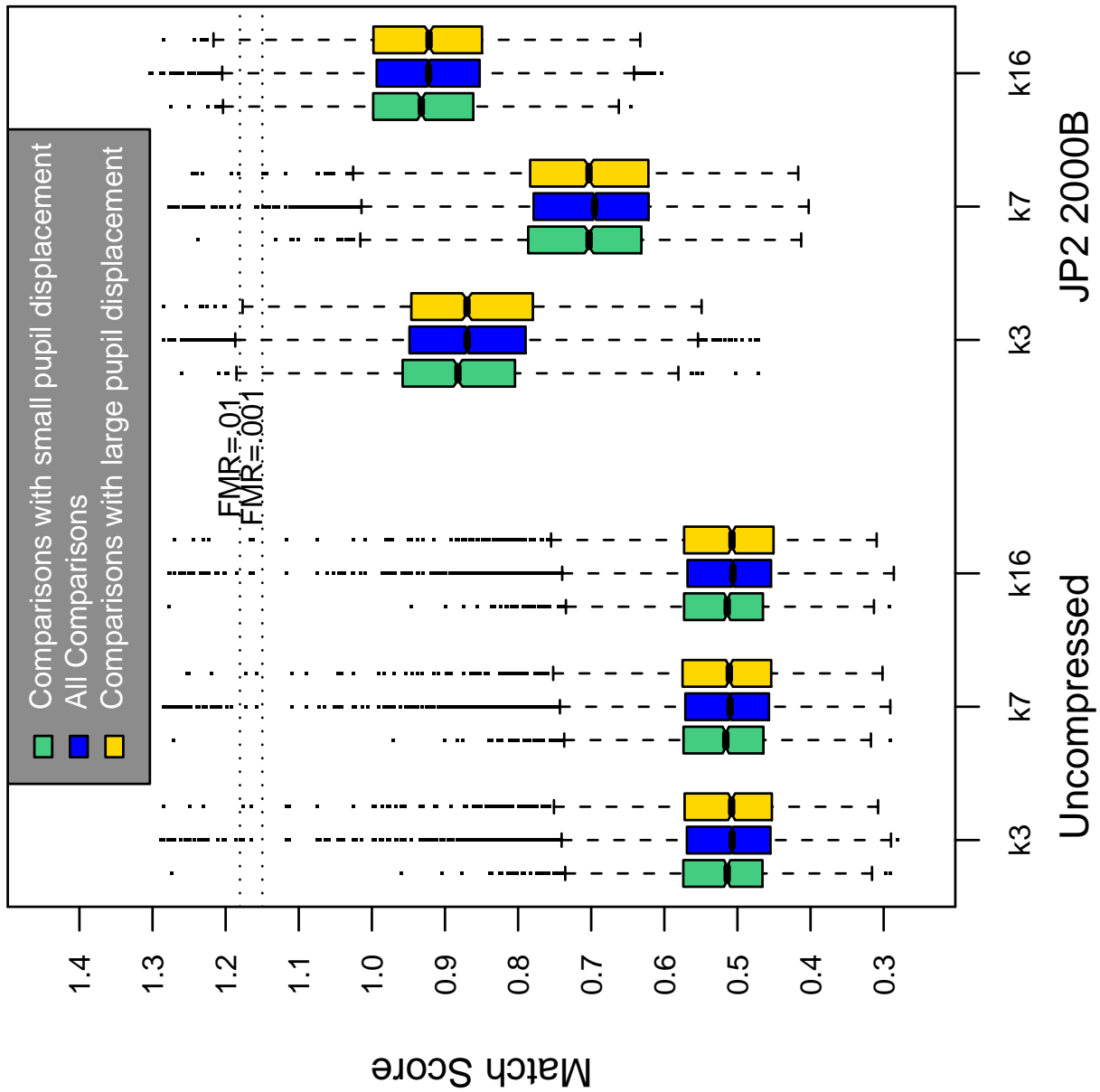


Table 214: Effect of pupil displacement on the genuine score distribution for I2

A = SAGEM	B = COGENT	C = CROSSMATCH	D = CAMBRIDGE	E = L1	x1 = PRIMARY
F = RETICA	G = LG	H = HONEYWELL	I = IRITECH	J = NEUROTECHNOLOGY	x2 = SECONDARY
KIND 1 = RAW 640x480		KIND 3 = CROP	KIND 7 = CROP+MASK	KIND 16 = CONCENTRIC POLAR	

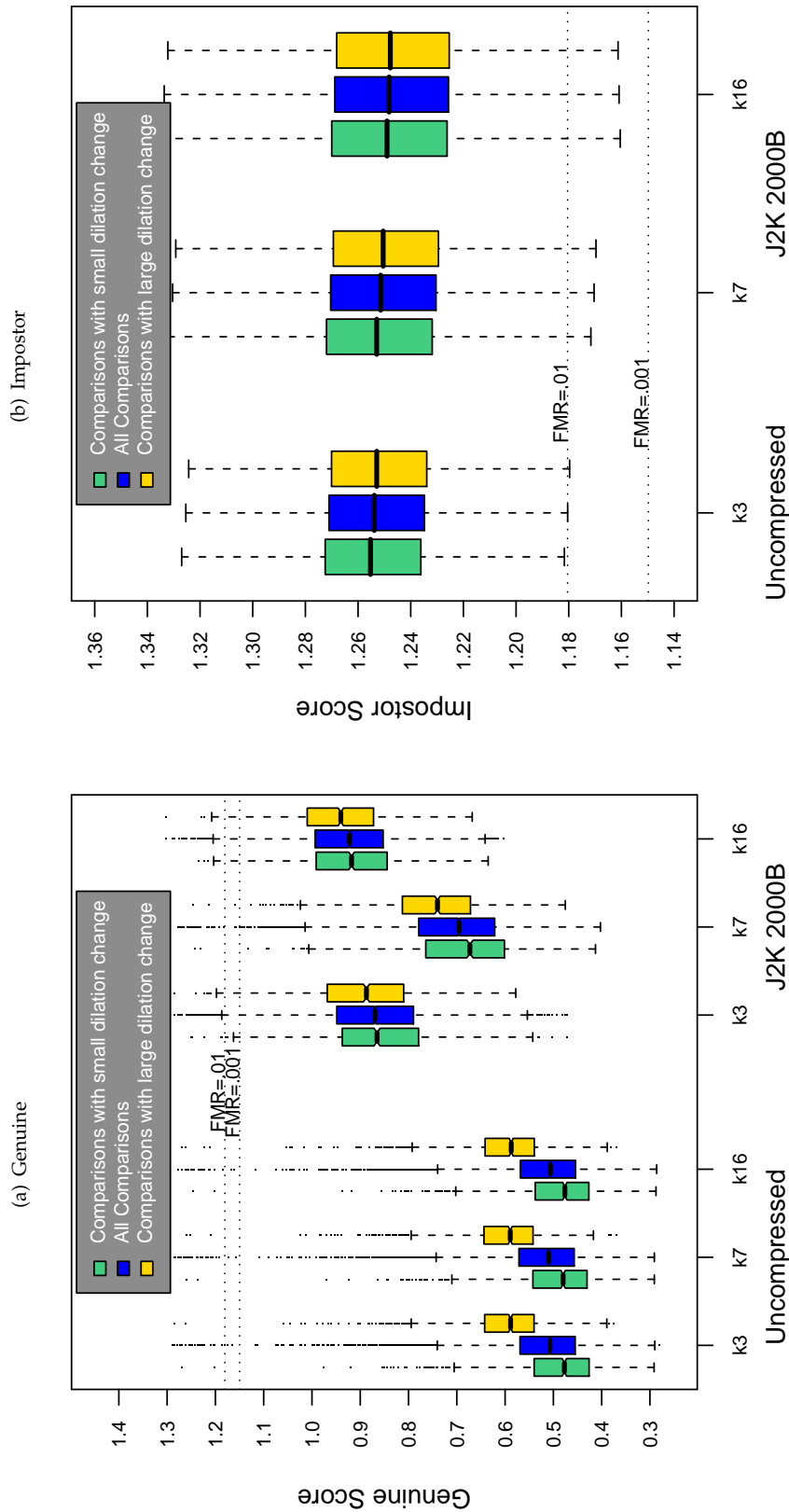


Table 215: The effect of dilation change on the two scores distributions for SDK 12.

A = SAGEM	B = COGENT	C = CROSSMATCH	D = CAMBRIDGE	E = L1	x1 = PRIMARY
F = RETICA	G = LG	H = HONEYWELL	I = IRITECH	J = NEUROTECHNOLOGY	x2 = SECONDARY
KIND 1 = RAW 640x480		KIND 3 = CROP	KIND 7 = CROP+MASK	KIND 16 = CONCENTRIC POLAR	

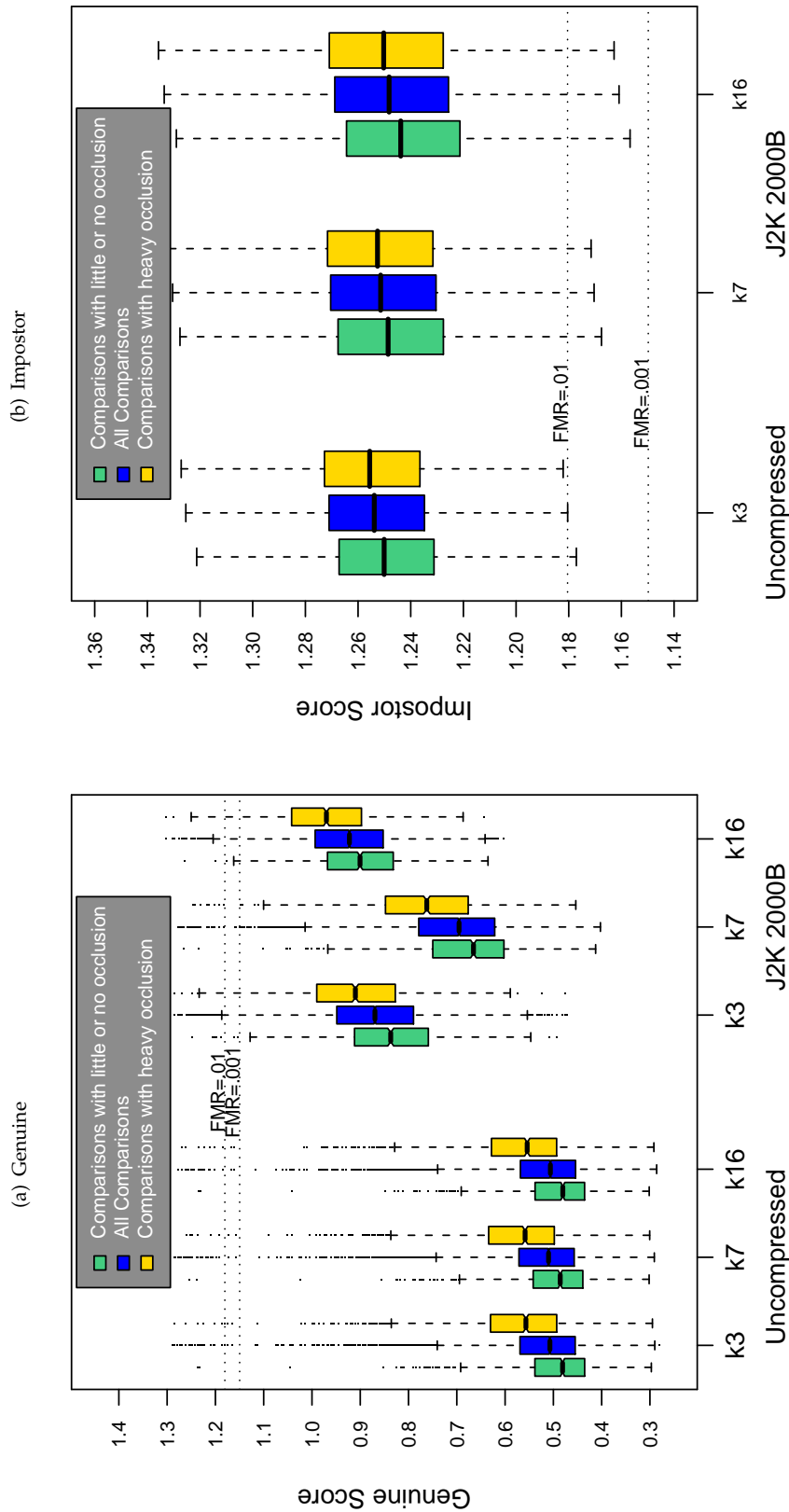
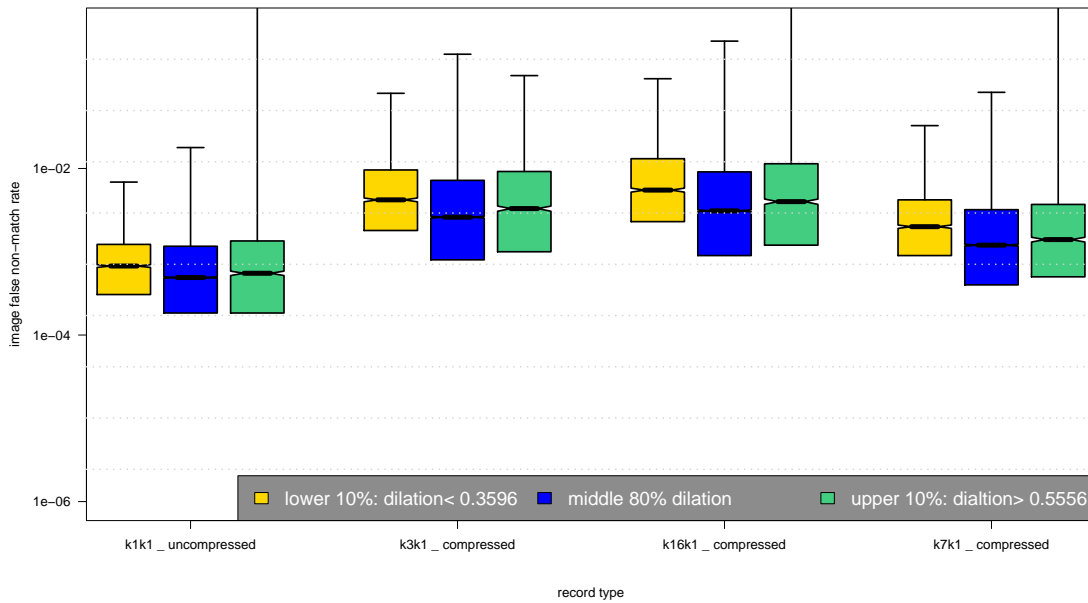
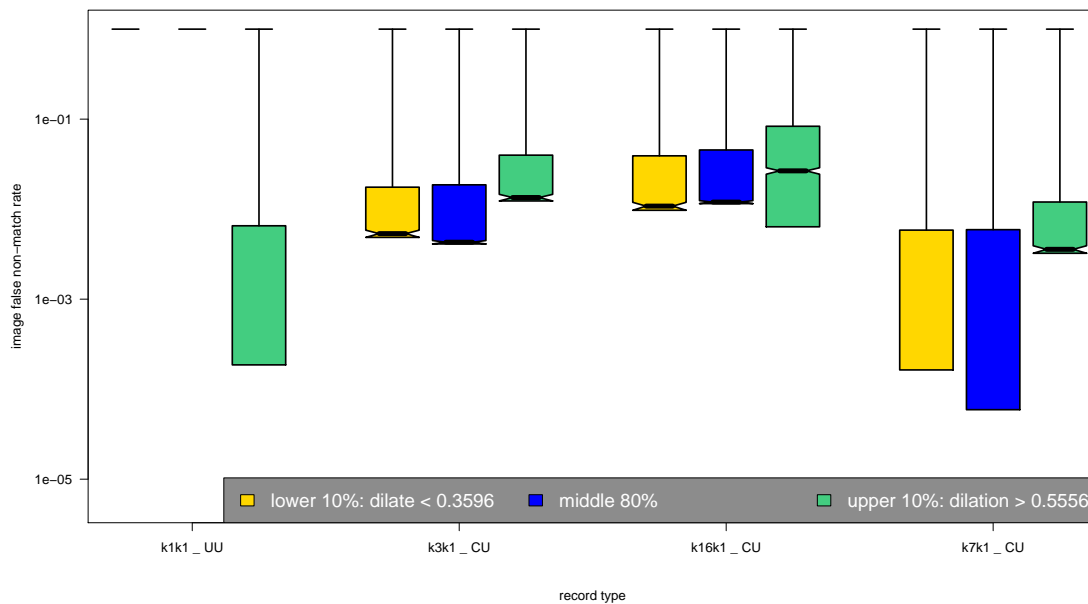


Table 216: The effect of eyelid occlusion on the two scores distributions for SDK 12.

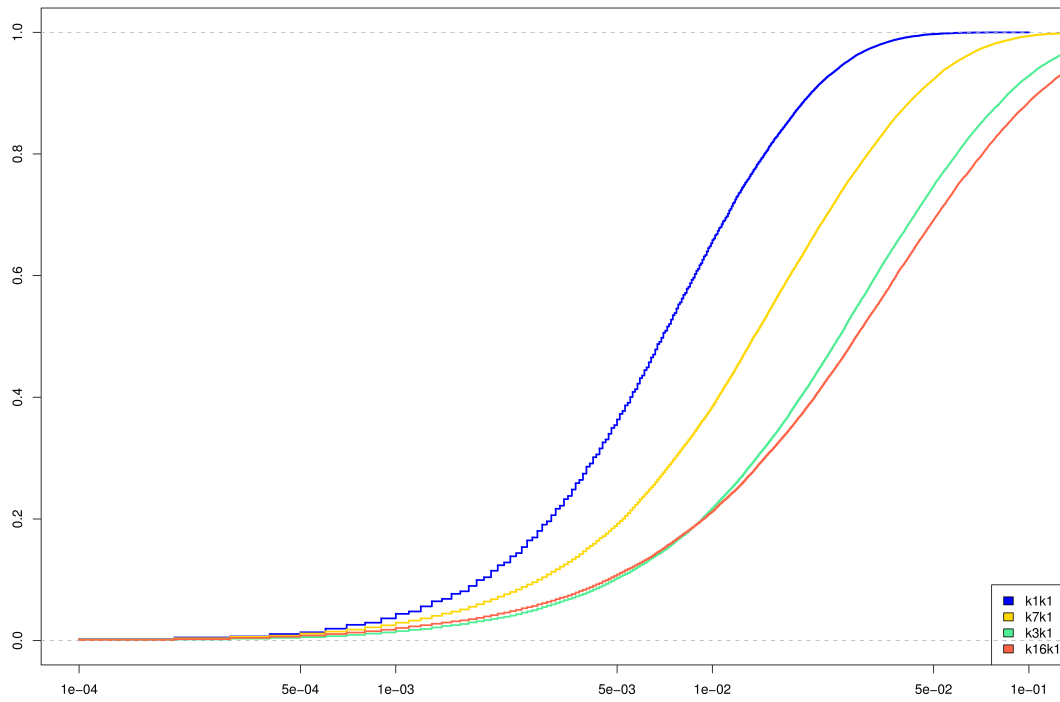
(a) iFMR using A1 dilation estimates



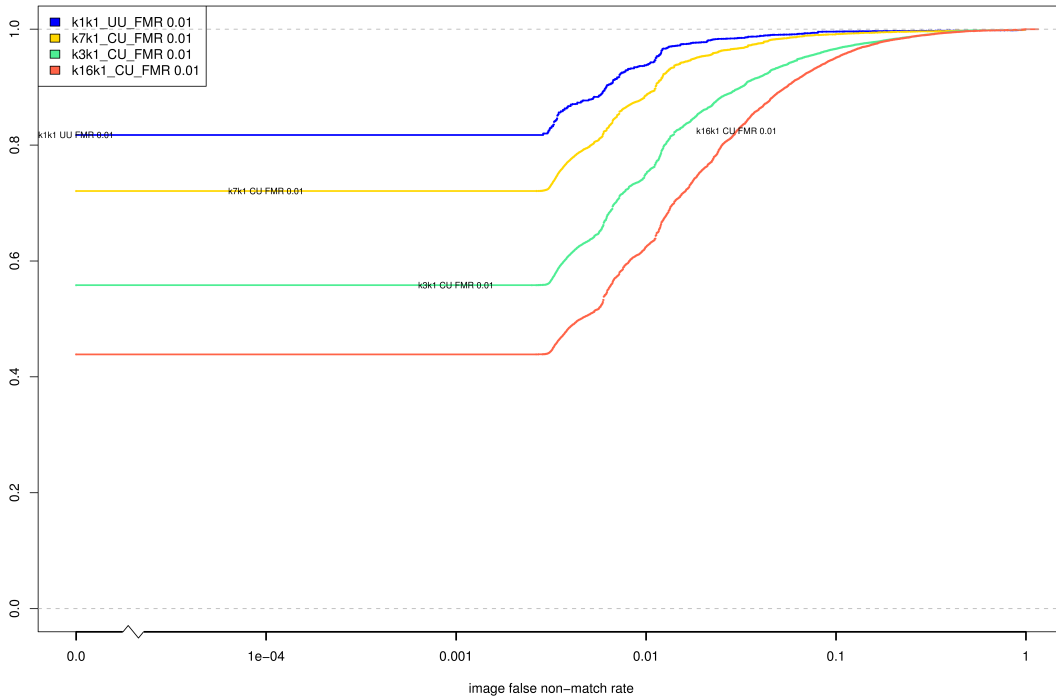
(b) iFNMR using A1 dilation estimates



(c) iFMR CDF



(d) iFNMR CDF



Compiled Results for Implementation J1

On June 25, 2009, NIST invited the IREX participants to submit a description of the SDKs submitted for the IREX effort. The intent was to allow providers to describe and contrast the feature sets, optimization, operational suitability and availability of the primary and secondary SDKs. NIST indicated that any submitted text would appear verbatim (with typesetting) in draft and final versions of the IREX report and that it would be attributed to the organization. This was optional and NIST put no constraints on the content beyond a 600 word limit, and a statement that anything labelled as confidential or proprietary would be omitted.

The provider of SDK J1, Neurotechnology, submitted the following to NIST - we are unable to validate this information.

Neurotechnology provides algorithms and software development products for fingerprint, face, iris and multi-modal biometrical identification, computer-based vision and object recognition to security companies, system integrators and hardware manufacturers. More than 2,000 system integrators and sensor providers in 98 countries license and integrate Neurotechnology products into their own applications, with millions of end-user installations worldwide.

VeriEye 2.1 algorithm implements advanced iris segmentation, enrollment and matching using robust digital image processing algorithms:

1. Robust eye iris detection. Irises are detected even when the images have obstructions, visual noise and different levels of illumination. Lighting reflections, eyelids and eyelashes obstructions are eliminated. Images with narrowed eyelids are also accepted.
2. Gazing-away iris images are correctly detected, segmented and transformed as if it were looking directly into the camera.
3. VeriEye uses active shape models that more precisely model the contours of the eye, as iris boundaries are not modeled by perfect circles.
4. Fast matching. Configurable matching speed varies from 50,000 to 150,000 comparisons per second (using only one core of Intel Core 2 Duo running at 2.66 GHz). The highest speed still preserves nearly the same recognition quality.
5. Reliability. VeriEye algorithm showed excellent performance in IREX when used with uncompressed images. This scenario is most common when biometric devices are used.
6. Small template size. One eye iris template size is 2.3kb. This allows to hold millions of records in a regular computer.

VeriEye is available as a software development kit (SDK) that allows development of PC and Web-based solutions on Microsoft Windows, Linux, Mac OS X platforms and various programming languages.

VeriEye SDK supports some third-parties iris cameras. At this report issuing date it supports Cross Match I Scan 2, Retica Mobile-Eyes, VistaFA2 Multimodal Iris & Face Camera as well as image input from other devices. We are looking for the opportunity to cooperate with other hardware manufacturers and support their devices.

VeriEye SDKs are available with highly competitive licensing options through Neurotechnology or from distributors worldwide. VeriEye Standard SDK costs 790 euros, and Extended SDK 1,290 euros. Prices for end-user product installation licenses depend on quantity and are in range from 396 to 43 euros or less per computer.

For more information and 30 days SDK trial downloads: www.neurotechnology.com.

A = SAGEM	B = COGENT	C = CROSSMATCH	D = CAMBRIDGE	E = L1	x1 = PRIMARY
F = RETICA	G = LG	H = HONEYWELL	I = IRITECH	J = NEUROTECHNOLOGY	x2 = SECONDARY
KIND 1 = RAW 640x480		KIND 3 = CROP		KIND 7 = CROP+MASK	
KIND 16 = CONCENTRIC POLAR					

IREX report showed that VeriEye constantly performed along with top algorithms except for the BATH dataset which provided iris images of unusually large irises radii. This was unexpected for VeriEye segmentation algorithm and ~2% of Failure to Enroll rate gave high False Rejection Rate of ~2.5% at zero False Acceptance Rate.

On August 17, 2009, NIST invited the IREX participants to submit a description their comments on a draft version of the IREX report. This was intended to allow participants to assist readers in the interpretation of a large and complicated testing effort. NIST indicated that any submitted text would appear verbatim (with typesetting) in the final version of the IREX report and that it would be attributed to the organization. Submission of content was optional and NIST put no constraints on the content beyond a word limit, and a statement that anything labelled as confidential or proprietary would be omitted.

The provider of SDK J1, Neurotechnology, elected not to submit any information

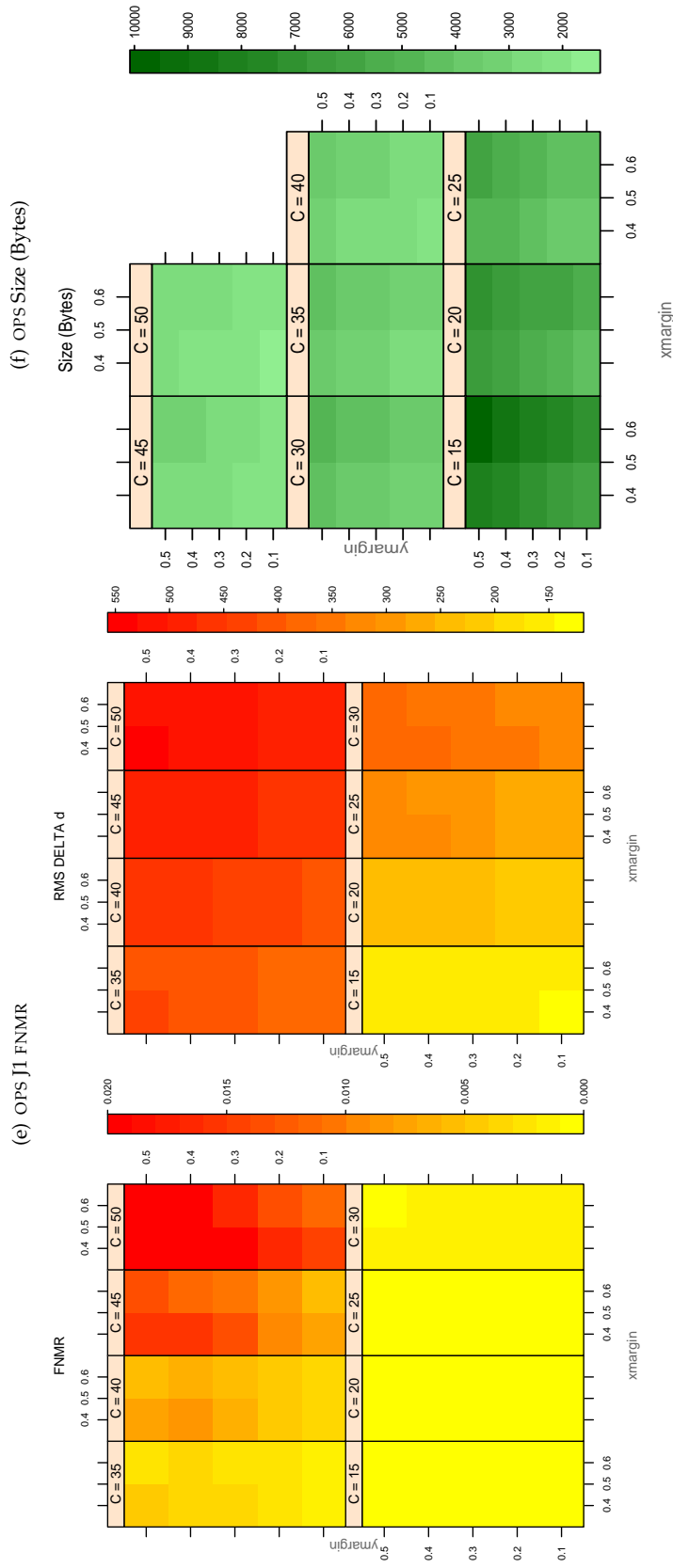


Table 217: For the IREX partition of the OPS database the plots at left show the dependence of cFNMR on the vertical and horizontal iris cropping margins for various compression ratios. This applies only for KIND 3 records. The margins are in units of iris radius. The use of conditional FNMR means that the plots exclude comparisons that were falsely rejected even before any compression was applied. On the **right side** is the rms difference between the crop+compress and the uncompressed comparison scores for each image pair. All computations are driven by the bounding box coordinates reported by the II SDK. The number of bits per pixel is $8/C$, where C is the compression ratio. The iris radius varies and because the cropping margins are fixed multiples of the radius the image size varies. The compressed size, in bytes, is the width times height divided by C . Values of cFNMR greater than 0.02 are shown as 0.02.

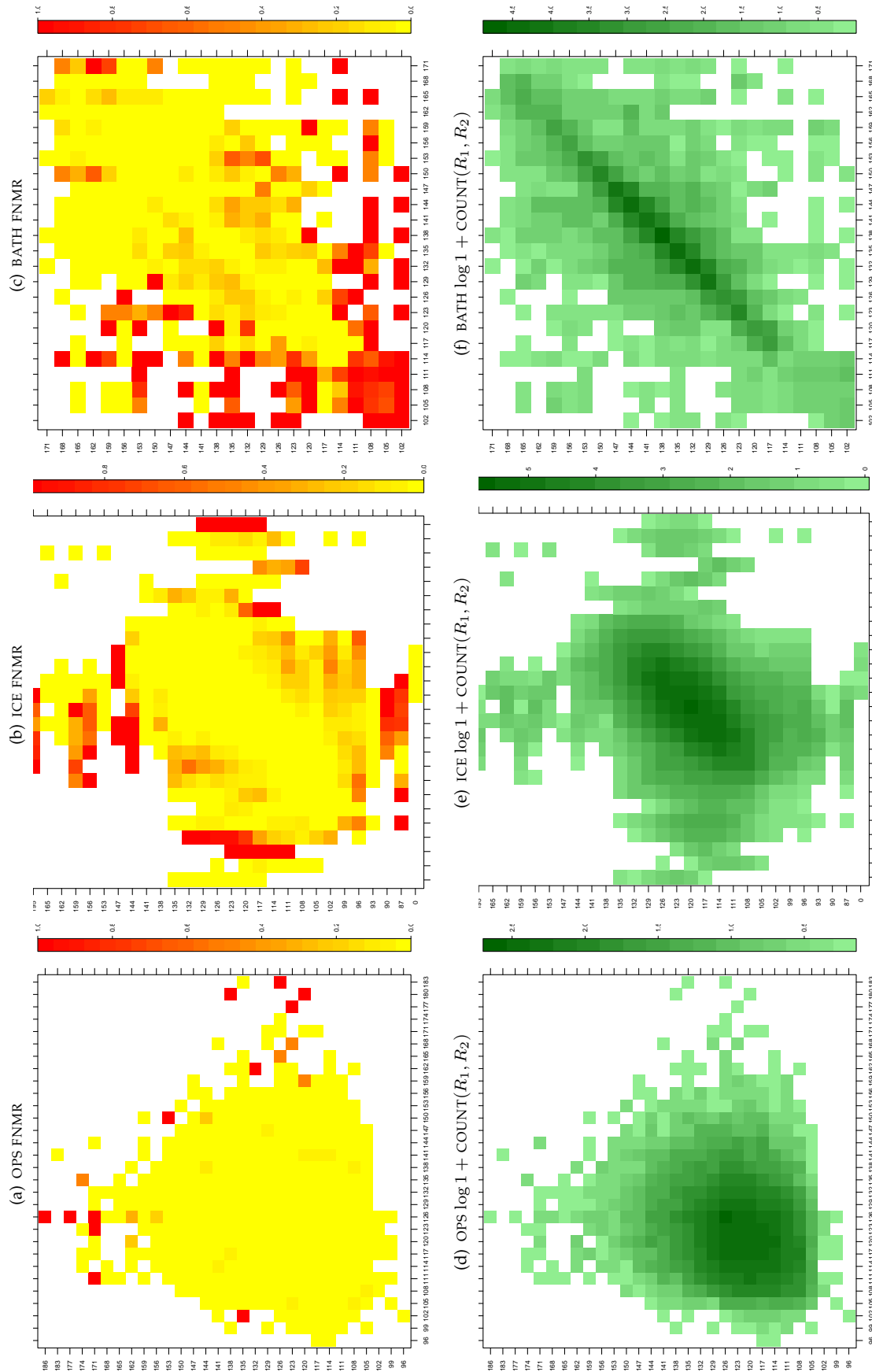


Table 218: For the three IREX databases: In the **top** row the color in each cell represents the occurrence of genuine comparisons with the given pair of radii. The *y*-axis represents enrollment samples with verification samples on the *x*-axis; In the **bottom** row the color scale plots $\log 1 + \text{COUNT}(R_1, R_2)$. The radii are quantized into three-pixel bins. The radii for DOD are on the range $96 \leq r \leq 186$ pixels. The radii for ICE are on the range $87 \leq r \leq 165$ pixels. The radii for BATH are on the range $100 \leq r \leq 170$ pixels.

A = SAGEM	B = COGENT	C = CROSSMATCH	D = CAMBRIDGE	E = L1	$x1$ = PRIMARY
F = RETICA	G = LG	H = HONEYWELL	I = IRITECH	J = NEUROTECHNOLOGY	$x2$ = SECONDARY
KIND 1 = RAW 640x480		KIND 3 = CROP	KIND 7 = CROP+MASK	KIND 16 = CONCENTRIC POLAR	

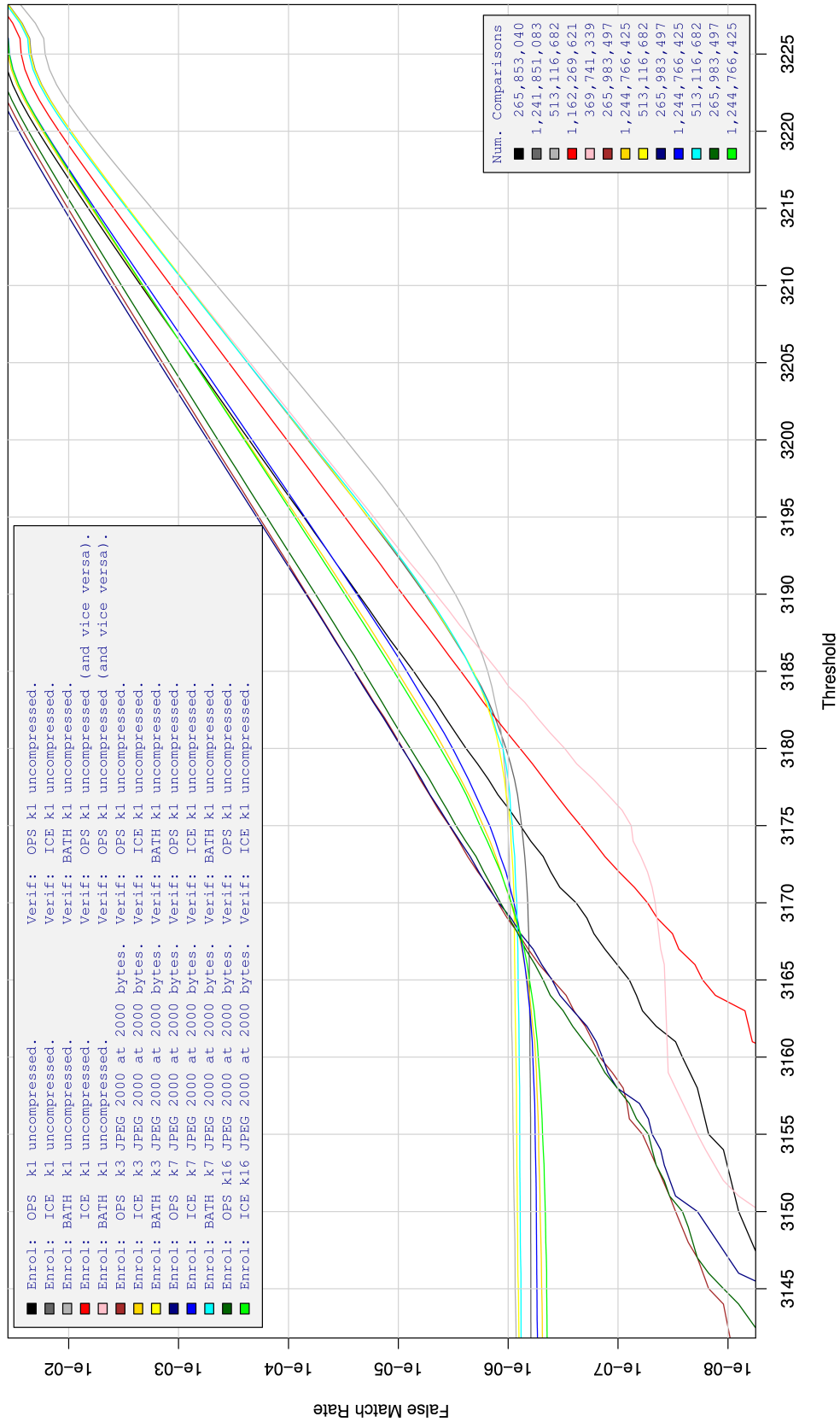


Table 219: For implementation J1, the dependency of FMR on threshold. for various combinations of enrollment and verification dataset, format, and compression.

A = SAGEM	B = COGENT	C = CROSSMATCH	D = CAMBRIDGE	E = L1	x1 = PRIMARY
F = RETICA	G = LG	H = HONEYWELL	I = IRITECH	J = NEUROTECHNOLOGY	x2 = SECONDARY
KIND 1 = RAW 640x480		KIND 3 = CROP		KIND 7 = CROP+MASK	
KIND 16 = CONCENTRIC POLAR					

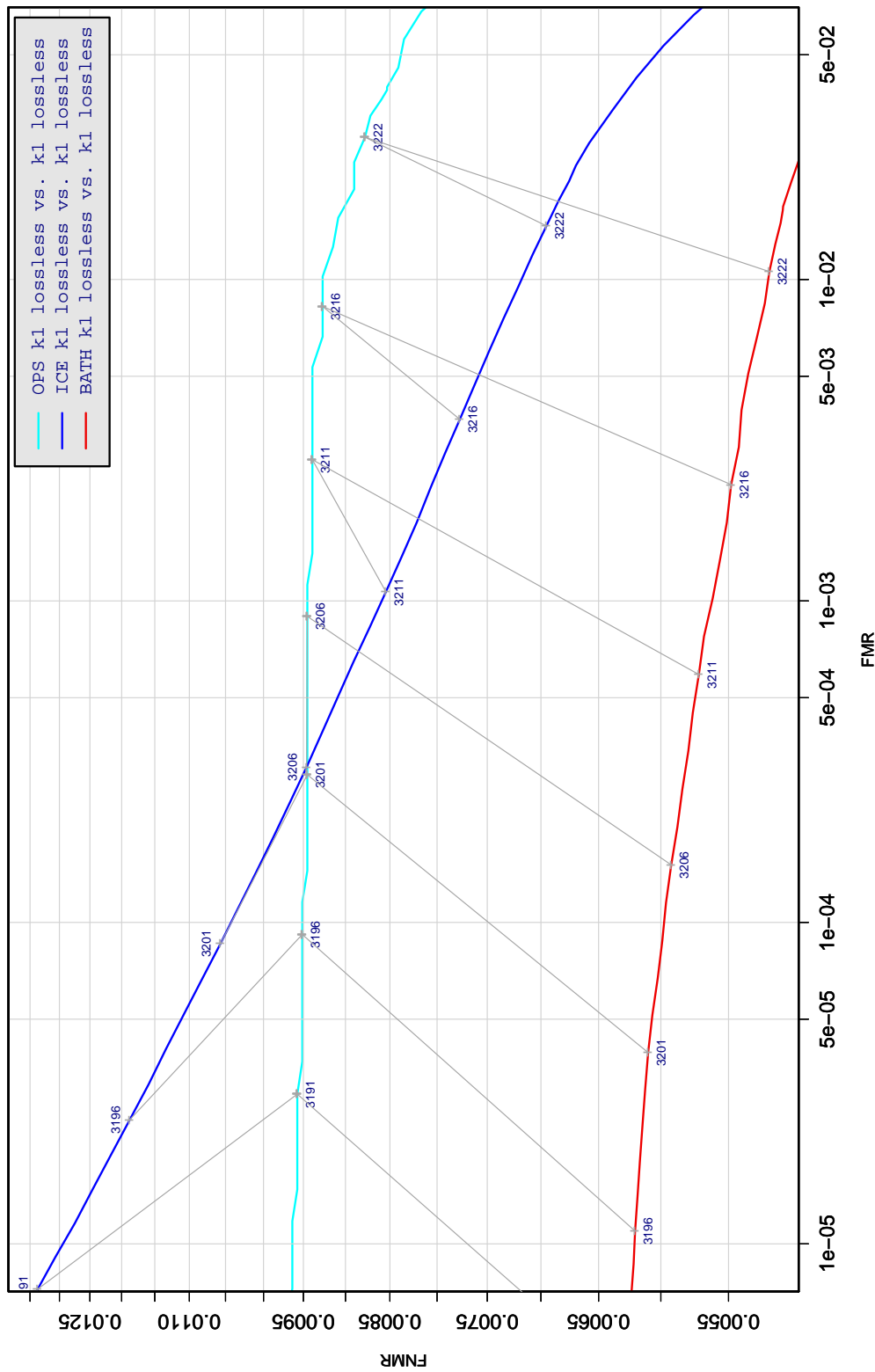


Table 220: DET curve for implementation J1 on three IREX databases. All comparisons are with uncompressed KIND 1 vs. KIND 1 images. The lines join points corresponding to the a fixed threshold. Non-vertical links indicate a change in FMR when the database changes. All results apply to native operation. Failures to produce a template i.e. FTE are ignored because the plots are intended to show *matching* effects, specifically to compare DET slopes and to show the effect of fixing a threshold.

A = SAGEM	B = COGENT	C = CROSSMATCH	D = CAMBRIDGE	E = L1	x1 = PRIMARY
F = RETICA	G = LG	H = HONEYWELL	I = IRITECH	J = NEUROTECHNOLOGY	x2 = SECONDARY
KIND 1 = RAW 640x480		KIND 3 = CROP	KIND 7 = CROP+MASK	KIND 16 = CONCENTRIC POLAR	

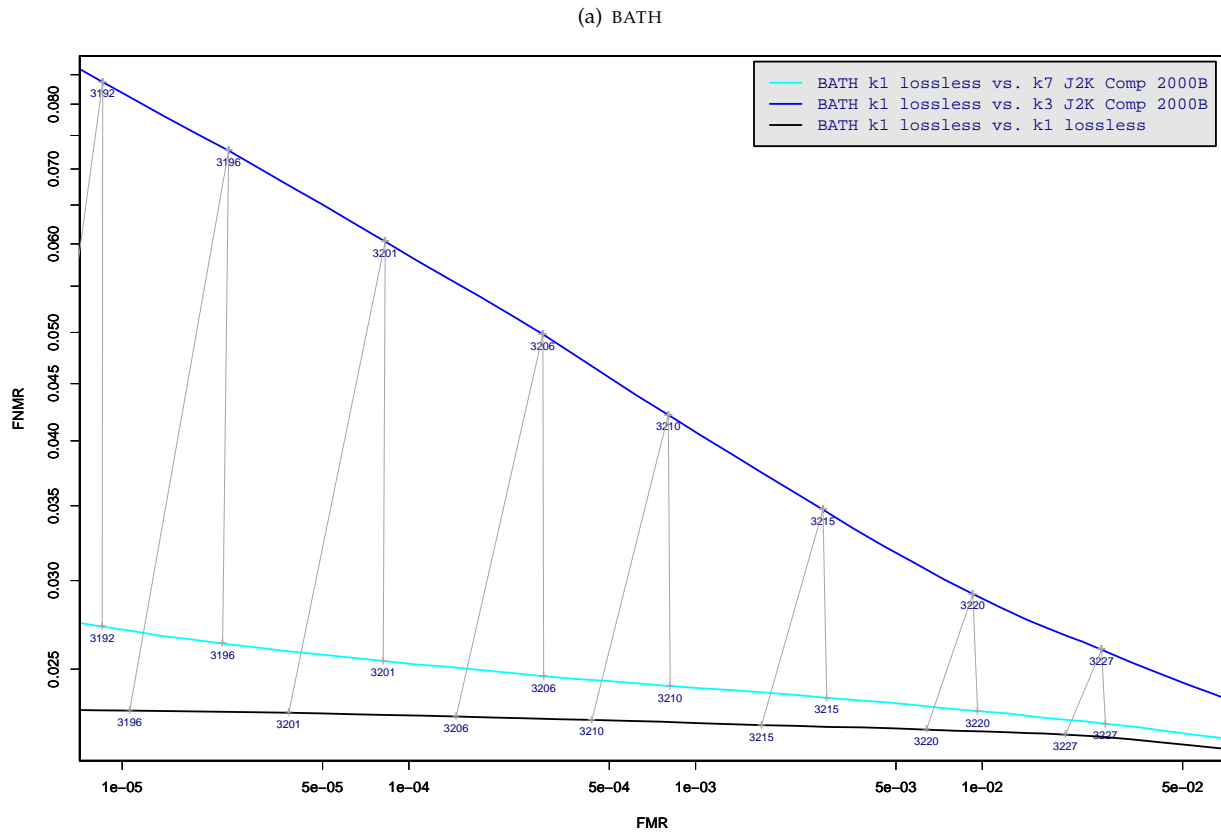


Table 221: DET curve for implementation J1 on the BATH database for the various supported KINDS . The DET characteristics are linked by lines joining points of equal threshold. Non-vertical links indicate a change in false acceptance when the data KIND changes. All results apply to native operation, and the effects of FTE are included.

A = SAGEM	B = COGENT	C = CROSSMATCH	D = CAMBRIDGE	E = L1	$x1$ = PRIMARY
F = RETICA	G = LG	H = HONEYWELL	I = IRITECH	J = NEUROTECHNOLOGY	$x2$ = SECONDARY
KIND 1 = RAW 640x480		KIND 3 = CROP	KIND 7 = CROP+MASK	KIND 16 = CONCENTRIC POLAR	

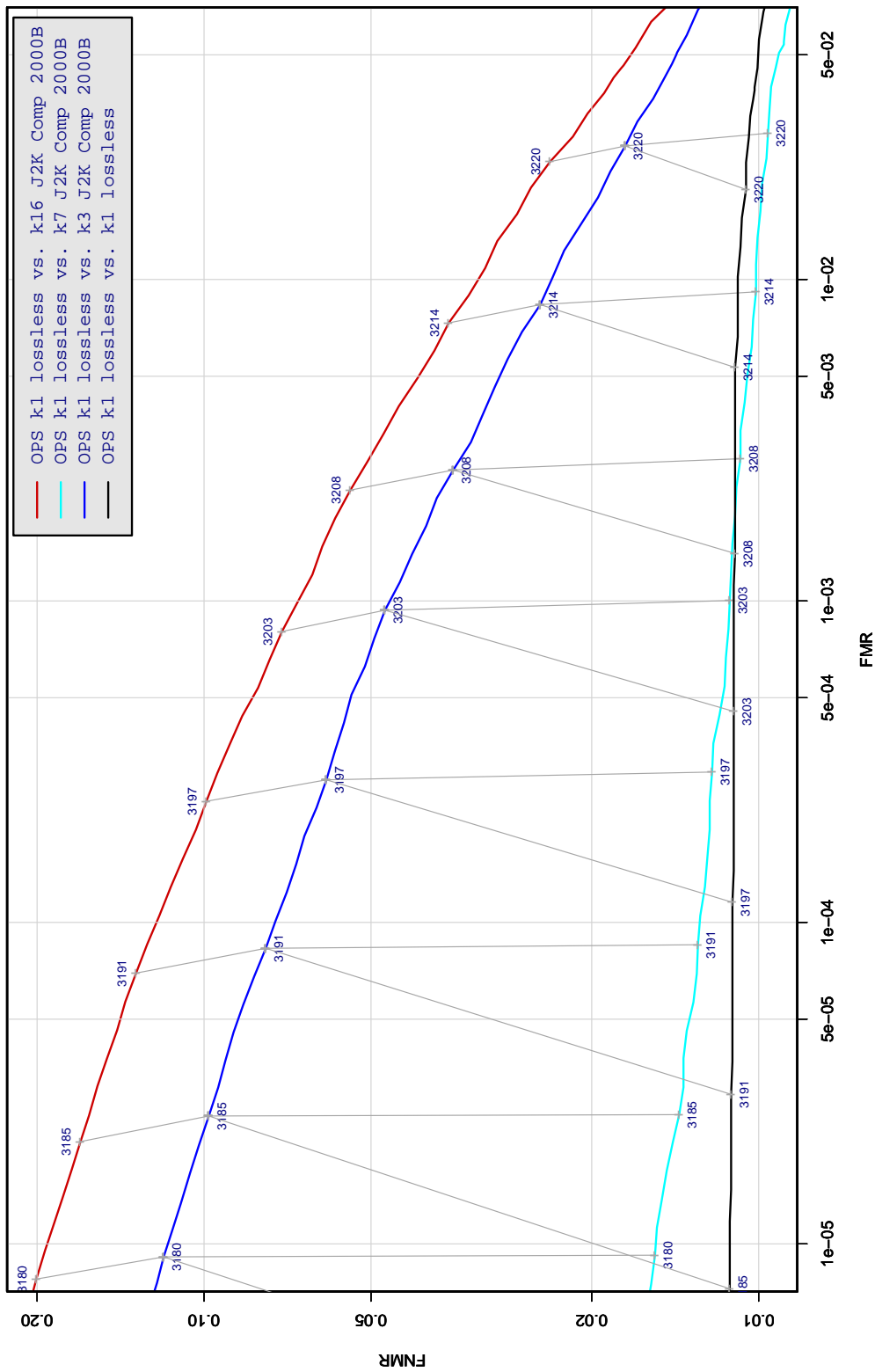


Table 222: DET curve for implementation J1 on the OPS database for the various supported KINDS . The DET characteristics are linked by lines joining points of equal threshold. Non-vertical links indicate a change in false acceptance when the data KIND changes. All results apply to native operation, and the effects of FTE are included.

A = SAGEM	B = COGENT	C = CROSSMATCH	D = CAMBRIDGE	E = L1	x1 = PRIMARY
F = RETICA	G = LG	H = HONEYWELL	I = IRITECH	J = NEUROTECHNOLOGY	x2 = SECONDARY
KIND 1 = RAW 640x480		KIND 3 = CROP		KIND 7 = CROP+MASK	KIND 16 = CONCENTRIC POLAR

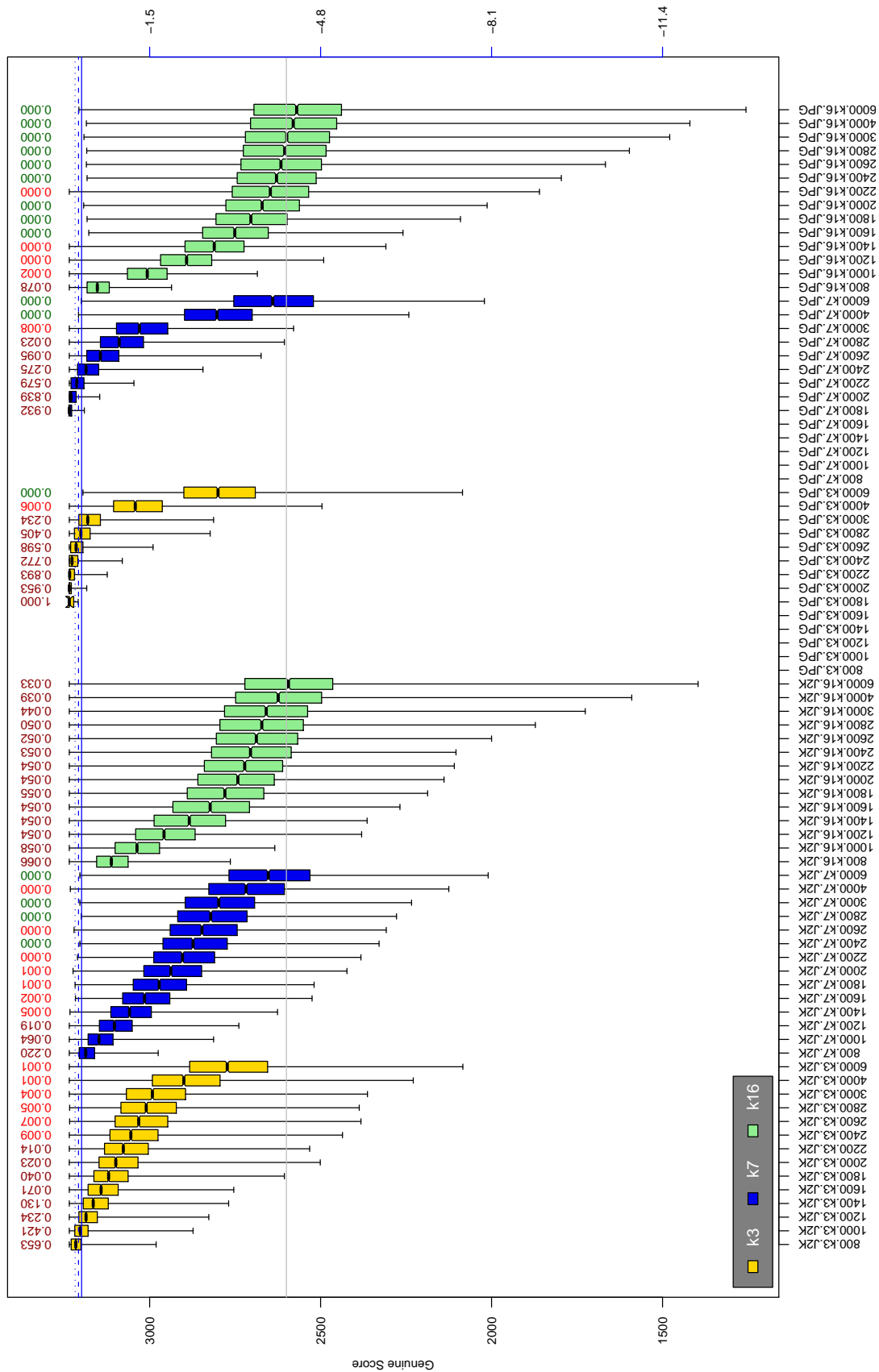


Table 223: The distribution of J1 native genuine comparison scores by size of the compressed image, KIND and the compression algorithm. The images are from the OPS dataset. The right axis scale gives the corresponding value for $d' = (s - \mu_I) / \sqrt{0.5(\sigma_I^2 + \sigma_C^2)}$ for genuine score s . The boxplots only include comparison scores if the uncompressed version of the same image was matched below the FMR = 0.001 threshold. Above the boxplots are FNR values at FMR = 10⁻³. The three blue lines correspond, from the top, to FMR of 10⁻², 10⁻³, and 10⁻⁴. The lower grey line refers to the median score obtained from comparison of uncompressed KIND 3 images. Any comparison for which either template had not been generated is excluded. Note that the iris record size on the horizontal axis is not evenly spaced above 3000 bytes.

A = SAGEM	B = COGENT	C = CROSSMATCH	D = CAMBRIDGE	E = L1	x1 = PRIMARY
F = RETICA	G = LG	H = HONEYWELL	I = IRITECH	J = NEUROTECHNOLOGY	x2 = SECONDARY
KIND 1 = RAW 640x480		KIND 3 = CROP	KIND 7 = CROP+MASK	KIND 16 = CONCENTRIC POLAR	

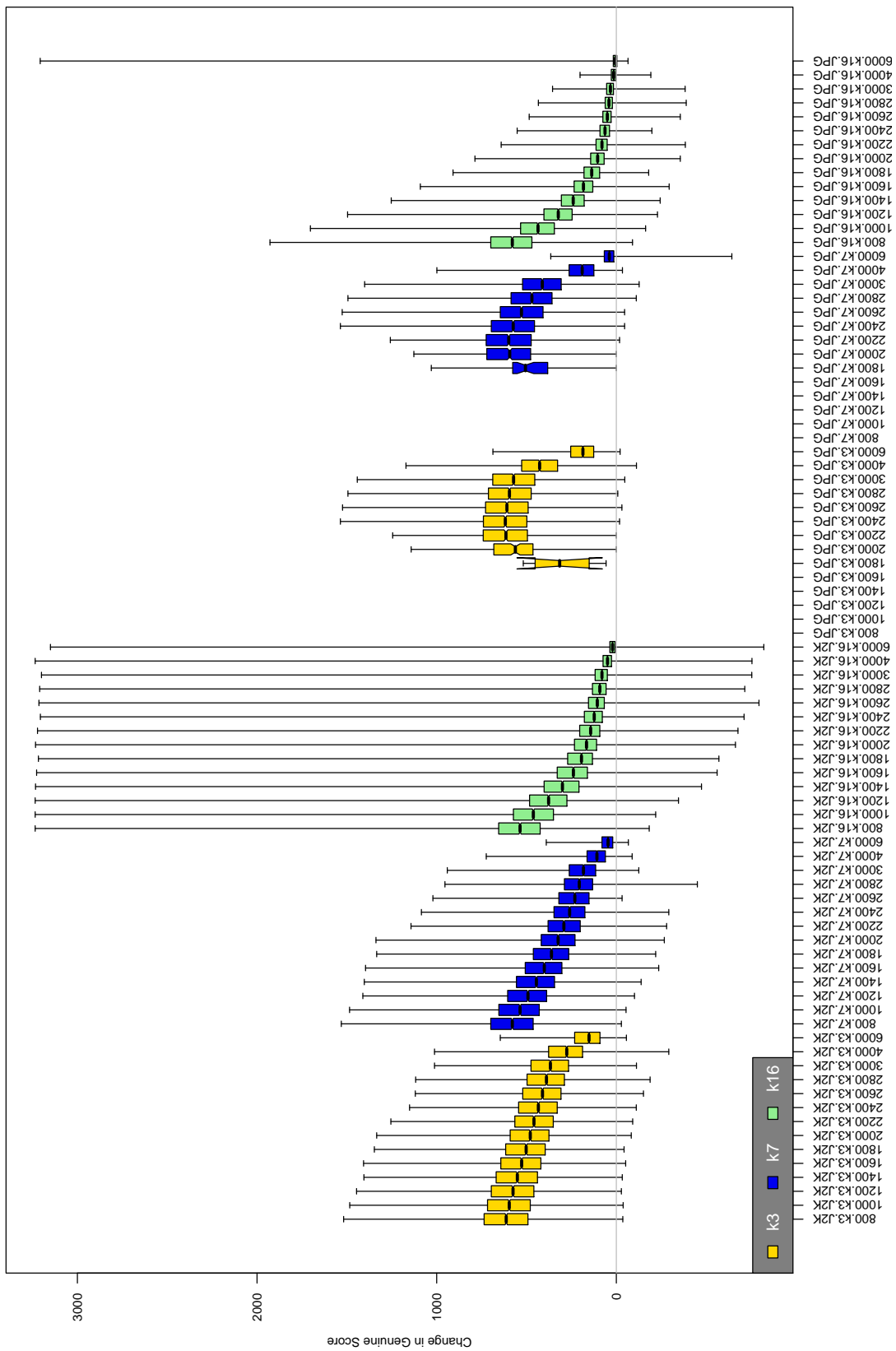


Table 224: The distribution of the *increase* in J1 native genuine comparison scores between the uncompressed “parent” and the compressed image, arranged by size, KIND and the compression algorithm. The images are from the OPS dataset. Any comparison involving a failed template is excluded. Note that the iris record size on the horizontal axis is not evenly spaced above 3000 bytes.

A = SAGEM	B = COGENT	C = CROSSMATCH	D = CAMBRIDGE	E = L1	x1 = PRIMARY
F = RETICA	G = LG	H = HONEYWELL	I = IRITECH	J = NEUROTECHNOLOGY	x2 = SECONDARY
KIND 1 = RAW 640x480		KIND 3 = CROP		KIND 7 = CROP+MASK	KIND 16 = CONCENTRIC POLAR

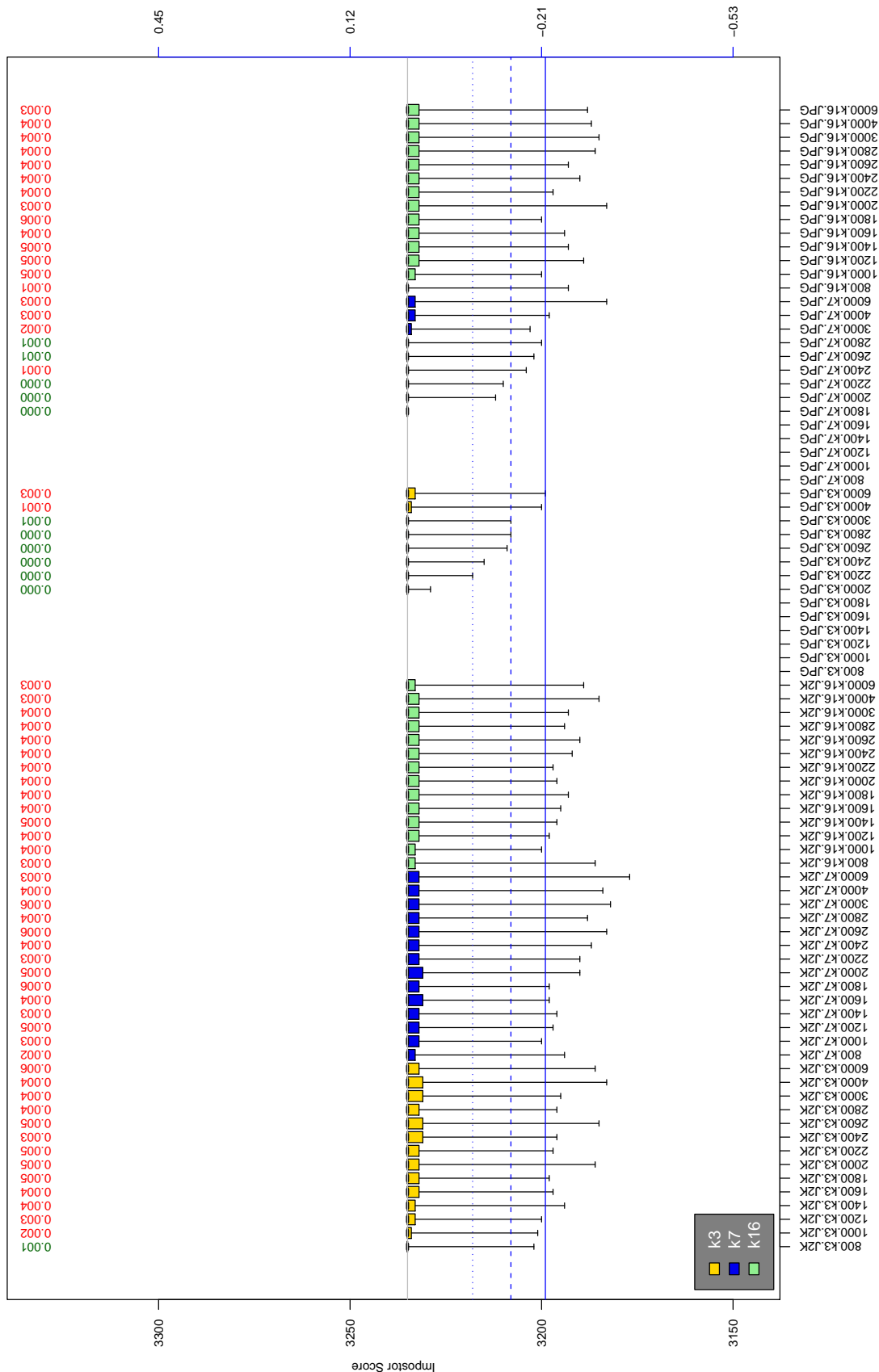


Table 225: The distribution of J1 native impostor comparison scores by size of the compressed image, KIND and the compression algorithm. The right axis scale gives the corresponding value for $d' = (s - \mu_1) / \sqrt{0.5(\sigma_1^2 + \sigma_2^2)}$ for impostor score s . The three blue lines correspond, from the top, to FMR of $10^{-2}, -3, -4$. The lower grey line refers to the median score obtained from comparison of uncompressed KIND 3 images. Any comparison involving a failed template is excluded. Above the boxplots are FMR values at the threshold that gives FMR = 10^{-3} on uncompressed images. These figures are computed from only 4000 comparisons so the FMR values and the tails of the impostor distribution are poorly characterized. Note that the iris record size on the horizontal axis is not evenly spaced above 3000 bytes.

A = SAGEM	B = COGENT	C = CROSSMATCH	D = CAMBRIDGE	E = L1	$x1$ = PRIMARY
F = RETICA	G = LG	H = HONEYWELL	I = IRITECH	J = NEUROTECHNOLOGY	$x2$ = SECONDARY
KIND 1 = RAW 640x480		KIND 3 = CROP	KIND 7 = CROP+MASK	KIND 16 = CONCENTRIC POLAR	

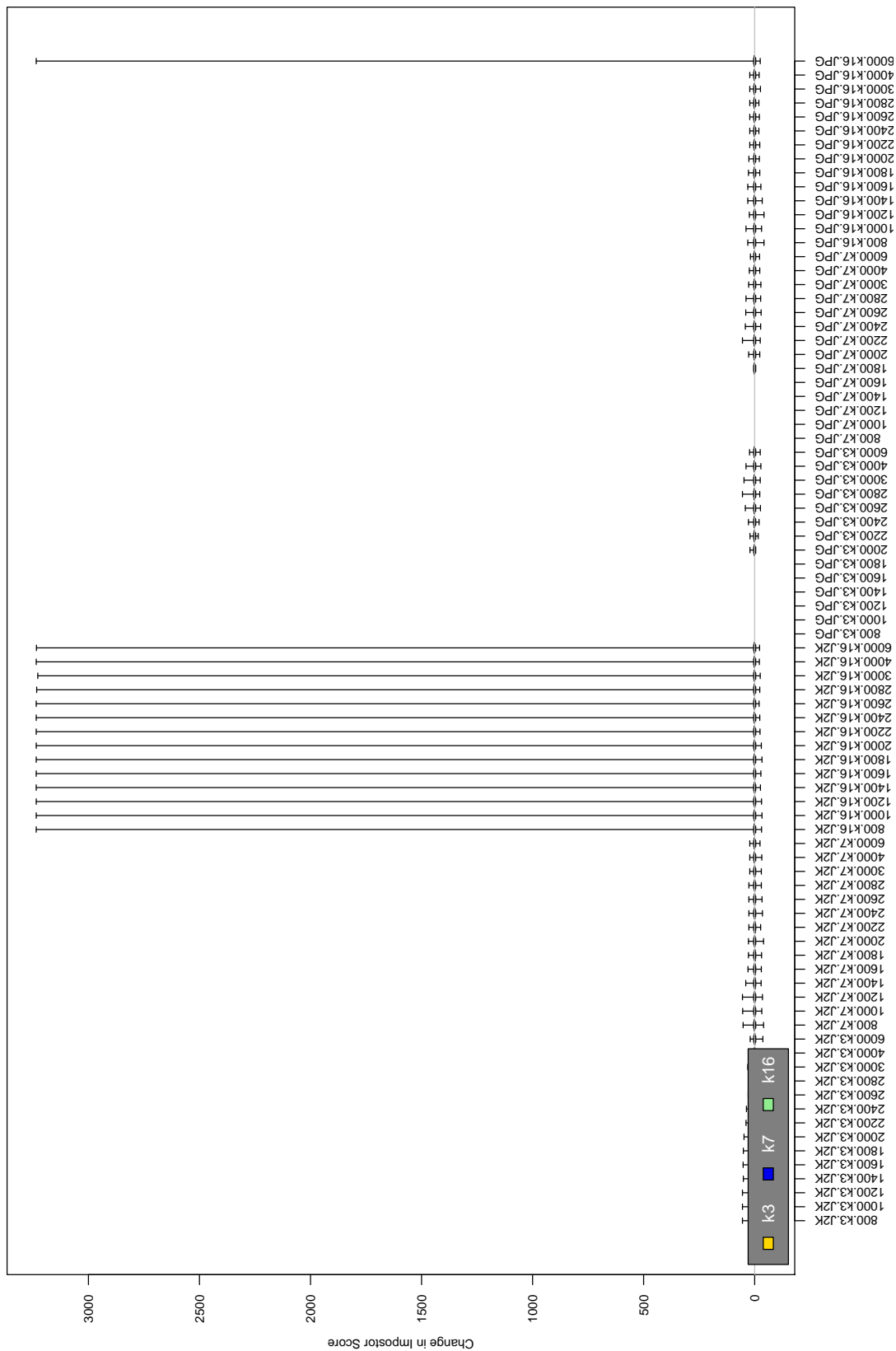


Table 226: The distribution of the increase in J1 native impostor comparison scores between the uncompressed “parent” and the compressed image, arranged by size, KIND and the compression algorithm. The images are from the OPS dataset. Any comparison involving a failed template is excluded. Note that the iris record size on the horizontal axis is not evenly spaced above 3000 bytes.

A = SAGEM	B = COGENT	C = CROSSMATCH	D = CAMBRIDGE	E = L1	x1 = PRIMARY
F = RETICA	G = LG	H = HONEYWELL	I = IRITECH	J = NEUROTECHNOLOGY	x2 = SECONDARY
KIND 1 = RAW 640x480		KIND 3 = CROP	KIND 7 = CROP+MASK	KIND 16 = CONCENTRIC POLAR	

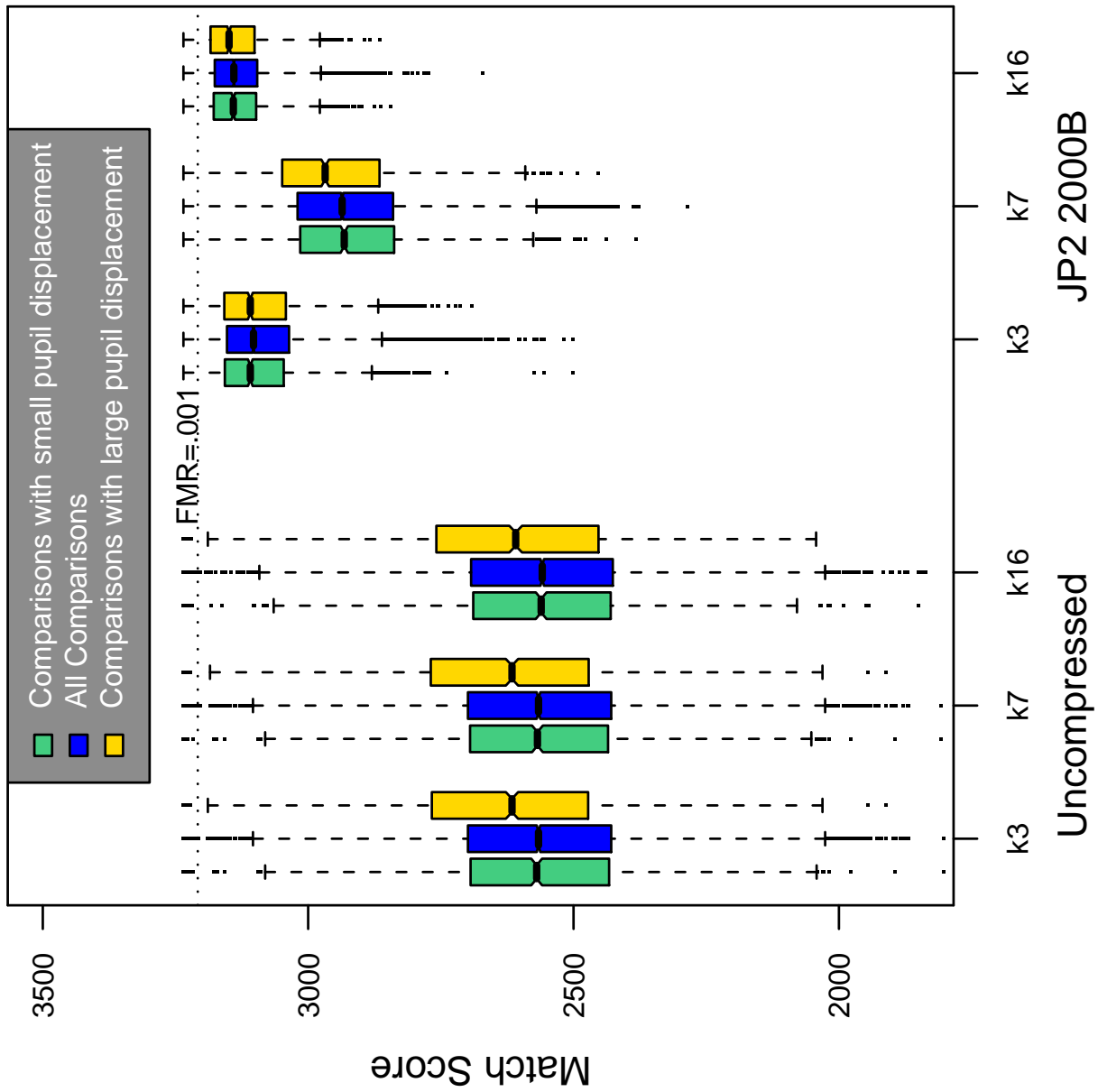


Table 227: Effect of pupil displacement on the genuine score distribution for J1

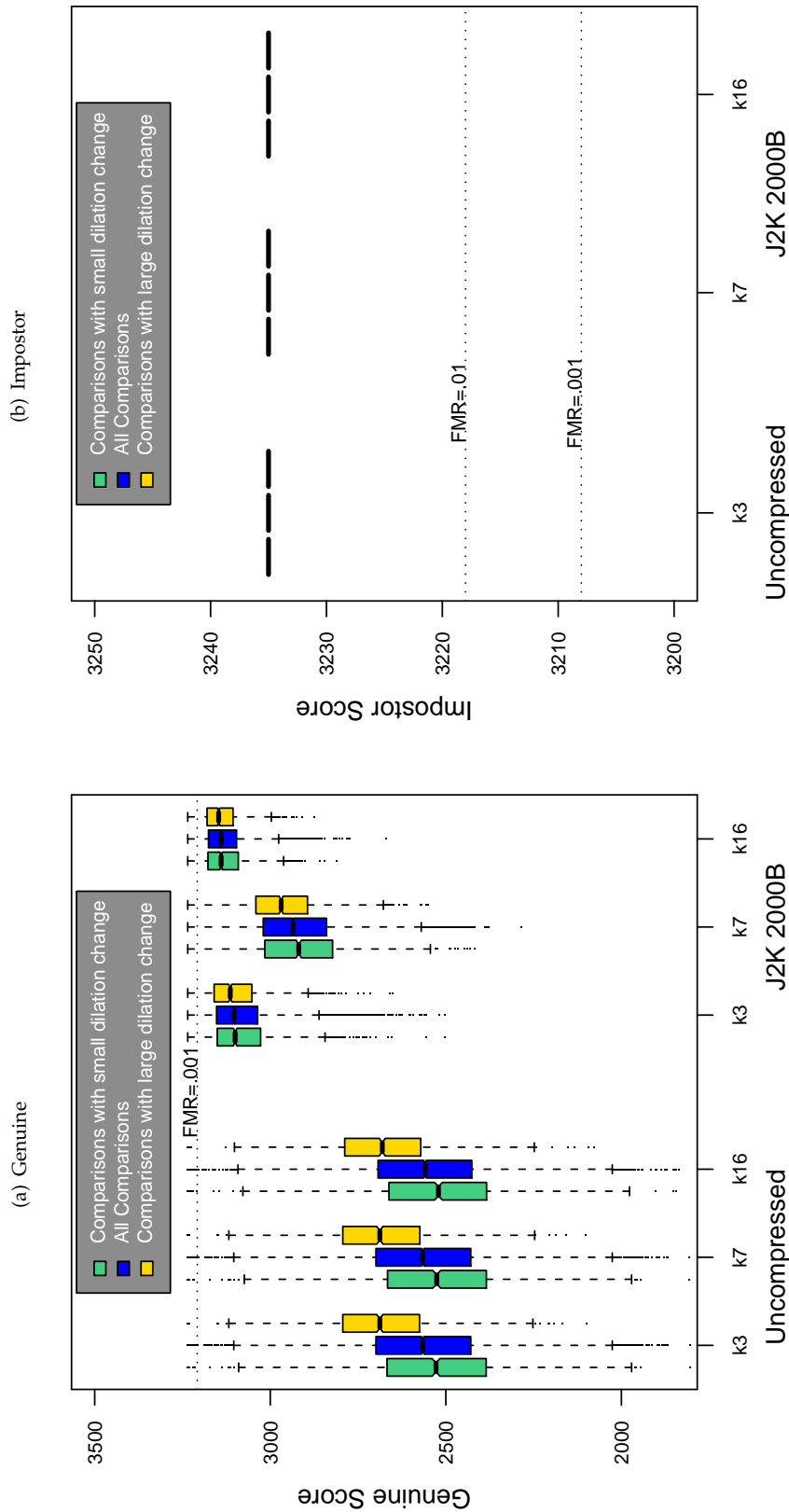


Table 228: The effect of dilation change on the two scores distributions for SDK J1.

A = SAGEM	B = COGENT	C = CROSSMATCH	D = CAMBRIDGE	E = L1	$x1$ = PRIMARY
F = RETICA	G = LG	H = HONEYWELL	I = IRITECH	J = NEUROTECHNOLOGY	$x2$ = SECONDARY
KIND 1 = RAW 640x480		KIND 3 = CROP	KIND 7 = CROP+MASK	KIND 16 = CONCENTRIC POLAR	

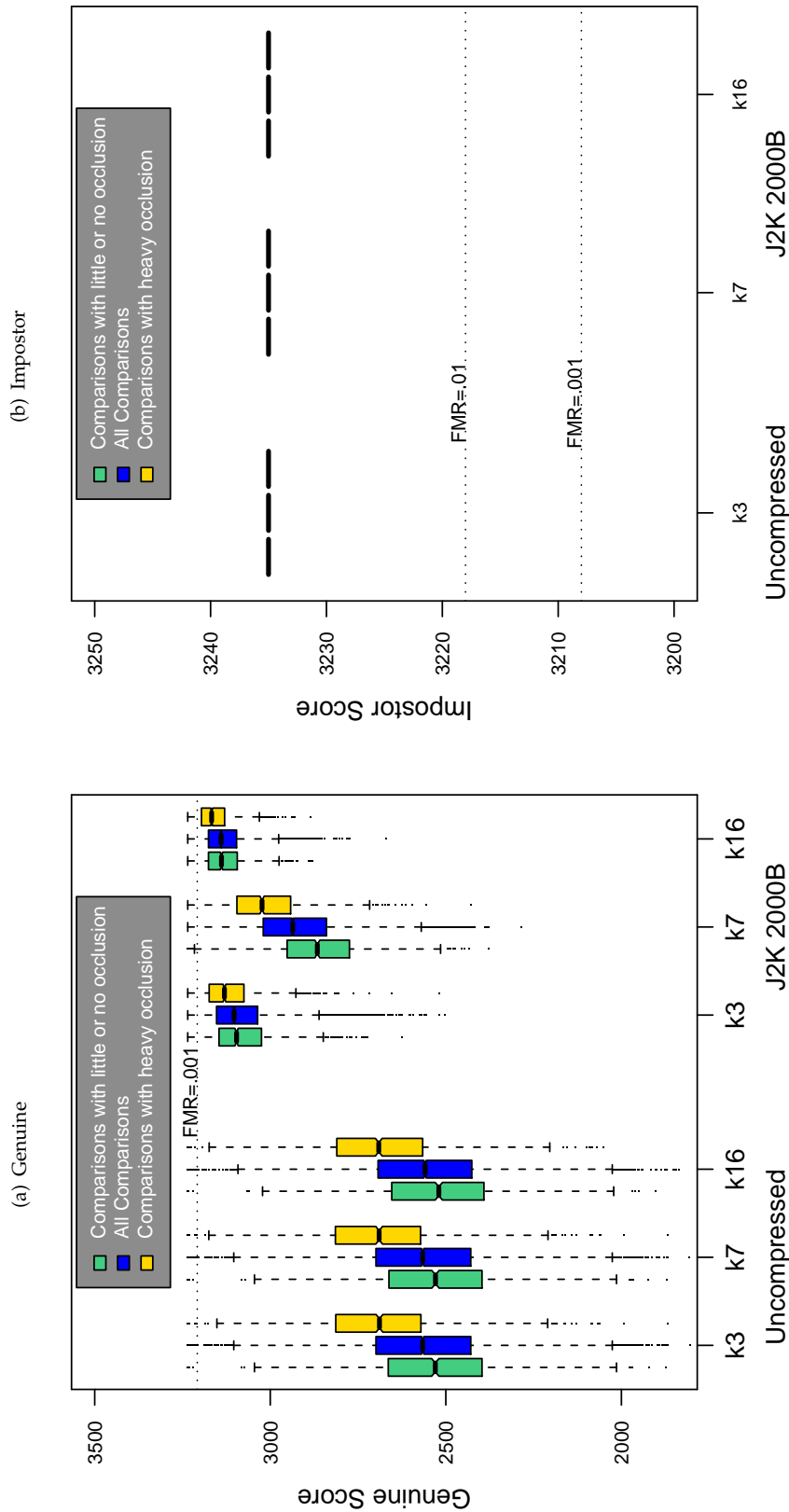
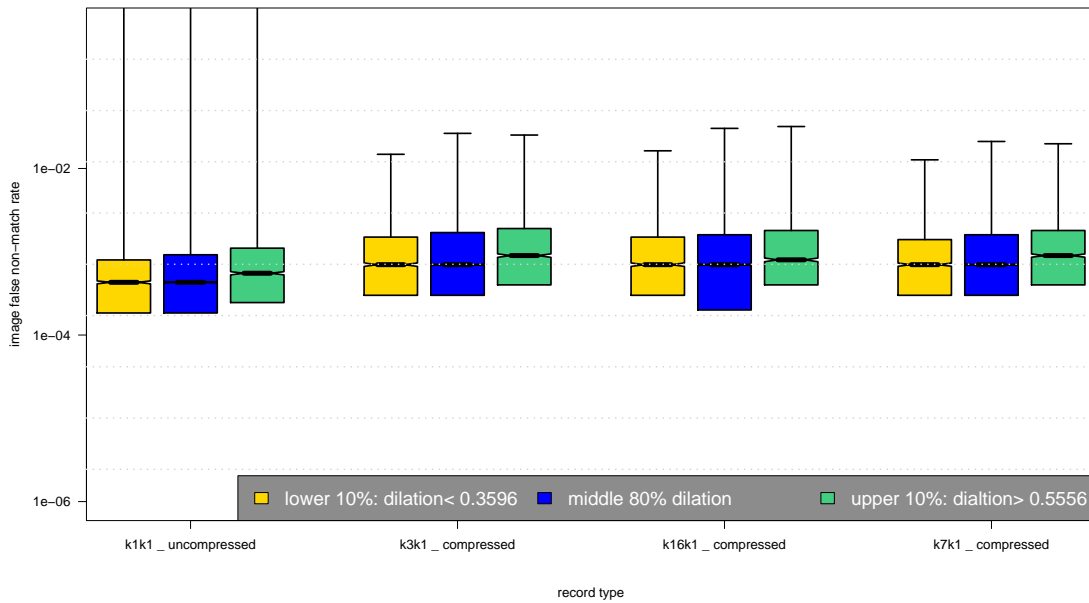
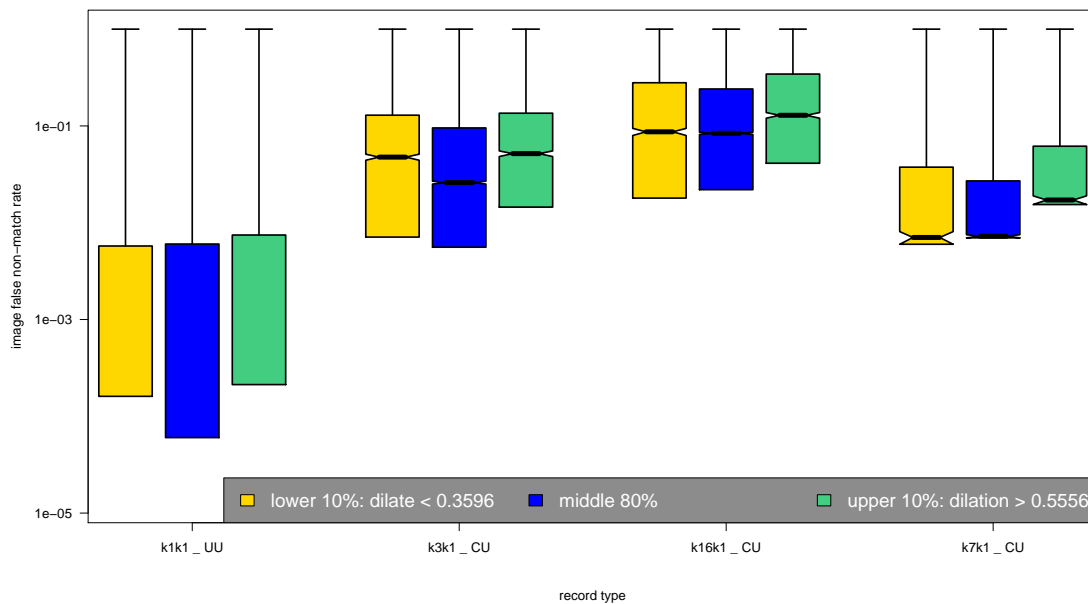


Table 229: The effect of eyelid occlusion on the two scores distributions for SDK J1.

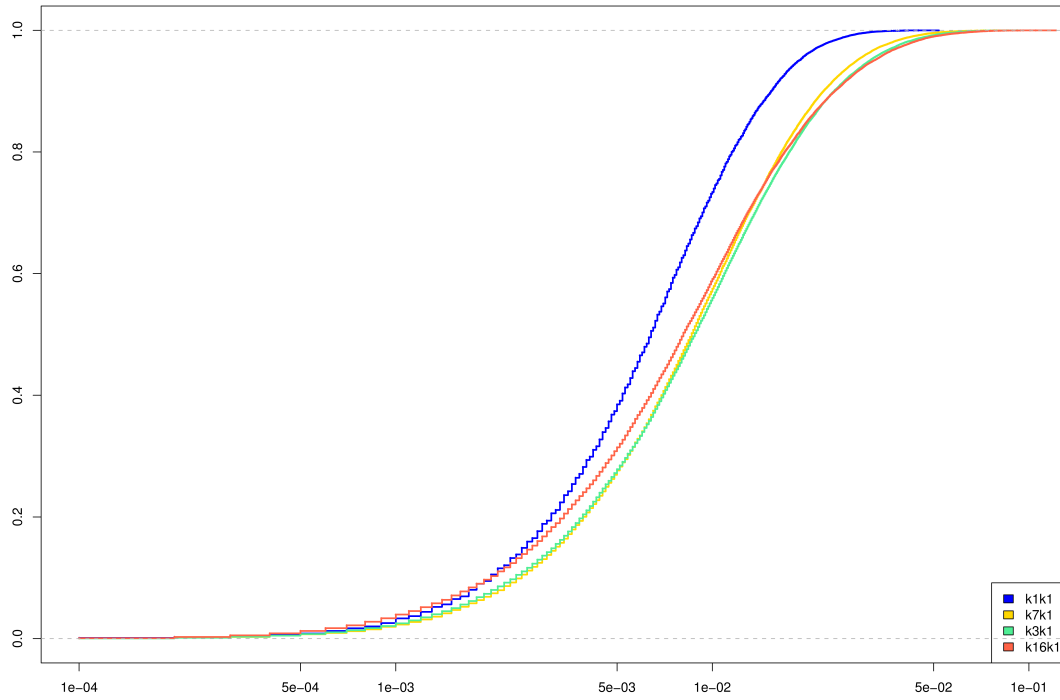
(a) iFMR using A1 dilation estimates



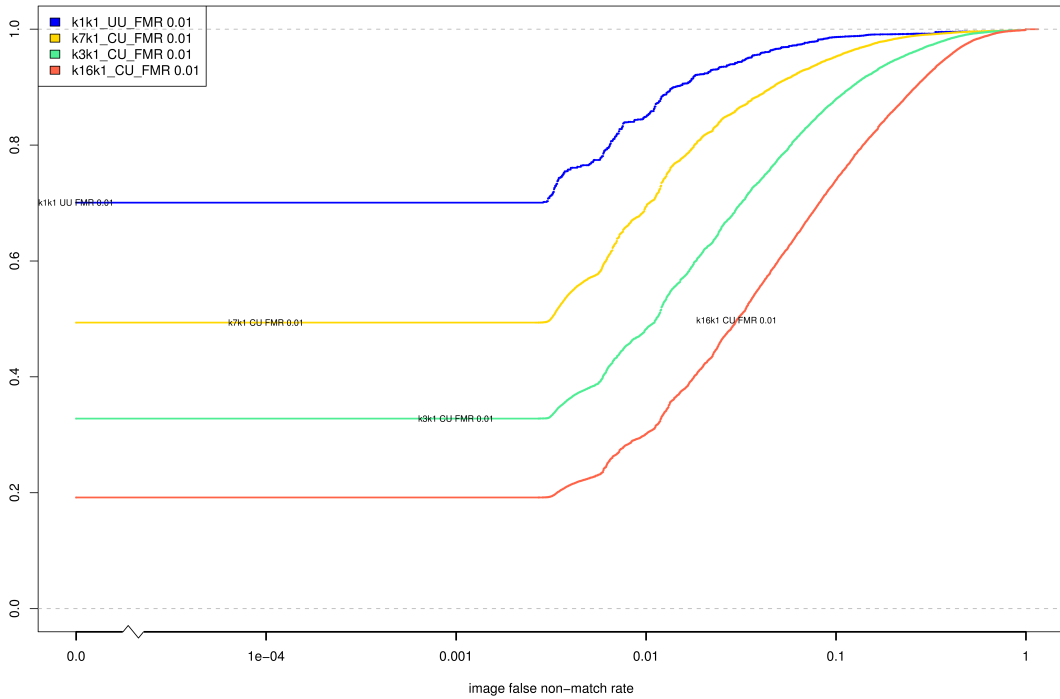
(b) iFNMR using A1 dilation estimates



(c) iFMR CDF



(d) iFNMR CDF



Compiled Results for Implementation J2

On June 25, 2009, NIST invited the IREX participants to submit a description of the SDKs submitted for the IREX effort. The intent was to allow providers to describe and contrast the feature sets, optimization, operational suitability and availability of the primary and secondary SDKs. NIST indicated that any submitted text would appear verbatim (with typesetting) in draft and final versions of the IREX report and that it would be attributed to the organization. This was optional and NIST put no constraints on the content beyond a 600 word limit, and a statement that anything labelled as confidential or proprietary would be omitted.

The provider of SDK J2, Neurotechnology, submitted the following to NIST - we are unable to validate this information.

Neurotechnology provides algorithms and software development products for fingerprint, face, iris and multi-modal biometrical identification, computer-based vision and object recognition to security companies, system integrators and hardware manufacturers. More than 2,000 system integrators and sensor providers in 98 countries license and integrate Neurotechnology products into their own applications, with millions of end-user installations worldwide.

VeriEye 2.1 algorithm implements advanced iris segmentation, enrollment and matching using robust digital image processing algorithms:

1. Robust eye iris detection. Irises are detected even when the images have obstructions, visual noise and different levels of illumination. Lighting reflections, eyelids and eyelashes obstructions are eliminated. Images with narrowed eyelids are also accepted.
2. Gazing-away iris images are correctly detected, segmented and transformed as if it were looking directly into the camera.
3. VeriEye uses active shape models that more precisely model the contours of the eye, as iris boundaries are not modeled by perfect circles.
4. Fast matching. Configurable matching speed varies from 50,000 to 150,000 comparisons per second (using only one core of Intel Core 2 Duo running at 2.66 GHz). The highest speed still preserves nearly the same recognition quality.
5. Reliability. VeriEye algorithm showed excellent performance in IREX when used with uncompressed images. This scenario is most common when biometric devices are used.
6. Small template size. One eye iris template size is 2.3kb. This allows to hold millions of records in a regular computer.

VeriEye is available as a software development kit (SDK) that allows development of PC and Web-based solutions on Microsoft Windows, Linux, Mac OS X platforms and various programming languages.

VeriEye SDK supports some third-parties iris cameras. At this report issuing date it supports Cross Match I Scan 2, Retica Mobile-Eyes, VistaFA2 Multimodal Iris & Face Camera as well as image input from other devices. We are looking for the opportunity to cooperate with other hardware manufacturers and support their devices.

VeriEye SDKs are available with highly competitive licensing options through Neurotechnology or from distributors worldwide. VeriEye Standard SDK costs 790 euros, and Extended SDK 1,290 euros. Prices for end-user product installation licenses depend on quantity and are in range from 396 to 43 euros or less per computer.

For more information and 30 days SDK trial downloads: www.neurotechnology.com.

A = SAGEM	B = COGENT	C = CROSSMATCH	D = CAMBRIDGE	E = L1	x1 = PRIMARY
F = RETICA	G = LG	H = HONEYWELL	I = IRITECH	J = NEUROTECHNOLOGY	x2 = SECONDARY
KIND 1 = RAW 640x480		KIND 3 = CROP		KIND 7 = CROP+MASK	
KIND 16 = CONCENTRIC POLAR					

IREX report showed that VeriEye constantly performed along with top algorithms except for the BATH dataset which provided iris images of unusually large irises radii. This was unexpected for VeriEye segmentation algorithm and ~2% of Failure to Enroll rate gave high False Rejection Rate of ~2.5% at zero False Acceptance Rate.

On August 17, 2009, NIST invited the IREX participants to submit a description their comments on a draft version of the IREX report. This was intended to allow participants to assist readers in the interpretation of a large and complicated testing effort. NIST indicated that any submitted text would appear verbatim (with typesetting) in the final version of the IREX report and that it would be attributed to the organization. Submission of content was optional and NIST put no constraints on the content beyond a word limit, and a statement that anything labelled as confidential or proprietary would be omitted.

The provider of SDK J2, Neurotechnology, elected not to submit any information

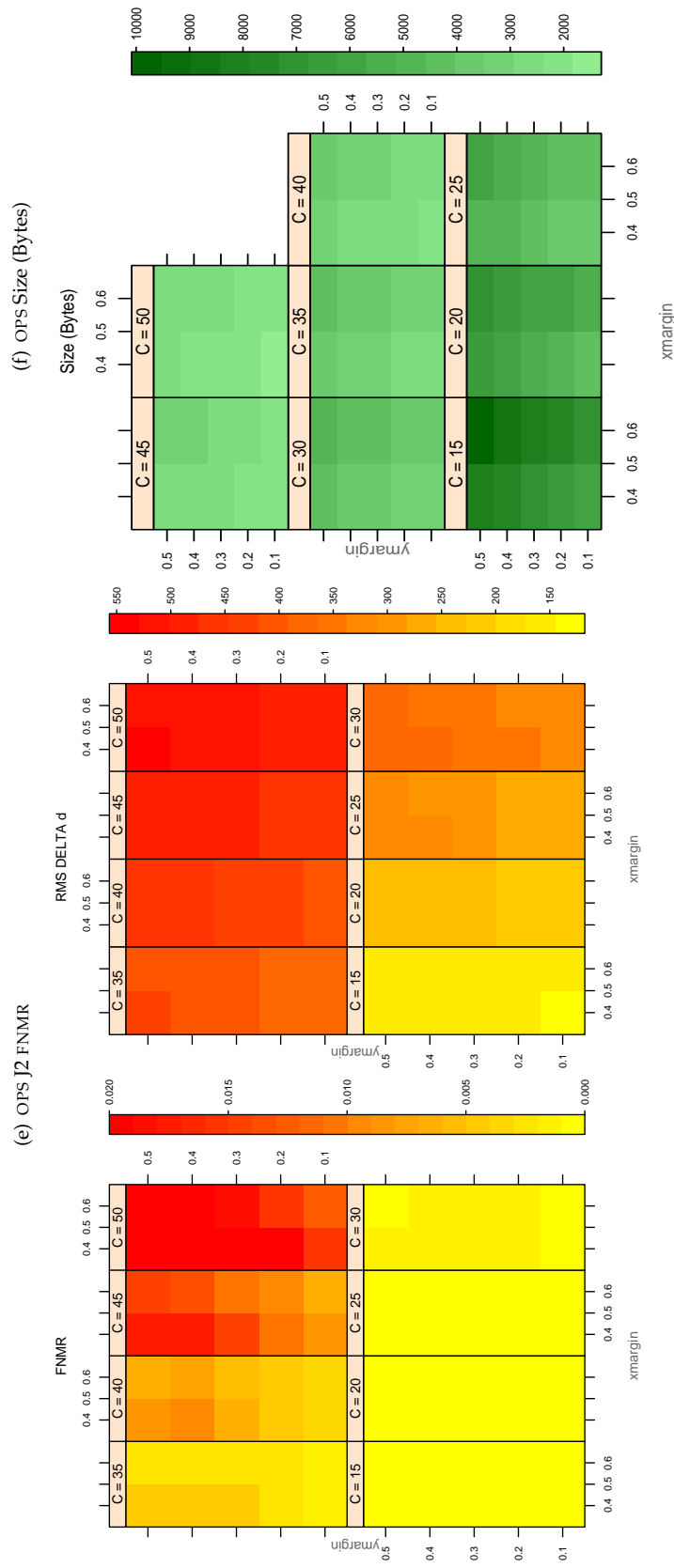


Table 230: For the IREX partition of the OPS database the plots at left show the dependence of cFNMNR on the vertical and horizontal iris cropping margins for various compression ratios. This applies only for KIND 3 records. The margins are in units of iris radius. The use of conditional FNMNR means that the plots exclude comparisons that were falsely rejected even before any compression was applied. On the **right side** is the rms difference between the crop+compress and the uncompressed comparison scores for each image pair. All computations are driven by the bounding box coordinates reported by the II SDK. The number of bits per pixel is $8/C$, where C is the compression ratio. The iris radius varies and because the cropping margins are fixed multiples of the radius the image size varies. The compressed size, in bytes, is the width times height divided by C . Values of cFNMNR greater than 0.02 are shown as 0.02.

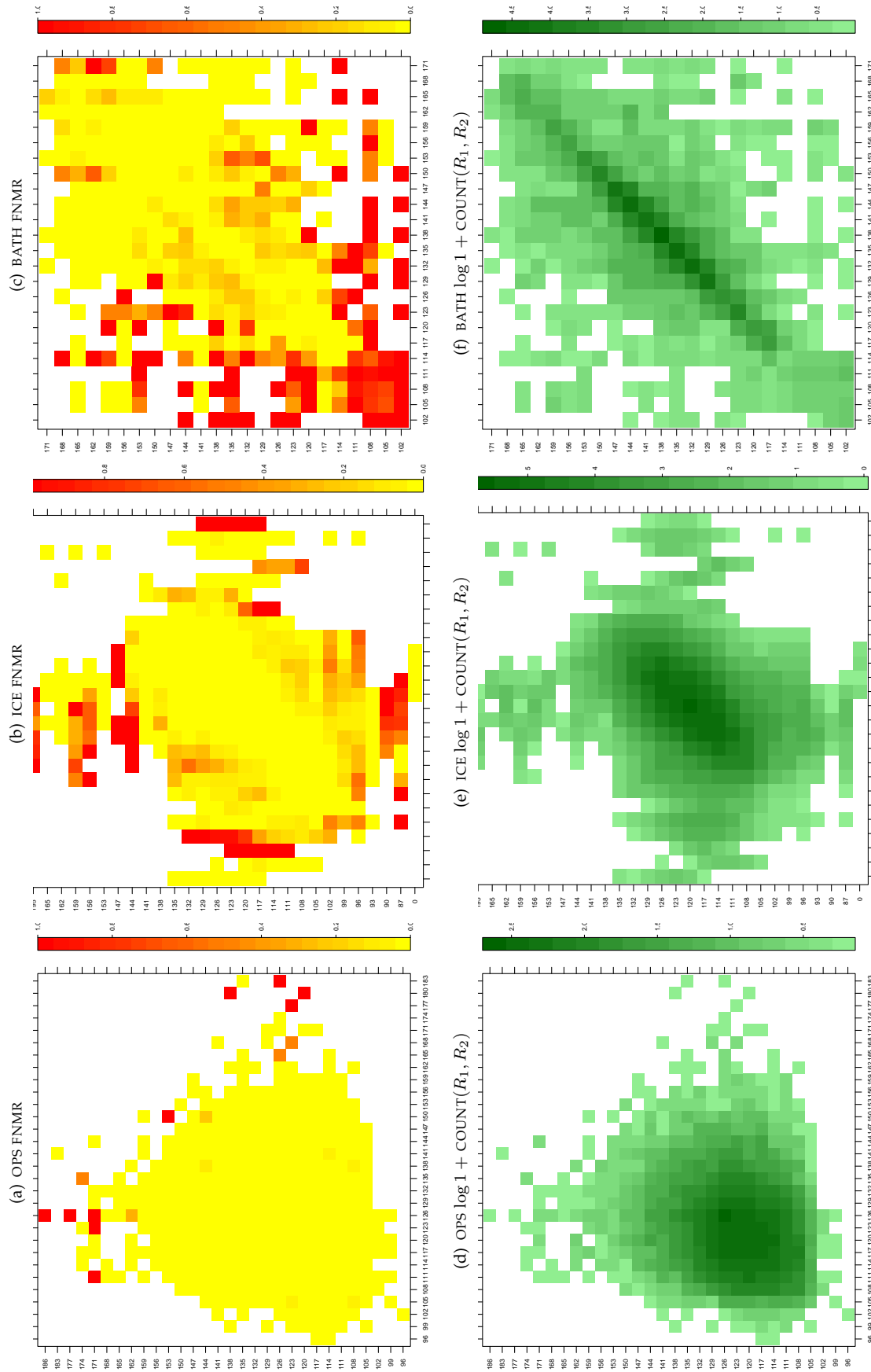


Table 231: For the three IREX databases: In the **top** row the color in each cell represents the occurrence of genuine comparisons with the given pair of radii. The *y*-axis represents enrollment samples with verification samples on the *x*-axis; In the **bottom** row the color scale plots $\log 1 + \text{COUNT}(R_1, R_2)$. The radii are quantized into three-pixel bins. The radii for DOD are on the range $96 \leq r \leq 186$ pixels. The radii for ICE are on the range $87 \leq r \leq 165$ pixels. The radii for BATH are on the range $100 \leq r \leq 170$ pixels.

A = SAGEM	B = COGENT	C = CROSSMATCH	D = CAMBRIDGE	E = L1	$x1$ = PRIMARY
F = RETICA	G = LG	H = HONEYWELL	I = IRITECH	J = NEUROTECHNOLOGY	$x2$ = SECONDARY
KIND 1 = RAW 640x480		KIND 3 = CROP		KIND 7 = CROP+MASK	KIND 16 = CONCENTRIC POLAR

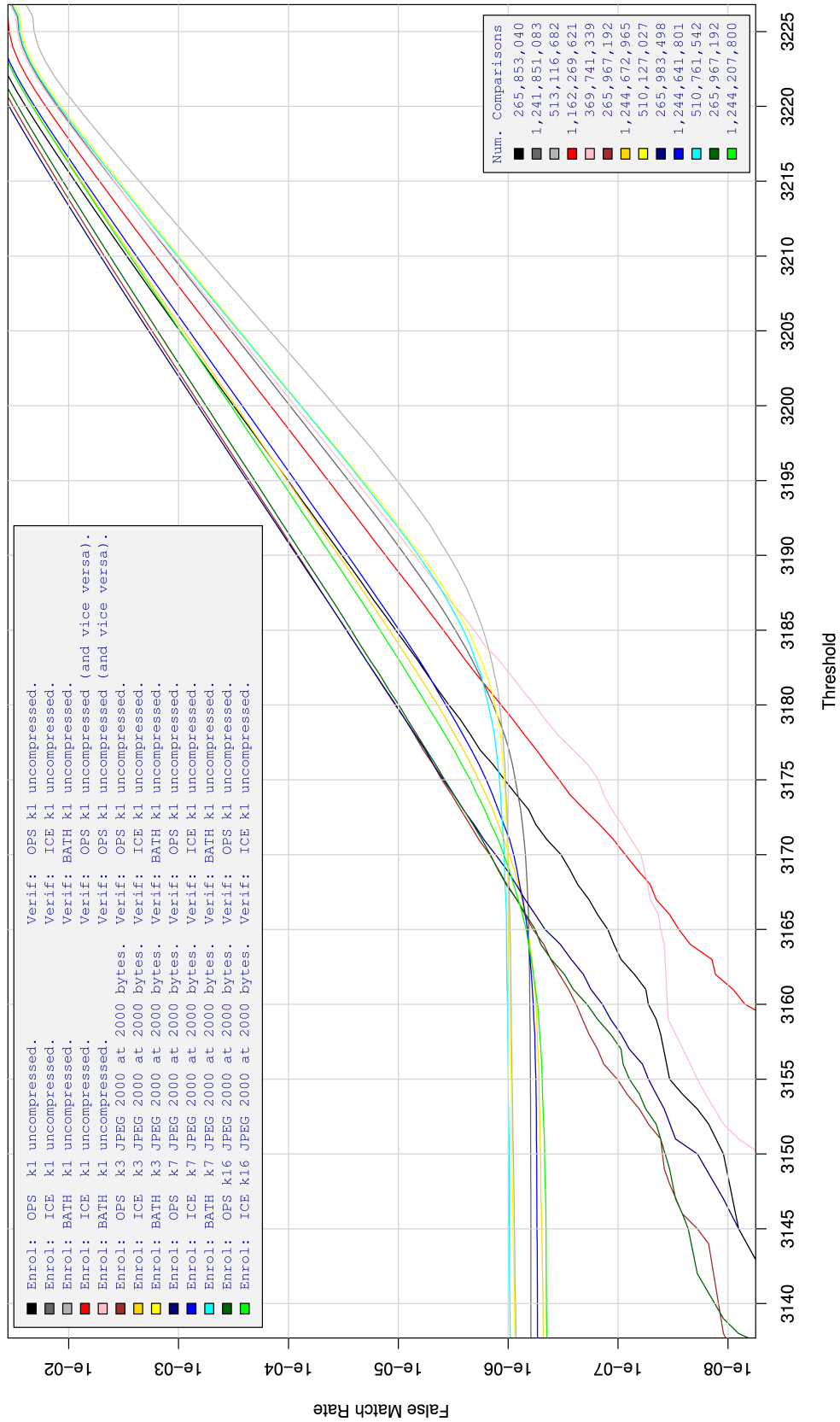


Table 232: For implementation J2, the dependency of FMR on threshold. for various combinations of enrollment and verification dataset, format, and compression.

A = SAGEM	B = COGENT	C = CROSSMATCH	D = CAMBRIDGE	E = L1	x1 = PRIMARY
F = RETICA	G = LG	H = HONEYWELL	I = IRITECH	J = NEUROTECHNOLOGY	x2 = SECONDARY
KIND 1 = RAW 640x480		KIND 3 = CROP		KIND 7 = CROP+MASK	
KIND 16 = CONCENTRIC POLAR					

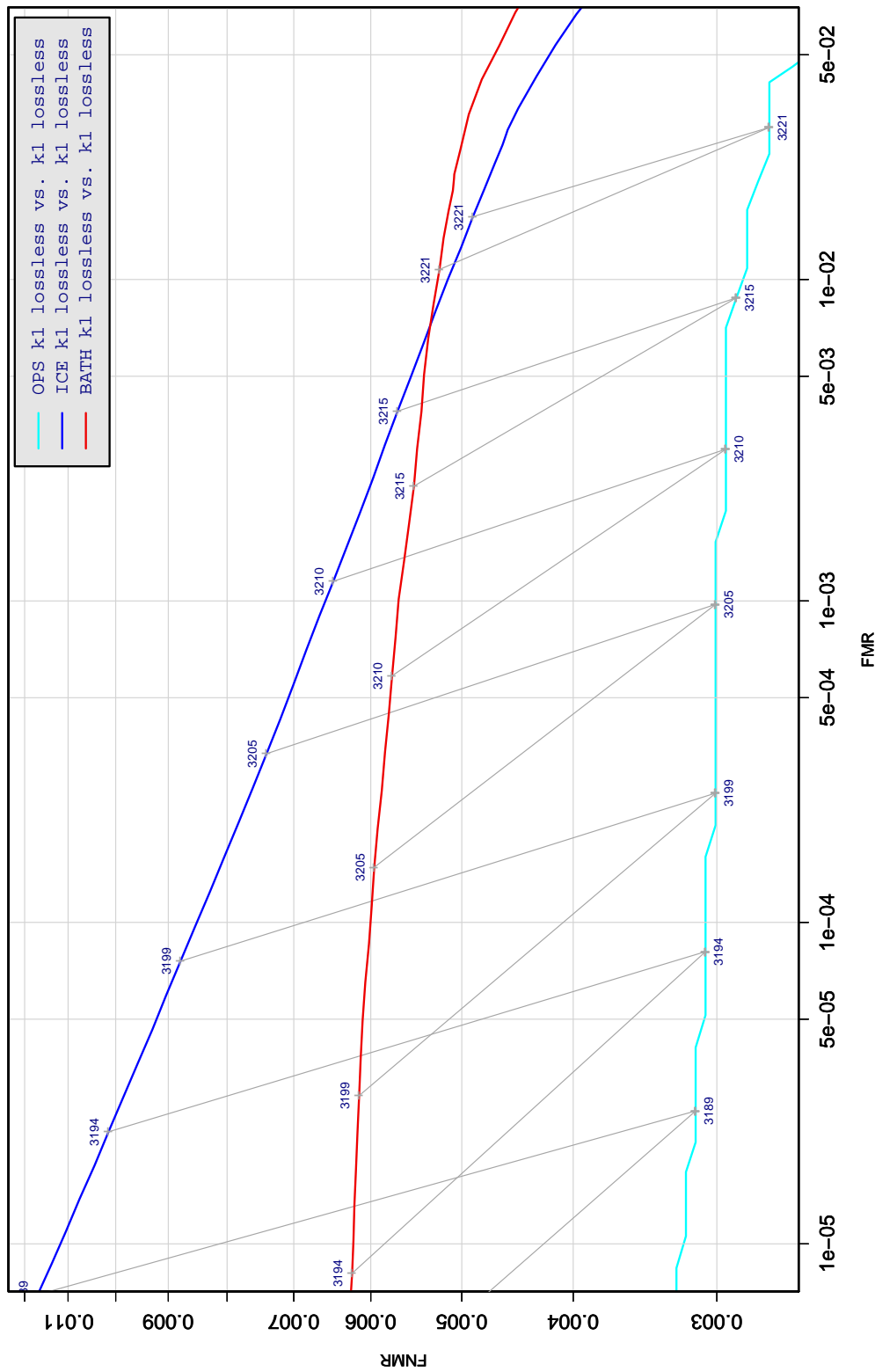


Table 233: DET curve for implementation J2 on three IREX databases. All comparisons are with uncompressed KIND 1 vs. KIND 1 images. The lines join points corresponding to the a fixed threshold. Non-vertical links indicate a change in FMR when the database changes. All results apply to native operation. Failures to produce a template i.e. FTE are ignored because the plots are intended to show *matching* effects, specifically to compare DET slopes and to show the effect of fixing a threshold.

A = SAGEM	B = COGENT	C = CROSSMATCH	D = CAMBRIDGE	E = L1	$x1$ = PRIMARY
F = RETICA	G = LG	H = HONEYWELL	I = IRITECH	J = NEUROTECHNOLOGY	$x2$ = SECONDARY
KIND 1 = RAW 640x480		KIND 3 = CROP	KIND 7 = CROP+MASK	KIND 16 = CONCENTRIC POLAR	

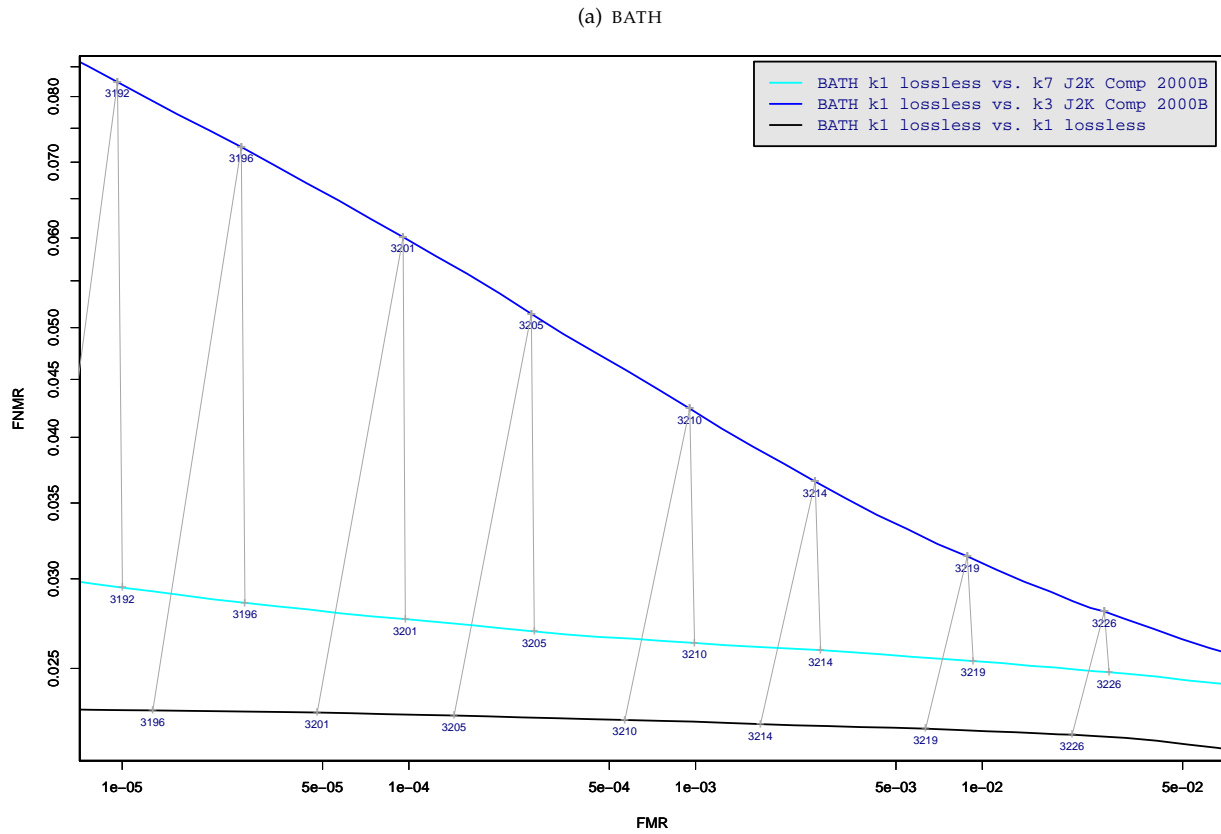


Table 234: DET curve for implementation J2 on the BATH database for the various supported KINDS . The DET characteristics are linked by lines joining points of equal threshold. Non-vertical links indicate a change in false acceptance when the data KIND changes. All results apply to native operation, and the effects of FTE are included.

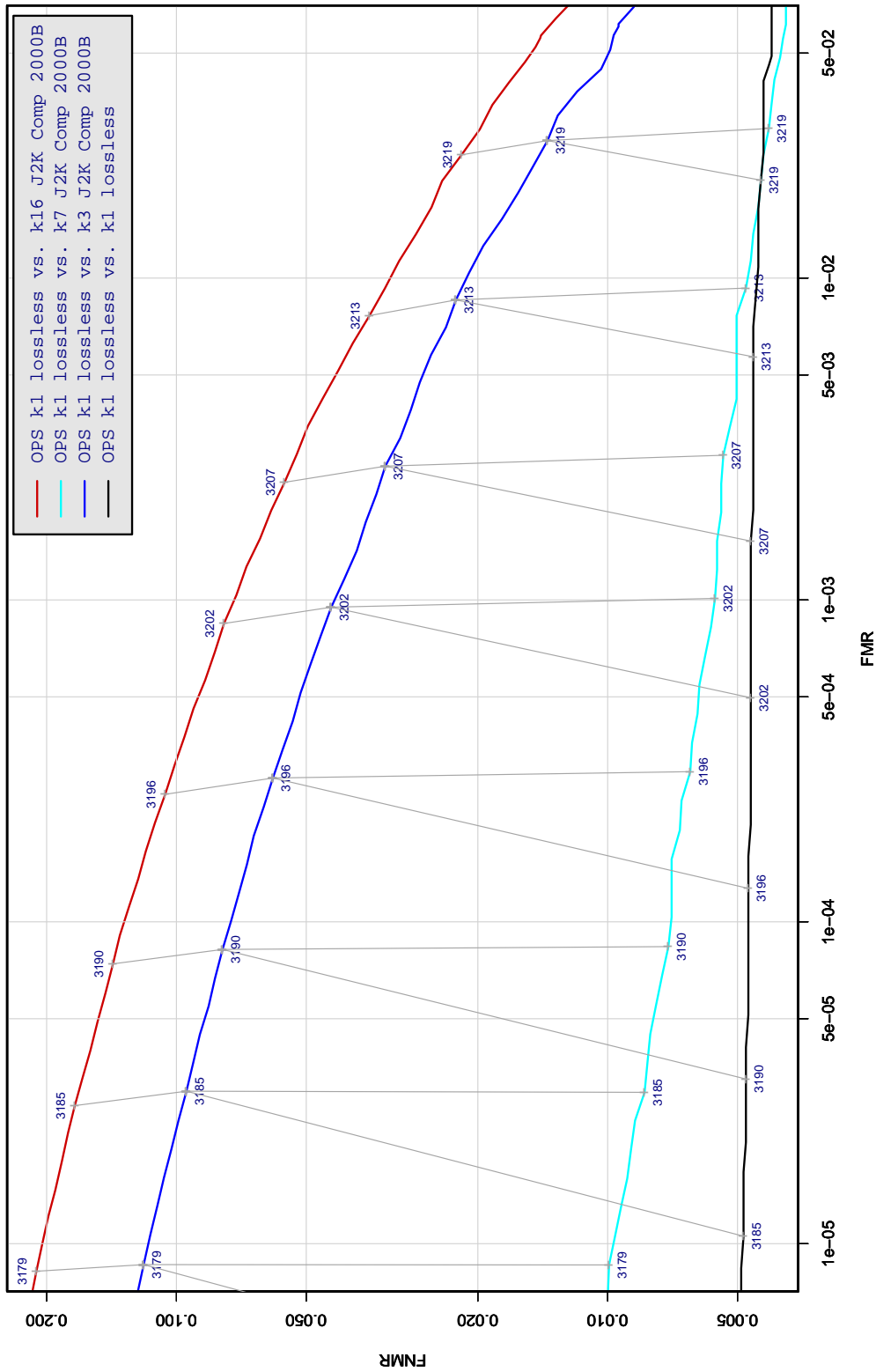


Table 235: DET curve for implementation J2 on the OPS database for the various supported KINDS . The DET characteristics are linked by lines joining points of equal threshold. Non-vertical links indicate a change in false acceptance when the data KIND changes. All results apply to native operation, and the effects of FTE are included.

A = SAGEM	B = COGENT	C = CROSSMATCH	D = CAMBRIDGE	E = L1	x1 = PRIMARY
F = RETICA	G = LG	H = HONEYWELL	I = IRITECH	J = NEUROTECHNOLOGY	x2 = SECONDARY
KIND 1 = RAW 640x480		KIND 3 = CROP		KIND 7 = CROP+MASK	
KIND 16 = CONCENTRIC POLAR					

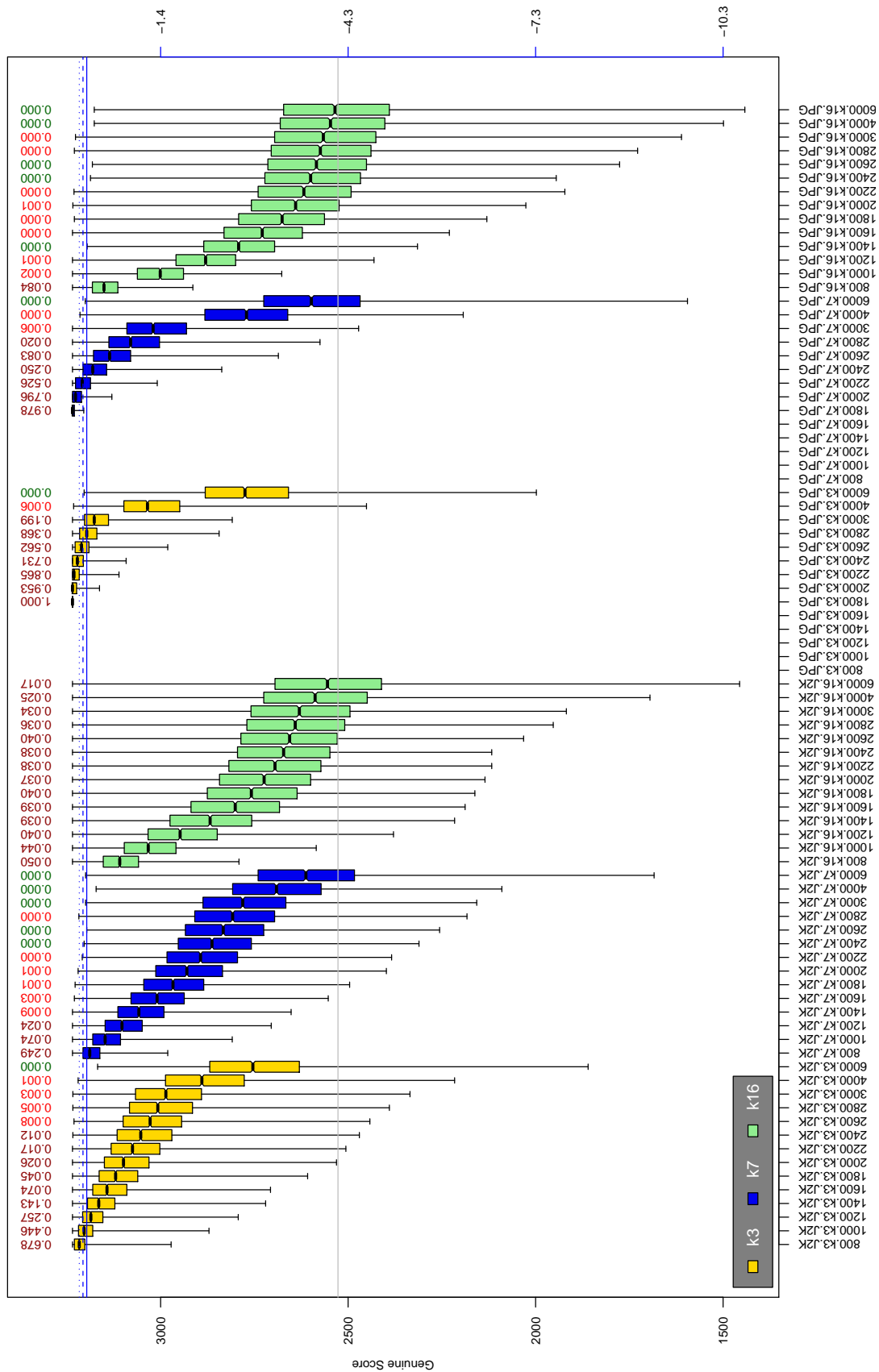


Table 236: The distribution of 12 native genuine comparison scores by size of the compressed image, KIND and the compression algorithm. The images are from the OPS dataset. The right axis scale gives the corresponding value for $d' = (s - \mu_I) / \sqrt{0.5(\sigma_I^2 + \sigma_C^2)}$ for genuine score s . The boxplots only include comparison scores if the uncompressed version of the same image was matched below the FMR = 0.001 threshold. Above the boxplots are FNR values at $FMR = 10^{-3}$. The three blue lines correspond, from the top, to FMR of $10^{(-2, -3, -4)}$. The lower grey line refers to the median score obtained from comparison of uncompressed KIND 3 images. Any comparison for which either template had not been generated is excluded. Note that the iris record size on the horizontal axis is not evenly spaced above 3000 bytes.

A = SAGEM	B = COGENT	C = CROSSMATCH	D = CAMBRIDGE	E = L1	$x1$ = PRIMARY
F = RETICA	G = LG	H = HONEYWELL	I = IRITECH	J = NEUROTECHNOLOGY	$x2$ = SECONDARY
KIND 1 = RAW 640x480		KIND 3 = CROP	KIND 7 = CROP+MASK	KIND 16 = CONCENTRIC POLAR	

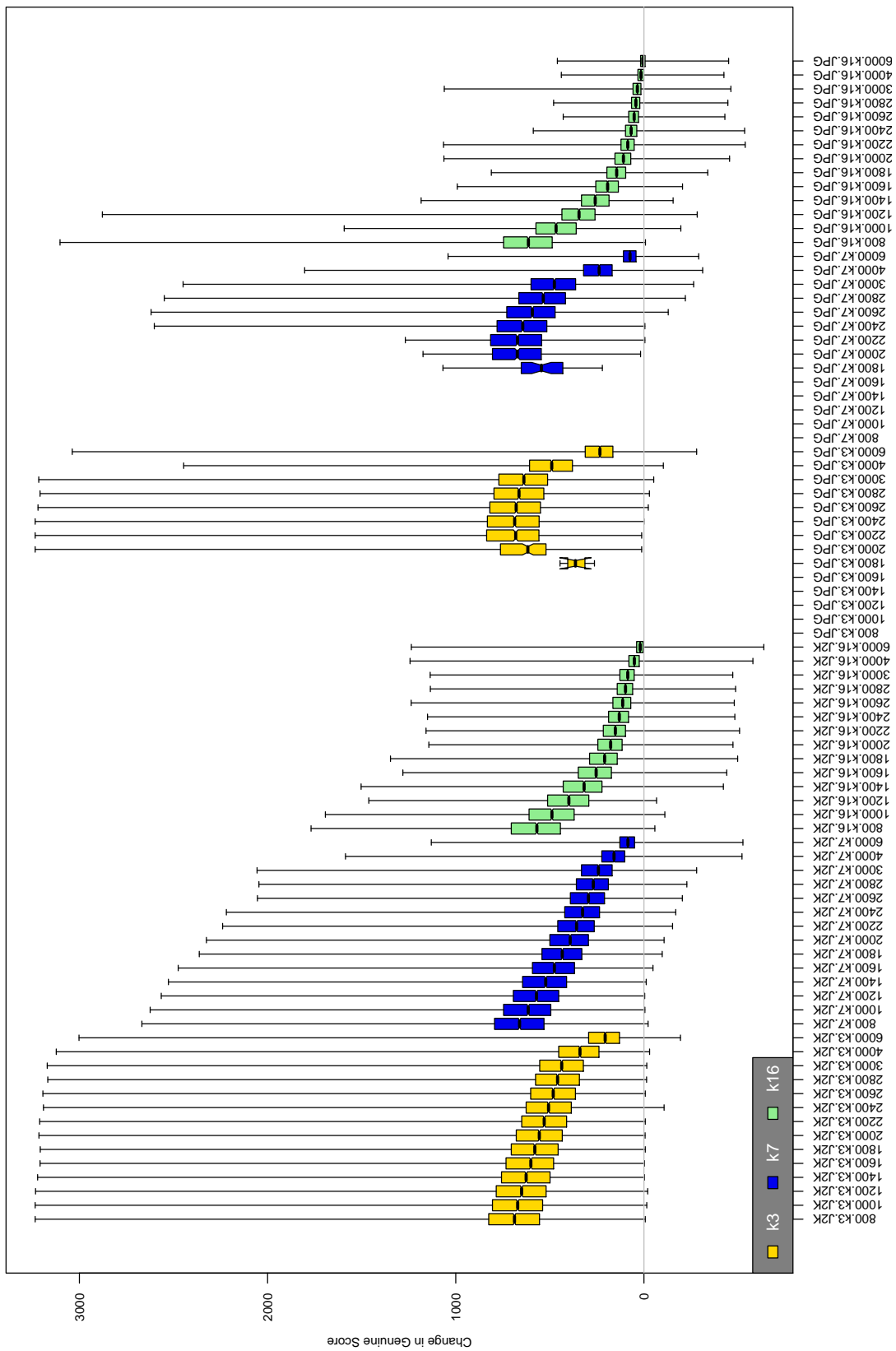


Table 237: The distribution of the *increase* in J2 native genuine comparison scores between the uncompressed “parent” and the compressed image, arranged by size, KIND and the compression algorithm. The images are from the OPS dataset. Any comparison involving a failed template is excluded. Note that the iris record size on the horizontal axis is not evenly spaced above 3000 bytes.

A = SAGEM	B = COGENT	C = CROSSMATCH	D = CAMBRIDGE	E = L1	x1 = PRIMARY
F = RETICA	G = LG	H = HONEYWELL	I = IRITECH	J = NEUROTECHNOLOGY	x2 = SECONDARY
KIND 1 = RAW 640x480		KIND 3 = CROP	KIND 7 = CROP+MASK	KIND 16 = CONCENTRIC POLAR	

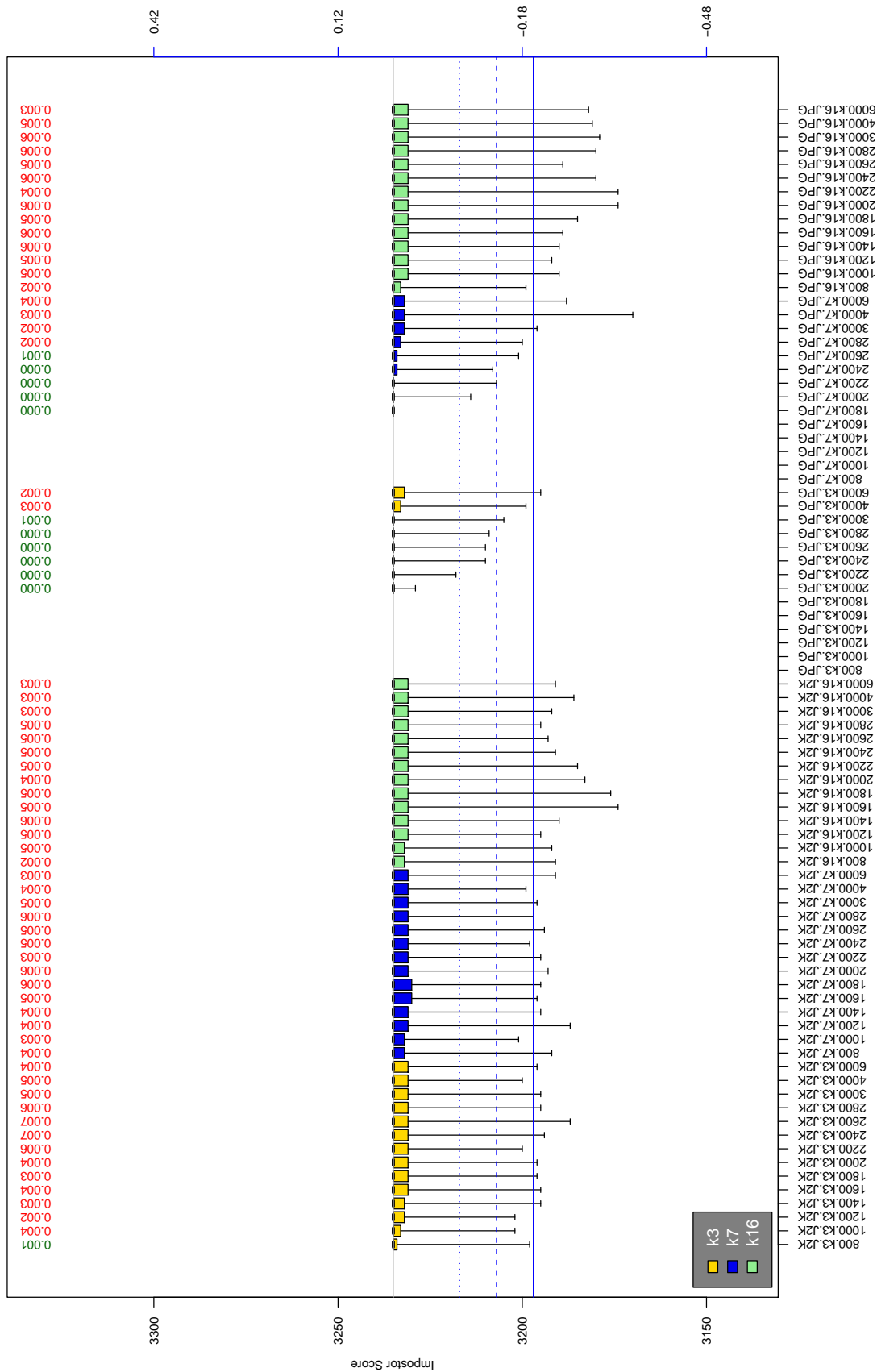


Table 238: The distribution of J2 native impostor comparison scores by size of the compressed image, KIND and the compression algorithm. The right axis scale gives the corresponding value for $d' = (s - \mu_1) / \sqrt{0.5(\sigma_1^2 + \sigma_2^2)}$ for impostor score s . The three blue lines correspond, from the top, to FMR of 10^{-2} , 10^{-3} , and 10^{-4} . The lower grey line refers to the median score obtained from comparison of uncompressed KIND 3 images. Any comparison involving a failed template is excluded. Above the boxplots are FMR values at the threshold that gives FMR = 10^{-3} on uncompressed images. These figures are computed from only 4000 comparisons so the FMR values and the tails of the impostor distribution are poorly characterized. Note that the iris record size on the horizontal axis is not evenly spaced above 3000 bytes.

A = SAGEM	B = COGENT	C = CROSSMATCH	D = CAMBRIDGE	E = L1	$x1$ = PRIMARY
F = RETICA	G = LG	H = HONEYWELL	I = IRITECH	J = NEUROTECHNOLOGY	$x2$ = SECONDARY
KIND 1 = RAW 640x480		KIND 3 = CROP		KIND 7 = CROP+MASK	KIND 16 = CONCENTRIC POLAR

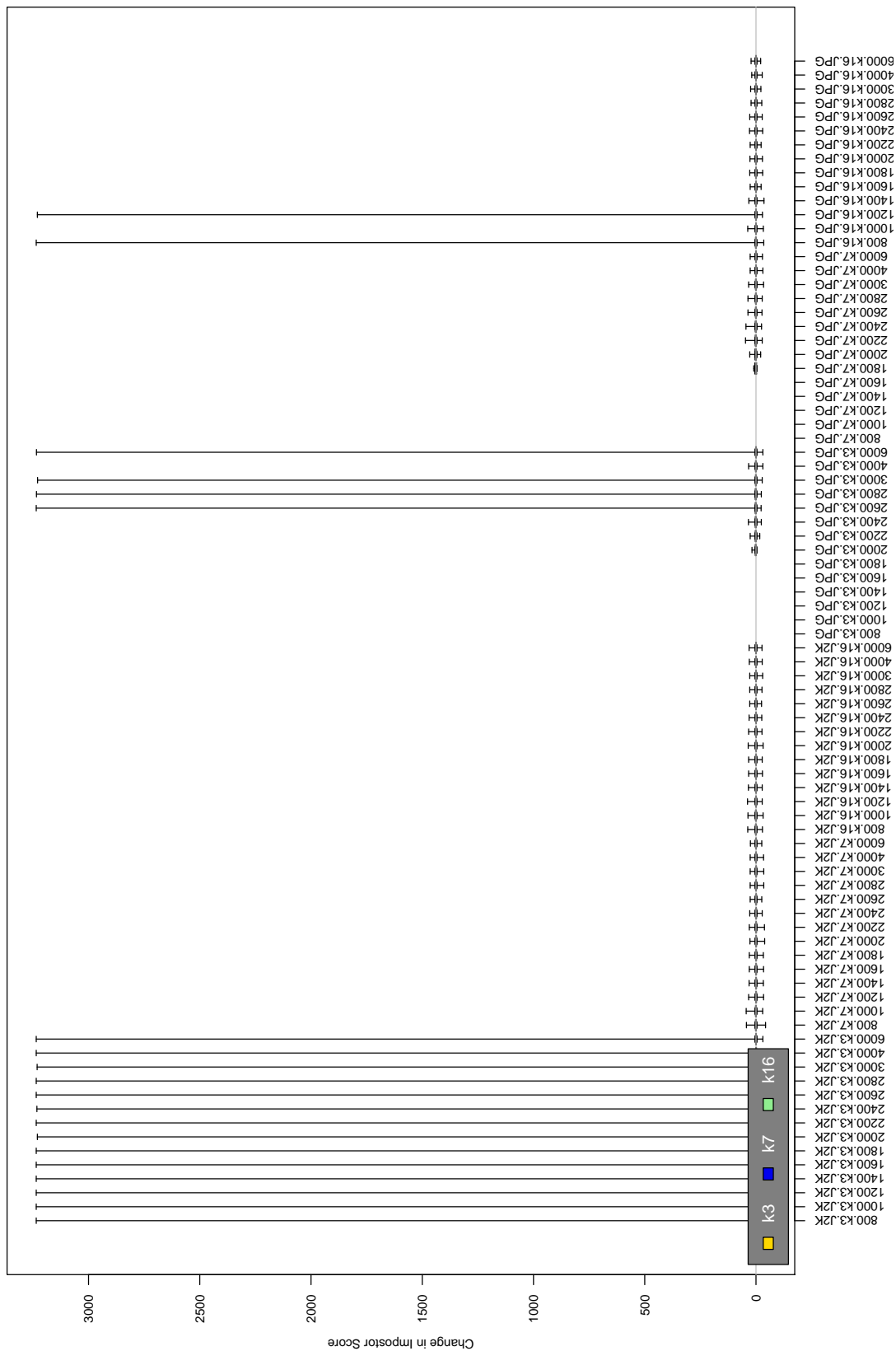


Table 239: The distribution of the increase in J2 native impostor comparison scores between the uncompressed “parent” and the compressed image, arranged by size, KIND and the compression algorithm. The images are from the OPS dataset. Any comparison involving a failed template is excluded. Note that the iris record size on the horizontal axis is not evenly spaced above 3000 bytes.

A = SAGEM	B = COGENT	C = CROSSMATCH	D = CAMBRIDGE	E = L1	x1 = PRIMARY
F = RETICA	G = LG	H = HONEYWELL	I = IRITECH	J = NEUROTECHNOLOGY	x2 = SECONDARY
KIND 1 = RAW 640x480		KIND 3 = CROP	KIND 7 = CROP+MASK	KIND 16 = CONCENTRIC POLAR	

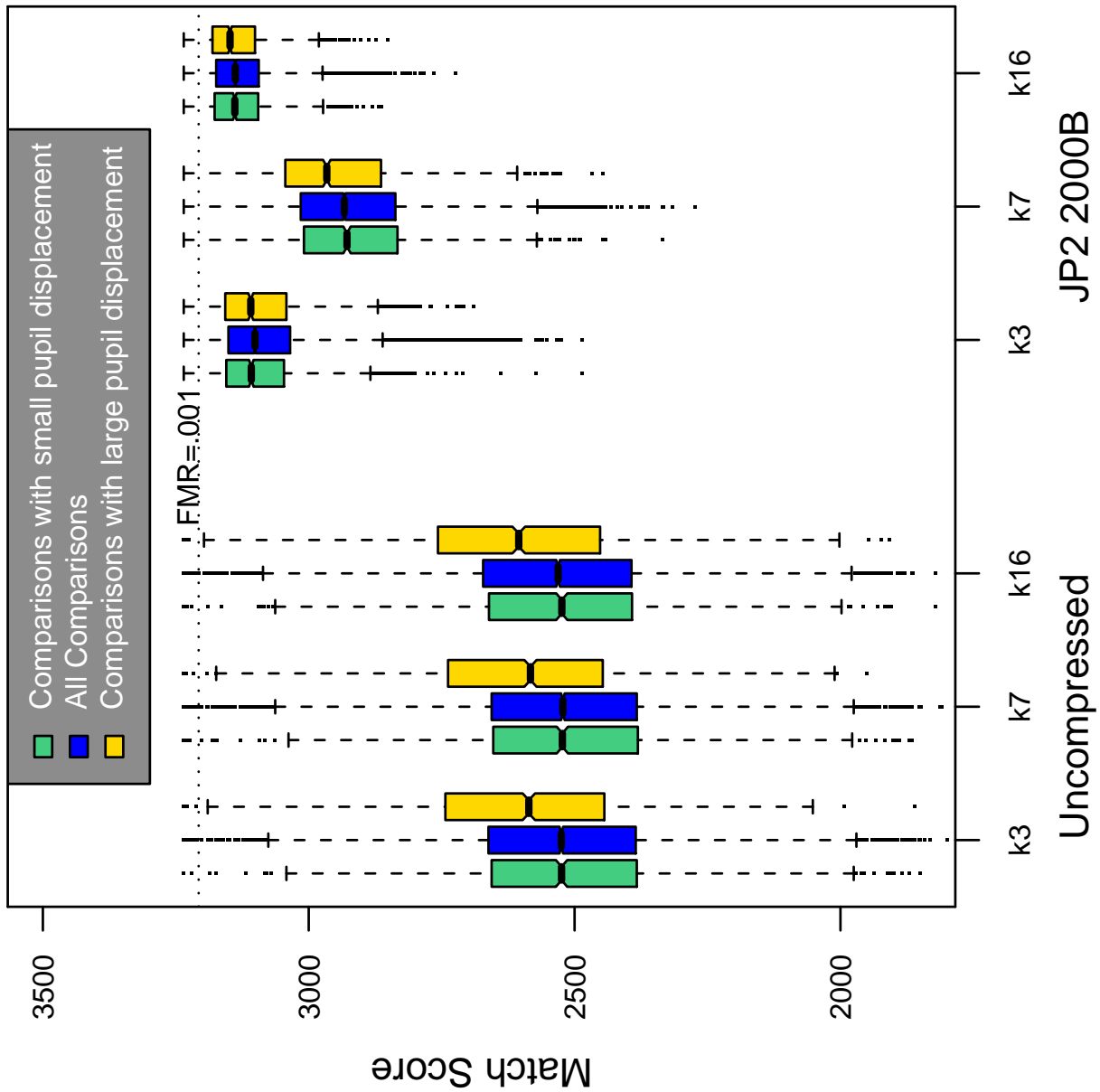


Table 240: Effect of pupil displacement on the genuine score distribution for J2

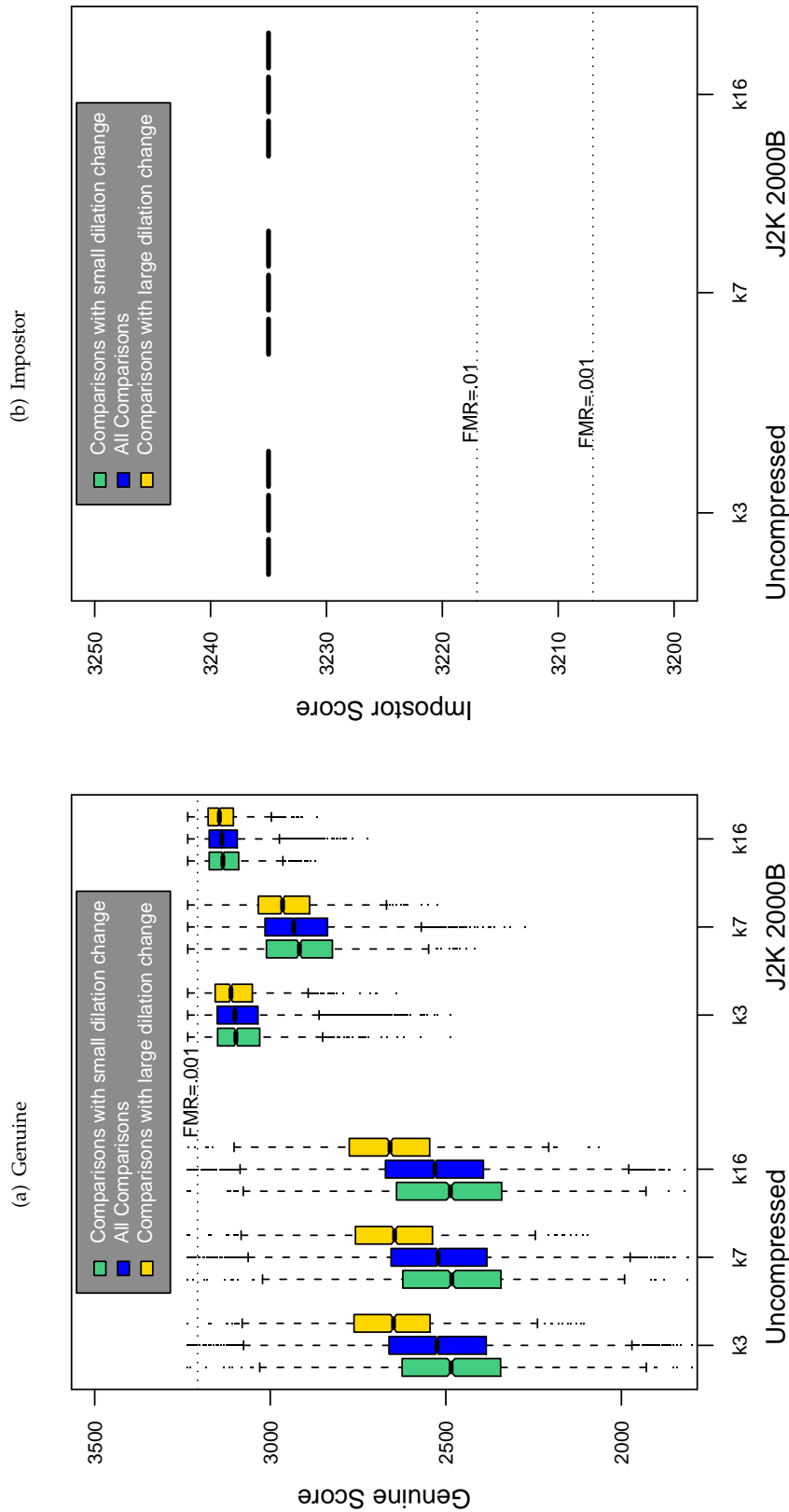


Table 241: The effect of dilation change on the two scores distributions for SDK J2.

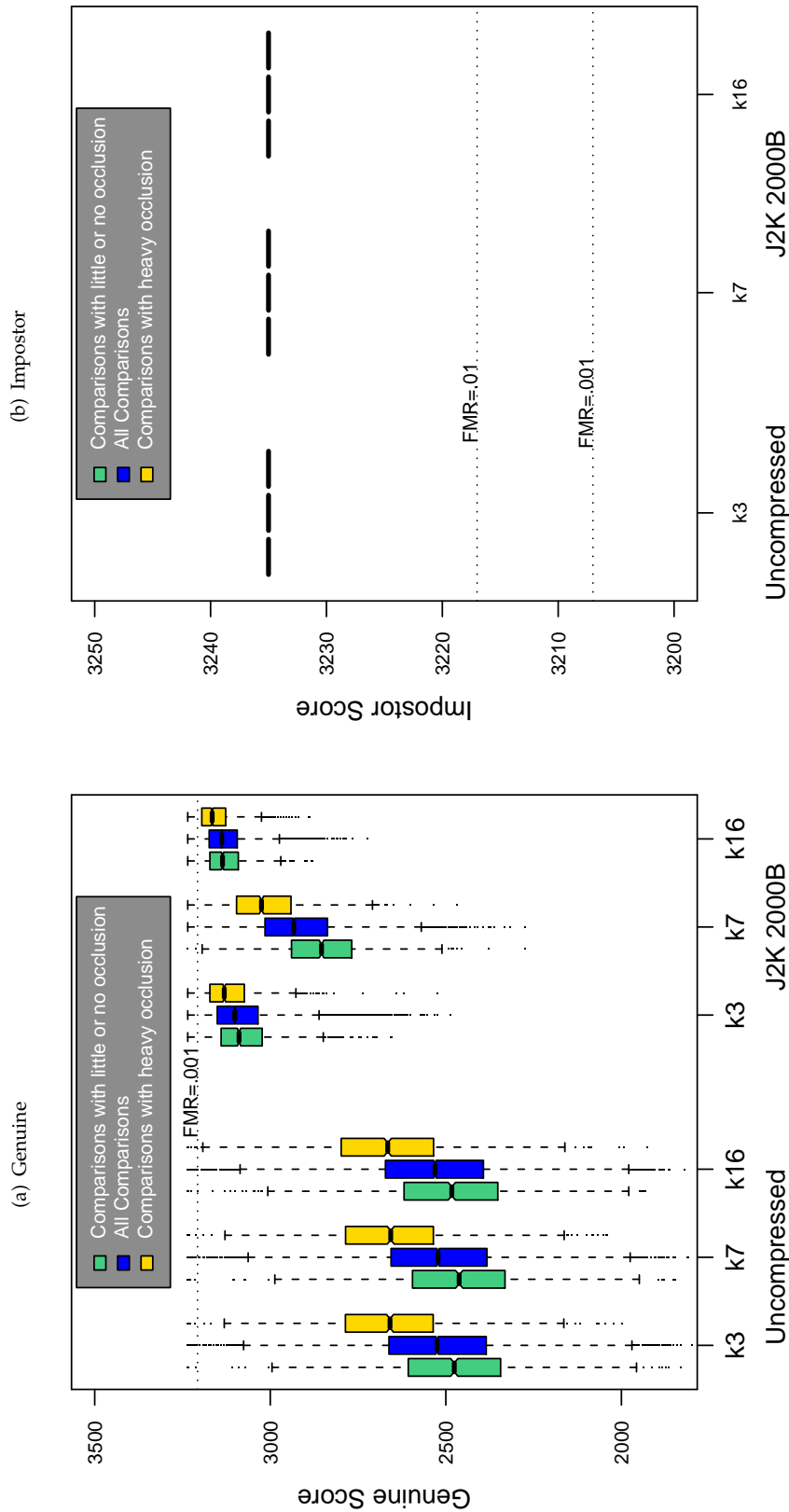
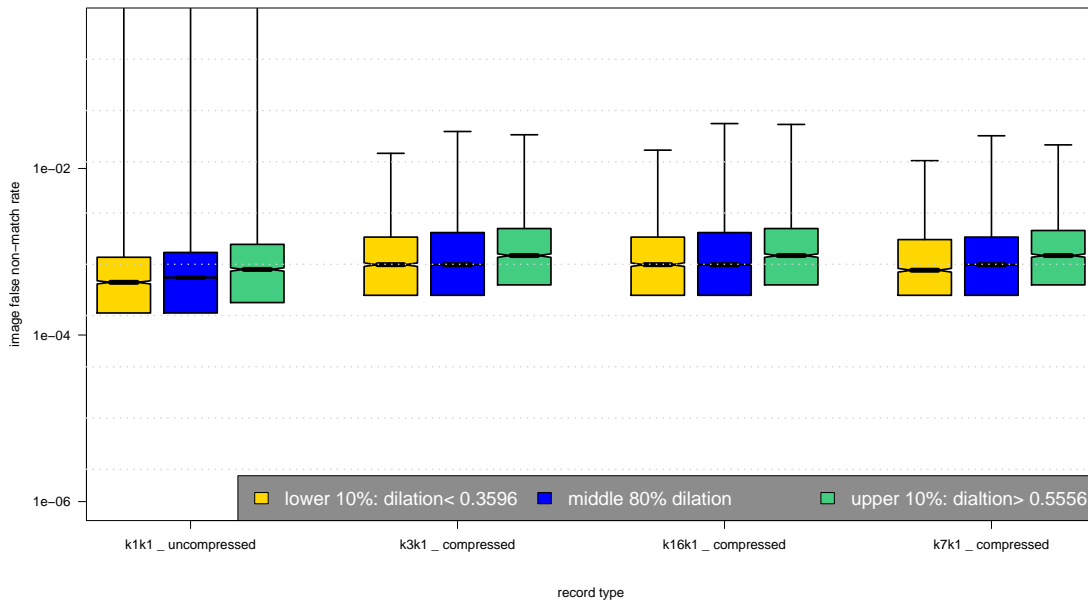
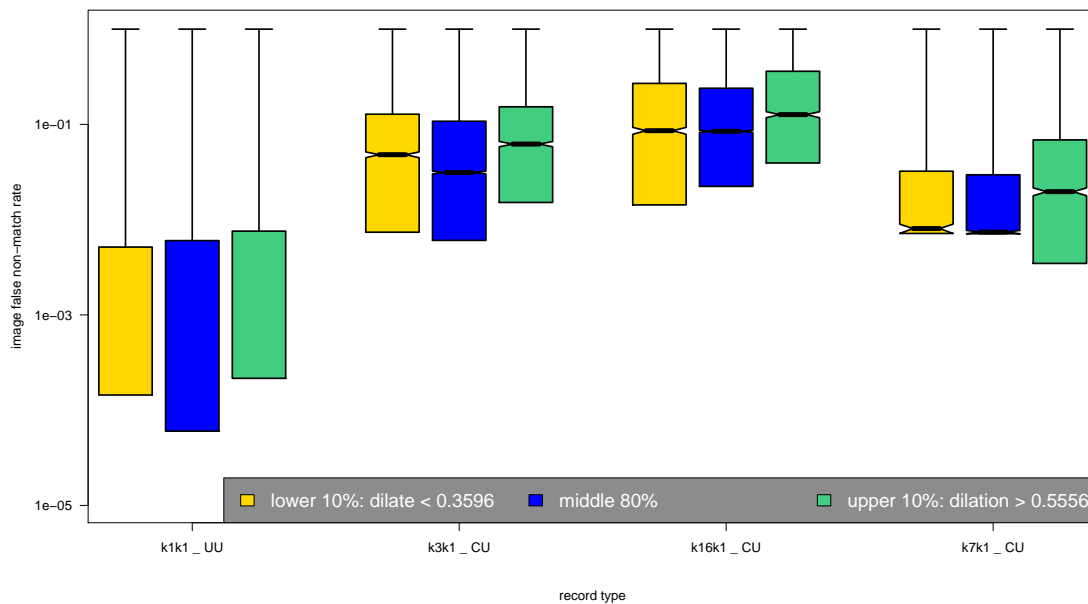


Table 242: The effect of eyelid occlusion on the two scores distributions for SDK J2.

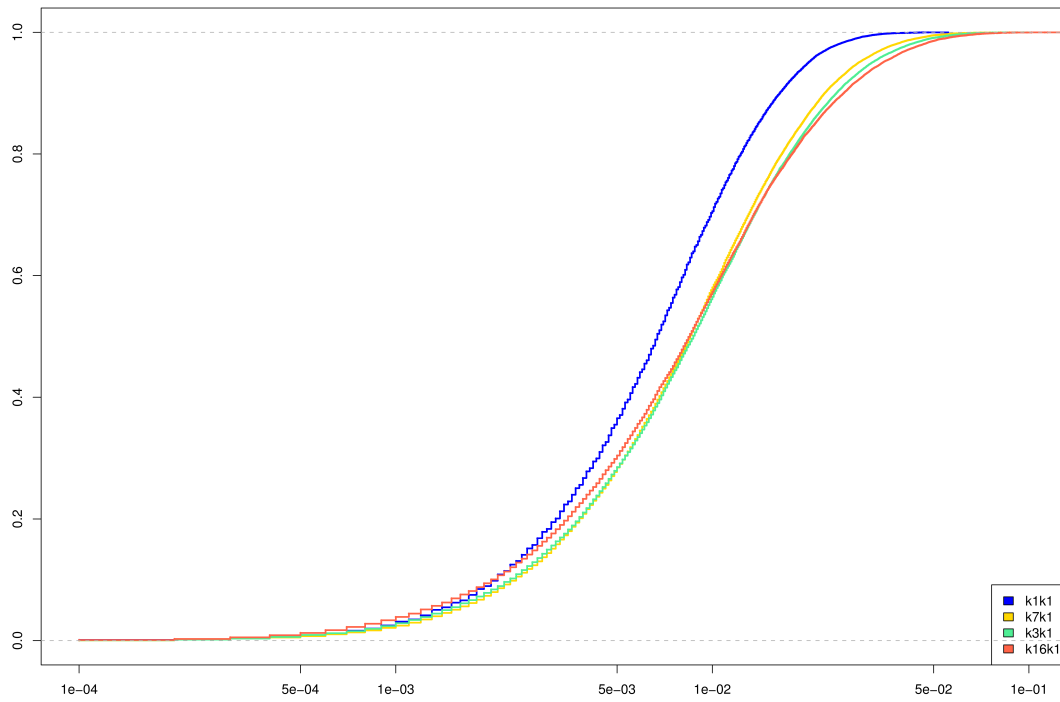
(a) iFMR using A1 dilation estimates



(b) iFNMR using A1 dilation estimates



(c) iFMR CDF



(d) iFNMR CDF

